

DOE/ID-10978
Revision 0
August 2003
Project No. 22522



U.S. Department of Energy
Idaho Operations Office

Performance Assessment for the INEEL CERCLA Disposal Facility Landfill



Idaho National Engineering and Environmental Laboratory

Performance Assessment for the INEEL CERCLA Disposal Facility Landfill

August 2003

**Prepared for the
U.S. Department of Energy
Idaho Operations Office**

ABSTRACT

This performance assessment for the INEEL CERCLA Disposal Facility (ICDF) landfill documents the projected radiological dose impacts associated with the disposal of low-level radioactive waste at the facility landfill. This assessment is conducted to evaluate compliance with the applicable radiological criteria of the Department of Energy and the Environmental Protection Agency for protection of the public and the environment. The calculations involve modeling the transport of radionuclides from buried waste to surface soil and subsurface media, and eventually to members of the public via air, groundwater, and food chain pathways. Projections of doses are calculated for both off-Site receptors and individuals who inadvertently intrude into the waste after site closure. The results of the calculations are used to evaluate the future performance of the disposal landfill. In addition, uncertainty and sensitivity analyses are performed. The comparison of the performance assessment results to the applicable performance objectives indicates that the performance objectives will be met.

EXECUTIVE SUMMARY

This report documents the projected impacts associated with disposal of low-level radioactive waste (LLW) at the INEEL CERCLA Disposal Facility (ICDF) landfill. The impacts were compared with applicable U.S. Department of Energy (DOE) and U.S. Environmental Protection Agency (EPA) standards.

The purpose of the ICDF landfill is to consolidate Idaho National Engineering and Environmental Laboratory (INEEL) Comprehensive Environmental Response, Compensation and Liability Act (CERCLA) wastes into one engineered facility. The LLW radiological performance assessment for the ICDF landfill presents a comprehensive, systematic analysis of the long-term impacts of LLW disposal in an arid, near-surface environment. Occupational radiological doses and impacts of nonradioactive, hazardous constituents are beyond the scope of this radiological performance assessment and will be considered in other assessments.

For the purpose of assessing the performance of LLW disposed of at the ICDF landfill, three time periods are of concern:

1. The institutional control period (100 years following closure of landfill in 2018), which follows site closure and during which periodic maintenance and monitoring activities are conducted. The facility is assumed to be closed, stabilized, and maintained but is still part of the INEEL reservation and is fenced and patrolled.
2. The compliance period (from 100 to 1,000 years following closure), during which the facility is assumed to be no longer maintained by the DOE and may be accessible to the public. Radiological impacts are assessed for a period of 1,000 years, the maximum time of compliance for DOE LLW performance assessments.
3. The postcompliance period (beyond 1,000 years). Analyses were also carried out to the time of maximum potential impact.

Two receptor types were assessed. The first was a member of the public. During the operational and institutional control periods, this individual resided at the INEEL Site boundary. During the postinstitutional control period, the member of the public resided 100 m from the downgradient edge of the ICDF waste. The receptor is exposed to contaminants through the groundwater all-pathways scenario, which assumes the receptor consumes (1) contaminated groundwater, (2) leafy vegetables and produce that were irrigated with contaminated groundwater, and (3) milk and meat from animals that consume contaminated water and pasture grass irrigated with contaminated groundwater.

The second type of receptor evaluated was an inadvertent intruder. This hypothetical receptor was assumed to intrude inadvertently onto the ICDF landfill during the postinstitutional control period. Two general kinds of intruder scenarios were evaluated: chronic and acute. The chronic scenario was a post-well-drilling scenario. This scenario included the doses from ingestion of contaminated food, inhalation of contaminated air, and external exposure. The

acute scenario was a well-drilling scenario. These scenarios included the doses from inhalation of contaminated air and external exposure. In both the acute and chronic scenarios, the doses were evaluated using the RESRAD computer code (Yu et al. 1993).

The performance assessment process consists of conceptual models that link radionuclide inventory, release (or source term), environmental transfer, and impact assessment (see Figure ES-1) and culminate in radiological doses to receptors. The waste inventory used in the performance assessment was derived from the INEEL CERCLA Disposal Facility Adjusted Design Inventory (EDF-ER-264).

The performance assessment focuses on two transport pathways to calculate exposure to off-Site members of the public; groundwater transport and atmospheric transport. The groundwater transport pathway describes the movement of radionuclides that leach from the landfill and move vertically down through the unsaturated zone to the aquifer. The atmospheric transport pathway considers radionuclides that diffuse to the landfill surface and are subsequently dispersed in the atmosphere.

The exposure pathways evaluated include ingestion of contaminated food and water, inhalation of radionuclides, and external exposure to radionuclides in the air and on the ground (or soil) surface. The agricultural products consumed by members of the public are contaminated via food chain transport of radionuclides deposited from air onto soil or plant surfaces, from radionuclides deposited onto soil or plant surfaces by irrigation water, or from the direct ingestion of contaminated water.

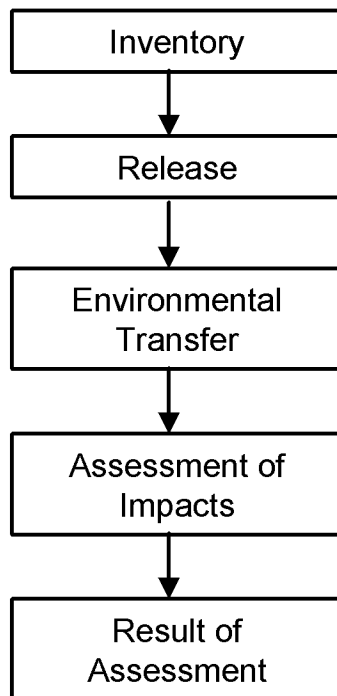


Figure ES-1. Performance assessment process.

The source of radionuclides for airborne transport during the operational and institutional control periods was diffusion of radioactive gases from the waste to the surface and transport of radioactive particles from the waste to surface soil by plant roots and harvester ants. The entire inventory of C-14, tritium, and Kr-85 was conservatively assumed to diffuse to the surface where it was dispersed to downwind receptors using the CAP88-PC computer code and INEEL meteorological data. Radon diffusion from the waste through the cover was evaluated using the RESRAD code for comparison with the 40 CFR 61, Subpart Q, standard for radon flux.

Impacts from the subsurface migration of radionuclides dissolved in groundwater were estimated using computer models that described release of radionuclides from the soils disposed of to the ICDF landfill and transported through the unsaturated zone to aquifer compliance locations.

A two-compartment source term model was developed that assumed the waste was homogeneous soils, available for transport from the source to the vadose zone in year 2018. The leachate was assumed to move from the waste area into a clay layer that provides additional attenuation and a change in the flux to the vadose zone due to generally much higher sorption. The computer code GWSCREEN used the source term model as a flux input and calculated the transport through the vadose zone and into the aquifer. Concentrations were estimated in the aquifer at a hypothetical receptor well located 100 m downgradient from the edge of the ICDF waste per DOE O 435.1. Decay and sorption were included throughout the model and reduced or slowed the migration of radionuclides in the subsurface.

This representation of subsurface transport is greatly simplified over the true processes that occur, reflecting the lack of definitive understanding of water movement in the subsurface beneath the ICDF landfill. As a result, the predictive concentrations used in this radiological performance assessment are affected by the uncertainties regarding these processes. An uncertainty analysis was performed on the hydrological transport model to assess the uncertainty of the calculations. The results indicate the precision of the model is roughly a factor of four thousand during the 1,000-year compliance period.

The results of the atmospheric, all-pathways, inadvertent intruder, and groundwater protection analyses are shown in Table ES-1, based on a maximum time of compliance of 1,000 years. These results indicate that the atmospheric, all-pathways, chronic intrusion, acute intrusion, and groundwater protection performance objectives will be met.

If the time of compliance were extended to 10,000 years, the performance objectives for the atmospheric, all-pathways, inadvertent intruder, and groundwater protection scenarios would still be met. In summary, there is a reasonable expectation that the performance objectives identified will not be exceeded as a result of postclosure of the ICDF landfill facility.

Table ES-1. Comparison of performance objectives and ICDF landfill performance assessment results.

Performance Objective	Standard	ICDF Performance Assessment Result
All-pathways (DOE O 435.1)	25 mrem/yr EDE ^a	0.05 mrem/yr (4.55 mrem/yr after 1,000-year time of compliance)
Atmospheric (40 CFR 61 Subpart H)	10 mrem/yr EDE (entire INEEL site)	0.01 mrem/yr during the operational and institutional control periods 0.01 mrem/yr during the postinstitutional control period
Atmospheric (40 CFR 61 Subpart Q)	20 pCi/m ² -s radon flux	0.17 pCi/m ² -s
Chronic inadvertent intruder (DOE O 435.1)	100 mrem/yr EDE	3.3 mrem/yr
Acute inadvertent intruder (DOE O 435.1)	500 mrem EDE	12.6 mrem
Groundwater protection	4 mrem/yr beta-gamma CDE ^b	0.4 mrem/yr (40 mrem/yr after 1,000-year time of compliance)
	20,000 pCi/L tritium	NA – screened out
	1 pCi/L I-129	0.10 pCi/L (9.8 pCi/L after the 1,000-year time of compliance)
	8 pCi/L Sr-90	NA – screened out
	5 pCi/L Ra-226 and -228	2.4×10^{-6} pCi/L (0.029 pCi/L after 1,000-year time of compliance)
	15 pCi/L gross alpha	0.011 pCi/L (0.2 pCi/L after 1,000-year time of compliance)
	20 µg/L uranium	0.083 µg/L (1.6 µg/L after 1,000-year time of compliance)

a. EDE = effective dose equivalent.

b. CDE = committed dose equivalent.

CONTENTS

ABSTRACT.....	iii
EXECUTIVE SUMMARY	v
ACRONYMS	xvii
1. INTRODUCTION.....	1-1
1.1 General Approach	1-1
1.2 General Facility Description	1-2
1.2.1 Waste Acceptance Criteria.....	1-6
1.2.2 General Land Use Patterns.....	1-6
1.3 LLW Disposal Facility Life Cycle	1-7
1.4 Related Documents.....	1-8
1.5 Performance Criteria	1-11
1.5.1 Public Protection Performance Objectives	1-11
1.5.2 Water Resource Impact Assessment.....	1-12
1.5.3 Intruder Analysis	1-14
1.5.4 ALARA Analysis	1-14
1.6 Summary of Key Assumptions	1-15
1.6.1 Source Inventory and Release Rates	1-16
1.6.2 Subsurface Models	1-17
1.7 Quality Assurance Measures.....	1-17
2. DISPOSAL FACILITY CHARACTERISTICS	2-1
2.1 Site Characteristics	2-1
2.1.1 Geography and Demography	2-1
2.1.2 Meteorology and Climatology	2-7
2.1.3 Ecology.....	2-9
2.1.4 Geology, Seismology, and Volcanology	2-13
2.1.5 Hydrology	2-26
2.1.6 Geochemistry	2-32
2.1.7 Natural Resources	2-38
2.1.8 Natural Background Radiation.....	2-40
2.2 Principal Facility Design Features	2-40
2.2.1 Water Infiltration.....	2-41
2.2.2 Disposal Unit Cover Integrity	2-46

2.2.3	Structural Integrity	2-50
2.2.4	Inadvertent Intruder Barrier	2-53
2.3	Waste Characteristics	2-53
2.3.1	Methods and Assumptions Used to Determine the Inventory.....	2-54
2.3.2	Initial Design and Adjusted Design Inventories.....	2-58
2.4	Summary of the ICDF Landfill Design Hydrologic Modeling Analyses	2-63
3.	ANALYSIS OF PERFORMANCE.....	3-1
3.1	Overview of Analysis	3-1
3.2	Analysis of Performance: Subsurface Transport Pathways	3-2
3.2.1	Conceptual Model of Facility Performance	3-2
3.2.2	Exposure Pathways and Scenarios	3-5
3.2.3	Radionuclide Inventories and Source Term.....	3-10
3.2.4	Environmental Transport of Radionuclides	3-25
3.3	Radon Analysis	3-35
3.4	Biotic Pathways.....	3-36
3.5	Atmospheric Pathways	3-37
4.	RESULTS OF ANALYSIS	4-1
4.1	Source Term.....	4-1
4.2	Groundwater Pathway Environmental Transport.....	4-1
4.3	Radon Flux Analysis	4-10
4.4	Atmospheric Emissions Dose Analysis	4-11
4.5	Groundwater Pathway Dose Analyses.....	4-11
4.5.1	All-Pathways Doses	4-11
4.5.2	Assessment of Groundwater Protection.....	4-13
4.6	Sensitivity/Uncertainty Analysis.....	4-14
4.6.1	Groundwater Pathway Sensitivity/Uncertainty	4-14
4.6.2	Sensitivity Analysis	4-26
5.	INADVERTENT INTRUDER ANALYSES	5-1
5.1	Intruder Inventory	5-1
5.1.1	Screening Procedure.....	5-1

5.1.2	Screening Results	5-2
5.2	Intruder Scenarios	5-4
5.2.1	Acute Intruder Scenarios	5-5
5.2.2	Chronic Intruder Scenarios	5-6
5.2.3	Acute Scenario Used in the Performance Assessment	5-7
5.2.4	Chronic Scenario Used in the Performance Assessment	5-8
5.3	Modeling of Intruder Scenarios.....	5-10
5.3.1	Time Periods Modeled.....	5-10
5.3.2	Input Parameters Used to Model the Acute Drilling Scenario.....	5-10
5.3.3	Input Parameters Used to Model the Chronic Postdrilling Scenario	5-10
5.4	Results	5-13
5.4.1	Acute Drilling Scenario	5-13
5.4.2	Chronic Postdrilling Scenario	5-13
5.5	Sensitivity and Uncertainty	5-14
6.	INTERPRETATION OF RESULTS.....	6-1
6.1	All-Pathways Dose	6-1
6.2	Radon Flux Results	6-3
6.3	Air Pathway Results	6-3
6.4	Groundwater Protection Results.....	6-3
6.5	Inadvertent Intruder Analysis Results	6-4
7.	PERFORMANCE EVALUATION.....	7-1
7.1	Comparison of Results to Performance Objectives	7-1
7.1.1	Analysis of I-129 in the Drinking Water Pathway	7-1
7.1.2	Use of Performance Assessment Results	7-1
7.2	Further Work.....	7-2
8.	WASTE ACCEPTANCE CRITERIA FOR THE ICDF	8-1
8.1	Intruder-Based WAC.....	8-1
8.2	Waste Acceptance Criteria Based on Groundwater Pathway	8-3
8.3	Sensitivity of Groundwater I-129 WAC to Cover Life	8-3
8.4	WAC Modifications Based on ICDF PA.....	8-5

9.	ALARA ANALYSIS.....	9-1
10.	PREPARERS	10-1
11.	REFERENCES.....	11-1
	Appendix A—Cover Design Life.....	A-1
	Appendix B—Monte Carlo Simulation of the ICDF Cover System for Infiltration and Longevity	B-1
	Appendix C—K _d Values for INTEC Groundwater Modeling	C-1

FIGURES

ES-1.	Performance assessment process.....	vi
1-1.	Map showing location of Idaho Nuclear Technology and Engineering Center.	1-3
1-2.	Location of the ICDF Complex.....	1-4
1-3.	Detailed layout of ICDF Complex.	1-5
1-4.	Land use designations in and around the INEEL.	1-8
2-1.	Map of the INEEL and the Eastern Snake River Plain.....	2-2
2-2.	Approximate distribution of vegetation at the INEEL.....	2-10
2-3.	Generalized geological map of the INEEL area.....	2-14
2-4.	Plan view of cross section shown in Figure 2-5.....	2-16
2-5.	North-south geological cross section at INTEC.....	2-17
2-6.	Locations of geologic cross sections and existing wells.....	2-19
2-7.	An east-west geologic cross section through the ICDF.....	2-20
2-8.	Seismicity and earthquake epicenter map showing the ESRP in relation to the Intermountain Seismic Belt and the Centennial Tectonic belt (WCFS 1996).....	2-22
2-9.	Earthquake epicenters in the INEEL region, 1850–1995.	2-23
2-10.	Volcanic rift zones at the INEEL.	2-25
2-11.	Surface water features on the INEEL.	2-27
2-12.	Water levels in PW series perched water wells and discharge in the Big Lost River at Lincoln Boulevard.....	2-30
2-13.	Schoeller diagram of water quality at INTEC for perched water, service waste water, the SRPA, and the Big Lost River.	2-34

2-14. Piper diagram of water chemistry from perched water, the SRPA, and the Big Lost River.....	2-36
2-15. Trilinear diagram of anion composition of perched water, Big Lost River water, and SRPA water.....	2-37
2-16. Landfill double composite liner system.....	2-42
2-17. Landfill cover section.....	2-44
2-18. Simplified depiction of the infiltration limiting final cover for the ICDF landfill.....	2-45
2-19. Schematic of the final landfill cover functional sections.....	2-46
2-20. Conceptual model and finite difference grid used for the ICDF STOMP fate and transport modeling.....	2-65
3-1. Overview of the analysis of performance for the ICDF landfill performance assessment.....	3-1
3-2. Conceptual model for the ICDF landfill performance assessment while the cover is intact.....	3-3
3-3. Conceptual model for the ICDF landfill performance assessment after cover failure.....	3-3
3-4. Conceptual model for GWSCREEN groundwater transport model.....	3-17
3-5. Conceptual model for the source term.....	3-23
3-6. Results of calibration of GWSCREEN to STOMP.....	3-32
4-1. Radionuclide flux from the base of the ICDF landfill (below the clay liner) to the top of the vadose zone as a function of time for the seven important nuclides in the ICDF landfill. Simulation start time is the year 2018.....	4-2
4-2. Radionuclide flux to the aquifer as a function of time for the seven important nuclides in the ICDF landfill. Simulation start time is the year 2018.....	4-3
4-3. Radionuclide concentrations in the aquifer as a function of time at the 180-m receptor (100 m downgradient from the edge of the source). Simulation start time is the year 2018.....	4-4
4-4. Concentration of Np-239 and significant progeny in the aquifer as a function of time at the 180-m (100 m downgradient from the edge of source) receptor location. Simulation start time is the year 2018.....	4-5
4-5. Concentration of Pu-239 and significant progeny in the aquifer as a function of time at the 180-m (100 m downgradient from the edge of source) receptor location. Simulation start time is the year 2018.....	4-6
4-6. Concentration of Pu-240 and significant progeny in the aquifer as a function of time at the 180-m (100 m downgradient from the edge of source) receptor location. Simulation start time is the year 2018.....	4-7

4-7.	Concentration of U-234 and significant progeny in the aquifer as a function of time at the 180-m (100 m downgradient from the edge of source) receptor location. Simulation start time is the year 2018.	4-8
4-8.	Concentration of U-238 and significant progeny in the aquifer as a function of time at the 180-m (100 m downgradient from the edge of source) receptor location. Simulation start time is the year 2018.	4-9
4-9.	All-pathways dose as a function of time at the 180-m (100 m downgradient from the edge of source) receptor location. The simulation starts at the end of operations (year 2018).	4-12
4-10.	Iodine-129 concentrations in the aquifer at the compliance point (100 m downgradient from the downgradient edge of the facility) as a function of time for the seven cover integrity scenarios described in Table 4-6. The deterministic results are based on Scenario 4.	4-16
4-11.	Frequency distribution of 500 samples of background percolation.	4-20
4-12.	Frequency distribution of 500 samples of longitudinal dispersivity in the aquifer.	4-20
4-13.	Frequency distribution of 500 samples of longitudinal dispersivity in the unsaturated zone.	4-21
4-14.	Frequency distribution of 500 samples of the iodine sorption coefficient in waste and interbed material.	4-22
4-15.	Frequency distribution of 500 samples of the iodine sorption coefficient in clay material.	4-23
4-16.	Frequency distribution of 500 samples of the cover lifetime.	4-23
4-17.	Distribution of all-pathways doses as a function of time at the 180-m (100 m downgradient from the edge of source) receptor location. The start time of the simulation is the year 2018.	4-24
4-18.	Cumulative frequency distribution of the I-129 concentration in the aquifer at the 180-m (100 m downgradient from the edge of source) receptor location for 1,000 years and 3,000 years following closure of the facility in the year 2018.	4-26
5-1.	Conceptual profile of ICDF landfill.	5-4
5-2.	Graphical representation of the acute drilling scenario (figure does not depict actual landfill site with final cover and side slopes that would deter drill rig from driving onto cover).	5-8
5-3.	Graphical representation of the chronic intruder postdrilling scenario (figure does not depict actual landfill site with final cover and steep side slopes that would deter family from taking up residence).	5-9

TABLES

1-1.	Performance objectives for the ICDF landfill performance assessment.	1-15
2-1.	Regional population of the INEEL; selected years 1990–2025.	2-4

2-2.	Threatened or endangered species, sensitive species, and species of concern that may be found on the INEEL	2-12
2-3.	Groundwater chemistries from the ESRP aquifer at the INEEL	2-33
2-4.	INEEL production wells and annual volume pumped	2-39
2-5.	Summary of predicted cover settlement	2-51
2-6.	Design and adjusted design inventories used for the ICDF landfill fate and transport analyses—radionuclide contaminants	2-58
3-1.	Element-independent parameter values used in the all-pathways dose calculation	3-6
3-2.	Element-specific parameter values used in the all-pathways dose calculation	3-6
3-3.	Radionuclide inventories and half-lives. Nuclides with half-lives less than 1 year were removed from further consideration and are shown in bold	3-12
3-4.	Phase II screening results for nuclides with half-lives >1 year using the NCRP screening factors.....	3-16
3-5.	Parameter values for Phase III screening of the ICDF landfill waste inventories	3-19
3-6.	Phase III groundwater pathway screening results using the GWSCREEN model	3-20
3-7.	Fixed and calibrated parameter values for calibration of GWSCREEN with STOMP	3-31
3-8.	Nuclide-independent parameter values for the GWSCREEN landfill performance assessment simulation	3-33
3-9.	Nuclide-dependent transport parameters	3-34
3-10.	Data used in the radon flux calculations	3-36
4-1.	Unsaturated transit times and peak ICDF and aquifer radionuclide fluxes.....	4-2
4-2.	Maximum radionuclide concentrations and time of maximum at the 180-m (100 m downgradient from the edge of source) receptor location	4-10
4-3.	Radon flux (pCi/m ² -s) from soil surface.....	4-11
4-4.	Maximum all-pathways doses and time of maximum at the 180-m (100 m downgradient from the edge of source) receptor location	4-13
4-5.	Comparison of groundwater protection criteria	4-14
4-6.	Description of cover integrity scenarios used to evaluate sensitivity of I-129 concentrations to cover integrity	4-15
4-7.	Parameter distributions used in the uncertainty sensitivity analysis	4-18

4-8.	Percentiles of the all-pathways dose at 1,000 years (year 3018).....	4-25
4-9.	Rank correlation coefficients and percent contribution to variance for the total (all nuclides) all-pathways dose at 1,000; 3,000; and 10,000 years	4-28
5-1.	Screening results for nuclides with half-lives >1 year using the NCRP screening factors.....	5-3
5-2.	Input parameters used in acute drilling scenarios.....	5-11
5-3.	Input parameters used in chronic drilling scenarios	5-12
5-4.	Acute and chronic intruder doses	5-13
6-1.	Maximum all-pathways doses and time of maximum at the 180-m (100 m downgradient from the edge of source) receptor location	6-2
6-2.	Comparison of groundwater protection criteria.	6-4
7-1.	Comparison of the ICDF landfill performance assessment results and the applicable performance objectives for the 0- to 1000-year time of compliance. Peak results are shown in parentheses	7-2
8-1.	Development of ICDF radionuclide WAC based on the chronic and acute intruder drilling scenarios	8-2
8-2.	Groundwater pathway WAC calculations for the PA contaminants of concern based on 25 mrem/yr performance objective	8-4
8-3.	Groundwater pathway WAC calculations for the PA contaminants of concern based on the groundwater MCLs.....	8-4
8-4.	Peak I-129 concentration and WAC values based on meeting the I-129 MCL of 1 pCi/L for the different cover integrity scenarios	8-5
8-5.	Development of ICDF radionuclide WAC based on the minimum WAC from the chronic and acute intruder drilling scenarios and groundwater pathway PA results and the ICDF design WAC.....	8-6

ACRONYMS

ADI	adjusted design inventory
ALARA	as low as reasonably achievable
bgs	below ground surface
BLM	U.S. Bureau of Land Management
CDC	Conservation Data Center
CDE	committed dose equivalent
CERCLA	Comprehensive Environmental Response, Compensation and Liability Act
CFA	Central Facilities Area
CFR	Code of Federal Regulations
CWID	CERCLA Waste Inventory Database
D&D&D	deactivation, decontamination, and decommissioning
DOE	U.S. Department of Energy
DOE-ID	U.S. Department of Energy Idaho Operations Office
DSR	dose-to-source ratio
EBR-I	Experimental Breeder Reactor-I
EDE	effective dose equivalent
EPA	U.S. Environmental Protection Agency
ESRP	Eastern Snake River Plain
FFA/CO	Federal Facility Agreement and Consent Order
GCL	geomembrane/geosynthetic clay liner
GSD	geometric standard deviation
HDPE	high-density polyethylene
ICDF	INEEL CERCLA Disposal Facility
ICP	Idaho Closure Project
ICPP	Idaho Chemical Processing Plant

ICRP	International Commission on Radiation Protection
IDAPA	Idaho Administrative Procedures Act
IDFG	Idaho Department of Fish and Game
IDI	initial design inventory
IDW	investigation-derived waste
INEEL	Idaho National Engineering and Environmental Laboratory
INPS	Idaho Native Plant Society
INTEC	Idaho Nuclear Technology and Engineering Center
LCRS	leachate collection recovery system
LLW	low-level waste
LFRG	Low-Level Waste Federal Review Group
MCL	maximum contaminant level
MEPAS	Multimedia Environmental Pollutant Assessment System
NCRP	National Council on Radiation Protection
NESHAP	National Emission Standards for Hazardous Air Pollutants
NRC	U.S. Nuclear Regulatory Commission
OU	operable unit
PA	performance assessment
PCB	polychlorinated biphenyl
PLDRS	primary leak detection recovery system
PMP	probable maximum precipitation
PNNL	Pacific Northwest National Laboratory
PPE	personal protective equipment
RCRA	Resource Conservation and Recovery Act
RD/RA	remedial design/remedial action
RESL	Radiological and Environmental Sciences Laboratory

RI/BRA	remedial investigation/baseline risk assessment
RI/FS	remedial investigation/feasibility study
ROD	Record of Decision
RWMC	Radioactive Waste Management Complex
SBL	soil bentonite liner
SDA	Subsurface Disposal Area
SF	screening factor
SLDRS	secondary leak detection recovery system
SRPA	Snake River Plain Aquifer
SSSTF	Staging, Storage, Sizing, and Treatment Facility
STOMP	Subsurface Transport Over Multiple Phases
SWW	service wastewater
T/E	threatened or endangered
TRA	Test Reactor Area
TSCA	Toxic Substances Control Act
UCL	upper confidence limit
USFS	U.S. Forest Service
USFWS	U.S. Fish and Wildlife Service
USGS	U.S. Geological Survey
VWG	Volcanism Working Group
WAC	Waste Acceptance Criteria
WAG	waste area group
WS	water supply

Performance Assessment for the INEEL CERCLA Disposal Facility Landfill

1. INTRODUCTION

The U.S. Department of Energy Idaho Operations Office (DOE-ID) authorized a remedial design/remedial action (RD/RA) for the Idaho Nuclear Technology and Engineering Center (INTEC) in accordance with the Waste Area Group (WAG) 3, Operable Unit (OU) 3-13 Record of Decision (ROD) (DOE-ID 1999). The ROD requires the removal and on-Site disposal of some of the Comprehensive Environmental Response, Compensation and Liability Act (CERCLA) remediation wastes generated within the boundaries of the Idaho National Engineering and Environmental Laboratory (INEEL).

The ROD requirements necessitated the construction of the INEEL CERCLA Disposal Facility (ICDF), which will be the disposal facility for the CERCLA generated waste streams. The ICDF is an on-Site, engineered facility, located south of INTEC, that meets the substantive requirements of Resource Conservation and Recovery Act (RCRA) Subtitle C, Toxic Substances Control Act (TSCA) polychlorinated biphenyl (PCB) landfill design and construction requirements. Designed and operated to accept not only WAG 3 wastes, but also wastes from other INEEL CERCLA actions, the ICDF Complex includes the necessary subsystems and support facilities to provide a complete waste disposal system.

The major components of the ICDF Complex include the landfill, an evaporation pond comprised of two cells, and the Staging, Storage, Sizing, and Treatment Facility (SSSTF). The ICDF landfill will accept only radioactive low-level, mixed low-level, hazardous, and TSCA wastes generated from INEEL CERCLA activities. Current projections of site-wide CERCLA waste volumes total about 389,923 m³ (510,000 yd³) (DOE-ID 1999). Most of the waste will be contaminated soil, but debris and CERCLA investigation-derived waste (IDW) are also included in the waste inventory.

Construction of the landfill has occurred and wastes are planned to be deposited in the ICDF Complex by the end of FY 2003. The ICDF landfill is scheduled to accept solid waste for a 15-year operations period with a postclosure period of 30 years and a landfill cover design life of 1,000 years.

This performance assessment (PA) documents the projected radiological dose impacts associated with the disposal of radioactive low-level waste (LLW) at the ICDF landfill. This radiological performance assessment is conducted to evaluate compliance with applicable radiological criteria of the U.S. Department of Energy (DOE) and the U.S. Environmental Protection Agency (EPA) for protection of the public and environment. The radiological performance assessment fulfills the requirements of DOE O 435.1, "Radioactive Waste Management." This PA includes calculations, for the 1,000-year period after closure, of potential doses to representative future members of the public, and potential releases from the landfill to demonstrate a reasonable expectation that the performance objectives are not exceeded as a result of the operation and closure of the ICDF landfill. The calculations involve modeling the transport of radionuclides from buried waste, to surface soil and subsurface media, and eventually to members of the public via air, groundwater, and food chain pathways. Projections of doses are made for both off-Site receptors and individuals inadvertently intruding onto the site after closure. In addition, uncertainty and sensitivity analyses are performed.

1.1 General Approach

A performance assessment is "an analysis of a radioactive waste disposal facility conducted to demonstrate there is a reasonable expectation that performance objectives established for the long-term protection of the public and the environment will not be exceeded following closure of the facility" (DOE O 435.1). Performance objectives include public and intruder radiological dose limits and drinking water radiological dose limits established by DOE orders. The performance objectives are (1) dose to the

public less than 25 mrem/yr from all pathways; (2) dose to representative public via air pathways less than 10 mrem/yr; and (3) radon less than average flux of 20 pCi/m²-s at the surface. In the context of this radiological performance assessment, the waste management system consists of the proposed disposal of LLW, the LLW disposal facility, and its environs. The radiological performance assessment is a tool used to predict the potential environmental consequences of the LLW disposal facility; its intent is to determine whether waste management activities will accomplish the goal of effectively containing LLW. This goal is accomplished if compliance with performance objectives is demonstrated in the performance assessment.

The LLW radiological performance assessment for the ICDF landfill presents a comprehensive, systematic analysis of the long-term impacts of LLW disposal in an arid, near-surface environment. Related assessment activities (e.g., safety assessments, risk assessments, characterizations for siting or construction, engineering evaluations, and cost/design studies) have been evaluated in other documents related to the ICDF Complex. Although occupational doses to workers are an important area of concern for facility operations, they are addressed by regulations and guidance different than those covering performance assessments. Furthermore, compliance with occupational criteria is not necessarily demonstrated by the type of calculations performed for radiological performance assessments. Additionally, this document excludes the potential impacts of chemical toxicity of radiological constituents and nonradiological hazardous constituents that may be in the waste.

A companion document, the *Composite Analysis for the INEEL CERCLA Disposal Facility Landfill* (DOE-ID 2003a), assesses the cumulative impacts from active and planned LLW disposal facilities and all other sources of radioactive contamination that could interact with the ICDF landfill to affect the dose to future members of the public. It is different from the performance assessment in that it addresses other INEEL radiological sources outside the ICDF landfill. Two other documents, *Performance Assessment for the Tank Farm Facility at the Idaho National Engineering and Environmental Laboratory* (DOE-ID 2001a) and *Composite Analysis for Tank Farm Closure* (DOE-ID 2002a) provide the framework and much of the substantive content for the site characteristics for the ICDF landfill performance assessment and composite analysis.

1.2 General Facility Description

The ICDF Complex was constructed at INTEC, as shown in Figure 1-1, to allow on-Site disposal of WAG 3 and other CERCLA-generated wastes at the INEEL. The purpose of the ICDF Complex is to consolidate INEEL CERCLA wastes into one engineered facility to reduce the footprint of contamination across the INEEL. The ICDF landfill meets the substantive requirements of RCRA Subtitle C design and construction, with a capacity of about 389,923 m³ (510,000 yd³) (DOE-ID 1999).

The site selected for the ICDF Complex is adjacent to Lincoln Boulevard and situated at the southwest corner of the INTEC facility, outside the facility fence (Figures 1-2 and 1-3). The SSSTF is the northernmost Complex component, directly to the west of the INTEC facility fence. To the south of the SSSTF is the ICDF landfill. To the east of the landfill is the evaporation pond, which is composed of two cells, referred to as the east and west cells. Fencing will be maintained around the ICDF Complex to provide security of the components and control of the waste handling practices. The location of the ICDF Complex allows for easy access from Lincoln Boulevard, the main INEEL road between facilities. This will allow controlled yet straightforward access to the ICDF Complex components, as needed, for WAG waste management.

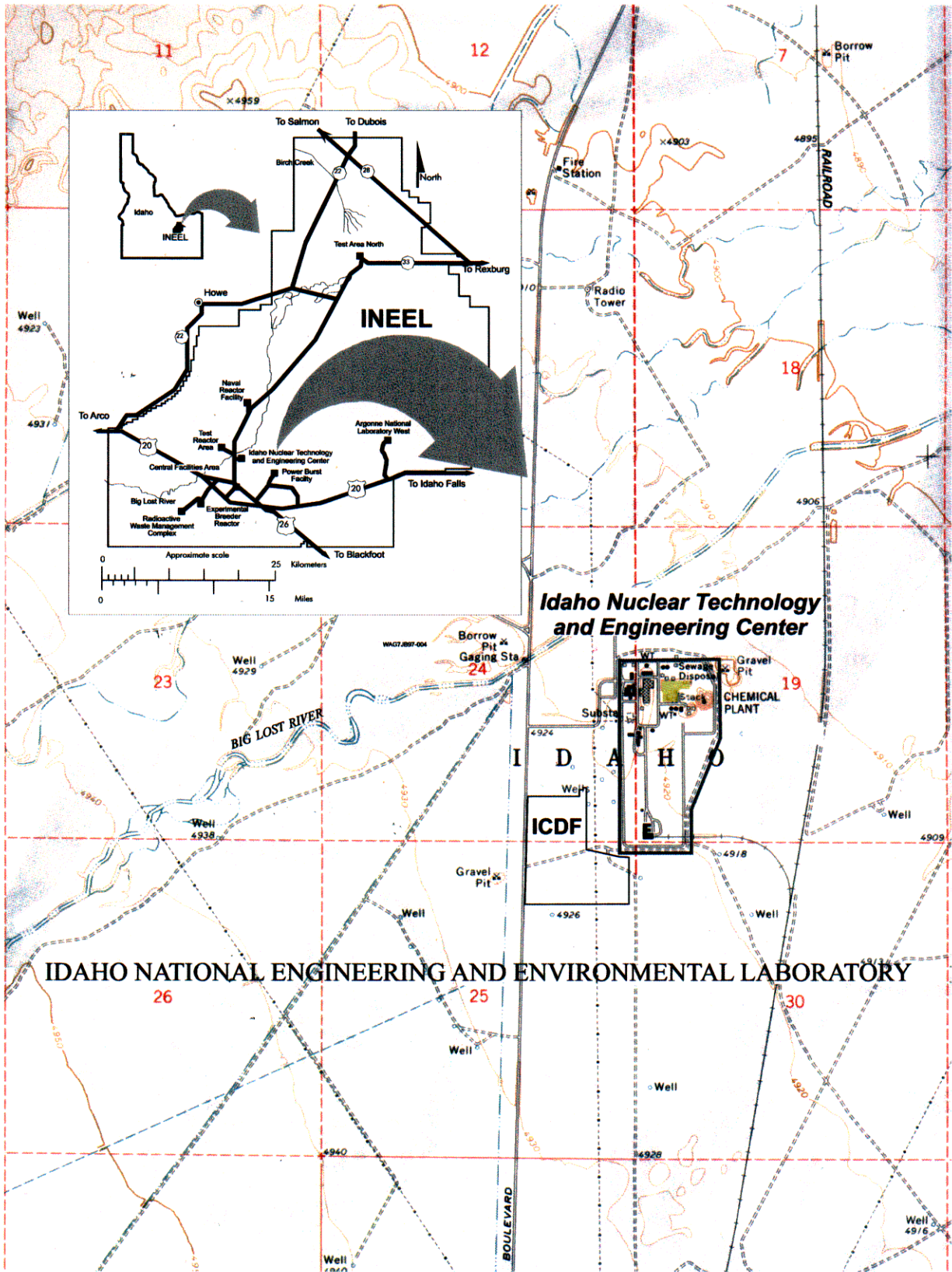


Figure 1-1. Map showing location of Idaho Nuclear Technology and Engineering Center.

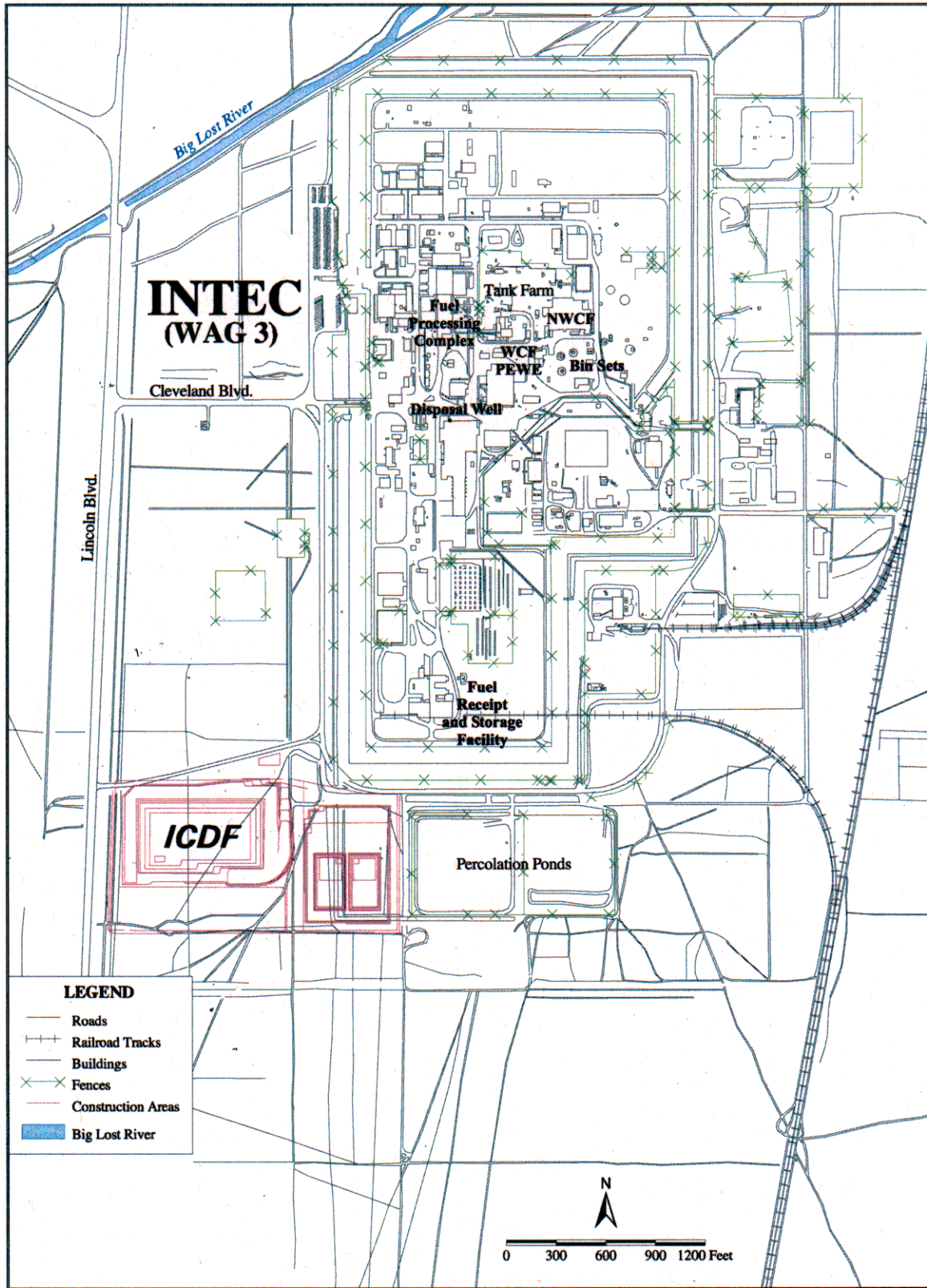


Figure 1-2. Location of the ICDF Complex.

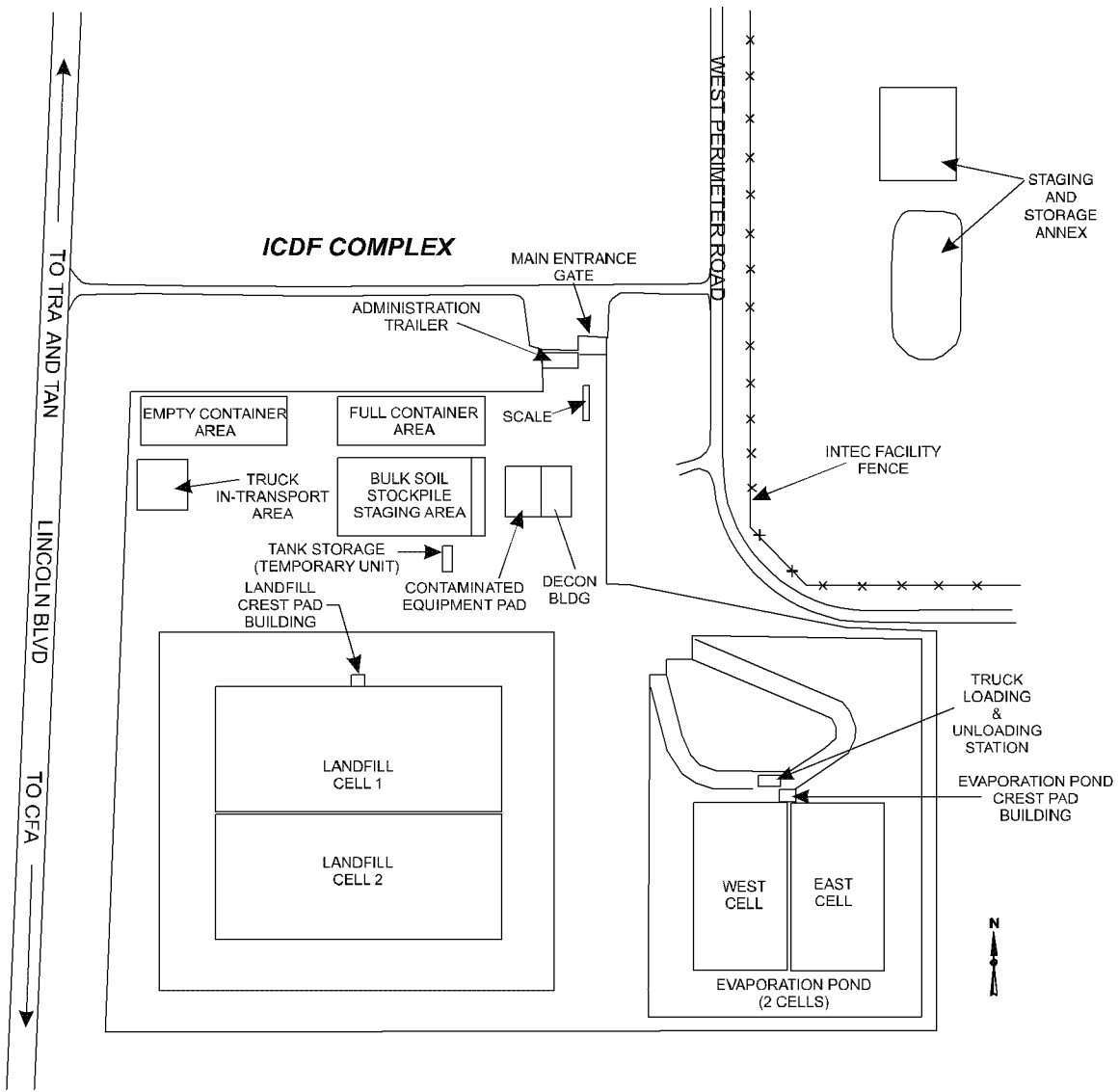


Figure 1-3. Detailed layout of ICDF Complex.

The landfill is designed to be protective of the Snake River Plain Aquifer (SRPA), such that groundwater contamination does not exceed a cumulative carcinogenic risk of $1E-04$, a cumulative noncarcinogenic hazard index of one, or applicable State of Idaho groundwater quality standards. The landfill has been designed with an operational life of 15 years, a postclosure period of 30 years, and a landfill cover design life of 1,000 years. The landfill cover has been designed to minimize infiltration and run-on and maximize run-off by maintaining a sloped surface, storing water for later release to the atmosphere, lateral drainage, and providing a low-permeability composite liner barrier system. The final cover has also been designed to protect the disposed waste for a period of 1,000 years. Design requirements include a liner system and leachate collection and removal system. The liner system is comprised of (1) a top liner designed and constructed of materials (e.g., a membrane) to prevent the migration of hazardous constituents into such liner during the active and postclosure care period, and (2) a composite bottom liner with the lower component constructed of at least 0.91 m (3 ft) of compacted soil material with a hydraulic conductivity of no more than $1E-07$ cm/sec. The leachate collection and

removal system has been designed and constructed, and will operate and be maintained to collect and remove leachate from the landfill during the active life and postclosure care period.

For more complete details on the landfill design refer to the ICDF Remedial Design/Construction Work Plan (DOE-ID 2002b) and Appendix A and Appendix B of this document.

1.2.1 Waste Acceptance Criteria

Landfill-specific Waste Acceptance Criteria (WAC) (e.g., numerical chemical and radiological concentrations) have been developed for the landfill and are included in the WAC document (DOE-ID 2002c). Development of the radiological acceptance criteria for the landfill included calculations to determine concentrations in the ICDF landfill leachate that are protective of the SRPA, human health, and the environment. The ICDF Complex users must specify waste content and obtain approval from the ICDF Complex operations manager prior to shipment. Wastes that can be accepted at the ICDF landfill include

- WAG 3 CERCLA remediation wastes, including soils, drill cuttings, building debris, boxed soils, and secondary remediation wastes, such as personal protective equipment.
- Wastes generated in the ICDF Complex and from CERCLA investigative, remedial, and removal activities at the INEEL WAGs. These wastes will include soils, drill cuttings, building debris, stabilized wastes, and secondary remediation and investigation wastes.
- Secondary CERCLA wastes from waste processing and decontamination activities in the ICDF Complex.

The ICDF landfill WAC document provides limits for the quantities of radioactive materials that may be accepted for disposal at the ICDF landfill (DOE-ID 2002c). These limits are based on the remedial action objectives outlined in the OU 3-13 ROD (DOE-ID 1999), which include prevention of the release of leachate to underlying groundwater that would result in exceeding a cumulative carcinogenic risk of $1E-04$ or applicable State of Idaho groundwater quality standards. In addition, the expected leachate concentrations must be compatible with the earthen and synthetic materials proposed for the ICDF landfill liner system. For radionuclides, the maximum allowable concentrations in leachate for liner compatibility would result in an absorbed dose of $1,000,000 \text{ rad/cm}^2$ while the design inventory concentrations would result in $17,000 \text{ rad/cm}^2$ (DOE-ID 2002c).

Waste material will go through an acceptance process at the ICDF Complex that includes weighing, profiling, verification, acceptance, quality assurance, and database management before the material will proceed to the ICDF landfill and evaporation pond.

1.2.2 General Land Use Patterns

The *INEEL Comprehensive Facility and Land Use Plan* (DOE-ID 1996a) and the INTEC Final ROD (DOE-ID 1999) describe the land use for the INEEL and INTEC. Land use at the INEEL is currently government-controlled industrial use. Presently, access to INEEL facilities requires proper clearance, training, or escort and controls to limit the potential for unacceptable exposures. A security force is used to limit access to approved personnel and visitors.

The primary use of INEEL land is to support facility and program operations dedicated to nuclear energy research, spent nuclear fuel management, hazardous and mixed waste management and minimization, cultural resources preservation, and environmental engineering, protection, and

remediation. Large tracts of land are reserved as buffer and safety zones around the boundary of the INEEL. Portions within the central area are reserved for INEEL operations. The remaining land within the core of the reservation, which is largely undeveloped, is used for environmental research, ecological preservation, and sociocultural preservation. Figure 1-4 illustrates the different land use classifications in and around the INEEL.

Approximately 77% of the land in the five counties surrounding the INEEL is considered open rangeland, forest, or barren (DOE-ID 1995). Roughly 21% of the land in these counties is used for farming. Somewhat less than 2% of the land in the surrounding counties is surface water or wetland, and only about 0.3% of the land in the counties is considered urban. The land outside the INEEL boundary closest to the INTEC is primarily Bureau of Land Management (BLM) -controlled with small pockets of State-controlled or private, noncultivated land.

Future land use is addressed in the INEEL future land use scenarios document (DOE-ID 1995) and in the *INEEL Comprehensive Facility and Land Use Plan* (DOE-ID 1996a). Future land use during the 1,000-year compliance period most likely will remain essentially the same as the current use: a research facility within the INEEL boundaries and agriculture and open land surrounding the INEEL. Other potential, but less likely land uses within the INEEL include agriculture and the return of the areas on-Site to their natural, undeveloped state.

Planning assumptions for land use within and adjacent to the INEEL are that the INEEL will remain under government control for at least the next 100 years and no new major, private developments (residential or nonresidential) are expected in areas adjacent to the INEEL. This PA assumes that the institutional control period begins at the end of closure for the ICDF landfill. The anticipated date of closure for the ICDF landfill is 2018. Closure and postclosure requirements for the ICDF Complex as specified in the ROD (DOE-ID 1999) will (1) ensure that the final cover is designed to serve as an intrusion barrier for a period of 1,000 years; (2) place permanent land use restrictions, zoning restrictions, and deed restrictions on the ICDF Complex and its adjacent buffer zone to permanently preclude industrial or residential development until unacceptable risk no longer remains at the site; and (3) provide access controls, monitoring, and maintenance for as long as the contents of the landfill remain a threat to human health or the environment if uncontrolled.

1.3 LLW Disposal Facility Life Cycle

The long-term life cycle of the ICDF landfill consists of

- Waste Disposal Operations, years 1–15 (2003–2018)
- Institutional Control, years 15–115 (2018–2118)
- Compliance Period, years 115–1,000 (2118–3018).

The closure strategy for the landfill assumes an engineered cover with institutional and land use controls. The cover is designed to last through the performance period of 1,000 years. However, a conservative cover lifetime is evaluated in this performance assessment. The “conservative case” assumes the landfill cover lasts for 500 years, limiting the net infiltration rate to 0.01 cm/yr and then the landfill cover is assumed to degrade over the next 500 years with net infiltration rate increasing from 0.01 cm/yr to 1 cm/yr (the natural background infiltration rate) as a linear increasing rate.

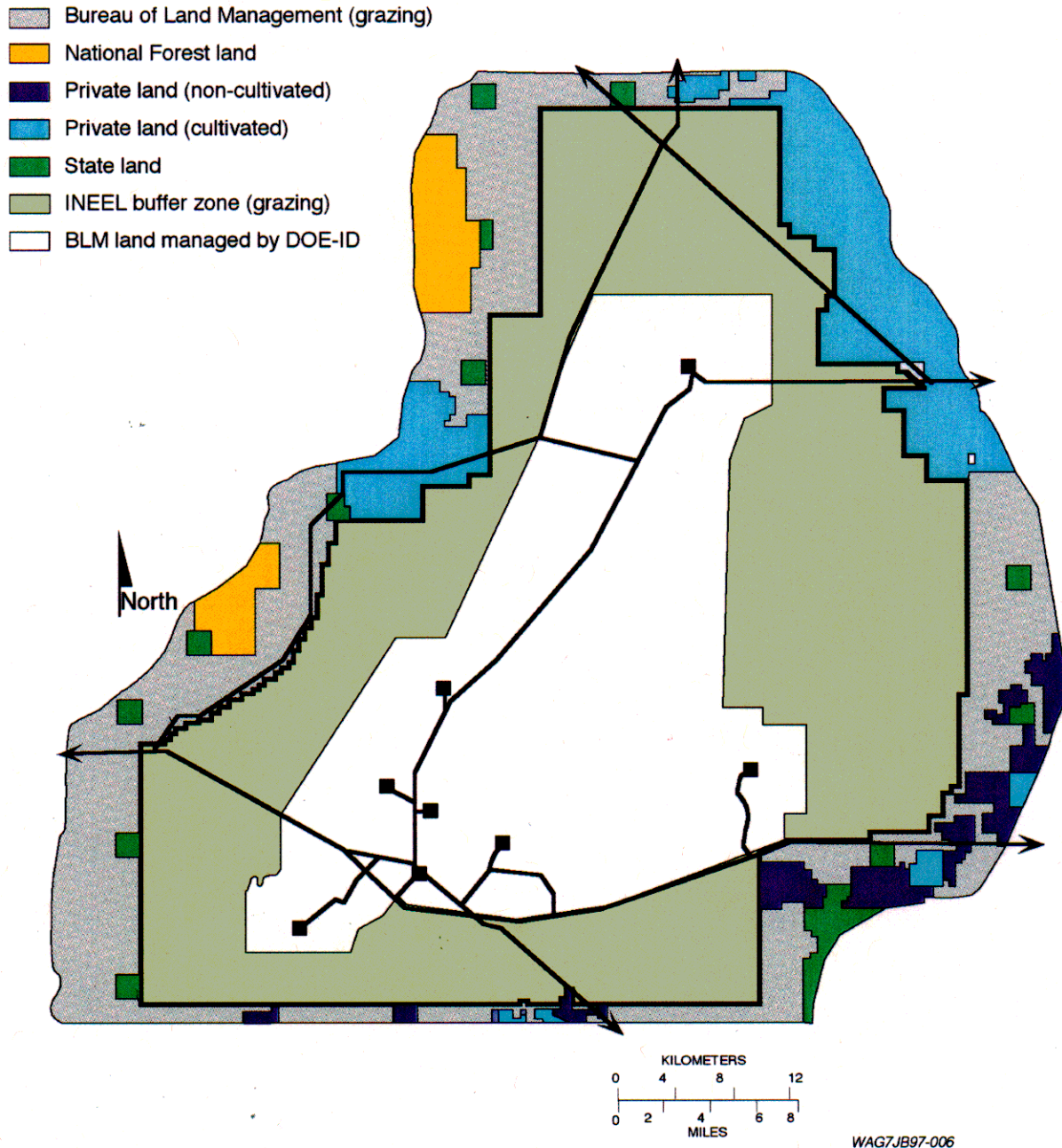


Figure 1-4. Land use designations in and around the INEEL.

1.4 Related Documents

The following discussion describes the regulatory framework in which this performance assessment was prepared. The EPA proposed listing the INEEL on the National Priorities List of the National Oil and Hazardous Substances Pollution Contingency Plan July 14, 1989 [54 FR 19820]. After considering the 60-day public comment period following the proposed INEEL listing, EPA issued a final ruling that listed the INEEL as a National Priorities List site in the FR, November 21, 1989 (54 FR 48184).

The Federal Facility Agreement and Consent Order (FFA/CO) between the EPA-Region X, the State of Idaho Department of Health and Welfare, and the DOE-ID was developed to establish the procedural framework and schedule for developing, prioritizing, implementing, and monitoring response actions at the INEEL in accordance with CERCLA, RCRA, and the Idaho Hazardous Waste Management Act (DOE-ID 1991). The FFA/CO identified 10 WAGs to be addressed through the CERCLA process with INTEC designated as WAG 3. A Comprehensive Remedial Investigation/Feasibility Study (RI/FS) (DOE-ID 1997a) identified release sites at INTEC that pose a threat to human health and/or the environment requiring remedial action to mitigate these risks. In accordance with the signed OU 3-13 ROD (DOE-ID 1999) the ICDF Complex was identified as a selected remedy for the OU 3-13 Group 3, "Other Surface Soils." As part of the selected remedy for Group 3, the ICDF Complex was constructed at INTEC to allow on-Site disposal of WAG 3 and other CERCLA-generated wastes at the INEEL.

The ICDF was designed and constructed to meet Idaho Administrative Procedures Act (IDAPA) 58.01.05.008 [40 CFR 264.301] for hazardous waste, 40 CFR 761.75 for PCB, and DOE Order 435.1 for radioactive waste landfill design and operating substantive requirements. The ICDF landfill will operate, close, and postclose in accordance with the substantive requirements of IDAPA 58.01.05.008 (40 CFR 264 Subparts G, F, and N), and maintain site access restrictions and institutional controls throughout the postclosure period. Permanent land use restrictions will be placed on the ICDF Complex, which will be closed in place, for as long as land use and access restrictions are required to be protective of human health and the environment. Maintenance will be performed on the final cover for the closed ICDF landfill as necessary to prevent the release of leachate to underlying groundwater that would result in exceedance of groundwater quality standards (i.e., maximum contaminant levels [MCLs]) in the SRPA. The final landfill cover has been designed to protect against inadvertent intrusion for a period of at least 1,000 years. Remedial actions taken under the ROD (DOE-ID 1999) will be reviewed under the CERCLA 5-year review process to ensure their protectiveness. Five-year reviews will also ensure that any changes in the physical configuration of the ICDF landfill where there is suspicion of a release of hazardous or radioactive substances will be managed to achieve remediation goals established in the ROD (DOE-ID 1999). The 5-year reviews will continue as long as contaminants exist at levels that result in restricted or limited site usage.

Waste disposal constraints for the ICDF landfill are outlined in *Waste Acceptance Criteria for ICDF Landfill* (DOE-ID 2002c). This document will be updated based on the results of this performance assessment. The *ICDF Operations and Maintenance Plan* (DOE-ID 2003b) contains the standard operating procedures and associated job safety analyses for all operations and maintenance activities to be conducted at the ICDF Complex. The *ICDF Complex Waste Verification Sampling and Analysis Plan* (DOE-ID 2003c) establishes the requirements for verification of untreated waste destined for disposal at the ICDF landfill and identifies the process to confirm that key parameters (those that limit waste acceptance in the landfill) in the waste do not exceed the limits on the Material Profile.

In accordance with DOE O 5400.1, a groundwater protection management plan has been instituted for the site and is described in the following reports: *INEL Groundwater Protection Management Plan* (DOE-ID 1993a), *Idaho National Engineering Laboratory Groundwater Monitoring Plan* (DOE-ID 1993b), and *Idaho National Engineering Laboratory Groundwater Monitoring Plan Update* (DOE-ID 2002d). Groundwater protection requirements applicable to operation, closure, and long-term performance of the landfill include prevention of the release of leachate to underlying groundwater that would result in exceeding applicable State of Idaho groundwater quality standards (i.e., MCLs) in the SRPA (DOE-ID 1999).

INEEL activities must comply with two stormwater pollution prevention plans: one for industrial activities (DOE-ID 1998), the other for construction activities (DOE-ID 1993c). The plans address stormwater discharges associated with industrial activities to waters of the United States. EPA's goal in

requiring these plans is to improve water quality by reducing pollutants in stormwater discharges. Another report that supports this PA is the *Idaho Chemical Processing Plant Safety Document* (INEEL 1998).

The Remedial Design/Construction Work Plan (DOE-ID 2002b) provides the framework for design and construction, and the Remedial Action Work Plan (DOE-ID 2003d) describes the operation of the ICDF Complex. Primary reference sources for the ICDF landfill design criteria are

- DOE-ID, 1999, *Final Record of Decision, Idaho Nuclear Technology and Engineering Center, Operable Unit 3-13*, DOE/ID-10660, Rev. 0, Department of Energy Idaho Operations Office; U.S. Environmental Protection Agency, Region 10; and State of Idaho Department of Health and Welfare, October 1999.
- DOE-ID, 2000, *Remedial Design/Remedial Action Scope of Work for Waste Area Group 3, Operable Unit 3-13*, DOE/ID-10721, Rev. 1, U.S. Department of Energy Idaho Operations Office, February 2000.
- DOE-ID, 2000, *Conceptual Design Report for the INEEL CERCLA Disposal Facility and Evaporation Pond*, DOE/ID-10806, Rev. 0, U.S. Department of Energy Idaho Operations Office, November 2000.
- DOE-ID, 2002, *INEEL CERCLA Disposal Facility Remedial Design/Construction Work Plan*, DOE/ID-10848, Rev. 1, Department of Energy Idaho Operations Office, May 2002.
- DOE-ID, 2003, *INEEL CERCLA Disposal Facility Remedial Action Work Plan*, DOE/ID-10984, Rev. 0, U.S. Department of Energy Idaho Operations Office, February 2003.
- TFR-71, 2002, “WAG 3 INEEL CERCLA Disposal Facility and Evaporation Pond,” Rev. 2, U.S. Department of Energy Idaho Operations Office, May 2002.
- TFR-2520, 2002, *Technical and Functional Requirements for the ICDF Complex Control System*, Rev. 0, U.S. Department of Energy Idaho Operations Office, May 2002.
- 40 CFR 264.301, 2001 “Standards for Owners and Operators of Hazardous Waste Treatment, Storage, and Disposal Facilities,” Subpart N, “Landfills,” Section 301, “Design and Operating Requirements,” Code of Federal Regulations, Office of the Federal Register, July 1, 2001.
- 40 CFR 761.75, 2000, “Polychlorinated Biphenyls (PCBs) Processing, Distribution in Commerce and Use Prohibitions,” Section 75, “Chemical Waste Landfills,” *Code of Federal Regulations*, Office of the Federal Register, July 1, 2000.

Other documents used in the development of this performance assessment include

- DOE O 435.1, Change 1, 2001, “Radioactive Waste Management Manual,” U.S. Department of Energy, August 18, 2001.
- DOE-ID, 2001, *Performance Assessment for the Tank Farm Facility at the Idaho National Engineering and Environmental Laboratory*, DOE/ID-10966, U.S. Department of Energy Idaho Operations Office, December 2001.

- DOE-ID, 2002, *Composite Analysis for the Tank Farm Closure*, DOE/ID-10974, U.S. Department of Energy Idaho Operations Office, March 2002.
- Maheras, S. J., A. S. Rood, S. O. Magnuson, M. E. Sussman, and R. N. Bhatt, 1994, *Radioactive Waste Management Complex Low-Level Waste Radiological Performance Assessment*, INEEL, EGG-WM-8773, 1994.
- Maheras, S. J., A. S. Rood, S. O. Magnuson, M. E. Sussman, and R. N. Bhatt, 1997, *Addendum to Radioactive Waste Management Complex Low-Level Waste Radiological Performance Assessment* (EGG-WM-8773), INEL/EXT-97-00462, 1997.
- Case, M. J., A. S. Rood, J. M. McCarthy, S. O. Magnuson, B. H. Becker, and T. K. Honeycutt, 2000, *Technical Revision of the Radioactive Waste Management Complex Low-Level Waste Radiological Performance Assessment for Calendar Year 2000*, INEEL/EXT-2000-01089, 2000.

1.5 Performance Criteria

The ICDF landfill performance assessment estimates radiological exposure to future members of the public for a 1,000-year period after closure of the facility to demonstrate there is a reasonable expectation that performance criteria established for the long-term protection of the public and the environment will not be exceeded. Performance criteria consist of specific performance objectives identified in DOE M 435.1-1.

The following sections describe each performance objective used to assess the long-term performance of the ICDF landfill. Performance objectives not explicitly called out in the Manual (e.g., site-specific regulatory agency agreements) are also discussed.

1.5.1 Public Protection Performance Objectives

The first applicable performance objective from DOE M 435.1-1 IV P.(1)(a) states:

Dose to representative members of the public shall not exceed 25 mrem (0.25 mSv) in a year total effective dose equivalent from all exposure pathways, excluding the dose from radon and progeny in air.

This performance objective is interpreted as requiring the performance analysis to provide a reasonable expectation that the “all-pathways” dose to a hypothetical future member of the public will not exceed 25 mrem effective dose equivalent (EDE), which includes the 50-year committed effective dose equivalent from ingestion and inhalation of radionuclides, plus the external EDE received during the exposure period (1 year) from all exposure pathways, excluding the dose from radon and progeny in air. “All pathways” include any and all modes by which a receptor at the point of public access could be exposed, including the air pathway. The analysis is to cover 1,000 years following closure of the disposal facility. Analysis beyond 1,000 years to calculate the maximum dose and the time of that dose shall be included in the sensitivity/uncertainty analyses as a means of increasing confidence in the outcome of the modeling. However, it should be noted that calculations for greater than 1,000 years have inherently large uncertainties due to extrapolating such calculations over longer time frames. The point of compliance for this performance objective should normally be at the point of highest calculated dose beyond a 100-m buffer zone surrounding the waste.

The second performance objective (DOE M 435.1-1 IV.P.(I)(b)) states:

Dose to representative members of the public via the air pathway shall not exceed 10 mrem (0.10 mSv) in a year total effective dose equivalent, excluding the dose from radon and its progeny.

Consistent with the National Emission Standards for Hazardous Air Pollutants (NESHAP) (40 CFR 61, Subpart H), radon-220, radon-222, and their progeny need not be included in the air pathway analysis for comparison with the 10-mrem/yr effective dose equivalent performance objective; separate controls for the emission of radon are discussed below. For the air pathway dose analysis, the point of compliance should be the point of highest calculated dose beyond a 100-m buffer zone surrounding the waste. A larger or smaller buffer zone may be used with justification. The 10-mrem/yr limit should be recognized to refer to all sources, not just the disposal facility. Therefore, if the performance assessment assumes a point of compliance that corresponds to the future land use boundary, a limit that is a fraction of the 10-mrem/yr dose limit should be used in recognition of the potential presence of other sources. Estimates of dose from current INEEL facilities are added to the ICDF landfill estimated dose and compared with the 10-mrem/yr dose limit.

The third performance objective (DOE M 435.1-1 IV.P.(I)(c)) states:

Release of radon shall be less than an average flux of 20 pCi/m²/s (0.74 Bq/m²/s) at the surface of the disposal facility. Alternately, a limit of 0.5 pCi/l (0.0185 Bq/l) of air may be applied.

For radon, a separate limit is applied. In most cases, the limit to be applied should be an average ground-surface emanation rate of 20 pCi/m²-s directly over the disposal unit. There may be special cases involving the disposal of material that radiologically resembles uranium or thorium mill tailings in isolated locations that warrant using an alternative limit. The alternative limit is an incremental increase in the air concentration of radon of 0.5 pCi/L at the point of assessment at the boundary of the facility.

1.5.2 Water Resource Impact Assessment

DOE O 5820.2A, which has been superseded by DOE O 435.1, contained a performance objective for protection of groundwater resources. DOE M 435.1-1 does not contain a specific performance objective (e.g., dose or concentration standard) for water resource impacts. The approach in DOE M 435.1-1 was chosen by the DOE for consistency with Nuclear Regulatory Commission (NRC) methods for LLW disposal and radiation protection principles articulated by the National Council on Radiation Protection and Measurements and the International Commission on Radiological Protection (ICRP). In accordance with these principles, it is appropriate to assign a fraction (e.g., 25 mrem) of the 100-mrem/yr public dose performance measure to a particular practice (e.g., radioactive waste disposal), but it is not recommended to further fraction performance objectives to specific pathways (e.g., groundwater). Thus, exposure by water pathways is included in the all-pathways analysis, but there is no specific performance objective for exposure by water pathways. In the case of the air pathway, the 10 mrem per year performance objective is based on a specific federal regulatory requirement. There is no comparable requirement for water resources.

DOE M 435.1-1, IV.P(2)(g) states:

For the purposes of establishing limits on radionuclides that may be disposed of near-surface, the performance assessment shall include an assessment of impacts to water resources.

For water resources protection, impacts were assessed on a site-specific basis in accordance with a hierarchical set of criteria. This approach recognizes that there are no federal requirements for protection of water resources for a radioactive waste disposal facility. The site-specific hierarchical approach, rather than mandating specific performance measures for all sites, is consistent with the EPA strategy for groundwater protection. EPA recognizes that groundwater protection is a regional and local matter. Accordingly, the hierarchy for establishing water resources protection is as follows:

- First, the disposal facility must comply with any applicable state or local law, regulation, or other legally applicable requirement for water resource protection.
- Second, the disposal facility must comply with any formal agreement applicable to water resource protection that is made with appropriate state or local officials.
- Third, if neither of the above conditions apply, the site should select assumptions for use in the performance assessment based on criteria established in the site groundwater protection management program and any formal land use plans.
- If none of the above conditions apply, the site may select assumptions for use in the performance assessment for the protection of water resources that are consistent with the use of water as a drinking water source.

For assessments addressing use of groundwater as a drinking water source, the point of assessment should normally be the location of highest groundwater concentration outside a 100-m buffer zone.

In terms of protecting the groundwater as a resource, assuming some volume averaging based on projected use may be appropriate. Applying the performance measure at an assumed wellhead mixed with a reasonable volume of groundwater, based on site-specific assumptions regarding groundwater use, is appropriate. This assumes mixing is consistent with state or local laws, regulations, or agreements.

1.5.2.1 Groundwater Protection. DOE O 435.1 and the supporting manual and guidance do not specify radiation dose or concentration limits that would constitute performance objectives for protection of groundwater. DOE M 435.1-1 uses a hierarchical approach that requires an analysis of potential applicable state and local requirements or agreements for groundwater protection. The ROD requires that the SRPA meets the IDAPA MCLs. Therefore, under this hierarchical approach the MCLs are the applicable limits.

Groundwater protection is evaluated by comparing predicted concentrations in groundwater with MCLs for radionuclides. Four types of concentrations are calculated: gross alpha concentration (excluding uranium and radon), Ra-226/Ra-228 concentration, committed dose equivalent (CDE) from beta-gamma-emitting radionuclides, and total uranium mass concentration. Note that the beta-gamma groundwater protection standard is CDE whereas the all-pathways dose is total EDE. The EDE is calculated using dose conversion factors from Federal Guidance Report 11 (EPA 1988) whereas CDE values are calculated using data for the 168-hour week from National Bureau of Standards Handbook 69 (DOC 1963).

The use of MCLs as the performance objective for groundwater protection is consistent with the CERCLA ROD for OU 3-13, which states the cumulative carcinogenic risk from all-pathways will be less than or equal to 1E-04 and/or applicable State of Idaho groundwater quality standards.

1.5.3 Intruder Analysis

For intruder analyses, institutional controls shall be assumed to be effective in deterring intrusion for at least 100 years following closure. The intruder analyses shall use performance measures for chronic and acute exposure scenarios, respectively, of 100 mrem (1 mSv) in a year and 500 mrem (5 mSv) total effective dose equivalent excluding radon in air.

Intruder analyses are to be performed as one of the mechanisms for establishing concentration limits for waste considered acceptable for near-surface disposal. The DOE intends to exercise control of the closure site until it can be safely released pursuant to DOE O 5400.5 (or 10 CFR 834 when promulgated). Hence, intrusion is an accidental, temporary event. However, for purposes of conducting intruder analyses, the intrusion event should be considered to occur because of a lapse in institutional controls that would be remedied within a few years. The focus of the intruder analysis should be on the selection of reasonable scenarios and reasonably conservative parameters. Intrusion is assumed to occur no sooner than 100 years following facility closure and should not be analyzed beyond 1,000 years postclosure. Intruder scenarios need to consider the following: (1) intruders may carry out activities for no more than 1 year before discovery; (2) an intruder may perform reasonable activities consistent with regional social customs; well drilling, excavation, and construction practices; and the regional environmental conditions projected for the time that intrusion is assumed to occur; (3) intrusion events may involve random contact with the waste, and the intruder will usually take reasonable investigative actions upon discovery of unusual activities; (4) intrusion events that contact the waste may be assumed to be limited to drilling or simple excavation scenarios involving use of relatively unsophisticated tools and commonplace machinery; and (5) doses calculated for an intruder will depend on waste disposal facility design and operating practices, and may be reduced by practices such as disposal below depths normally associated with common construction activities, use of intruder barriers or durable waste forms or containers, or distributed disposal of higher-activity waste.

The 500-mrem EDE should be used in assessing acute exposure from individual events that reasonably could occur at the site considering regional social customs and regional construction practices (e.g., well drilling and excavation).

The 100-mrem/yr EDE should be used in assessing chronic exposure from residing at or frequently visiting the disposal site. In the analysis of chronic exposure of a hypothetical intruder, doses should be assumed to come from external exposure to, and inhalation and ingestion of materials exhumed from the site. Exposure may occur through a variety of pathways, but need not include the consumption of contaminated groundwater or the irrigation of crops with contaminated groundwater. Groundwater consumption and crop irrigation are excluded because the impacts of groundwater contamination are evaluated separately in the all-pathways analysis, the water resource protection analysis, or both. Similarly, intruder doses need not include consideration of doses from airborne radon and its short-lived progeny because these are dealt with in the air pathway analysis. Doses from the progeny of radon that are deposited in the disposal facility should be included in the intruder analyses.

1.5.4 ALARA Analysis

DOE's approach to radiation protection for LLW disposal is based on two key components. One component is the performance objectives described in Section 1.5.1, which specify maximum doses for various pathways. The other component requires doses to be maintained "as low as reasonably achievable" (ALARA).

The goal of the ALARA process is attainment of the lowest practical dose level after taking into account social, technical, economic, and public policy considerations. Therefore, in addition to providing

a reasonable expectation that the performance objectives described in Section 1.5.1 will not be exceeded, the performance assessment also needs to show that LLW disposal is being conducted in a manner that maintains releases of radionuclides to the environment ALARA. An ALARA analysis for the ICDF landfill may be found in Section 9.

Table 1-1 summarizes the specific performance objectives discussed above pertinent to the ICDF landfill performance assessment.

Table 1-1. Performance objectives for the ICDF landfill performance assessment.

Performance Objective	Dose or Concentration Limit	Receptor/Scenario
All pathways (DOE O 435.1)	25 mrem/yr EDE	Hypothetical future member of the public exposed at maximum point of impact at INEEL boundary for first 100 years then 100 m from ICDF at maximum dose location.
Atmospheric (40 CFR 61 Subpart H)	10 mrem/yr EDE	Representative member of the public exposed at maximum point of impact at INEEL boundary for first 100 years then 100 m from ICDF at maximum dose location.
Atmospheric (40 CFR 61 Subpart Q)	20 pCi/m ² -s radon flux or 0.5 pCi/L radon concentration	Representative member of the public exposed at ICDF surface or boundary of facility.
Chronic inadvertent intrusion (DOE O 435.1)	100 mrem/yr EDE	Inadvertent intruder at ICDF.
Acute inadvertent intrusion (DOE O 435.1)	500 mrem EDE	Inadvertent intruder at ICDF.
Groundwater protection (40 CFR 141) (IDAPA 58.01.11) ^a	4 mrem/yr CDE for β , γ ^b MCL ^c of 15 pCi/L for gross α ^d MCL of 5 pCi/L Ra-226 and Ra-228 MCL of 8 pCi/L Sr-90 MCL of 20,000 pCi/L H-3	Dose to a member of the public at INEEL boundary until 2118. Then it is 100 m downgradient. MCLs are in groundwater at INEEL boundary until 2118. Then 100 m downgradient of ICDF.

a. As promulgated as of October 1999.

b. Proposed rule, Federal Register Vol. 65, No. 78, April 21, 2000, pp. 21576–21628 (65 FR 78).

c. MCL = maximum contaminant level.

d. Includes Ra-226, excludes radon and uranium.

1.6 Summary of Key Assumptions

In order to evaluate the performance of the ICDF landfill, simplifying assumptions were made in the performance assessment. The following sections summarize the key assumptions that are most critical to the analysis of performance.

- In October 1999, DOE, EPA, and Idaho Department of Environmental Quality signed a ROD (DOE-ID 1999) that stipulated the need for an on-Site landfill to dispose of WAG 3 other surface soils release sites and CERCLA remediation wastes generated within the boundaries of the INEEL.

The landfill is to be an engineered facility meeting RCRA Subtitle C, Idaho Hazardous Waste Management Act, and TSCA PCB landfill design and construction requirements.

- The remedial action objectives outlined in the ROD specify institutional controls beyond the year 2095 to prevent disturbance of the capped area and to be protective of human health and environment as long as the contents of the landfill remain a threat to human health or environment if uncontrolled. The remedial action objectives of the ROD will be achieved by the following three phases: “(1) DOE Operational Phase, expected until year 2045, (2) Government Control Phase, expected between years 2045 and 2095, (3) Post Governmental, beyond 2095 continue institutional controls at all capped areas to prevent disturbance of capped areas to ensure the Snake River Plain Aquifer groundwater does not exceed MCLs” (DOE-ID 1999).
- The ICDF landfill cover has been designed to last for 1,000 years. However, the analysis for this performance assessment assumes the cover will perform as designed for 500 years (one-half the design life) until the year 2518 and then fail over a 500-year period from 2518 until 3018. During the period from year 2518 until 3018, the cover gradually deteriorates and the infiltration through the cover linearly increases from 0.01 cm/yr in year 2518 until it returns to its background rate (1 cm/yr) in year 3018. Appendix A provides detailed information on the expected long-term performance of the landfill cover.

1.6.1 Source Inventory and Release Rates

The following summarizes the critical assumptions related to the source inventory and the release rates. In each case the assumption is summarized and the significance with respect to the analysis of performance is discussed.

- The entire waste is assumed to be compacted soil. This is a conservative assumption with respect to the leaching of contaminants from the facility. There is relatively little uncertainty in this assumption because the waste will be predominantly soils that will be compacted during emplacement in the facility. All containerized and grouted wastes should be more stable than the compacted soil. Therefore, treating the waste as 100% compacted soil is a conservative assumption.
- Because the maximum or the 95% upper confidence limit (UCL) concentrations have been used to estimate soil concentrations, the entire volume of soil is assumed to be contaminated by a concentration equal to the maximum or 95% UCL. This is a conservative estimate of the contaminant inventory. Actual inventory is expected to be significantly lower.
- The engineered disposal system will completely isolate all radionuclides from the subsurface up to the time of closure of the facility in the year 2018. Failure of the engineered system has not been evaluated; however, the leachate collection system is a fairly simple design and it is reasonable to expect that it will operate as designed.
- Radionuclides that leach from the waste soil travel vertically and mix instantaneously in the engineered clay layer below the waste. First-order processes describe releases from the waste and clay layer. This assumption is reasonable based on the design of the facility. The clay layer will provide significant sorption of most of the radionuclides, thereby providing protection to the groundwater quality.

1.6.2 Subsurface Models

The following summarizes the critical assumptions related to the subsurface models. In each case the assumption is summarized and the significance with respect to the analysis of performance is discussed.

- The cover only restricts water flow through the waste. While the cover is in place, most moisture is retained in the soil and released through evapotranspiration or runs off the cover into the surrounding soil where it infiltrates. A small amount passes through the cover and into the waste. The enhanced infiltration around the cover results in vadose zone water travel times that are equivalent to background vadose zone water travel times during operations and the periods of institutional control and postinstitutional control. Therefore the cover is assumed to significantly reduce the rate of contaminant release from the ICDF landfill but not the time to the first arrival of contaminants to the aquifer.
- Water travel times through the vadose zone fractured basalt are instantaneous; therefore, the vadose zone travel times are controlled by the thickness of the sedimentary interbeds.
- The aquifer is composed of an equivalent homogeneous porous medium of infinite lateral extent and finite thickness. The predicted ICDF performance is much more sensitive to the source release than to the mixing in the aquifer; therefore, this assumption is not expected to significantly influence the predicted performance of the ICDF.

1.7 Quality Assurance Measures

Quality requirements for Idaho Closure Project (ICP) programs, which the ICDF landfill falls under, are specified in *Project Management Plan, Environmental Restoration Program Management*, PLN-694, November 30, 2000. Appendix A of this project management plan describes the quality assurance systems used to manage, perform, and assess work of the ICP Directorate. This plan, along with the *Quality Assurance Project Plan for Waste Area Groups 1, 2, 3, 4, 5, 6, 7, 10 and Inactive Sites* (DOE-ID 2002e), hereinafter referred to as the QAPjP, establishes the quality requirements for environmental restoration.

Primarily, this appendix communicates that all personnel participating in environmental restoration activities are responsible for meeting the performance goals of the ICP Directorate. The requirements of the DOE orders, codes, standards, and regulations governing quality programs imposed by the contract with DOE-ID are addressed by company policies and procedures. The ICP Program complies with the applicable portions of these documents. The QAPjP addresses the quality requirements for environmental data.

The degree of rigor applied to environmental restoration activities and deliverables is based on risk as permitted by the graded approach philosophy contained in Attachment I of DOE Order 414.1A, "Quality Assurance." The *Code of Federal Regulations* (CFR), Title 10, "Energy," Part 830, "Nuclear Safety Management," Subsection 120, "Quality Assurance" (10 CFR 830.120) applies to facilities and activities of ICP that are designated nuclear or radiological, or that encompass performed work in support of a nuclear facility.

Each project is evaluated to determine whether it meets the definition of nuclear or radiological and assignment of quality levels is based on that evaluation. Presently, most of the items and activities of ICP have been designated Quality Level 3. Items determined to be Quality Level 1 or 2 are captured on a Q-List as required by company policies and procedures.

The following codes, standards, and regulations establish the quality assurance requirements for the ICP Directorate. Company policies and procedures delineate the requirements of DOE Order 414.1A, and 10 CFR 830.120 applicable to ICP items and activities. In addition, the FFA/CO requires a QAPjP that meets the guidance and specifications in Quality Assurance Management Staff QAMS-005/80, “Interim Guidelines and Specifications for Preparing Quality Assurance Project Plans,” (EPA 1983) and subsequent amendments. Presently, the EPA QA/R-5, “EPA Guidance for Quality Assurance Project Plans for Environmental Data Operations,” (EPA 1994) is being used as the standard for developing and maintaining the QAPjP. Other codes, standards, and regulations pertinent to ICP are listed in company policies and procedures.

2. DISPOSAL FACILITY CHARACTERISTICS

This section provides descriptive information and data for the INEEL Site, environment, and the ICDF, and the ICDF's LLW waste characteristics. This information provides the basis for the performance assessment ICDF conceptual model and an understanding of the method of analysis.

2.1 Site Characteristics

The following sections discuss the location of the disposal facility, the general land surface features of the site, the population distribution in the area, and uses of adjacent lands.

2.1.1 Geography and Demography

2.1.1.1 Disposal Site Location. The INEEL is located in southeastern Idaho, on the north-central part of the Eastern Snake River Plain (Figure 2-1). Included in its 2.305 km² (890 mi²) of area are portions of five Idaho counties (Bingham, Bonneville, Butte, Clark, and Jefferson). The nearest INEEL boundaries are 51 km (32 mi) west of Idaho Falls, 37 km (23 mi) northwest of Blackfoot, 71 km (44 mi) northwest of Pocatello, and 11 km (7 mi) east of Arco, Idaho. There are no permanent residents within an 17.7-km (11-mi) radius of INTEC. The INEEL is approximately equidistant from the three larger metropolitan areas of Salt Lake City, UT, 339 km (211 mi); Boise, ID, 413 km (257 mi); and Butte, MT, 344 km (214 mi) (DOE-ID 1993b).

The ICDF Complex has been constructed at INTEC, as shown in Figure 1-1, to allow on-Site disposal of WAG 3 and other INEEL CERCLA-generated wastes. The purpose of the ICDF is to consolidate INEEL CERCLA wastes into one engineered facility to reduce the footprint of contamination across the INEEL. INTEC occupies approximately 80 ha (200 ac) in the south-central portion of the INEEL and consists of more than 150 buildings. Primary facilities at INTEC include storage, treatment, and laboratory facilities for spent nuclear fuel, mixed HLW, and mixed transuranic waste (sodium-bearing waste). Located outside the INTEC perimeter fence are parking areas, a helicopter landing pad, the wastewater treatment lagoon, various pits, and percolation ponds. These areas occupy approximately 22 ha (55 ac). The site selected for the ICDF Complex (Figure 1-1) is adjacent to Lincoln Boulevard and situated at the southwest corner of the INTEC facility, outside the facility fence.

The SSSTF is the northernmost ICDF Complex component, directly to the west of the INTEC facility fence. To the south of the SSSTF is the ICDF landfill, which is composed of two cells. Cell 1, the northernmost cell, will be constructed first and expanded into Cell 2 when Cell 1 nears capacity. To the east of the landfill is the evaporation pond, which is also composed of two cells, referred to as the east and west cells. The evaporation pond is directly south of the INTEC facility fence, and also sits just west of the existing INTEC percolation ponds. Two crest pad buildings have been constructed to provide shelter for leachate transfer equipment. One crest pad building, located on the northern side of the landfill, is for the landfill; the other, located on the northern side of the evaporation pond, is for the evaporation pond. Fencing will be maintained around the ICDF Complex to provide security of the components and control of the waste handling practices that take place. The proximity of the ICDF Complex to the INTEC facility allows for utilities to be extended to serve the SSSTF and the ICDF landfill and evaporation pond.

The location of the ICDF Complex allows for easy access from Lincoln Boulevard, the main INEEL road between facilities. This will allow controlled yet straightforward access to the ICDF Complex components, as needed, for INEEL CERCLA waste management.

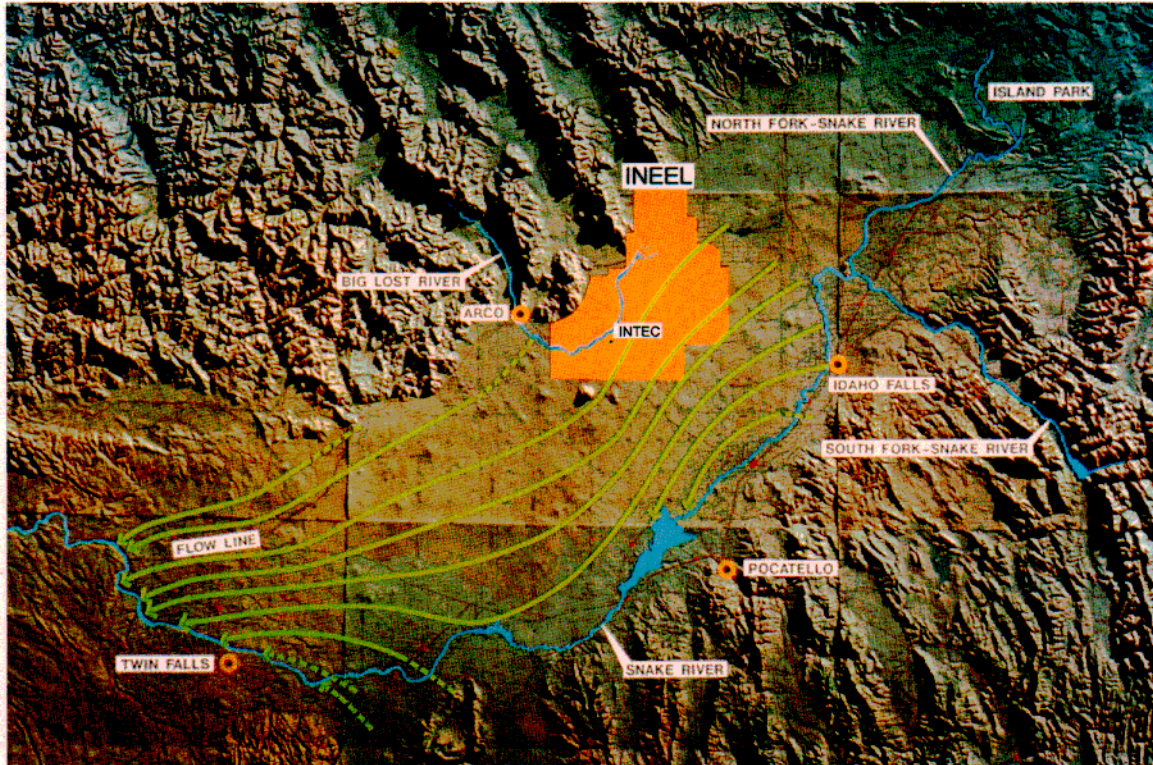


Figure 2-1. Map of the INEEL and the Eastern Snake River Plain.

The ICDF is located in an area meeting low-level waste landfill siting requirements. Additional specific siting criteria for the location of the ICDF landfill include

- Outside the 100-year floodplain
- Outside cultural and historic resources
- Within the WAG 3 area of contamination
- Outside of wetland areas
- Not in active seismic zones
- Not in high surface erosion zones
- Not in an area of high historic groundwater table.

2.1.1.2 Disposal Site Description. The land surface of the INEEL is relatively flat. The predominant relief on the INEEL is the result of volcanic buttes and unevenly surfaced and fissured basalt flows. Elevations on the INEEL range from 1,585 m (5,200 ft) in the northeast to 1,448 m (4,750 ft) in the southwest with the average being approximately 1,520 m (5,000 ft). INTEC is located on an alluvial plain approximately 61 m (200 ft) from the Big Lost River channel (near the channel intersection with INEEL's Lincoln Boulevard in the south-central portion of the INEEL). Elevation at INTEC is 1,498 m (4,914 ft). Gravelly, medium-to-coarse textured soils derived from the alluvial deposits occur in the vicinity of INTEC. The underlying basalt is covered with as much as 15.2 m (50 ft) of these soils and the land

surface is flat. The natural plant life is limited by soil type, meager rainfall, and extended drought periods and consists mainly of sagebrush and various grasses.

The INEEL is located in the Mud Lake-Lost River Basin (also known as the Pioneer Basin). This closed drainage basin includes three main streams: the Big and Little Lost Rivers and Birch Creek. The Big Lost River flows southeast from Mackay Dam, past Arco, and onto the Snake River Plain near the INEEL's southwestern boundary. The Birch Creek and Little Lost River channels enter the INEEL from the northwest. These three streams drain the mountain areas to the north and west of INEEL, although most flow is diverted for irrigation in the summer months before it reaches the site boundaries. Flow that reaches the INEEL infiltrates the ground surface along the length of the streambeds, in the spreading areas behind the diversion dam at the southern end of the INEEL, and, if the stream flow is sufficient, in the ponding areas (playas or sinks) in the northern portion of the INEEL. During dry years, there is little or no surface water flow on the INEEL. Because the Mud Lake-Lost River Basin is a closed drainage basin, water does not flow off the INEEL but rather infiltrates the ground surface to recharge the aquifer, or is consumed by evapotranspiration.

Existing man-made surface water features at INTEC consist of two percolation ponds used for disposal of water from the service waste system, and sewage treatment lagoons and infiltration trenches for treated wastewater. INTEC also is surrounded by a stormwater drainage ditch system (DOE-ID 1998). Stormwater runoff from most areas of INTEC flows through ditches to an abandoned gravel pit on the northeast side of INTEC. From the gravel pit, the runoff infiltrates the ground. The system is designed to handle a 25-year, 24-hour storm event. Because the land is relatively flat (slopes of generally less than 1%) and annual precipitation is low, stormwater runoff volumes are small and are generally spread over large areas where they may evaporate or infiltrate the ground surface.

The Snake River Plain has a relatively low rate of seismicity, whereas the surrounding Basin and Range has a fairly high rate of seismicity (WCFS 1996). The primary seismic hazards from earthquakes to INEEL facilities consist of the effects from ground shaking and surface deformation (surface faulting, tilting). Other potential seismic hazards such as avalanches, landslides, mudslides, and soil liquefaction are not likely to occur at the INEEL because the local geological conditions and terrain are not conducive to these types of hazards. Based on the seismic history and geologic conditions, earthquakes greater than moment magnitude of 5.5 and associated strong ground shaking and surface fault rupture are not likely to occur within the Snake River Plain (WCFS 1996). However, moderate to strong ground shaking could affect the INEEL from earthquakes in the Basin and Range. Section 2.1.4.2 provides detailed discussions on seismology.

Volcanic hazards include the effects of lava flows, fissures, uplift, subsidence, volcanic earthquakes, and ash flows or airborne ash deposits. Most of the basalt volcanic activity occurred from 4 million to 2,100 years ago in the INEEL area. The most recent and closest volcanic eruption occurred at the Craters of the Moon National Monument, 43 km (26.8 mi) southwest of INTEC (Kuntz et al. 1992). Based on probability analysis of the volcanic history in and near the south-central INEEL area, the Volcanism Working Group (VWG) estimated that the conditional probability that basaltic volcanism would affect a south-central INEEL location is less than once per 100,000 years or longer (VWG 1990). The probability is associated primarily with the Axial Volcanic Zone and the Arco Volcanic Rift Zones. INTEC is located in a lesser lava flow hazard area of the INEEL, more than 8 km (5 mi) from the Axial Volcanic Zone and any volcanic vent younger than 400,000 years. The probability that basaltic volcanism would affect a south-central INEEL location is less than once per 400,000 years or longer.

2.1.1.3 Population Distribution. Population growth surrounding the INEEL (i.e., within a seven-county region comprised of Bannock, Bingham, Bonneville, Butte, Clark, Jefferson, and Madison counties, and the Fort Hall Indian Reservation and Trust Lands) has paralleled statewide growth from

1960 to 1990. During this time, the regional population increased an average of approximately 1.3% annually, while the annual growth rate for the state was 1.4% (BEA 1997). From 1990 to 1995, state population growth accelerated to over 3% per year, and the regional population growth remained under 2% (DOC 1997a, 1997b). Population growth for both the state and regional populations are projected to slow after the year 2000. Table 2-1 lists 1990 and 2000 census data for the counties surrounding the INEEL, and growth projections for 2010 and 2025. The projections are based on an annual growth rate of 1.5%.

Bannock and Bonneville counties have the largest populations in the region, and together account for almost 64% of the total regional population in the year 2000. Butte and Clark are the most sparsely populated counties and together contain less than 1% of the regional population. The largest cities in the region are Pocatello (Bannock County) and Idaho Falls (Bonneville County), with year 2000 populations of approximately 51,466 and 50,730, respectively (DOC 2001). The nearest populated area to the INEEL is Atomic City, population about 25, located approximately 1.6 km (1 mi) from the southern INEEL boundary and about 18 km (11 mi) from INTEC.

No permanent residents live within a 16-km (10-mi) circle centered at INTEC on the INEEL. No cities or towns are within 16 km (10 mi) of the ICDF landfill. However, several INEEL facilities, such as Central Facilities Area (CFA), Test Reactor Area (TRA), and Radioactive Waste Management Complex (RWMC) are within 16 km (10 mi) of the ICDF landfill. Also, the Experimental Breeder Reactor I (EBR-I), a National Historic Landmark, is located southwest and within 16 km (10 mi) of the ICDF landfill.

Variations in populations are caused by the daily influx of the INEEL workforce. About 4,110 workers are employed within 16 km (10 mi) of INTEC. U. S. Highways 20 and 26 pass through the site and are within 16 km (10 mi) of INTEC. Traffic on these highways, other than the daily Site traffic, is related to travel between cities surrounding the Site and the many recreational opportunities in the area. The projected INEEL workforce for the year 2004 is 7,250 (DOE 1995).

Table 2-1. Regional population of the INEEL; selected years 1990–2025.

County	1990 ^a	2000 ^b	2010	2025
Bannock	66,026	75,565	86,899	106,451
Bingham	37,583	41,735	47,995	58,794
Bonneville	72,207	82,522	94,900	116,252
Butte	2,918	2,899	3,333	4,083
Clark	762	1,022	1,175	1,439
Jefferson	16,543	19,155	22,028	26,984
Madison	23,674	27,467	31,587	38,694
Total	219,713	250,365	287,917	352,667

a. Source: DOC (1990).
b. Source: DOC (2001).

2.1.1.4 Uses of Adjacent Lands. The INEEL occupies approximately 2,305 km² (890 mi²) of land in Bingham, Bonneville, Butte, Clark, and Jefferson counties in southeastern Idaho. Approximately 2% of this land (4,613 ha [11,400 ac]) has been developed to support INEEL facility and program operations associated with energy research and waste management activities (DOE 1995). INEEL operations are performed within the Site's primary facility area (CFA, TRA, INTEC, etc.), which occupies 822 ha (2,032 ac). A 140,000-ha (340,000-ac) security and safety buffer zone is located around the core development area, which also accommodates environmental research and ecological and socio-cultural preservation.

Approximately 6% of the INEEL 14,000 ha (34,000 ac) is devoted to utility rights-of-way and public roads, including Highway 20 (which runs east and west and crosses the southern portion of the INEEL), Highway 26 (which runs southeast and northwest intersecting Highway 20), and Idaho State Highways 22, 28, and 33 (which cross the northeastern part of INEEL) (DOE 1995).

Up to 140,000 ha (340,000 ac) of the INEEL is leased for cattle and sheep grazing (DOE 1995); the Bureau of Land Management administers grazing permits. However, grazing of livestock is prohibited within one-half mile of any primary facility boundary and within 3.2 km (2 mi) of any nuclear facility. In addition, 400 ha (900 ac) located at the junction of Idaho State Highways 28 and 33 are used by the U.S. Sheep Experiment Station as a winter feedlot (DOE-ID 1996a). Figure 1-4 shows land use in the vicinity of the INEEL.

On July 17, 1999, the Secretary of Energy and representatives of the U.S. Fish and Wildlife Service, Bureau of Land Management, and Idaho State Fish and Game Department designated 29,649 ha (73,263 ac) of the INEEL as the Sagebrush Steppe Ecosystem Reserve (DOE 1999). In 1995, the National Biological Service listed the ungrazed sagebrush steppe ecosystem in the Intermountain West and big sagebrush (*Artemisia tridentata*) in Idaho's Snake River Plain as critically endangered (Noss et al. 1995). The INEEL Sagebrush Steppe Ecosystem Reserve was designated to ensure this portion of the ecosystem receives special scientifically controlled consideration. Conservation management in this area is intended to maintain the current vegetation and provide the opportunity for study of an undisturbed sagebrush steppe ecosystem. Traditional rangeland uses, such as livestock grazing, which currently exist in a portion of the area, will be allowed to continue under this management designation. The designated INEEL Sagebrush Steppe Ecosystem Reserve is located in the northwest portion of the area. The southern boundary of the Reserve, which runs east and west along section lines, is about 18 km (11 mi) north of INTEC at the closest point (DOE 2002).

Recreational uses of the INEEL include public tours of general facility areas and the EBR-I, a National Historic Landmark. Controlled hunting also is permitted on the INEEL, but is restricted to one-half mile inside the Site boundary. These restricted hunts are intended to assist the Idaho Department of Fish and Game (IDFG) in reducing crop damage caused by wild game on adjacent private agricultural lands. The INEEL is designated as a National Environmental Research Park, functioning as a field laboratory set aside for ecological research and evaluation of the environmental impacts from nuclear energy development (DOE 1999).

The INEEL is located on Federal land that is recognized as part of the Shoshone-Bannock Tribes aboriginal territory and contains cultural resources important to the tribes. Protection of these cultural resources, access to sacred sites, sites of traditional use, and repatriation of native American human remains and cultural items are of paramount importance to the tribes and DOE.

Land use at the INEEL is in a state of transition. Emphasis is moving toward nuclear energy research, radioactive and hazardous waste management, environmental restoration and remedial technologies, and technology transfer, resulting in more development of the INEEL within some facility

areas and less development in others. DOE has projected land use scenarios at the INEEL for the next 25, 50, 75, and 100 years. Future development is projected to take place in the central portion of the INEEL within existing facility areas.

For further review, see the *Long-Term Land Use Future Scenarios for the Idaho National Engineering Laboratory* (DOE-ID 1995) and the *Idaho National Engineering and Environmental Laboratory Comprehensive Facility and Land Use Plan* (DOE-ID 1996a).

Approximately 75% of the land adjacent to the INEEL is owned by the federal government and administered by the Bureau of Land Management. Land uses on this federally held land consist of wildlife management, mineral and energy production, grazing, and recreation. The State of Idaho owns approximately 1% of the adjacent land. This land is also used for wildlife management, grazing, and recreation. The remaining 24% of the land adjacent to the INEEL is privately owned and is primarily used for grazing and crop production (SAR-II-8.4).

Small communities and towns located near the INEEL boundaries include Mud Lake and Terreton to the east; Arco, Butte City, and Howe to the west; and Atomic City to the south. The larger communities of Idaho Falls/Ammon, Rexburg, Blackfoot, and Pocatello/Chubbuck are located to the east and southeast of the INEEL Site. The Fort Hall Indian Reservation is located southeast of the INEEL Site.

All county plans and policies encourage development adjacent to previously developed areas to minimize the need to extend infrastructure improvements and to avoid urban sprawl. Because the INEEL is remotely located from most developed areas, INEEL lands and adjacent areas are not likely to experience residential and commercial development, and no new development is planned near the INEEL Site. However, recreational and agricultural uses are expected to increase in the surrounding area in response to greater demand for recreational areas and the conversion of rangeland to cropland (DOE-ID 1993b).

The four most prominent tourist/recreation areas or attractions in the INEEL area include

- Yellowstone National Park, which is approximately 117 km (72.5 mi) northeast of the INEEL, and 160 km (99.5 mi) from INTEC
- EBR-I, which is situated on the INEEL
- Craters of the Moon National Monument, which is located approximately 30 km (19 mi) southeast of the INEEL
- The resort areas of Ketchum and Sun Valley, which are approximately 95.8 km (59.5 mi) west of the INEEL (115.9 km [72 mi] from INTEC) (SAR-II-8.4).

Other recreation and tourist attractions in the region surrounding the INEEL site include Hell's Half Acre Wilderness Study Area, Black Canyon Wilderness Study Area, Camas National Wildlife Refuge, Market Lake State Wildlife Management Area, North Lake State Wildlife Management Area, Yellowstone National Park, Targhee and Challis National Forests, Sawtooth National Recreation Area, Sawtooth Wilderness Area, Sawtooth National Forest, Grand Teton National Park, Jackson Hole recreation complex, and the Snake River.

Planning assumptions in the *INEEL Comprehensive Facility and Land Use Plan* (DOE-ID 1996a) are that the INEEL will remain under government control for at least the next 100 years. Future

government management and control becomes increasingly uncertain with time. No residential development will be allowed to occur within INEEL boundaries during the next 100 years.

INTEC was one of the facilities that had a future use scenario projected in the *Long-Term Land Use Future Scenarios for the Idaho National Engineering Laboratory* (DOE-ID 1995). The scenarios are broken down into the present situation, as well as for the next 25, 50, 75, and 100 years:

- Present: Interim storage of spent nuclear fuels, disposition of fuels, managing waste and improving waste, and water management techniques
- 25-year: Continue use as industrial area, planned new waste treatment facility
- 50-year: Approaching end of useful life if no new mission identified, decontamination and decommissioning with all or selected areas for restricted industrial use
- 75-year: Standby mode for restricted industrial use, reuse permitted but no new development outside existing fence line
- 100-year: Continuation as a restricted industrial area
- Implement institutional controls (to include a DOE-ID Directive limiting access) to prevent perched water use while INTEC operations continue and to prevent future drilling into or through the perched zone (through noticing this restriction to local county governments, ShoBan Tribal Council, General Services Administration, BLM, and other agencies as necessary).

2.1.2 Meteorology and Climatology

Meteorological data have been collected periodically at over 45 locations on and near the INEEL since 1949. The longest and most complete record of air temperature and precipitation observations (over 35 years) at the INEEL was collected from the weather station at CFA. The CFA station is located approximately 5 km (3 mi) south of INTEC. Differences in climate between the CFA monitoring station and INTEC are minimal. INTEC and CFA are at approximately the same terrain elevation and have the same exposure to wind, snow, and cloud cover.

The National Oceanic and Atmospheric Administration Air Resources Laboratories conducts most of the meteorological monitoring within 80 km (50 mi) of the INEEL. An overview of climatological data is available from data summaries collected from the CFA monitoring station. A summary of the climatology of the INEEL is available in *Climatology of the Idaho National Engineering Laboratory* (Clawson et al. 1989).

2.1.2.1 Temperature. Temperatures at the INEEL vary widely over the course of the year. Records for CFA indicate that the highest and lowest daily temperatures range from 38°C (101°F) to -44°C (-47°F), respectively. The average annual temperature at the INEEL exhibits a gradual seven-month increase, beginning with the first week in January and continuing through the third week in July. During the months of April through October, the average monthly temperature varies from 5 to 20°C (41 to 68°F). The temperature then decreases over the course of five months until the minimum average temperature is again reached in January. During the months of November through March, the average monthly temperature varies from -9 to -1°C (15 to 30°F). On average, 42% of the days in a year contain a freeze/thaw cycle, in which the maximum air temperature exceeds 0°C (32°F), and the minimum air temperature is at or below 0°C (32°F). Inversion conditions (warmer air temperature with increasing

altitude) and lapse conditions (cooler air temperature with increasing altitude) occur approximately 46% and 54% of the time, respectively.

2.1.2.2 Wind. The prevailing wind direction at INTEC and at most locations on the INEEL is southwesterly. In summer, a very sharp reversal in wind direction occurs daily; winds from the southwest predominate during daylight hours, and northeasterly winds predominate at night. The reversals normally occur shortly after sunrise and sunset. The average wind speed at the 6-m (20-ft) level at CFA ranges from 8.2 km/h (5.1 mph) in December to 15 km/h (9.3 mph) in March and April. The highest hourly-average wind speed at the 6-m (20-ft) level was 108 km/h (67 mph), and the maximum instantaneous gust at the same level was 125.5 km/h (78 mph). Strong wind gusts can occur in the immediate vicinity of thunderstorms. On the average, these gusts occur 2 or 3 days per month during June, July, and August. Calm conditions prevail 11% of the time.

2.1.2.3 Precipitation. The average annual precipitation at CFA is 22 cm (8.7 in.). The highest recorded annual amount of precipitation recorded was 36.6 cm (14.4 in.) in 1963, and the lowest amount was 11.4 cm (4.5 in.) in 1966. The majority of precipitation occurs in May and June, with an average precipitation for each of these months of 3 cm (1.2 in.). Precipitation amounts in excess of 2.54 cm (1 in.) per day have been recorded eight times at CFA, with the maximum being 4 cm (1.64 in.). The maximum hourly precipitation observed at CFA is 1.37 cm (0.54 in.). Snowfall is a substantial contributor to total annual precipitation and ranges from 17 to 152 cm/yr (6.7 to 60 in./yr), with an annual average of 70 cm (28 in.). The maximum average monthly snowfall is 16.3 cm (6.4 in.), occurring in December.

2.1.2.4 Evaporation. The potential annual evaporation from a saturated ground surface at the INEEL is approximately 91 cm (36 in.), with 80% of the evaporation occurring between May and October. During July, the warmest month of the year, the daily potential evaporation rate is approximately 0.6 cm (0.2 in.) (Hull 1989). Evaporation occurring during the remainder of the year is small. Actual evaporation rates are much lower than potential rates because the ground surface is rarely saturated. Transpiration by the native vegetation of the Snake River Plain is estimated at 15 to 23 cm/yr (5.9 to 9.1 in./yr). From late winter to spring, precipitation is most likely to infiltrate into the ground because of the low evapotranspiration rates (Mundorff et al. 1964). For evaporation from surface water bodies (ponds), a pan evaporation rate of approximately 109 cm/yr (43 in./yr) has been estimated (Clawson et al. 1989).

2.1.2.5 Relative Humidity. The highest relative humidity is observed in the winter, with the average midday relative humidity at about 55%. The lowest is observed in the summer, when the midday average is approximately 18%. An absolute maximum relative humidity value of 100% was observed in every month of the year except July, and the lowest observed was 4% in July and August. This is indicative of the very dry summers experienced at the INEEL.

2.1.2.6 Special Phenomena. Several other types of meteorological phenomena such as thunderstorms, hail, and tornadoes occur at the INEEL. The INEEL may experience an average of two to three thunderstorm days during each of the summer months from June through August with considerable year to year variation. Thunderstorms over the INEEL are usually much less severe than what is normally experienced in the mountains surrounding the ESRP or areas of the Rocky Mountains. Precipitation from many thunderstorms evaporates before reaching the ground (virga). The frequent result is little or no measurable precipitation. Occasionally, however, rain amounts exceeding the long-term average may result from a single thunderstorm. Small hail has been observed to occasionally occur in conjunction with thunderstorms. The size of the hail is usually smaller than ¼ in. in diameter. The diameter may range up to ¾ in. on very rare occasions. No hail damage has ever been reported at the INEEL.

Most tornado activity in the U.S. occurs east of the Rocky Mountains. In Idaho, tornadoes have been reported only in the spring and summer seasons (April through August). Records from 1950 through 1989 indicate a total of five funnel clouds and no tornadoes sighted within the boundaries of the INEEL. The chance of a tornado developing at the INEEL is extremely remote.

2.1.3 Ecology

The following sections discuss the plant and animal species and communities that may be found on the Site including threatened, endangered, and sensitive species.

2.1.3.1 Flora. The INEEL represents the largest remnant of undeveloped, ungrazed sagebrush steppe ecosystem in the Intermountain West (DOE-ID 1996a). This ecosystem has been listed as critically endangered with less than two percent of its original coverage remaining (Noss et al. 1995, Saab and Rich 1997).

In 1975, the INEEL Site was dedicated as one of five DOE National Environmental Research Parks. It is an outdoor laboratory used to study ecological relationships and the effects of human activities on natural systems. In addition, it provides a unique setting for scientific investigation because the public has been excluded from much of the area for the past 25 years. Ecological data collected from the Idaho National Environmental Research Park provide a basis for analyzing environmental changes over time and assessing the effect of human influence on the environment.

Research on the flora and fauna of the INEEL Site has largely been conducted by or in conjunction with the DOE Radiological and Environmental Sciences Laboratory (RESL). The physical aspects of the INEEL Site and its flora and fauna are typical of cold, high altitude, sagebrush ecosystems found in the western United States.

Much of the following discussion of the flora and fauna at the INEEL is from the *Environmental Resource Document for the Idaho National Engineering Laboratory* (Irving 1993). This report contains additional detailed information and references to specific ecological studies.

Extensive surveys of INEEL vegetation were carried out in 1952, 1958, and 1967 using 150 permanent transects established and maintained for this purpose (Harniss and West 1973). McBride et al. (1978) and Jeppson and Holte (1978) also have described vegetation.

More recently, Anderson et al. (1996a) broadly described ten vegetation classes and plant communities that occur on the INEEL (Figure 2-2). These communities do not represent homogeneous community types, but integrated communities that share dominant species and are more similar to each other than to communities represented by other vegetation classes. Sagebrush steppe is the dominant community on the INEEL. Other community types include juniper woodlands, grasslands, low shrubs on lava, sagebrush-rabbitbrush, sagebrush-winterfat, salt desert shrub, wetlands, playas, bare ground or disturbed areas, and lava. Figure 2-2 depicts the distribution of vegetation at the INEEL.

Several studies have been conducted at the INEEL on the plant rooting depths, especially for the RWMC Subsurface Disposal Area (SDA). Studies of plant uptake of radionuclides at the INEEL have focused primarily on (a) determining if deep-rooted plants are a mechanism for waste pit intrusion and subsequent uptake of radionuclides and (b) analyzing inventories of radionuclides in aerial portions of plants. Aerial portions of plants are important because they can potentially transport subsurface contaminants through dispersal of leaves, consumption by herbivores, use by birds as nesting materials, and wildfire.

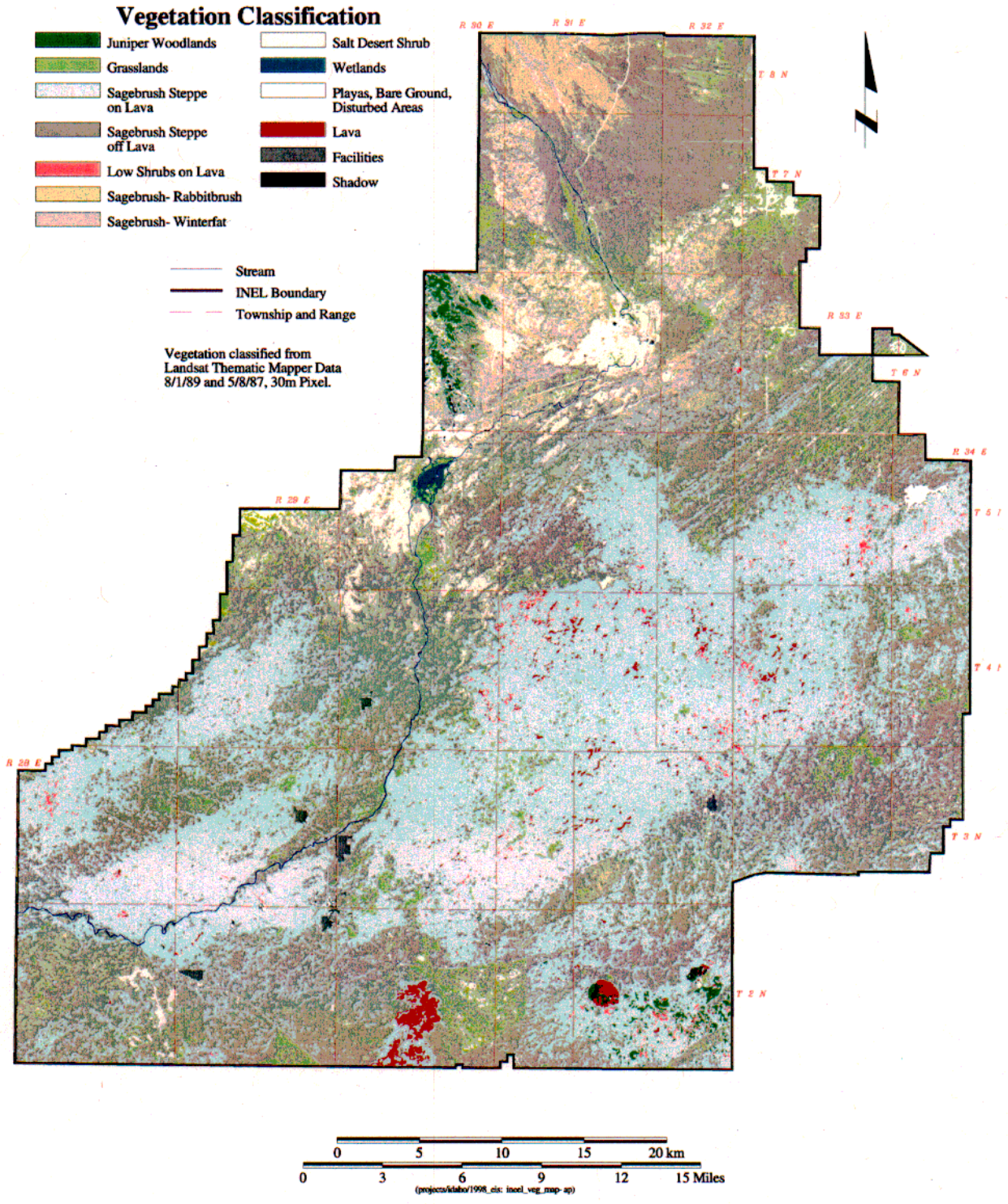


Figure 2-2. Approximate distribution of vegetation at the INEEL.

One RWMC SDA study comparing radionuclide uptake by crested wheat grass (rooting depth 1 to 1.5 m [3 to 4.9 ft]) with that by Russian thistle (rooting depth 1 to 5 m [3 to 16 ft]) showed higher radionuclide concentrations in the deeper-rooted species (Arthur 1982). Examples of other deep-rooting species are rabbitbrush and sagebrush. General examples of shallow-rooting plant types are grasses and annual forbs.

Reynolds and Fraley (1989) found that the roots of big sagebrush extended to a depth of 225 cm (89 in.), green rabbitbrush to a depth of 190 cm (75 in.), and Great Basin wild rye had roots up to 200 cm (79 in.) deep at the SDA. Maximum lateral spread of the roots of both big sagebrush and Great Basin wild rye was 90 cm (35.5 in.) and occurred at a depth of 40 cm (15.8 in.). In addition, studies indicate root penetration of up to 1.6 m (5.2 ft) for sodar and crested wheat grass at the INEEL (Markham 1987).

2.1.3.2 Fauna. The INEEL supports a variety of wildlife including small mammals, birds, reptiles, and a few large mammals.

Aquatic life on the INEEL is limited and depends mainly upon the flow of the Big Lost River. During several months of the year, and even during some entire years, the river does not flow. However, during spring runoff and periods of high rainfall, the diversion system (at the southern boundary of the INEEL) and the Big Lost River sinks (at the northern boundary of the INEEL) support water flow during periods of water accumulation. This normally occurs less than 2 or 3 months in the spring. Fish species observed in the Big Lost River on the INEEL include rainbow trout, mountain whitefish, eastern brook trout, Dolly Varden char, Kokanee salmon, and the shorthead sculpin (Overton et al. 1976).

A total of 219 vertebrate species have been recorded on the INEEL. Vertebrate species include six species of fish, one amphibian, nine reptiles, 164 birds, and 39 mammals (Reynolds et al. 1986). Several vertebrate species present on the INEEL are considered sagebrush-obligate species, meaning that they rely upon sagebrush for survival. Among others, these species include sage sparrow (*Amphispiza belli*), Brewer's sparrow (*Spizella breweri*), northern sagebrush lizard (*Sceloporus graciosus*), sage grouse (*Centrocercus urophasianus*), and pygmy rabbit (*Brachylagus idahoensis*).

A total of 740 insect species have been recorded at the INEEL; 226 of these species have not yet been identified beyond the family level. The majority of the abundant species belong to the orders Hymenoptera (wasps and ants) and Diptera (flies).

Studies have been performed on burrowing characteristics of small mammals such as ground squirrels, deer mice, and voles (Arthur et al. 1983; Markham 1987; Reynolds and Laundre 1988). Results of the studies indicate burrows no deeper than 140 cm (55 in.) at the INEEL.

2.1.3.3 Threatened, Endangered and Sensitive Species. A list of threatened or endangered (T/E) and sensitive species that may occur on the INEEL is given in Table 2-2. The list was originally compiled from the U.S. Fish and Wildlife Service (USFWS) (USFWS 1996, 1997); the IDFG Conservation Data Center (CDC) threatened, endangered, and sensitive species for the State of Idaho (CDC 1994); and RESL documentation for the INEEL (Reynolds 1994; Reynolds et al. 1986). This list (USFWS 2001) was most recently updated in February 2002.^a

The only species documented at the INEEL and currently recognized as threatened or endangered under the Endangered Species Act is the bald eagle, which was recently down-listed to threatened. The peregrine falcon, recently removed from the federal list, remains on the endangered list for the State of Idaho.

a. Updated by N. L. Hampton, BBWI, February 4, 2002.

Table 2-2. Threatened or endangered species, sensitive species, and species of concern that may be found on the INEEL.

Common Name ^a	Scientific Name	Federal Status ^{b,c}	State Status ^c	BLM Status ^c	USFS ^f Status ^c
<u>Plants</u>					
Lemhi milkvetch	<i>Astragalus aquilonius</i>	—	S	S	S
Painted milkvetch ^e	<i>Astragalus ceramicus</i> var. <i>apus</i>	SC	R	—	—
Plains milkvetch	<i>Astragalus gilviflorus</i>	—	1	S	S
Winged-seed evening primrose	<i>Camissonia pterosperma</i>	—	S	S	—
Nipple cactus ^e	<i>Coryphantha missouriensis</i>	—	R	—	—
Spreading gilia	<i>Ipomopsis (=Gilia) polycladon</i>	—	2	S	—
King's bladderpod	<i>Lesquerella kingii</i> var. <i>cobrensis</i>	—	M	—	—
Tree-like oxlytheca ^e	<i>Oxytheca dendroidea</i>	—	R	R	—
Inconspicuous phacelia ^d	<i>Phacelia inconspicua</i>	C	SSC	S	S
Ute ladies' tresses ^d	<i>Spiranthes diluvialis</i>	LT	—	—	—
Puzzling halimolobos	<i>Halimolobos perplexa</i> var. <i>perplexa</i>	—	M	—	S
Slender moonwort ^d	<i>Botrychium lineare</i>	R	GP1	—	—
<u>Birds</u>					
Peregrine falcon	<i>Falco peregrinus</i>	R	E	—	—
Merlin	<i>Falco columbarius</i>	—	P	S	—
Gyr falcon	<i>Falco rusticolus</i>	—	SSC	S	—
Bald eagle	<i>Haliaeetus leucocephalus</i>	LT	T	—	—
Ferruginous hawk	<i>Buteo regalis</i>	W	SSC	S	—
Black tern	<i>Chlidonias niger</i>	—	SSC	—	—
Northern pygmy owl ^d	<i>Glaucidium gnoma</i>	W	SSC	—	—
Burrowing owl	<i>Athene(=Speotyto) cucularia</i>	SC	—	S	—
Common loon	<i>Gavia immer</i>	W	SSC	—	—
American white pelican	<i>Pelicanus erythrorhynchos</i>	—	SSC	—	—
Great egret	<i>Casmerodius albus</i>	—	SSC	—	—
White-faced ibis	<i>Plegadis chihi</i>	SC	—	—	—
Long-billed curlew	<i>Numenius americanus</i>	SC	—	S	—
Loggerhead shrike	<i>Lanius ludovicianus</i>	SC	NL	S	—
Northern goshawk	<i>Accipiter gentilis</i>	W	P	—	S
Swainson's hawk	<i>Buteo swainsoni</i>	—	—	S	—
Trumpeter swan	<i>Cygnus buccinator</i>	SC	SSC	S	S
Sharptailed grouse	<i>Tympanuchus phasianellus</i>	SC	—	S	S
Boreal owl	<i>Aegolius fumereus</i>	W	SSC	S	S
Flammulated owl	<i>Otus flammeolus</i>	W	SSC	—	S
Yellow-billed cuckoo ^d	<i>Coccyzus americanus</i>	C	—	—	—
Greater sage grouse	<i>Centrocercus urophasianus</i>	SC	—	—	—
<u>Mammals</u>					
Gray wolf ^g	<i>Canis lupus</i>	LE/XN	E	—	—
Pygmy rabbit	<i>Brachylagus (=Sylvilagus) idahoensis</i>	W	GSC	S	—
Townsend's Western big-eared bat	<i>Corynorhinus (=Plecotus) townsendii</i>	SC	SSC	S	S
Merriam's shrew	<i>Sorex merriami</i>	—	U	—	—
Long-eared myotis	<i>Myotis evotis</i>	W	U	—	—
Small-footed myotis	<i>Myotis ciliolabrum (=subulatus)</i>	W	U	—	—
Western pipistrelle ^d	<i>Pipistrellus hesperus</i>	W	SSC	—	—
Fringed myotis ^d	<i>Myotis thysanodes</i>	W	SSC	—	—
California myotis ^d	<i>Myotis californicus</i>	W	U	—	—
<u>Reptiles and amphibians</u>					
Northern sagebrush lizard ^h	<i>Sceloporus graciosus</i>	SC	—	—	—

Table 2-2. (continued).

Common Name ^a	Scientific Name	Federal Status ^{b,c}	State Status ^c	BLM Status ^c	USFS ^f Status ^c
Ringneck snake ^d	<i>Diadophis punctatus</i>	C	SSC	S	—
Night snake ^e	<i>Hypsiglena torquata</i>	—	—	R	—
<u>Insects</u>					
Idaho pointheaded grasshopper ^d	<i>Acrolophitus punchellus</i>	W	—	—	—
<u>Fish</u>					
Shorthead sculpin ^d	<i>Cottus confusus</i>	—	SSC	—	—

a. This list was compiled by N. Hampton from letters from the U.S. Fish and Wildlife Service (USFWS) (1996, 1997, 2001) for threatened or endangered, and sensitive species listed by the IDFG Conservation Data Center (CDC 1994 and IDFG Web site) and Radiological Environmental Sciences Laboratory documentation for the INEEL (Reynolds et al. 1986).

b. The USFWS no longer maintains a candidate (C2) species listing but addresses former listed species as “species of concern” (USFWS 1996). The C designation replaces C2.

c. Status codes: INPS=Idaho Native Plant Society; S=sensitive; 2=State Priority 2 (INPS); M=State of Idaho monitor species (INPS); U= undetermined, 1=State Priority 1 (INPS); LE=listed endangered; P=protected nongame species, E=endangered; T = threatened; XN = experimental population, nonessential; SC=species of concern, SSC=species of special concern; W = watch species and C = candidate for listing, see item b, formerly Category 2 (defined in CDC 1994). BLM=Bureau of Land Management; R = removed from sensitive list (nonagency code added here for clarification).

d. No documented sightings at the INEEL, however, the ranges of these species overlap the INEEL and are included as possibilities to be considered for field surveys.

e. Recent updates that resulted from Idaho State Sensitive Species meetings (BLM, USFWS, INPS, and USFS) (IDFG Website).

f. U.S. Forest Service (USFS) Region 4.

g. Anecdotal evidence indicates that isolated wolves may occur on the INEEL. However, no information exists to substantiate hunting or breeding on site (Morris 1999).

h. The sagebrush lizard was placed on the list as a result of a miscommunication, however, it remains on the official USFWS update periodically issued for the INEEL (N. Hampton BBWI, lecture at IDFG by Dr. Charles Peterson, Idaho State University, January 10, 2002, Idaho Falls, ID)..

A number of former C2 species recorded at the INEEL no longer have status under the Endangered Species act, but remain species of concern. These include the burrowing owl (*Athene cunicularia*), white-faced ibis (*Plegadis chichi*), trumpeter swan (*Cygnus buccinator*), long-billed curlew (*Numenius americanus*), loggerhead shrike (*Lanius excubitor*), greater sage grouse (*Centrocercus urophasianus*), sharp-tailed grouse (*Tympanuchus phasianellus*), and Townsend’s big-eared bat (*Corynorhinus townsendii*). Painted milk-vetch (*Astragalus ceramicus* var. *apus*) also remains on the USFWS periodic update for the INEEL (USFWS 2001), but has been removed from the State of Idaho list. The sagebrush lizard (*Sceloporous graciosus*) was designated as a candidate for listing through a miscommunication,^b but remains as a species of concern on the periodic T/E update for the INEEL (USFWS 2001).

Five additional species documented at the INEEL also appear on the federal watch list and the USFWS list of species of concern for the INEEL (USFWS 2001) including the ferruginous hawk (*Buteo regalis*), pygmy rabbit (*Brachylagus idahoensis*), Merriam’s shrew (*Sorex merriami*), long-eared myotis (*Myotis evotis*), and small-footed myotis (*Myotis ciliolabrum*).

2.1.4 Geology, Seismology, and Volcanology

The following sections discuss the regional and site-specific geology, seismology, and volcanology.

2.1.4.1 Regional and Site-Specific Geology. The INEEL is located on the west-central part of the ESRP, a northeast-trending structural basin about 322 km (200 mi) long and 80 to 112 km (50 to 70 mi) wide (Figure 2-3). The INEEL is underlain by a sequence of Tertiary and Quaternary volcanic rocks and sedimentary interbeds that are more than 3,048 m (10,000 ft) thick (Whitehead 1992).

b. N.L. Hampton, BBWI, lecture at IDFG by Dr. Charles Peterson, Idaho State University, January 10, 2002, Idaho Falls, ID.

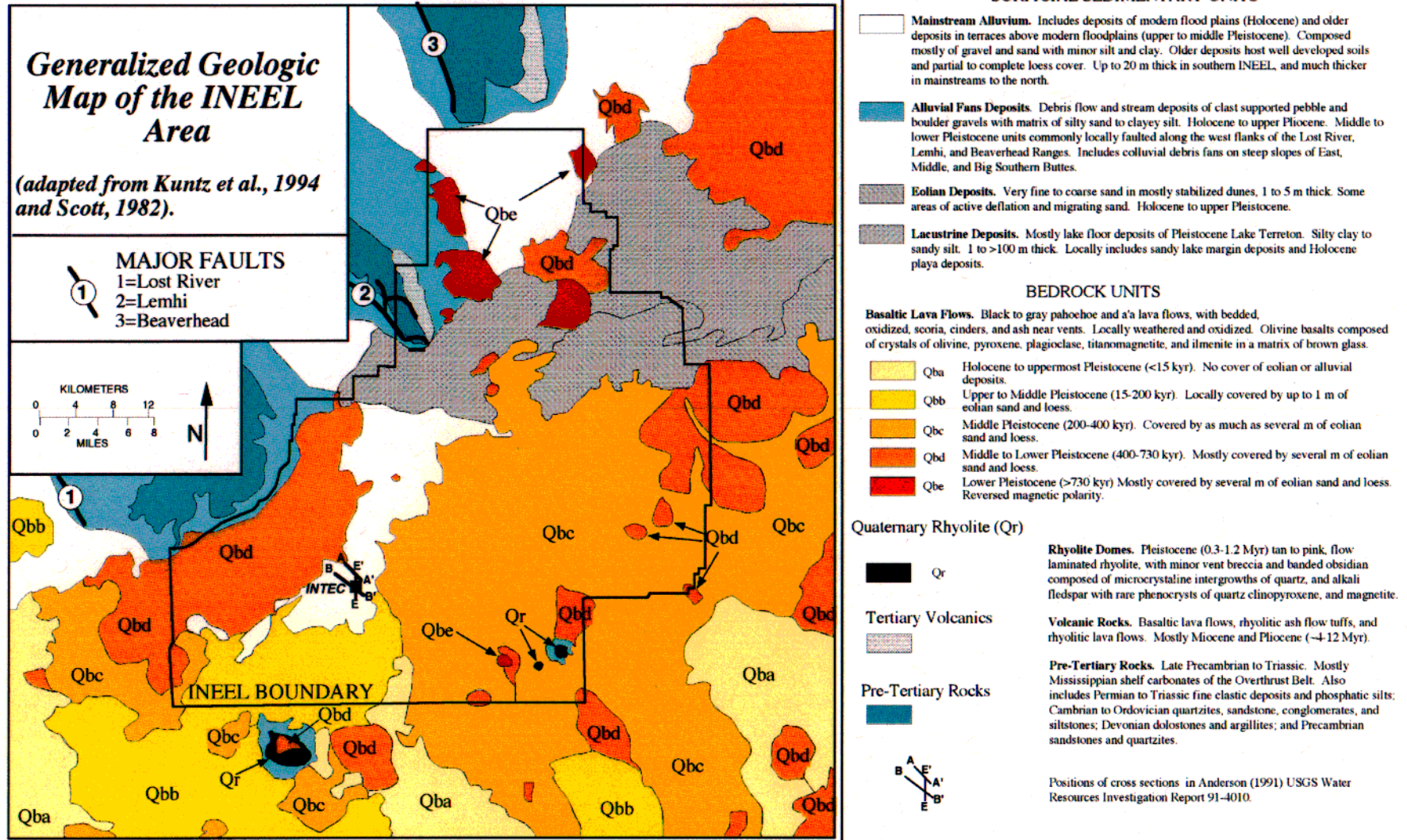


Figure 2-3. Generalized geological map of the INEEL area.

The volcanic rocks consist mainly of basalt flows in the upper part of the sequence and rhyolitic ash-flow tuffs in the lower part. Basalt and interbeds generally range in age from about 200 thousand to 4 million years before present (Anderson et al. 1997), and underlie the plain to depths ranging from about 670 m to 1,158 m (2,200 to 3,800 ft) below land surface.

Hundreds of basalt flows, basalt-flow groups, and sedimentary interbeds underlie the INEEL. Basalt makes up about 85% of the volume of deposits in most areas. A basalt flow is a solidified body of rock formed by the surficial outpouring of molten lava from a vent or fissure (Bates and Jackson 1980). A basalt-flow group consists of one or more distinct basalt flows deposited during a single, brief eruptive event. All basalt flows of a group erupted from the same vent or several nearby vents; represent the accumulation of one or more lava flows from the same magma; and have similar geologic ages, paleomagnetic properties, potassium contents, and natural-gamma emissions (Anderson and Bartholomay 1995). The basalt flows consist mainly of medium- to dark-gray vesicular to dense olivine basalt. Individual flows generally range from 3 to 15 m (10 to 50 ft) thick, and are locally interbedded with scoria and thin layers of sediment. Sedimentary interbeds are as thick as 15 m (50 ft) and consist of well sorted to poorly sorted deposits of clay, silt, sand, and gravel. In places, the interbeds contain or consist mainly of scoria and basalt rubble. Sedimentary interbeds accumulated on the ancestral land surface for hundreds to hundreds of thousands of years during periods of volcanic quiescence, and are thickest between basalt-flow groups.

At least 178 basalt-flow groups and 103 sedimentary interbeds underlie the INEEL above the effective base of the aquifer (Anderson et al. 1996b, 1997). Basalt-flow groups and sedimentary interbeds are informally referred to as A through S5. Basalt-flow groups A through L and related sediment range in age from about 200 to 800 thousand years and make up the unsaturated zone and the uppermost part of the aquifer in most areas of the INEEL. Most wells in the southern and eastern parts of the INEEL are completed in basalt-flow groups AB through I and the related sediments. Flow groups AB through I and related sediments range in age from about 200 to 640 thousand years and make up a stratigraphic section characterized by horizontal to slightly inclined layers. Anderson et al. (1997) estimated the geologic ages of basalts and sediments in the unsaturated zone and the SRPA from about 200 thousand to 1.8 million years; average accumulation rates are reflective of a subsidence rate of 50 m (164 ft)/100,000 yr.

The nomenclature for the stratigraphy underlying the INTEC facility and the surrounding area is based on work presented by Anderson (1991) and Anderson et al. (1996b). A north-south geologic cross section, illustrated in Figures 2-4 and 2-5, show the complexity of the subsurface at INTEC.

The stratigraphy of the aquifer at and near INTEC is dominated by thick, massive basalt flows of flow group I and thin, overlying flows of flow groups B through H. Significant changes in the flow thickness are often related to changes in the lithology of the flow or are caused by the flow margins in which the flow appears as a lobe of basalt. The lithologic changes that may cause a change in the flow thickness are the existence of pyroclastic deposits on or within a flow, or a flow being very vesicular, and thus, more susceptible to the effects of erosion.

Based on the Anderson (1991) geologic cross section, the unsaturated zone and upper regional aquifer underlying INTEC are comprised of nineteen basalt-flow groups, eleven sedimentary interbeds, and surficial alluvium. The sediments, as interpreted, appear to be primarily made up of sands and silts with some small clay lenses. The majority of the sediments are thin 0.3- to 1.5-m (1- to 5-ft) layers of silt between the major basalt flows. Sediments were most likely deposited in eolian or fluvial type environments. Two major sediment sequences are shown on the cross sections: the upper sequence associated with the "CD," thick "D" and "DE2" sands and silts; and the lower sediments associated with the "DE6," "DE7," and "DE8" stratigraphic units.

The cross sections show a very thick sequence of sediments, particularly in the northern end of the south-north section, which are stratigraphically shown as the "CD," "D," and "DE2" units. These sediments appear to be a thick sequence of sands over silts and clays. The sediments associated with the

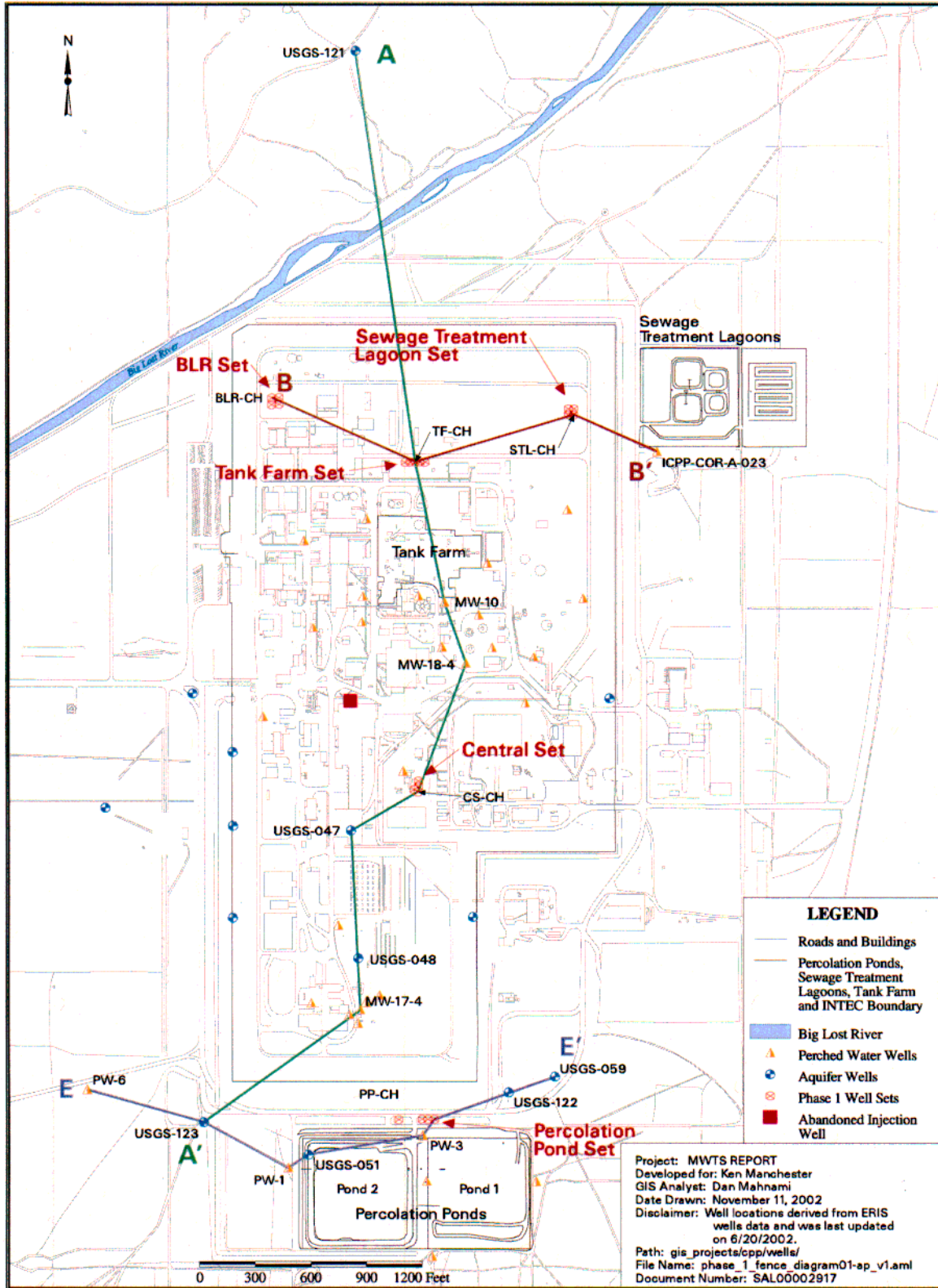


Figure 2-4. Plan view of cross section shown in Figure 2-5.

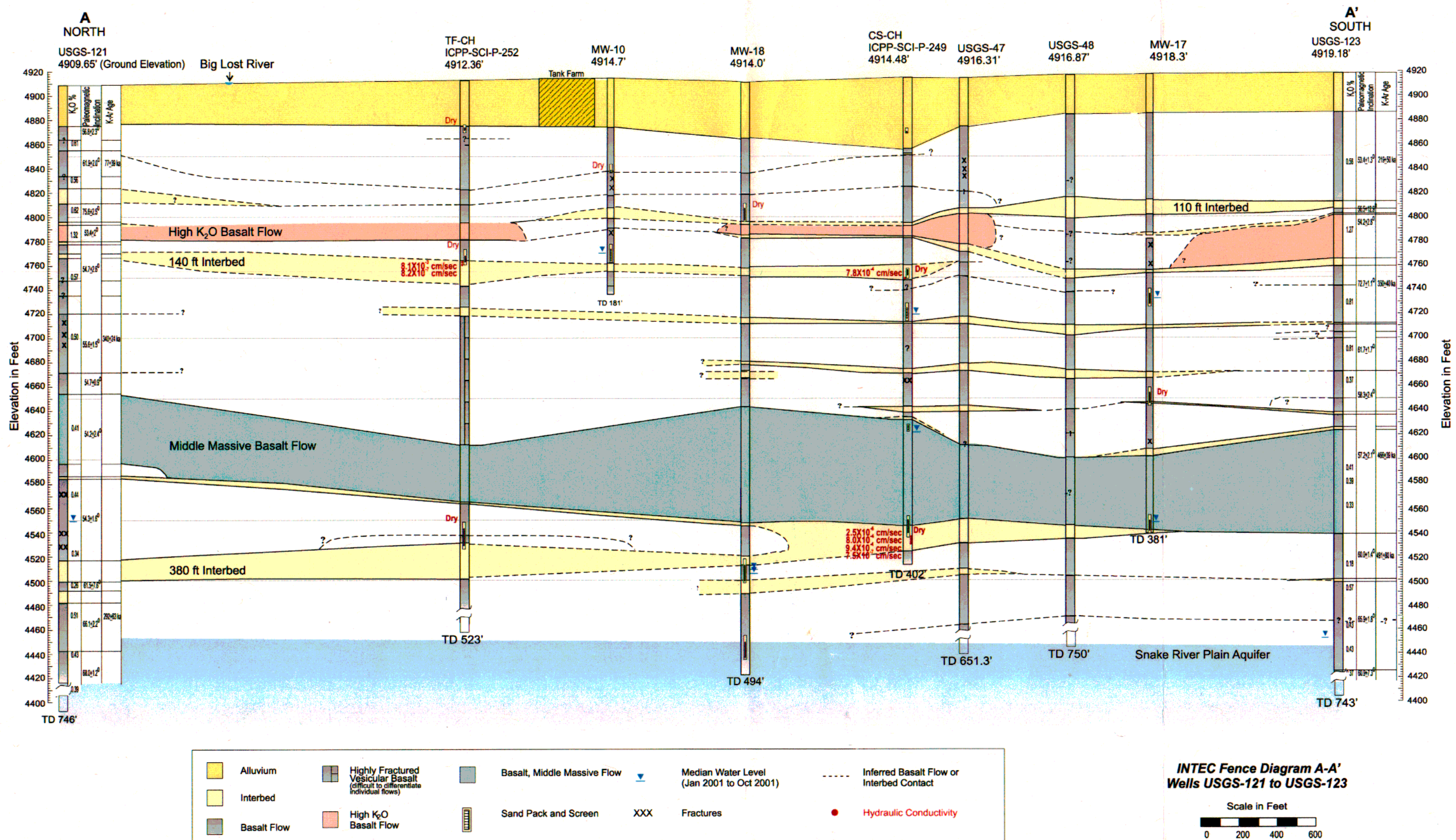


Figure 2-5. North-south geological cross section at INTEC.

“DE6,” “DE7,” and “DE8” stratigraphic units appear to be made up of gravels, silts, and clays. These sediments were most likely deposited in a fluvial environment and may indicate a braided stream deposit.

The geology beneath the ICDF Complex has been characterized from information gathered from logs (lithologic, geophysical, and video) as well as tests (geotechnical and hydrologic) from the drilling of numerous SRPA and perched water wells and coreholes located in the vicinity of the ICDF Complex and INTEC. The locations of wells closest to the ICDF Complex are shown in Figure 2-6. An east-west geologic cross-section through the ICDF Complex (A-A' in Figure 2-6) is shown in Figure 2-7.

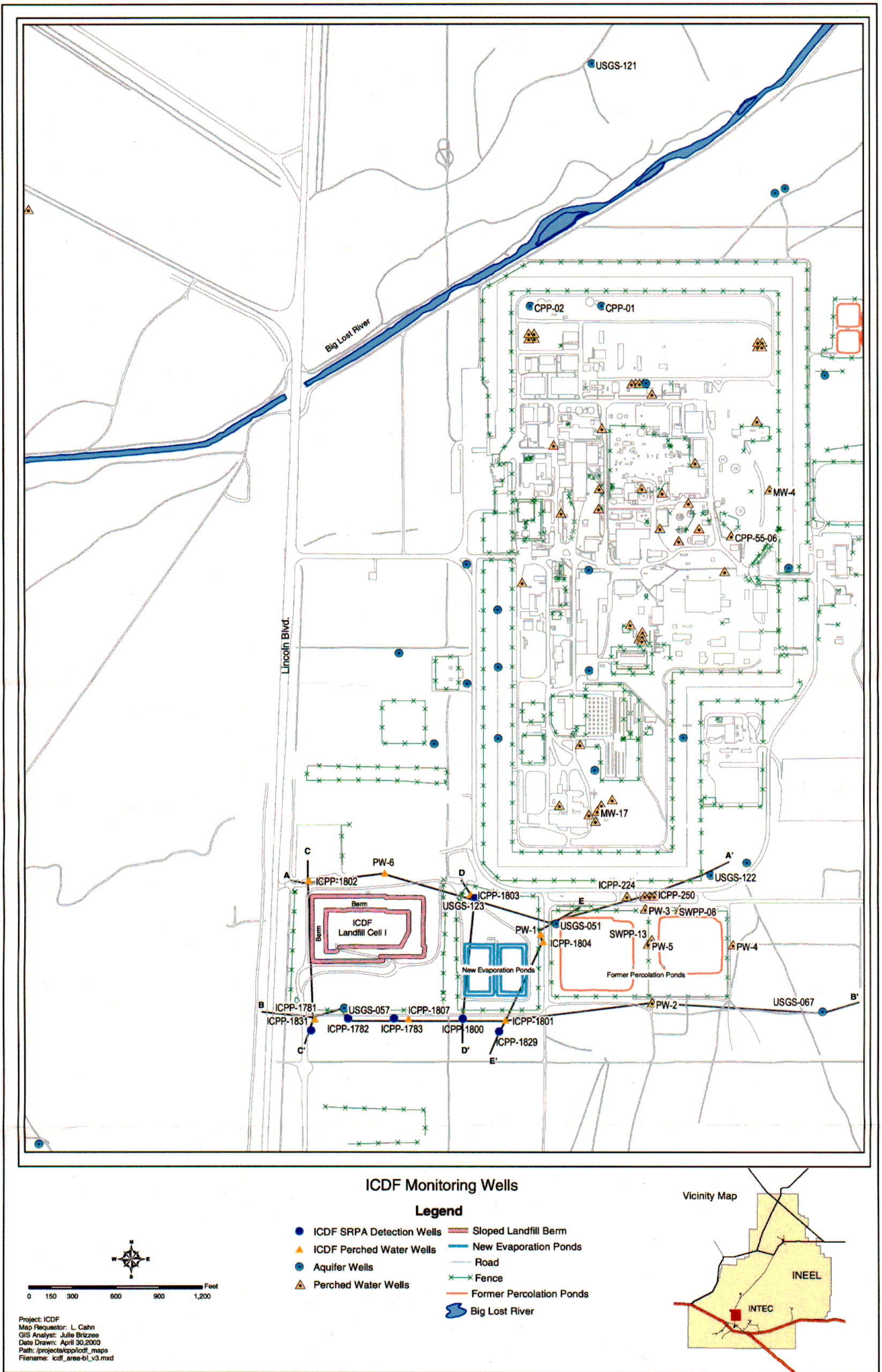
The subsurface beneath the ICDF Complex, as shown in Figure 2-7, is characterized by approximately 9 to 16.8 m (30 to 55 ft) of alluvial materials underlain by a series of basalt flows and discontinuous sedimentary interbeds. The surface alluvium at the ICDF Complex has been mapped as a flood delta or fan related to late Pleistocene cataclysmic flooding, most likely from the Pinedale Glaciation (Rathburn 1991). The Pinedale Glaciation occurred between 12,000 and 35,000 years ago. An intermittent layer of fine sand, silt, and clay known as “old alluvium” in the literature (designation SM to CL) ranges in thickness from 0 to 4 m (0 to 13 ft) and occurs at the top of basalt. The thickness correlates to low spots and depressions and tends to increase to the south and west of the ICDF Complex. It is less prevalent in the northwest area. Sand lenses were periodically found within this layer. The sediments overlie vesicular dark gray, olivine basalt bedrock that may be weathered and fractured in the first several feet near the interface (DOE-ID 2000a).

As can be seen in Figure 2-7, two very distinctive massive basalt flows can be used as marker beds and traced between most boreholes underneath the ICDF Complex. The depth at which these distinctive flows occur varies between boreholes. The CD basalt flow occurs at a depth between approximately 41 to 53 m (135 and 175 ft), and the DE5 basalt occurs at a depth between approximately 98 and 120 m (320 and 395 ft) in USGS-57. The CD basalt flow is characterized by a higher-than-average natural-gamma count. Above the CD basalt flow is a fairly continuous series of thin interbeds interspersed with thin basalt flows. This is the most continuous interbed underlying the ICDF Complex and is the location of perched water that forms intermittently in response to wastewater discharges to the percolation ponds. As can be seen in Figure 2-7, the other interbeds are discontinuous, less massive, and cannot be traced horizontally between boreholes. The DE5 basalt is among the thickest and most massive of the basalt flows found in the subsurface underlying the ICDF Complex and has a typical thickness of nearly 30 m (100 ft).

Well USGS-51 is completed in the SRPA and is just east of the ICDF Complex, between the ICDF Complex and the west percolation pond. In this well, there are at least six sedimentary interbeds and 13 basalt flow groups. Narrow interbeds ranging from 1.2 to 4.5 m (4 to 15 ft) thick are interspersed with basalt flow groups ranging from 2.4 to 29 m (8 to 96) ft thick (Anderson 1991).

Holocene surficial geology and archaeology suggest that fluvial and eolian deposition and tectonic subsidence in the INEEL area have been in approximate net balance for at least the past 10,000 years. A reversal of the long-term, regional pattern of ESRP subsidence, sedimentation, and volcanism into an erosional rather than a depositional regime would require major changes from the Holocene tectonic or climatic configuration of the ESRP. Worldwide geologic evidence indicates that the Quaternary epoch (approximately the past 2 millions years) has been a time of major climatic fluctuations. During colder and wetter periods, glaciers occupied high-elevation areas. Lowland areas such as the ESRP received thick, widespread loess blankets. Lowland areas also were periodically impacted by local catastrophes (such as the large, late-Pleistocene, glacial outburst flood(s) that traveled down the Big Lost River valley), eroded upland surfaces on the ESRP, and deposited sediment in the INTEC area. If the future ESRP climate were to become warmer and more arid, the probable consequences would be decreased vegetation and increased eolian transport of fine-grained sediment, mainly as longitudinal dunes of fine sand.

Figure 2-6. Locations of geologic cross sections and existing wells.



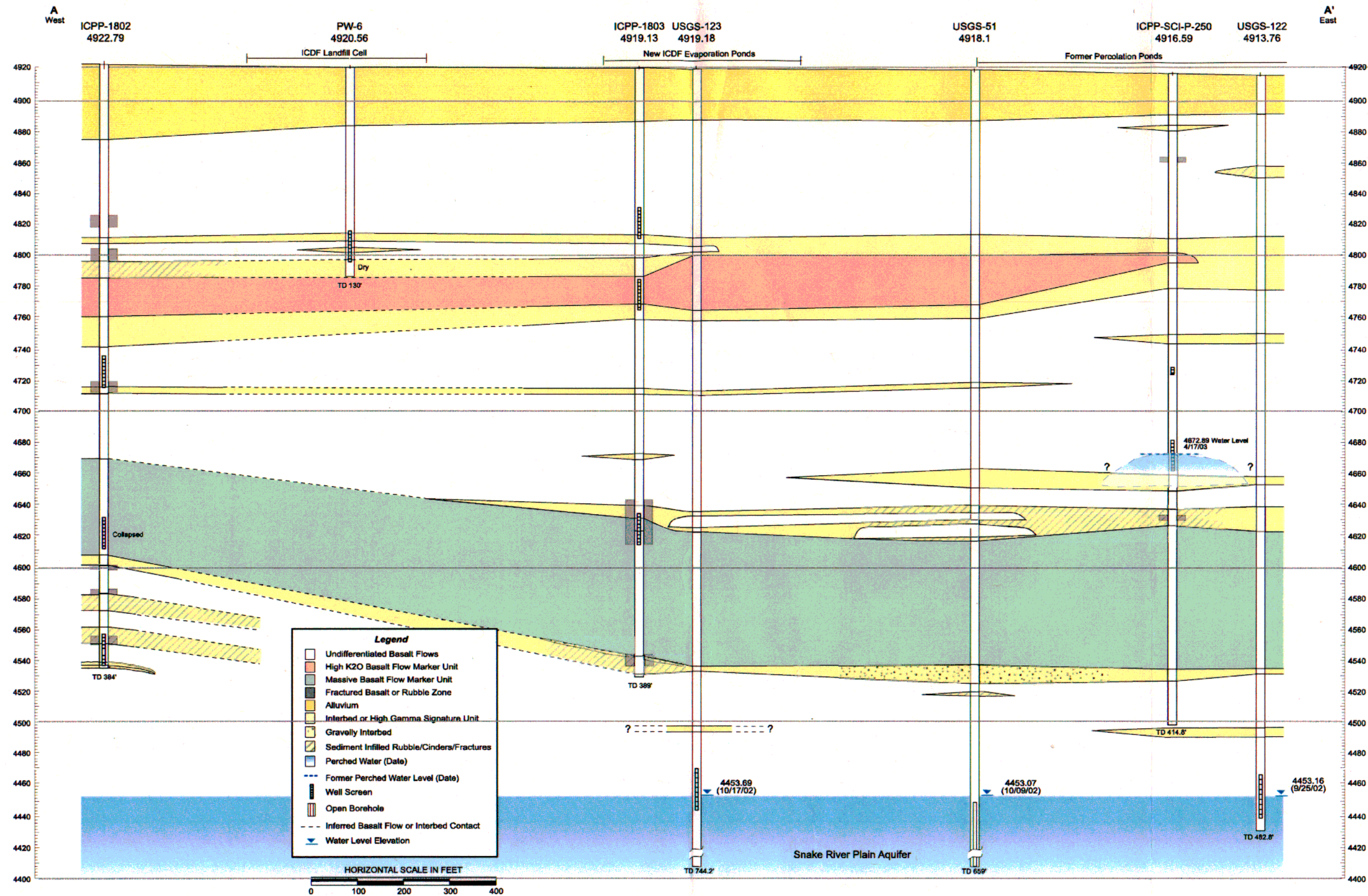


Figure 2-7. An east-west geologic cross section through the ICDF.

Future climate fluctuations on the ESRP, to either colder/wetter or warmer/drier conditions, are not expected to erode the INTEC land surface. Quaternary geologic and Holocene archaeological data suggest the INEEL area will probably continue its long-term history of regional subsidence and net accumulation of sedimentary and volcanic materials, although sedimentation patterns on the ESRP will change in response to future climate fluctuations.

Surface soil erosion at INTEC could occur as a consequence of faulting and uplift, but this erosion would involve a major change in the Quaternary tectonic configuration of the ESRP. Therefore, this scenario is improbable within the next 10,000 years, considering

- The regional seismicity and tectonic history of the INEEL area
- The absence of Quaternary tectonic faults on the ESRP in the vicinity of the INTEC
- The long response time for significant erosion to occur as a result of protracted faulting and uplift.

In summary, the following impacts from volcanic and tectonic activity are relevant to INTEC radiological performance assessment:

- During the past 4 million years, the ESRP and the INTEC area have undergone regional subsidence, basaltic volcanism, and fluvial and eolian sedimentation. Erosion has not been a significant process on the ESRP.
- Surficial- and subsurface-geologic data indicate that the INTEC area has both subsided and accumulated basalt lava flows and sediments at an average rate of 0.3 mm (0.01 in.)/yr. Significant uplift or erosion has not interrupted this long-term trend.
- Lava inundation or magma intrusion associated with volcanism from the nearby Arco Volcanic Rift Zone is improbable considering the volcanic history of the area. Lava inundation or magma intrusion would not likely result in the release of radionuclides to the environment.

2.1.4.2 Seismology. The seismically active Intermountain seismic belt and Centennial Tectonic seismic belts surround the ESRP. The Intermountain seismic belt is a zone of concentrated seismicity that extends from northwestern Montana through eastern Idaho and Utah into southern Nevada. The Centennial seismic belt, also a seismically active zone, extends from the Hebgen Lake, Montana, area westward into central Idaho.

The INEEL, U.S. Geological Survey (USGS), Montana Bureau of Mines and Geology, U.S. Bureau of Reclamation, and the University of Utah Seismograph Stations have compiled earthquake data from 1884 to 1989 (shown in Figure 2-8). The distribution of epicenters indicates that the Snake River Plain is devoid of earthquakes relative to the active areas surrounding it, with the possible exception of the 1905 earthquake located at Shoshone, Idaho (WCFS 1996). Historical records suggest that the epicenter for the 1905 earthquake is not located within the Snake River Plain but rather near the Idaho-Utah border. Figure 2-9 shows earthquake epicenters in the INEEL region from 1850 to 1995.

A large earthquake, in the vicinity of the INEEL but outside the Snake River Plain, occurred in the Centennial seismic belt on October 28, 1983, with a surface-wave magnitude of 7.3. The earthquake resulted from slippage along the Lost River fault—a northwest rupture along a normal fault with relative vertical movement downward to the west. The epicenter for this event was located in the Thousand Springs Valley near the western flank of Borah Peak, approximately 89 to 97 km (55 to 60 mi) from INEEL facilities. There was substantial damage to masonry structures in the local communities of

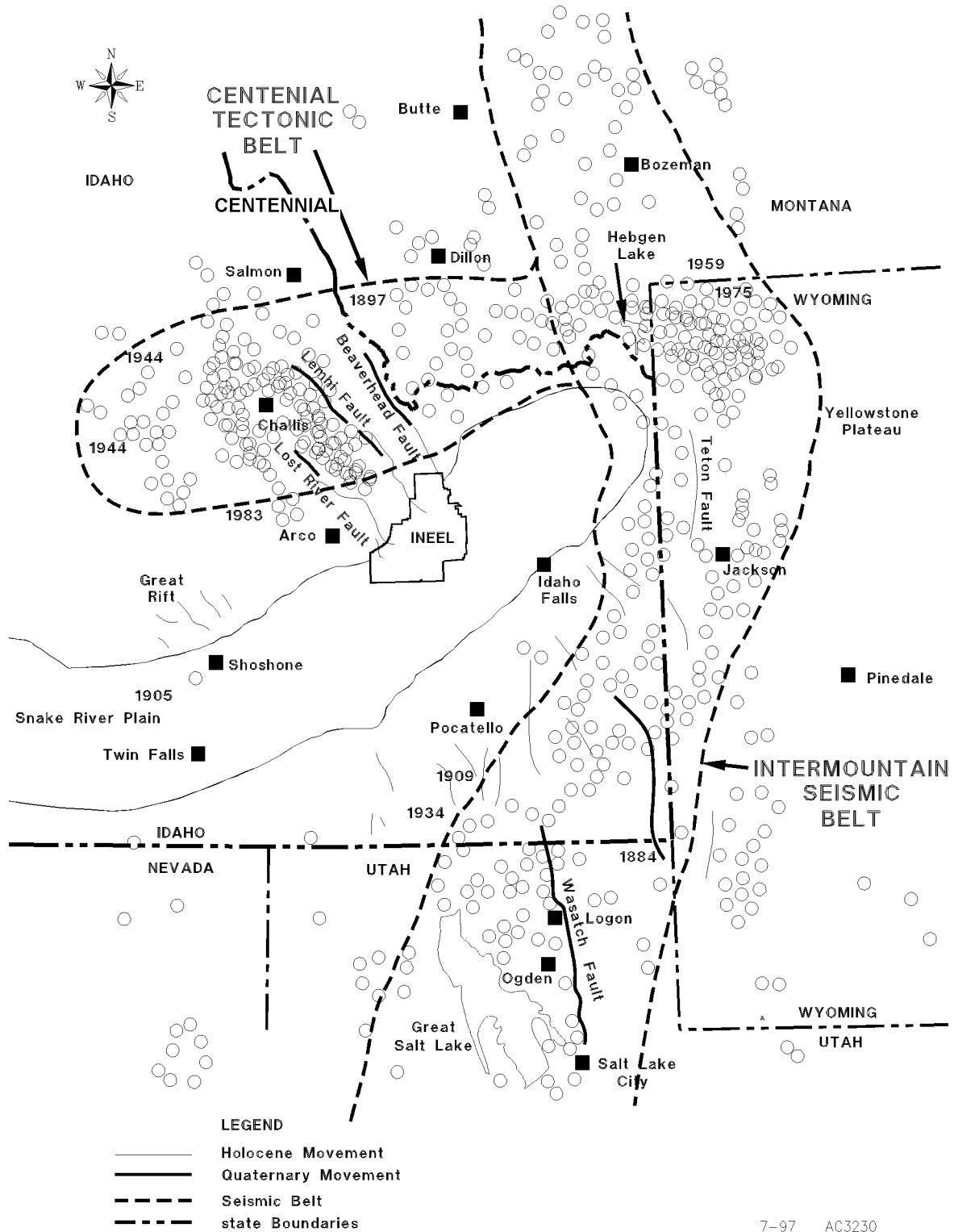


Figure 2-8. Seismicity and earthquake epicenter map showing the ESRP in relation to the Intermountain Seismic Belt and the Centennial Tectonic belt (WCFS 1996).

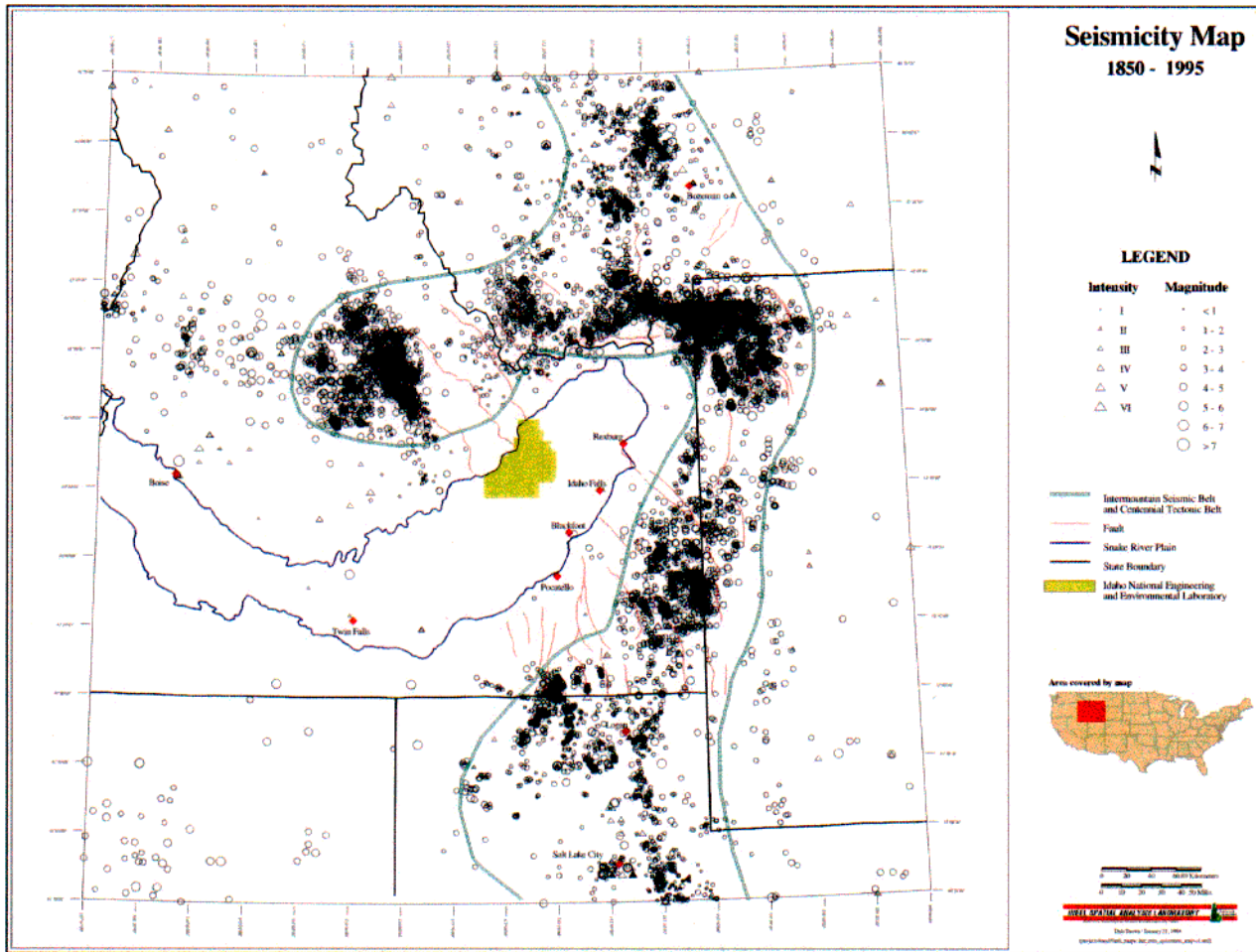


Figure 2-9. Earthquake epicenters in the INEEL region, 1850–1995.

Mackay and Challis near the epicentral area. Although the earthquake ground motions were felt at the INEEL Site, only minor nonnuclear building damage occurred in the form of hairline cracks and settlement (Gorman and Guenzler 1983). INTEC did not experience structural failures or waste spills as a result of the earthquake, and waste storage facilities do not show evidence of permanent movement or resulting damage. Peak ground accelerations ranging from 0.022 to 0.078 g were recorded at several INEEL facility areas. The INEEL was located in Modified Mercalli Intensity Zone VI during the earthquake (Jackson 1985).

The largest historic earthquake in the region occurred on August 17, 1959, at Hebgen Lake, Montana, located approximately 193 km (120 mi) northeast of the INEEL Site. The event had a surface-wave magnitude (M) of 7.5 and was felt at the INEEL, but caused no damage there.

The INEEL has maintained a seismic network for monitoring earthquake activity on and around the ESRP since December 1971. Currently, the seismic network consists of 24 seismic stations and 21 strong-motion accelerographs. The seismic stations continually record seismic data, and their data are used to calculate the locations and magnitudes of microearthquakes (M < 3.5) that occur locally. When triggered, the strong-motion accelerographs record earthquake ground motions from local moderate to large earthquakes.

The INEEL seismic network has compiled earthquake data from 1972 to present. During this period, approximately 15 microearthquakes have been located within the ESRP, indicating that infrequently-occurring, small magnitude earthquakes ($M < 1.3$) are characteristic of ESRP seismicity (Jackson et al. 1993; Pelton et al. 1990). These data are in agreement with the historical earthquake data compiled for the surrounding region (Figure 2-9). Recent modifications to the seismic network, such as placing sensors in 18- to 21-m (59- to 69-ft) boreholes, will lower the magnitude threshold of detecting microearthquakes within the ESRP.

Because the seismically active Intermountain and Centennial seismic belts surround the ESRP and several Quaternary faults are located near the western boundary of the INEEL, seismic hazard assessments have been updated for all facility areas at the INEEL (WCFS 1996; Payne et al. 2000; SAR-II-8.4). These assessments were being performed to quantitatively estimate peak ground motions that INEEL facilities may experience from nearby large magnitude earthquakes. Most of the INEEL including the ICDF landfill is located in Seismic Zone 2B, and a small portion is located in Zone 3. The seismic design levels for INEEL facilities exceed those required for these classifications.

Uplift and erosion of the INTEC area could result from faulting and uplift of the southern Lost River Fault, if the fault encroached southward onto the ESRP to a position several kilometers west of INTEC. Assuming immediate initiation of this faulting and maximum uplift rates from the most recently active fault segments of the nearby Basin and Range Province (1 to 2 m [3 to 7 ft]/1,000 yr), significant uplift and erosion of the INTEC area would require times of 10,000 to 100,000 years.

Additional up-to-date information on seismic hazards for the INEEL is presented in WCFS 1996 and Chapter 2 of Three Mile Island-2 Safety Analysis Report 2003 (SAR-II-8.4). Most of the INEEL is underlain by a 0- to 1-km (0- to 0.6-mi) thick sequence of Tertiary and Quaternary basalt lava flows and interbedded sediments. Based on drill hole information, regional mapping along the margins of the ESRP, and geophysical information, the basalt/sediment sequence is underlain by an older section (up to several kilometers thick) of late Tertiary rhyolitic volcanic rock. These two volcanic sequences are a consequence of the passage of the Yellowstone mantle plume (hotspot) through the INEEL area of the ESRP in late Tertiary time (Malde 1991). The Tertiary rhyolitic volcanic rocks were erupted at 6.5 to 4.3 million annum (Ma), when the hotspot resided beneath the INEEL area. They are comprised mostly of ash-flow tuffs erupted during large, violent explosive episodes and large rhyolitic lava flows. They are analogous to the ash flow tuffs and lava flows that erupted from calderas in the Yellowstone Plateau at 2.0 to 0.6 Ma.

These types of large-scale explosive eruptions can occur only directly over the mantle hotspot because large inputs of heat into the lower and middle crust are required to generate such large volumes of rhyolitic magma. Because the hotspot is now situated beneath the Yellowstone National Park, recurrence of this type of volcanic activity in the INEEL area is nearly impossible. Residual heat in the upper mantle after passage of the hotspot has continued to produce basaltic magmas that have risen to the surface and erupted onto the subsiding ESRP. Basaltic eruptions in the INEEL area began at about 4 Ma, soon after passage of the hotspot, and have continued. The most recent activity occurred along the Great Rift about 2,100 years ago.

Basalt vents on the ESRP include broad, low-relief shield volcanoes, small spatter cones, and spatter ramparts along eruptive fissures. Lava fields related to single vents range in surface area from 2 to 400 km² (0.7 to 154 mi²) and in volume from 0.05 to 7 km³ (0.01 to 1.7 mi³) (Kuntz et al. 1992). Volcanic vents are not randomly distributed on the ESRP; they are concentrated in northwest-trending linear zones known as volcanic rift zones (Figure 2-10).

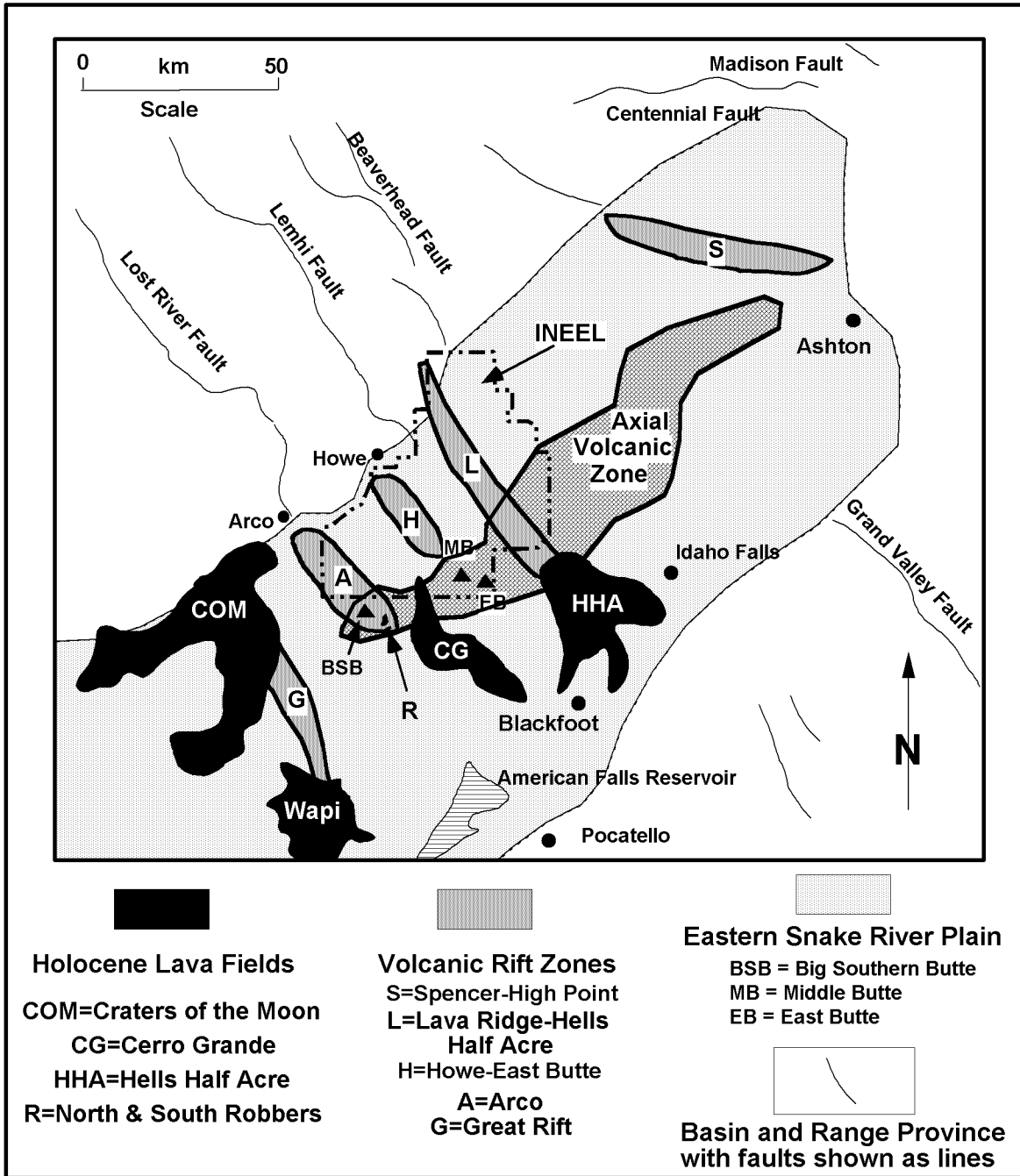


Figure 2-10. Volcanic rift zones at the INEEL.

In addition, vents are concentrated in a northeast-trending zone, known as the Axial Volcanic Zone, along the central axis of the ESRP. The Axial Volcanic Zone is a constructional highland caused by more voluminous magma output along the axis of the ESRP.

Based on radiometric age determinations of basalt lava flows, the Arco Volcanic Rift Zone north of Big Southern Butte was active between 600 and 100 thousand annum (ka) (Kuntz et al. 1992). The Cerro Grande and North and South Robbers flows (10,500 to 12,000 ka) near Big Southern Butte occur at the intersection of the Arco Volcanic Rift Zone and the Axial Volcanic Zone. Except for volcanism along the

Great Rift, all of the Holocene volcanic fields of the ESRP occur along the Axial Volcanic Zone (Figure 2-10). Recurrence of volcanism in the ESRP has a greater likelihood of occurring along the Great Rift or the Axial Volcanic Zone.

Additional information on the site volcanism is presented in “Quaternary volcanism, tectonics, and sedimentation in the INEL area” (Hackett and Smith 1992).

2.1.5 Hydrology

The following sections discuss the surface water and groundwater of the ICDF landfill site and vicinity.

2.1.5.1 Surface Water. Natural surface water near or on the INEEL consists mainly of three streams draining intermountain valleys to the north and northwest of the Site: the Big Lost River, the Little Lost River, and Birch Creek (Figure 2-11). Streamflows are often depleted before reaching the INEEL by irrigation and hydropower diversions, and infiltration losses along the channel bed. When water does flow onto the INEEL, it either evaporates or infiltrates into the ground because the Pioneer Basin in which these streams terminate is a closed topographic depression on the Eastern Snake River Plain.

Stream flows from the Little Lost River and Birch Creek very seldom reach the INEEL. The Little Lost River drains the slopes of the Lemhi and Lost River mountain ranges. Water in the Little Lost river is diverted for irrigation north of Howe, Idaho, and does not flow onto the INEEL. The Little Lost River is considered to have negligible potential for flooding on the INEEL (Kjelstrom and Berenbrock 1996). Birch Creek originates from springs below Gilmore Summit in the Beaverhead Mountains and flows in a southeasterly direction onto the Snake River Plain. The water in the creek is diverted north of the INEEL for irrigation and hydropower purposes. In the winter months when the water is not used for irrigation, typically November through April, flows from Birch Creek are returned to an anthropogenic channel on the INEEL, 6.4 km (4 mi) north of Test Area North, and recharge the SRPA by infiltration.

The Big Lost River is the major surface water feature on the INEEL and at its closest point is roughly 60 m (200 ft) from the northwest facility boundary of INTEC and about 1 km (0.6 mi) from the ICDF landfill location. Major control on the Big Lost River upstream of the INTEC site includes the Mackay Dam and the INEEL diversion dam. The Big Lost River waters are impounded and regulated by Mackay Dam, located approximately 6.4 km (4 mi) northwest of Mackay, Idaho, for irrigation purposes downstream. The Big Lost River flows from the dam southeastward through the Big Lost River valley, past Arco and onto the ESRP. Streamflows are often depleted before reaching the INEEL by irrigation diversions and infiltration losses along the river. When flow in the Big Lost River actually reaches the INEEL, it is either diverted at the INEEL diversion dam or flows northward across the INEEL in a shallow, gravel-filled channel. The main channel branches into several channels 29 km (18 mi) northeast of the INEEL diversion dam, referred to as the Big Lost River Sinks and terminates in a series of three shallow playas that are connected by branching channels. All flow of the Big Lost River that enters onto the INEEL, except for evapotranspiration losses, is recharged to the subsurface. The stretch of the Big Lost River on the INEEL is ephemeral with no recreational or consumptive uses (e.g., irrigation, manufacturing, or drinking) of the water. In addition, there are no identified future uses of surface water that may enter onto the INEEL.

The need for flood control on the INEEL was first recognized in the early 1950's when downstream facilities were threatened by localized flooding as a result of ice jams in the Big Lost River. The INEEL diversion dam was constructed in 1958 and enlarged in 1984 to divert high runoff flows from downstream INEEL facilities. The diversion dam consists of a small earthen diversion dam and headgate that diverts water from the main channel, through a connecting channel, and into a series of four natural

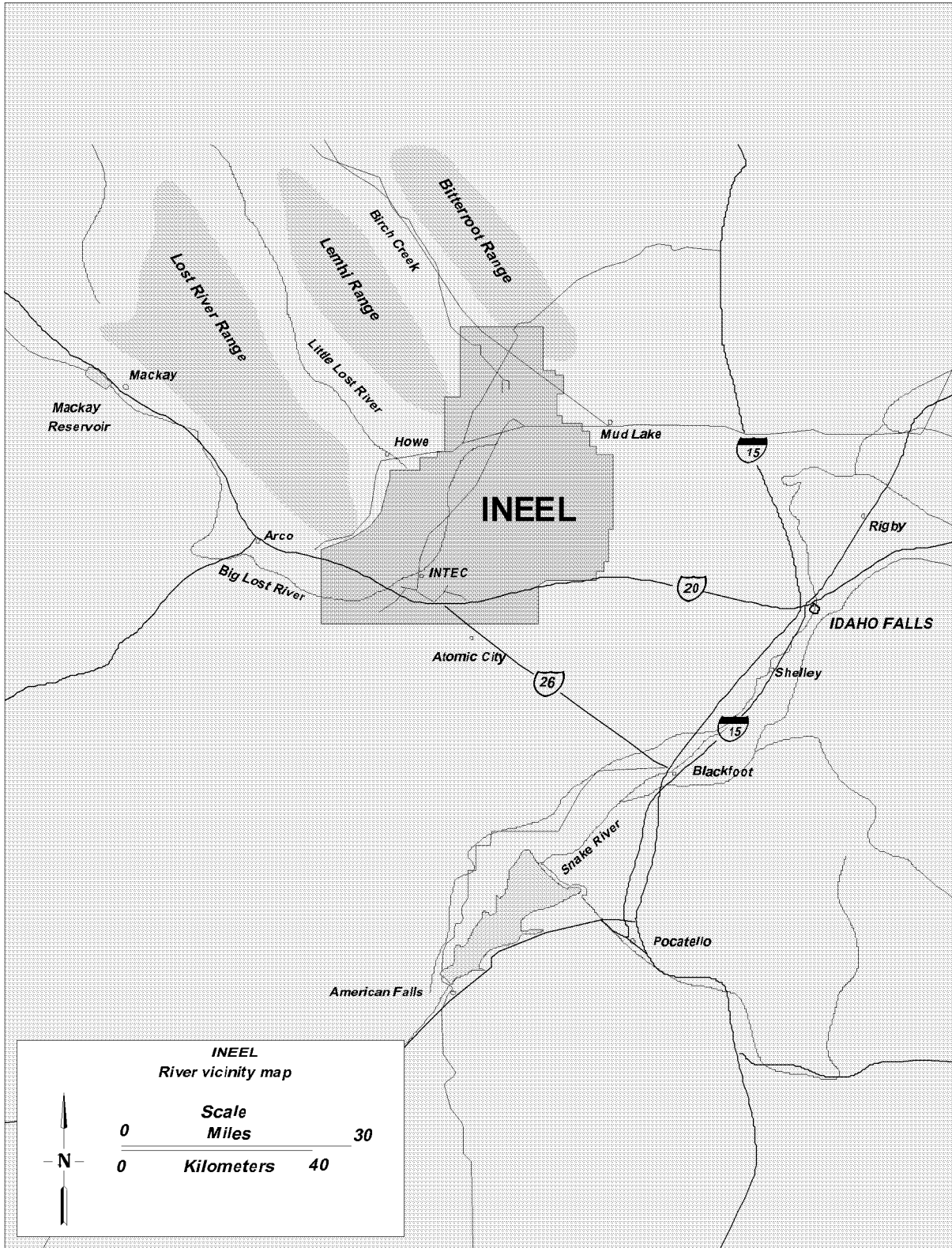


Figure 2-11. Surface water features on the INEEL.

depressions, called spreading areas. Gates placed on two large, corrugated steel culverts, which are 1.8 m (6 ft) in diameter, control flow downstream onto the INEEL. When the gates are wide open, the maximum flow through the diversion dam downstream onto the INEEL is 900 ft³/sec (cfs) (Lamke 1969). Flow in the diversion channel is uncontrolled at discharges that exceed the capacity of the culverts. The diversion channel is capable of carrying 7,200 cfs from the Big Lost River channel into the spreading areas. Two low swales located southwest of the main channel will carry an additional 2,100 cfs for a combined diversion capacity of 9,300 cfs (Bennett 1986). The capacity of the spreading areas is 58,000 acre-ft at an elevation of 1,539 m (5,050 ft) (McKinney 1985). An overflow weir in spreading area D allows water to drain southwest off the INEEL. Runoff from the Big Lost River has never been sufficient to exceed the capacity of the spreading area and overflow the weir.

2.1.5.1.1 Big Lost River 100-Year Floodplain—The ICDF landfill is located outside the 100-year floodplain of the Big Lost River. A USGS floodplain study (Berenbrock and Kjelstrom 1998) routed the 100-year peak flow estimate of 7,200 cfs (Kjelstrom and Berenbrock 1996) downstream onto the INEEL. The flood-routing study did not include the INEEL diversion dam in the model simulation. The study assumes 1,000 cfs of the peak flow will flow down the diversion channel and the remainder flow of 6,200 cfs is routed downstream onto the INEEL using a one-dimensional code that does not account for infiltration, side or overbank losses. This conservative floodplain study indicates a potential for flooding in the north end of INTEC. All other INEEL facilities including the ICDF landfill are located outside of the Big Lost River 100-year floodplain. The extent of flooding in the northern portion of INTEC would reach a peak elevation of 1,497 m (4911.6 ft) (Berenbrock and Kjelstrom 1998). The ICDF landfill site location at an average elevation of 1,500 m (4922 ft) and about 1 km (0.6 mi) south of the Big Lost River is located outside of the Big Lost River 100-year floodplain. A recent evaluation of the INTEC geomorphic setting, (based on soil profiles taken along the Big Lost River and used to develop a late Quaternary soil chronosequence) indicates that INTEC is sited on geomorphic surfaces that are well in excess of 10,000 years in age. This evaluation suggests that the hazard of significant flooding of this area by the Big Lost River is low under natural channel conditions (Ostenaar et al. 1999).

2.1.5.1.2 Runon/Runoff from 25-year, 24-hour Storm Event—A statistical analysis of meteorological data from CFA for the period 1950 through 1995 estimates 4.3 cm (1.7 in.) of precipitation for a 25-year, 24-hour storm event and 5.6 cm (2.2 in.) of precipitation for a 100-year, 24-hour storm event (Sagendorf 1996). A hydrological evaluation of the internal and external drainage systems at INTEC was performed to determine if it is adequate for handling runon/runoff from a 25-year, 24-hour storm event (Burgess 1991). The study concluded the internal and external drainage systems could safely carry runon/runoff from this storm event with minor maintenance and upgrades made to the existing ditches and culverts. The ICDF landfill has been designed to accommodate the runon/runoff from a 25-year, 24-hour storm event (DOE-ID 2001a; EDF-ER-270).

2.1.5.1.3 Man-made Surface Water Features—Man-made surface water features in the vicinity of the INTEC consist of two percolation ponds (scheduled to go offline December 2003) used for disposal of water in the service waste system (formerly injected into the aquifer via the Idaho Chemical Processing Plant [ICPP] injection well) and sewage treatment lagoons and infiltration trenches for treated water. In addition to these features, several landscaped areas at the INTEC historically have been watered during the summer months, and a network of ditches is used to channel runoff from the facilities after precipitation events. Some of the precipitation runon/runoff is channeled to an old gravel pit in the northeastern portion of INTEC.

2.1.5.2 Groundwater

2.1.5.2.1 Perched Water—Perched water in the vicinity of INTEC has been investigated during both the WAG 3 Remedial Investigation/Feasibility Study (RI/FS) (DOE-ID 1997a) and as part

of an ongoing effort to support the WAG 3 perched water remedy (DOE-ID 2003e). There are several perched water zones underlying the INTEC facility. These perched zones can be divided into an upper and lower perched water zone. The upper basalt perched water zone was initially discovered in the late 1950s. Perched water was encountered in Wells USGS-50 and USGS-52 at 38.4 and 53.0 m (126 and 174 ft) below ground surface (bgs), respectively. The occurrence of this perched water was attributed to operational practices based on the presence of radioactive and chemical contaminants. Since then, numerous monitoring wells have been installed in the upper perched water zone to identify the source of recharge, delineate the perched water bodies, and determine the nature and extent of contamination.

A lower perched water zone also was identified in the basalt at depths between 104 and 122 m (340 and 400 ft) bgs (Robertson et al. 1974). This water was first discovered in 1956 while drilling Well USGS-40; perched water was encountered at a depth of 106 m (348 ft). An analysis of this perched water detected abnormally high total dissolved solids (303 mg/L), sodium (25 mg/L), and chloride (81 mg/L), indicating the water is of waste origin (Olmsted 1962). According to Robertson et al. (1974), this was a reasonable level for the perched water because of the presence of a clay bed at 113 m (370 ft) bgs. In the late 1950s, only wells drilled in the northern INTEC area encountered the lower perched groundwater zone. Since 1984, a lower perched groundwater zone also has formed in the southern INTEC area because of the disposal of process wastewater through the percolation ponds. The location of this lower perched water zone is indicated by Well MW-17 and borehole neutron logs from Well USGS-51.

The percolation ponds have been the primary source of recharge to perched water adjacent to the ICDF Complex. Geotechnical borings to the top of bedrock beneath the ICDF Complex did not identify any saturated water bodies. There was an increase in moisture content related to the fine-grained sediments overlying the basalt. Moisture content varied indirectly with the amount of sand present and ranged in value from 8 to 30%. Under the ICDF Complex, perched water has been documented to occur at the primary series of interbeds above the upper marker basalt bed. This perched water forms in response to wastewater discharge to the western-most of the two percolation ponds. The perched water is transient and dissipates when discharge is switched from the west to the east percolation pond.

The USGS drilled shallow boreholes (SWP series, or SWPP series) in 1983 prior to the construction of the unlined INTEC percolation ponds. The water levels in each PW series perched water well around the percolation ponds are plotted at the top of Figure 2-12, with the scale on the left vertical axis. The wells to the west of the percolation ponds and closest to the ICDF Complex are PW-1 and PW-6. These wells behave similarly and have periodically gone dry. PW-6, which is the farthest from the percolation ponds, is shown as a thick red line and went dry from 1989 to 1990, from 1995 to 1997, and has been dry since mid-2000. PW-1, which is just west of the west percolation pond and is shown as a thick navy blue line on Figure 2-12, went dry in 1995 and again in 2000. PW-4, which is just east of the east percolation pond, is shown as a thin brown line on Figure 2-12. The water levels in this well behave opposite to the water levels in PW-1, which is just west of the west percolation pond. When water levels are low in PW-4, they are high in PW-1 and vice versa. For example, from 1986 to 1988, wastewater was discharged to the west (#2) percolation pond (Cecil et al. 1991), and water levels were high in PW-1 and PW-6 and low in PW-4. Figure 2-12 also demonstrates that when water levels are increasing in PW-4, they are decreasing in PW-1 and vice versa. These two wells respond to switches in discharges between the ponds. For example, in late fall 1995, water was switched from the east percolation pond (Pond #1) to the west percolation pond (Pond #2). At the same time, the water levels began to increase in PW-1 and decrease in PW-4 in response. Likewise, water was switched from the west pond to the east pond in February 2000, and PW-1 and PW-4 responded quickly.

In contrast, water levels in PW-2 and PW-5 remain relatively flat (shown as a thin pink and green line on Figure 2-12). PW-2 is just south of the two ponds and equidistant from both ponds, and PW-5 is in between the two ponds.

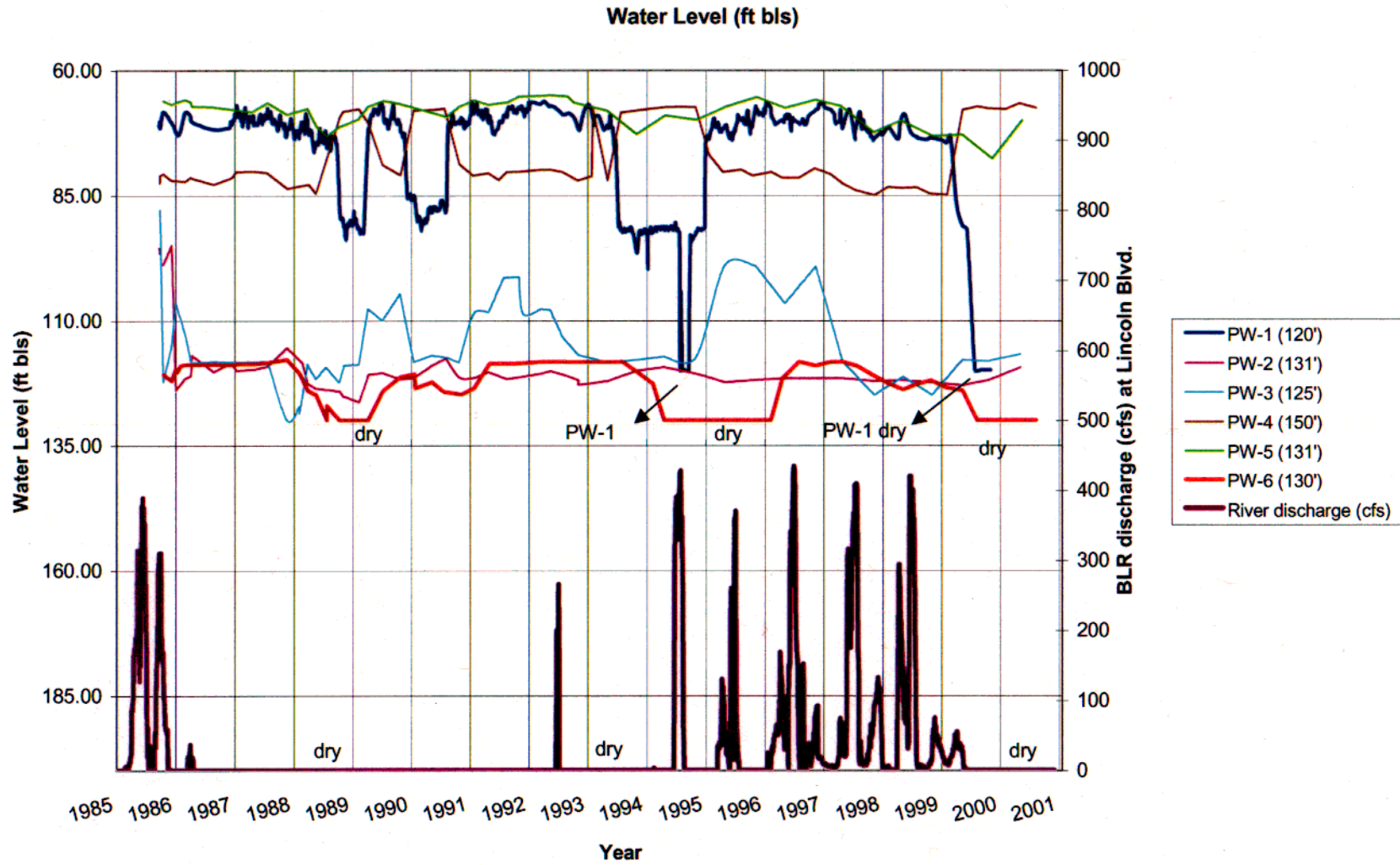


Figure 2-12. Water levels in PW series perched water wells and discharge in the Big Lost River at Lincoln Boulevard.

On the bottom portion of Figure 2-12, discharge in the Big Lost River measured daily at the USGS Lincoln Boulevard gauging station is plotted. The station is adjacent to INTEC. The right vertical axis is river discharge in cubic ft per second (cfs). There is no correlation between the flow in the Big Lost River and water in the perched water wells around the percolation ponds and the ICDF Complex. There was no flow in the Big Lost River near INTEC from mid-1987 to mid-1993. All of the PW perched water wells had water in them during this period with the exception of PW-6, which went dry for about a year in the middle of this period. PW-6 then had water in it during the time the Big Lost River was mostly dry. When the Big Lost River started to flow again in 1985, both PW-1 and PW-6 went dry. The upper perched water wells around the ICDF Complex and the percolation ponds are not influenced by flow in the Big Lost River, but rather are influenced by discharge to the percolation ponds.

The above interpretation of perched water monitoring time histories in the southern area of INTEC demonstrates the formation of perched water near the ICDF Complex is linked to leakage from wastewater discharge to the percolation ponds and not from the Big Lost River. It is also evident that the perched water is transient and the wells closest to the ICDF Complex can dry up in response to shutting off discharges to the western percolation pond. The percolation ponds were shut down permanently in August 2002, and it is expected that the perched water in wells near the ICDF Complex will dissipate. PW-6, which is the farthest away from the percolation ponds and is on the edge of the ICDF landfill, is already dry.

2.1.5.2.2 Regional Aquifer—The SRPA, one of the largest and most productive groundwater resources in the United States, underlies the INEEL. The aquifer is listed as a Class I aquifer, and EPA has designated it as a sole source aquifer. The SRPA consists of a series of saturated basalt flows and interlayered pyroclastic and sedimentary materials that underlie the ESRP. The SRPA is approximately 322 km (200 mi) long, 64 to 97 km (40 to 60 mi) wide, and covers an area of 24,853 km² (9,600 mi²). It extends from Bliss, Idaho, on the southwest to near Ashton, Idaho, northeast of the INEEL. Aquifer boundaries are formed by contacts with less permeable rocks at the margins of the plain (Mundorff et al. 1964).

Permeability of the aquifer is controlled by the distribution of highly fractured basalt flow tops and interflow zones with some additional permeability contributed by vesicles and intergranular pore spaces. The variety and degree of interconnected water-bearing zones complicates the direction of groundwater movement locally throughout the aquifer (Barraclough et al. 1981). Although a single lava flow may not be a good aquifer, a series of flows may include several excellent water-bearing zones. If the sequence of basalt flows beneath the Snake River Plain is considered to constitute a single aquifer, it is one of the world's most productive (Mundorff et al. 1964).

Robertson et al. (1974) estimated that as much as a 2 billion acre-ft of water may be in storage in the aquifer, of which about 500 million acre-ft are recoverable. The aquifer discharges about 7.6 million acre-ft of water annually to springs and rivers. Pumpage from the aquifer for irrigation totals about 1.9 million acre-ft annually (Hackett et al. 1986). Groundwater withdrawn from wells and springs supplies 100% of the drinking water consumed within the ESRP.

Recharge to the aquifer occurs mostly through infiltration of irrigation water (5.1 million acre-ft) and from valley underflow (1.5 million acre-ft) from the 90,610 km² (35,000 mi²) of recharge area in the surrounding mountains to the north and northeast of the plain (Hackett et al. 1986). Recharge from river seepage amounts to about 1.3 million acre-ft, and direct recharge from precipitation falling on the plain is estimated at 0.8 million acre-ft (Hackett et al. 1986).

The USGS has maintained a groundwater monitoring network at the INEEL to characterize the occurrence, movement, and quality of water and to delineate the movement of facility-related wastes in

the SRPA since 1949. This network consists of a series of wells from which periodic water-level and water-quality data are obtained. In addition to the independent USGS groundwater monitoring, the INTEC implemented a groundwater monitoring program in October 1991 of selected wells in fulfillment of the RCRA and DOE O 5400.1 groundwater monitoring requirements.

In the vicinity of INTEC, 16 aquifer tests resulted in transmissivity estimates ranging 5 orders of magnitude from a maximum transmissivity of $7.0 \times 10^4 \text{ m}^2/\text{d}$ ($7.5 \times 10^5 \text{ ft}^2/\text{d}$) at Well CPP-3 (the former INTEC injection well) to a minimum transmissivity of $0.93 \text{ m}^2/\text{d}$ ($10 \text{ ft}^2/\text{d}$) at Well USGS-114 (Ackerman 1991). Based on the transmissivity testing, the average hydraulic conductivity of the SRPA basalts at INTEC was estimated by Ackerman to be approximately $4.0 \times 10^2 \pm 7.9 \times 10^2 \text{ m/d}$ ($1.3 \times 10^3 \pm 2.6 \times 10^3 \text{ ft/d}$). Using the average hydraulic conductivity, a hydraulic gradient of 1.2 m/km (6.3 ft/mi) at INTEC, and an estimated effective porosity of 10%, the calculated seepage velocity in the vicinity of the INTEC is approximately 3 m/d (10 ft/d). The hydraulic gradient in the SRPA around INTEC is very flat and flow is generally south-southwest.

The water quality in the SRPA at and downgradient from the INTEC has been adversely impacted due to past facility operations. The majority of INTEC-related SRPA contamination is due to the past disposal of wastes through the ICPP injection well. Contamination in the aquifer is also due to downward migration of contaminants from surface soils and perched groundwater zones. The injection well was the primary source for waste disposal from 1952 through February 1984 and used intermittently for emergency situations until 1986. The average discharge to the well during this period was approximately 1.4 billion L/yr (363 million gal/yr) or about 3.8 million L/d (1 million gal/d). It has been estimated a total of 22,000 Ci of radioactive contaminants have been released in $4.2 \times 10^{10} \text{ L}$ ($1.1 \times 10^{10} \text{ gal}$) of water. The vast majority of this radioactivity is attributed to H-3 (approximately 96%) with minor components of I-129 and Sr-90.

2.1.6 Geochemistry

A number of studies have characterized the groundwater geochemistry of the ESRP aquifer (McLing 1994; Wood and Low 1988). These studies indicate that groundwater beneath the INEEL has multiple source regions and that these source regions have subtle chemical signatures (Johnson et al. 2000) that are defined by the geologic media in which the water originates. Waters originating from the Basin and Range valleys north of the INEEL are largely composed of Paleozoic carbonates and siliciclastic sediments and are therefore enriched in Ca-Mg-HCO₃. In contrast, waters originating in the volcanics of the Yellowstone Plateau contain more Na-K relative to those derived from the sedimentary terrain to the west. The largest source of recharge to the ESRP aquifer is the Yellowstone Plateau. However, recharge derived from the Basin and Range valleys north of the INEEL dominates in the western parts of INEEL.

Groundwater beneath the ICDF is mostly derived through a fast flow corridor originating in the Little Lost River valley (Roback et al. 2001). This fast flow corridor is potentially important to contaminant transport from the INTEC facility (Cecil and Green 1999). Water chemistry along this fast flow zone is dominated by Ca-Mg-HCO₃ derived from water rock interactions that occurred in the recharge zones located in the mountains north of the site. The water is thus over-saturated with respect to calcite (McLing 1994) and authogenic (secondary) calcite is precipitated from the water as cement in the sedimentary interbeds and as fracture and vesicle fillings within the basalt (McLing 1994).

The aquifer water is also saturated with atmospheric gasses due to the largely unconfined nature of the system. Consequently, except for areas that are locally contaminated by organic constituents, the groundwater is fully oxidized (McLing 1994). While pH varies across the ESRP aquifer system, the variation is generally small with pHs ranging from 7.5 to 8.3 (Table 2-3). Because most recharge to the

Table 2-3. Groundwater chemistries from the ESRP aquifer at the INEEL.

Well Name	Groundwater chemistries in mg/L from selected wells near the INTEC								Temperature (Celsius)
	Na	K	Ca	Mg	Cl	SO ₄	HCO ₃	pH	
USGS-17	7.78	3.12	44.5	12.9	5.7	14	152	8.21	15.5
USGS-5	8.15	2.6	43.5	15.6	8.8	11	139	7.58	11
Site 9	13.2	3.34	39	17.2	13	11	139	7.58	13.2
USGS-15	25	1.81	52.2	17.26	25	19	221	8.2	12.3
USGS-89	21.7	4.5	29	18.7	38	34	98	8.3	14
NRF-2	18	1.8	70	22	46	39	177	7.7	12.5

system comes in the form of snowmelt at high altitudes, groundwater entering the aquifer is quite cold ~9.0°C (Smith and McLing 2001). Groundwater warms predictably as residence time increases in the aquifer (Table 2-3), resulting from an extremely high geothermal gradient beneath the ESRP (Blackwell 1989; Blackwell and Steele 1992). The high geothermal gradient is the result of the passage of the Yellowstone Hot Spot and its associated volcanic activity. However, there are areas within the ESRP aquifer that have anomalously high thermal signatures, which may result from upwelling of deep geothermal waters (Johnson et al. 2000). A summary of water chemistries from wells located in the western part of the INEEL is presented in Table 2-3.

Preexisting contamination beneath the ICDF, in the perched water from the percolation ponds and in the aquifer from the injection well, has been well documented. The chemical signatures of perched water and aquifer water at INTEC and their relationship to contaminant sources are discussed.

Sodium and chloride, two primary nonradioactive contaminants, were discharged to the percolation ponds and stemmed from the ion-exchange process. Although concentrations vary over the years, average concentration of sodium in wastewater was 103 mg/L during 1971 to 1973 (Barraclough and Jensen 1976). During 1996 to 1998, approximately 321,143 kg (708,000 lb) of sodium was discharged to the ponds. The discharge weighted average ranged from 163 mg/L in 1996 to 124 mg/L in 1998 (Bartholomay and Tucker 2000). Sodium ranged from 120 mg/L in PW-6 to 210 mg/L in PW-1. Similar concentrations were reported in SWP-8 and SWP-13 (Tucker and Orr 1998). Barraclough and Jensen (1976) reported background concentrations of sodium in the SRPA as 8 to 10 mg/L.

Discharge of chloride also varies over the years. About 1.63 million kg (3.6 million lb) of chloride was discharged to the ponds between 1989 and 1991, and 1.59 million kg (3.5 million lb) was discharged between 1996 and 1998. The discharge weighted average concentration was 267 mg/L. With the exception of two concentrations from well PW-6, chloride concentrations in perched water (SWP wells and PW wells) near the ponds reflect chloride concentrations in wastewater. Barraclough and Jensen (1976) reported that the background concentration of chloride in the SRPA is between 8 and 15 mg/L.

Schoeller diagrams are graphical methods used to demonstrate patterns in water chemistry. These diagrams display the composition of cations and anions in such a way that groupings and trends become readily apparent. Figure 2-13 is a Schoeller diagram that shows the concentrations of major ions for different INTEC waters. The Schoeller diagram emphasizes the absolute concentrations of ions in water. All of the water in the shallow perched water around the percolation ponds is high in sodium and chloride. PW-1 (orange triangles), PW-2 (pink X), PW-4 (brown diamonds), and PW-5 (green asterisk) are all very similar waters and plot almost on top of each other. These data are from October 1991, when there was water in the perched water wells around the ICDF Complex. In contrast, water from farther to the north of the percolation ponds and the ICDF Complex is lower in sodium and chloride. Recent samples

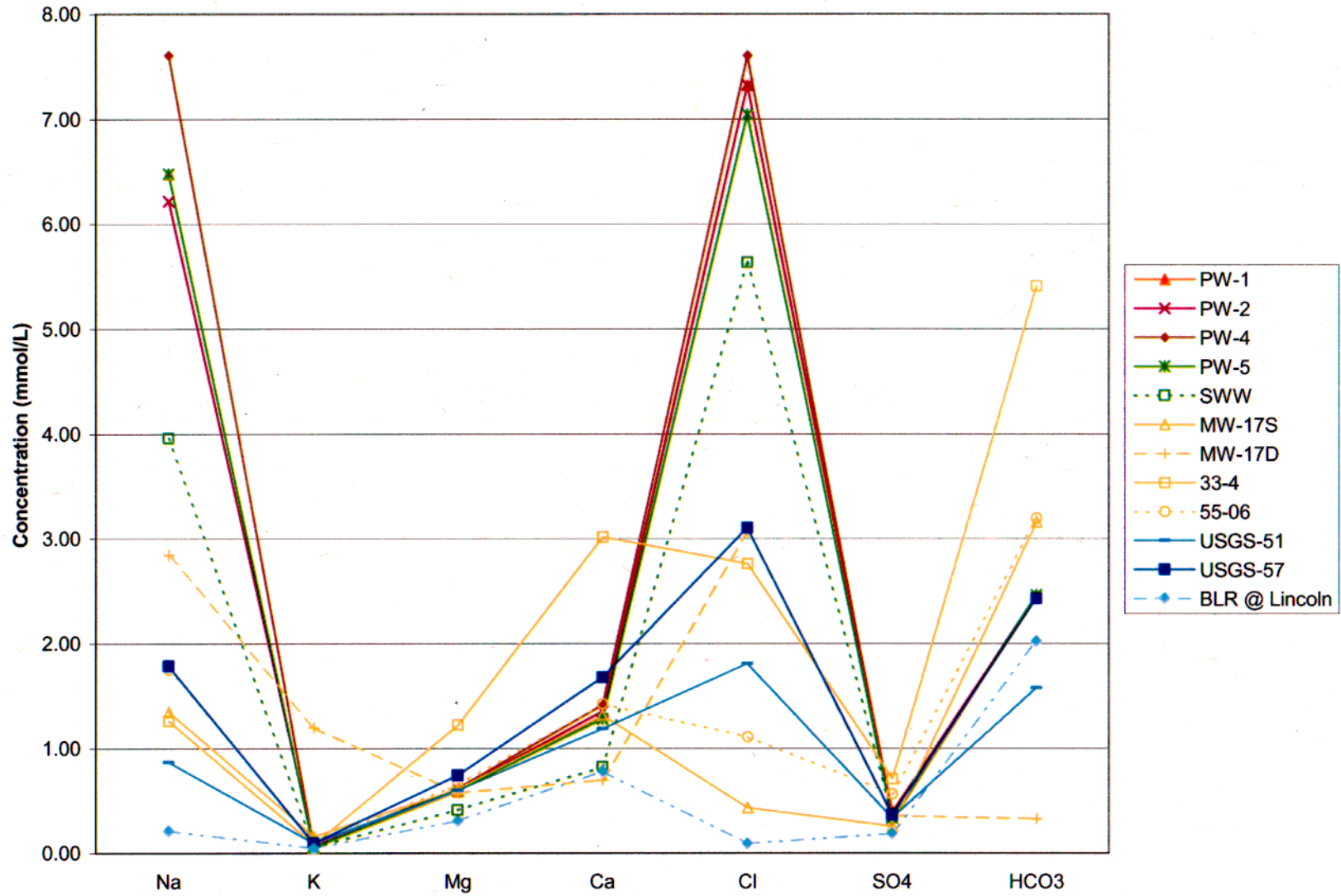


Figure 2-13. Schoeller diagram of water quality at INTEC for perched water, service waste water, the SRPA, and the Big Lost River.

(January 2000) from the service wastewater (SWW) line that goes to the percolation ponds are shown by a dashed green line with open squares. The process has been improved over the past decade, and the SWW water quality is lower in sodium and chloride than when the perched water samples were taken in 1991. Although the concentrations are lower in the 2000 SWW samples, the wastewater is of similar composition to the 1991 perched water samples. For comparison, samples from Well 33-4, which is near the tank farm (plotted with yellow squares), and Well 55-06, which is in the eastern portion of INTEC (plotted with yellow circles), are also plotted.

Monitoring Well MW-17 is north of the percolation ponds near the Building 603 fuel storage basins and was originally completed in three perched water zones. MW-17S monitors shallow perched water, is screened from 55.4 to 58.4 m (181.7 to 191.7 ft), and currently has water in it. MW-17P, which is currently dry, is screened from 80.4 to 83.4 m (263.8 to 273.8 ft). MW-17D monitored deep perched water and is screened from 109.7 to 116 m (360 to 381 ft). It is also currently dry. Data from a January 1995 sampling at MW-17S are plotted on Figure 2-13 as yellow triangles and at MW-17D as yellow plus signs. It is interesting to note that MW-17S was very low in all ions, whereas MW-17D had slightly elevated sodium and chloride but not as high as in the PW wells. This may indicate that water in MW-17D mixed with water from the service wastewater.

For comparison, water from SRPA monitoring Wells USGS-51 and USGS-57, located just east and south, respectively, of the ICDF Complex near PW-1, are plotted as solid blue lines. The chemistry in the SRPA near the ICDF Complex is very different from that in perched water wells in the same area.

Similarly, water from the Big Lost River at the Lincoln Boulevard bridge, plotted as a dashed light blue line, is also distinctly different from the perched water. In addition, there is a distinct difference in water chemistry between the perched water near the ICDF Complex, which stems from the percolation ponds, and the northern perched water from Well 55-06 and from around the tank farm (Well 33-4).

The Piper diagram is another method used to show differences or similarities between water samples. It is based on the ionic composition (millequivalents per liter [meq/L]) of a water sample and emphasizes the ratios between ions. Samples from the perched water around the ICDF Complex and the percolation ponds are shown as circles on the Piper diagram in Figure 2-14 and are high in chloride.

In this type of diagram, the similarity between perched water at the percolation ponds, the service wastewater, and MW-17D is more evident than it was on the Schoeller diagram. The differences between these two diagrams indicate that water from the percolation ponds has mixed with another source at MW-17D, which has diluted the concentrations of major ions but left their ratios the same.

The Big Lost River and the INTEC water supply samples are very similar. In comparison, USGS-57 has higher chloride. The northern perched water is higher in chloride than the Big Lost River but lower in chloride than the perched water from the percolation ponds.

A trilinear anion diagram of perched water, Big Lost River water, and groundwater is shown in Figure 2-15. The upgradient aquifer (water supply [WS]) and Big Lost River are very similar with essentially no nitrate. The perched water around the percolation ponds is also low in nitrate but elevated in chloride. The northern perched zone has intermediate chloride but much more nitrate than other water sources. This nitrate could be from the sewage treatment plant or nitric acid from spills in the tank farm.

The USGS monitored the PW wells around the percolation ponds for Sr-90, H-3, and Cs-137 among other constituents of wastewater discharged to the percolation ponds. USGS data indicate H-3 and Sr-90 contamination in the perched water at similar concentrations to wastewater that was discharged to the ponds (Tucker and Orr 1998). Chloride, manganese, and iron exceeded the federal secondary drinking water standards. Sr-90, H-3, and nitrate have exceeded the primary drinking water standard in the past (DOE 1995).

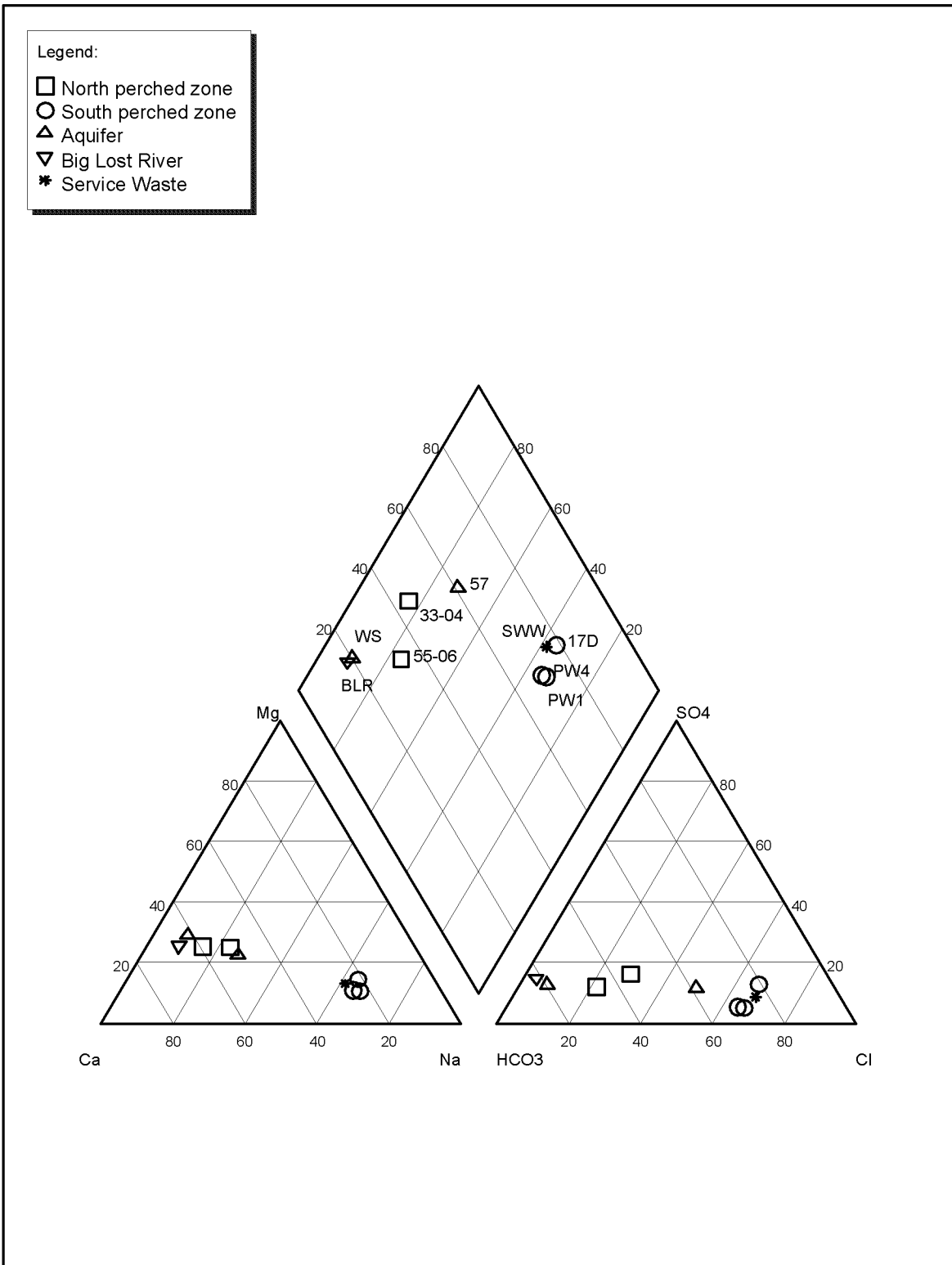


Figure 2-14. Piper diagram of water chemistry from perched water, the SRPA, and the Big Lost River.

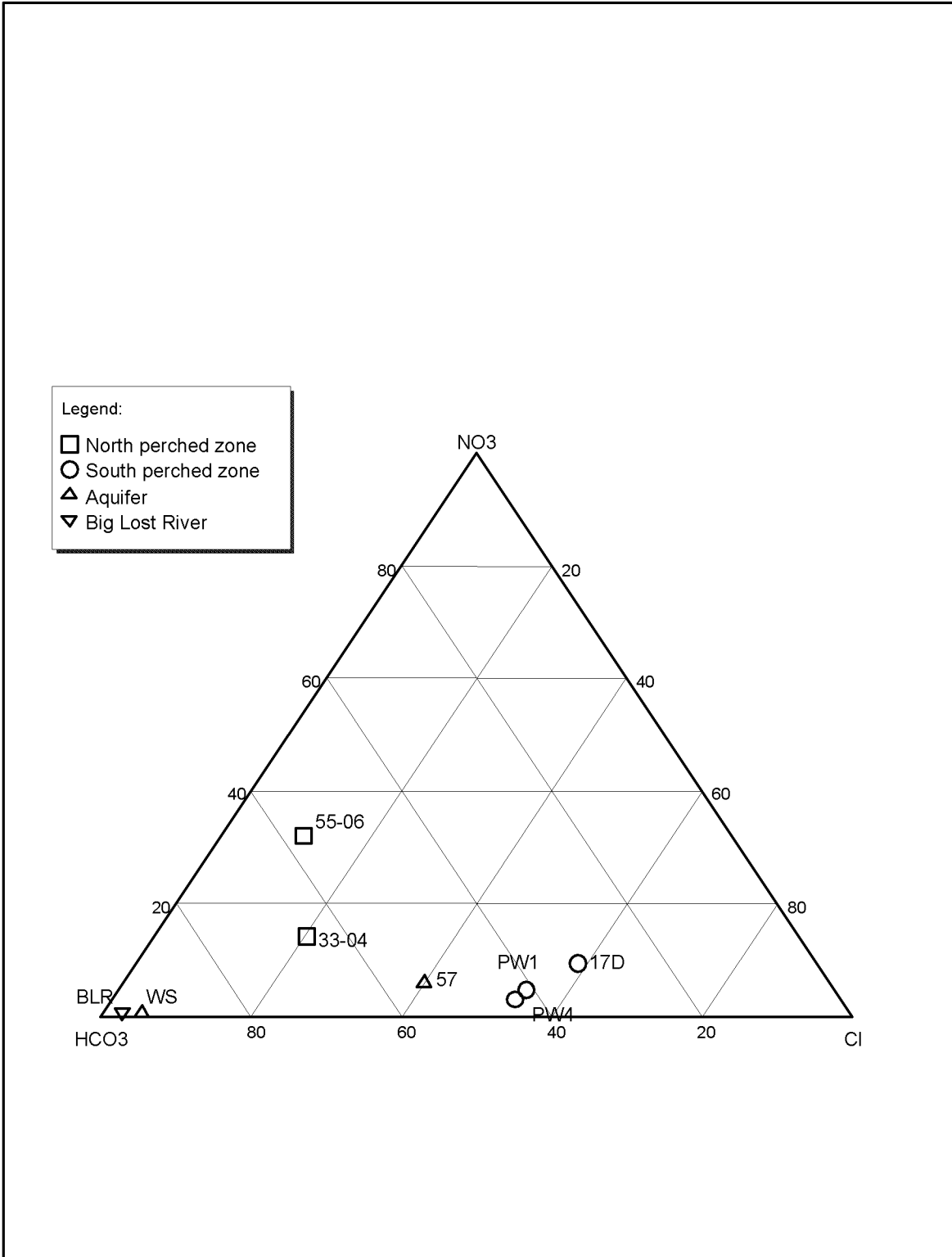


Figure 2-15. Trilinear diagram of anion composition of perched water, Big Lost River water, and SRPA water.

The percolation ponds adjacent to the ICDF Complex were taken out of service in August 2002. Water levels in the perched water around the ICDF Complex are expected to decrease over time, because the percolation ponds were the primary source of water. In other perched water wells at the INEEL (WAG 2, for example), contaminant concentrations have been known to spike as wells begin to go dry. Dramatic increases in concentrations are possible for the new perched water wells at the ICDF Complex as water levels decline. It is critical that this information be factored into any analysis of significant increases in order to avoid a false conclusion regarding a release from the ICDF landfill.

The above water chemistry discussions have demonstrated that the formation of perched water at the ICDF Complex was linked to leakage from wastewater discharge to the percolation ponds and not from the Big Lost River. As discussed previously, the percolation ponds were shut down permanently in August 2002. The perched water in wells near the ICDF Complex is dissipating.

2.1.7 Natural Resources

The following section discusses the natural geologic and water resources of the INEEL.

2.1.7.1 Geologic Resources. Geologic resources at the INEEL are very limited in nature. INEEL mineral resources include sand, gravel, pumice, silt, clay, and aggregate. These resources are extracted at several quarries or pits at the INEEL and used for road construction and maintenance, waste burial activities, and ornamental landscaping. The geologic history of the ESRP makes the potential for petroleum products at the INEEL very low. The potential for geothermal energy exists at the INEEL; however, a study by Mitchell et al. (1980) identified no economic geothermal resources.

2.1.7.2 Water Resources. The SRPA, one of the largest and most productive groundwater resources in the United States, underlies the INEEL and adjacent properties. The aquifer is listed as a Class I aquifer and was designated by the EPA as a sole source aquifer in 1991 (EPA 1990). Groundwater from this aquifer supplies most of the water for the area surrounding the INEEL and essentially all drinking water consumed within the ESRP (SAR-II-8.4). The water from the aquifer is used for agriculture, food processing, aquaculture, and domestic, rural, public, and livestock water supplies. In total, nearly 17.8 trillion liters (4.7 trillion gallons) of water are drawn from the aquifer annually, with the majority going to agriculture (DOE-ID 1998).

Irrigated agriculture provides a significant portion of the economic base for the people of southern Idaho, and the SRPA plays a major role in meeting irrigation requirements. The aquifer provides groundwater for irrigation of over one third of the 1.2 million hectares (3 million acres) of the ESRP that are irrigated. It is estimated that over 127,000 people depend on the aquifer for domestic and municipal water needs. Total domestic water consumption is approximately 5.7 million m³/yr (46,000 acre-ft/yr); groundwater discharge from well pumpage equals approximately 2.37 billion m³/yr (1.92 million acre-ft/yr) (EPA 1990).

In addition to providing water for INEEL Site operations and agriculture, the aquifer supplies water for other industries. Water discharged from springs in the Twin Falls-Hagerman area is used to raise fish commercially. The spring water flow of 47.0 m³/s (1,660 ft³/s) constitutes 76% of the water used for the commercial production of fish in Idaho. Most of these fish farms discharge water directly into the Snake River. The discharges from Hagerman Springs also significantly contribute to the flow of the Snake River downstream of Twin Falls, Idaho.

Groundwater in the aquifer generally flows from the northeastern recharge areas to the southwestern discharge areas. Nearly 8.0E+09 m³ (6.5E+06 acre-ft/yr) of water is discharged by the aquifer annually. Most of the discharge occurs as spring flow between Hagerman and Twin Falls. About 2.6E+06 m³/yr (2.1E+06 acre-ft/yr) of irrigation water is pumped from the SRPA in a typical year. About half of this water reenters the ground as return flow to the aquifer (SAR-II-8.4).

The altitude of the regional groundwater surface underlying the INEEL ranges from about 1,400 m (4,600 ft) in the north to about 1,300 m (4,400 ft) near the southwest boundary of the INEEL. The average hydraulic gradient slopes to the south and southwest on the INEEL at about 0.8 m/km (4 ft/mi). Within the INEEL boundaries, the depth below the land surface to the regional groundwater table ranges from 60 m (200 ft) in the northeast to 300 m (900 ft) in the west-southwest (SAR-II-8.4).

The SRPA is the only source of water used at the INEEL. The combined groundwater withdrawal averages approximately 3E+07 L/d (7E+06 gal/d) or 1E+07 m³/yr (8,000 acre-ft/yr). Table 2-4 lists the INEEL production wells, the depth of the well, the depth to water at the well, and the annual volume of water withdrawn from the well. All wells withdraw water from the main body of the SRPA. The water withdrawn from each well is used for potable water on the Site, for ground maintenance, and for necessary facility operations (SAR-II-8.4).

Table 2-4. INEEL production wells and annual volume pumped.^{a,b}

Well Name	Depth of Well (ft bgs)	Depth to Water (ft bgs)	Annual Volume (gal)
ANP-01	360	208	2.561E+06
ANP-02	340	211	1.433E+06
ANP-08	309	218	3.908E+05
Badging Facility Well	644	489	5.760E+04
CFA-1	639	468	1.473E+07
CFA-2	681	471	1.448E+05
CPP-01	586	460	1.834E+08 ^c
CPP-02	605	460	1.834E+08 ^c
CPP-04	700	462	1.834E+08 ^c
CPP-05	695	447	1.834E+08 ^c
EBR-I	1075	596	4.491E+04
EBR II-1	745	632	2.767E+06 ^d
EBR II-2	753	630	2.767E+06 ^d
FET-1	330	199	1.427E+06
FET-2	455	200	5.067E+05
Fire Station Well	516	420	1.057E+04
NRF-1	535	363	2.594E+06
NRF-2	529	362	9.368E+06
NRF-3	546	363	9.802E+04
NRF-4	597	363	1.649E+07
Rifle Range Well	620	508	9.115E+04
RWMC Production	685	568	4.824E+05
SPERT-1	653	456	3.871E+05
SPERT-2	1,217	463	3.450E+05
TRA-01	600	453	3.595E+07
TRA-03	602	456	2.074E+06
TRA-04	965	463	9.006E+07

a. All wells are withdrawing water from the main body of the SRPA and are used as drinking water wells with the exception of Wells ANP-08, Fire Station Well, and NRF-4, which are production wells for facility operations.

b. Source: SAR-II-8.4.

c. Total for Wells CPP-01, CPP-02, CPP-04, and CPP-05.

d. Total for both Wells EBR II-1 and EBR II-2.

The underflow of the INEEL (i.e., the amount of water passing directly under the INEEL boundaries) is approximately $1.8\text{E}+12$ L/yr ($4.7\text{E}+11$ gal/yr). The INEEL consumption is less than 1% of the INEEL underflow and less than 0.1% of the total annual aquifer discharge (SAR-II-8.4).

2.1.8 Natural Background Radiation

Monitoring and assessment activities are conducted to characterize existing radiological conditions at the INEEL and the surrounding environment. Results of these activities show that exposures resulting from airborne radionuclide emissions are well within applicable standards and are a small fraction of the dose from background sources.

DOE has compared radiation levels monitored on and near the INEEL with those monitored at distant locations to determine radiological conditions. Results from onsite and boundary community locations include contributions from background conditions and INEEL emissions. These data show that over the most recent 5-year period for which results are available (1992 through 1996), average radiation exposure levels for boundary locations were no different than those at distant stations. The average annual dose measured by the Environmental Science and Research Foundation Inc. during 1996 was 123 mrem for distant locations and 124 mrem for boundary community locations (DOE-ID 1997b). The corresponding 5-year averages were 127 mrem/yr for the distant group and 125 mrem/yr for the boundary group. These differences are well within the range of normal variation.

The offsite population could receive a radiation dose as a result of radiological conditions directly attributable to INEEL operations. The dose associated with radiological emissions is assessed annually to demonstrate compliance with the NESHAP (40 CFR 61, Subpart H). The effective annual dose equivalent to the maximally exposed individual resulting from radionuclide emissions from INEEL facilities during 1995 and 1996 has been estimated at 0.018 mrem and 0.031 mrem, respectively (DOE-ID 1996b, 1997c). These doses are well below both the EPA dose limit (10 mrem/yr) and the dose received from background sources (about 360 mrem/yr).

The annual collective dose to the population surrounding the INEEL, based on 1990 U.S. Census Bureau data, was estimated at 0.3 person-rem. This estimate is based on the air emissions from all facilities that were expected to become operational before June 1, 1995 (DOE 1995). The dose applies to a total population of about 120,000 people, resulting in an average individual dose of less than 0.003 mrem. For comparison, this population receives an annual collective dose from background sources of about 43,000 person-rem. In 1999, the population doses were updated in the High-Level Waste Environmental Impact Statement (DOE 2002); as a result, the dose was estimated at about 0.09 person-rem per year.

2.2 Principal Facility Design Features

The ICDF landfill will be a modular design, consisting of two cells, with a total capacity of $389,923\text{ m}^3$ ($510,000\text{ yd}^3$). The landfill is lined with a double composite liner system and include leachate collection and leak detection recovery systems. After the landfilled waste is placed to its final grades, it will be covered with a robust cover barrier system engineered to minimize infiltration for 1,000 years and conceivably years beyond (EDF-ER-281). The landfill is designed for an operational life of 15 years, a postclosure period of 30 years, and an expected landfill cover design life of 1,000 years.

The ICDF landfill complies with the substantive requirements of the RCRA Subtitle C and TSCA design standards specified in IDAPA 58.01.05.008 (40 CFR 264 Subpart N) and the PCBs Chemical Waste Landfill Design requirements (40 CFR 761.75). It also complies with the requirements of RCRA Subtitle C closure requirements specified in IDAPA 58.01.05.008 (40 CFR 264.310).

The following subsections address the principal design features of the facility that contribute to the long-term isolation of disposed waste. These features serve to (1) minimize the infiltration of water through disposal units; (2) ensure integrity of disposal unit covers; (3) provide for the structural stability of backfill, waste, and covers; and (4) provide a barrier against intrusion.

2.2.1 Water Infiltration

Minimization of infiltration of water through the disposal units of the ICDF landfill is accomplished by incorporation of both a bottom liner system and a surface cover in the facility design. Information on the design features of the bottom liner and surface cover are provided in the following subsections.

2.2.1.1 Landfill Bottom Liner. The ICDF landfill will be lined with a double composite liner system with leak detection to minimize and detect percolation of liquids into the subsurface. The composite landfill liner system consists of a primary high-density polyethylene (HDPE) geomembrane/geosynthetic clay liner (GCL) composite barrier and secondary HDPE geomembrane/soil bentonite liner (SBL) barrier. The primary composite barrier is designed to keep leachate from leaking into the underlying primary leak detection recovery system (PLDRS). The secondary barrier provides a means of identifying a leak from the primary system and provides an absorptive capacity of contaminants with a SBL. The composite liner system (i.e., primary geomembrane/GCL and secondary geomembrane/SBL) provides an added protection from leaks. The lower liner at the composite will mitigate leaks from the upper layer, reducing flow through a hole or defect by keeping the hole or defect from becoming larger over time.

The SBL was designed to have a maximum saturated permeability of 1×10^{-7} cm/sec and a thickness of 0.9 m (3 ft). Studies of SBLs have shown that this permeability significantly reduces the amount of percolation (Peyton and Schroeder 1990).

The permeability of the local clay borrow ranges from 1×10^{-6} cm/sec to 1×10^{-7} cm/sec (DOE-ID 2000a). A soil amendment study was performed to determine the amount of bentonite needed in the clay to achieve the permeability requirement in the laboratory (EDF-ER-272). The study concluded that mixing the clay borrow (i.e., base soil) with 5% of bentonite by dry weight produced a SBL material having a maximum permeability of 1×10^{-8} cm/sec in the laboratory.

Between the primary and secondary barriers is a drainage material to detect leaks from the overlying primary barrier and divert the liquid to a main sump. Liquids in the sump can be removed by pumps through riser pipes installed in the landfill. The primary leak detection recovery system has been designed with a high transmissivity so that liquids can flow with little resistance to a central sump.

The recommended EPA action leakage rate is defined in the final rule 40 CFR 264.302 as the “maximum design flow rate that the leak detection system can remove without the fluid head on the bottom liner exceeding 1 ft”. Based on this leakage rate, the action leakage rate for the ICDF landfill cell is 5,224 L/d (1,380 gal/d) and includes a factor of safety of two in accordance with EPA guidelines. Based on the design of the PLDRS the leakage rate dictated the sump and pump size.

The ICDF landfill also includes a secondary leak detection recovery system (SLDRS) located directly beneath the lowest barrier, which is the SBL. The SLDRS is positioned above a tertiary HDPE geomembrane located beneath the center of the landfill. Liquids would have to pass through two HDPE geomembranes, a GCL, and a 3-ft-thick low-permeable SBL before being detected in the SLDRS. The SLDRS will provide vadose zone monitoring and early detection.

The SLDRS was placed in a limited aerial extent only in the region of greatest probability of leachate collection and bottom liner leakage. The greatest probability of bottom liner leakage is near the leachate collection recovery system (LCRS) sump. The hydraulic head is usually greatest over the liner near the LCRS sump and the greatest density of seams in the geomembrane usually occurs at this location. Because the SLDRS was placed directly beneath and in contact with the bottom liner of the landfill, water capture in the SLDRS sump will be almost exclusively from leaks through the liner system. The SLDRS was extended under the center of the landfill along its north-south axis. This region would be the second greatest probability of bottom liner leakage. However, since a partial SLDRS will be installed, there is some possibility that water outside of the landfill cell could seep in along its edges. For this reason, chemical analysis of any water captured in the SLDRS sump will be used to distinguish between leaks and outside groundwater influences.

Leachate generated in the landfill will be managed with an LCRS. The LCRS consists of high-permeable gravel overlying the primary HDPE geomembrane on the landfill floor and a synthetic geocomposite material on the side slopes. The LCRS will divert leachate to a perforated pipe located along the center north-south axis of the landfill. Leachate then flows through the pipe to the LCRS sump where it can be pumped to the evaporation pond.

The LCRS design consisted of sizing the LCRS based on expected precipitation event and leachate generation to maintain less than 1 ft of hydraulic head over the liner system. The LCRS design is provided in the following three design studies: EDF-ER-269 Leachate Generation Study, EDF-ER-280 Landfill Leachate Collection System Design Analysis, and EDF-ER-274 Leachate/Contaminant Reduction Time Study.

A profile of the landfill liner system is provided in Figure 2-16.

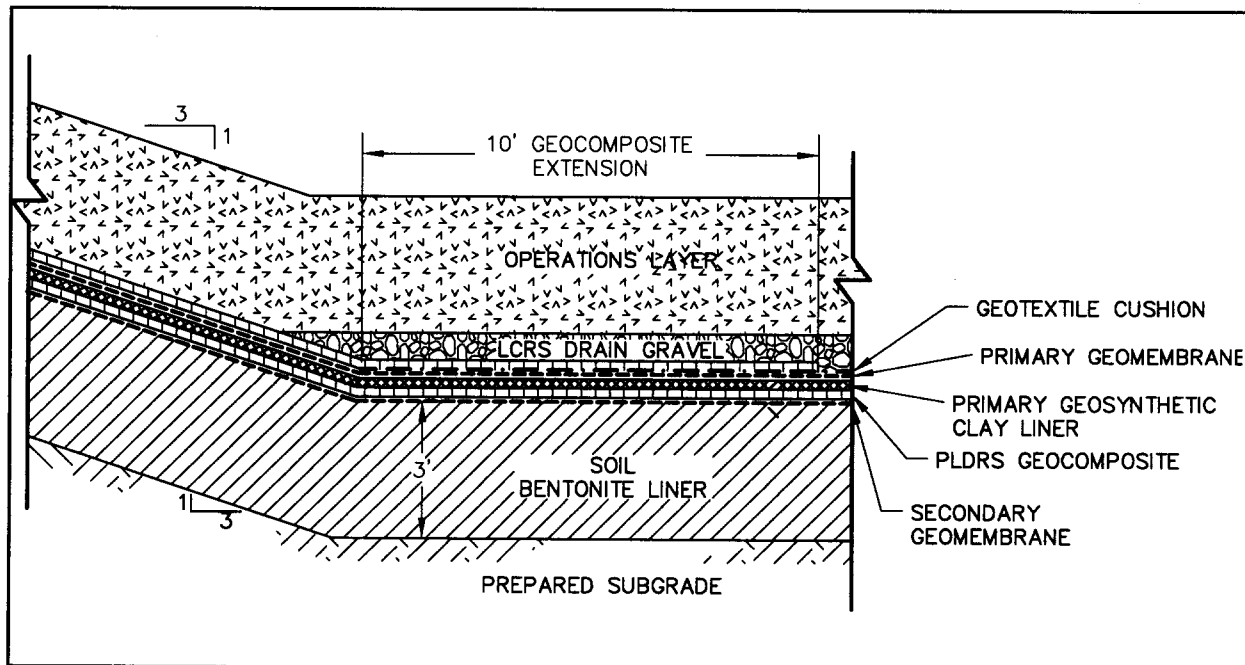


Figure 2-16. Landfill double composite liner system.

2.2.1.2 Landfill Surface Cover. Upon closure, a cover will be installed over the landfill. The ICDF landfill cover is designed as an infiltration limiting cover, to minimize long-term infiltration to the waste, thus reducing leachate generation and contaminant migration. The cover system will minimize infiltration and maximize run-off by maintaining a sloped surface, storing water for later release to the atmosphere, lateral drainage, and providing a low-permeability composite liner barrier system. The low infiltration rate to the waste is attributed to the design of the final cover, which consists of three distinct functional elements, described below:

- Upper section: The upper water storage component provides water storage during wet periods for later release into the atmosphere during dry periods. The upper section comprises a surface consisting of a vegetated soil/gravel matrix system sloped to minimize infiltration and maximize run-off. Vegetation is used to enhance the evapotranspiration properties of the upper cover portion. Beneath the soil/gravel matrix is a layer of silty loam-type soil that provides water storage during wet periods for later release into the atmosphere during dry periods. Coupled with a capillary break provided by the underlying sand and gravel layers, it will store moisture from long-term, low-probability precipitation events for later release to the atmosphere by evapotranspiration. The evapotranspiration layer in the cover is an integral component that provides long-term minimization of migration of liquids through the closed landfill while functioning for the long term with minimal maintenance. Results from hydrologic modeling of the final cover indicate that the minimum water storage layer thickness needed to maximize water storage is 2 m (6.5 ft). Sensitivity analysis shows clearly that increasing the water storage thickness beyond the optimal thickness increases water storage capacity, but does not reduce the percolation rate.

The ICDF landfill cover surface grade and erosion protection meet or exceed the requirements of RCRA Subtitle C design standards specified in IDAPA 58.01.05.008 (40 CFR 264.310). The function of the surface cover is to promote surface water drainage, minimize erosion, and provide a medium for vegetation. The surface will be sloped so that surface water run-off is directed to the side slopes of the landfill lined with basalt riprap armoring. The landfill side slopes will be sloped at 2.5H:1V (2.5 horizontal to 1 vertical) from the edge of the cover to the existing ground surface as shown in Figure 2-17. The riprap side slope armor will dissipate the energy from water run-off from the cover until it reaches the existing ground surface at a distance of over 30.5 m (100 ft) from the edge of the waste mass. A final grade of 7% was determined for the cover (EDF-ER-267). This will ensure that a minimum slope of 3% is maintained after consolidation to promote surface water drainage off the cover system through its 1,000-year life.

- Middle section: The biointrusion layer provides protection from burrowing animals and a capillary break. Biointrusion protection is provided by a layer of 5- to 12.7-cm (2- to 5-in.) diameter gravel. Two filter layers of sand and gravel provide smooth transitions between the biointrusion gravel layer and the over- and under-lying layers. The filter layers above the biointrusion layer prevent fine-grained soil from the upper section from migrating into the coarser materials. The filter layers also provide capillary breaks due to the contrast in unsaturated permeabilities. The capillary breaks provide redundancy for limiting infiltration in the cover. The relatively coarser materials in the middle section compared to the upper section will also provide lateral drainage in the event breakthrough occurs through the upper cover layers.
- Lower section: The lower section includes a composite liner system that has a permeability less than or equal to the permeability of the landfill bottom liner system that complies with IDAPA 58.01.05.008 (40 CFR 264.310). The composite liner system consists of a single HDPE geomembrane over an SBL. The composite system will intercept water in the event breakthrough occurred from the upper cover sections and divert it laterally through the overlying sand and gravel layers.

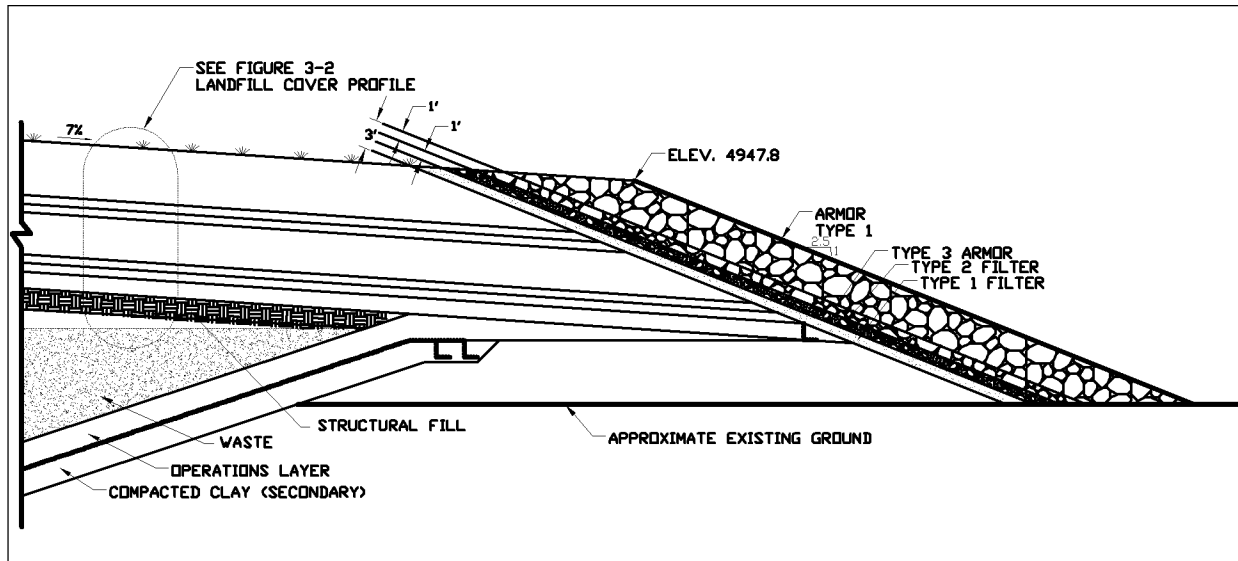


Figure 2-17. Landfill cover section.

The geomembrane and SBL designed for the bottom liner system will function for the cover as well. Consequently, similar analyses used for the bottom liner are applicable for the cover system.

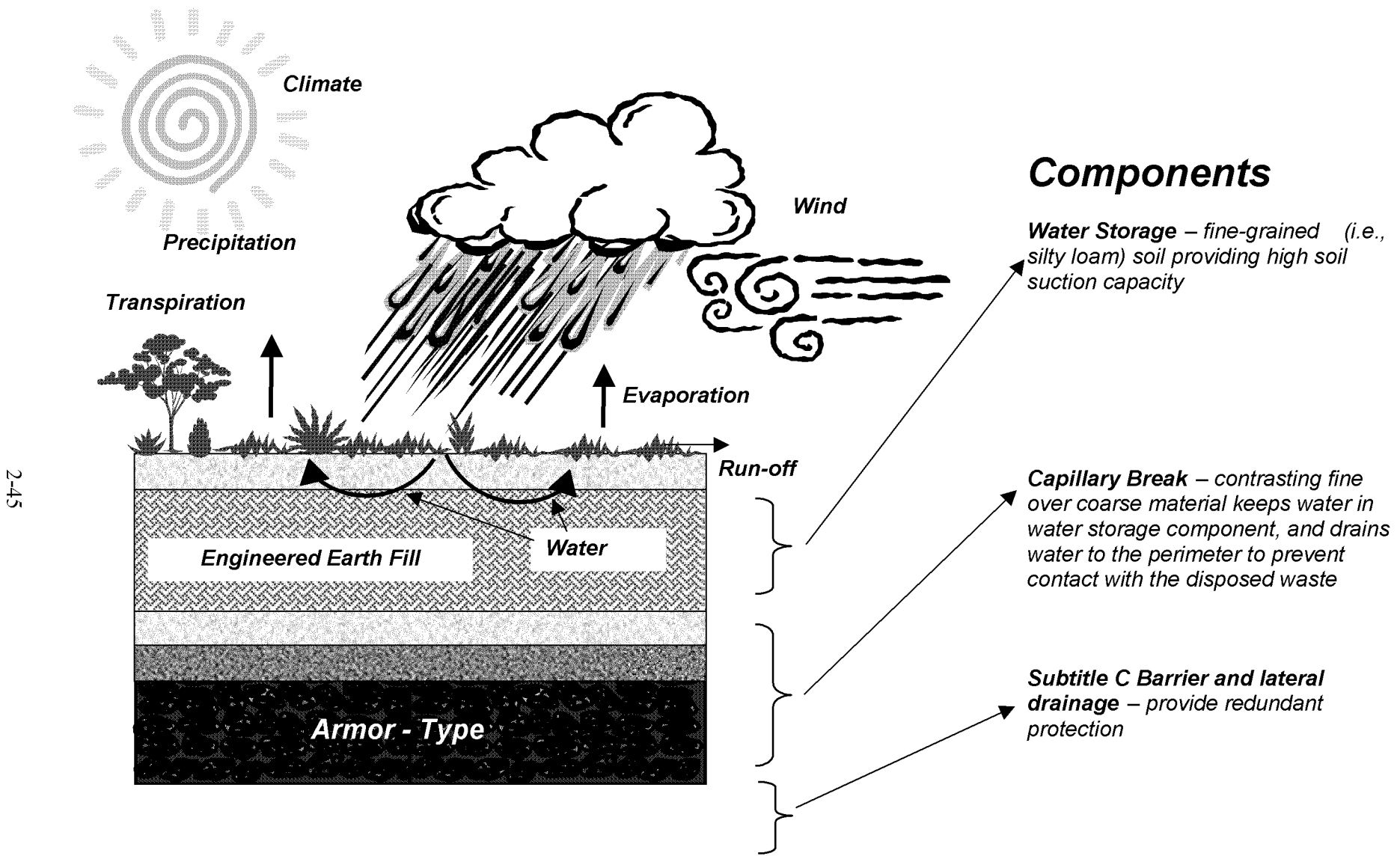
Each component in the cover profile is shown in Figures 2-18 and 2-19.

The results of hydrologic modeling of the cover predict a very low infiltration rate (less than 0.1 mm/yr) over the next 1,000 years at the base of the cover system (EDF-ER-279).

The facility will have a storm water drainage system that is designed to (1) direct storm water and snow melt runoff around the ICDF and (2) minimize soil erosion on and around the facility (EDF-ER-270). Erosion control measures include silt fences, planted vegetation, and temporary straw bale check structures. Runoff is directed with the use of ditches. The ditches are sized to accept runoff from offsite areas in addition to drainage produced from Cell 1 and the future construction of Cell 2.

The design storm for determining adequate ditch sizes is the 25-year, 24-hour event in accordance with INEEL design standards. Design of the storm water drainage system is considered conservative since an assumption was made that the covers placed over Cells 1 and 2 would be completely impervious and shed all precipitation. Overland flow enters the ditch system by flowing over the banks of the proposed channel. After collection, flows will be routed to the southeast corner of the site. Channel discharge is accomplished through a spillway section located at the downstream end of the channel. The spillway section is 4.6 m (15 ft) wide and lined with riprap to help minimize the effects of soil erosion. Discharge will continue as sheet flow over the continued property east of the ditch.

Existing surface conditions at the ICDF site consist of relatively flat terrain overlain with native sagebrush. The land slopes downward at approximately 0.3% in the northeast direction. Soil conditions are porous with a relatively low percentage of clay material. Natural depressions are present throughout the drainage basin. There are no natural channels or drainage ways on or near the ICDF Complex. The basin area, including the ICDF Complex is approximately 22.3 ha (55 ac). The existing paved roadway located west of the ICDF serves as a barrier to any additional flows west of the roadway. An investigation was performed to determine water surface elevations in the channels surrounding the ICDF under severe site conditions. Such conditions include accumulation of ice within the channel cross section, a frozen land surface resulting in decreased infiltration, and accumulation of snow on the drainage area prior to the



2-45

Figure 2-18. Simplified depiction of the infiltration limiting final cover for the ICDF landfill.

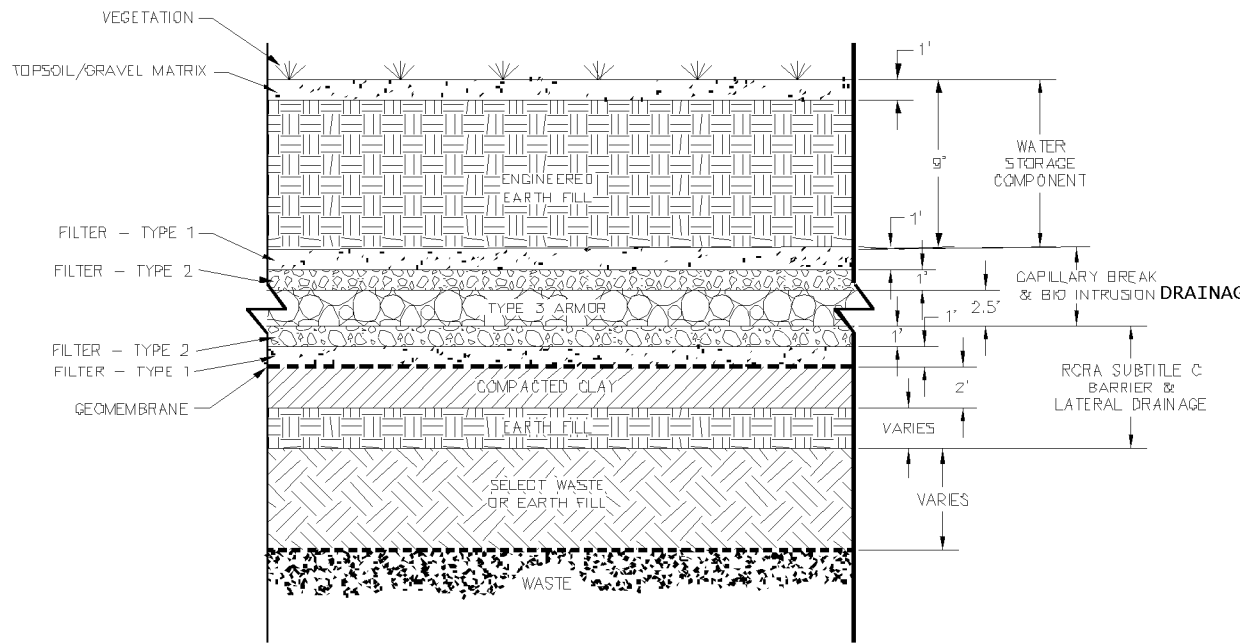


Figure 2-19. Schematic of the final landfill cover functional sections.

rainfall event. Under these conditions, the drain channels surrounding the ICDF have been shown to adequately transport the increased flows without overtopping. In the event that the channels should overtop, the embankment surrounding the ICDF would prevent runoff from entering into the cells. The perimeter ditch channels are located approximately 36.6 m (120 ft) away from the ICDF cell, which would preclude any subsurface infiltration into the cell due to the limited hydraulic gradient between the ditch and the ICDF cell locations.

2.2.2 Disposal Unit Cover Integrity

2.2.2.1 Upper Section. Surface water and wind erosion analyses were performed to determine the amount of soil loss from the cover due to sheet flow (EDF-ER-281). Erosion due to surface water was completed using the Modified Universal Soil Loss Equation as recommended by the NRC for long-term (i.e., 1,000-year) soil loss (NRC 1986). The surface of the cover was assumed to be fine-grained soils such as those found at the Rye Grass Flats area at INEEL without accounting for the protection of the soil/gravel matrix. The analysis consisted of determining the probable maximum precipitation (PMP) event and calculating soil loss per year using the Modified Universal Soil Loss Equation. Approximately 0.6 m (2 ft) of soil could erode from the surface of the cover over a 1,000-year time period. The minimum water storage layer thickness needed to maximize water storage is 2 m (6.5 ft) based on the Hydrologic Modeling of the Final Cover (EDF-ER-268). The water storage layer will be constructed with an additional 0.76 m (2.5 ft) of material to provide a sacrificial layer in the event that the surface would erode due to water erosion.

Extensive wind tunnel studies performed at Hanford facility show that a mixture of fine-grained soil and pea gravel significantly reduced erosion due to wind forces. Soil/pea gravel armoring can reduce erosion rates from 96.5 to more than 99% at wind speeds of 45, 56, and 67 mph (Ligotke 1993). The average wind speed at INEEL based on the period of record is 9 mph with peak gusts up to 82 mph (NOAA 2001). Based on these studies, a soil/pea gravel matrix will provide sufficient protection against aeolian forces for the ICDF cover through its 1,000-year life, and conceivably beyond.

The cover settlement has been evaluated in the landfill compaction subsidence study (EDF-ER-267). Based on the settlement determined in this study and the other design considerations (subsidence, erosion, and abrasion), a final grade of 7% was determined for the cover. This will ensure that a minimum slope of 3% is maintained after consolidation to promote surface water drainage off the cover system through its lifetime.

The landfill cover surface will be seeded and fertilized to promote plant growth. Vegetation will minimize erosion and accelerate removal of water from the water storage layer. Long-term considerations include periods of drought or fire so erosion and hydrologic modeling studies have assumed a poor stand of vegetation. The vegetation will consist of local plant species based on vegetation studies performed for disturbed areas at INEEL (DOE-ID 1989). Vegetation based on native plant species will include

- Secar Bluebunch Wheatgrass
- Bottlebrush Squirreltail
- Sandberry Bluegrass
- Sodar Streambank Wheatgrass
- Green Rabbit Brush.

The maximum allowable noxious weed percentage (by dry weight) will be 0.5%. The maximum allowable wet and other crop percentage will be 1.5%. The engineered seed mix will provide superior vegetation providing more transpiration and erosion control than the surrounding natural vegetation.

The ICDF Complex is situated outside the Big Lost River floodplain. The ICDF landfill lies within alluvial, aeolian, and lacustrine sediments deposited over millions of years ago by the Big Lost River system. A massive precipitation event may conceivably create floodwaters that would impact the permanent cover barrier. The rock armor on the permanent cover side slopes has been sized based on the PMP event. The PMP for INEEL is 9 in. of rain in 1 hour. The average annual rainfall is 8.6 in. per year based on the 44-year period of record at the CFA at INEEL. The PMP would generate a probable maximum flood event from the surface cover of approximately 13,600 gallons per minute across a 100-ft section of the cover. Flood waters at the base of the cover would have to rise over 10 ft above the existing ground surface to overtop the rock armoring on the landfill cover side slopes. The existing ground surface surrounding the ICDF landfill has little relief (less than 2%). Consequently, floodwaters would be relatively slow moving as compared to run-off from a 7% sloping surface like the ICDF cover. Beyond the geological deposits left by the Big Lost River system, there is no evidence that a large precipitation event would cause massive flooding of the magnitude necessary to erode the permanent ICDF side slope rock armor.

Basalt is a durable volcanic rock that provides excellent erosion protection; however, it may vary in its density and competency. Durability and abrasion-type tests will be performed on the rock armor selected for the ICDF cover prior to construction to determine its long-term durability. Based on the results of these tests, rock armor will be oversized if necessary to ensure that it performs its function for the life of the cover system.

Tornado-type winds are expected to be extremely rare at the ICDF Complex. The cover side slope armor consisting of large heavy basalt riprap will resist tornado-type winds. The surface of the permanent cover will consist of vegetation and a soil/pea gravel matrix. The soil/pea gravel matrix has been shown to be resistant to high wind forces generated in wind tunnel tests performed at the Hanford Facility.

Cover slope stability calculations were completed for both static and pseudostatic cases to determine short- and long-term stability (EDF-ER-268). The peak-ground acceleration generated by a DOE performance category 4 earthquake was used to ensure pseudostatic stability for the cover performance period. This performance category is a high hazard category for a magnitude of an earthquake that would have a reoccurrence interval of 1 in 10,000 years.

2.2.2.2 Middle Section. Sands and gravels will be used in the cover system for the biointrusion and filter layers. The source of these materials will be alluvial deposits at the INEEL. The alluvial deposits at the INEEL comprise granite, quartz, and other durable minerals that make them ideally suited for long-term applications.

2.2.2.3 Lower Section. Stresses will be induced in the cover SBL and geomembrane components due to settlement in the foundation soils, waste, and the cover itself. The settlement calculation for the foundation and liner soils is provided in the subsurface consolidation design study (EDF-ER-266). The amount of settlement in the waste and cover itself are provided in the landfill compaction/subsidence study (EDF-ER-267). When the cover settles, the geomembranes will compress, resulting in a reduction in stress. However, the SBL could crack due to excessive settlement. The proposed cover surface will have a slope of 7%. The cover could accommodate an additional settlement (after surface consolidation, cover settlement, and the maximum strains are accounted for) of 4 m (13 ft). Approximately 54% (i.e., 2.1 m [7 ft]) of the allowable settlement are predicted over the long term. Consequently, the strain in the SBL will not cause cracking and increased permeability.

The geomembrane liner will be subject to puncture from the filter layers loaded by overlying materials. A nonwoven geotextile was installed between the geomembrane and filter gravel to provide a cushion. The required puncture resistance of the geotextile was determined based on the analysis performed for the bottom liner system. The round alluvium sand and gravels excavated from the landfill was screened to remove particles over 5 cm (2 in.) in diameter for the filter layer. The minimum puncture resistance is 56 kg (124 lb), including a factor of safety of two based on the maximum particle size in the LCRS (EDF-ER-281).

Geomembranes are susceptible to wind uplift, causing damage prior to placing overlying soil layers. The geomembrane in the cover will be anchored with overlying cover materials after the liner system is installed, protecting from wind uplift. However, there will be short periods of time when the geomembranes will be exposed to winds such as during the liner installation (EDF-ER-281).

The geomembrane overlying the SBL was terminated in trenches constructed around the perimeter of the cover. The ends of the liners was buried under 0.6 m (2 ft) of earth to protect from wind uplift and pull out (EDF-ER-281).

The SBL can sustain irreversible damage caused by freeze-thaw cycles. Water added during construction for compaction can freeze, increasing the hydraulic permeability through formation of cracks, microcracks, and interconnected macropores (Benson and Othman 1993). Extreme frost penetration at INEEL is estimated to be 114 cm (45 in.). The ICDF landfill SBL will be protected from frost by 4.7 m (15.5 ft) of overlying soil layers in the cover.

The HDPE membranes have been used in landfills for containment for several decades. The engineering properties of these materials are well understood. They are manufactured to perform a specific function including hydraulic barriers, erosion control, and drainage. Long-term degradation issues include the following: radioactive degradation, biological degradation, chemical degradation, thermal degradation, oxidation degradation, and ultraviolet degradation. Each of these issues is discussed in turn below.

2.2.2.3.1 Radioactive Degradation—The HDPE has a higher resistance to radiation exposure than other liner materials including polyester, polyurethane, and polypropylene (Farnsworth and Hymas 1989). Studies performed on thin films (i.e., 0.002 in.) of different types of HDPE material show that it can become brittle when irradiated at doses between 4,400,000 and 78,000,000 rad/cm². Polymeric material manufacturers reported that it begins losing its tensile strength and ductility near 1,000,000 rad/cm² of total radiation exposure. The normal allowable maximum human exposure is 200 rad/cm² for comparison. Samples of HDPE liner exposed to radiation doses up to 37,000,000 rad/cm² have a reduction in tensile strength of approximately 25%. Even with the reduction of tensile strength, the geomembrane remains intact and could continue to perform its function as a barrier layer. The HDPE geomembranes currently in use today are manufactured with additives to improve ductility and durability such as carbon black and antioxidants. These additives allow higher radiation doses than standard HDPE material alone. The anticipated dose to the primary geomembrane in the ICDF landfill is 12,000 rad/cm² during its operational life. A maximum radiation dose of 1,000,000 rad/cm² for the landfill liner system during its service life is recommended (EDF-ER-278).

2.2.2.3.2 Biological Degradation—Biological degradation consists of fungi or bacteria attaching themselves to the polymer, resulting in a change of geomembrane properties. Other types of biological degradation could be from insects or burrowing animals. Tests performed with rats indicate that they were not able to chew their way through geomembranes. Tests performed in the laboratory and in the field show that geomembranes are very resistant to a wide spectrum of biological degradation including manufactured biological additives capable of destroying high-molecular weight polymers like those used in the geomembranes (EPA 1989a). Therefore, degradation due to biological attack is very unlikely.

2.2.2.3.3 Chemical Degradation—The HDPE geomembrane material that will be used in the ICDF landfill is considered to be the most chemically inert liner material commercially available. Numerous studies using EPA Method 9090 and permeability tests, among other testing procedures, have been performed for waste disposal facilities and in the laboratory, providing a good understanding of the compatibility behavior of these liner materials. Published studies provide a good tool for establishing compatibility without relying on Method 9090 or permeability testing, which can be time-intensive and require synthetically generating hazardous leachate. A detailed description of the chemical compatibility with the expected leachate composition is described in the liner/leachate compatibility study (EDF-ER-278).

The maximum recommended concentration of chemical categories were provided to supply the WAC regarding liner compatibility. General chemical categories rather than individual constituents provide a worst-case scenario due to possible synergistic effects of mixed compounds. However, to provide numerical WAC, individual constituents in the ICDF design inventory were evaluated to determine maximum allowable ICDF landfill concentrations with regard to liner compatibility. The maximum allowable ICDF landfill waste concentrations are provided in (DOE-ID 2002c).

2.2.2.3.4 Thermal Degradation—Polymeric materials exposed to heat may be subjected to changes in the physical, mechanical, or chemical properties. The amount of change is dependent on the time and severity of exposure. Compatibility and environmental stress rupture tests are performed by submerging geomembrane material in a solution of leachate or surface active agents typically heated to over 49° (120°F). HDPE geomembranes perform very well under these conditions. Most likely, the highest temperatures that the HDPE geomembrane in the ICDF landfill will be subject to occur during construction from exposure to the sun. After installation, the geomembrane used in the landfill will be buried and remain at a temperature between 10 and 21°C (50 and 70°F). Thus, thermal degradation will not occur over the long term.

Behavior of polymeric materials due to cold temperatures is different than when exposed to heat. Cold will not degrade a geomembrane. Geomembranes have been used for landfill and liquid containment systems in the arctic without degradation. Geomembranes behave differently in cold temperatures in that they become stiff and difficult to work with during installation. However, this was not be an issue, as construction was completed over the summer.

2.2.2.3.5 Oxidation Degradation—Oxidation degradation results in a loss of mechanical properties and ductility of the geomembrane. Oxidation can occur when exposed to high temperatures (i.e., 200°F). Oxidation degradation can also occur when the geomembrane is exposed to the sun for long periods of time. Burying geomembranes under soil minimizes geomembrane contact with oxygen and significantly reduces or eliminates oxidation degradation. Geomembrane manufacturers also add antioxidant agents in the geomembrane to reduce the potential for oxidation degradation.

2.2.2.3.6 Ultraviolet Degradation—Polymers degrade when exposed to ultraviolet light due to photo oxidation. Additives in the geomembranes such as carbon black are used to retard ultraviolet degradation. The geomembrane in the landfill will be covered by soil, eliminating ultraviolet degradation.

As long as antioxidants are present in the geomembrane, the physical and mechanical properties of the geomembrane can be preserved. Accelerated aging studies have been performed on HDPE geomembranes to estimate the length of time it requires to deplete the antioxidants in geomembranes. The results of the study indicate that 80 years at an ambient temperature of 20°C (68°F) would be required to deplete the antioxidants in an HDPE geomembrane (Hsuan and Guan 1998).

2.2.3 Structural Integrity

The ICDF landfill will contain CERCLA-generated contaminated bulk soil, debris (i.e., rubble, concrete, wood, drums, boxes, personal protective equipment [PPE], and metals), and treated waste that are generated at the INEEL and meet the Agency-approved WAC for the ICDF landfill (DOE-ID 2002c). Total subsidence in the cover will be a cumulative of settlement amounts due to deformation in the landfill components listed below:

- Consolidation of the waste that is soil
- Consolidation of the waste due to degradation of waste debris
- Consolidation due to voids left in containerized waste
- Consolidation of the compacted clay liner and foundation soils
- Consolidation of the cover itself.

The total predicted settlement in the ICDF landfill cover is summarized in Table 2-5.

Table 2-5. Summary of predicted cover settlement.

Landfill Component	Long-term Predicted Settlement (ft)
Foundation and liner	1.2
Waste as soil	0 ^a
Waste as degradable debris	Varies (dependent on debris thickness)
Cover	0.1
Total predicted cover settlement without degradable debris	1.3

a. Settlement will be immediate during operation and cover construction.

The majority of the waste in the landfill will be soil comprised of the sands and gravels found in the near surface soils around the INEEL Site (DOE-ID 2000a). The waste soils will be compacted to minimize settlement. Additionally, settlement in the waste will be immediate as the waste is placed in the landfill and during construction of the cover.

A portion of the waste placed in the landfill will be nonsoil material. These materials will be debris such as rubble, concrete, wood, PPE, metals, containerized waste, and treated waste that are generated at the INEEL and meet the Agency-approved WAC for the ICDF. Debris can be categorized as nondegradational and degradational. Nondegradational debris includes materials such as asphalt and concrete. Material such as wood, plastic, and metal can degrade due to biochemical, oxidation, and corrosion-type reactions creating voids in the waste that may result in long-term settlement. Containerized waste (e.g., drums) may contain a void space up to 5% (DOE-ID 2002c) that can collapse due to loads from the overlying waste. Debris will be preprocessed if necessary to minimize mechanical compression resulting from distortion, bending, or reorientation. The volume of waste consists predominantly of contaminated soils so the volume of debris is expected to be minimal. Debris will be placed to maximize compaction efforts and minimize subsidence.

In municipal and construction debris landfills, where degradable debris accounts for a majority of the air space, long-term secondary settlement can be on the order of 15% of the waste thickness.^c This amount of settlement is higher than that expected for the ICDF landfill because the landfill will contain only contaminated soil and debris without municipal solid waste. Additionally, the actual volume of degradable debris is expected to be small in the ICDF landfill (EDF-ER-264). The amount of settlement caused by degrading debris will be a function of its thickness in the landfill. The maximum amount of settlement due to degradable-type debris potentially could be on the order of 1.5 m (5 ft) for a debris thickness of 10 m (34 ft) (the total thickness of waste in the landfill). Additionally, the cover could settle an additional 0.3 m (1 ft) due to 55-gallon drums collapsing over time. However, waste to be containerized and disposed in 55-gallon drums will be kept at a minimum through the waste acceptance process.

The soils underlying the landfill consist of dense alluvial deposits overlying basalt bedrock ranging in thickness from 4.6 to 7.6 m (15 to 25 ft). The alluvium consists of gravels, gravel-sand mixtures, and sand-gravel-cobble mixtures to poorly sorted gravels with sand and silt. An intermittent layer of fine sand, silt, and clay (i.e., “old alluvium”) between the bedrock and gravels ranges in thickness from 0.6 to 21 m

c. Fassett, unpublished paper titled: “Geotechnical Properties of Municipal Solid Waste and Their Use in Landfill Design,” 1993.

(2 to 7 ft) based on the borings located within the landfill footprint. The SRPA is located approximately 134 m (440 ft) below the bottom of the landfill (EDF-ER-275).

The existing sand and gravelly foundation soils will provide a structurally stable subgrade for the ICDF landfill liner system. Additionally, the foundation layer is relatively thin, dense, and not influenced by a changing groundwater table. As a worst-case estimate, total settlement was determined on the assumption that the SBL is overlying 4.6 m (15 ft) of the “old alluvium” soil. This will provide a conservative settlement estimate, because the “old alluvium” will have the largest amount of consolidation. This also takes into account the small amount of immediate settlement in the gravels and secondary consolidation that could occur. Note that these assumptions are to provide a conservative subsurface consolidation amount and may not be valid for other calculations.

The foundation is loaded by the waste, operations layer, and the landfill cover. The stress increase caused by this load is calculated at various depths utilizing published solutions to the Boussinesq Equation. Terzaghi’s consolidation theory is then used to determine the settlement in the subgrade soils caused by the increase in effective stress due to the load (Holtz and Kovacs 1981). The maximum long-term differential settlement in the liner and foundation soils is estimated to be 0.4 m (1.2 ft) (EDF-ER-266).

The loads will be the largest near the middle of the landfill rather than on the sideslopes, resulting in potential differential settlement. Given that the settlement on the sides of the landfill will be very small, the total settlement calculated at the middle of the landfill floor will be the maximum differential settlement. Differential settlement will create strain in the liner system components. The predicted 0.001% strain on the liner component of the landfill is below the allowable 0.1% strain for SBL, the 1.0% strain for GCLs, and the 20% strain for geomembranes (EDF-ER-266).

To provide adequate drainage, the minimum bottom slope of 1% is required for leak detection recovery systems in landfills (40 CFR 264.301). The current practice and minimum technology guidance for bottom slopes of landfills is a minimum of 2% (EPA 1989a). The ICDF landfill floor was designed at a 2.5% slope, steeper than 2% to allow for differential settlement. A maximum differential settlement of 0.4 m (1.2 ft) near the middle of the landfill floor would result in a floor slope of approximately 2%, meeting the regulatory requirement and suggested minimum landfill slope guidance.

The cover is comprised mainly of earthen materials that will settle due to this weight. The cover layers comprised of fine-grain soil will consolidate the most over the long term. These include the soil bentonite liner barrier layer and engineered structural fill water storage layer. Cover settlement is calculated to be 0.03 m (0.1 ft) (EDF-ER-267).

The integrity of the cover must be maintained for the long term (the design life of 1,000 years). This is achieved by overbuilding the cover to accommodate predicted settlement and minimize strain in the cover components.

Landfill covers must maintain a positive slope to promote surface water runoff (40 CFR 264.310). The EPA recommends a final top slope between 3 and 5%, after settlement has occurred (EPA 1989b). The proposed cover surface will have a slope of 7% (EDF-ER-281) and a length of 118 m (387 ft) measured on its shortest side. A cover slope constructed at a maximum slope of 7% has been shown to be stable and resistant to wind and water erosion (EDF-ER-281). This cover can accommodate settlement (i.e., after subsurface consolidation, cover settlement, and the maximum strain are accounted for) of 4 m (13 ft) (EDF-ER-267).

2.2.4 Inadvertent Intruder Barrier

To deter the inadvertent intrusion of humans into the waste, a marker system will be used to warn future generations of the dangers of the buried waste. Permanent markers that identify the potential exposure hazards will be installed at all corner boundaries for each cell of the landfill (DOE-ID 2002c). The DOE intends to maintain active control of INEEL (using fences, patrols, alarms, and monitoring instruments) per the ROD requirements discussed previously in Section 1.2.2 (DOE-ID 1999). During the operational phase, a 1.8-m (6-ft) woven mesh fence will be placed around the site to prevent animals and unauthorized persons from entering. If these measures should cease, other passive-type measures will warn the inadvertent intruder from waste buried beneath the permanent cover barrier. The measures may include recognizable warning markers and other physical features. Site information will be provided on an Internet website, U.S. Geological Survey maps, libraries, and other information repositories that would be readily available to the public (EDF-ER-281). Land use restrictions and institutional controls will be placed on the ICDF landfill and its adjacent buffer zone to permanently preclude development until unacceptable risk no longer remains at the site (DOE-ID 2001a, 1999)

The ICDF landfill will have a steep rocky side slope of basalt riprap. This feature clearly delineates the boundaries of the surface barrier by providing a distinct contrast with the surrounding flat terrain. The side slopes are engineered structures that will be obvious that the structure had been built by humans. These distinct riprap side slopes in combination with warning signs will minimize the risk of human intrusion. The riprap basalt is a durable volcanic rock; however, it may vary in its density and competency. Durability and abrasion-type tests will be performed on the rock armor selected for the ICDF cover prior to construction to determine its long-term durability. Based on the results of these tests, rock armor will be oversized if necessary to ensure that it performs its function for the life of the cover system.

As discussed above, the ICDF landfill cover also contains a biointrusion layer consisting of gravel. The function of this layer is to prevent small burrowing animals and ants from penetrating the underlying cover components and the waste material. Past barrier studies at INEEL, Hanford, and other facilities have shown that a thin layer of gravel is effective in preventing animals and ants from penetrating underlying waste materials (Morris and Bleu 1997; Wing 1993). The biointrusion material will consist of gravel screened from the local available alluvium at INEEL. The alluvium gravels at INEEL are composed of granite, quartz, and other durable minerals that make it ideally suited for long-term applications.

2.3 Waste Characteristics

According to the OU 3-13 ROD (DOE-ID 1999), the ICDF landfill has an authorized capacity of 389,000 m³ (510,000 yd³). Approximately 358,903 m³ (469,400 yd³) of INEEL CERCLA remediation waste, about 92% of the authorized capacity, have already been identified for disposal in the ICDF landfill during the first 10 years of operation. This remediation waste includes 304,846 m³ (398,700 yd³) of predominately contaminated soils with minor debris and 54,057 m³ (70,700 yd³) of debris from deactivation, decontamination, and decommissioning (D&D&D) activities. In addition to remediation waste, an additional 61 m³ (80 yd³) of IDW generated as part of the OU 3-14 tank farm investigation will be disposed in the ICDF landfill.

The ICDF Remedial Action Work Plan (DOE-ID 2003d) discusses the objectives and methods of conducting treatability studies on waste material. The wastes are primarily soils containing radionuclides and RCRA heavy metals, namely mercury. To dispose of these waste soils, the heavy metals must be removed or stabilized such that the final treated form does not leach any of the heavy metals above the standards defined by the EPA in 40 CFR 268.49. The treatment method in this treatability study is a Portland cement-based chemical fixation system that stabilizes the heavy metals in a nonleachable form.

This study will use actual waste material. The waste samples will be subjected to a matrix of tests wherein the Portland cement will be supplemented with chemical additives and the waste loading. The treated waste samples will be analyzed via the toxicity characteristic leaching procedure and the paint filter test for free liquids to determine if the treated material would meet disposal criteria.

Any soil treatment will occur at the SSSTF, which is a part of the ICDF Complex. The majority of wastes (primarily soils) that would be processed through the facility and designated option paths for these wastes have been identified (EDF-ER-296). Soils associated with CPP-92, CPP-98, CPP-99, and CFA-04 are being considered for treatment. The estimated volume of soil to be treated is 1,079 m³ (1,412 yd³). A portion of the decontamination facility will be used for stabilizing the waste.

A small fraction of the wastes is already in metal containers. However, for the PA analyses, it is assumed that the entire waste is compacted soil. This is a conservative assumption with respect to the leaching of contaminants from the facility.

There are relatively few uncertainties related to the waste characteristics of the wastes to be disposed of to the ICDF landfill. The waste will be predominantly soils that will be compacted during emplacement in the facility. All containerized and grouted wastes should be more stable than the compacted soil. Therefore, treating the waste as 100% compacted soil is a conservative assumption. There is relatively large uncertainty in the radionuclide inventory contained in the soils. As will be explained below, the total inventory was conservatively estimated in order to compensate for this uncertainty.

2.3.1 Methods and Assumptions Used to Determine the Inventory

This section of the PA summarizes the basic methodology used to calculate the “initial design inventory” (IDI) (EDF-ER-264) and “adjusted design inventory” (ADI). The ADI is the waste inventory used for the ICDF landfill design analysis as well as the ICDF landfill PA waste inventory used for the analysis presented in this document. The methods and assumptions developed for the IDI and ADI are described in the next two sections.

2.3.1.1 Initial Design Inventory. This section contains a summary of the assumptions and methods used to develop the IDI presented in EDF-ER-264. The approach was intended to provide a conservative estimate of the waste inventory that is expected to be disposed in the landfill during the first 10 years of operation.

To the extent analytical data were available on the contaminant concentration of the waste, those data were used to help determine the waste inventory. When analytical data were not available, contaminant concentrations for each release site were estimated based on process knowledge, releases from similar sites, scaling factors, or average contaminant concentrations from the waste. Since much of the design inventory is conservatively estimated, it provides a conservative initial approximation of the wastes to be disposed in the ICDF landfill.

The design inventory includes only waste from the CERCLA remediation sites that have been identified in the CERCLA Waste Inventory Database (CWID) Report (DOE-ID 2000b) for disposal in the ICDF landfill. A total of 304,846 m³ (398,700 yd³) of contaminated soil and debris has been identified from 35 release sites for disposal in the ICDF landfill during the first 10 years of operation. From WAGs 1, 2, 3, 5, and 7 D&D&D sites, a total of 54,057 m³ (70,700 yd³) of waste debris has been identified.

As previously explained, in addition to the waste from these sites, 61 m³ (80 yd³) of IDW from the OU 3-14 tank farm investigation and 55,057 m³ (70,700 yd³) of debris from D&D&D are also expected to

be generated and disposed in the ICDF landfill. The authorized capacity identified in the OU 3-13 ROD for the ICDF landfill is 389,900 m³ (510,000 yd³).

The CERCLA Waste Inventory Database Report (DOE-ID 2000b) provides the available analytical data for the radiological contaminants that have been analyzed for each release site. Specifically, it contains analytical data on the following radionuclides that have been detected at one or more release sites at the INEEL:

Ag-108m, Am-241, Ce-144, Co-57, Co-60, Cs-134, Cs-137, Eu-152, Eu-154,
Eu-155, H-3, I-129, K-40, Np-237, Pu-238, Pu-239, Pu-239/240, Ra-226,
Ru-106, Sb-125, Sr-90, Tc-99, Th-228, Th-230, Th-232, U-234, U-235, U-238.

Based upon typical reactor operations, however, it is likely that other radionuclides may be present in the waste stream (DOE-ID 1997d). To estimate the concentration of the potentially present radionuclides at a given release site, a scaling factor was developed based on Cs-137 concentrations and the irradiation of a typical 200-g fuel element. This approach will identify the radionuclides that were potentially present in the waste stream and estimate their concentrations relative to the Cs-137 concentration. It will not account for naturally occurring radionuclides such as uranium, thorium, etc. and their progeny.

The design inventory is primarily based on the analytical data contained in the CWID, which is described in DOE-ID (2000b), hereafter referred to as the CWID Report. All data having detectable concentrations (i.e., all data that were not flagged with a "U" qualifier) were used in development of the design inventory. This includes data that have other data validation qualifiers, such as "R," "J," "B," etc. For radionuclides, the concentrations in the design inventory were decayed to a common date of January 1, 2002.

For the sites having detectable contamination based on analytical data, either the maximum concentration or the 95% UCL concentration was used for the design inventory. The 95% UCL concentration was selected if the following two conditions were satisfied: (1) a minimum of eight detectable concentrations was available and (2) the 95% UCL concentration was less than the maximum concentration. If either of these conditions was not satisfied, then the maximum concentration was used for the design inventory. The methodology used to calculate the 95% UCL concentrations is provided in Appendix A of EDF-ER-264.

If analytical data were not available for a given release site, but the contaminant may be present based on process knowledge, the concentration was estimated using data from the CWID report. The estimated concentrations were based on the weighted average of the mean concentrations from those release sites where the contaminant was detected. The weighted average concentrations were determined using the following equation:

$$C_{WA} = \frac{\sum_0^i C_n X_n + C_l X_l + \dots C_l X_l}{\sum_0^i X_n + X_l + \dots X_l} \quad (2-1)$$

where

- C_{WA} = concentration, weighted average
- C = concentration
- X = contaminated volume.

Importantly, the mean concentrations provided in the summary tables of the CWID report were calculated using only the analytical results where there were detectable concentrations. In other words, the nondetectable results were not used in calculating the mean concentrations. This approach provides a conservative estimate of the mean concentration (i.e., biased high).

Finally, additional data for some of the release sites were identified that are not currently in the CWID. If sources of information were used other than CWID, the source of the data is referenced in the associated summary table.

Cesium-137 was selected as the indicator radionuclide for the scaling because (1) the majority of the sites have data on Cs-137 and (2) it is a relatively immobile contaminant in nature and should still be present in the waste volume. An evaluation showed the CWID report (DOE-ID 2000b) and other referenced documents contained analytical data for Cs-137 on all but three sites. The Cs-137 concentrations at these three sites (CPP-69, CPP-98, and CPP-99) were estimated based upon the Cs-137 concentrations at similar release sites. Site CPP-69 was assumed to be the same as Site CPP-11 and Sites CPP-98 and CPP-99 were assumed to be the same as CPP-97. In addition, radiological contamination was not expected at Sites CPP-44, CPP-55, CPP-93, and TSF-03; and, as a result, Cs-137 data are not available. For these sites, a background concentration of 0.82 pCi/g was used for Cs-137 in the design inventory.

The Cs-137 concentrations used in the design inventory were determined following the approach described above. Either the maximum concentration or the 95% UCL concentration (if eight or more detectable measurements are available) was used in the design inventory for Cs-137. The concentrations for the other radionuclides where analytical data are not available were determined using a scaling factor based upon the site-specific Cs-137 concentration.

The development of scaling factors for each radionuclide is described in EDF-ER-264. Basically, the computer-modeled activities from a typical 200-g fuel element following irradiation to determine the scaling factors necessary to estimate the activities of the other radionuclides based upon the Cs-137 concentration. The theoretical activities of the waste from a typical reactor operation are identified in Table A-1a, Appendix A-2 of the CWID report (DOE-ID 2000b). These activities were then adjusted to account for 22 years of radioactive decay from the time period of 1980 to January 1, 2002. The radioactive decay was performed using the Radioactive Decay Calculator[®] (version 2.01), which accounts for all daughter products and ingrowth radionuclides. The resulting activities calculated for January 1, 2002, were then divided by the Cs-137 activity to develop a specific scaling factor for each radionuclide. The scaling factors for each radionuclide are provided in EDF-ER-264, Table D-1 of Appendix D.

The EDF-ER-264, Appendix D, identifies the design inventory for radionuclides on a site-by-site basis. Details concerning radionuclide concentration and activity are provided in EDF-ER-264, Tables D-2 and D-3, respectively. These tables use the concentrations derived from the scaling factors except when actual analytical data were available. If data were available, either the maximum concentration or the 95% UCL concentration (if eight or more detectable measurements are available) was used in the design inventory for the given radionuclide except for Sr-90, Tc-99, and U-234. For these radionuclides, the concentrations determined using the scaling factors were significantly higher than the analytical data available in measured concentrations in CWID (DOE-ID 2000b). As a result, the design inventory used the scaled-determined concentrations for these radionuclides as a more conservative estimate. The sites and associated radionuclides having sufficient data to calculate the 95% UCL concentrations are identified in EDF-ER-264, Table D-4.

2.3.1.1.1 Data Use—The approach used to develop the design inventory was to use the existing data to the maximum extent possible in order to provide waste characteristic estimates. When data were not available, however, conservative assumptions were used to estimate the potential contaminant characteristics of the waste for the design inventory. This is important because the design inventory is not only based on the analytical data, but also includes an evaluation of each release site to determine the type and concentration of contaminants that may be reasonably expected to be present in the waste.

The following bullets summarize the approach and assumptions used to develop the design inventory:

- All data with detectable concentrations (i.e., all data that were not flagged with a “U” qualifier) were used in development of the design inventory. This includes data with other data validation qualifiers, such as “R,” “J,” “B,” etc.
- Contaminant estimates for the release sites having analytical data were based either on the maximum concentration (if less than eight detectable measurements were available) or the 95% UCL concentration (if eight or more detectable measurements).
- A conservative approach was used to estimate the 95% UCL concentration. The mean concentrations of the samples were determined using only the data having detectable measurements, and the standard deviation was calculated using all the data. This approach results in a conservative estimate for both the mean and standard deviation (see discussion in Appendix A of EDF-ER-264).
- Contaminant estimates for the release sites without analytical data were based on the weighted-average of the mean concentrations from the sites having analytical data for that contaminant. As an additional conservative estimate, the mean concentrations were calculated using only the data having detectable measurements (i.e., no “U” flagged data used in the calculations).
- The amount of contaminant at each release site was determined by multiplying the contaminant concentration estimates (described above) by the entire soil volume identified in the CWID report (DOE-ID 2000b). This assumes that the entire volume of soil is contaminated by a concentration equal to the maximum or 95% UCL.
- For radionuclides, concentrations for all possible contaminants were determined based upon a scaling factor applied to the site-specific Cs-137 concentrations and, when available, the analytical data. A comparison of the analytical data to the scaled data determined that the scaled data provide a reasonable estimate of the radionuclide concentration within the waste. When both analytical and scaled data were available, the more conservative (i.e., higher) concentration was used in the design inventory.
- Concentration estimates for Sr-90, Tc-99, and U-234 were based on the scaled data rather than the analytical data. For these radionuclides, the scaled data generally provide a more conservative estimate of the contaminant concentration.

Given the limited characterization data on the waste, it is not possible to quantify the differences between the contaminant concentration in the design and adjusted design inventories to the actual waste. Based upon the above assumptions, however, it appears that the design inventory provides a reasonably conservative estimate of the wastes to be disposed in the ICDF landfill during the first 10 years of operation. The adjusted design inventory provides an additional 60% conservatism.

2.3.1.2 Adjusted Design Inventory. This section documents the change from the IDI document (EDF-ER-264) to the ADI for use in the design analysis calculations as well as the performance assessment and the composite analysis. The history of the ICDF landfill ADI is summarized below:

1. EDF-ER-264 documents the original ICDF inventory for the ICDF Complex 30% design. It provides estimates for the IDI and is based on 315,761 m³ (413,000 yd³) of soil at 1,500 kg/m³ bulk soil density for the waste.
2. After the ICDF Complex 60% design was completed, the capacity of the facility was estimated to be 389,923 m³ (510,000 yd³). This is 23.5% greater than the estimated volume of contaminated soil (510,000/413,000 = 1.235). For analysis purposes, it was assumed that 23.5% more contaminated soil would be placed in the ICDF landfill than originally planned.
3. In preparation for the 60% design, the bulk soil density of the contaminated soil to be placed in the ICDF was re-estimated and increased from 1,500 to 1,946 kg/m³. The design inventory was based on soil concentrations; therefore, the increase in the soil bulk density results in an increase in the estimated inventory for the ICDF landfill. This is an increase of 29.7% (1,946/1,500 = 1.297).

2.3.2 Initial Design and Adjusted Design Inventories

The ADI is presented in Table 2-6. The inventory values are based on the methodology discussed in Section 2.3.1.2. The table includes the IDI for easy comparison.

The IDI provides a conservative estimate of the contaminant concentration and mass that are expected to be present in the wastes, and destined for disposal in the ICDF landfill, during the first 10 years of operation. In addition, the ADI increases the mass of soil by 23.5% and the radionuclide inventory by 60.2%. This additional safety factor provides an extra level of conservatism for the PA analysis.

The ADI is the inventory used for the performance assessment source term. The ADI will be referred to as the ICDF PA inventory for the remainder of this document.

Table 2-6. Design and adjusted design inventories used for the ICDF landfill fate and transport analyses—radionuclide contaminants.

Radionuclide	Initial Design Inventory 1/1/2002 (Ci)	Adjusted Design Inventory or ICDF PA Inventory 1/1/2002 (Ci)
H-3	2.35E+01	3.76E+01
Be-10	5.41E-07	8.67E-07
C-14	2.18E-05	3.50E-05
K-40	9.08E-01	1.45E+00
Sc-46	1.35E-20	2.16E-20
Cr-51	1.09E-54	1.75E-54
Mn-54	9.15E-09	1.47E-08
Co-57	1.75E-03	2.80E-03
Co-58	2.78E-17	4.46E-17
Fe-59	2.14E-35	3.42E-35
Co-60	9.16E+01	1.47E+02
Zn-65	1.28E-09	2.05E-09
Se-79	7.86E-02	1.26E-01

Table 2-6. (continued).

Radionuclide	Initial Design Inventory 1/1/2002 (Ci)	Adjusted Design Inventory or ICDF PA Inventory 1/1/2002 (Ci)
Kr-81	2.51E-09	4.02E-09
Kr-85	5.49E+02	8.79E+02
Rb-86	0.00E+00	0.00E+00
Rb-87	5.28E-06	8.46E-06
Sr-89	2.84E-44	4.54E-44
Sr-90	1.08E+04	1.74E+04
Y-90	1.08E+04	1.74E+04
Y-91	1.96E-37	3.15E-37
Nb-92	3.01E-19	4.82E-19
Zr -93	4.06E-01	6.50E-01
Nb-93m	6.40E-03	1.02E-02
Nb-94	4.18E-06	6.70E-06
Zr-95	1.39E-25	2.22E-25
Nb-95	2.27E-33	3.64E-33
Nb-95m	8.72E-36	1.40E-35
Tc-98	8.37E-08	1.34E-07
Tc-99	2.73E+00	4.37E+00
Rh-102	1.41E-05	2.26E-05
Ru-103	9.51E-30	1.52E-29
Rh-103m	1.34E-58	2.14E-58
Ru-106	5.75E-03	9.21E-03
Rh-106	5.39E-03	8.63E-03
Ag-106	0.00E+00	0.00E+00
Pd-107	2.90E-03	4.64E-03
Ag-108	1.75E-09	2.80E-09
Ag-108m	3.79E-01	6.07E-01
Ag-109m	2.33E-12	3.73E-12
Cd-109	2.33E-12	3.73E-12
Ag-110	2.45E-11	3.93E-11
Ag-110m	2.63E-09	4.21E-09
Ag-111	0.00E+00	0.00E+00
Cd-113m	7.68E-01	1.23E+00
In-114	8.93E-55	1.43E-54
In-114m	9.35E-55	1.50E-54
Cd-115m	2.02E-54	3.23E-54
In-115	2.74E-12	4.39E-12
In-115m	0.00E+00	0.00E+00
Sn-117m	0.00E+00	0.00E+00
Sn-119m	7.03E-08	1.13E-07
Sn-121m	1.27E-02	2.04E-02
Sn-123	3.99E-17	6.39E-17
Te-123	2.14E-15	3.43E-15
Te-123m	1.40E-23	2.24E-23

Table 2-6. (continued).

Radionuclide	Initial Design Inventory 1/1/2002 (Ci)	Adjusted Design Inventory or ICDF PA Inventory 1/1/2002 (Ci)
Sb-124	9.82E-41	1.57E-40
Sn-125	0.00E+00	0.00E+00
Sb-125	4.39E+00	7.04E+00
Te-125m	1.07E+00	1.72E+00
Sn-126	6.98E-02	1.12E-01
Sb-126	9.77E-03	1.56E-02
Sb-126m	6.98E-02	1.12E-01
Te-127	4.43E-20	7.10E-20
Te-127m	4.50E-20	7.21E-20
Xe-127	7.49E-73	1.20E-72
Te-129	3.20E-71	5.12E-71
Te-129m	5.08E-71	8.13E-71
I-129	6.15E-01	9.85E-01
Xe-129m	0.00E+00	0.00E+00
I-131	0.00E+00	0.00E+00
Xe-131m	1.27E-112	2.04E-112
Cs-132	0.00E+00	0.00E+00
Xe-133	0.00E+00	0.00E+00
Cs-134	5.31E+00	8.51E+00
Cs-135	1.70E-02	2.72E-02
Cs-136	0.00E+00	0.00E+00
Ba-136m	0.00E+00	0.00E+00
Cs-137	1.16E+04	1.85E+04
Ba-137m	1.09E+04	1.75E+04
La-138	0.00E+00	0.00E+00
Ba-140	0.00E+00	0.00E+00
La-140	1.25E-105	2.01E-105
Ce-141	8.55E-72	1.37E-71
Ce-142	0.00E+00	0.00E+00
Pr-143	0.00E+00	0.00E+00
Ce-144	8.56E-04	1.37E-03
Pr-144	8.39E-04	1.34E-03
Pr-144m	1.20E-05	1.92E-05
Nd-144	1.55E-10	2.48E-10
Pm-146	2.75E-03	4.41E-03
Sm-146	2.02E-10	3.23E-10
Nd-147	0.00E+00	0.00E+00
Pm-147	1.81E+02	2.90E+02
Sm-147	1.94E-06	3.11E-06
Pm-148	1.88E-59	3.02E-59
Pm-148m	3.90E-58	6.25E-58
Sm-148	4.78E-13	7.66E-13
Sm-149	2.43E-12	3.89E-12

Table 2-6. (continued).

Radionuclide	Initial Design Inventory 1/1/2002 (Ci)	Adjusted Design Inventory or ICDF PA Inventory 1/1/2002 (Ci)
Eu-150	8.20E-09	1.31E-08
Sm-151	1.60E+02	2.56E+02
Eu-152	4.58E+02	7.34E+02
Gd-152	1.29E-14	2.06E-14
Gd-153	9.53E-12	1.53E-11
Eu-154	3.89E+02	6.23E+02
Eu-155	8.36E+01	1.34E+02
Eu-156	0.00E+00	0.00E+00
Tb-160	1.50E-34	2.41E-34
Tb-161	0.00E+00	0.00E+00
Ho-166m	1.28E-06	2.05E-06
Er-169	0.00E+00	0.00E+00
Tm-170	3.02E-26	4.84E-26
Tm-171	7.55E-13	1.21E-12
Hf-181	3.69E-37	5.92E-37
Tl-207	8.65E-06	1.39E-05
Tl-208	9.38E-05	1.50E-04
Tl-209	4.98E-10	7.98E-10
Pb-209	2.30E-08	3.68E-08
Pb-210	5.17E-07	8.29E-07
Pb-211	8.67E-06	1.39E-05
Pb-212	2.62E-04	4.20E-04
Pb-214	2.66E-06	4.26E-06
Bi-210	5.17E-07	8.29E-07
Bi-211	8.67E-06	1.39E-05
Bi-212	2.62E-04	4.20E-04
Bi-213	0.00E+00	0.00E+00
Bi-214	2.66E-06	4.26E-06
Po-210	4.81E-07	7.70E-07
Po-211	3.24E-10	5.19E-10
Po-212	1.55E-04	2.49E-04
Po-213	2.06E-08	3.30E-08
Po-214	2.66E-06	4.26E-06
Po-215	8.67E-06	1.39E-05
Po-216	2.62E-04	4.20E-04
Po-218	2.66E-06	4.26E-06
At-217	2.43E-08	3.89E-08
Rn-218	5.97E-117	9.56E-117
Rn-219	9.60E-06	1.54E-05
Rn-220	2.62E-04	4.20E-04
Rn-222	2.94E-06	4.71E-06
Fr-221	2.43E-08	3.89E-08
Fr-223	1.34E-07	2.14E-07

Table 2-6. (continued).

Radionuclide	Initial Design Inventory 1/1/2002 (Ci)	Adjusted Design Inventory or ICDF PA Inventory 1/1/2002 (Ci)
Ra-222	5.54E-117	8.87E-117
Ra-223	9.60E-06	1.54E-05
Ra-224	2.62E-04	4.20E-04
Ra-225	2.43E-08	3.89E-08
Ra-226	2.24E-01	3.60E-01
Ra-228	7.21E-11	1.16E-10
Ac-225	2.43E-08	3.89E-08
Ac-227	9.68E-06	1.55E-05
Ac-228	7.21E-11	1.16E-10
Th-226	1.03E-117	1.65E-117
Th-227	8.61E-06	1.38E-05
Th-228	1.56E-02	2.50E-02
Th-229	2.43E-08	3.89E-08
Th-230	8.22E-02	1.32E-01
Th-231	7.62E-02	1.22E-01
Th-232	7.38E-02	1.18E-01
Th-234	8.12E-04	1.30E-03
Pa-231	3.31E-05	5.30E-05
Pa-233	2.06E-02	3.31E-02
Pa-234m	8.12E-04	1.30E-03
Pa-234	1.30E-06	2.08E-06
U-230	0.00E+00	0.00E+00
U-232	2.53E-04	4.06E-04
U-233	1.21E-05	1.94E-05
U-234	2.86E+00	4.57E+00
U-235	5.22E-02	8.37E-02
U-236	9.58E-02	1.53E-01
U-237	0.00E+00	0.00E+00
U-238	9.25E-01	1.48E+00
U-240	1.20E-11	1.93E-11
Np-235	3.22E-11	5.16E-11
Np-236	3.28E-08	5.26E-08
Np-237	3.05E-01	4.88E-01
Np-238	1.03E-07	1.65E-07
Np-239	1.58E-04	2.53E-04
Np-240	1.32E-14	2.12E-14
Np-240m	1.20E-11	1.93E-11
Pu-236	2.62E-06	4.20E-06
Pu-237	5.73E-59	9.18E-59
Pu-238	1.11E+02	1.77E+02
Pu-239	3.16E+00	5.06E+00
Pu-240	7.11E-01	1.14E+00
Pu-241	3.03E+01	4.85E+01

Table 2-6. (continued).

Radionuclide	Initial Design Inventory 1/1/2002 (Ci)	Adjusted Design Inventory or ICDF PA Inventory 1/1/2002 (Ci)
Pu-242	1.14E-04	1.83E-04
Pu-243	3.03E-16	4.85E-16
Pu-244	1.20E-11	1.93E-11
Pu-246	6.55E-26	1.05E-25
Am-241	1.13E+01	1.81E+01
Am-242m	2.14E-05	3.43E-05
Am-242	2.15E-05	3.44E-05
Am-243	1.58E-04	2.53E-04
Am-245	0.00E+00	0.00E+00
Am-246	6.55E-26	1.05E-25
Cm-241	6.14E-81	9.84E-81
Cm-242	2.55E-17	4.09E-17
Cm-243	1.68E-06	2.70E-06
Cm-244	8.54E-04	1.37E-03
Cm-245	3.80E-08	6.09E-08
Cm-246	8.48E-10	1.36E-09
Cm-247	3.03E-16	4.85E-16
Cm-248	9.25E-17	1.48E-16
Cm-250	2.62E-25	4.20E-25
Bk-249	1.02E-21	1.64E-21
Bk-250	3.67E-26	5.88E-26
Cf-249	1.95E-16	3.13E-16
Cf-250	9.98E-17	1.60E-16
Cf-251	4.51E-19	7.22E-19
Cf-252	1.06E-20	1.70E-20

2.4 Summary of the ICDF Landfill Design Hydrologic Modeling Analyses

In developing the design for the ICDF landfill, several design calculations, studies, and evaluations were performed to determine key design parameters. A summary of the ICDF landfill design hydrologic modeling analyses is presented below.

Concentrations of selected design inventory constituents in ICDF landfill leachate were evaluated to estimate leachate chemical characteristics during the 15-year operations period and the 30-year postclosure period. The evaluation is presented in EDF-ER-274. The purpose of the study was to estimate leachate constituent concentrations to support various design evaluations, including

- Identifying a conservative estimate of the leachate chemical characteristics as a basis for assessment of landfill liner/leachate compatibility
- Identifying a conservative estimate of the leachate chemical composition to assess worker exposure to landfill contaminants in the leachate evaporation ponds.

Following the postclosure period, the concentrations of the constituents moving out of the facility and being transported through the vadose zone to the aquifer were evaluated to determine whether the ICDF is protective of the SRPA. The vadose zone and aquifer modeling is documented in EDF-ER-275.

Four evaluations were used for the ICDF design hydrologic evaluation and a summary of each follows. The first evaluation identified potential maximum leachate concentrations in the landfill. The geochemical model PHREEQC (v 2.5) (Parkhurst and Appelo 1999) was used to simulate the chemical nature of the leachate at the approximate moisture content of the compacted waste soil. The geochemical modeling indicates that pore water within the compacted waste soil is expected to be a brackish to saline water (approximately 0.5 molar ionic strength) dominated by sodium and sulfate and buffered by carbonates to a pH of around 8.0.

The second evaluation identified the potential loss of constituents from the waste soil in leachate during the 15-year operating period. A spreadsheet-based analytical solution was developed for this evaluation. The analytical solution indicates that as much as 20% of the inventory masses of the most mobile constituents (e.g., iodine and technetium) may be removed from the landfill during the operating period, about 5% of the Tc-99, and less than 1% of the uranium isotopes and Np-237 are expected to be removed from the landfill during the 15-year operating period.

The third evaluation identified the potential concentration of leachate constituents outside of the landfill during the 30-year postclosure period. A numerical simulation model was used to estimate the volume and characteristics of the leachate. The numerical model used was version 2.0 of the Subsurface Transport Over Multiple Phases (STOMP) finite difference code developed by Pacific Northwest National Laboratory (PNNL) to conduct the simulations. A description of the STOMP code is found in the Theory Guide (PNNL 1996) and the User's Guide (PNNL 2000). The numerical simulations of constituent transport during the 30-year postclosure period indicated that less than 1% of the contaminant mass would be expected to leave the landfill as leachate during the postclosure period.

The fourth evaluation was the vadose zone and aquifer ICDF fate and transport modeling effort, which used the STOMP version 2.0 code as well. This code was selected over simpler codes for its ability to simulate flow and transport through the hydraulically complex INEEL unsaturated zone. In particular, the INEEL unsaturated zone consists of engineered barrier layers under the waste and alternating basalt and interbed layers down to the aquifer. Each of the sediment and rock layers has significantly different hydraulic and transport characteristics. This heterogeneity is difficult for numerical models to accurately simulate. STOMP has been shown to have this capability. The conceptual model and numerical discretization used for the ICDF design fate and transport modeling is shown in Figure 2-20. Fate and transport modeling was conducted to predict potential concentrations in the SRPA over time from the ICDF landfill (EDF-ER-275). The concentrations were predicted for a hypothetical SRPA monitoring well located 20 m downgradient from the ICDF Complex. Various infiltration rates were assumed in order to determine design requirements of the ICDF landfill. The modeling predicts that the ICDF Complex will be protective of the SRPA if it operates as designed, and detectable concentrations of radioactive contaminants from the Complex are not expected in the tertiary leachate detection system for over 100 years.

Due to the high degree of uncertainty regarding the actual rate of waste soil placement in the landfill and the actual placement of specific waste soil, conservative assumptions were made that are believed to maximize apparent leachate concentrations for these evaluations.

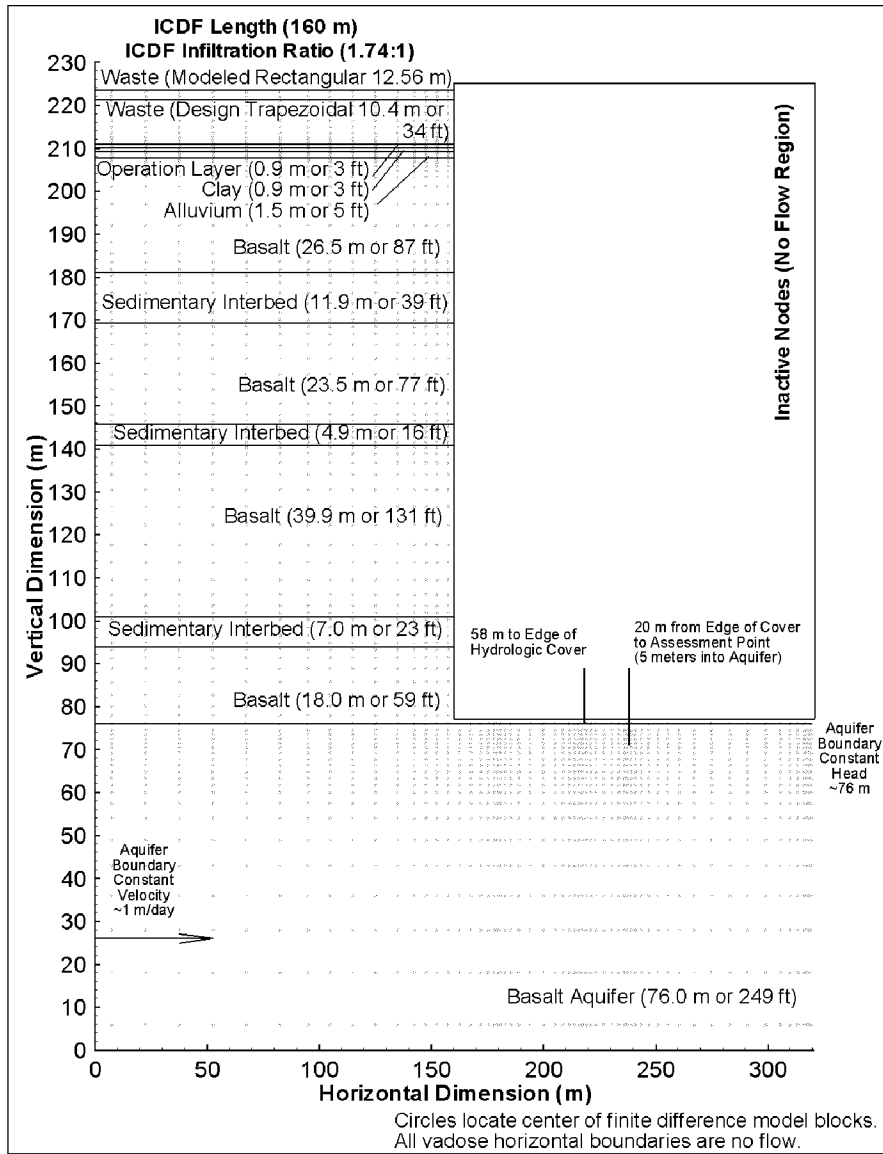


Figure 2-20. Conceptual model and finite difference grid used for the ICDF STOMP fate and transport modeling.

3. ANALYSIS OF PERFORMANCE

The following sections document the technical basis for determining the long-term performance of the ICDF landfill based on the radionuclide inventory of the proposed waste disposal.

3.1 Overview of Analysis

The methods used to analyze the long-term performance of the ICDF landfill are described in this section. Performance is defined in terms of off-Site exposure and dose from radionuclides that may migrate from the ICDF landfill. Analysis of performance therefore requires estimates of the (1) inventory of radionuclides in the facility, (2) release rate of radionuclides from the facility, and (3) concentrations of radionuclides released from the facility in environmental media (air, soil, water). The estimates of radionuclide concentrations in environmental media are used to estimate doses to a hypothetical individual based on an exposure scenario. The exposure scenario is the link between contaminated environmental media and possible detriment to a person exposed to contaminated media. The various pathways of possible exposure are illustrated in Figure 3-1. The analysis begins with the LLW inventories in the ICDF landfill. Radionuclides then migrate from the facility along transport pathways and contaminate environmental media (air, soil, water). Contaminated environmental media may be ingested or inhaled directly, or may be used to produce food products that also become contaminated and are later ingested.

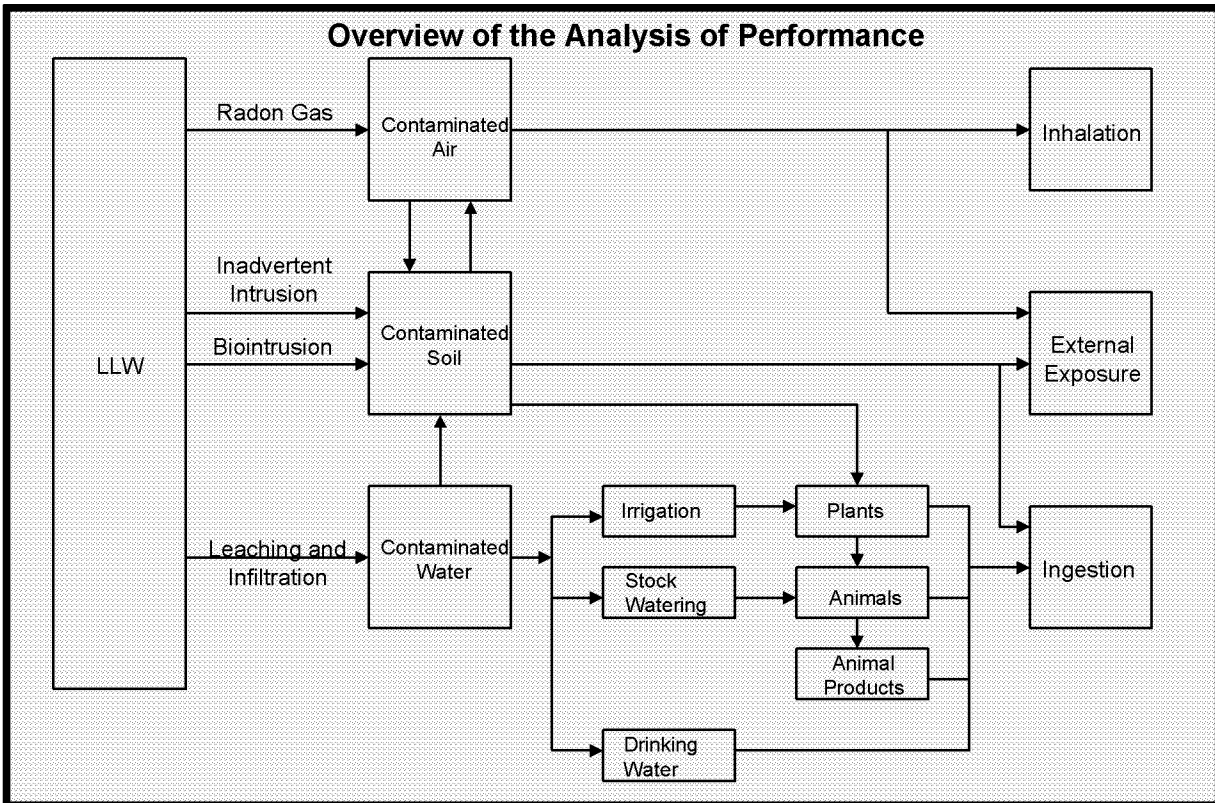


Figure 3-1. Overview of the analysis of performance for the ICDF landfill performance assessment.

This description of the analysis of performance is split into four major sections. In Section 3.2, subsurface transport pathways are covered; in Section 3.3, radon transport pathways are covered; in Section 3.4, biotic pathways are covered; and in Section 3.5, air transport pathways are covered. In each transport pathways section, the source term, radionuclide transport methods, parameter values, relevant exposure scenarios, and dose analysis are described.

3.2 Analysis of Performance: Subsurface Transport Pathways

The analysis of performance for the subsurface transport pathways is described in this section. The section begins with a conceptual model of the facility and surrounding environment.

3.2.1 Conceptual Model of Facility Performance

The subsurface flow and transport conceptual model for the performance assessment is illustrated in Figure 3-2 for the institutional control period and in Figure 3-3 for the postinstitutional control period. In general, the conceptual model was based on the conceptual model used in the engineering design of the ICDF landfill; however, some significant differences exist. These differences are discussed later in this section. The conceptual model contains the following assumptions:

- Radionuclides remain contained within the disposal structure up to the time of closure of the facility in the year 2018.
- A cover placed over the facility limits infiltration into the waste to 0.01 cm/yr. The cover has been designed to last for 1,000 years (EDF-ER-281). However, the conservative analysis for this performance assessment assumes the cover will perform as designed for 500 years (one-half the design life) until the year 2518 and then fail over a 500-year period from 2518 until 3018. During the period from year 2518 until 3018, the cover gradually deteriorates and the infiltration through the cover linearly increases from 0.01 cm/yr in year 2518 until it returns to its background rate (1 cm/yr) in year 3018.
- The cover only restricts water flow through the waste. While the cover is in place, most moisture runs off the cover into the surrounding soil where it infiltrates. A small amount (0.01 cm/yr) passes through the cover and into the waste. The enhanced infiltration around the cover results in vadose zone water travel times that are equivalent to background vadose zone water travel times. (See Figure 3-2 and Figure 3-3 for the conceptual models during and after the period that the cover remains intact.)
- Vadose zone water travel times are unchanged by the presence of the cover.
- The waste is homogeneously mixed with soil. No release from the ICDF landfill is assumed during its operational lifetime (2003 to 2018).
- Radionuclides that leach from the waste soil travel vertically and mix instantaneously in a clay layer below the waste.
- Release from the waste and clay layer is described by first-order processes.
- Vadose zone water travel times through fractured basalt are instantaneous, leaving only travel times through the sedimentary interbeds to be important.
- The aquifer is composed of an equivalent homogeneous porous medium of infinite lateral extent and finite thickness.

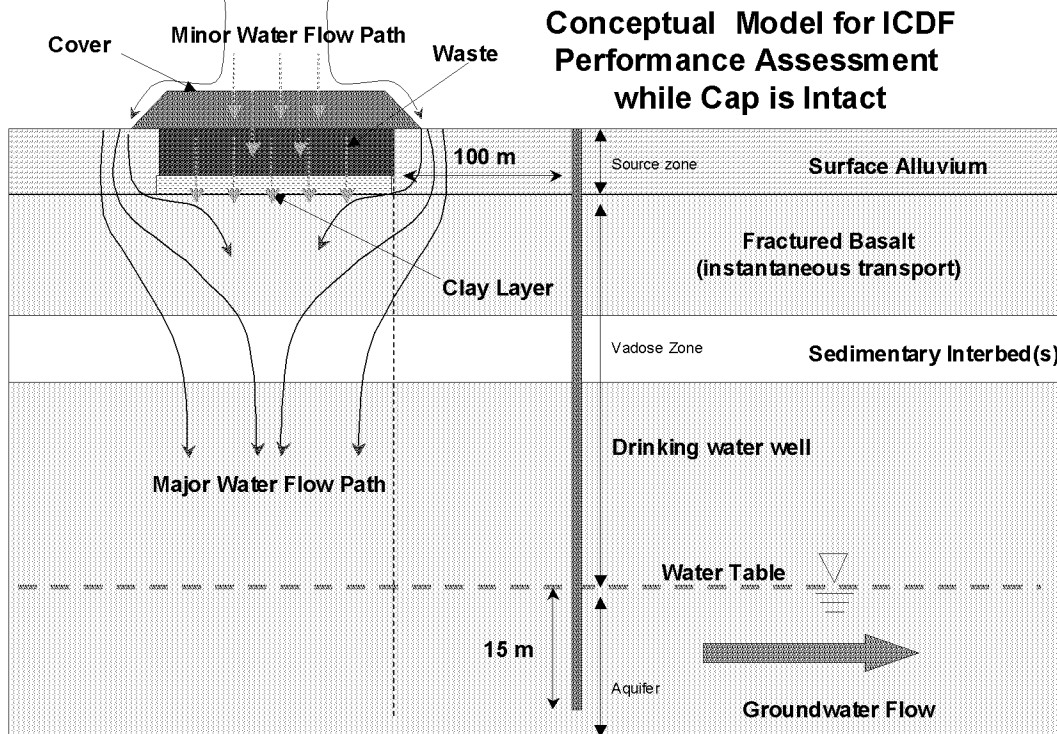


Figure 3-2. Conceptual model for the ICDF landfill performance assessment while the cover is intact.

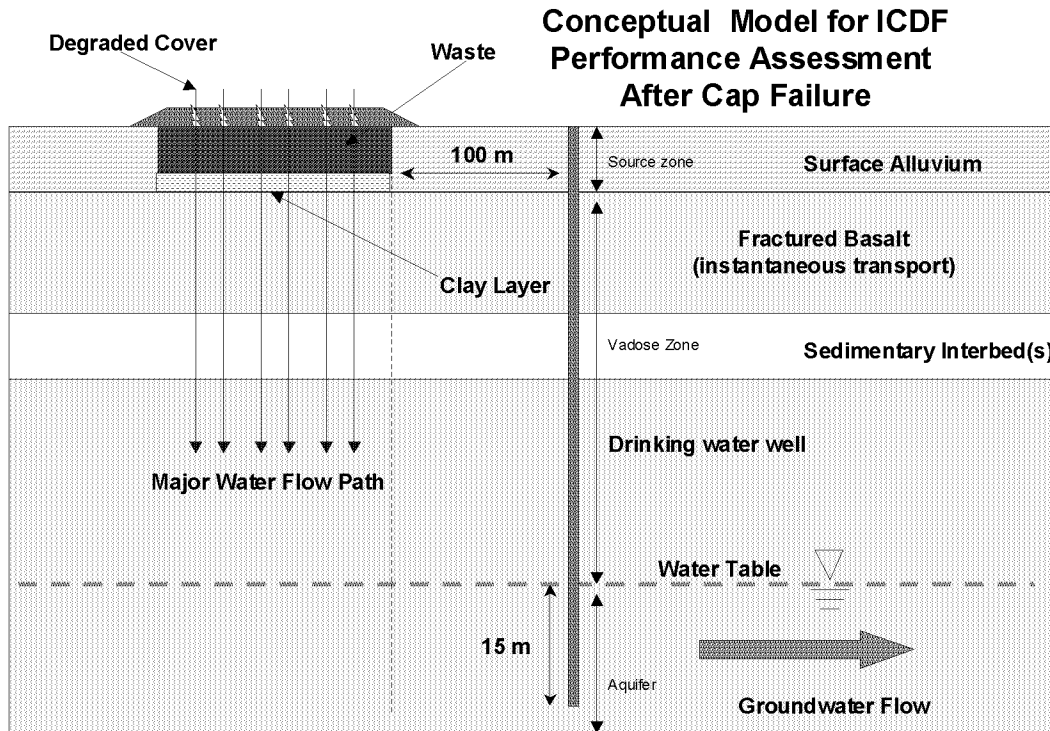


Figure 3-3. Conceptual model for the ICDF landfill performance assessment after cover failure.

Differences between the performance assessment conceptual model and the conceptual model used in the engineering design of the facility were mainly related to the influence of the cover on water travel times through the subsurface. The ICDF landfill design model assumes the cover remains intact for all future times and that infiltration in the subsurface is directly proportional to the infiltration through the cover. The performance assessment conceptual model assumes the cover remains intact for 500 years. After 500 years, the cover degrades over the next 500 years, with the net infiltration rate increasing from 0.01 cm/yr to 1 cm/yr (background infiltration rate) as a linear increasing rate. Additionally, the performance assessment conceptual model assumes the background infiltration rate and not infiltration through the cover dictate infiltration (that is, travel times) in the subsurface. The PA assumption that the cover does not influence water travel times in the vadose zone results in a conservative estimate of transport from the ICDF landfill compared to the ICDF landfill design model assumptions. It is therefore expected that performance assessment doses will exceed engineering design model doses.

3.2.1.1 Model Selection for Implementation of Conceptual Model. Design of the engineered barrier for the ICDF facility utilized the STOMP code (PNL 1996) for flow and transport calculations. The STOMP code is fully capable of addressing the conceptual model described earlier; however, the conceptual model may easily be represented by a far more simple computer model that may also be more conducive to Monte Carlo sensitivity-uncertainty analysis. The computer model selected for these calculations was GWSCREEN Version 2.5 (Rood 1999). This model adapts well to the conceptual model for transport in the unsaturated and saturated zone. GWSCREEN was developed for assessment of the groundwater pathway from leaching of radioactive and nonradioactive substances from surface or buried sources. The code was designed for implementation in the Track 1 and Track 2 assessment of CERCLA sites identified as low probability hazard at the INEEL (DOE-ID 1994). The code uses a mass conservation approach to model three processes: contaminant release from a source volume, vertical contaminant transport in the unsaturated zone, and 2- or 3-dimensional contaminant transport in the saturated zone. Optionally, the source term may be calculated external to GWSCREEN. In this case, fluxes to the vadose zone must be provided to GWSCREEN.

The computational framework for GWSCREEN has its roots in the methodology presented by the Nuclear Regulatory Commission (Codell et al. 1982; Kozak et al. 1990). Similar methodologies have also been employed in several other assessment codes including the Remedial Action Priority System (Whelan et al. 1996) and DECHEM (Killough et al. 1991). The groundwater transport model used in GWSCREEN has been used at the INEEL for scoping and assessment purposes (Codell et al. 1982; Rood et al. 1989) and has been shown to give reasonable results when calibrated to measured data.

GWSCREEN has been validated against other codes using similar algorithms and techniques (Smith and Whitaker 1993). The code was originally designed for assessment and screening of the groundwater pathway when field data are limited. It was intended to simulate relatively simple conceptual systems and may serve as a predictive tool when the system can be described as such. Furthermore, GWSCREEN under simple conceptual systems is well suited for regulatory compliance calculations such as the ICDF landfill performance assessment. The conceptual representation of the site as presented in EDF-ER-275 lends itself very well to the GWSCREEN framework. Although the design conceptual model in EDF-ER-275 included more complexity than the GWSCREEN representation (for example, explicit treatment of basalt layers), the net effect of these complexities is overridden by the parameters and assumptions that drive the system. In particular, the assumed time of cover integrity and the assumed infiltration rate account for much of the behavior of the model. Using similar assumptions about infiltration and cover integrity, both model applications (STOMP and GWSCREEN) were shown to provide comparable results.

Three applications of GWSCREEN were used in the ICDF PA: (1) a deterministic simulation of nuclide screening, (2) a deterministic simulation of ICDF performance, and (3) a stochastic simulation of ICDF performance. The screening application of GWSCREEN used the built-in source term model and conservative assumptions and parameter values to identify those nuclides that have potential for significant dose. For the performance assessment applications, the built-in source term model in GWSCREEN was disabled. Radionuclide fluxes to the unsaturated zone were provided by an external source term model described in Section 3.2.3.2.

3.2.2 Exposure Pathways and Scenarios

Exposure scenarios are the link between contaminated environmental media and the exposure of a hypothetical receptor. They are essentially statements and parameter values that describe the behavior of a hypothetical receptor. Two scenarios were considered for the subsurface transport pathways: the all-pathways scenario and the drinking water scenario.

3.2.2.1 All-Pathways Scenario. The methodology used to calculate the all-pathways dose is based on the methodology presented in NRC (1977) and Peterson (1983). The all-pathways scenario assumes a receptor consumes (1) contaminated groundwater, (2) leafy vegetables and produce that were irrigated with contaminated groundwater, and (3) milk and meat from animals that consume contaminated water and pasture grass irrigated with contaminated groundwater. The receptor is located 100 m downgradient from the downgradient edge of the ICDF landfill for all times following facility closure in the year 2018. Tables 3-1 and 3-2 contain the parameter values used in the all-pathways dose calculation followed by equations used to calculate the dose from each exposure pathway. Values listed in Table 3-2 are only for the nuclides that were deemed significant through the screening process (see Section 3.2.3).

The dose from human consumption of drinking water is calculated using

$$D = C_{GW} \times U_W \times DCF \quad (3-1)$$

where

- D = dose (cumulative effective dose equivalent) from one year's consumption of contaminated media, in this case groundwater (rem/yr)
- C_{GW} = radionuclide concentration in groundwater (Ci/L)
- U_W = human consumption rate of water (L/yr)
- DCF = ingestion dose conversion factor (rem/Ci).

Table 3-1. Element-independent parameter values used in the all-pathways dose calculation.

Parameter	Symbol	Units	Value	Reference
Water ingestion rate (human)	U	L/yr	7.30E+02	EPA (1989c)
Water ingestion rate (beef cow)	Q _w	L/d	5.00E+01	NRC (1977)
Water ingestion rate (milk cow)	Q _w	L/d	6.00E+01	NRC (1977)
Feed consumption, beef cow (dry weight)	Q _F	kg/d	1.20E+01	NCRP (1984)
Feed consumption, milk cow (dry weight)	Q _F	kg/d	1.60E+01	NCRP (1984)
Meat consumption	U _B	kg/yr	8.50E+01	Rupp (1980)
Milk consumption	U _M	L/yr	1.12E+02	Rupp (1980)
Produce consumption	U _P	kg/yr	1.76E+02	Rupp (1980)
Leafy vegetable consumption	U _{LV}	kg/yr	1.80E+01	Rupp (1980)
Irrigation rate	I	L/m ² -d	8.47E+00	Site-specific
Washoff constant	K	1/mm	2.50E-02	Peterson (1983)
Yield, leafy vegetables (wet weight)	R/Y _v	kg/m ²	7.60E-02	Calculated from Baes and Orton (1979) and Baes et al. (1984)
Yield, produce (wet weight)	R/Y _v	kg/m ²	3.20E-02	Calculated from Baes and Orton (1979) and Baes et al. (1984)
Yield, pasture grass (dry weight)	R/Y _v	kg/m ²	2.00E+00	Calculated from Baes and Orton (1979) and Baes et al. (1984)
Areal density (dry weight)	P	kg/m ²	2.25E+02	DOE-ID (1987)
Irrigation time	T _i	d	9.00E+01	Site-specific
Buildup time	t _b	d	3.65E+02	Site-specific
Fraction of year irrigated	f _i	—	2.50E-01	Site-specific
Translocation factor (leafy veg)	T	—	1.00E+00	Ng et al. (1978)
Translocation factor (produce)	T	—	1.00E-01	Ng et al. (1978)
Washing factor (leafy veg.)	DF	—	5.00E-01	Ng et al. (1978)
Washing factor (produce)	DF	—	1.00E+00	Ng et al. (1978)
Fraction of produce produced locally	FV	—	7.00E-01	EPA (1989d)
Fraction of beef produced locally	FB	—	4.42E-01	EPA (1989d)
Fraction of milk produced locally	FM	—	3.99E-01	EPA (1989d)

Table 3-2. Element-specific parameter values used in the all-pathways dose calculation.^a

Element	Meat Transfer Coefficient (d/kg)	Milk Transfer Coefficient (d/L)	Concentration Ratio (wet weight)	Concentration Ratio (dry weight)
Actinium	2.50E-05	2.00E-05	1.50E-04	3.50E-03
Iodine	7.00E-03	1.00E-02	2.10E-02	1.50E-01
Lead	3.00E-04	2.50E-04	3.90E-03	4.50E-02
Neptunium	5.50E-05	5.00E-06	4.30E-03	1.00E-01
Plutonium	5.00E-07	1.00E-07	1.90E-05	4.50E-04
Protactinium	1.00E-05	5.00E-06	1.10E-04	2.50E-03
Radium	2.50E-04	4.50E-04	6.40E-04	1.50E-02
Technicium	8.50E-03	1.00E-02	6.40E-01	9.50E+00
Thorium	6.00E-06	5.00E-06	3.60E-05	8.50E-04
Uranium	2.00E-04	6.00E-04	1.70E-03	8.50E-03

a. All values from Baes et al. (1984).

The beef and dairy exposure route assumes cattle drink contaminated stock water and the receptor in turn consumes the contaminated beef and milk from the cattle. Meat and milk are treated separately. The dose is calculated using

Meat:

$$D = C_{GW} \times Q_w \times F_f \times U_B \times DCF \times FB \quad (3-2)$$

Milk:

$$D = C_{GW} \times Q_w \times F_m \times U_M \times DCF \times FM \quad (3-3)$$

where

- Q_w = consumption rate of water by beef or milk cattle (L/d)
- F_f = meat transfer coefficient (d/kg)
- U_B = human consumption rate of meat (kg/yr)
- FB = fraction of beef produced locally (unitless)
- F_m = milk transfer coefficient (d/L)
- U_M = human consumption rate of milk (L/yr)
- FM = fraction of milk produced locally (unitless).

The dose to humans from ingestion of contaminated leafy vegetables and produce is calculated assuming two contamination routes: (1) direct deposition of contaminated irrigation water on plants and (2) deposition of contaminated irrigation water on soil followed by root uptake by plants. Leafy vegetables and produce are treated separately. The dose through direct deposition is calculated using

Leafy Vegetables - Direct Deposition:

$$D = \frac{C_{GW} \times I \times r}{Y_v} \times \frac{1 - e^{-(\lambda_r + KI)t_i}}{\lambda_r + KI} \times U_{LV} \times DCF \times DF \times T \times FV \quad (3-4)$$

Produce - Direct Deposition:

$$D = \frac{C_{GW} \times I \times r}{Y_v} \times \frac{1 - e^{-(\lambda_r + KI)t_i}}{\lambda_r + KI} \times U_P \times DCF \times DF \times T \times FV \quad (3-5)$$

where

- I = irrigation rate (L/m²-d)
- r = interception fraction (unitless)

- Y_v = agricultural yield (kg/m², wet weight)
 λ_r = radioactive decay constant (d⁻¹)
 k = washoff constant (mm⁻¹)
 t_i = irrigation time (d).
 U_{LV} = human consumption rate of leafy vegetables (kg/yr)
 DF = fraction of activity remaining after preparation and processing (unitless)
 T = translocation factor (unitless)
 FV = fraction of leafy vegetables and produce produced locally (unitless)
 U_p = human consumption rate of produce (kg/yr).

The product kI is also known as the weathering rate constant because of washoff (Peterson 1983). This quantity describes the rate at which material is removed from plant surfaces by water and is analogous to λ_e , the weathering rate constant used in nonirrigation situations. The value of kI is calculated using

$$kI = 0.025 \text{ mm}^{-1} \times \frac{8.47L}{m^2 \cdot d} \times \frac{1m^3}{1,000L} \times \frac{1,000mm}{1m} = 0.212/d \quad (3-6)$$

The dose from deposition of contaminated irrigation water on soil followed by root uptake by plants and human consumption of plants is calculated using the following equations. Credit is not taken for leaching of radionuclides from the root zone of plants.

Leafy Vegetables - Root Uptake:

$$D = \frac{C_{GW} \times I \times f_I}{P} \times \frac{1 - e^{-\lambda_r t_{bi}}}{\lambda_r + kI} \times CR \times U_{LV} \times DCF \times FV \quad (3-7)$$

Produce - Root Uptake:

$$D = \frac{C_{GW} \times I \times f_I}{P} \times \frac{1 - e^{-\lambda_r t_{bi}}}{\lambda_r + kI} \times CR \times U_p \times DCF \times FV \quad (3-8)$$

where

- f_I = fraction of the year that crops are irrigated (unitless)
 P = areal density [kg (dry weight soil)/m²]
 CR = concentration ratio [pCi/kg (wet weight plant) / pCi/kg (dry weight soil)]
 t_b = build-up time for radionuclides in soil (d).

The dose to humans from ingestion of contaminated animal products is also calculated assuming two contamination routes: (1) direct deposition and (2) root uptake; meat and milk are treated separately. All food (pasture or stored feed) eaten by cattle is assumed to be contaminated. The dose through direct deposition is calculated using

Meat - Direct Deposition:

$$D = \frac{C_{GW} \times I \times r}{Y_v} \times \frac{1 - e^{-(\lambda_r + KI)t_i}}{\lambda_r + KI} \times Q_F \times F_f \times U_B \times \frac{10^{-6} \mu\text{Ci}}{\text{pCi}} \times DCF \times \frac{1,000 \text{mrem}}{\text{rem}} \times FB \quad (3-9)$$

Milk - Direct Deposition:

$$D = \frac{C_{GW} \times I \times r}{Y_v} \times \frac{1 - e^{-(\lambda_r + KI)t_i}}{\lambda_r + KI} \times Q_F \times F_m \times U_M \times DCF \times FM \quad (3-10)$$

where

Y_v = agricultural yield (kg/m², dry weight)

Q_F = animal consumption rate of pasture and feed [kg (dry)/d].

The dose through deposition on soil followed by root uptake is calculated using the following equations. As with produce and leafy vegetables, credit is not taken for leaching of radionuclides from the root zone of plants.

Meat - Root Uptake:

$$D = \frac{C_{GW} \times I \times f_l}{P} \times \frac{1 - e^{-\lambda_r t_{bi}}}{\lambda_r} \times CR \times Q_F \times F_f \times U_B \times DCF \times FB \quad (3-11)$$

Milk - Root Uptake:

$$D = \frac{C_{GW} \times I \times f_l}{P} \times \frac{1 - e^{-\lambda_r t_{bi}}}{\lambda_r} \times CR \times Q_F \times F_f \times U_B \times DCF \times FB \quad (3-12)$$

where

CR = concentration ratio [pCi/kg (dry weight plant) / pCi/kg (dry weight soil)].

Note that the term, CR in Equations 3-11 and 3-12 represents the concentration ratio for forage in dry weight. Dry-weight based CR s are needed because animal consumption rates are based on dry weight of forage. Secondary and indirect pathways, such as inhalation of contaminated irrigation water, inhalation of contaminated dust, or external exposure from radionuclides deposited on the soil, were omitted from this scenario. These pathways were either not viewed as credible (e.g., a farmer standing under a center pivot irrigator while it was running and inhaling contaminated irrigation water) or would contribute relatively minor amounts when compared to direct pathways such as direct ingestion of contaminated water.

All-pathways doses were calculated for a unit groundwater concentration (1 Ci/L) and tabulated. These values could then be scaled to the actual groundwater concentration calculated for each nuclide. For the radionuclides of concern, the all-pathways doses for unit concentrations are presented in Section 3.2.4.3 (Table 3-9).

3.2.2.2 Drinking Water Scenario. For the drinking water scenario, the receptor is assumed to consume 2 L of water per day for 365 days per year from a well located 100 m downgradient from the downgradient edge of the ICDF landfill. This scenario is used to compute the dose from direct ingestion of man-made beta-gamma emitting nuclides and compare to the proposed maximum contaminant level of 4 mrem/yr effective dose equivalent. Additionally, gross alpha activity concentrations, Ra-226/Ra-228, and total uranium mass concentrations are also computed at this location.

3.2.3 Radionuclide Inventories and Source Term

The inventory for the ICDF landfill consisted of 210 individual radionuclides. The large number of radionuclides presents difficulties in estimating future dose impacts and dilutes resources from those nuclides that are most important. Therefore, contaminant screening was performed to reduce the number of nuclides to a manageable level and focus resources on those nuclides that are most important. Contaminant screening is discussed below followed by a description of the mathematical model for the source term.

3.2.3.1 Inventory Screening Methodology and Procedure—Contaminant screening typically is applied using two methods: absolute criteria and relative ranking. The absolute criteria method computes a conservative estimate of the individual nuclide dose. This dose is then compared against a criterion. If the dose is greater than the criterion then the nuclide is retained for further evaluation. If the dose is less than the criterion, then the nuclide is screened out and not considered in any further evaluations.

In relative ranking, each nuclide is ranked according to the ratio of the individual nuclide dose to the total dose for all nuclides. Nuclides retained for further evaluation are then selected based on a user-defined criterion. The criterion usually states what fraction of the total dose a nuclide must be above to be retained for further analysis. While this process from the outside appears to be simple and attractive, it contains a number of serious pitfalls. Namely, the procedure used to calculate the dose must realistically simulate nuclide behavior in the environment and must be consistent across all exposure scenarios. A conservative estimate of the dose is not appropriate for relative ranking because nuclide dose is highly dependent on its environmental behavior. Nuclides with lower relative doses may be eliminated prematurely because of unrealistically high doses from other nuclides, which, under realistic conditions, may not be important at all. Based on the above discussion, the screening method will use an absolute criterion coupled with a conservative fate and transport model and exposure scenario.

Screening was performed in three phases. Phase I screening eliminated nuclides based on their half-life. Phase II screening used screening factors developed by the National Council on Radiation Protection (NCRP) (NCRP 1996) to screen radionuclides. Phase III screening used a simple and conservative application of the GWSCREEN (Rood 1999) model to calculate a screening dose. The GWSCREEN application considers dilution, dispersion, and unsaturated transit time, whereas the NCRP does not. The Phase III screening application of GWSCREEN was substantially different than its application in the fate and transport calculations for the performance assessment described later in this chapter.

3.2.3.1.1 Phase I Inventory Screening—Some nuclides can be eliminated from consideration early in the screening process based on their half-life. Nuclides with half-lives of less than

1 year were eliminated from further consideration based on a conservative estimate of the unsaturated travel time. Assuming a 10-m-thick sedimentary interbed thickness (average interbed thickness in the INTEC area is ~11 m), and the Track 2 (DOE-ID 1994) default infiltration rate (10 cm/yr) and moisture content of 30% yields a mean unsaturated travel time of 30 years. After 30 years, a nuclide with a 1-year half-life would only have 9.3×10^{-10} of its original activity. Therefore, nuclides with half-lives of 1 year or less are not expected to contribute significantly to dose from the groundwater pathway. The 1-year half-life is the same screening cutoff that the NCRP has implemented in its groundwater screening models.

Nuclide inventories and Phase I screening results are presented in Table 3-3. Of the 210 nuclides listed in the inventory, 88 nuclides remained after the Phase I screen. Two other nuclides were omitted because they are essentially stable isotopes (La-138 and Ce-142) leaving 86 nuclides to evaluate in the Phase II screening. Many of the nuclides screened were short-lived progeny of longer-lived parent nuclides. These short-lived progeny generally do not exist without the presence of their parent. It is important to note that these nuclides were only screened from the initial inventory and that both the Phase II screening (NCRP screening methodology) and the Phase III screening (GWSCREEN methodology) includes the ingrowth of these progeny from their parent nuclides over time.

3.2.3.1.2 Phase II Inventory Screening—The NCRP provides a series of simple screening techniques and factors that can be used to demonstrate compliance with environmental standards or other administratively set reference levels for releases of radionuclides to the atmosphere, surface water, or groundwater. The screening factor is essentially a dose conversion factor having units of total EDE per unit of activity (Sv/Bq). These factors incorporate radionuclide fate and transport processes and an assumed exposure scenario to calculate the annual total EDE to a hypothetical receptor per unit of activity in the radionuclide inventory. The screening factors applicable to groundwater exposure consider leaching and subsequent dilution of radionuclides in groundwater from a generic waste site. Factors are calculated for six delay times: 0, 2, 10, 30, 100, and 1,000 years. During the delay time, radionuclide inventories are only depleted by radioactivity decay. The maximum of the six values is then reported in the screening factor tables for groundwater.

The exposure scenario essentially has the entire waste inventory susceptible to leaching over the period of 1 year into a water volume equal to the annual average per capita use of groundwater in rural regions of the United States (91,000 L). The receptor is then assumed to drink 800 L of this contaminated water over the period of a year and their dose is computed for that intake.

The screening factor for groundwater is given by (NCRP 1996):

$$SF = \lambda_L A_o \frac{U_{DW}}{V} \sum_{i=0}^N X_i DCF_{ing,i} \quad (3-13)$$

where

- SF = groundwater screening factor (Sv/Bq)
- λ_L = leach rate constant (yr^{-1})
- A_o = initial activity (Bq)
- U_{DW} = consumption of drinking water (assumed to be 800 L/yr)
- V = dilution volume (assumed to be 91,000 L)

Table 3-3. Radionuclide inventories and half-lives. Nuclides with half-lives less than 1 year were removed from further consideration and are shown in bold.

Radionuclide	Half-life (years)	ICDF PA Inventory (Ci)	Is half-life less than 1 year?	Radionuclide	Half-life (years)	ICDF PA Inventory (Ci)	Is half-life less than 1 year?	Radionuclide	Half-life (years)	ICDF PA Inventory (Ci)	Is half-life less than 1 year?
Ac-225	2.74E-02	3.89E-08	Yes	I-131	2.20E-02	0.00E+00	Yes	Rn-219	1.25E-07	1.54E-05	Yes
Ac-227	2.18E+01	1.55E-05		In-114	2.28E-06	1.43E-54	Yes	Rn-220	1.76E-06	4.20E-04	Yes
Ac-228	6.99E-04	1.16E-10	Yes	In-114m	1.36E-01	1.50E-54	Yes	Rn-222	1.05E-02	4.71E-06	Yes
Ag-106	4.56E-05	0.00E+00	Yes	In-115	4.60E+15	4.39E-12		Ru-103	1.08E-01	1.52E-29	Yes
Ag-108	4.51E-06	2.80E-09	Yes	In-115m	5.12E-04	0.00E+00	Yes	Ru-106	1.01E+00	9.21E-03	
Ag-108m	1.27E+02	6.07E-01		K-40	1.28E+09	1.45E+00		Sb-124	1.65E-01	1.57E-40	Yes
Ag-109m	1.25E-06	3.73E-12	Yes	Kr-81	2.10E+05	4.02E-09		Sb-125	2.77E+00	7.04E+00	
Ag-110	7.79E-07	3.93E-11	Yes	Kr-85	1.07E+01	8.79E+02		Sb-126	1.24E+01	1.56E-02	
Ag-110m	6.84E-01	4.21E-09	Yes	La-138	stable	0.00E+00		Sb-126m	3.61E-05	1.12E-01	Yes
Ag-111	2.04E-02	0.00E+00	Yes	La-140	4.59E-03	2.01E-105	Yes	Sc-46	2.30E-01	2.16E-20	Yes
Am-241	4.32E+02	1.81E+01		Mn-54	8.56E-01	1.47E-08	Yes	Se-79	6.50E+04	1.26E-01	
Am-242	1.83E-03	3.44E-05	Yes	Nb-92	3.60E+07	4.82E-19		Sm-146	7.00E+07	3.23E-10	
Am-242m	1.52E+02	3.43E-05		Nb-93m	1.46E+01	1.02E-02		Sm-147	1.06E+11	3.11E-06	
Am-243	7.38E+03	2.53E-04		Nb-94	2.03E+04	6.70E-06		Sm-148	1.20E+13	7.66E-13	
Am-245	2.40E-04	0.00E+00	Yes	Nb-95	9.60E-02	3.64E-33	Yes	Sm-149	4.00E+14	3.89E-12	
Am-246	4.75E-05	1.05E-25	Yes	Nb-95m	9.88E-03	1.40E-35	Yes	Sm-151	9.00E+01	2.56E+02	
At-217	1.01E-09	3.89E-08	Yes	Nd-144	5.00E+15	2.48E-10		Sn-117m	3.72E-02	0.00E+00	Yes
Ba-136m	1.01E-08	0.00E+00	Yes	Nd-147	3.01E-02	0.00E+00	Yes	Sn-119m	8.02E-01	1.13E-07	Yes
Ba-137m	4.85E-06	1.75E+04	Yes	Np-235	1.08E+00	5.16E-11		Sn-121m	7.60E+01	2.04E-02	
Ba-140	3.50E-02	0.00E+00	Yes	Np-236	1.15E+05	5.26E-08		Sn-123	3.54E-01	6.39E-17	Yes
Be-10	1.60E+06	8.67E-07		Np-237	2.14E+06	4.88E-01		Sn-125	2.64E-02	0.00E+00	Yes
Bi-210	1.37E-02	8.29E-07	Yes	Np-238	5.80E-03	1.65E-07	Yes	Sn-126	1.00E+05	1.12E-01	
Bi-211	4.05E-06	1.39E-05	Yes	Np-239	6.45E-03	2.53E-04	Yes	Sr-89	1.38E-01	4.54E-44	Yes
Bi-212	1.15E-04	4.20E-04	Yes	Np-240	1.24E-04	2.12E-14	Yes	Sr-90	2.86E+01	1.74E+04	
Bi-213	8.68E-05	0.00E+00	Yes	Np-240m	1.41E-05	1.93E-11	Yes	Tb-160	1.98E-01	2.41E-34	Yes
Bi-214	3.78E-05	4.26E-06	Yes	Pa-231	3.73E+04	5.30E-05		Tb-161	1.89E-02	0.00E+00	Yes
Bk-249	8.76E-01	1.64E-21	Yes	Pa-233	7.39E-02	3.31E-02	Yes	Tc-98	4.20E+06	1.34E-07	
Bk-250	3.68E-04	5.88E-26	Yes	Pa-234	7.64E-04	2.08E-06	Yes	Tc-99	2.13E+05	4.37E+00	
C-14	5.73E+03	3.50E-05		Pa-234m	2.22E-06	1.30E-03	Yes	Te-123	1.00E+13	3.43E-15	
Cd-109	1.27E+00	3.73E-12		Pb-209	3.71E-04	3.68E-08	Yes	Te-123m	3.28E-01	2.24E-23	Yes
Cd-113m	1.37E+01	1.23E+00		Pb-210	2.23E+01	8.29E-07		Te-125m	1.59E-01	1.72E+00	Yes
Cd-115m	1.22E-01	3.23E-54	Yes	Pb-211	6.86E-05	1.39E-05	Yes	Te-127	1.07E-03	7.10E-20	Yes
Ce-141	8.90E-02	1.37E-71	Yes	Pb-212	1.21E-03	4.20E-04	Yes	Te-127m	2.98E-01	7.21E-20	Yes
Ce-142	stable	0.00E+00		Pb-214	5.10E-05	4.26E-06	Yes	Te-129	1.32E-04	5.12E-71	Yes
Ce-144	7.78E-01	1.37E-03	Yes	Pd-107	6.50E+06	4.64E-03		Te-129m	9.20E-02	8.13E-71	Yes
Cf-249	3.51E+02	3.13E-16		Pm-146	5.53E+00	4.41E-03		Th-226	5.87E-05	1.65E-117	Yes

Table 3-3. (continued).

Radionuclide	Half-life (years)	ICDF PA Inventory (Ci)	Is half-life less than 1 year?	Radionuclide	Half-life (years)	ICDF PA Inventory (Ci)	Is half-life less than 1 year?	Radionuclide	Half-life (years)	ICDF PA Inventory (Ci)	Is half-life less than 1 year?
Cf-250	1.31E+01	1.60E-16		Pm-147	2.62E+00	2.90E+02		Th-227	5.13E-02	1.38E-05	Yes
Cf-251	9.00E+02	7.22E-19		Pm-148	1.47E-02	3.02E-59	Yes	Th-228	1.91E+00	2.50E-02	
Cf-252	2.64E+00	1.70E-20		Pm-148m	1.13E-01	6.25E-58	Yes	Th-229	7.34E+03	3.89E-08	
Cm-241	9.58E-02	9.84E-81	Yes	Po-210	3.79E-01	7.70E-07	Yes	Th-230	7.70E+04	1.32E-01	
Cm-242	4.47E-01	4.09E-17	Yes	Po-211	1.64E-08	5.19E-10	Yes	Th-231	2.91E-03	1.22E-01	Yes
Cm-243	2.85E+01	2.70E-06		Po-212	9.44E-15	2.49E-04	Yes	Th-232	1.40E+10	1.18E-01	
Cm-244	1.81E+01	1.37E-03		Po-213	1.33E-13	3.30E-08	Yes	Th-234	6.60E-02	1.30E-03	Yes
Cm-245	8.50E+03	6.09E-08		Po-214	5.20E-12	4.26E-06	Yes	Tl-207	9.07E-06	1.39E-05	Yes
Cm-246	4.75E+03	1.36E-09		Po-215	6.34E-11	1.39E-05	Yes	Tl-208	5.80E-06	1.50E-04	Yes
Cm-247	1.56E+07	4.85E-16		Po-216	4.63E-09	4.20E-04	Yes	Tl-209	4.18E-06	7.98E-10	Yes
Cm-248	3.39E+05	1.48E-16		Po-218	5.80E-06	4.26E-06	Yes	Tm-170	3.52E-01	4.84E-26	Yes
Cm-250	6.90E+03	4.20E-25		Pr-143	3.71E-02	0.00E+00	Yes	Tm-171	1.92E+00	1.21E-12	
Co-57	7.42E-01	2.80E-03	Yes	Pr-144	3.29E-05	1.34E-03	Yes	U-230	5.69E-02	0.00E+00	Yes
Co-58	1.94E-01	4.46E-17	Yes	Pr-144m	1.37E-05	1.92E-05	Yes	U-232	7.20E+01	4.06E-04	
Co-60	5.27E+00	1.47E+02		Pu-236	2.85E+00	4.20E-06		U-233	1.59E+05	1.94E-05	
Cr-51	7.39E-02	1.75E-54	Yes	Pu-237	1.24E-01	9.18E-59	Yes	U-234	2.44E+05	4.57E+00	
Cs-132	1.77E-02	0.00E+00	Yes	Pu-238	8.78E+01	1.77E+02		U-235	7.04E+08	8.37E-02	
Cs-134	2.06E+00	8.51E+00		Pu-239	2.41E+04	5.06E+00		U-236	2.34E+07	1.53E-01	
Cs-135	2.30E+06	2.72E-02		Pu-240	6.57E+03	1.14E+00		U-237	1.85E-02	0.00E+00	Yes
Cs-136	3.60E-02	0.00E+00	Yes	Pu-241	1.44E+01	4.85E+01		U-238	4.47E+09	1.48E+00	
Cs-137	3.02E+01	1.85E+04		Pu-242	3.76E+05	1.83E-04		U-240	1.61E-03	1.93E-11	Yes
Er-169	2.57E-02	0.00E+00	Yes	Pu-243	5.65E-04	4.85E-16	Yes	Xe-127	9.97E-02	1.20E-72	Yes
Eu-150	5.00E+00	1.31E-08		Pu-244	8.26E+07	1.93E-11		Xe-129m	2.43E-02	0.00E+00	Yes
Eu-152	1.36E+01	7.34E+02		Pu-246	2.97E-02	1.05E-25	Yes	Xe-131m	3.24E-02	2.04E-112	Yes
Eu-154	8.80E+00	6.23E+02		Ra-222	1.20E-06	8.87E-117	Yes	Xe-133	1.44E-02	0.00E+00	Yes
Eu-155	4.96E+00	1.34E+02		Ra-223	3.13E-02	1.54E-05	Yes	Y-90	7.31E-03	1.74E+04	Yes
Eu-156	4.16E-02	0.00E+00	Yes	Ra-224	9.91E-03	4.20E-04	Yes	Y-91	1.60E-01	3.15E-37	Yes
Fe-59	1.22E-01	3.42E-35	Yes	Ra-225	4.05E-02	3.89E-08	Yes	Zn-65	6.69E-01	2.05E-09	Yes
Fr-221	9.13E-06	3.89E-08	Yes	Ra-226	1.60E+03	3.60E-01		Zr-93	1.53E+06	6.50E-01	
Fr-223	4.14E-05	2.14E-07	Yes	Ra-228	5.75E+00	1.16E-10		Zr-95	1.75E-01	2.22E-25	Yes
Gd-152	1.10E+14	2.06E-14		Rb-86	5.11E-02	0.00E+00	Yes				
Gd-153	6.61E-01	1.53E-11	Yes	Rb-87	4.73E+10	8.46E-06					
H-3	1.23E+01	3.76E+01		Rh-102	2.90E+00	2.26E-05					
Hf-181	1.16E-01	5.92E-37	Yes	Rh-103m	1.07E-04	2.14E-58	Yes				
Ho-166m	1.20E+03	2.05E-06		Rh-106	9.51E-07	8.63E-03	Yes				
I-129	1.57E+07	9.85E-01		Rn-218	1.11E-09	9.56E-117	Yes				

- X_i = annual average fraction of the original parent activity for decay chain member i
 DCF_{ing} = ingestion dose conversion factor (Sv/Bq)
 N = number of progeny in the decay chain.

Assuming there is 100% containment of the waste during the delay time, and the release of radioactivity is averaged over the first year of the release following the delay time, the fraction of the original parent activity leached to the dilution volume over a year for the parent (X_0) is given by

$$X_0 = \frac{\left(1 - e^{-(\lambda_L + \lambda_0^r)T_{avg}}\right) e^{-\lambda_0^r T_{del}}}{T_{avg} (\lambda_L + \lambda_0^r)} \quad (3-14)$$

where

- λ_0^r = radioactive decay rate constant for parent (yr^{-1})
 T_{avg} = averaging time (1 yr)
 T_{del} = delay time (yr).

A typographical error in Equation 3-14 was noted in the NCRP text. The fraction of progeny activity relative to the parent that is leached to the dilution volume is given by

$$X_i = \frac{I}{T_{avg}} \left(\prod_{j=1}^K \lambda_j^r f_j \right) \sum_{h=0}^N \frac{\left(1 - e^{-\lambda_h^r T_{avg}}\right) e^{-\lambda_h^r T_{del}}}{\lambda_h^r \prod_{\substack{p=0 \\ p \neq h}}^K (\lambda_p^r + \lambda_h^r)} \quad (3-15)$$

where

- f_j = fraction of parent decaying to j th progeny
 λ_h^r = radioactive decay rate constant for j th progeny parent (yr^{-1}).

The leach rate constant is taken from formulation described in Baes and Sharp (1983) and used in the models RESRAD (Yu et al. 1993), Multimedia Environmental Pollutant Assessment System (MEPAS) (Whelan et al. 1996), and GWSCREEN (Rood 1999). The leach rate constant is given by

$$\lambda_L = \frac{I}{H \theta \left(1 + \frac{K_d \rho}{\theta} \right)} \quad 3-16$$

where

- I = assumed infiltration rate (0.18 m yr⁻¹)
- H = assumed waste thickness (0.5 m)
- ρ = bulk density (cm³/g)
- K_d = sorption coefficient (cm³/g)
- θ = moisture content (0.3 m³/m³).

Values for the sorption coefficient used in the NCRP screening were taken from Kennedy and Strenge (1992). The assumed infiltration rate represents the upper-bound infiltration rate determined for low-level radioactive waste sites located in the southeastern United States.

The assumption is made in Equation 3-13 that the unsaturated travel time is instantaneous. For the INEEL, this is an extremely conservative assumption because unsaturated contaminant travel times have been estimated to take from several years to hundreds of thousands of years depending on the sorption properties of the contaminant. Under these assumptions, the NCRP groundwater screening model provides a conservative estimate of the potential dose.

Nuclides with an NCRP screening dose of less than 1 mrem (1×10^{-5} Sv) were removed from further consideration. These nuclides are identified in Table 3-4 along with their NCRP screening dose value. The NCRP screening dose is calculated by multiplying the radionuclide inventory by the NCRP screening dose factor. For example, the NCRP screening dose for Ac-227 is

$$SD = 1.55 \times 10^{-5} \text{ Ci} \times 3.7 \times 10^{10} \frac{\text{Bq}}{\text{Ci}} \times 8.1 \times 10^{-12} \frac{\text{Sv}}{\text{Bq}} = 4.65 \times 10^{-6} \text{ Sv} \quad (3-17)$$

For some nuclides, NCRP screening factors were unavailable. Typically this meant the nuclide had an extremely long half-life such that it was essentially a stable isotope (Nd-144, $T_{1/2} = 5 \times 10^{15}$ years), or exposure via groundwater was limited by the physical form of the nuclide (Kr-85). In these two cases, the nuclide was screened from the inventory because ingestion dose factors were unavailable.

Of the 86 nuclides remaining from the Phase I screening, 49 nuclides were screened in Phase II leaving 37 nuclides remaining. These 37 nuclides were then put through the Phase III screening, which is the last step of the screening process.

Table 3-4. Phase II screening results for nuclides with half-lives >1 year using the NCRP screening factors.

Radionuclide	Groundwater Ingestion NCRP Screening Factor (Sv/Bq)	Screening Dose (Sv)	Is Screening Dose <1 mrem? (1×10^{-5} Sv)	Radionuclide	Groundwater Ingestion NCRP Screening Factor (Sv/Bq)	Screening Dose (Sv)	Is Screening Dose <1 mrem? (1×10^{-5} Sv)
Ac-227	8.1E-12	4.65E-06	Yes	Pa-231	1.5E-11	2.94E-05	No
Ag-108m	4.2E-14	9.43E-04	No	Pb-210	5.4E-12	1.66E-07	Yes
Am-241	5.9E-13	3.95E-01	No	Pd-107	2.2E-15	3.78E-07	Yes
Am-242m	1.6E-12	2.03E-06	Yes	Pm-146	2.5E-15	4.08E-07	Yes
Am-243	6.0E-13	5.63E-06	Yes	Pm-147	1.7E-15	1.82E-02	No
Be-10	1.4E-14	4.49E-10	Yes	Pu-236	8.5E-14	1.32E-08	Yes
C-14	1.6E-13	2.07E-07	Yes	Pu-238	1.7E-12	1.11E+01	No
Cd-109	2.8E-14	3.87E-15	Yes	Pu-239	2.0E-12	3.74E-01	No
Cd-113m	6.7E-13	3.05E-02	No	Pu-240	2.0E-12	8.42E-02	No
Cf-249	2.7E-12	3.13E-17	Yes	Pu-241	6.1E-14	1.09E-01	No
Cf-250	7.1E-13	4.20E-18	Yes	Pu-242	1.9E-12	1.28E-05	No
Cf-251	2.7E-12	7.22E-20	Yes	Pu-244	2.2E-12	1.57E-12	Yes
Cf-252	3.5E-13	2.20E-22	Yes	Ra-226	4.6E-12	6.12E-02	No
Cm-243	1.5E-13	1.50E-08	Yes	Ra-228	5.4E-13	2.31E-12	Yes
Cm-244	1.1E-13	5.57E-06	Yes	Rb-87	4.9E-14	1.53E-08	Yes
Cm-245	5.1E-13	1.15E-09	Yes	Rh-102	8.4E-15	7.01E-09	Yes
Cm-246	2.9E-13	1.46E-11	Yes	Ru-106	6.5E-14	2.22E-05	No
Cm-247	3.0E-13	5.38E-18	Yes	Sb-125	3.6E-15	9.37E-04	No
Cm-248	1.1E-12	6.03E-18	Yes	Sb-126	1.3E-32	7.53E-24	Yes
Cm-250	6.3E-12	9.78E-26	Yes	Se-79	2.2E-14	1.02E-04	No
Co-60	5.8E-14	3.15E-01	No	Sm-146	2.8E-13	3.35E-12	Yes
Cs-134	4.2E-15	1.32E-03	No	Sm-147	2.6E-13	3.00E-08	Yes
Cs-135	1.4E-14	1.41E-05	No	Sm-148	none	1.00E-99	Yes
Cs-137	7.7E-14	5.28E+01	No	Sm-149	none	1.00E-99	Yes
Eu-150	1.1E-14	5.34E-12	Yes	Sm-151	1.0E-15	9.48E-03	No
Eu-152	9.1E-15	2.47E-01	No	Sn-121m	1.1E-14	8.30E-06	Yes
Eu-154	1.1E-14	2.54E-01	No	Sn-126	1.1E-13	4.55E-04	No
Eu-155	9.5E-16	4.71E-03	No	Sr-90	3.5E-12	2.25E+03	No
Gd-152	2.2E-13	1.68E-16	Yes	Tc-98	8.7E-12	4.32E-08	Yes
H-3	5.9E-14	8.21E-02	No	Tc-99	3.2E-12	5.17E-01	No
Ho-166m	1.8E-14	1.36E-09	Yes	Te-123	8.1E-15	1.03E-18	Yes
I-129	1.9E-10	6.92E+00	No	Th-228	2.1E-15	1.94E-06	Yes
In-115	1.6E-13	2.60E-14	Yes	Th-229	3.6E-13	5.18E-10	Yes
K-40	5.4E-13	2.91E-02	No	Th-230	5.2E-13	2.53E-03	No
Kr-81	none	0.00E+00	Yes	Th-232	4.8E-13	2.10E-03	No
Kr-85	none	0.00E+00	Yes	Tm-171	1.0E-13	4.48E-15	Yes
Nb-92	none	1.00E-99	Yes	U-232	3.3E-11	4.96E-04	No
Nb-93m	1.4E-15	5.31E-07	Yes	U-233	1.1E-11	7.91E-06	Yes
Nb-94	2.7E-14	6.70E-09	Yes	U-234	4.2E-12	7.11E-01	No
Nd-144	none	1.00E-99	Yes	U-235	1.4E-11	4.33E-02	No
Np-235	6.5E-15	1.24E-14	Yes	U-236	3.4E-12	1.93E-02	No
Np-236	1.8E-14	3.50E-11	Yes	U-238	1.4E-10	7.67E+00	No
Np-237	2.4E-10	4.33E+00	No	Zr-93	1.7E-15	4.09E-05	No

3.2.3.1.3 Phase III Inventory Screening—Phase III screening used a conservative implementation of the groundwater screening model GWSCREEN Version 2.5 (Rood 1999) to calculate groundwater concentrations and ingestion doses for nuclides that were not screened in Phase II screening. The GWSCREEN model was developed to address CERCLA sites at the INEEL. The code, coupled with a set of default parameter values identified in the CERCLA Track 2 risk assessment process (DOE-ID 1994), provides conservative estimates of groundwater concentrations and ingestion doses at the INEEL.

The GWSCREEN conceptual model is illustrated in Figure 3-4. Radionuclides disposed in the ICDF landfill are assumed to be mixed homogeneously with soil and placed in a volume represented by the volume of the ICDF landfill. One-dimensional transport in a 11.6-m-thick unsaturated zone composed of sedimentary interbeds is assumed. The thickness of the sedimentary interbeds assumed for the screening application of GWSCREEN is about one-half the thickness used in the design of the ICDF (EDF-ER-275). The thinner sedimentary interbed thickness is conservative because radionuclide transit times in the unsaturated zone are shorter. The receptor well is placed on the downgradient edge of the source. Note that the receptor distance is measured from the center of the source; therefore, the distance to the receptor well is $160 \text{ m} \div 2 = 80 \text{ m}$. The conceptual model assumes no containment by containers or engineered barriers. The waste is then assumed to be exposed to infiltrating water and contaminants are leached from the waste and move into the subsurface. The Track 2 default infiltration rate is 10 cm/yr.

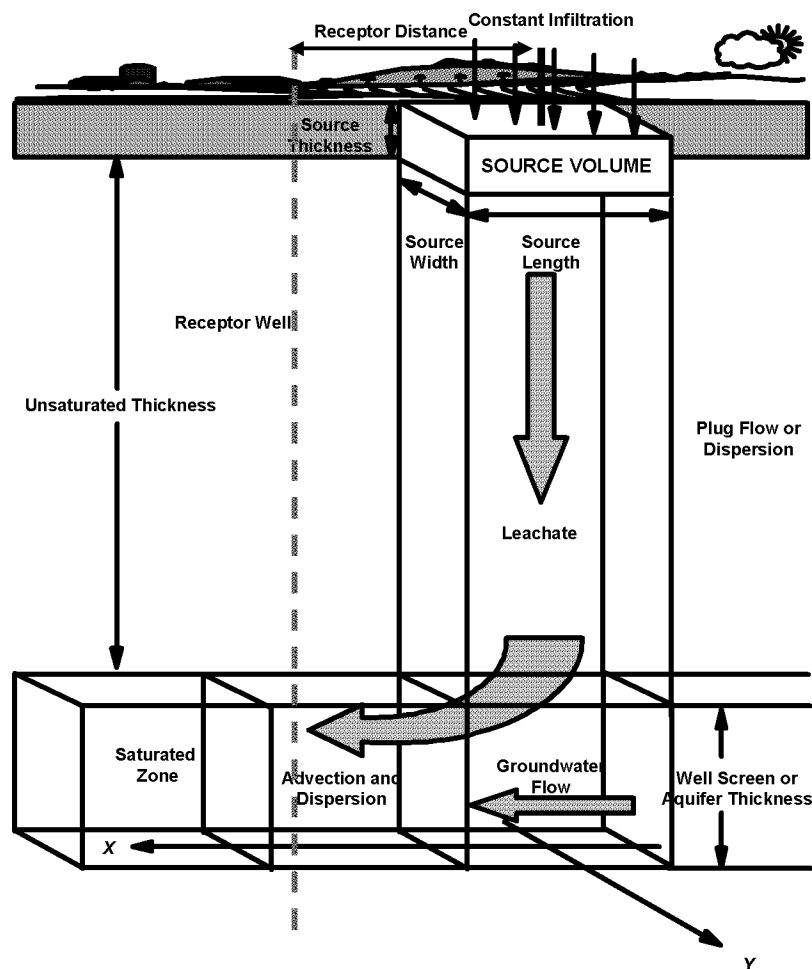


Figure 3-4. Conceptual model for GWSCREEN groundwater transport model.

No dispersion in the unsaturated zone is assumed. The subsurface environment beneath the INEEL is composed of basalt flows separated by sedimentary interbeds. The basalt flows are oftentimes fractured, allowing water to move freely in the vertical direction. The Track 2 methodology (DOE-ID 1994) recognized this feature of the system and assumed water transport time through the fractured basalt is relatively instantaneous and ultimately controlled by the presence of sedimentary interbeds. Therefore, only transport through sedimentary interbeds is considered when computing contaminant transport in the unsaturated zone. The aquifer was assumed to be homogeneous isotropic media of infinite lateral extent and finite thickness. Contaminants entering the aquifer from the unsaturated zone mix with water in the aquifer over a depth defined by a typical well screen of 15 m. Concentrations are then evaluated at the downgradient edge of the source. This receptor is the point where the highest concentrations in the aquifer are computed.

The GWSCREEN model also considers transport of radioactive progeny. For simplicity, progeny are assumed to travel at the same rate as their parent. Under most circumstances, this assumption leads to conservative dose estimates at the receptor point. However, when considering the transport of a short-lived immobile parent that has a long-lived mobile progeny, results can be distorted and in many cases are not conservative. This situation occurs for the Pu-241⇒Am-241⇒Np-237 and Pu-238⇒U-234 decay chains. In general, the short-lived immobile parent nuclide never leaves the waste zone and instead decays to its more mobile long-lived progeny. The sorption characteristics of the progeny then determine the overall transit time of the decay chain along with accompanying radiation dose. For conservatism, the entire activity of the short-lived immobile parent is converted to the equivalent progeny activity by

$$A_{Prog} = A_{Parent} \frac{T_{parent}}{T_{Prog}} \tag{3-18}$$

where

- A_{Prog} = equivalent activity of the long-lived mobile progeny (Ci)
- A_{Parent} = original activity of the short-lived immobile parent (Ci)
- T_{Prog} = half-life of the long-lived mobile progeny (years)
- T_{Parent} = half-life of the short-lived immobile parent (years).

The receptor scenario assumes the person drinks 2 L of water per day for 365 days per year. Ingestion doses are computed using dose conversion factors published in FGR 11 (EPA 1988) and include contributions from all progeny.

The screening criteria for Phase III were set at 1/10th of the allowable drinking water dose for beta-gamma emitters of 4 mrem/yr as stated in 40 CFR 141. Although this standard applies only to beta-gamma-emitting nuclides and is calculated using ICRP 2 methodology (ICRP 1960), the 0.4 mrem screening criteria coupled with other conservative assumptions were believed to be stringent enough to avoid screening any nuclides of importance from the inventory.

Input data for the GWSCREEN screening simulation (Table 3-5) were primarily obtained from the Track 2 guidance document (DOE-ID 1994). The dimension of the waste disposal site, Darcy velocity in the aquifer, and the sedimentary interbed thickness in the unsaturated zone are site-specific values. Site-specific values were obtained from the ICDF landfill flow and transport modeling documentation (EDF-ER-275).

Table 3-5. Parameter values for Phase III screening of the ICDF landfill waste inventories.

Parameter	Value	Reference
Length parallel to groundwater flow	160 m	Fate and transport modeling design of the ICDF landfill cover (EDF-ER-275)
Width perpendicular to groundwater flow	194 m	Fate and transport modeling design of the ICDF landfill cover (EDF-ER-275)
Background percolation rate	0.1 m/yr	DOE-ID (1994)
Thickness of source	12.56 m	Fate and transport modeling design of the ICDF landfill cover (EDF-ER-275)
Water-filled porosity – source	0.3	DOE-ID (1994)
Water-filled porosity – unsaturated zone	0.3	DOE-ID (1994)
Unsaturated interbed thickness (transport time through basalt assumed to be instantaneous)	11.6 m	Average thickness of sediments in the INTEC area (see Section 3); also about 1/2 the thickness used in the ICDF design (EDF-ER-275)
Bulk density-source	1.5 g/cm ³	DOE-ID (1994)
Bulk density-unsaturated zone	1.9 g/cm ³	DOE-ID (1994)
Bulk density-saturated zone	1.9 g/cm ³	DOE-ID (1994)
Well screen thickness ^a	15 m	DOE-ID (1994)
Receptor distance parallel to groundwater flow (measured from center of source)	80 m	Based on guidance in DOE-ID (1994)
Receptor distance perpendicular to groundwater flow (measured from center of source)	0 m	DOE-ID (1994)
Water ingestion rates for receptor	2 L/d	DOE-ID (1994)
Exposure frequency	365 d/yr	DOE-ID (1994)
Darcy velocity in aquifer	21.9 m/yr	Fate and transport modeling design of the ICDF landfill cover (EDF-ER-275)
Longitudinal dispersivity	9 m	DOE-ID (1994)
Transverse dispersivity	4 m	DOE-ID (1994)
Aquifer porosity	0.06	Fate and transport modeling design of the ICDF landfill cover (EDF-ER-275)

a. A vertically averaged solution is used per Track 2 Guidance. Thickness of the vertical section is taken to be the well screen thickness.

Nuclide-specific data are reported in the results table. The primary source of sorption coefficient data was DOE-ID (1994) (the Track 2 screening process). If a value for a given nuclide did not exist in DOE-ID (1994), then other sources were consulted, including Sheppard and Thibault (1990), NCRP (1996), and DOE-ID (1997a). The sorption coefficients or K_d values were assumed to be applicable to sedimentary rocks and materials that make up the surface alluvium and interbeds. Sorption coefficients in fractured basalt, which makes up most of the aquifer, tend to be lower than in sedimentary materials because surface area of available sorption sites is lacking. The ratio of the aquifer basalt-to-soil K_d value was estimated in the INTEC Remedial Investigation/Baseline Risk Assessment (RI/BRA) (DOE-ID 1997a) to be 0.04. The ratio was multiplied by all sediment K_d values to obtain the aquifer K_d values used in the GWSCREEN simulation. The infiltration rate is set at 10 cm/yr, which is a factor of 10 times the undisturbed soil infiltration assumed for INEEL soils.

Using the 0.4 mrem/yr screening criteria, 29 of the 37 nuclides were screened and removed from further consideration (Table 3-6). One exception, however, was made in the case of Th-230. This nuclide had a screening dose close to the criteria (0.55 mrem/yr) and has never been shown to be a large dose contributor in other performance assessments at the INEEL (Maheras et al. 1994; Case et al. 2000). Because the overall importance of this nuclide in performance assessments appears to be small and its screening dose was close to the 0.4 mrem/yr screening criteria, this nuclide was eliminated from further evaluation. Therefore, seven nuclides were retained for a detailed analysis of dose. These nuclides are I-129 (82 mrem/yr), Pu-239 (51 mrem/yr), Np-237 (14 mrem/yr), U-234 (12 mrem/yr), Pu-240 (7.9 mrem/yr), U-238 (3.3 mrem/yr), and Tc-99 (0.85 mrem/yr).

Table 3-6. Phase III groundwater pathway screening results using the GWSCREEN model.

Radionuclide	Progeny	Ingestion DCF (rem/Ci) ^a	K _d (mL/g) ^b	Decay chain member dose (mrem)	Total dose (mrem) ^c
Ag-108m		7.62E+03	90		1.6E-50
Am-241 (Np-237) ^d		3.64E+06	8	9.75E-05	9.8E-02
	U-233	2.89E+05	6	7.87E-08	
	Th-229	4.03E+06	100	5.91E-09	
Cd-113m		1.61E+05	6		2.1E-30
Co-60		2.69E+04	10		0.0E+00
Cs-134		7.33E+04	500		0.0E+00
Cs-135		7.07E+03	500		2.2E-05
Cs-137		5.00E+04	500		0.0E+00
Eu-152		6.48E+03	340 (1)		0.0E+00
Eu-154		9.55E+03	340 (1)		0.0E+00
Eu-155		1.53E+03	340 (1)		0.0E+00
H-3		6.40E+01	0		9.6E-02
I-129		2.76E+05	0		8.1E+01
K-40		1.86E+04	15		1.1E-01
Np-237		4.44E+06	8	1.59E-02	1.6E+01
	U-233	2.89E+05	6	1.05E-05	
	Th-229	4.03E+06	100	7.91E-07	
Pa-231		1.06E+07	550 (2)	6.38E-09	1.7E-05
	Ac-227	1.48E+07	450 (2)	1.09E-08	
Pm-147		1.05E+03	240 (3)		0.0E+00
Pu-238 (U-234) ^d		2.83E+05	6	1.72E-04	1.7E-01
	Th-230	5.48E+05	100	2.81E-07	
	Ra-226	1.33E+06	100	1.68E-07	
	Pb-210	7.27E+06	100	8.78E-07	
Pu-239		3.54E+06	22	4.21E-02	4.2E+01
	U-235	2.67E+05	6	5.54E-08	
	Pa-231	1.06E+07	550 (2)	1.39E-09	
	Ac-227	1.48E+07	450 (2)	2.34E-09	
Pu-240		3.54E+06	22	6.52E-03	6.5E+00

Table 3-6. (continued).

Radionuclide	Progeny	Ingestion DCF (rem/Ci) ^a	K _d (mL/g) ^b	Decay chain member dose (mrem)	Total dose (mrem) ^c	
Pu-241 (Np-237) ^d	U-236	2.69E+05	6	3.17E-07		
	Th-232	2.73E+06	100	2.84E-14		
	Ra-228	1.44E+06	100	1.50E-14		
	Th-228	8.08E+05	100	8.38E-15		
			4.44E+06	8	1.03E-05	1.0E-02
	U-233	2.89E+05	6	6.84E-09		
	Th-229	4.03E+06	100	5.14E-10		
Pu-242		3.36E+06	22	1.65E-06	1.7E-03	
Ra-226	U-238	2.70E+05	6	3.41E-13		
	U-234	2.83E+05	6	2.48E-15		
	Th-230	5.48E+05	100	4.82E-18		
	Ra-226	1.33E+06	100	4.31E-18		
	Pb-210	7.27E+06	100	2.30E-17		
			1.33E+06	100	1.92E-08	1.3E-04
		Pb-210	7.27E+06	100	1.06E-07	
Ru-106		2.74E+04	55 (3)		0.0E+00	
Sb-125		2.81E+03	50		0.0E+00	
Se-79		8.70E+03	4		1.6E-02	
Sm-151		3.89E+02	240 (3)		0.0E+00	
Sn-126		1.95E+04	130 (3)		8.3E-04	
Sr-90		1.42E+05	12 (1)		5.8E-25	
Tc-99		1.46E+03	0.2 (1)		9.5E-01	
Th-230		5.48E+05	100	3.56E-05	6.1E-01	
Th-232	Ra-226	1.33E+06	100	8.82E-05		
	Pb-210	7.27E+06	100	4.82E-04		
			2.73E+06	100	1.94E-04	3.5E-01
U-232	Ra-228	1.44E+06	100	1.02E-04		
	Th-228	8.08E+05	100	5.73E-05		
			1.31E+06	6	1.02E-11	1.1E-08
U-234	Th-228	8.08E+05	100	4.34E-13		
			2.83E+05	6	1.25E-02	1.3E+01
	Th-230	5.48E+05	100	2.04E-05		
U-235	Ra-226	1.33E+06	100	1.22E-05		
	Pb-210	7.27E+06	100	6.38E-05		
			2.67E+05	6	2.17E-04	2.2E-01
U-236	Pa-231	1.06E+07	550	3.02E-06		
	Ac-227	1.48E+07	450	5.03E-06		
			2.69E+05	6	3.99E-04	4.0E-01
	Th-232	2.73E+06	100	1.83E-11		

Table 3-6. (continued).

Radionuclide	Progeny	Ingestion DCF (rem/Ci) ^a	K _d (mL/g) ^b	Decay chain member dose (mrem)	Total dose (mrem) ^c
U-238	Ra-228	1.44E+06	100	9.62E-12	3.9E+00
	Th-228	8.08E+05	100	5.39E-12	
	U-234	2.70E+05	6	3.88E-03	
	U-234	2.83E+05	6	1.57E-05	
	Th-230	5.48E+05	100	1.28E-08	
	Ra-226	1.33E+06	100	5.33E-09	
Zr-93	Pb-210	7.27E+06	100	2.73E-08	1.0E-04
	Zr-93	1.66E+03	600		

a. Dose conversion factors from EPA (1988).

b. Unless otherwise noted, all K_d values from DOE-ID (1994). Noted sources are (1) DOE-ID (1997a); (2) Sheppard and Thibault (1990); (3) NCRP (1996).

c. Drinking water doses were based on ingestion of 2 L of water per day for 365 days per year.

d. The nuclide in the parentheses was the decay chain modeled in the simulation. All parent activity was converted to equivalent activity of this daughter.

3.2.3.2 Source Term Model. The mathematical model for the source term is based on a two-compartment, first-order kinetic model. A first-order model has the following limitations and assumptions:

1. Contaminants entering the compartment are instantaneously mixed within the compartment.
2. Release from the compartment is proportional to the amount of activity within the compartment and described by a first-order rate constant.

The two compartments considered in the model are the waste and the clay liner. The source term model provided radionuclide fluxes from the base of the clay liner to the top of the unsaturated zone. The conceptual model is illustrated in Figure 3-5. The differential equations that describe the mass balance in the compartments are

$$\frac{dQ_w}{dt} = -(K_1 + \lambda_d)Q_w \quad (3-19)$$

$$\frac{dQ_c}{dt} = -(K_2 + \lambda_d)Q_c + K_1Q_w \quad (3-20)$$

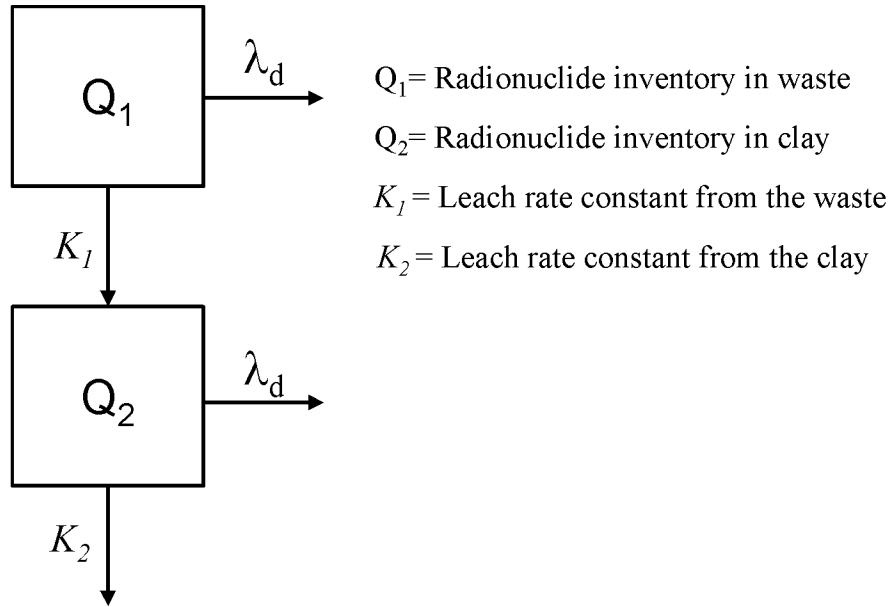


Figure 3-5. Conceptual model for the source term.

(Decay is considered in both compartments as indicated by the rate constant, λ_d .)

With the following initial conditions:

$$Q_1(t=0) = Q_0 \quad (3-21)$$

$$Q_2(t=0) = 0 \quad (3-22)$$

where

t = time (yr)

Q_1 = total activity in waste compartment (Ci)

Q_2 = total activity in clay compartment (Ci)

Q_0 = initial inventory in waste compartment (Ci)

K_1 = leach rate constant for waste compartment (yr^{-1})

K_2 = leach rate constant for clay (yr^{-1})

λ_d = decay rate constant (yr^{-1}).

The solution to the system of equations is

$$F(t) = K_2 Q_2(t) \quad (3-23)$$

$$Q_1(t) = Q_0 e^{-(K_1 + \lambda_d)t} \quad (3-24)$$

$$Q_2(t) = \frac{K_1 Q_0}{(K_2 + \lambda_d) - (K_1 + \lambda_d)} (e^{-(K_1 + \lambda_d)t} - e^{-(K_2 + \lambda_d)t}) \quad (3-25)$$

$$K_1 = \frac{P}{T_1 \left(1 + \frac{K_{d1} \rho_1}{\theta_1}\right) \theta_1} \quad (3-26)$$

$$K_2 = \frac{P}{T_2 \left(1 + \frac{K_{d2} \rho_2}{\theta_2}\right) \theta_2} \quad (3-27)$$

$$\lambda_d = \frac{\ln(2)}{t_{1/2}} \quad (3-28)$$

where

- $F(t)$ = contaminant flux from compartment 2 to the unsaturated zone (Ci/yr)
- P = infiltration rate (m/yr)
- T_1 = thickness of compartment 1 (m)
- T_2 = thickness of compartment 2 (m)
- K_{d1} = soil to water contaminant distribution coefficient (cm³/g) in compartment 1
- K_{d2} = soil to water contaminant distribution coefficient (cm³/g) in compartment 2
- θ_1 = soil moisture content in compartment 1 (unitless)
- θ_2 = soil moisture content in compartment 2 (unitless)
- ρ_1 = soil bulk density in compartment 1 (g/cm³)
- ρ_2 = soil bulk density in compartment 2 (g/cm³)
- $t_{1/2}$ = radioactive decay half-life (yr).

Equations 3-23 through 3-28 were used to calculate fluxes to the unsaturated zone for constant infiltration rates. These fluxes were useful for calibrating the model to the ICDF landfill design model. For the performance assessment, infiltration through the waste varied as a function of time depending on the assumed state of integrity of the cover. Therefore, Equations 3-19 and 3-20 were solved numerically using a 4th order Runge Kutta solver described in Press et al. (1992). Prior to failure of the cover, infiltration through the waste was 0.01 cm/yr. After failure of the cover, infiltration returns to its background value of 1.0 cm/yr.

3.2.4 Environmental Transport of Radionuclides

The conceptual model described in Section 3.2.1 adapts very well to the conceptual model for transport in the unsaturated and saturated zone in the GWSCREEN code (Rood 1999). The built-in source model in GWSCREEN is disabled in this application and radionuclide fluxes to the unsaturated zone are provided by the source term model described in Section 3.2.3.2. Transport in the unsaturated zone is described by a simple plug flow model or a semi-analytical solution to the contaminant mass flux equations for a 1-dimensional environment. In this application, the dispersive solution is used. Transport in the saturated zone is calculated with a 2-dimensional or 3-dimensional semi-analytical solution to the advection dispersion equation in groundwater. In this application, the 3-dimensional solution (averaged over the well screen depth) was used. Dispersion in the aquifer may be described by fixed dispersivity values or three, spatially-variable dispersivity functions.

The dispersion model for unsaturated transport incorporates the same assumptions about flow as the plug flow model. Flow is assumed to be steady state, unidirectional (downward) and under unit gradient conditions. The unsaturated zone is assumed to be a homogeneous isotropic medium of infinite extent. Solid and liquid contaminant phases are assumed to be in equilibrium and related by the linear distribution coefficient. The mass balance equation describing transport in one-dimension is

$$\frac{\partial C}{\partial t} + \frac{U_u}{R_{du}} \frac{\partial C}{\partial x} = \frac{D_x}{R_{du}} \frac{\partial^2 C}{\partial x^2} - \lambda_d C \quad (3-29)$$

where

- C = concentration (mg or Ci/m³)
- R_{du} = retardation in the unsaturated zone
- U_u = unsaturated pore velocity (flow in the positive x direction, m/yr)
- D_x = dispersion coefficient in the x direction (m²/yr)
- t = time (yr)
- x = distance traversed parallel to direction of flow (m).

The solution to Equation (3-29) for an instantaneous release at $x = 0$ is

$$C(x, t) = \frac{1}{\theta_u R_{du} \sqrt{4\pi D_x t / R_{du}}} \exp\left(\frac{(x - U_u t / R_{du})^2}{4D_x t / R_{du}} - \lambda_d t\right) \quad (3-30)$$

The contaminant flux per unit area at a distance x for a vertical plane source oriented perpendicular to flow is given by Equation (3-31).

$$F_a = \theta_u \left(U_u C - D_x \frac{\partial C}{\partial x} \right) \quad (3-31)$$

The total contaminant flux (mass or activity per unit time) at a distance x resulting from an instantaneous release of a unit quantity of contaminant at $x=0$ and $t=0$ would be (Codell et al. 1982):

$$F_a(x, t) = \frac{x + \frac{U_u t}{R_{du}}}{4\sqrt{D_x \pi t^3 / R_{du}}} \exp \left[\frac{-\left(x - \frac{U_u t}{R_{du}}\right)}{4D_x t / R_{du}} - \lambda_d t \right] \quad (3-32)$$

Equation (3-32) is formulated in terms of an instantaneous release. Solutions for arbitrary sources can be arrived at through the use of the convolution integral (Codell et al. 1982):

$$\Theta = \int_0^t F_s(\tau) \Theta_i(t - \tau) d\tau \quad (3-33)$$

where

$F_s(\tau)$ = the arbitrary source release at time τ

$\Theta_i(t - \tau)$ = the solution of $F_a(x, t - \tau)$, for an instantaneous source of strength $F_s(\tau)$ released at $t = 0$.

Equation (3-33) is solved using either Gauss-Legendre or Simpson rule integration. In this application, the Simpson rule integration is used. The source in Equation (3-32) [$F(\tau)$] is calculated from the source term model. The flux (mass or activity per unit time) at time t is subsequently passed to the aquifer model.

The saturated zone model is based on an analytic solution to the advection dispersion equation for contaminants in a saturated porous medium. This solution is published in Codell et al. (1982) and has been used for assessment of radionuclide transport in groundwater. The model contains the following assumptions and limitations:

1. The model uses a Cartesian coordinate system (x, y, z) as a frame of reference. The positive x direction is in the direction of flow.
2. The flow is uniform and unidirectional. No sources or sinks are accounted for.
3. The aquifer is modeled as an isotropic, homogeneous porous medium of infinite lateral extent and finite thickness.
4. Molecular diffusion is assumed to be negligible.
5. The source can be represented by a rectangular area of length, L , and width, W , and centered at the origin (0,0,0).
6. The dispersion coefficients remain constant over time.
7. Transport is limited to a single specie that may decay or degrade as a function of time. Radioactive progeny are assumed to travel at the same rate as their parent.
8. The contaminant is assumed to move as a dissolved substance. Transport in liquid organic and vapor phases are not considered.

9. Solid and liquid phases are in equilibrium and concentrations are related by the linear distribution coefficient (K_d).

The mass balance equation that describes contaminant transport for the stated assumptions is

$$\frac{\partial C}{\partial t} + \frac{U}{R_d} \frac{\partial C}{\partial x} = \frac{D_x}{R_d} \frac{\partial^2 C}{\partial x^2} + \frac{D_y}{R_d} \frac{\partial^2 C}{\partial y^2} + \frac{D_z}{R_d} \frac{\partial^2 C}{\partial z^2} - \lambda_d C \quad (3-34)$$

where

- C = concentration (mg or Ci/m³)
- U = average linear velocity or groundwater pore velocity (m/yr)
- D_x, D_y, D_z = dispersion coefficient in the x, y, and z direction (m²/yr)
- R_d = retardation factor in the aquifer
- t = time (yr)
- x = distance from center of area source to receptor parallel to groundwater flow (m)
- y = distance from center of area source to receptor perpendicular to groundwater flow (m)
- z = distance downward from the surface of the aquifer (m).

The retardation factor in the aquifer is given by

$$R_d = 1 + K_{da} \frac{\rho_a}{\eta} \quad (3-35)$$

where

- η = the effective porosity of the aquifer (m³/m³)
- K_{da} = the distribution coefficient in the aquifer (mL/g)
- ρ_a = the bulk density in the aquifer (g/cm³).

The dispersion coefficients (D_x, D_y, D_z) are given by

$$D_x = \alpha_L U \quad D_y = \alpha_T U \quad D_z = \alpha_V U \quad (3-36)$$

where

- α_L = the longitudinal dispersivity (m)
- α_T = the transverse dispersivity (m)

α_v = the vertical dispersivity (m).

The vertically averaged Green's function solution to Equation (3-34) for instantaneous release of mass M_a at $t = 0$ at the surface of an area defined by L and W and initial concentration of zero everywhere in the model domain is given by

$$C(x, y, t) = \frac{M_a}{\eta R_d} \frac{1}{2L} \frac{1}{b} \left(\operatorname{erf} \left(\frac{x + \frac{L}{2} - \frac{Ut}{R_d}}{\sqrt{\frac{4D_x t}{R_d}}} \right) - \operatorname{erf} \left(\frac{x - \frac{L}{2} - \frac{Ut}{R_d}}{\sqrt{\frac{4D_x t}{R_d}}} \right) \right) \times \frac{1}{2W} \left(\operatorname{erf} \left(\frac{\frac{W}{2} + y}{\sqrt{\frac{4D_y t}{R_d}}} \right) + \operatorname{erf} \left(\frac{\frac{W}{2} - y}{\sqrt{\frac{4D_y t}{R_d}}} \right) \right) e^{-\lambda_d t} \quad (3-37)$$

where

- b = the well screen thickness or mixing depth (m)
- M_a = the initial total mass in the volume defined by $L \times W \times b$
- erf = the error function
- L = length of source parallel to groundwater flow (m)
- W = width of source perpendicular to groundwater flow (m).

The terms L and W represent the length parallel to groundwater flow and the width perpendicular to groundwater flow, respectively. For conservatism, the L and W terms are assumed to be the same as the actual length and width of the facility. Therefore, there is the implicit assumption that water in the vadose zone only travels vertically and transverse dispersion in the unsaturated zone is zero.

For the 3-D solution, Equation (3-37) is multiplied by Z_1 .

$$Z_1 = \left(1 + 2 \sum_{m=1}^{\infty} \exp \left(-\frac{m^2 \pi^2 D_z t}{b^2 R_d} \right) \cos \left(m\pi \frac{z}{b} \right) \right) \quad (3-38)$$

where

- z = receptor distance below the surface of the aquifer (m).

The 3-D solution gives the concentration at a point specified by (x, y, z) in the aquifer. Often, the average concentration over a screened interval is more useful than concentration at a point. The average concentration over a screened well interval, b_w (from the surface of the aquifer to depth b_w), for the three-dimensional solution is given by

$$C_{3Davg}(x, y, z, t) = \frac{\int_0^{b_w} C(x, y, z, t) dz}{b_w} \quad (3-39)$$

For an arbitrary release, the concentration may be found by the convolution integral (Equation 3-33) replacing F_s with F_a (the flux to the aquifer) and where Θ represents Equation (3-37).

To evaluate the movement of radioactive progeny, the model makes the simplifying assumption that radioactive progeny travel at the same rate as the parent. This assumption has been shown to be conservative (Codell et al. 1982) and greatly simplifies the calculations. The concentration of the i^{th} progeny in a decay chain at the receptor location is

$$C_i = C_{parent} \frac{DIF_i R_{d\ parent}}{DIF_{parent} R_{d_i}} \quad (3-40)$$

where

- DIF_i = decay-ingrowth factor of the i^{th} progeny
- DIF_{parent} = decay-ingrowth factor of the parent
- R_{d_i} = retardation factor of the i^{th} progeny
- $R_{d\ parent}$ = retardation factor of the parent
- C_{parent} = groundwater concentration of the parent (Ci/m^3).

The decay ingrowth factor for an n member chain is given by (Scrable et al. 1974)

$$DIF_i(t) = \frac{\lambda_i}{\lambda_1} \left[\frac{\left(\prod_{i=1}^{n-1} \lambda_i \right) \sum_{i=1}^n \frac{e^{-\lambda_i t}}{\prod_{\substack{j \neq i \\ j=1}}^n (\lambda_j - \lambda_i)}}{\prod_{\substack{j \neq i \\ j=1}}^n (\lambda_j - \lambda_i)} \right] \quad (3-41)$$

where

- λ_1 = decay constant for the parent (yr)
- λ_i = decay constant for the i^{th} progeny (yr)
- t = time from waste emplacement or release to from the source (years).

3.2.4.1 Groundwater Model Calibration to Facility Design Model. Design of the ICDF landfill included fate and transport modeling (EDF-ER-275) using the STOMP model (PNNL 1996). Fate and transport modeling was done to determine if the facility is performing adequately by comparing estimated groundwater concentrations and doses to facility performance standards.

The conceptual model for the design of the ICDF landfill considered an essentially 1-dimensional representation of the unsaturated zone and 2-dimensional representation in the aquifer. Dimensions represented in the aquifer included horizontal (parallel to groundwater flow) and vertical directions. In the unsaturated zone, basalt layers were explicitly treated along with sedimentary interbeds. The source term considered a wedge-shaped source with an engineered cover and clay liner. Water flux in the unsaturated zone was specified by the flux of water passing through the cover. The water flux was assumed to remain constant for all times, and, therefore, the cover is assumed to remain intact for all time.

The STOMP model is a considerably more complex subsurface flow and transport model compared to GWSCREEN. However, many of the model options were not utilized and the facility design conceptual model could easily be represented by the far simpler GWSCREEN model. Run times for STOMP were considerably longer than GWSCREEN (6 to 10 hours compared to several minutes for GWSCREEN), making it not amenable to parametric uncertainty analysis using Monte Carlo sampling. Therefore, the GWSCREEN model was used as our performance assessment model. The GWSCREEN model output was calibrated to STOMP model output in order to achieve consistency in the modeling approaches. This is not to say that there are not differences in the model assumptions between the performance assessment and the facility design modeling. There are differences between the two modeling exercises; however, the performance assessment and facility design modeling serve different purposes. What is important is that, for the same set of assumptions, both models should produce similar results. The calibration of GWSCREEN to STOMP also serves as an independent check of the STOMP runs.

The inverse modeling tool UCODE (Poeter and Hill 1998) was used to facilitate model calibration. UCODE uses nonlinear regression techniques to minimize the weighted residuals between an “observation” and a “model estimate.” In this case, the observation was a STOMP concentration in the aquifer and the model estimate was a corresponding GWSCREEN concentration. Four parameters were considered in the calibration: thickness of the unsaturated sedimentary interbeds, dispersivity in the unsaturated zone, longitudinal dispersivity in the aquifer, and vertical dispersivity in the aquifer. Recall that the STOMP model is only 2-dimensional in the aquifer and basically represents a vertical cross section through the center of the facility parallel to groundwater flow. This geometry is equivalent to an infinitely long area source. Therefore, the transverse dispersivity in GWSCREEN was set to a very small value (0.01 m) so that losses from the edge of the source were minimal.

For calibration, a constant infiltration rate of 1.74 cm/yr was assumed and four surrogate contaminants having different sorption properties were considered (Table 3-7). For each surrogate, a unit concentration in the source term was assumed (1 Ci/g). Therefore, the total inventory was $1 \text{ Ci/g} \times 1.946 \text{ g/cm}^3 \times 3.9 \times 10^{11} \text{ cm}^3 = 7.59 \times 10^{11} \text{ Ci}$. The volume of waste ($3.9 \times 10^{11} \text{ cm}^3$) was based on source dimensions of 160 m \times 194 m \times 12.56 m. For the GWSCREEN calibration, source dimensions of 160 m \times 194 m \times 12.0 m were assumed.

Figure 3-6 shows the results of the calibrations for the four surrogate radionuclides. In general, very good agreement was reached between STOMP and GWSCREEN. Mean ratios of GWSCREEN concentration to STOMP concentrations were 1.12, 0.95, 1.03, and 0.90 for surrogates 1, 2, 3, and 4, respectively.

Table 3-7. Fixed and calibrated parameter values for calibration of GWSCREEN with STOMP.

Parameter	Value	Comments
Source length (m)	160	Fixed value
Source width (m)	194	Fixed value
Source thickness (m)	12.56	Fixed value
Clay layer thickness (m)	0.9	Fixed value
Infiltration rate (cm/y)	1.74	Fixed value
Bulk density in source (g/cm ³)	1.946	Fixed value
Bulk density - unsaturated zone (g/cm ³)	1.359	Fixed value
Bulk density - clay layer (g/cm ³)	1.586	Fixed value
van Genuchten α (1/m) in waste	1.066	Fixed value
van Genuchten n in waste	1.53	Fixed value
Saturated hydraulic conductivity in waste (m/yr)	31.5	Fixed value
Total porosity of waste (m ³ /m ³)	0.266	Fixed value
Residual moisture content of waste (m ³ /m ³)	0.072	Fixed value
van Genuchten α (1/m) in clay	0.8	Fixed value
van Genuchten n in clay	1.09	Fixed value
Saturated hydraulic conductivity in clay (m/yr)	0.0315	Fixed value
Total porosity of clay (m ³ /m ³)	0.39	Fixed value
Residual moisture content of clay (m/m)	0.07	Fixed value
van Genuchten α (1/m) in unsaturated interbeds	1.066	Fixed value
van Genuchten n in unsaturated interbeds	1.523	Fixed value
Saturated hydraulic conductivity in interbeds (m/yr)	21.3	Fixed value
Total porosity of interbeds (m ³ /m ³)	0.487	Fixed value
Residual moisture content of interbeds (m/m)	0.072	Fixed value
Transverse dispersivity (m)	0.01	Fixed value
Aquifer thickness (m)	76	Fixed value
Well screen thickness (m)	15	Fixed value
Darcy velocity in aquifer (m/yr)	21.9	Fixed value
Porosity of aquifer (m ³ /m ³)	0.06	Fixed value
Bulk density of aquifer (g/cm ³)	2.491	Fixed value
Receptor location (meters from center of source)	158	Fixed value
Sorption coefficients for surrogate 1 (mL/g)	0.0; 0.0	Waste/interbed K_d ; clay K_d (fixed)
Sorption coefficients for surrogate 2 (mL/g)	0.0; 1.0	Waste/interbed K_d ; clay K_d (fixed)
Sorption coefficients for surrogate 3 (mL/g)	0.2; 1.0	Waste/interbed K_d ; clay K_d (fixed)
Sorption coefficients for surrogate 4 (mL/g)	6.0; 63.0	Waste/interbed K_d ; clay K_d (fixed)
Unsaturated thickness (m)	22.7	Calibrated value
Unsaturated dispersivity (m)	2.92	Calibrated value
Longitudinal dispersivity in the aquifer (m)	3.31	Calibrated value
Vertical dispersivity in the aquifer (m)	2.87	Calibrated value

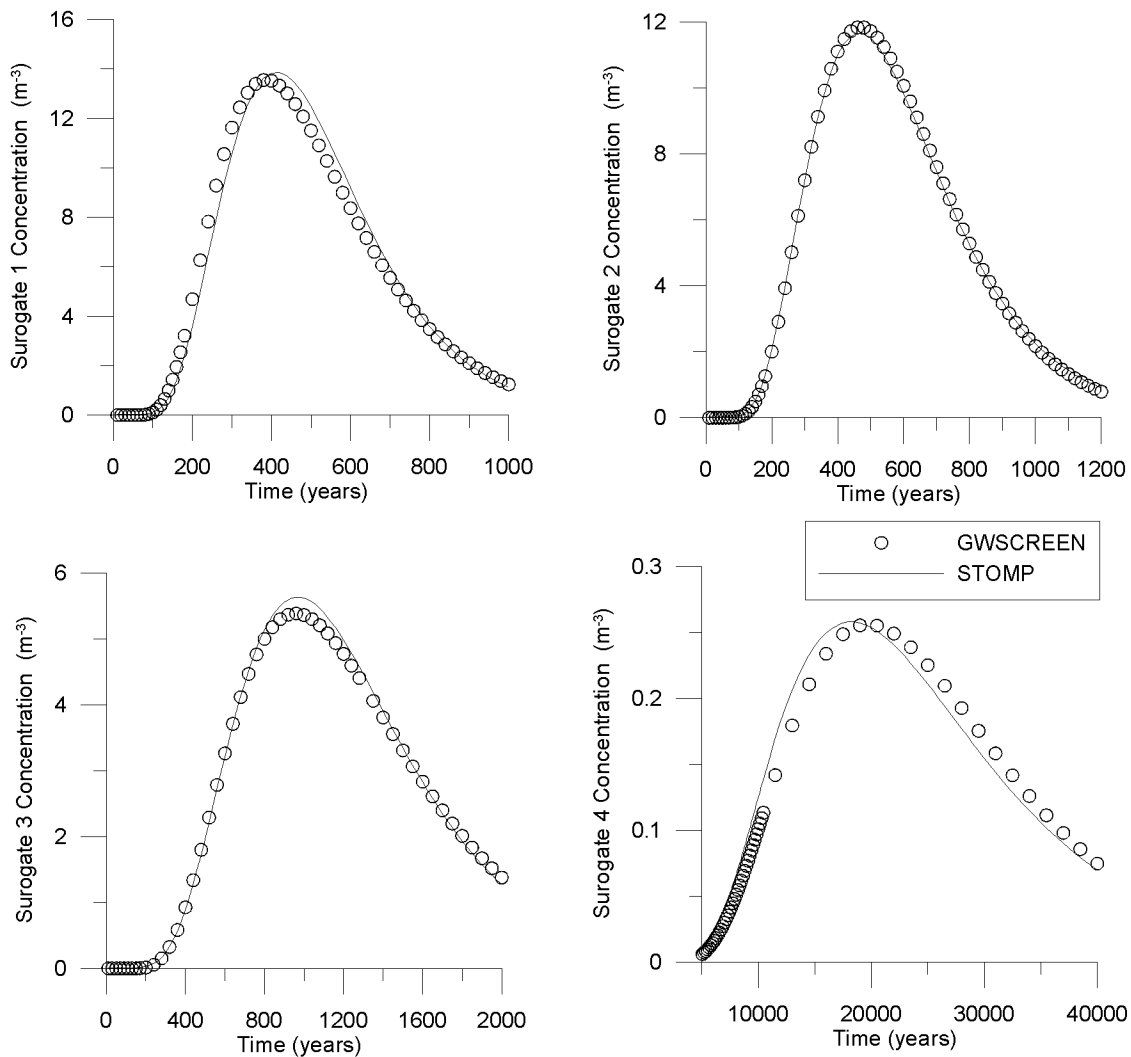


Figure 3-6. Results of calibration of GWSCREEN to STOMP.
 (A unit concentration (1 Ci/g) source term was assumed for all calibration runs.)

3.2.4.2 Parameter Values for Subsurface Pathways Models. Parameter values for the subsurface pathway models are summarized in Table 3-8 (nuclide independent parameters) and Table 3-9 for nuclide dependent parameters. Many of the nuclide independent parameters values are the same as reported in the previous table for model calibration parameters (Table 3-7). However, enough are different or require additional explanation that a new table was warranted. Sorption coefficient data were obtained in a letter from T. Jenkins, DOE-ID, to M. Doornbos, INEEL, July 3, 2001. This letter contains the K_d values that were used in the INTEC modeling. The contents of this letter are presented in Appendix C. Dose conversion factors were obtained from EPA (1988).

3.2.4.3 Dose Calculations. The all-pathways dose was calculated by multiplying the groundwater concentration (Ci/m^3) by the all-pathways dose for a unit concentration ($\text{rem}\cdot\text{m}^3/\text{Ci}\cdot\text{yr}$), which yields the annual dose at the given time:

$$D_{ap} = DU_{ap} \times C \tag{3-42}$$

Table 3-8. Nuclide-independent parameter values for the GWSCREEN landfill performance assessment simulation.

Parameter	Value	Reference/Comments
Source length (m)	160	EDF-ER-275, ICDF only
Source width (m)	194	EDF-ER-275, ICDF only
Source thickness (m)	12.56	EDF-ER-275, ICDF only
Clay layer thickness (m)	0.9	EDF-ER-275, ICDF only
Infiltration rate through cover and into waste, 0-500 years (cm/yr)	0.01	Applies only to the ICDF source term model; infiltration through the vadose zone remains at its background rate of 1 cm/yr (EDF-ER-279)
Infiltration rate through cover and into waste, 500-1,000 years (cm/yr)	Linear increase from 0.01 to 1 cm/yr	Applies only to the ICDF source term model; infiltration through the vadose zone remains at its background rate of 1 cm/yr
Infiltration rate through cover, 1,000-∞ years or background infiltration rate (cm/yr)	1.0	Cover returns to estimated background infiltration after failure, ICDF only
Infiltration in vadose zone 0-∞ (cm/yr)	1.0	Estimated background infiltration
Bulk density in source (g/cm ³)	1.946	EDF-ER-275, ICDF only
Bulk density - unsaturated zone (g/cm ³)	1.359	EDF-ER-275
Bulk density - clay layer (g/cm ³)	1.586	EDF-ER-275, ICDF only
van Genuchten α (1/m) in waste	1.066	EDF-ER-275, ICDF only
van Genuchten n in waste	1.53	EDF-ER-275, ICDF only
Saturated hydraulic conductivity in waste (m/yr)	31.5	EDF-ER-275, ICDF only
Total porosity of waste (m ³ /m ³)	0.266	EDF-ER-275, ICDF only
Residual moisture content of waste (m ³ /m ³)	0.072	EDF-ER-275, ICDF only
van Genuchten α (1/m) in clay	0.8	EDF-ER-275, ICDF only
van Genuchten n in clay	1.09	EDF-ER-275, ICDF only
Saturated hydraulic conductivity in clay (m/yr)	0.0315	EDF-ER-275, ICDF only
Total porosity of clay (m ³ /m ³)	0.39	EDF-ER-275, ICDF only
Residual moisture content of clay (m ³ /m ³)	0.07	EDF-ER-275, ICDF only
van Genuchten α (1/m) in unsaturated interbeds	1.066	EDF-ER-275
van Genuchten n in unsaturated interbeds	1.523	EDF-ER-275
Saturated hydraulic conductivity in interbeds (m/yr)	21.3	EDF-ER-275
Total porosity of interbeds (m ³ /m ³)	0.487	EDF-ER-275
Residual moisture content of interbeds (m ³ /m ³)	0.072	EDF-ER-275
Transverse dispersivity in aquifer (m)	$\alpha \times 0.2$	Whelen et al. (1996) (α = longitudinal dispersivity)
Aquifer thickness (m)	76	DOE-ID (1994)
Well screen thickness (m)	15	DOE-ID (1994)
Darcy velocity in aquifer (m/yr)	21.9	EDF-ER-275
Porosity of aquifer (m ³ /m ³)	0.06	EDF-ER-275
Bulk density of aquifer (g/cm ³)	2.491	EDF-ER-275
Receptor location (meters south from center of source)	180	DOE PA Guidance (DOE M 435.1-1)
Unsaturated thickness (m)	22.7	Calibrated value
Unsaturated dispersivity (m)	2.92	Calibrated value
Longitudinal dispersivity in the aquifer (m)	3.31	Calibrated value for ICDF, scale-dependent value for all other sources
Vertical dispersivity in the aquifer (m)	$\alpha \times 1.16 \times 10^{-3}$	Whelen et al. (1996) (α = longitudinal dispersivity)

Table 3-9. Nuclide-dependent transport parameters.

Nuclide/Progeny	Half-Life (yr)	Number of Progeny	Waste/Interbed K_d (mL/g) ^{a,c}	Clay K_d (mL/g) ^a	Ingestion DCF (rem/Ci) ^b	All-Pathways Dose/Unit Concentration (rem-m ³ /Ci-yr) ^d
I-129	1.57×10^7	0	0.1	1	2.76E+05	4.54E+05
Np-237	2.14×10^6	2	8	55	4.44E+06	3.42E+06
U-233	1.59×10^5		6	63	2.89E+05	2.34E+05
Th-229	7,430		100	1700	4.03E+06	3.10E+06
Pu-239	21,400	3	140	1700	3.54E+06	2.71E+06
U-235	7.04×10^8		6	63	2.67E+05	2.16E+05
Pa-231	32,800		550	2700	1.06E+07	8.10E+06
Ac-227	21.8		450	2400	1.48E+07	1.13E+07
Pu-240	6,570	4	140	1700	3.54E+06	2.71E+06
U-236	2.34×10^7		6	63	2.69E+05	2.17E+05
Th-232	1.41×10^{10}		100	1700	2.73E+06	2.09E+06
Ra-228	5.75		100	9100	1.44E+06	1.15E+06
Th-228	1.91		100	1700	8.08E+05	6.19E+05
Tc-99	2.13×10^5	0	0.2	1	1.46E+03	3.37E+03
U-234	2.44×10^5	3	6	63	2.83E+05	2.29E+05
Th-230	75,400		100	1700	5.48E+05	4.19E+05
Ra-226	1,600		100	1900	1.33E+06	1.06E+06
Pb-210	22		100	710	7.27E+06	5.76E+06
U-238	4.47×10^9	4	6	63	2.70E+05	2.18E+05
U-234	2.44×10^5		6	63	2.83E+05	2.29E+05
Th-230	75,400		100	1700	5.48E+05	4.19E+05
Ra-226	1,600		100	1900	1.33E+06	1.06E+06
Pb-210	22		100	710	7.27E+06	5.76E+06

a. From letter from T. Jenkins, DOE ID, to M. Doornbos, BBWI, July 3, 2001 (Appendix C).

b. Dose conversion factors from EPA (1988).

c. The aquifer basalt K_d is always 1/25 the waste/interbed K_d .

d. All pathway DCFs include short-lived progeny that are assumed to be in secular equilibrium with the parent in the environment.

where

D_{ap} = the all-pathways dose (rem/yr)

DU_{ap} = the all-pathways dose for a unit concentration (rem-m³/Ci-yr)

C = the groundwater concentration (Ci/m³).

Drinking water doses were calculated by

$$D_{dw} = C \times 2 \frac{L}{day} \times \frac{m^3}{1000 L} 365 \frac{d}{year} \times DCF \quad (3-43)$$

where

- D_{dw} = the drinking water dose (rem)
 C = groundwater concentration (Ci/m³)
 DCF = the ingestion dose conversion factor (rem/Ci).

3.3 Radon Analysis

The projected waste inventory is not a significant radon source. Radium-226 concentrations in the ICDF landfill waste (0.5 pCi/g) are less than background concentrations found in INEEL soils (0.75 to 1.4 pCi/g assuming secular equilibrium with Th-230) (Rood et al. 1996). However, because the performance objectives include a radon flux limit or a maximum concentration in air at the point of compliance 1,000 years after closure (40 CFR 61), a radon analysis was performed.

The RESRAD computer code (Yu et al. 1993) was used to estimate the surface radon flux. RESRAD was selected for use in the PA dose and radon flux calculations because

1. RESRAD is the only code designated by DOE in Order 5400.5 for the evaluation of radioactively contaminated sites.
2. The EPA Science Advisory Board reviewed the RESRAD model and used RESRAD in their rulemaking on radiation site cleanup regulations.
3. NRC has approved the use of RESRAD for dose evaluation by licensees involved in decommissioning.
4. RESRAD has been applied to over 300 sites in the U.S. and other countries.
5. The RESRAD code has been verified and has undergone several benchmarking analyses, and has been included in the IAEA's VAMP and BIOMOVs II projects to compare environmental transport models.
6. RESRAD can incorporate site-specific data, which enables more realistic dose assessments.
7. RESRAD meets appropriate quality assurance requirements.

RESRAD was specifically used to estimate the radon flux and exposure analyses because it includes a radon pathway suitable for buried waste.

The data used to estimate the radon flux included site-specific data shown in Table 3-10, as well as default data in the RESRAD code.

Table 3-10. Data used in the radon flux calculations.

Parameter	Value	Comments
Total porosity	0.39	EDF-ER-275
Volumetric water content	0.39	EDF-ER-275
Soil density	1.586 g/cm ³	EDF-ER-275
U-234 concentration in 2018	6 pCi/g	Based on the adjusted design inventory, waste bulk density of 1,946 kg/m ³ , and waste volume of 389,923 m ³
U-238 concentration in 2018	2 pCi/g	Same comment as above
Ra-226 concentration in 2018	0.47 pCi/g	Same comment as above
Th-230 concentration in 2018	0.17 pCi/g	Same comment as above
Waste area	37,637 m ²	Based on waste volume of 389,923 m ³ and an average waste depth of 10.36 m (EDF-ER-275)
Waste thickness	10.36 m	EDF-ER-267
Cover thickness	0.6096 m	Based on the most limiting layer in the design cover, the soil bentonite layer over design in EDF-ER-279
Uranium leach rate	4.5E-06/yr	Based on a K _d ^a of 1,000 mL/g and an infiltration rate 0.70 m/yr
Thorium leach rate	4.5 E-06/yr	Based on a K _d ^a of 1,000 mL/g and an infiltration rate 0.70 m/yr
Radium leach rate	8.97E-05/yr	Based on a K _d ^a of 50 mL/g and an infiltration rate 0.70 m/yr

a. K_d values are RESRAD default values that provide a conservative estimate of radon flux and are not the values used in the groundwater modeling.

The cover depth used in the analysis represents the thickness of the compacted clay layer (soil bentonite layer) in the landfill cover. This layer is very impermeable, having the lowest theoretical saturated hydraulic conductivity (7E-08 cm/s) of the materials used in the lower barrier and lateral drainage component of the design cover (EDF-ER-279). Thus, it represents the most limiting barrier to radon diffusion.

3.4 Biotic Pathways

The biotic transport and uptake of radionuclides have been studied rather extensively at the INEEL. Groves and Keller (1983) identified 10 species of small mammals nesting on or near the RWMC. Four species were the most numerous: deer mice (*Peromyscus maniculatus*), montane voles (*Microtus montanus*), Ord's kangaroo rats (*Dipodomys ordii*), and Townsend's ground squirrels (*Spermophilus townsendii*). Reynolds and Wakkinen (1987) studied the burrow depths of these four species in undisturbed soils. None of the deer mice burrows extended past 60 cm (20 in.), none of the montane vole burrows extended past 70 cm (30 in.), and none of the Ord's kangaroo rat burrows extended past 100 cm (40 in.). The maximum reported burrow depths for undisturbed soil was 138 cm (54.3 in.) for the Townsend's ground squirrel.

Harvester ants (*Pogonomyrmex salinus*) also were considered. Harvester ants burrow deeper than the small mammals. Blom, Clark, and Johnson (1991) state that harvester ants have been found as deep as 2.7 m (8.9 ft) in Wyoming and at the Hanford Site.

Reynolds and Fraley (1989) studied plant root profiles near the RWMC and determined the maximum rooting depth for big sagebrush (*Artemisia tridentata*) was 225 cm (88.6 in.), green rabbitbrush (*Chrysothamnus viscidiflorus*) was 190 cm (75 in.), and Great Basin wild rye (*Leymus cinereus*) was 200 cm (80 in.).

Although biotic transport of radionuclides can be significant at the INEEL, the depth of biointrusion at the ICDF landfill is precluded by the depth of the final cover at the facility and the incorporation of a biobarrier component (EDF-ER-279). The final cover depth will be at least 5.3 m (17.5 ft). Approximately 0.6 m (2 ft) of soil could erode from the surface of the cover during the 1,000-year period of concern (EDF-ER-281). Even then, the animal burrows and plant roots would not reach the waste. Therefore, biointrusion was not considered further.

3.5 Atmospheric Pathways

This section describes the methodology and data used to calculate doses from atmospheric emissions from the ICDF landfill. The doses are based, in part, on the emissions dose assessments performed for the NESHAP Annual Report (DOE-ID 2001b).

This atmospheric pathways analysis assumes that the primary radionuclides emitted via air from the waste are the gaseous forms of tritium, C-14, and Kr-85. For this analysis, it was assumed that the entire inventory of these radionuclides was released to the surface during a 1-year period. The annual emission rate was then input into CAP-88PC (Parks 1997) for diffusion and dose calculations.

As required for NESHAP compliance dose assessments, the receptor location for the operational and institutional control periods was at the point of the maximally exposed individual at Frenchman's Cabin, about 8 km SSW of the RWMC outside the INEEL boundary (Case et al. 2000). The receptor location during the postinstitutional control period was 100 m from the ICDF landfill.

Data used for the CAP88-PC simulations are those used for current NESHAP calculations and include inhalation, ingestion, and external exposure pathways. The results were summed with the latest estimate of the INEEL baseline dose of 0.01 mrem/yr (DOE-ID 2001b). The atmospheric data, environmental data, and the computer code used in the analyses are also discussed in Case et al. (2000).

4. RESULTS OF ANALYSIS

This section describes the results of the analysis described in Section 3. Included are

- Intermediate results from the source term model used to estimate subsurface radionuclide fluxes (Section 4.1)
- Environmental transport of radionuclides via groundwater (Section 4.2)
- Radon flux analysis (Section 4.3)
- Atmospheric emissions dose analysis (Section 4.4)
- Groundwater pathway dose analysis for the all-pathways and drinking water scenario (Section 4.5)
- Analysis of the sensitivity and uncertainty of the groundwater modeling results (Section 4.6).

4.1 Source Term

Estimated fluxes of radionuclides as a function of time from the base of the ICDF landfill (below the clay liner) are illustrated in Figure 4-1 and tabulated in Table 4-1. Fluxes were calculated, using the source term model described in Section 3.2.1. Radionuclide flux from the ICDF landfill is minimal during the first 500 years because the landfill cover limits infiltration to 0.01 cm/yr (0.004 in./yr) and its integrity is assumed to be maintained. After 500 years, the landfill cover is assumed to degrade over the next 500 years and net infiltration through the landfill cover over this time linearly returns to the natural background infiltration rate of 1 cm/yr (0.4 in./yr). Radionuclide leach rates increase almost proportionally to the increase in infiltration. Background infiltration (1 cm/yr) through the waste is assumed to continue for infinity. Fluxes of I-129 and Tc-99 quickly drop after 2,000 years because the source at that time is almost completely depleted. Actinide fluxes continue increasing up to about 10,000 years except for Pu-239, which peaks around 30,000 years. With a half-life of 6,570 years, Pu-240 decreases after 10,000 years because of decay in the landfill.

4.2 Groundwater Pathway Environmental Transport

Radionuclide fluxes at the vadose zone-aquifer interface (Figure 4-2) were calculated with GWSCREEN calibrated to the STOMP model output. Radionuclide fluxes for I-129 and Tc-99 to the aquifer are about a factor of two lower than fluxes across the ICDF landfill-vadose zone interface. For the plutonium isotopes, this difference is several orders of magnitude. The greater difference is because significant decay of plutonium isotopes occurs during transport in the unsaturated zone. For the uranium isotopes and Np-237, the difference between the flux at the ICDF landfill-vadose zone boundary and the flux at the aquifer was about a factor of 1.5.

Radionuclide concentrations in groundwater are illustrated in Figure 4-3 for all principal radionuclides. The concentration of actinides and their associated daughter products are shown in Figures 4-4 through 4-8. In general, daughter product concentrations were considerably less than their parent concentrations and do not reach secular equilibrium. Radionuclide concentrations in the aquifer closely resemble the behavior of radionuclide fluxes to the aquifer mainly because transit times in the aquifer are short.

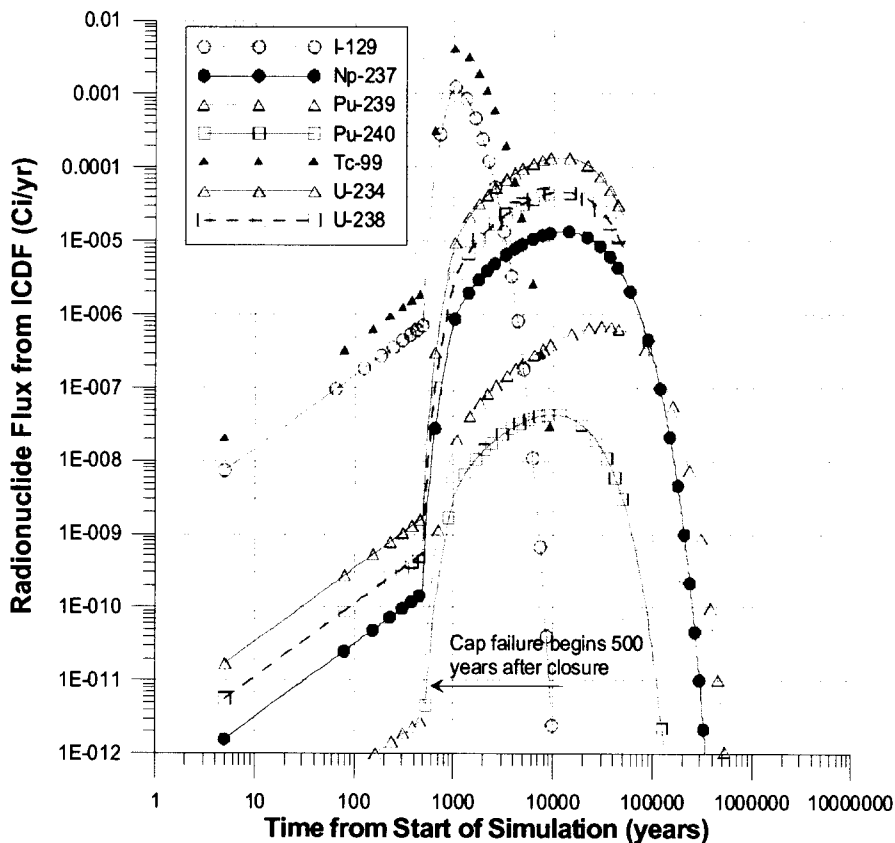


Figure 4-1. Radionuclide flux from the base of the ICDF landfill (below the clay liner) to the top of the vadose zone as a function of time for the seven important nuclides in the ICDF landfill. Simulation start time is the year 2018.

Table 4-1. Unsaturated transit times and peak ICDF and aquifer radionuclide fluxes.

Nuclide	Peak Aquifer Flux (Ci/yr)	Peak ICDF Flux (Ci/yr)	Mean Unsaturated Transit Time ^a (yr)
I-129	6.2×10^{-4}	1.2×10^{-3}	840
Np-237	8.9×10^{-6}	1.3×10^{-5}	22,236
Pu-239	3.1×10^{-10}	6.8×10^{-7}	151,650
Pu-240	2.4×10^{-15}	4.3×10^{-8}	85,178
Tc-99	2.0×10^{-3}	4.0×10^{-3}	1,111
U-234	9.5×10^{-5}	1.4×10^{-4}	16,648
U-238	3.3×10^{-5}	4.6×10^{-5}	16,850

a. The mean unsaturated transit time was calculated using (Whelan et al. 1999):

$$T_{unsat} = \frac{\sqrt{\left(\frac{X_u U_u}{R_{du}}\right)^2 + \left(\frac{4\lambda_d D_x X_u^2}{R_{du}}\right) + \left(\frac{D_x}{R_{du}}\right)^2} - \left(\frac{D_x}{R_{du}}\right)}{\left(\frac{4\lambda_d D_x}{R_{du}}\right) + \left(\frac{U_u}{R_{du}}\right)^2}$$

where X_u = the unsaturated thickness and D_x is the unsaturated dispersion coefficient. Other terms are previously defined in Section 3.2.

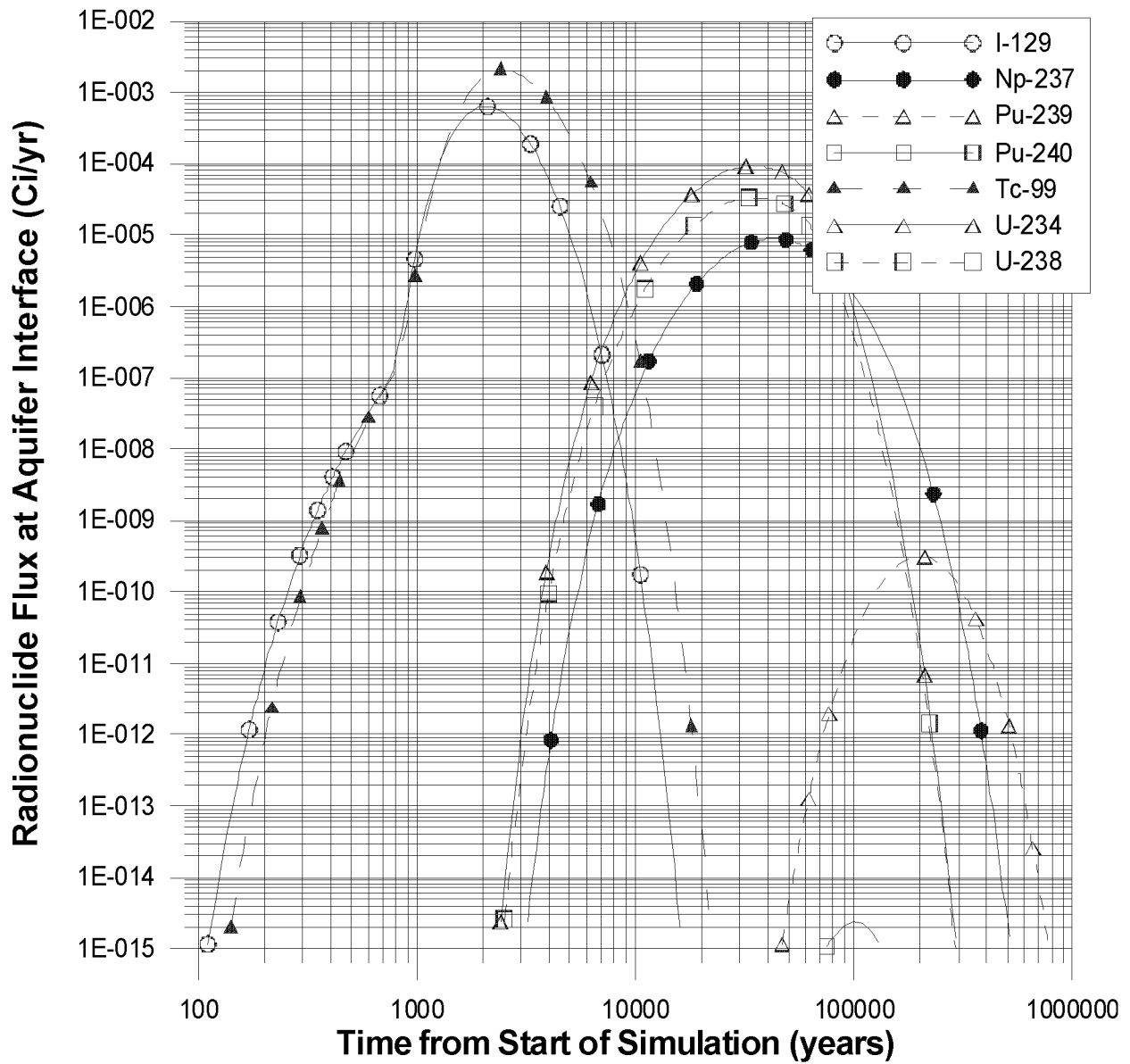


Figure 4-2. Radionuclide flux to the aquifer as a function of time for the seven important nuclides in the ICDF landfill. Simulation start time is the year 2018.

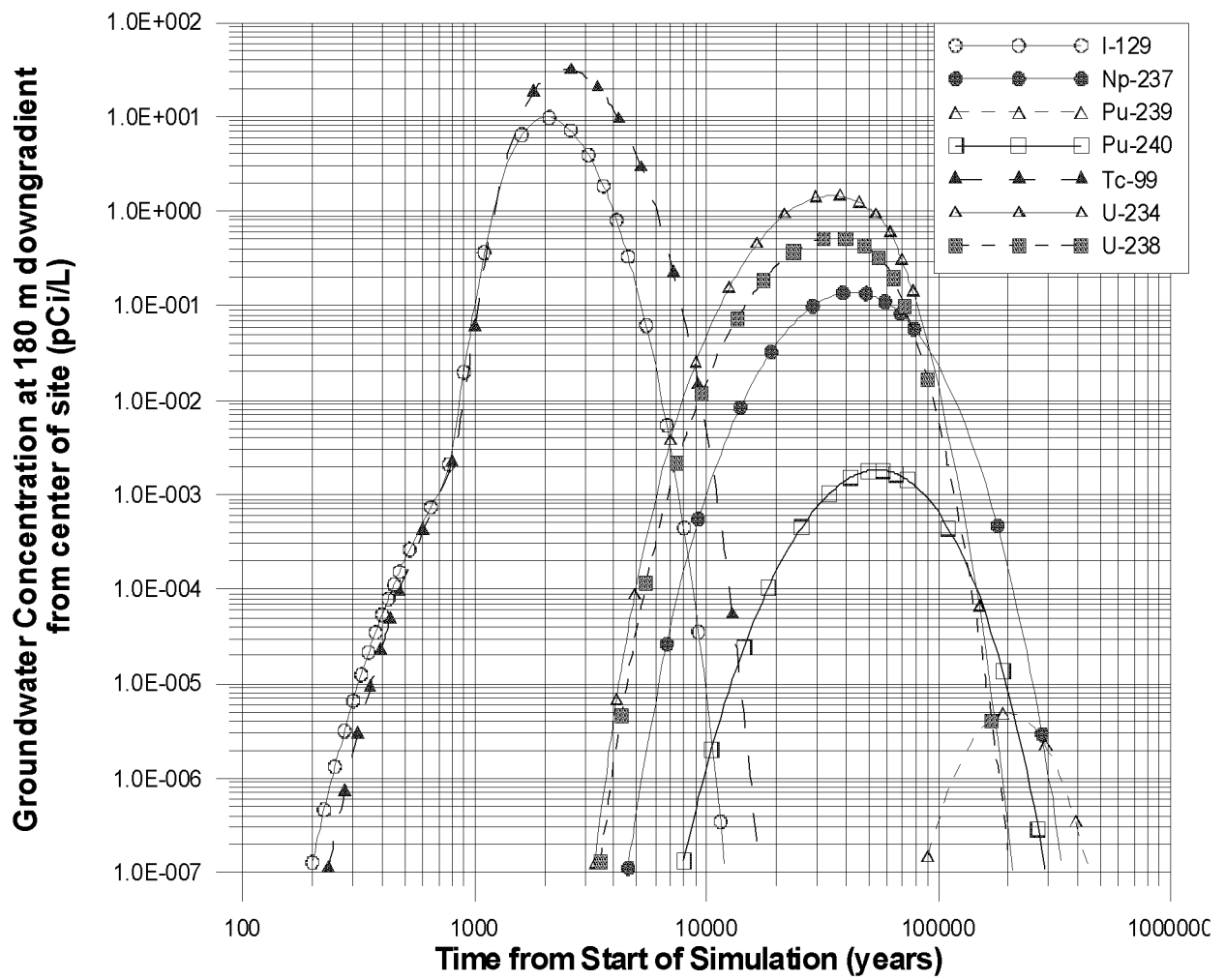


Figure 4-3. Radionuclide concentrations in the aquifer as a function of time at the 180-m receptor (100 m downgradient from the edge of the source). Simulation start time is the year 2018.

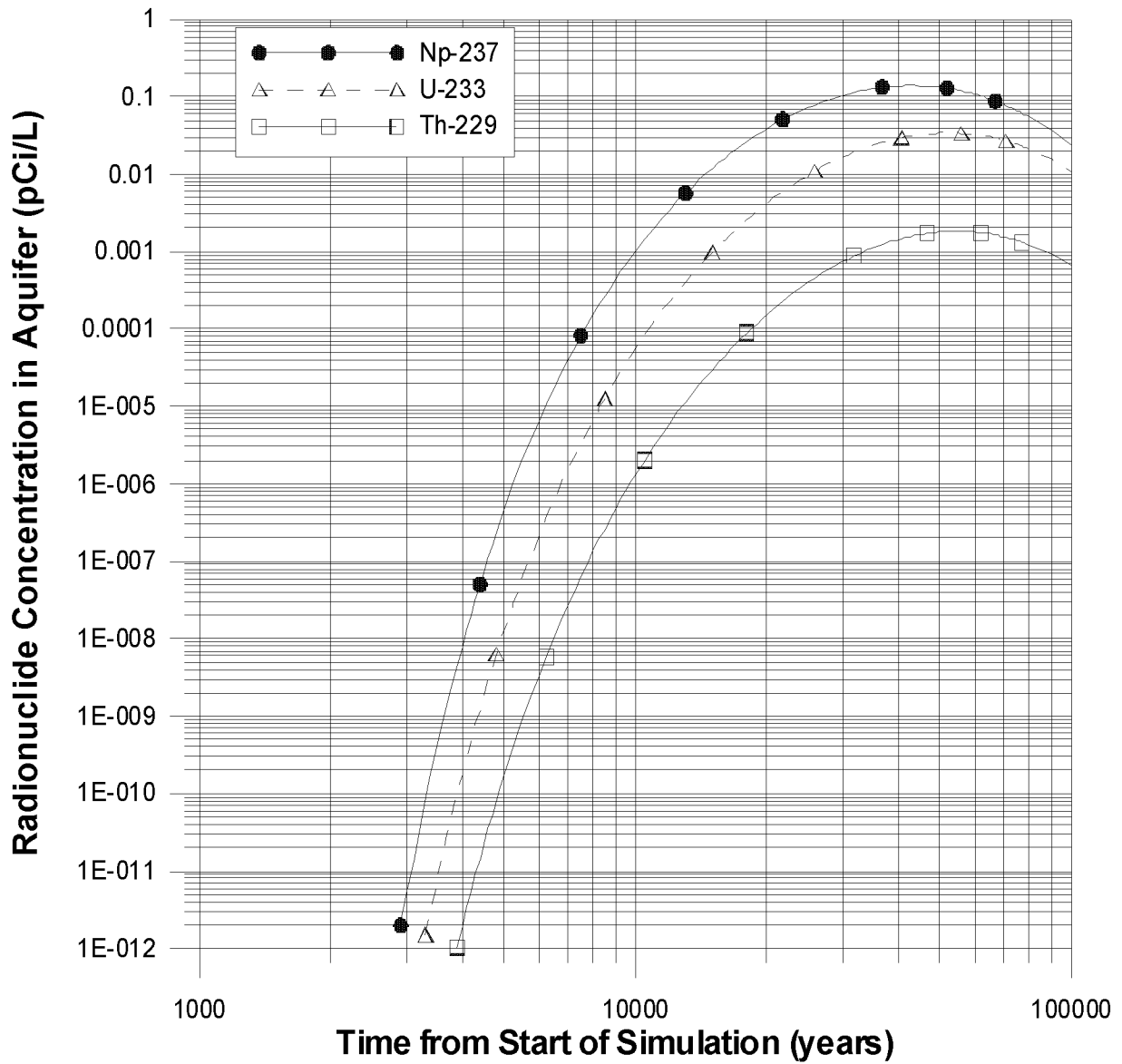


Figure 4-4. Concentration of Np-239 and significant progeny in the aquifer as a function of time at the 180-m (100 m downgradient from the edge of source) receptor location. Simulation start time is the year 2018.

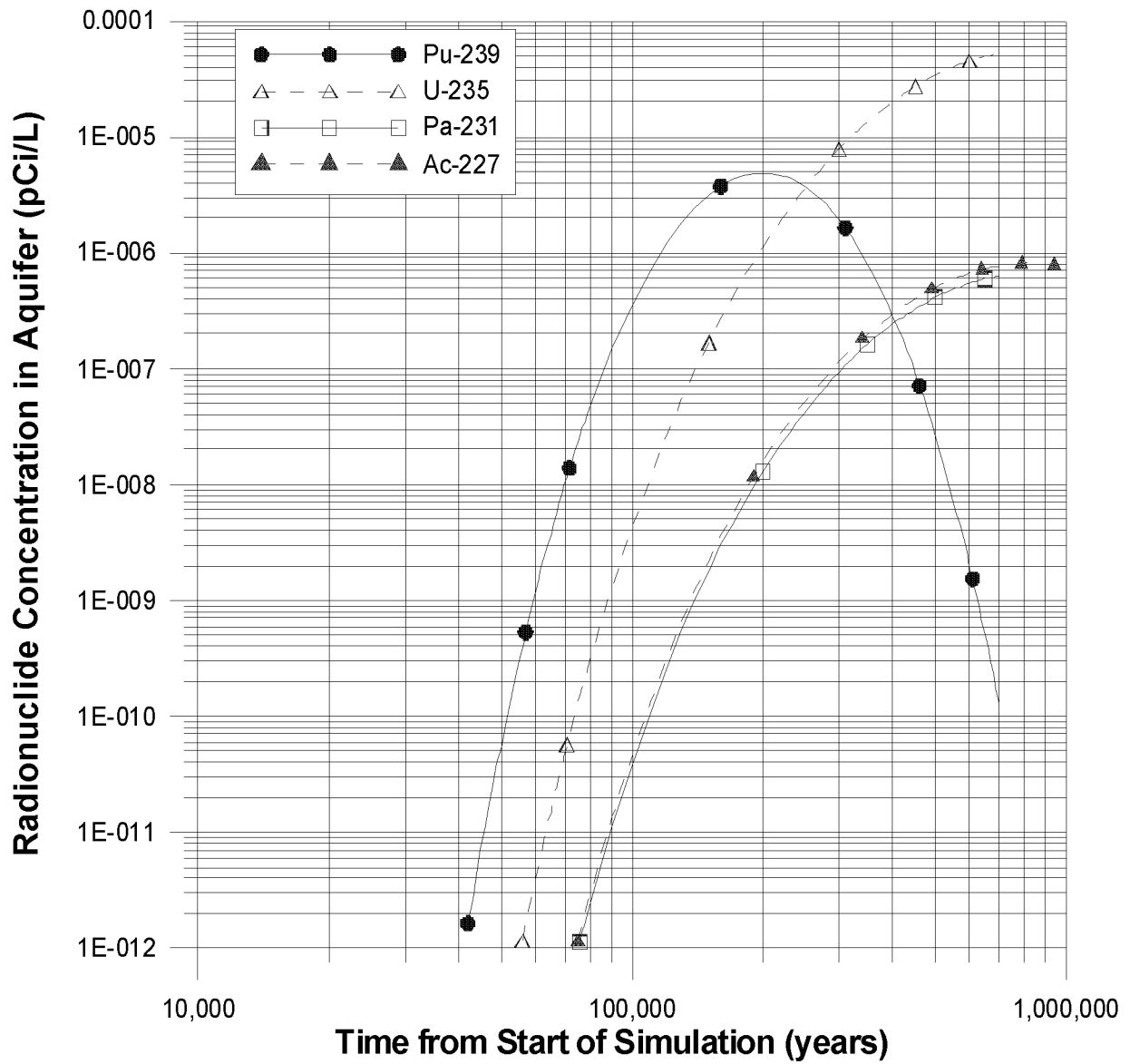


Figure 4-5. Concentration of Pu-239 and significant progeny in the aquifer as a function of time at the 180-m (100 m downgradient from the edge of source) receptor location. Simulation start time is the year 2018.

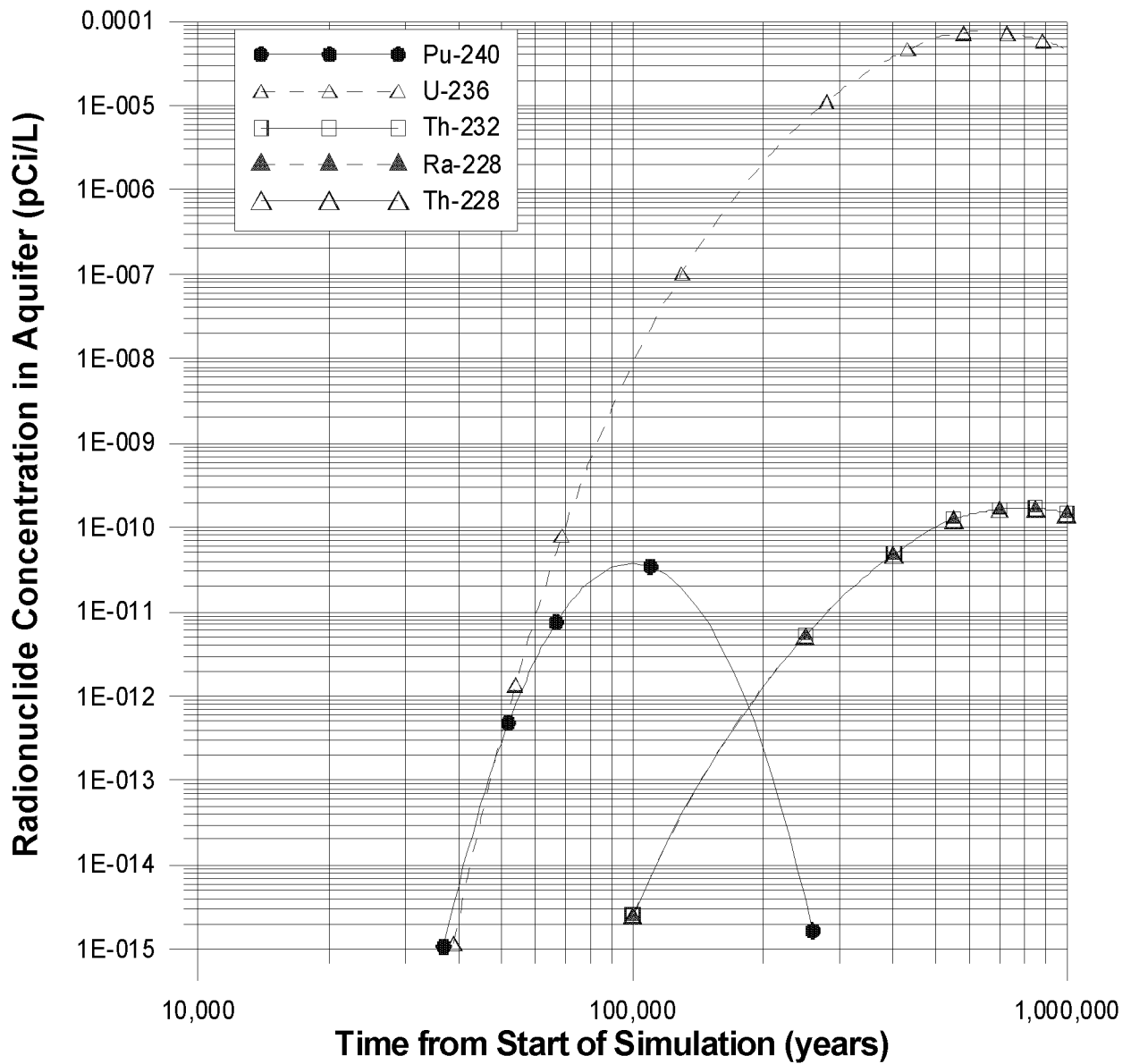


Figure 4-6. Concentration of Pu-240 and significant progeny in the aquifer as a function of time at the 180-m (100 m downgradient from the edge of source) receptor location. Simulation start time is the year 2018.

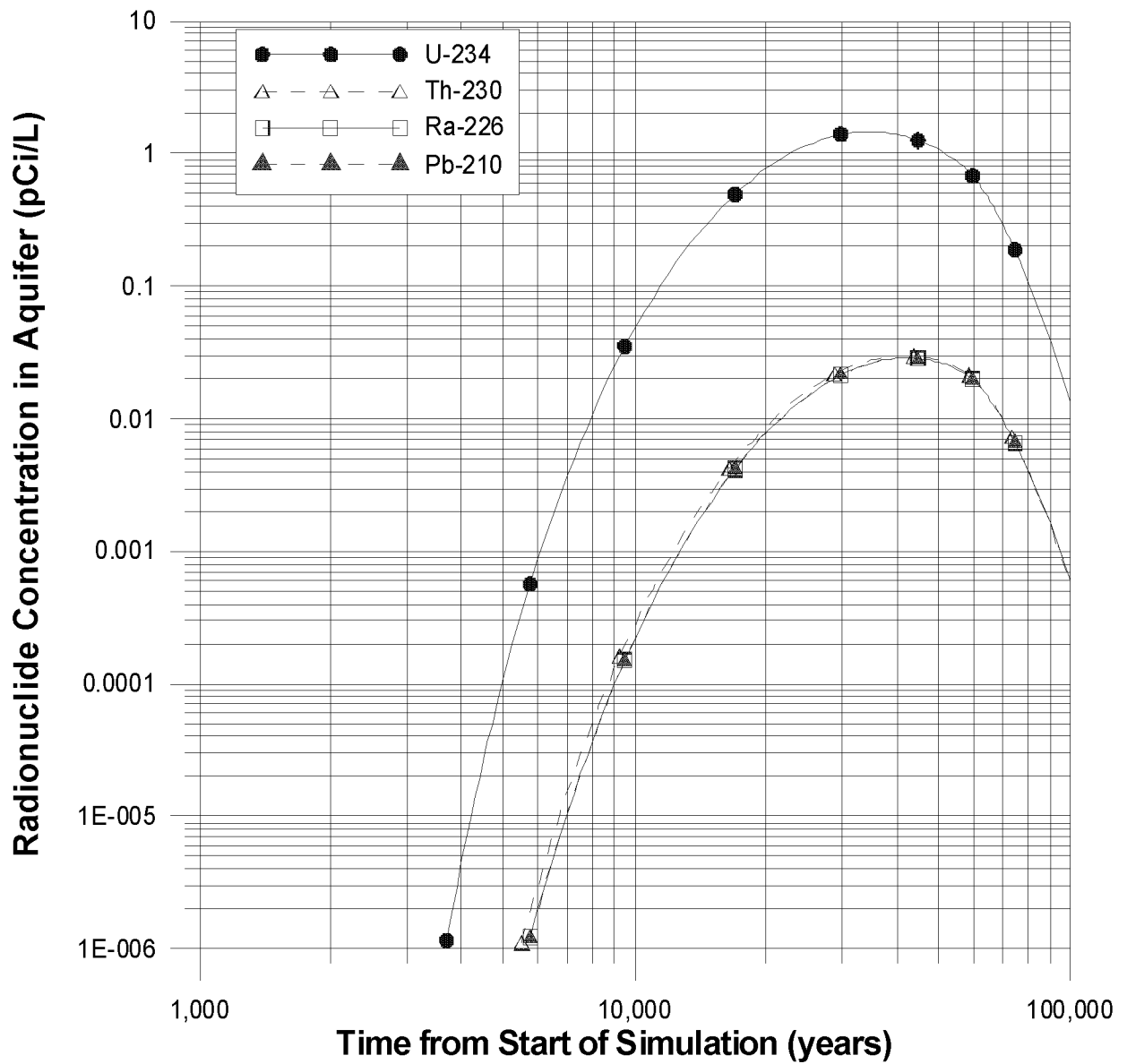


Figure 4-7. Concentration of U-234 and significant progeny in the aquifer as a function of time at the 180-m (100 m downgradient from the edge of source) receptor location. Simulation start time is the year 2018.

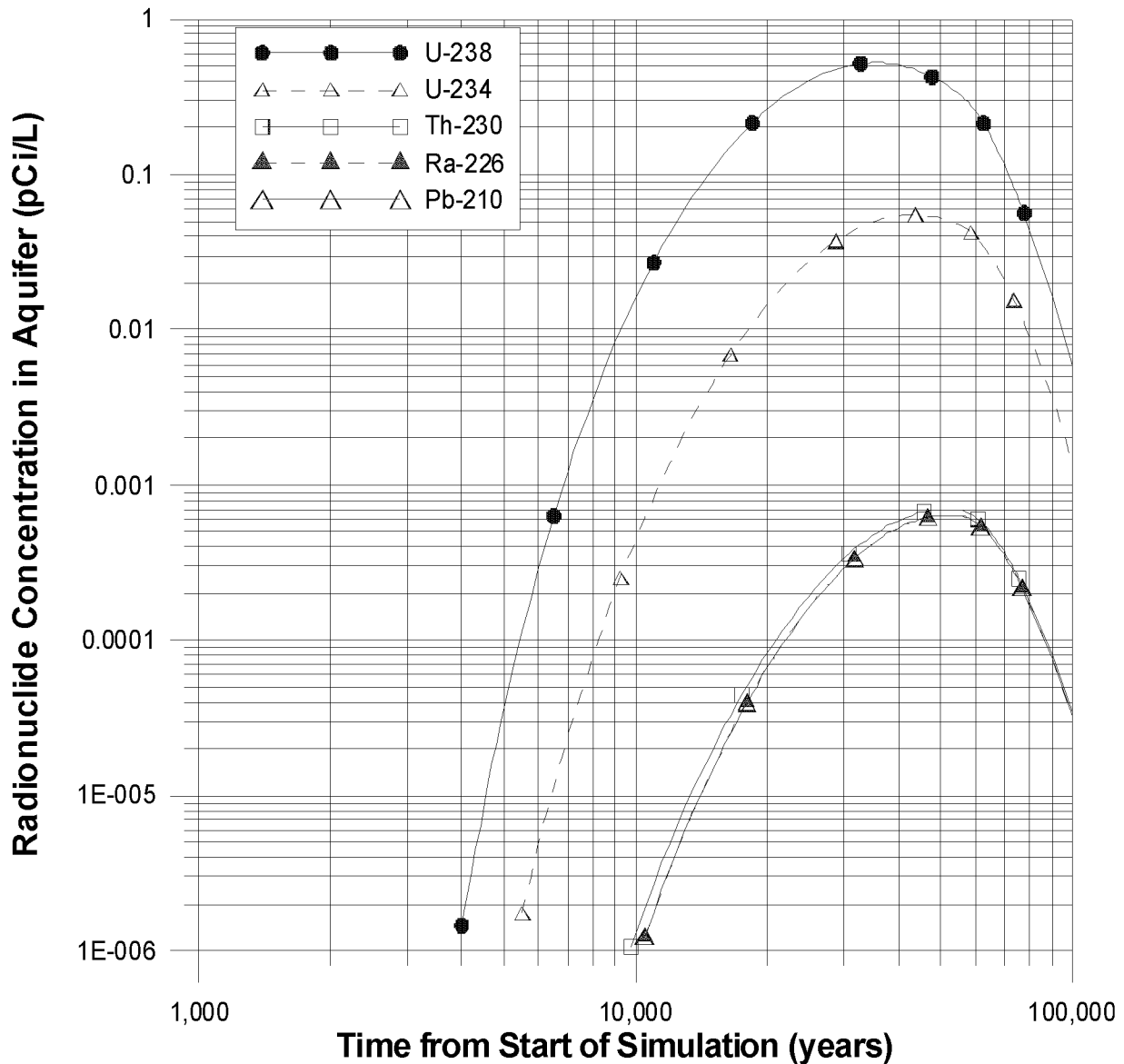


Figure 4-8. Concentration of U-238 and significant progeny in the aquifer as a function of time at the 180-m (100 m downgradient from the edge of source) receptor location. Simulation start time is the year 2018.

Maximum concentrations and time of maximum concentration are presented in Table 4-2. Because the landfill cover is assumed to remain intact for 500 years and then degrade over the next 500 years such that background infiltration (1.0 cm/yr) is achieved at 1,000 years after cover placement, radionuclide concentrations are minimal during the 0- to 1,000-year time window. Iodine-129 reaches its maximum value in the year 4,118 (2,100 years from the start of the simulation) and technetium-99 reaches its maximum in the year 4,518 (2,500 years from the start of the simulation). All actinide concentrations are insignificant during the 1,000-year window of compliance.

Table 4-2. Maximum radionuclide concentrations and time of maximum at the 180-m (100 m downgradient from the edge of source) receptor location.

Nuclide	Progeny	Maximum Concentration (pCi/L)	Time of Maximum (yr) ^a
I-129		9.8	2,100
Np-237		0.14	42,750
	U-233	0.034	51,750
	Th-229	1.8×10^{-3}	54,750
Pu-239		4.9×10^{-6}	200,000
	U-235	5.5×10^{-5}	810,000
	Pa-231	6.6×10^{-7}	810,000
	Ac-227	8.1×10^{-7}	810,000
Pu-240		3.8×10^{-11}	100,000
	U-236	7.4×10^{-5}	630,000
	Th-232	1.7×10^{-10}	790,000
	Ra-228	1.7×10^{-10}	790,000
	Th-228	1.7×10^{-10}	790,000
Tc-99		32	2,500
U-234		1.5	34,750
	Th-230	0.03	41,750
	Ra-226	0.029	42,750
	Pb-210	0.029	41,750
U-238		0.53	35,750
	U-234	0.055	43,750
	Th-230	7.0×10^{-4}	50,750
	Ra-226	6.4×10^{-4}	51,750
	Pb-210	6.4×10^{-4}	51,750

a. The time represents the number of years from the start of the simulation (2018).

4.3 Radon Flux Analysis

As described in Section 3.3, the projected waste inventory is not a significant radon source. Radium-226 concentrations in the ICDL landfill waste (0.5 pCi/g) are less than background concentrations found in INEEL soils (0.75 to 1.4 pCi/g) assuming secular equilibrium with Th-230 (Rood et al. 1996). However, because the performance objectives include a radon flux limit (40 CFR 61), radon analyses were performed.

The RESRAD computer code (Yu et al. 1993) was used to perform radon flux analyses during the period of closure and institutional control (2018–2118) and for 1,000 years after this period (2118–3118). In addition, radon flux calculations were performed at 10,000 years and 100,000 years to determine the effects of progeny ingrowth on radon flux. Results are shown in Table 4-3.

Table 4-3. Radon flux (pCi/m²-s) from soil surface.

Time:	2018	2118	2518	3018	6018	7018	12018	102018
Ra-226	1.69E-01	1.60E-01	1.30E-01	1.00E-01	3.52E-02	1.24E-02	9.06E-04	3.30E-24
Th-230	0.00E+00	2.58E-03	1.16E-02	2.05E-02	3.91E-02	4.48E-02	4.51E-02	1.35E-02
U-234	0.00E+00	4.13E-05	9.62E-04	3.53E-03	2.34E-02	4.99E-02	1.19E-01	5.77E-01
U-238	0.00E+00	1.31E-09	1.55E-07	1.16E-06	2.47E-05	9.29E-05	4.88E-04	3.25E-02
Total	1.69E-01	1.63E-01	1.43E-01	1.24E-01	9.77E-02	1.07E-01	1.66E-01	6.23E-01

The peak radon flux, within the 1,000-year compliance period, was estimated to be 0.17 pCi/m²-s at the time of facility closure. This flux is well below the 40 CFR 61, Subpart Q, standard of 20 pCi/m²-s. The peak radon flux value is associated with Ra-226 disposed in the facility.

Beyond the 1,000-year compliance period, radon flux was observed to increase after 10,000 years primarily due to ingrowth of U-234 progeny. However, the flux rates are still well below the standard of the 20 pCi/m²-s.

4.4 Atmospheric Emissions Dose Analysis

Based on calculations using CAP88-PC (Parks 1997), the release of the entire H-3, C-14, and Kr-85 inventory from disposed waste during operational and institutional control periods (2003-2118) would result in a maximum dose to a member of the general public of 4.60E-04 mrem/yr. The hypothetical individual resides at location of maximum concentration, approximately 13,900 m SSW of the INTEC facility along Highway 20/26 (Abbott 1998). The dose represents doses received through the ingestion, inhalation, and external exposure pathways. The dose is predominantly due to internalization of Kr-85 via inhalation and ingestion pathways. Combined with the current baseline INEEL dose of 1.01E-02 mrem/yr at the same location (DOE-ID 2001b), the maximum total dose (1.02E-02 mrem/yr) estimated for the release of radioactive gases during the operational and institutional control periods is well below the 40 CFR 61, Subpart H, standard of 10 mrem/yr.

CAP88-PC was also used to model the release of the entire H-3 and Kr-85 inventory from disposed waste during the postinstitutional-control period (after 2118). However, the exposed individual was located 100 m from the ICDF landfill. The maximum projected dose (6.67E-03 mrem/yr) incorporates doses from ingestion, inhalation, and external exposure pathways. The dose primarily represents the intake of tritium via ingestion pathways. The dose is significantly below the 40 CFR 61, Subpart H, standard of 10 mrem/yr.

4.5 Groundwater Pathway Dose Analyses

4.5.1 All-Pathways Doses

The all-pathways committed effective dose equivalent as a function of time is presented in Figure 4-9. All-pathways doses are low (0.05 mrem/yr) during the 0- to 1,000-year compliance window and are dominated by I-129. Maximum total (all nuclide) all-pathways past the 1,000-year compliance window is 4.6 mrem/yr. Maximum all-pathways actinide dose is 1 mrem/yr and occurs 38,750 years following closure of the facility (2018). Actinide doses are dominated by U-234 and Np-237. Maximum doses and time of maximum dose are tabulated in Table 4-4 and do not exceed the 25 mrem/yr all-pathways dose constraint at any time in the future. The all-pathways doses in Table 4-4 are divided into three time frames. The first time frame is years 2018 through 2118, which represents the time period of institutional control. The point of compliance during institutional control is the INEEL Site boundary.

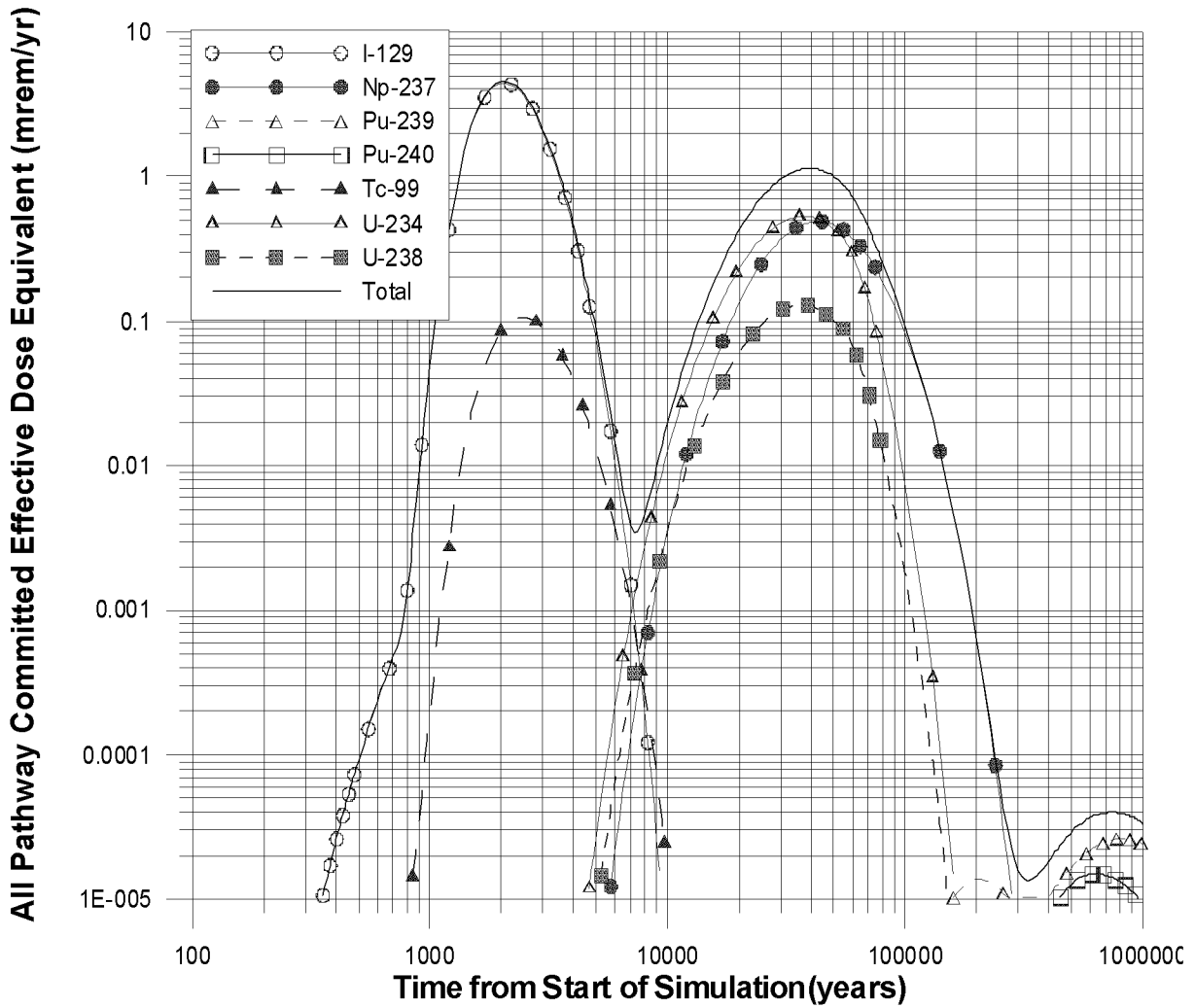


Figure 4-9. All-pathways dose as a function of time at the 180-m (100 m downgradient from the edge of source) receptor location. The simulation starts at the end of operations (year 2018).

Table 4-4. Maximum all-pathways doses and time of maximum at the 180-m (100 m downgradient from the edge of source) receptor location.

Period	PA All-Pathways Dose			Years to Peak (yr)
	Institutional Control Period (Receptor 4)	Compliance Period (Receptor 2)	Postcompliance Period (Receptor 2)	
Years	2018–2118	2118–3018	3018–inf.	
<u>Nuclide</u>	(mrem/yr)	(mrem/yr)	(mrem/yr)	
I-129	0	0.05	4.5	2,100
Np-237	0	0	0.49	42,750
Pu-239	0	0	0.000026	790,000
Pu-240	0	0	0.000015	620,000
Tc-99	0	0.00020	0.11	2,500
U-234	0	0	0.53	34,750
U-238	0	0	0.13	35,750
Maximum dose (all nuclides)	0	0.05	4.55	2,100
Maximum actinide dose	0	0	1.14	38,750

The period from year 2118 to year 3018 represents the compliance period and the point of compliance is 100 m south of the downgradient edge of the ICDF landfill. During the institutional control period from the years 2018 through 2118, the dose at the off-INEEL receptor is predicted to be zero for the ICDF PA. During the compliance period from year 2118 through year 3018, the predicted peak dose at 100-m downgradient from the edge of the ICDF landfill is 0.05 mrem/yr in year 2018. Of this dose, 99.6% is from I-129. After the compliance period has ended in year 3018, the peak dose predicted 100 m downgradient of the ICDF landfill, is 4.6 mrem/yr, 2,100 years after closure of the ICDF landfill (year 4118). Of this dose, 98% is from I-129.

The compliance dose for the PA is 25 mrem/yr total EDE. Therefore, the ICDF landfill PA analysis indicates that the ICDF landfill will meet the all-pathways dose performance objective over all time periods.

4.5.2 Assessment of Groundwater Protection

Groundwater protection is evaluated by comparing predicted concentrations in groundwater, or doses from groundwater ingestion, with MCLs for radionuclides. Four types of concentrations/doses are calculated: gross alpha concentration (excluding uranium and radon), Ra-226/Ra-228 concentrations, CDE from beta-gamma-emitting radionuclides, and total uranium mass concentration. Note that the beta-gamma groundwater protection standard is CDE whereas the all-pathways dose is total EDE. The EDE was calculated using dose conversion factors from Federal Guidance Report 11 (EPA 1988) whereas the CDE values were calculated using data for the 168-hour week from National Bureau of Standards Handbook 69 (DOC 1963) as stipulated in 40 CFR 141. The MCL concentration for beta-gamma-emitting radionuclides is the concentration in drinking water that, if consumed at 2 L/day for 365 d/yr, would yield a CDE of 4 mrem/yr. The I-129 concentration that corresponds to 4 mrem/yr CDE is 1 pCi/L. During the compliance period (years 2018–3018) the maximum CDE from beta-gamma-emitting radionuclides (I-129 and Tc-99) at the point of compliance was 0.41 mrem/yr which is about an order of magnitude less than the MCL of 4 mrem/yr CDE (Table 4-5). I-129 accounts for over 99.99% of this dose. During the postcompliance period, the maximum CDE was 39 mrem/yr which is almost an order of magnitude greater than the 4 mrem/yr CDE limit. I-129 accounts for over 99.5% of this dose.

Table 4-5. Comparison of groundwater protection criteria.

Groundwater Performance Measure	0 to 1,000 Year (year 2018-3018)	>1,000 Year (year 3018 and beyond)	Comments
Beta-gamma dose ≤ 4 mrem/yr CDE	0.41	39	Almost all of the dose is due to I-129
Gross alpha activity ≤ 15 pCi/L	0.0	2.3	—
Uranium concentration < 20 µg/L	0.0	1.6	—
Ra-226/Ra-228 concentration ≤ 5 pCi/L	0.0	0.029	Ingrowth from U-238, U-234, and Th-232 parents

Gross alpha activity reaches a maximum of 2.2 pCi/L, 34,800 years after the closure of the landfill. Ra-226 and Ra-228 reach a maximum concentration of 0.029 pCi/L 41,800 years after closure of the landfill. Both the gross alpha activity concentration and the Ra-226/-228 concentration were below the standard of 15 and 5 pCi/L, respectively.

4.6 Sensitivity/Uncertainty Analysis

The following discussion represents the results of a sensitivity/uncertainty analysis performed for the groundwater pathway dose analysis. A sensitivity/uncertainty analysis was not conducted for the atmospheric and radon flux analyses, as the results were significantly below applicable performance objectives.

4.6.1 Groundwater Pathway Sensitivity/Uncertainty

Performance objectives for the groundwater pathway were achieved during the 1,000-year time of compliance using the models of performance described in Section 3.2. Performance objectives were achieved in part by the actions of the engineered cover that limited infiltration through the waste for a sufficiently long period such that maximum radionuclide fluxes reached the aquifer well after the 1,000-year compliance period. All-pathways doses did not exceed the 25 mrem/yr standard for *any* time in the future. However, the I-129 concentration in the aquifer at the 100-m compliance point exceeded its MCL of 1 pCi/L after the 1,000-year time of compliance by about an order of magnitude. Based on the deterministic analysis, I-129 has the potential to exceed the performance criteria and the performance of the cover appears to be a critical parameter in determining whether the facility meets the performance standards during the 1,000-year compliance period. Therefore, the sensitivity/uncertainty analysis will first address I-129 concentrations in the aquifer for different cover integrity scenarios. A second analysis will examine the overall uncertainty in the all-pathways dose for all nuclides using a parametric uncertainty analysis. The parametric uncertainty analysis will identify the most sensitive parameters at the time of maximum dose during the 1,000-year compliance time.

4.6.1.1 Sensitivity of I-129 Concentrations to Cover Integrity. Seven cover integrity scenarios were evaluated in the sensitivity analysis (Table 4-6). Each scenario is described by two time periods: (1) time from cover emplacement to start of cover degradation and (2) time over which cover degradation occurs. In all cases, the cover is installed in the year 2018. The cover restricts the water flux through the waste to 0.01 cm/yr while the cover remains intact. The cover begins degrading at the time specified by the scenario (Column 3 in Table 4-6). Infiltration is assumed to linearly increase from the designed-based cover infiltration (0.01 cm/yr) to background infiltration (1.0 cm/yr) over the scenario-specific time specified in Column 4 of Table 4-6.

Table 4-6. Description of cover integrity scenarios used to evaluate sensitivity of I-129 concentrations to cover integrity.

Scenario Number	Description	Time cover remains intact (years)	Time cover degrades over (years)
1	Design Case – Cover life of 1,000 yr with 4,000 yr of cover degradation	1,000	4,000
2	Performance Case – Cover life of 1,000 yr with 1,000 yr of cover degradation	1,000	1,000
3	Enhanced Degradation Case – Cover life of 750 yr with 750 yr of cover degradation	750	750
4	Conservative Case – Cover life of 500 yr with 500 yr of cover degradation (equivalent to the scenario used in the deterministic results)	500	500
5	Rapid Degradation Case – Cover life of 250 yr with 250 yr of cover degradation	250	250
6	Extreme Degradation Case – Cover life of 100 yr with 100 yr of cover degradation	100	100
7	Catastrophic Failure Case – Cover life of 100 yr with 20 yr of cover degradation	100	20

The deterministic results presented in Sections 4.2 and 4.5 are equivalent to the Conservative Case scenario (Scenario 4). Iodine-129 concentrations as a function of time were calculated for each cover scenario and the results are shown in Figure 4-10. In general, cover longevity affects the time of maximum concentration in the aquifer; the time over which the cover degrades affects the peak concentration. In all cases except the Design Case and the Catastrophic Failure Case, the cover degradation time is equal to the time the cover remains intact. In the Design Case, the cover remains intact for 1,000 years and then degrades to background infiltration over the next 4,000 years. The relatively longer degradation time for the Design Case results in a slower release of I-129 over time and a substantially lower peak concentration compared to the other cases.

4.6.1.2 Parametric Uncertainty Analysis. To address uncertainty of the remaining nuclides and the overall all-pathways dose, a parametric uncertainty analysis was performed. Parametric uncertainty analysis uses an estimated frequency distribution of values for each model parameter considered to be uncertain and produces a frequency distribution of model predictions or output. Parameter uncertainty was performed for the all-pathways groundwater exposure scenario using Monte Carlo simulation combined with simple random sampling. In Monte Carlo simulation, parameter values are randomly sampled from distributions developed by the analyst. The model is then run and the output variable stored. The process is repeated for multiple model realizations (typically greater than 100) resulting in an empirical distribution of the output variable. The parameter uncertainty presented here is not intended to be definitive; rather, it represents the response of the model output to the current state-of-knowledge of model input. As the knowledge base of model input changes, so will the uncertainty estimate. The analysis therefore serves as a template for uncertainty and sensitivity analyses in performance assessments.

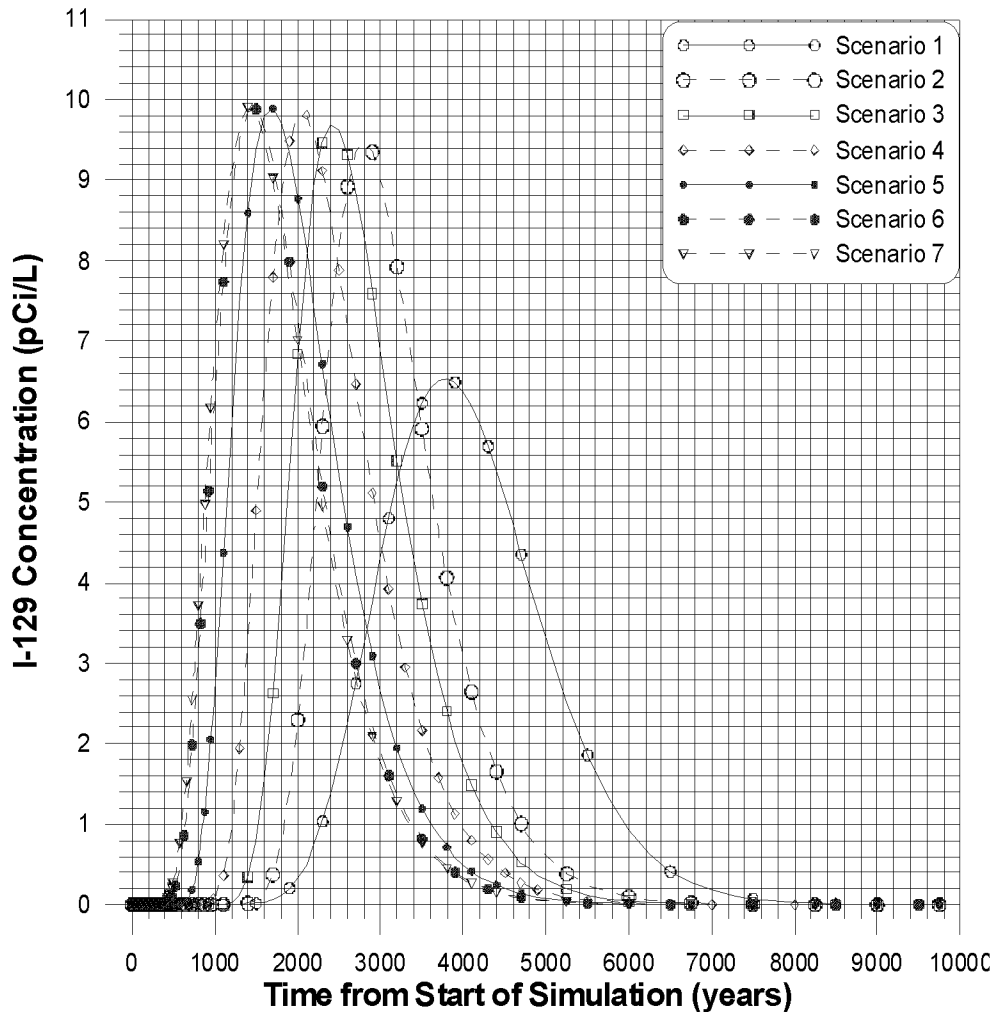


Figure 4-10. Iodine-129 concentrations in the aquifer at the compliance point (100 m downgradient from the downgradient edge of the facility) as a function of time for the seven cover integrity scenarios described in Table 4-6. The deterministic results are based on Scenario 4.

A Perl^d script (EDF-2114^e) was used as the Monte Carlo driver for the simulation and performed the following functions for each Monte Carlo trial:

- Sample parameter values from assigned distributions
- Write input files for the source term model and generate release files for each of the nuclides
- Write a GWSCREEN input file and execute GWSCREEN
- Extract and store output from the GWSCREEN model run.

d. Perl (Practical Extraction Reporting Language) is a scripting language available on most Unix workstations and recently made available for Windows-based machines.

e. EDF-2114, “Documentation of a Perl Script for Performing Monte Carlo Uncertainty Analysis Using GWSCREEN for the ICDF Performance Assessment,” Idaho National Engineering and Environmental Laboratory (in preparation).

Uncertainty was not evaluated for the food chain pathway or the resident exposure scenario. The food chain pathway includes exposure to radionuclides derived from the groundwater other than direct ingestion. Food chain exposure pathways include transfer of radioactivity to crops via irrigation with contaminated water and transfer of radioactivity to livestock via ingestion of contaminated water and animal feed. Equations and parameter values for this pathway are described in Section 3.2.2. Food chain doses were incorporated into the total dose (including direct ingestion) by calculating an all-pathways dose conversion factor as described in Section 3.2.4.3. Uncertainty in the food chain pathway model could be determined external to these calculations because the parameters that describe food chain transport (concentration factors, animal transfer factors, and animal ingestion rates) are generally independent from those used to calculate fate and transport. There is, however, correlation between soil depletion rates and contaminant leaching, which must be accounted for in the simulation. The Perl script that was written is certainly amenable to inclusion of this pathway; however, our primary emphasis here was to evaluate the uncertainty in radionuclide groundwater concentrations, which therefore only requires evaluation of groundwater transport model uncertainty.

Uncertainties in the exposure scenario parameters (which mostly consist of human ingestion rates of water and food products) were also ignored. The reason for this is that the exposure scenario represents a hypothetical future resident whose behavior is neither predictable nor measurable. In contrast, the transport of radionuclides represents real physical processes that can be measured (albeit with difficulty) and predicted with mathematical models. The same cannot be said of the hypothetical resident. The resident exposure scenario is only a means to translate concentrations of radionuclides in the environment to relevant health impacts that can be compared with regulatory standards. For these reasons, all exposure scenario parameters were considered fixed.

Uncertainty was also not considered for the inventory. The inventories used in this performance assessment were based on either maximum or the 95% upper confidence limit of concentrations in soils (EDF-ER-264). Therefore, the inventory has already been designed to be biased high and any stochastic treatment of it would result in doses that were lower.

Output from the Monte Carlo simulation consists of an empirical distribution containing n values. These values are arranged in ascending order and reported in terms of their ordered-statistics^f or percentiles. For example, the 5th percentile represents the 5th highest value of 100 values. In this way, statements about model precision can be made. For example, suppose the output distribution contained 100 values. The 5th highest value (out of the 100 values) was 2 and the 95th highest value was 45. We could then state that 90% of the model predictions fell between 2 and 45, or that 95% of the model predictions were less than 45.

Five hundred model realizations were run for the Monte Carlo simulation. This was a convenient number to choose because run times were relatively short (several hours) and confidence intervals around the percentiles on the tails could be reasonably well defined. Using the nonparametric ordered-statistics described in Hahn and Meeker (1991), confidence intervals for an empirical distribution containing 500 values were determined. Given a distribution of 500 values, the 95% confidence interval around the 95th percentile value (475th highest value) is ~93rd percentile and ~97th percentile.

Parameter distributions are summarized in Table 4-7 and discussed in subsequent sections. In some cases, distributions were assumed based on current knowledge of the parameter. In general, all parameter distributions developed for environmental systems tend to have some degree of subjectivity within them because there is typically not enough data to develop a purely quantitative distribution (Till and

f. The ordered-statistics are the ordered ranking of all n values comprising an empirical distribution.

Table 4-7. Parameter distributions used in the uncertainty sensitivity analysis.

Parameter	Distribution Type	Units	Distribution Parameters
Background percolation rate	Triangle	m/yr	Minimum 0.005; mode 0.01; maximum 0.02
Cover infiltration	Log triangle	m/yr	Minimum 5.0E-05; mode 1.0E-04; maximum 1.0E-03
Cover lifetime	Triangular	yr	Minimum 100; mode 1000; maximum 2500
Longitudinal dispersivity (aquifer)	Triangle	m	Minimum 1.7; mode: 3.3; maximum 6.6
Unsaturated dispersivity	Triangle	m	Minimum 1.5; mode 2.9; maximum 5.8
Darcy velocity in aquifer	Triangle	m/yr	Minimum 11; mode 22; maximum 44
Waste and interbed iodine K_d	Lognormal	mL/g	Geometric mean 0.1; geometric standard deviation 1.6
Waste and interbed neptunium K_d	Lognormal	mL/g	Geometric mean 8; geometric standard deviation 1.5
Waste and interbed plutonium K_d	Lognormal	mL/g	Geometric mean 140; geometric standard deviation 1.3
Waste and interbed technetium K_d	Lognormal	mL/g	Geometric mean 0.2; geometric standard deviation 1.5
Waste and interbed uranium K_d	Lognormal	mL/g	Geometric mean 6; geometric standard deviation 1.9
Waste and interbed ^a radium K_d	Lognormal	mL/g	Geometric mean 100; geometric standard deviation 6.3
Waste and interbed ^a actinium K_d	Lognormal	mL/g	Geometric mean 100; geometric standard deviation 2.0
Waste and interbed ^a thorium K_d	Lognormal	mL/g	Geometric mean 100; geometric standard deviation 1.9
Waste and interbed ^a lead K_d	Lognormal	mL/g	Geometric mean 100; geometric standard deviation 3.8
Waste and interbed ^a protactinium K_d	Lognormal	mL/g	Geometric mean 550; geometric standard deviation 2.0
Clay iodine K_d	Lognormal	mL/g	Geometric mean 1; geometric standard deviation 1.7
Clay neptunium K_d	Lognormal	mL/g	Geometric mean 55; geometric standard deviation 6.7
Clay plutonium K_d	Lognormal	mL/g	Geometric mean 1,700; geometric standard deviation 1.6
Clay technetium K_d	Lognormal	mL/g	Geometric mean 1; geometric standard deviation 1.03
Clay uranium K_d	Lognormal	mL/g	Geometric mean 63; geometric standard deviation 2.1

a. The waste and interbed K_d s are not used for daughter products in GWSCREEN. Daughter product sorption is only considered in the aquifer and used to partition the daughter product according to the parent nuclide concentration. The sampled K_d is used to calculate the K_d in the aquifer which is 1/25 the K_d in the interbeds.

Meyer 1983). The distribution is a statement of belief about the parameter's true but unknown value. Log-transformed distributions were assigned to many of the parameters because their minimum and maximum values spanned a factor of five or greater. When the span of a distribution exceeds a factor of five, log-transformed data are typically better at characterizing the distribution than linear-scale data. Triangular or log-triangular distributions were assigned to some of the parameters. These distributions are useful when there are only estimates of a central (mean or mode), minimum, and maximum value of a parameter. A discussion and justification for each parameter follows.

4.6.1.2.1 Background Percolation Rates—The background percolation rate is the amount of water that enters the vadose zone from undisturbed land. Infiltration through the cover and into the waste is addressed separately. After the cover fails, infiltration returns to background levels. Background percolation rates in undisturbed soils have been estimated to range between 0.4 and 1.2 cm/yr (Cecil et al. 1992). A value of 1 cm/yr was used for the deterministic calculations. A factor of two uncertainty was assumed for the background infiltration rate, which approximately bounds the range of infiltration rates reported by Cecil. A triangular distribution was assigned having a minimum value of 0.5 cm/yr, a mode value of 1 cm/yr, and a maximum value of 2 cm/yr (Figure 4-11).

4.6.1.2.2 Cover Percolation Rates—The cover is designed to minimize infiltration into the waste; therefore, percolation through the cover was assumed to be minimal while the cover remains intact. After failure, infiltration through the cover returns to background levels. The background percolation rate defined earlier is used as the infiltration rate following cover failure. Prior to cover failure, the infiltration rate through the cover was assumed to be represented by a log-triangular distribution having mode equal to the “best estimate” infiltration rate (1×10^{-4} m/yr), a maximum of 1×10^{-3} m/yr, and a minimum of 5×10^{-5} m/yr.

4.6.1.2.3 Dispersivity in the Aquifer—Dispersivity is a parameter that describes the spreading that occurs while a contaminant is advected in a fluid medium. This parameter was used as a means of calibrating the GWSCREEN model to STOMP and calibrated values of 3.31 m, 0.01 m, and 2.87 m for the longitudinal, transverse, and vertical dispersivity, respectively, were obtained from the calibration. The small value for the transverse dispersivity was because the STOMP model was only two-dimensional. The small transverse dispersivity essentially reduced the GWSCREEN simulation into an area source with infinite width (perpendicular groundwater flow) problem. For the deterministic calculations, the calibrated longitudinal dispersivity value of 3.31 m was used. However, transverse and vertical dispersivity values were based on the ratios of transverse/longitudinal (0.2) and vertical/longitudinal dispersivity (1.16×10^{-3}) reported in the MEPAS (Whelan et al. 1996) manual. Because little information was available from which to develop a distribution, the distribution assigned was based on a reasonable expectation of expected uncertainties. The range and the shape of the distribution of dispersivity was based on the range and shape used in the RWMC performance assessment (Case et al. 2000). The longitudinal dispersivity was assumed to vary by a factor of two from its median value. Transverse and vertical dispersivity were then calculated from the longitudinal dispersivity based on the ratios provided in Whelan et al. (1996). A triangular distribution was assigned to α_L having a minimum of value of 1.7 m, a mode value of 3.3 m, and a maximum value of 6.6 m (Figure 4-12).

4.6.1.2.4 Dispersivity in Unsaturated Zone—Like dispersivity in the aquifer, dispersivity in the unsaturated zone was treated as a calibration parameter. Again, a factor of two uncertainty was assumed. A triangular distribution was defined having a minimum of 1.5 m, a mode of 2.9 m (the calibrated value), and maximum of 5.8 m (Figure 4-13).

4.6.1.2.5 Darcy Velocity in the Aquifer—The Darcy velocity in the aquifer is described by Darcy’s Law and is given by

$$q = K \frac{dh}{dx} \quad (4-1)$$

where

$$q = \text{Darcy velocity (m/y)}$$

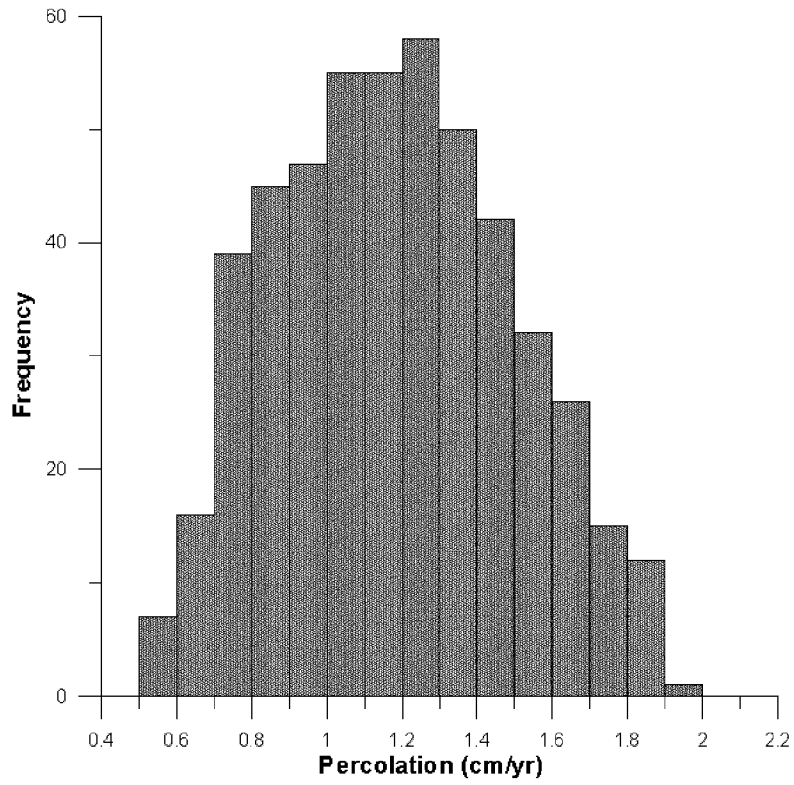


Figure 4-11. Frequency distribution of 500 samples of background percolation.

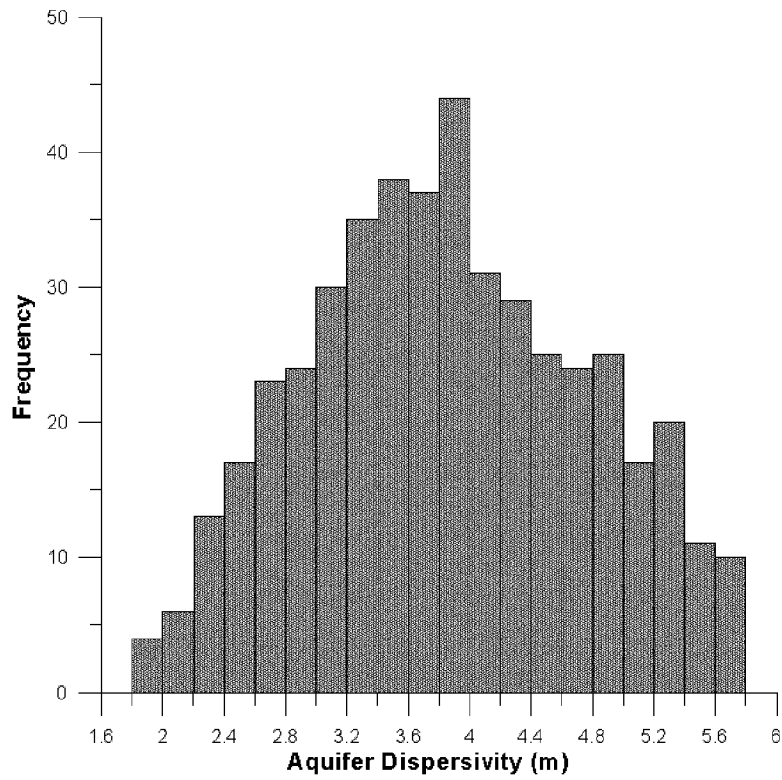


Figure 4-12. Frequency distribution of 500 samples of longitudinal dispersivity in the aquifer.

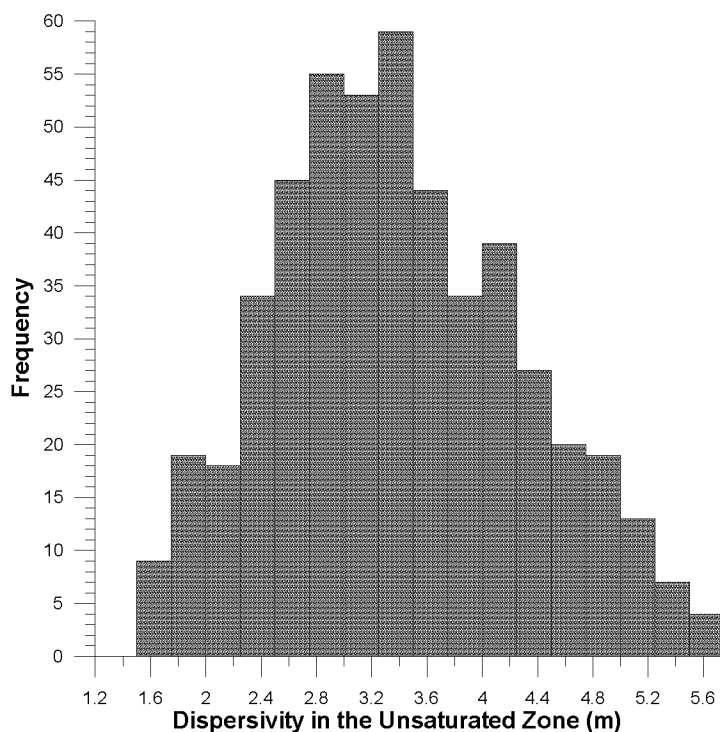


Figure 4-13. Frequency distribution of 500 samples of longitudinal dispersivity in the unsaturated zone.

K = saturated hydraulic conductivity (m/yr)

dh/dx = change in elevation head with respect to distance or the hydrologic gradient (m/m).

The average value for K in the INTEC area was estimated to be $\sim 400 \pm 800$ m/d ($1.46 \times 10^5 \pm 2.92 \times 10^5$ m/yr) (Ackerman 1991). The hydraulic gradient across the site ranges from about 1-4 ft/mi ($dh/dx = 1.9 \times 10^{-4}$ to 7.6×10^{-4}) (Barraclough et al. 1967); therefore, the Darcy velocity is roughly 28 to 110 m/yr. The ICDF engineering design report (EDF-ER-275) used a Darcy velocity of 22 m/yr and this value was also used for the deterministic results. This value is on the low side of estimated Darcy velocities and would tend to produce conservative results because there would be less water for dilution. Based on the relative close proximity of the receptor (100 m downgradient) to the source and that variations in Darcy velocity would be less over that distance compared to the entire Site, an uncertainty of a factor of two was applied to the Darcy velocity. Assuming the deterministic value of 22 m/yr represents the mode of a triangular distribution, the minimum of the distribution is then $22 \text{ m/yr} \div 2 = 11 \text{ m/yr}$ and the maximum is $22 \text{ m/yr} \times 2 = 44 \text{ m/yr}$.

4.6.1.2.6 Sorption Coefficients—Distributions of sorption coefficients were separated into those for waste/interbed materials and those for clay material. The sorption coefficient in the aquifer was always 1/25th the sorption coefficient in the interbed material. Lognormal distributions were assigned in all cases.

Lognormal distributions are appropriate when the range of possible parameter values spans orders of magnitude as is the case with most sorption coefficient data. The geometric mean was assumed to be the deterministic value. The geometric standard deviation (GSD) was based on the distribution of measured K_d values for either sand or clay materials as reported in Sheppard and Thibault (1990). Waste and interbed materials were assumed to be similar to sand. Sheppard and Thibault (1990) report the

standard deviation of sorption coefficient logarithms in their results. This value can be converted to a GSD by taking its exponent. Some of the calculated GSD values were larger than 20 and included values that are clearly outside the range of values observed or considered credible at the INEEL. Because this range was so large, it was decided that the GSD would be defined by the geometric standard deviation of the distribution of geometric means and not by the underlying distribution of individual K_d values. The GSD of the geometric means is then given by

$$GSD_{\mu} = \exp\left(\frac{\sigma}{\sqrt{n}}\right) \quad (4-3)$$

where

- σ = standard deviation of the natural logarithms
- n = number of observations.

Because of the importance of I-129 in the dose estimates, the distribution of iodine sorption coefficients for waste/interbed material and clay is illustrated in Figures 4-14 and 4-15.

4.6.1.2.7 Engineered Cover Lifetime—In the deterministic simulation, the cover was assumed to last 500 years. This assumption was considered a conservative estimate of the cover lifetime because the cover has been designed to last at least 1,000 years. For the uncertainty analysis, 1,000 years was assumed to be the most likely value of a triangular distribution (Figure 4-16) having a minimum value of 100 years (corresponding to the extreme degradation case) and a maximum lifetime

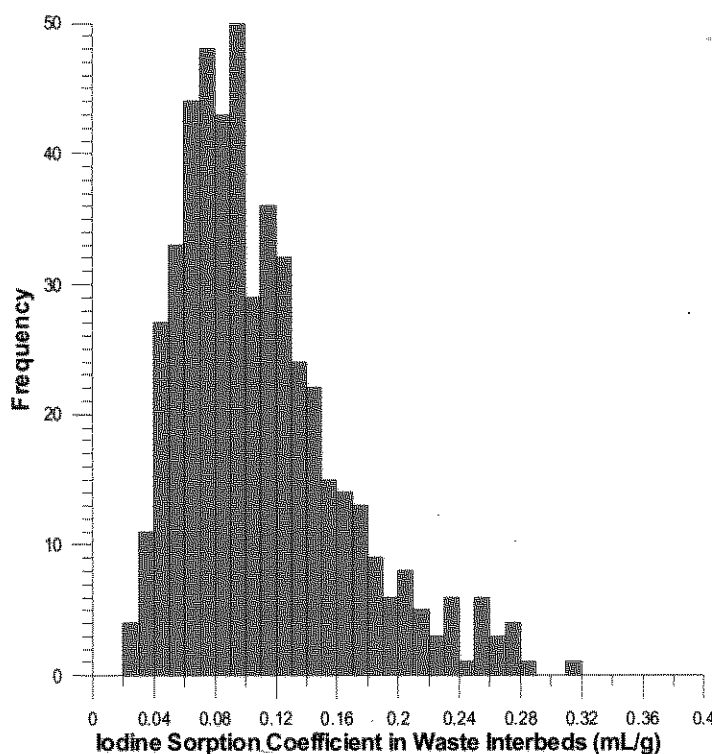


Figure 4-14. Frequency distribution of 500 samples of the iodine sorption coefficient in waste and interbed material.

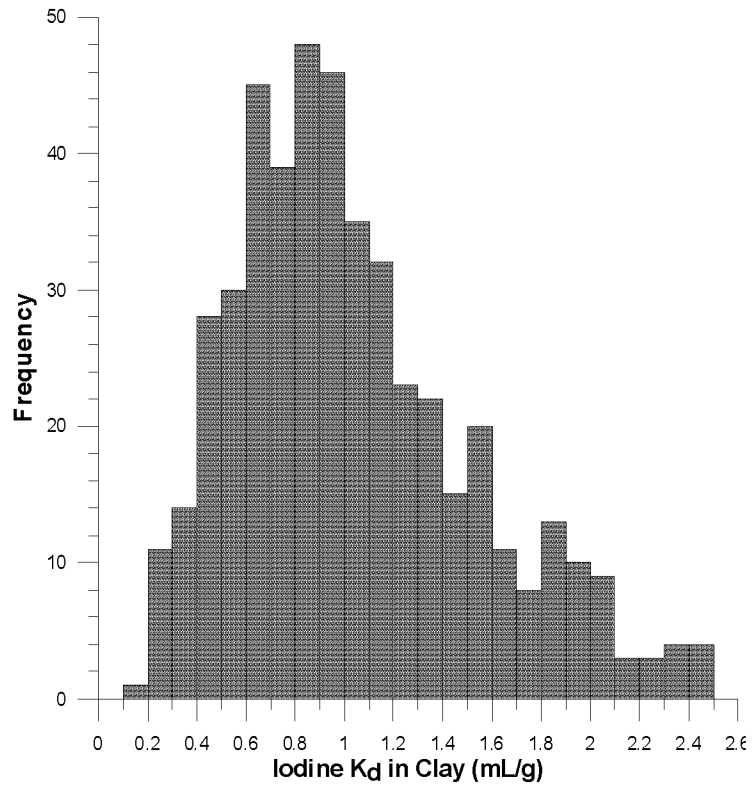


Figure 4-15. Frequency distribution of 500 samples of the iodine sorption coefficient in clay material.

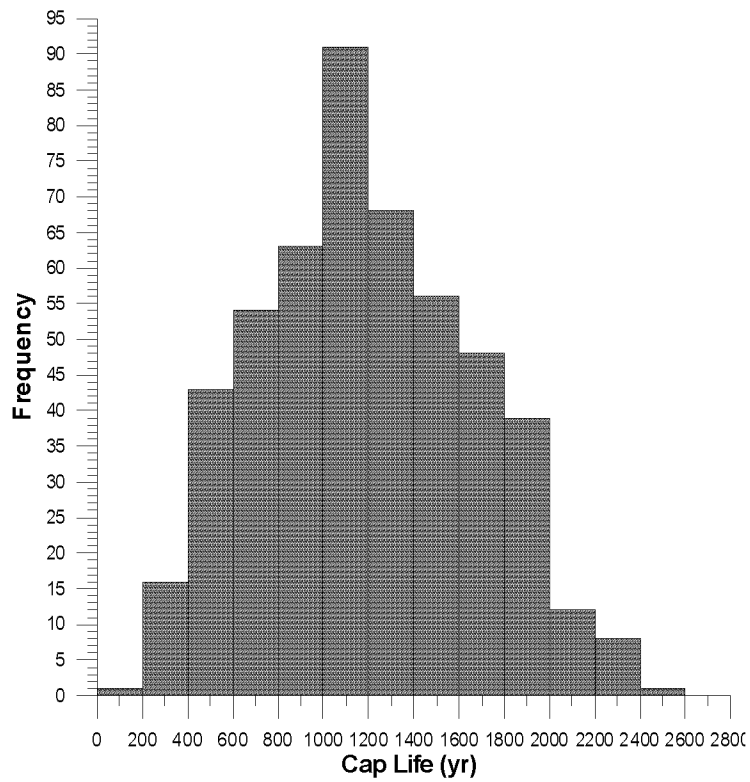


Figure 4-16. Frequency distribution of 500 samples of the cover lifetime.

of 2,500 years. In all cases, the time the cover degrades is equal to the cover integrity lifetime. Therefore, the maximum possible sampled lifetime of the cover would be $2,500 \text{ years} \times 2 = 5,000 \text{ years}$, which is the same overall cover lifetime for the Design Case scenario (1000 years + 4000 year degradation time = 5000 years).

4.6.1.3 Results. Results for the uncertainty analysis are expressed in terms of percentiles of the distribution of the output variable. The percentiles represent an ordered ranking of the values. For example, the 25th percentile represents the 25th highest value, the 50th percentile represents the 50th highest value, and the 95th percentile represents the 95th highest value. The output variable is the total dose. Figure 4-17 shows the distribution of the all-pathways dose as a function of time. The dotted red line represents the median (50th percentile) value. The gray shaded area represents where 90% of the model predictions were. The base of the gray area represents the 5th percentile and the top of the area represents the 95th percentile. Ninety-fifth percentile doses are highest in the year 2500 and reach a maximum of 5.8 mrem/yr. Doses are dominated by I-129. Maximum dose during the 1,000-year time frame of compliance occurred at 1,000 years and had a median value of 0.006 mrem/yr and a 95th percentile value of 0.52 mrem/yr (Table 4-8).

The tails of the distribution are typically sensitive to the number of model realizations. While the increasing number of realizations can improve stability in the tails of the distribution, the important information is the confidence interval around a percentile on the tail of the distribution. For example, the confidence interval around the 5th and 95th percentile value is important to the decision-maker. Hahn and Meeker (1991) provide tabulated values of nonparametric confidence intervals of percentiles for empirical

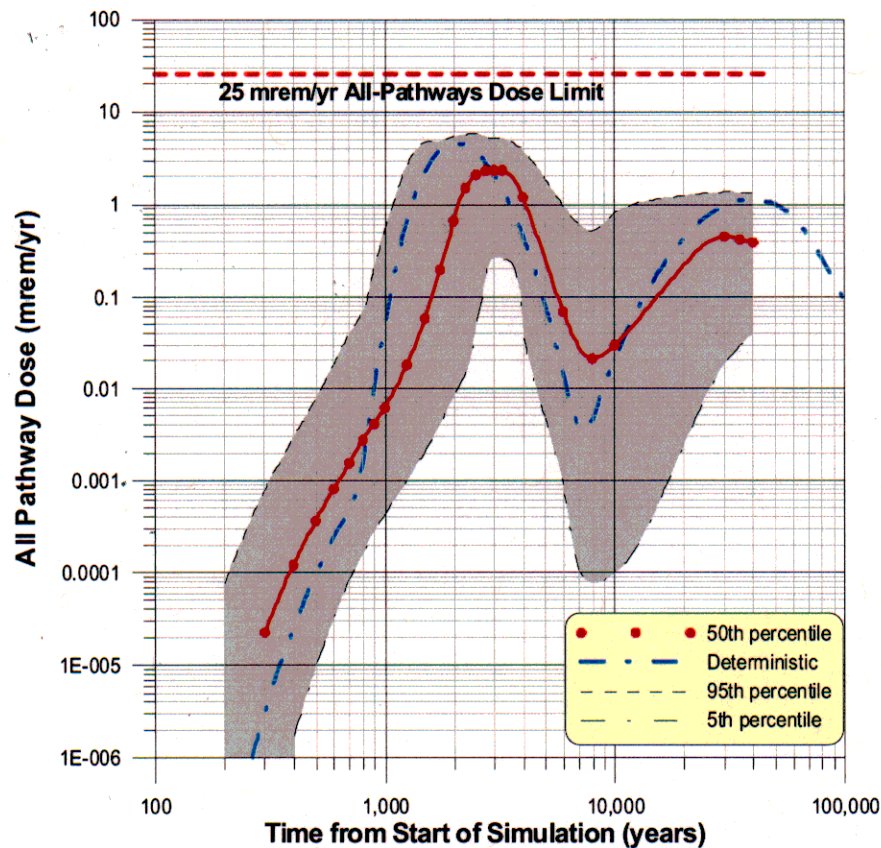


Figure 4-17. Distribution of all-pathways doses as a function of time at the 180-m (100 m downgradient from the edge of source) receptor location. The start time of the simulation is the year 2018.

Table 4-8. Percentiles of the all-pathways dose at 1,000 years (year 3018).

Percentile	All-Pathways Dose (mrem/yr)	Percentile	All-Pathways Dose (mrem/yr)
100.0%	6.5E+00	50.0%	6.0E-03
97.0%	1.3E+00	45.0%	4.6E-03
95.0%	5.2E-01	40.0%	3.7E-03
93.0%	2.6E-01	35.0%	3.3E-03
90.0%	1.4E-01	30.0%	2.6E-03
85.0%	5.8E-02	25.0%	2.1E-03
80.0%	3.7E-02	20.0%	1.5E-03
75.0%	2.7E-02	15.0%	1.2E-03
70.0%	2.2E-02	10.0%	8.3E-04
65.0%	1.5E-02	5.0%	4.3E-04
60.0%	1.2E-02	3.0%	3.0E-04
55.0%	8.1E-03	0.0%	4.1E-05

distributions containing n values. In this case, $n = 500$. The 95% confidence interval around the 95th percentile for 500 model realizations ranged from the 93rd to 97th percentile. The confidence interval around the 5th percentile for 500 model realizations ranged from the 3rd to the 7th percentile. The upper-bound 95% confidence interval for the 95th percentile is the primary interest for this project. The 95% confidence interval around the 95th percentile dose at 1,000 years ranges from ~ 0.26 to ~ 1.3 mrem. Therefore, with 95% confidence, the analysis shows that there is less than a 5% probability that the model predicted all-pathways dose will exceed 1.3 mrem/yr at 1,000 years. Considering the entire distribution of values, the results of the modeling indicate 95% confidence that 95% of the model predicted doses at 1,000 years are between $3.0E-04$ mrem/yr and 1.3 mrem/yr.

In later years ($t > 10,000$ years), doses are dominated by the actinides. Beyond 10,000 years, the 50th percentile dose at the time of maximum dose (at 30,000 years) was 0.45 mrem/yr with the 5th and 95th percentile values of 0.018 to 1.4 mrem/yr, respectively.

Iodine-129 is the major dose contributor and concentrations exceeded the 1 pCi/L MCL after the 1,000-year compliance time. Figure 4-18 shows the cumulative frequency distribution for I-129 concentrations in the aquifer at the end of the compliance time (1,000 years) and at the time of maximum all-pathways dose (deterministic time was 3,000 years). At 1,000 years, there is about a 5% probability that the I-129 concentration will exceed 1 pCi/L. At 3,000 years, there is a greater than 90% probability that the I-129 concentration will exceed 1 pCi/L.

The results presented here indicate the precision of the model is about a factor of 4,000 at the 1,000-year time of compliance. Parameters that contributed to this somewhat large level of uncertainty are discussed in the sensitivity analysis presented in the next section.

It is important to note that the above statements only relate to the model predicted doses and not to any real or actual doses. That is, the parametric uncertainty analysis only evaluates the precision of the model. Model accuracy can only be evaluated by comparing model predictions with measured data. Because the assessment is prospective, measured data with which to compare model predictions do not exist.

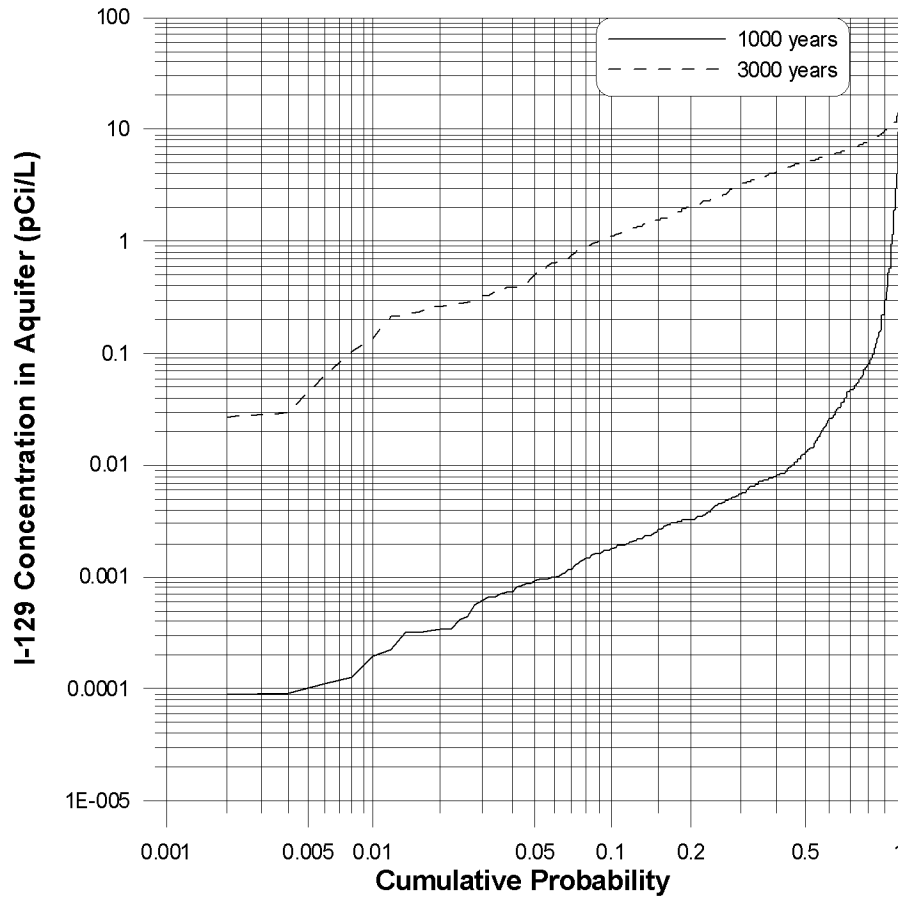


Figure 4-18. Cumulative frequency distribution of the I-129 concentration in the aquifer at the 180-m (100 m downgradient from the edge of source) receptor location for 1,000 years and 3,000 years following closure of the facility in the year 2018.

4.6.2 Sensitivity Analysis

A quantitative sensitivity analysis was performed using the data generated during the Monte Carlo uncertainty analysis. Some aspects of parameter sensitivity were addressed in a previous section (4.6.1.1). This analysis employed a one-factor-at-a-time approach to evaluate the sensitivity of I-129 groundwater concentrations to different cover integrity scenarios. In the approach presented here, the Monte Carlo sampling techniques described earlier were used to propagate input parameter uncertainty into the predicted dose estimates. Then, using regression techniques, rank correlation coefficients were calculated between each parameter and the corresponding predicted dose. Parameter sensitivities are then established by the degree of correlation between the parameter and the output variable (predicted dose).

4.6.2.1 Methodology. The methods used to evaluate parameter sensitivity are described in Crystal Ball[®] software package (Decisioneering Inc. 1993). The rank correlation coefficients provide a quantitative measure of the sensitivity of the predicted dose to variations in the input parameters. Rank correlation replaces each input parameter and endpoint value pair, with its ranking within the distribution. Linear correlation of the rankings is then performed. Consider a simulation of n Monte Carlo trials where the parameters, a , b , and c are defined stochastically. The output variable defined as y , is calculated n times during the simulation. The results may be tabulated as follows:

$$\begin{array}{ccccccc}
a_1 & b_1 & c_1 & \Rightarrow & y_1 & & \\
a_2 & b_2 & c_2 & \Rightarrow & y_2 & & \\
a_3 & b_3 & c_3 & \Rightarrow & y_3 & & \\
. & & & & & & \\
. & & & & & & \\
. & & & & & & \\
a_n & b_n & c_n & \Rightarrow & y_n & &
\end{array}$$

The subscript 1, 2, 3, ...n refer to the Monte Carlo trial number. To calculate the rank correlation coefficient, the values of a_i , b_i , c_i , and y_i are replaced by their ranking within the distribution of values. For example, suppose for the third Monte Carlo Trial, the values a_3 , b_3 , c_3 , are selected yielding an output value of y_3 . Suppose 500 trials are performed and the value of a_3 was ranked at 23, that is, it is the 23rd highest value within the distribution 500 values of a . The value of a_3 is replaced by 23. Likewise, the values of b_3 , c_3 , and y_3 are replaced by their respective ranks. Linear correlation is then performed between the ranks of each of the parameters and output variable, y .

The advantage of rank correlation over simple linear correlation is that it is nonparametric. That is, it is not dependent on the underlying distribution of either the input or output variables. The rank correlation coefficient is given by (Press et al. 1992):

$$r_s = \frac{\sum_i (R_i - \bar{R})(S_i - \bar{S})}{\sqrt{\sum_i (R_i - \bar{R})^2} \sqrt{\sum_i (S_i - \bar{S})^2}} \tag{4-4}$$

where

- r_s = the rank correlation coefficient
- R_i = the rank of the input parameter value
- S_i = the rank of the corresponding output value.

The advantage of using Monte Carlo techniques over that of a one-factor-at-a-time approach is that interaction between parameters are included in the analysis. For example, the sensitivity of the dose due to parameter Y may depend on the value chosen for parameter X . Rank correlation coefficients provide a meaningful measure of the degree to which parameters and the endpoint (all-pathways dose) *change together*. The rank correlation coefficient takes on a value between -1 and $+1$. Perfect correlation is achieved when the absolute value of the correlation coefficient equals 1. Degree of correlation (and thereby degree of sensitivity) decreases with a decrease in the absolute value of the correlation coefficient. A positive correlation coefficient indicates that an increase in the value of the parameter results in an increase in the computational endpoint. A negative correlation coefficient indicates that an increase in the value of the parameter results in a decrease in the computational endpoint.

Another way to visualize the sensitivity analysis results is to compute the percent contribution each parameter has to the total variance. The contribution to the total variance was *approximated* using a simple technique described in the Crystal Ball® software (Decisioneering Inc. 1993) where the rank correlation coefficient for each parameter is squared and normalized to 100%. The output variable for this analysis is total (all nuclides) all-pathways dose at a specific time. Based on the results of the uncertainty analysis, three time periods were chosen 1,000; 3,000; and 10,000 years.

4.6.2.2 Sensitivity Analysis Results. Results of the sensitivity analysis at 1,000 years (Table 4-9) indicate that the total all-pathways dose is most sensitive to the cover infiltration rate, followed by the iodine K_d in waste and interbed material, and the estimated lifetime of the cover. The sign of the rank correlation coefficient indicates total dose is inversely related to the iodine K_d and is positively related to the cover infiltration rate. The remaining parameters each contributed less than 1% to the total variability, with the exception of the aquifer Darcy velocity (3.3%), iodine K_d in clay (6.25%) and the background infiltration rate (11%). Combined, these three parameters contributed ~20.6% to the total variability observed in the all-pathways dose at 1,000 years. Note that the longitudinal, transverse, and vertical dispersivity have essentially the same rank correlation coefficient. This is because the transverse and vertical dispersivity are correlated to the longitudinal dispersivity as described in an earlier section.

The relative importance of the parameters changes for the all-pathways dose at 3,000 and 10,000 years (Table 4-9). At 3,000 years, the Darcy velocity in the aquifer is identified as the most important parameter followed by the iodine K_d in the waste and interbeds. The all-pathways dose at 10,000 years is most sensitive to the uranium K_d , which accounts for 77% of the variability.

Table 4-9. Rank correlation coefficients and percent contribution to variance for the total (all nuclides) all-pathways dose at 1,000; 3,000; and 10,000 years.

Variable	1,000 years		3,000 years		10,000 years	
	Rank Correlation Coefficient	% Contribution to Variance	Rank Correlation Coefficient	% Contribution to Variance	Rank Correlation Coefficient	% Contribution to Variance
Background percolation	3.01E-01	10.953%	1.23E-01	7.447%	3.28E-01	11.784%
Longitudinal dispersivity	6.28E-02	0.479%	-4.33E-02	0.926%	-4.20E-02	0.194%
Transverse dispersivity	6.28E-02	0.478%	-4.33E-02	0.925%	-4.20E-02	0.193%
Vertical dispersivity	6.28E-02	0.478%	-4.33E-02	0.925%	-4.20E-02	0.194%
Dispersivity in unsaturated zone	7.92E-02	0.761%	3.27E-02	0.529%	1.36E-01	2.033%
Darcy velocity	-1.66E-01	3.321%	-3.64E-01	65.51%	-7.16E-02	0.562%
Iodine K_d in clay	-2.27E-01	6.247%	1.18E-02	0.069%	8.97E-03	0.009%
Neptunium K_d in clay	-3.06E-02	0.113%	-2.97E-02	0.437%	-3.98E-02	0.174%
Plutonium K_d in clay	-4.61E-02	0.258%	-3.74E-02	0.691%	6.16E-03	0.004%
Technicium K_d in clay	3.80E-02	0.175%	-2.49E-02	0.308%	1.10E-02	0.013%
Uranium K_d in clay	-6.47E-02	0.508%	2.27E-02	0.255%	-2.17E-01	5.168%
Iodine K_d in waste/interbed	-3.51E-01	14.922%	-1.61E-01	12.757%	9.17E-02	0.923%
Neptunium K_d in waste/interbed	-8.29E-03	0.008%	-8.00E-02	3.161%	-2.37E-02	0.061%
Plutonium K_d in waste/interbed	-1.05E-02	0.013%	-8.17E-02	3.298%	9.39E-02	0.966%
Technicium K_d in waste/interbed	-5.26E-02	0.335%	-2.02E-03	0.002%	-4.79E-02	0.252%
Uranium K_d in waste/interbed	-2.94E-03	0.001%	3.37E-02	0.562%	-8.40E-01	77.353%
Cover lifetime	-3.38E-01	13.812%	6.65E-02	2.189%	-3.08E-02	0.104%
Cover infiltration	6.23E-01	47.137%	-4.52E-03	0.01%	-1.05E-02	0.012%

The sensitivity analysis results illustrate that identifying the most important parameters depends on the scope of the assessment question. If the assessment question is limited to the dose in the 0- to 1,000-year time frame, then the important parameters are the cover infiltration rate, and the iodine K_d value in the waste and interbeds (1,000-year results). If the assessment question includes the maximum dose regardless of the time of occurrence, then the Darcy velocity in the aquifer and the iodine K_d value would be identified as important (3,000-year results). If the assessment question is limited to actinide doses only, then the uranium K_d value would be identified as the most important parameter (10,000-year results). Given that the compliance window for DOE low-level waste performance assessment is 1,000 years, the 1,000-year sensitivity analysis results are most applicable. Therefore, all-pathways doses in the 0- to 1,000-year time frame are most sensitive to the cover infiltration rate and the waste/interbed iodine K_d value.

5. INADVERTENT INTRUDER ANALYSES

Intruder scenarios considered in this PA are limited to those previously described for low-level radioactive waste performance assessments (NRC 1982; Kennedy and Peloquin 1988). These intruder scenarios include both acute and chronic exposure scenarios. Acute exposure scenarios involve exposures of short duration, and include an intruder-construction scenario, a discovery scenario, and a drilling scenario.

Chronic, longer-duration, intruder scenarios include the intruder-agriculture, intruder-resident, and postdrilling scenarios. The *Technical Revision of the Radioactive Waste Management Complex Low-Level Waste Radiological Performance Assessment for Calendar Year 2000* (Case et al. 2000) considered two additional intruder scenarios at the INEEL: chronic intruder-radon and chronic biointrusion. All eight of these scenarios were screened for use in this PA and are discussed in this section.

The intruder scenarios used to support the waste classification limits in 10 CFR 61 were the intruder-construction, intruder-discovery, and intruder-agriculture scenarios. The more restrictive of the scenarios, intruder-construction and intruder-agriculture, were used for setting the Class A and Class C waste classification limits. The intruder-discovery scenario was used for setting the Class B waste limits for short-lived radionuclides (Oztunali and Roles 1986; NRC 1982).

This section

- Discusses the screening methods used to develop the source term used in the intruder analyses
- Presents the basis for the selection of appropriate intruder scenarios for the ICDF landfill PA and describes the selected intruder scenarios
- Discusses the computer code, RESRAD, and input parameters used to model the scenarios
- Presents the doses to inadvertent intruders for acute and chronic scenarios, based on a maximum time of compliance of 1,000 years
- Provides a discussion of sensitive parameters and uncertainty in the calculations.

5.1 Intruder Inventory

The inventory for the ICDF landfill consists of 210 individual radionuclides. The large number of radionuclides presents difficulties in estimating future dose impacts and dilutes resources from those nuclides that are most important. Therefore, contaminant screening was performed to reduce the number of nuclides to a manageable level and focus resources on those nuclides that are most important.

5.1.1 Screening Procedure

The methods presented in NCRP (1996) for ground burial screening were used.

5.1.1.1 Screening of Short-lived Radionuclides. Some nuclides can be eliminated from consideration early in the screening process based on their half-life. Nuclides with half-lives of less than 1 year were eliminated from further consideration, assuming the same screening cutoff the NCRP has implemented in its ground burial screening models. Many of the nuclides removed from consideration were radioactive progeny of longer-lived parents (e.g., Ac-228, Bi-214, Po-210). This screening only

eliminated these nuclides from the disposed inventory; however, they are still considered in the decay chains of longer-lived parents. Table 3-3 presents the results of the screening of short-lived radionuclides.

5.1.1.2 Screening Dose Calculations. The NCRP provides a series of simple screening factors (SFs) that can be used to demonstrate compliance with environmental standards or other administratively set reference levels for releases of radionuclides to the atmosphere, surface water, or ground. The screening factor is essentially a dose conversion factor having units of total EDE per unit of activity (Sv/Bq). These factors incorporate radionuclide fate and transport processes and an assumed exposure scenario to calculate the annual total EDE to a hypothetical receptor per unit of activity in the radionuclide inventory. A complete discussion of the assumptions used in the screening dose calculations for ground disposal may be found in NCRP (1996).

The SFs provided for the ground burial screening include direct, inhalation, soil ingestion, groundwater ingestion, and vegetable ingestion components. For the purpose of selecting radionuclides for intruder analyses, the SFs used in this assessment only included the surface pathways (direct, inhalation, soil, and vegetables) and did not include the groundwater SF. This pathway was addressed in the groundwater dose analysis and is discussed in Section 3.2.

The effective screening value for each radionuclide is calculated using the formula

$$D_i = M_{0,i} \times SF_i \quad (5-1)$$

where

D_i	=	screening value for radionuclide i (Sv)
$M_{0,i}$	=	inventory (Bq)
SF_i	=	screening factor for radionuclide i and all progeny for the period of maximum exposure (Sv/Bq).

The NCRP method decays the initial inventory for 10 years, representing the administrative control period. Because the intruder scenarios do not begin until after 100 years of institutional control, the inventory was decayed for an additional 90 years for this assessment.

Nuclides with an NCRP screening dose of less than 1 mrem (1×10^{-5} Sv) were removed from further consideration. These nuclides are identified in Table 5-1 along with their NCRP screening dose value. The NCRP screening dose is calculated by multiplying the radionuclide inventory by the NCRP screening dose factor.

For some nuclides, NCRP screening factors were unavailable. This typically meant that the nuclide had an extremely long half-life such that it was essentially a stable isotope (Nd-144, radiological decay half-life = 5×10^{15} years). In the case of Ru-106, the half-life is a little over 1 year and therefore would not be present in sufficient quantities to impact total dose. In these cases, the nuclide was screened from the inventory because dose factors were unavailable.

5.1.2 Screening Results

Of the 86 nuclides remaining from the short-lived radionuclides screening presented in Section 3.2.3.1.1, 46 nuclides were screened using the NCRP screening methodology described above, leaving 40 nuclides remaining. These 40 nuclides were then included in the inventory used for intruder analyses.

Table 5-1. Screening results for nuclides with half-lives >1 year using the NCRP screening factors.

Radionuclide	Ground Burial Surface Pathways		Is Screening Dose <1 mrem (1×10^{-5} Sv)?	Radionuclide	Ground Burial Surface Pathways		Is Screening Dose <1 mrem (1×10^{-5} Sv)?
	NCRP Screening Factor (Sv/Bq) ^a	Screening Dose (Sv)			NCRP Screening Factor (Sv/Bq)	Screening Dose (Sv)	
Ac-227	5.69E-11	1.86E-06	yes	Pa-231	1.6E-10	3.03E-04	No
Ag-108m	1.6E-11	2.19E-01	no	Pb-210	1.6E-11	2.90E-08	Yes
Am-241	7.8E-12	4.52E+00	no	Pd-107	2.6E-14	4.43E-06	Yes
Am-242m	5.0E-11	4.24E-05	no	Pm-146	2.1E-12	4.33E-09	yes
Am-243	1.0E-11	9.67E-05	no	Pm-147	0.0E+00	0.00E+00	yes
Be-10	4.2E-14	1.35E-09	yes	Pu-236	1.4E-12	6.93E-17	yes
C-14	1.7E-11	2.16E-05	no	Pu-238	6.2E-12	2.00E+01	no
Cd-109	0.0E+00	0.00E+00	yes	Pu-239	7.5E-12	1.40E+00	no
Cd-113m	3.0E-11	1.45E-02	no	Pu-240	7.4E-12	3.09E-01	no
Cf-249	3.1E-10	3.03E-15	yes	Pu-241	2.3E-13	5.40E-03	no
Cf-250	2.5E-12	1.25E-19	yes	Pu-242	7.1E-12	4.80E-05	no
Cf-251	1.0E-11	2.57E-19	yes	Pu-244	2.9E-11	2.06E-11	yes
Cf-252	0.0E+00	0.00E+00	yes	Ra-226	7.5E-11	9.65E-01	no
Cm-243	5.4E-12	5.98E-08	yes	Ra-228	2.9E-11	2.45E-15	yes
Cm-244	2.9E-12	4.68E-06	yes	Rb-87	1.2E-12	3.60E-07	yes
Cm-245	1.6E-11	3.69E-08	yes	Rh-102	1.8E-12	6.83E-16	yes
Cm-246	7.8E-12	3.89E-10	yes	Ru-106	none	1.00E-99	yes
Cm-247	1.5E-11	2.64E-16	yes	Sb-125	3.5E-13	1.50E-11	yes
Cm-248	2.9E-11	1.58E-16	yes	Sb-126	0.0E+00	0.00E+00	yes
Cm-250	1.8E-10	2.83E-24	yes	Se-79	7.0E-13	3.25E-03	no
Co-60	6.5E-12	2.58E-04	no	Sm-146	8.2E-13	9.80E-12	yes
Cs-134	1.0E-12	2.29E-14	yes	Sm-147	7.4E-13	8.53E-08	yes
Cs-135	1.7E-12	1.70E-03	no	Sm-148	none	1.00E-99	yes
Cs-137	1.4E-11	1.21E+03	no	Sm-149	none	1.00E-99	yes
Eu-150	1.3E-11	2.41E-14	yes	Sm-151	2.0E-15	9.48E-03	no
Eu-152	6.6E-12	1.83E+00	no	Sn-121m	9.9E-13	3.28E-04	no
Eu-154	5.4E-12	1.04E-01	no	Sn-126	3.0E-11	1.24E-01	no
Eu-155	1.7E-13	2.90E-06	yes	Sr-90	3.3E-11	2.36E+03	no
Gd-152	1.4E-12	1.05E-15	yes	Tc-98	3.8E-11	1.90E-07	yes
H-3	2.5E-13	2.20E-03	no	Tc-99	9.8E-12	1.58E+00	no
Ho-166m	1.6E-11	1.15E-06	yes	Te-123	3.3E-13	4.21E-17	yes
I-129	1.0E-11	3.64E-01	no	Th-228	7.1E-13	4.53E-18	yes
In-115	6.4E-13	1.04E-13	yes	Th-229	3.2E-11	4.51E-08	yes
K-40	8.1E-12	4.34E-01	no	Th-230	4.2E-11	2.07E-01	no
Kr-81	8.0E-14	1.19E-11	yes	Th-232	9.9E-11	4.31E-01	no
Kr-85	6.9E-15	6.67E-04	no	Tm-171	0.0E+00	0.00E+00	yes
Nb-92	none	1.00E-99	yes	U-232	3.4E-11	2.15E-04	no
Nb-93m	1.2E-14	6.55E-08	yes	U-233	4.0E-12	2.87E-06	yes
Nb-94	1.7E-11	4.20E-06	yes	U-234	1.6E-12	2.71E-01	no
Nd-144	none	1.00E-99	yes	U-235	6.0E-12	1.86E-02	no
Np-235	0.0E+00	0.00E+00	yes	U-236	1.3E-12	7.38E-03	no
Np-236	0.0E+00	0.00E+00	yes	U-238	3.0E-11	1.64E+00	no
Np-237	6.0E-11	1.08E+00	no	Zr-93	2.4E-14	5.84E-04	no

a. Includes inhalation, direct exposure, and ingestion of soil and produce. Does not include the groundwater pathway.

5.2 Intruder Scenarios

The intruder scenarios assume an individual inadvertently contacts the waste disposed of in the ICDF landfill as defined in and required by DOE O 435.1 IV.P.(2)(h). In order to do so, the intruder must compromise the cover placed over the waste, either through excavation or drilling. Figure 5-1 illustrates the conceptual profile of the disposal facility used in the intruder calculations. Details of the cover design may be found in EDF-ER-281.

The uppermost layer consists of engineered earth fill covered by 0.3 m (1 ft) of a vegetated topsoil/gravel mix. It is designed to promote surface water drainage and minimize erosion. The middle layer consists of a layer of 5- to 13-cm (2- to 5-in.) gravel to prevent biointrusion and layers of filter-type materials to prevent migration of fine-grained material and to provide capillary breaks. The bottom cover barrier layer is designed to intercept water in the event breakthrough occurs from upper cover sections and to divert it laterally. It includes filter material, a geomembrane, and compacted clay. The bottom layer also incorporates a layer of earth fill placed over the waste during operations. The thickness of this operational cover varies; however, EDF-ER-286 states that it is approximately 2 ft. To be conservative, it was assumed to be 1 ft thick.

Based on an erosion analysis, it was estimated that approximately 0.6 m (2 ft) of soil could erode from the surface of the cover over a 1,000-year period (EDF-ER-281). This erosion was considered in the conceptual model.

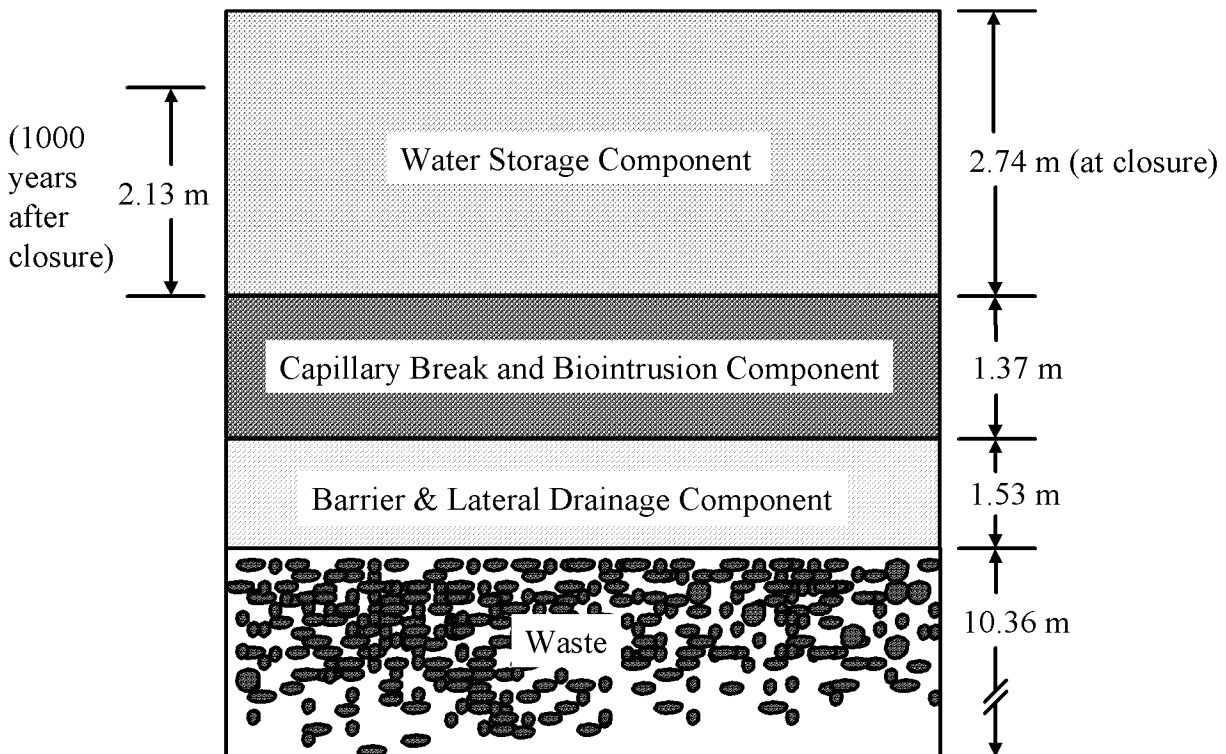


Figure 5-1. Conceptual profile of ICDF landfill.

5.2.1 Acute Intruder Scenarios

Two acute intruder scenarios were considered: (1) the intruder construction scenario and (2) the intruder-discovery scenario. These acute intruder scenarios are described below.

5.2.1.1 Intruder Construction Scenario. The intruder-construction scenario involves an inadvertent intruder who chooses to excavate or construct a building on the disposal site. In this scenario, the intruder is assumed to dig a basement excavation to a depth of approximately 3 m (10 ft) (Oztunali and Roles 1986). It is assumed that the intruder does not recognize the hazardous nature of the material excavated. He or she is exposed to radioactive constituents in the waste during the excavation of a basement. The intruder is also exposed to the exhumed waste by inhalation of resuspended contaminated soil and external irradiation from contaminated soil. Potato cellar excavation was also considered since these cellars are common in the agricultural region surrounding the INEEL. However, potato cellars are relatively shallow, with a typical depth of 1 m (3 ft) (Maheras et al. 1994, 1997). Therefore, the depth to the waste (5.6 m at closure and 5.0 m after 1,000 years) would preclude direct contact with the waste from the 3-m (10-ft) excavation. Moreover, the design of the cover would act to deter someone from digging at the site.

Due to the cover depth over the waste (i.e., greater than 3 m [10 ft]) and the impediments to digging inherent in the cover design, the intruder-construction scenario was not considered for further analysis.

5.2.1.2 Intruder-Discovery Scenario. The intruder-discovery scenario is conceptualized as a modification of the intruder-construction scenario. The basis for the intruder-discovery scenario is the same as the intruder-construction scenario, except that the exposure time is reduced (Oztunali and Roles 1986). The scenario involves the intruder excavating a basement to a 3-m (10-ft) depth. The intruder is assumed to recognize that he or she is digging into very unusual soil immediately upon encountering the biointrusion barriers in the cover, and leaves the site. Consequently, the exposure time is reduced.

It is difficult to imagine a credible discovery scenario that would have an intruder digging to a sufficient depth to contact the waste. Even if the top earth fill layer was breached, the shielding provided by the middle and bottom layers (~ 3 m or 10 ft) would result in insignificant doses for this scenario. It is considered highly improbable that an intruder would dig through 3 m (10 ft) of large gravel, compacted clay, and a geomembrane before realizing that he or she was encountering unusual soil conditions.

In addition, considering the limited exposure time of 6 hours assumed by Oztunali and Roles (1986), this scenario would not provide significant acute doses. Moreover, the intruder-discovery scenario does not have a defined chronic scenario that follows the acute scenario and only considers the exposure during excavation. For example, the chronic intruder-agriculture scenario would not follow the intruder-discovery scenario, further limiting the potential doses from this scenario.

Based on the disposal depth of the waste and limited potential doses, the intruder-discovery scenario for the landfill was not considered for further analysis.

5.2.1.3 Intruder-Drilling Scenario. The intruder-drilling scenario assumes the short-term exposure of a hypothetical intruder to drill cuttings from a borehole penetrating the waste disposal site. This scenario involves wastes buried below the depth of typical construction excavations.

Although the gravel might deter ordinary drilling efforts, the intruder-drilling scenario was retained for analysis in the ICDF landfill PA. It is the only acute scenario that could reasonably occur in which the waste could be contacted, moved to the surface, and expose the intruder.

5.2.2 Chronic Intruder Scenarios

Five potential chronic intruder exposure scenarios were considered: (1) the intruder-agriculture, (2) intruder-resident, (3) intruder-radon, (4) biointrusion, and (5) postdrilling scenarios. These scenarios are described below. Those scenarios not considered applicable to the ICDF landfill PA are screened out from further consideration.

5.2.2.1 Intruder-Agriculture Scenario. The chronic intruder-agriculture scenario is an extension of the acute intruder-construction scenario. It is assumed in this scenario that an intruder lives in the building constructed as part of the intruder-construction scenario and engages in agricultural activities on the contaminated site. The intruder is exposed to contamination by inhalation of resuspended contaminated soil, inhalation of gaseous radionuclides released from the waste, external irradiation, ingestion of contaminated soil, ingestion of contaminated beef and milk, and ingestion of contaminated vegetables. The intruder-resident scenario assumes the intruder constructs a residence on the waste after an excavation or some natural process exposes it.

As stated previously, the intruder-construction scenario was not considered applicable to the ICDF landfill PA. Thus, the intruder-agriculture scenario was not considered applicable and was removed from further analysis.

5.2.2.2 Intruder-Resident Scenario. The intruder-resident scenario assumes that the intruder constructs a residence on the waste after an excavation or some natural process exposes it. This scenario was not considered applicable to the ICDF landfill PA because of the depth of the waste and the shielding provided by the overlying cover. This shielding, along with the shielding provided by the house foundation, would reduce the external dose rates to very low levels. Therefore, the intruder-resident scenario was not considered for further analysis.

5.2.2.3 Intruder-Radon Scenario. The RWMC PA (Case et al. 2000) evaluated the intruder-radon scenario. The intruder-radon scenario assumes that an intruder excavates a 10- \times 10- \times 3-m (30- \times 30- \times 10-ft) basement over the waste while constructing a home. The intruder is exposed to Rn-222 and its short-lived progeny while residing in the home. The exposure from radon emanating from the waste and migrating into the home is evaluated.

DOE M 435.1-1 states that the intruder dose analyses are to exclude the total EDE contribution from radon in air. Therefore, the RWMC chronic intruder-radon scenario was not considered for further analysis.

5.2.2.4 Biointrusion Scenario. The biointrusion scenario, assessed in the RWMC PA (Maheras et al. 1997), assumes that an intruder moves onto the site but does not excavate into the waste. Rather, radioactivity is brought to the surface by plants through root uptake and by burrowing animals.

As discussed in Section 3.4, the depth of cover and the inclusion of biointrusion layers precludes contact with the waste by biota. Therefore, the biointrusion scenario was not considered further.

5.2.2.5 Postdrilling Scenario. The chronic postdrilling scenario is an extension of the acute drilling scenario. It assumes that the intruder occupies the site after drilling a water well and grows crops on a mixture of clean soil and contaminated drill cuttings. After exhumation of the waste, the exposure

pathways are the same as for the intruder-agriculture scenario. This intruder scenario was retained for further analysis.

5.2.3 Acute Scenario Used in the Performance Assessment

The acute drilling scenario assumes an inadvertent intruder drills a well into the contents of the ICDF landfill. The intruder is exposed to contaminated drill cuttings spread over the ground and contaminated airborne dust. In the standard drilling scenario used in many PAs, the intruder is assumed to be exposed to contaminated drill cuttings in a mud pit. However, site-specific information developed through interviews with local well drilling contractors in the Idaho Falls area indicates that drillers spread the cuttings over the ground and do not use mud pits (Seitz et al. 1991). The authors of the RWMC PA (Maheras et al. 1997; Case et al. 2000), used this site-specific deviation of the standard drilling scenario, and it also was incorporated into the ICDF landfill intruder-drilling scenario. The assumption that the drill cuttings are spread over the ground will result in higher dose estimates than if the cuttings were assumed to be in a mud pit because of the decrease in the shielding factor.

The drill cuttings are assumed to be spread over a 2,200-m² (24,000-ft²) lot, which corresponds to about one-half acre. Typical lot sizes located outside of the Idaho Falls city limits are 0.4 to 1.2 ha (1 to 3 acres). Therefore, a 2,200-m² (24,000-ft²) lot size was considered conservative for use in the RWMC Radiological PA (Maheras et al. 1997) and also was incorporated into the ICDF landfill intruder-drilling scenario.

Well drilling contractors in the Idaho Falls area have reported that two types of wells are typically drilled: small-diameter residential wells and large irrigation wells. The small residential wells are typically 15 to 20 cm (6 to 8 in.) in diameter, serve a single residence, and also may provide enough water for a family garden and small quantities of livestock. The large-diameter irrigation wells are drilled to serve systems that irrigate hundreds of acres; the wells are located in the middle of farm fields, not near the farmer's residence. Therefore, a farmer would not drill an irrigation well to acquire water for his residence. Large-diameter irrigation wells are currently drilled in 46-cm (18-in.) diameters, but drilling contractors indicated that 56-cm (22-in.) -diameter irrigation wells would be drilled in the future (Seitz et al. 1991). An acute drilling exposure could result from drilling either a 20-cm (8-in.) -diameter residential well or a 56-cm (22-in.) -diameter irrigation well. The larger 56-cm (22-in.) -diameter irrigation well was assessed for the acute intruder-drilling scenario.

The intruder is assumed to reside by the contaminated cuttings for 160 hours, the time local Idaho Falls well drilling contractors state it would take to drill and develop a 56-cm (22-in.) -diameter irrigation well (Seitz et al. 1991). Based on a waste thickness of 10.4 m (34 ft), the 56-cm (22-in.) well results in 2.5 m³ (88 ft³) of contaminated waste being brought to the surface during the acute drilling scenario. The exposure pathways for this acute drilling scenario include inhalation of resuspended drill cuttings and external exposure to the ground source. Figure 5-2 illustrates the acute intruder-drilling scenario.

The activity concentration of radionuclides in the drill cuttings was determined as follows:

$$C_{s,i} = \frac{C_{w,i}}{\rho} \quad (5-2)$$

where

$C_{s,i}$ = waste activity concentration of radionuclide i (pCi/g)

1×10^{12} = factor for converting Ci to pCi

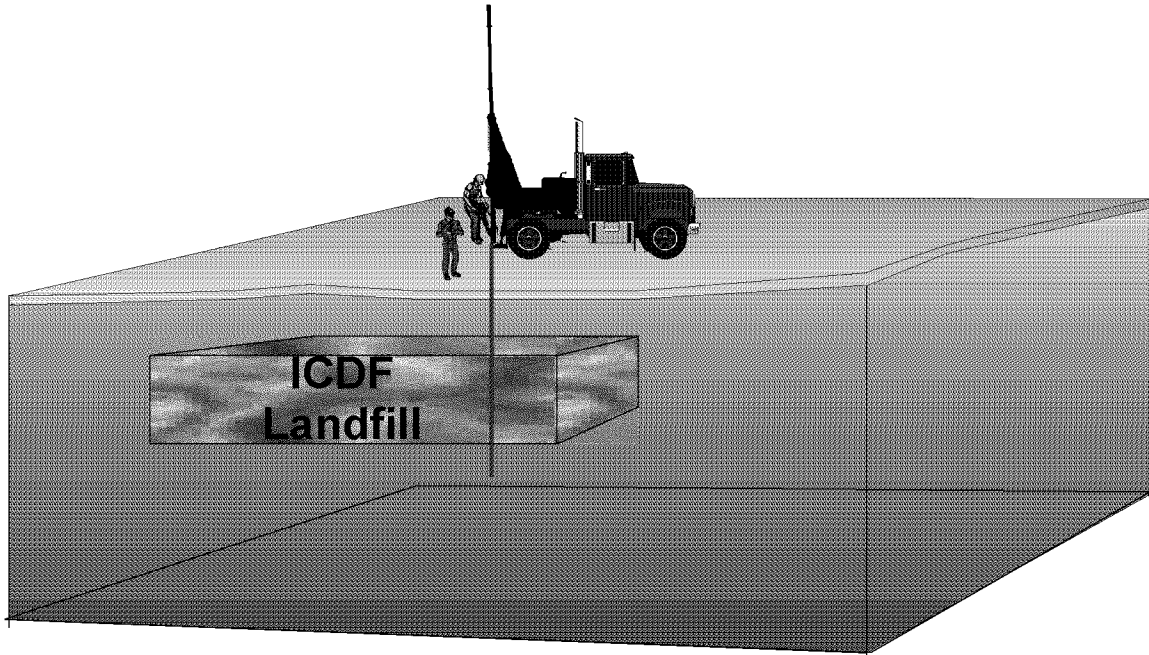


Figure 5-2. Graphical representation of the acute drilling scenario (figure does not depict actual landfill site with final cover and side slopes that would deter drill rig from driving onto cover).

$C_{w,i}$ = waste activity concentration of radionuclide i at the time of intrusion (Ci/m^3)

ρ = bulk density of the cuttings (g/m^3).

Using this equation, the radionuclide concentration in the soil will be the same for any given well radius, but the total amount of contaminated soil will vary with the well radius. This equation conservatively assumes that the radionuclide activity in the waste is not mixed with the soil in the drill cuttings. That is, that only the section containing waste is contained in the contaminated radius. The radionuclide activity would likely be mixed with the well cuttings.

The RESRAD code was used to estimate the dose from acute drilling. The code and input parameters are described in Section 5.3. The results of the analysis are given in Section 5.4.

5.2.4 Chronic Scenario Used in the Performance Assessment

The chronic postdrilling scenario assumes that an inadvertent intruder moves onto the ICDF landfill and drills a residential well into the waste. The drilling portion of the scenario evaluates a 20-cm (8-in.) residential well. This type of well serves a single residence and provides sufficient water for a family garden and small quantities of livestock. As described in the acute drilling scenario, large-diameter wells are drilled to serve irrigation systems (i.e., hundreds of acres) that are located in the middle of farm fields, not near a farmer's residence. Therefore, in the chronic postdrilling scenario, the residence/home garden is evaluated using the traditional drinking water well diameter of 20 cm (8 in.).

The drill cuttings that are brought to the surface are assumed to be spread over 2,200 m^2 (24,000 ft^2) or approximately one-half acre of land surface. The waste is assumed to be mixed to a depth of 61 cm (24 in.). The mixing depth of 61 cm (24 in.) is based on using a deep tilling plow to increase the depth of the root zone and to break up soil compaction. These plows are used in areas of southeast Idaho

with highly erodible soils to minimize erosion. Deep tilling plows have shanks that till to a depth of 61 cm (24 in.), are sold at Idaho Falls implement dealers, and was the tilling depth used in the RWMC PA and accepted by the Low-Level Waste Federal Review Group (LFRG) (Maheras et al. 1997). Based on a waste thickness of 10.4 m (34 ft), the 20-cm (8-in.) well results in 0.3 m³ (11 ft³) of contaminated waste being brought to the surface during the acute drilling scenario.

The chronic postdrilling scenario assumes that the intruder is exposed to the drill cuttings during plowing and cultivation (i.e., dust inhalation). In addition, the intruder is assumed to ingest contaminated food products from the garden and from beef and milk cattle consuming contaminated forage. The intake of contaminated forage by cattle was adjusted according to the fraction of feed grown on contaminated cuttings and the necessary remaining feed obtained from uncontaminated ground. Figure 5-3 provides an illustration of the chronic intruder postdrilling scenario.

The activity concentration of radionuclides in the contaminated zone was calculated as follows:

$$C_{s,i} = 1 \times 10^{12} \times C_{w,i} \times \frac{\pi r_{\text{well}}^2 t_w}{A_c D_c \rho} \quad (5-3)$$

where

- $C_{s,i}$ = soil activity concentration of radionuclide i, (pCi/g)
- 1×10^{12} = factor for converting Ci to pCi
- $C_{w,i}$ = waste activity concentration of radionuclide i at the time of intrusion (Ci/m³)
- r_{well} = radius of the well borehole (m)

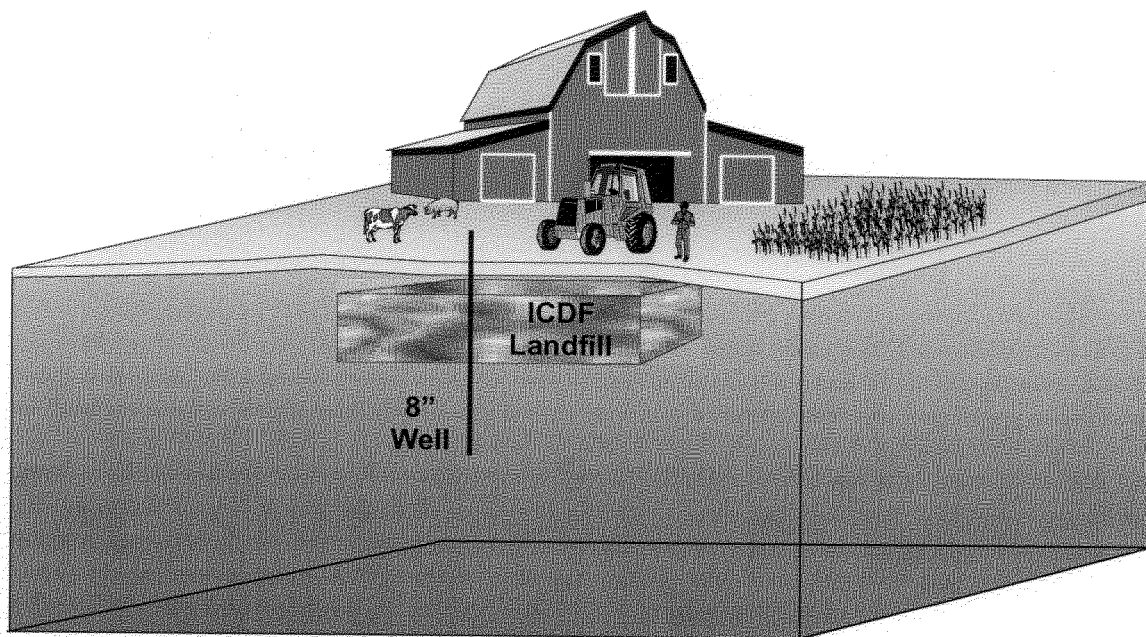


Figure 5-3. Graphical representation of the chronic intruder postdrilling scenario (figure does not depict actual landfill site with final cover and steep side slopes that would deter family from taking up residence).

- t_w = thickness of the waste zone (m)
- A_c = area over which contamination is spread (m^2)
- D_c = final depth of the contaminated zone after tilling (m)
- ρ = bulk density of the soil (g/m^3).

The RESRAD code was used to estimate the dose in the chronic postdrilling scenario. The code and input parameters are described in Section 5.3. The results of the analysis are given in Section 5.4.

5.3 Modeling of Intruder Scenarios

The RESRAD code was selected to calculate the doses from inadvertent intrusion into the waste. The code was selected for use for the reasons discussed in Section 3.3 and because it specifically models the exposure of a receptor to buried waste via inhalation, external exposure, ingestion (food, water and soil), and radon pathways. The code also addresses the gaseous forms of C-14 and tritium independent of particulate forms. In addition, RESRAD keeps track of progeny ingrowth and includes the progeny activity in the dose calculations.

5.3.1 Time Periods Modeled

Intruder doses were calculated at various times after site closure in the year 2018 after the 15-year operational period. The three time periods of concern are

- Institutional control (100 years following closure). During this period, maintenance and surveillance monitoring of the disposal facility would continue.
- Compliance Period (100 to 1,000 years following closure). During this period, the INEEL Site boundary would cease to exist and the area near the landfill would be available for unrestricted access and use by the public.
- Postcompliance Period (beyond 1,000 years). The maximum time of compliance for DOE O 435.1 is 1,000 years; however, calculations may be extended beyond this if doses appear to increase due to progeny ingrowth.

5.3.2 Input Parameters Used to Model the Acute Drilling Scenario

Table 5-2 presents the input parameters used in the RESRAD code to model the acute drilling scenario. In addition, the RESRAD default dose conversion library was used.

5.3.3 Input Parameters Used to Model the Chronic Postdrilling Scenario

Table 5-3 presents the input parameters used in the RESRAD code to model the chronic drilling scenario. In addition, the default dose conversion library was used.

Table 5-2. Input parameters used in acute drilling scenarios.

Parameter(s)	Value	Comments
Soil concentrations:	Estimated using Equation 5-2.	
Calculation times:	1, 100, 1,000, 10,000, & 100,000 yr	
Contaminated zone		
Area:	2200 m ²	Maheras et al. 1997
Thickness ^a :	0.115 cm	Footnote a
Cover and Contaminated Zone Hydrology		
Cover depth:	0 m	
Density of contaminated zone:	1.946 g/cm ³	EDF-ER-264
Contaminated zone erosion rate:	0 m/yr	
Contaminate zone total porosity:	0.4	Default
Contaminate zone field capacity:	0.2	Default
Contaminated zone hydraulic conductivity:	10 m/yr	Default
Contaminated zone <u>b</u> parameter:	5.3	Default
Humidity in air:	0.35 g/m ³	Case et al. 2000
Evapotranspiration coefficient:	0.5	Default
Wind speed:	0.0001 m/s	Min. wind speed for max.
Precipitation:	0.2212 m/yr	Average INEEL value
Irrigation:	0 m/yr	
Runoff coefficient:	0.2	Default
Occupancy, Inhalation, and External Gamma Data		
Inhalation rate:	8400 m ³ /yr	Default
Mass loading for inhalation:	0.001 g/m ³	Maheras et al. 1997
Exposure duration:	1 yr	
Indoor dust filtration factor:	0.4	Default
External gamma shielding factor:	0.7	Default
Indoor time fraction:	0	
Outdoor time fraction:	0.018	160 hrs/yr (Maheras et al. 1997)
Shape of the contaminated zone:	Circular	
Ingestion data, nondietary data		
Depth of soil mixing layer:	0.115 cm	Footnote a
Carbon-14 Data		
C-12 concentration in local water:	0.00002 g/cm ³	Default
C-12 concentration in contaminated soil:	0.03 g/g	Default
Fraction of vegetation C absorbed from soil:	0.02	Default
Fraction of vegetation C absorbed from air:	0.98	Default
Thickness of evasion layer of C-14 in soil:	0.3 m	Default
C-14 evasion flux rate from soil:	7.00E-07 1/sec	Default
C-12 evasion flux rate from soil:	1.00E-10 1/sec	Default
Grain faction in livestock feed		
Beef cattle:	0.8	Default
Milk cow:	0.2	Default
DCF Correction factor for gaseous forms of C-14:	123.4	Default
<p>a. Volume of waste (10.36 m thick) brought to surface via a 22-inch (0.5588 m) well: 2.54 m³ Thickness of waste brought to the surface: 0.115 cm</p>		

Table 5-3. Input parameters used in chronic drilling scenarios.

Parameter(s)	Value	Comments
Soil concentrations:	Estimated using Equation 5-3.	
Calculation times:	1, 100, 1,000, 10,000, & 100,000 yr	
Contaminated zone		
Area:	2200 m ²	Maheras et al. 1997
Thickness ^a :	0.61 m	Footnote a
Cover and Contaminated Zone Hydrology		
Cover depth:	0 m	
Density of contaminated zone:	1.5 g/cm ³	Footnote b
Contaminated zone erosion rate:	0 m/yr	
Contaminate zone total porosity:	0.4	Default
Contaminate zone field capacity:	0.2	Default
Contaminated zone hydraulic conductivity:	10 m/yr	Default
Contaminated zone ^b parameter:	5.3	Default
Humidity in air:	0.35 g/m ³	RWMC PA
Evapotranspiration coefficient:	0.5	Default
Wind speed:	3.3528 m/s	Average INEEL value
Precipitation:	0.2212 m/yr	Average INEEL value
Irrigation:	0 m/yr	
Runoff coefficient:	0.2	Default
Watershed area for nearby stream or pond	1.00E+06 m ²	Default
Accuracy for water/soil computations	1.00E-03	Default
Occupancy, Inhalation, and External Gamma Data		
Inhalation rate:	8400 m ³ /yr	Default
Mass loading for inhalation:	5.53E-05 g/m ³	Maheras et al 1997
Exposure duration:	1 yr	
Indoor dust filtration factor:	0.4	Default
External gamma shielding factor:	0.7	Default
Indoor time fraction:	0.5	Default
Outdoor time fraction:	0.25	Default
Shape of the contaminated zone:	Circular	
Ingestion Pathway, Dietary Data		
Fruit, vegetable, and grain consumption:	94 kg/yr	Case et al. 2000
Leafy vegetable consumption:	17 kg/yr	Case et al. 2000
Milk consumption:	89 L/yr	Case et al. 2000
Meat and poultry consumption:	55 kg/yr	Case et al. 2000
Soil ingestion	3.65 g/yr	Case et al. 2000
Ingestion pathway, nondietary data		
Livestock fodder intake for meat	5.4	Case et al. 2000
Livestock fodder intake for milk:	7.2	Case et al. 2000
Livestock water intake for meat:	50	Default
Livestock water intake for milk:	160	Default
Livestock intake of soil:	0.5	Default
Mass loading for foliar deposition:	0.0001	Default
Depth of soil mixing layer:	0.61	Maheras et al. 1997
Depth of roots:	0.15	Maheras et al. 1997
Groundwater Fractional Usage		
Livestock water:	1	Default
Irrigation water:	1	Default
Depth of soil mixing layer:	0.61 m	Maheras et al. 1997
Storage Times Before Use Data		
Fruit, non-leafy vegetables, and grain:	14 days	Default
Leafy vegetables:	1 days	Default
Milk:	1 days	Default
Meat:	20 days	Default
Well water:	1 days	Default
Surface water:	1 days	Default
Livestock fodder:	45 days	Default
Carbon-14 Data		
C-12 concentration in local water:	0.00002 g/cm ³	Default
C-12 concentration in contaminated soil:	0.03 g/g	Default
Fraction of vegetation C absorbed from soil:	0.02	Default
Fraction of vegetation C absorbed from air:	0.98	Default
Thickness of evasion layer of C-14 in soil:	0.3 m	Default
C-14 evasion flux rate from soil:	7.00E-07 1/sec	Default
C-12 evasion flux rate from soil:	1.00E-10 1/sec	Default
Grain fraction in livestock feed		
Beef cattle:	0.8	Default
Milk cow:	0.2	Default
DCF Correction factor for gaseous forms of C-14	123.4	Default

a. Plow depth.

b. Density of well drillings and surface soil = 1.5 g/cm³

5.4 Results

Table 5-4 presents the results of modeling the intruder scenarios using RESRAD. Acute and chronic intruder analyses for the 1,000-year compliance period are based on drilling a well through the waste in the ICDF landfill. Calculations are provided beyond 1,000 years, to 100,000 years, to detect potential increasing trends in doses due to ingrowth of radioactive daughters.

5.4.1 Acute Drilling Scenario

The acute intruder drilling scenario yielded a peak dose of 12.6 mrem in 2118, the end of institutional control (see Table 5-4). Inhalation accounted for the majority of the dose. Plutonium-238 and Am-241 were the dominant inhalation pathway radionuclides, contributing 49% and 11% of the total estimated dose, respectively. The dominant radionuclide for the external exposure pathway was Cs-137, which contributed 29% of the entire dose.

The dose was below the DOE O 435.1 acute exposure standard of 500 mrem. If the maximum time of compliance were extended past 1,000 years, the peak doses from the acute drilling scenario would be unaffected because the peak doses occurred at 100 years.

5.4.2 Chronic Postdrilling Scenario

The maximum chronic intruder postdrilling dose was calculated to be 3.3 mrem/yr and occurred in the year 2118 (100 years after closure of the ICDF landfill). External exposure and ingestion are the predominant exposure pathways. Strontium-90 and Cs-137 were the major contributors to the total predicted dose. External exposure from Cs-137 accounted for 46% of the total dose, while the ingestion pathway, via contaminated plants, dominated the dose from Sr-90, representing 53% of the total dose.

The dose was well below the DOE O 435.1 chronic exposure standard of 100 mrem/yr. If the maximum time of compliance were extended past 1,000 years, the peak doses from the chronic drilling scenario would be unaffected because the peak doses occurred at 100 years after institutional control ceased.

Table 5-4. Acute and chronic intruder doses.

Years	Acute Drilling Scenario Dose (mrem)	Chronic Drilling Scenario Dose (mrem/year)
100	12.6	3.3
500	1.9	0.007
1,000	1.2	0.006
3,000	0.8	0.005
5,000	0.7	0.005
10,000	0.7	0.006
100,000	0.6	0.02
Years/Standard	Acute Drilling Scenario Maximum Dose (mrem)	Chronic Drilling Scenario Maximum Dose (mrem/year)
100 to 1,000	12.6	3.3
100 to 1E+5	12.6	3.3
DOE O 435.1	500	100

5.5 Sensitivity and Uncertainty

This section presents the sensitivity and uncertainty associated with the inadvertent intruder analyses. Per the guidance of DOE M 435.1-1, the evaluation is limited to qualitative arguments.

Uncertainty exists in formulating the model used to quantify the behavior of the system. The uncertainty results from incomplete knowledge of the system or process and includes the uncertainty in the choice and specification of scenarios. Because the performance assessment addresses impacts that occur in the future, there is great deal of uncertainty associated with the predictions of potential land use and, therefore, the selection of the intruder scenario. It is impossible to determine if the intruder scenarios selected accurately simulate what will happen at the landfill following a period of institutional control. Because of this, the approach taken was to remove unimportant scenarios from further consideration and to select scenarios that reasonably bound potential doses.

Section 5.2 provides the basis for the selection of the acute drilling scenario and the chronic postdrilling scenario for evaluation in the performance assessment. Many of the standard scenarios were not considered applicable because of the depth (5.6 m) and design of the cover. Any scenario involving excavation of the cover was eliminated because of the impediments that would be encountered in the cover (i.e., rock armor, geomembrane, and compacted clay). In addition, even if the intruder ignored these barriers, the depth of the basement (typically 3 m) would preclude contact with the waste. It could be argued that significant erosion of the cover could result in a cover depth that would accommodate excavation to the waste layer. However, an erosion analysis of the cover concluded that approximately 0.6 m (2 ft) of soil could erode from the surface of the cover over a 1,000-year period (EDF-ER-281).

The acute and chronic intruder scenarios assume that an individual drills through the waste and brings waste material to the surface. Although these scenarios are more logical than the construction scenarios, they are still unlikely to occur and thus are very conservative in nature. It could be argued that the person drilling the well would be discouraged from drilling, particularly when encountering the biointrusion layer, which incorporates Type 3 armor comprised of 5- to 13-cm (2- to 5-in.) gravel, and unnatural materials, such as the geomembranes. In addition, it is unlikely that the site would be selected for well drilling as it is elevated above the surface and is obviously man-made. The sloped edges will be lined with basalt riprap armor, sharply defining the landfill as an obvious human artifact.

Additional conservatism was added to the intruder analyses through the use of the following assumptions that were made:

1. A 56-cm (22-in.) irrigation well, instead of a 15- to 20-cm (6- to 8-in.) residential well, was selected for the acute drilling scenario to assure that more waste material was brought to the surface.
2. A 20-cm (8-in.) residential well was selected over a more typical 15-cm (6-in.) well in the chronic postdrilling scenario to maximize the volume of waste brought to the surface.
3. In the acute drilling scenario, the material was spread over the surface of a half-acre lot, rather than in a mud pit, so that the intruder directly contacts the waste and the waste is not diluted.
4. The drill cuttings of waste were not diluted with other subsurface media acquired in the cuttings resulting in more conservative dose calculations.

Uncertainty exists in the selection of the model used to quantify the selected scenarios. Uncertainty in the model selected, RESRAD, can only be evaluated through model validation. Model validation answers the question “Does the model accurately simulate the behavior of the system?” While it is beyond the scope of this analysis to perform model validation, there are several features of the RESRAD model that provided confidence that it was appropriate to model the performance of the ICDF landfill (see Section 3.3). These features include the following:

1. RESRAD was developed for DOE to calculate radiation doses and excess lifetime cancer risk to a chronically exposed onsite resident, as well as to provide residual radioactive material guidelines.
2. Nine environmental pathways are considered: direct exposure; inhalation of particulates and radon; and ingestion of plant foods, meat, milk, aquatic foods, water, and soil.
3. The RESRAD code has been verified, has undergone several benchmarking analyses, and has been included in the IAEA's VAMP and BIOMOVs II projects to compare environmental transport models.
4. RESRAD can incorporate site-specific data, which enables more realistic dose assessments

Many uncertainties are associated with the parameter values selected for the model. Typically, parametric uncertainty is assessed through an uncertainty analysis, which involves quantifying the uncertainty of model output, based on the uncertainty of parameter values input into the model. Uncertainty analysis of the intruder scenarios was not conducted. Instead, to help ensure that the conclusions of the PA are reasonable, conservative values were selected, when appropriate, particularly for sensitive parameters. For example, one sensitive parameter in the modeling of the acute drilling scenario is the wind speed. Varying the wind speed produced extremely different results. Using the minimum wind speed allowed resulted in maximum inhalation doses due because minimum wind speed results in maximum airborne particulate concentrations at the site.

Another sensitive parameter, for both the acute and chronic intruder scenarios, is the leaching rate from the waste. When the leach rate was calculated by the RESRAD code, the source term was, in many cases, quickly depleted. This resulted in much lower doses than expected if leaching was suppressed. The source leach rate constant was thus set to a minimum rate of $1E-30 \text{ yr}^{-1}$ for each radionuclide to conservatively ensure that the maximum radionuclide concentrations were available over time for the intruder scenarios.

6. INTERPRETATION OF RESULTS

In this section, the results presented in Sections 4 and 5 are consolidated to provide the basis for evaluating the performance of the disposal facility. The goals of the interpretation of results are to

- Address the findings of the sensitivity and uncertainty analyses to provide an overall estimate of the expected performance of the disposal facility that is defensible for each of the performance criteria for the time of compliance at the points of compliance
- Provide a rational basis to conclude that the performance of the LLW disposal facility has been completely addressed
- Provide a rational basis to conclude that the analysis is logically interpreted
- Provide a rational basis to conclude that the results are correct representations of the facility performance
- Provide a rational basis to conclude that the results are sufficiently rigorous.

The interpretation of the results includes the findings for the

- All-pathways analysis
- Radon flux analysis
- Air pathway analysis
- Groundwater resource protection analysis
- Inadvertent intruder analysis.

6.1 All-Pathways Dose

All-pathways doses were predicted to be below the 25 mrem/yr standard for the 1,000-year compliance time frame (Table 6-1). As presented in Section 4.5.1, the predicted maximum all-pathways dose during the 1,000-year compliance period (year 2018–3018) was estimated to be 0.047 mrem/yr. Virtually all of the dose is attributed to I-129 during the 1,000-year compliance time period and for the next 3,000 years following closure of the facility. The maximum all-pathways dose for any time was 4.6 mrem/yr and occurred 2,100 years after closure of the facility. Doses from actinides reach a maximum of 1.1 mrem/yr approximately 38,750 years following closure of the facility. Actinide doses are dominated by U-234 and Np-237.

Table 6-1. Maximum all-pathways doses and time of maximum at the 180-m (100 m downgradient from the edge of source) receptor location.

Nuclide	0 to 1,000-year (year 2018–3018) All-Pathways Dose (mrem/yr)	>1,000-year (> year 3018) All-Pathways Dose (mrem/yr)	Time of Maximum Dose (years from end of operations)
I-129	0.047	4.5	2,100
Np-237	0	0.49	42,750
Pu-239	0	2.6×10^{-5}	790,000
Pu-240	0	1.5×10^{-5}	620,000
Tc-99	2.0×10^{-4}	0.11	2,500
U-234	0	0.53	34,750
U-238	0	0.13	35,750
Maximum actinide dose	0	1.1	38,750
Maximum dose (all nuclides)	0.047	4.6	2,100

The examination of model sensitivity and uncertainty incorporated two types of analyses: (1) a one-factor-at-a-time analysis and (2) a Monte Carlo analysis. A one-factor-at-a-time analysis is used to examine the impact of the output variable to variations in a single parameter. The output variable was the I-129 concentration in groundwater. Iodine-129 was chosen because it dominates the dose for the first 3000 years following closure of the facility. The sensitivity of the output variable to changes in the cover failure and degradation time was examined. A Monte Carlo uncertainty analysis was used to estimate an empirical probability distribution of the output variable based on a stochastic sampling of model input. It was useful for quantifying model precision and identifying which parameters the output variable was most sensitive to. The output variable for the Monte Carlo simulation was the total all-pathways dose.

The one-factor-at-a-time analysis indicated that changing the cover failure time shifts the maximum concentration in the aquifer along the time axis by the difference in the time of failure from the assumed base case value of 500 years. For example, if the failure time is 1,000 years (instead of 500 years), then all concentrations and doses occur about 500 years later than predicted in the base case. The magnitude of the concentration also decreases slightly because the time the cover degrades is proportional to the cover integrity time. That is, if the cover lasts 1,000 years then it is assumed to degrade over the next 1,000 years. The Design Case scenario assumed a 1,000-year cover lifetime with a 4,000-year cover degradation time. This scenario resulted in the most significant reduction in the peak concentration (almost a factor of 2) from the base case results.

To address uncertainty of the remaining nuclides and the overall all-pathways dose estimate, a parametric uncertainty analysis was performed. Parametric uncertainty analysis uses an estimated frequency distribution of values for each model parameter considered to be uncertain and produces a frequency distribution of model predictions or output. Details are presented in Section 4.6.1.2. The results presented indicate the precision of the model is roughly four orders of magnitude 1,000 years from site closure (year 3018). Based on the Monte Carlo uncertainty analysis, the analysis indicates with a 95% confidence that there is less than a 5% probability that the model-predicted all-pathways dose will exceed 1.3 mrem/yr for the 1,000-year compliance time.

The rather large uncertainty bounds of the all-pathways dose at 1,000 years (approximately a factor of 4,000, see Table 4-8 and Figure 4-17) indicate that doses in the 1,000-year time frame are extremely sensitive to model assumptions that govern release and transport of I-129. Contrast that with doses at, for example, 30,000 years, which spanned ~2 orders of magnitude, and are dominated by actinides. Intuitively, one might expect doses out at 30,000 years to have greater uncertainty than dose estimates made in the 0- to 1,000-year time frame. However, in this case, the dose in the 0- to 1,000-year time frame was shown to be particularly sensitive to the time of cover failure, cover infiltration rates, and the waste/interbed K_d for iodine. The cover failure time and waste/interbed iodine K_d were shown to have little impact on the dose beyond 10,000 years.

Note that the above statement only relates to the predicted doses and not to any real or actual doses. That is, the parametric uncertainty analysis only evaluates the precision of the model. Model accuracy can only be evaluated by comparing model predictions with measured data. Because the assessment is prospective, measured data with which to compare model predictions do not exist.

6.2 Radon Flux Results

As discussed in Section 4.3, the projected waste inventory is not a significant radon source. Radium-226 concentrations in the ICDF landfill waste (0.5 pCi/g) are less than background concentrations found in INEEL soils (0.75 to 1.4 pCi/g assuming secular equilibrium with Th-230) (Rood et al. 1996). In spite of this observation, a very conservative radon flux calculation was performed. It was assumed that the waste is covered by only 2 ft of clay, the most limiting material, in terms of hydraulic conductivity.

The peak result within the 1,000-year period of compliance, 0.17 pCi/m²-s, is well below the performance objective of 20 pCi/m²-s. Of the radionuclides disposed in the waste, the major dose contributor is Ra-226. The result, given the conservative nature of the calculations, should provide confidence in the long-term performance of the facility.

6.3 Air Pathway Results

As presented in Section 4.4, the air pathway analysis is based on the bounding assumption that the entire inventory of gaseous radionuclides (tritium, C-14, and Kr-85) is released from the cover surface in 1 year. The results (4.60E-04 mrem/yr at closure and 6.67E-03 mrem/yr at the end of institutional control) are below the current INEEL baseline dose (1.01E-02 mrem/yr) estimated for NESHAP compliance (DOE-ID 2001b). The major nuclide contributors to dose were Kr-85 during operations and tritium following institutional control. When summed with the baseline dose, the estimated doses are well below the 40 CFR 61 standard of 10 mrem/yr for the entire INEEL.

The results should be considered bounding, given the extremely conservative emissions assumption, and therefore provide assurance that the facility will not exceed atmospheric limits.

6.4 Groundwater Protection Results

As explained in Section 3.2, for the ICDF landfill flow and transport simulations it was assumed for the facility design analyses that all contaminants disposed of to the facility will be noncontainerized, compacted soils. After closure, the facility will be covered with an infiltration-reducing cover that will reduce the infiltration rate to 0.1 mm/yr for 500 years. After 500 years, the infiltration rate is assumed to increase to the undisturbed soils background infiltration rate of 1 cm/yr, for the rest of the time of evaluation. Beneath the waste will be engineered layers of soil. One layer will be a clay layer that will retard the transport of all sorbed contaminants leached from the waste to the vadose zone.

The vadose zone was simulated as a single homogeneous layer that includes 1-dimensional flow and transport with dispersion. The aquifer was simulated as a homogeneous and isotropic 1-dimensional flow and 3-dimensional transport problem. The point of compliance is the upper 15 m of the aquifer, 180 m from the center of the ICDF landfill, and 100 m downgradient from the edge of the waste. Details of the model are provided in Section 3.2.

Groundwater protection is evaluated by comparing predicted concentrations in groundwater with MCLs for radionuclides. Four types of concentrations are calculated: gross alpha concentration (excluding uranium and radon), Ra-226/Ra-228 concentration, committed dose equivalent (CDE) from beta-gamma-emitting radionuclides, and total uranium mass concentration. Note that the beta-gamma groundwater protection standard is CDE whereas the all-pathways dose is total EDE. The EDE (used in Section 4.5.1) was calculated using dose conversion factors from Federal Guidance Report 11 (EPA 1988) whereas CDE values were calculated using data for the 168-hour week from National Bureau of Standards Handbook 69 (DOC 1963).

Results of calculations (Table 6-2) for the ICDF landfill performance assessment indicate the 4 mrem/yr CDE beta-gamma drinking water standard is not exceeded during the 1000-year compliance period (year 2018-3018). Almost all the beta-gamma dose is from I-129. Beyond the 1000-year compliance period (>year 3018), the MCL for I-129 is exceeded at the 100 m compliance point. Gross alpha activity reaches a maximum of 2.3 pCi/L 34,750 years after the closure of the facility. Radium-226 and Ra-228 reach a maximum concentration of 0.029 pCi/L 41,750 years after closure of the facility. Both the gross alpha activity concentration and the Ra-226/Ra-228 concentration were below the standards of 15 and 5 pCi/L, respectively.

As with the all-pathways dose results, the I-129 is the primary contaminant of concern for the groundwater protection criteria.

Table 6-2. Comparison of groundwater protection criteria.

Groundwater Performance Measure	0 to 1,000 years (year 2018–3018)	>1,000 years (year 3018 and beyond)	Comments
Beta-gamma dose \leq 4 mrem/yr CDE	0.41 mrem/yr	39 mrem/yr	Almost all of the dose is due to I-129
Gross alpha activity \leq 15 pCi/L	0.0 pCi/L	2.3 pCi/L	—
Uranium concentration $<$ 20 μ g/L	0.0 μ g/L	1.6 μ g/L	—
Ra-226/Ra-228 concentration \leq 5 pCi/L	0 pCi/L	0.029 pCi/L	Ingrowth from U-238, U-234, and Th-232 parents

6.5 Inadvertent Intruder Analysis Results

The maximum dose calculated for the acute intruder-drilling scenario is 12.6 mrem, 100 years after facility closure. Inhalation accounts for the majority of the dose. Plutonium-238 and Am-241 are the dominant inhalation pathway radionuclides, contributing 49% and 11% of the total estimated dose, respectively. The dominant radionuclide for the external exposure pathway was Cs-137, which contributes 29% of the entire dose. The total dose is significantly less than the DOE O 435.1 performance objective of 500 mrem.

The maximum dose calculated for the chronic intruder postdrilling scenario is 3.3 mrem/yr, 100 years after facility closure. Inhalation is the predominant exposure pathway. Strontium-90 and Cs-137 are the major contributors to the total predicted dose. External exposure from Cs-137 accounts for 46% of the total dose, while the ingestion pathway, via contaminated plants, dominates the dose from Sr-90, representing 53% of the total dose.

Section 5 demonstrated that many of the standard intruder scenarios were not considered applicable to the ICDF landfill because of the depth of the waste and the nature of the cover materials. The well drilling scenario is considered to be very conservative because the engineered barriers presented in the cover would act to deter drilling. Additional conservatism has been incorporated in the calculations through the use of conservative assumptions (such as spreading the waste at the drilling site, rather than placing the drill cuttings into a mud pit). These layers of conservatism provide assurance that the results are bounding and that the ICDF landfill will perform within regulatory standards.

7. PERFORMANCE EVALUATION

This performance assessment documents the projected radiological impacts associated with the disposal of LLW at the ICDF landfill. The projected impacts are used to demonstrate compliance with applicable radiological dose criteria of the DOE and the EPA for protection of the public and the environment. This section compares the performance assessment results to the applicable performance objectives. Additionally, it addresses the implications and applications of the results of the performance assessment for site characterization, monitoring, operations, and regulatory issues.

7.1 Comparison of Results to Performance Objectives

Table 7-1 presents the results of the ICDF landfill performance assessment and compares them to the applicable performance objectives. The dose to a hypothetical member of the general public was assessed through reasonable yet conservative scenarios. These scenarios reflect the site-specific conditions at the ICDF landfill. The performance assessment results indicate the performance objectives are met for both the compliance time period (1,000 years from site closure or year 3018) and any time afterward. Therefore, there is a reasonable expectation that performance objectives established for the long-term protection of the public and the environment will not be exceeded following closure of the ICDF landfill.

7.1.1 Analysis of I-129 in the Drinking Water Pathway

During the compliance period (years 2018–3018) the I-129 peak aquifer concentration at the point of compliance is 0.1 pCi/L which is an order of magnitude below the I-129 MCL of 1.0 pCi/L. During the postcompliance period, the I-129 concentration is predicted to increase to 9.8 pCi/L in year 4118. This is greater than the I-129 MCL of 1 pCi/L.

7.1.2 Use of Performance Assessment Results

The results of the performance assessment are used for comparison with the performance objectives and to support the development of the Waste Acceptance Criteria (WAC). WAC (DOE-ID 2002c) have been developed and the results of this PA will be used to modify the WAC, where necessary. This PA analysis and the design analysis both use the same underlying inventory estimates and primarily the same assumptions, with the exception of the assumed infiltration rate through the landfill cover. For the design analysis (which the WAC are based on), it was assumed that the cover would reduce infiltration to 0.01 cm/yr for the entire time of evaluation. For this PA, it was assumed that the cover would reduce infiltration to 0.01 cm/yr during the first 500 years of the compliance period until the year 2518 and then fail over a 500-year period from 2518 until 3018. During the period from year 2518 until 3018, the cover gradually deteriorates and the infiltration through the cover linearly increases from 0.01 cm/yr in year 2518 until it returns to its background rate of 1 cm/yr in year 3018.

The results of this performance assessment will be used in the development of an environmental monitoring plan and an action plan. Because this is a radioactive waste management facility, it will meet the environmental monitoring requirements of DOE O 5400.1, “General Environmental Protection Program”; DOE O 5400.5, “Radiation Protection of the Public and the Environment”; and DOE O 435.1, “Radioactive Waste Management.” The monitoring will be designed to verify that the facility is performing as planned. The action plan will detail what action will be taken if the results of the monitoring indicate the facility is not performing as expected.

Table 7-1. Comparison of the ICDF landfill performance assessment results and the applicable performance objectives for the 0- to 1000-year time of compliance. Peak results are shown in parentheses.

Performance Objective	Standard	ICDF Performance Assessment Result
All-pathways (DOE O 435.1)	25 mrem/yr EDE	0.05 mrem/yr (4.55 mrem/yr after 1,000-year time of compliance)
Atmospheric (40 CFR 61 Subpart H)	10 mrem/yr EDE (entire INEEL Site)	0.01 mrem/yr during the operational and institutional control periods 0.01 mrem/yr during the postinstitutional control period
Atmospheric (40 CFR 61 Subpart Q)	20 pCi/m ² -s radon flux	0.17 pCi/m ² -s
Chronic inadvertent intruder (DOE O 435.1)	100 mrem/yr EDE	3.3 mrem/yr
Acute inadvertent intruder (DOE O 435.1)	500 mrem EDE	12.6 mrem
Groundwater protection	4 mrem/yr beta-gamma CDE	0.4 mrem/yr (40 mrem/yr after 1,000-year time of compliance)
	20,000 pCi/L H-3	NA – screened out
	1 pCi/L I-129	0.10 pCi/L (9.8 pCi/L after the 1,000-year time of compliance)
	8 pCi/L Sr-90	NA – screened out
	5 pCi/L Ra-226 and Ra-228	2.4×10^{-6} pCi/L (0.029 pCi/L after 1,000-year time of compliance)
	15 pCi/L gross alpha	0.011 pCi/L (0.2 pCi/L after 1,000-year time of compliance)
	20 µg/L uranium	0.083 µg/L (1.6 µg/L after 1,000-year time of compliance)

7.2 Further Work

The PA for the ICDF landfill is a working document. Annual reports will be used to evaluate new information with respect to the assumptions made in this PA. If there are major changes to the assumptions, then the performance of the ICDF landfill will be reevaluated. Further work will include, but not be limited to, the following:

- During disposal to the ICDF landfill, radiological soil surveys will be conducted and the projected radionuclide inventory will be refined accordingly. This will include sampling of the soils before disposal to the ICDF landfill and reestimation of the inventory.
- Because the prediction of flow and transport in the vadose zone has a high level of uncertainty, a tracer test has been conducted and the analyses from this test are pending. Tracers were introduced in the INTEC percolation pond and the sewage treatment pond. Monitoring is currently underway. In the future, when sufficient water is running in the Big Lost River, a tracer will be introduced in the river as well. The objective of the study is to follow the transport of the tracer through the vadose zone. The study will provide new information on (1) the horizontal spreading of contaminants in the vadose zone in the vicinity of surface water sources, (2) the velocity of movement in the horizontal directions, (3) the vertical transport velocity, and (4) the total travel time from the surface to the aquifer under relatively well-defined water flux conditions.

- The subsurface science initiative at the INEEL is actively involved in research to better understand the mechanisms controlling flow and transport of contaminants in the subsurface. The results of this research could modify the conceptual model upon which the ICDF landfill analyses are based. Therefore, the research progress will be monitored and results incorporated into the PA annual reviews. Examples of areas of interest include
 - Unsaturated hydraulic parameters
 - Distribution coefficients in sediments, basalt matrix, vertical fractures in the vadose zone, and rubble zones in the aquifer
 - Flow and transport in fractures
 - Flow and transport interactions at basalt-sediment interfaces
 - Facilitated transport
 - Performance of infiltration reducing covers on disposal facilities
 - Source term releases as influenced by geochemistry
 - Testing and development of new and better ways to measure parameters and monitor the movement of contaminants in the subsurface.

8. WASTE ACCEPTANCE CRITERIA FOR THE ICDF

The WAC were originally calculated for the ICDF landfill based on the ICDF landfill design process. In this section, WAC are calculated based on the ICDF PA intruder and groundwater pathway evaluations and then compared to the ICDF design WAC. The minimum WAC for each radionuclide from this comparison becomes the WAC.

8.1 Intruder-Based WAC

The WAC were developed from the acute and chronic intruder drilling scenarios as required and defined by DOE M 435.1-1 IV.P.(2)(h). The acute drilling scenario assumes an inadvertent intruder drills a well into the contents of the ICDF landfill. The intruder is exposed to contaminated drill cuttings spread over the ground and contaminated airborne dust. The intruder is assumed to reside by the contaminated cuttings for 160 hours, the time local Idaho Falls well drilling contractors state it would take to develop a 56-cm (22-in.) -diameter irrigation well 135 m (443 ft) deep. Based on a waste thickness of 10.4 m (34 ft), the 56-cm (22-in.) well results in 2.5 m³ (88 ft³) of contaminated waste out of a total 32.4 m³ (1,142 ft³) of contaminated cuttings being brought to the surface during the acute drilling scenario. The exposure pathways for this acute drilling scenario include inhalation of resuspended drill cuttings and external exposure to the ground source. The RESRAD code was used to estimate dose from acute drilling (Gilbert et al. 1989). The WAC are developed from these acute drilling results by taking the acute exposure limit of 500 mrem and dividing it by the dose-to-source ratio (DSR) for each radionuclide and multiplying by the ratio of the total depth of the well (135 m [443 ft]) to the depth of the waste zone (10.4 m [34 ft]).

The chronic postdrilling scenario assumes that an inadvertent intruder moves onto the ICDF landfill and drills a residential well into the waste. The drilling portion of the scenario evaluates a 20-cm (8-in.) residential well. This type of well serves a single residence and provides sufficient water for a family garden and small quantities of livestock. As described in the acute drilling scenario, large-diameter wells are drilled to serve irrigation systems (i.e., hundreds of acres) that are located in the middle of farm fields, not near a farmer's residence. Therefore, in the chronic postdrilling scenario, the residence/home garden is evaluated using the traditional drinking water well diameter of 20 cm (8 in.).

The drill cuttings that are brought to the surface are assumed to be spread over 2,200 m² (24,000 ft²) or approximately 1/2 acre of land surface. The waste is assumed to be mixed to a depth of 61 cm (24 in.). The mixing depth of 61 cm (24 in.) is based on using a deep tilling plow to increase the depth of the root zone and to break up soil compaction. These plows are used in areas of southeast Idaho with highly erodible soils to minimize erosion. Deep tilling plows have shanks that till to a depth of 61 cm (24 in.) and are sold at Idaho Falls implement dealers. This tilling depth was used and accepted by the LFRG in the RWMC PA (Maheras et al. 1994, 1997). Based on a waste thickness of 10.4 m (34 ft), the 20-cm (8-in.) well results in 0.3 m³ (11 ft³) of contaminated waste being brought to the surface during the acute drilling scenario (see Table 8-1) and mixed into the 1,342 m³ of agricultural soil.

The chronic postdrilling scenario assumes that the intruder is exposed to the contaminated agricultural soils during plowing and cultivation (i.e., dust inhalation). In addition, the intruder is assumed to ingest contaminated food products from the garden and from beef and milk cattle consuming contaminated forage. The intake of contaminated forage by cattle was adjusted according to the fraction of feed grown on contaminated cuttings and the necessary remaining feed obtained from uncontaminated ground. The RESRAD code was used to estimate dose from the chronic postdrilling scenario. The WAC are developed from these chronic drilling results by taking the chronic exposure limit of 100 mrem and dividing it by the DSR for each radionuclide and multiplying by the ratio of the mass of soil in mixing zone (2.01E+09 g) to the mass of the waste in well (6.54E+05 g) (see Table 8-1). A similar process was followed to determine the WAC based on the PA groundwater pathway results.

Table 8-1. Development of ICDF radionuclide WAC based on the chronic and acute intruder drilling scenarios.

Nuclide	Chronic DSR (mrem/yr per pCi/g)	PA Chronic ACW ^a (pCi/g)	Acute DSR (mrem/yr per pCi/g)	PA Acute ACW ^a (pCi/g)
Ag-108m	3.05E+00	1.01E+05	9.45E-05	6.90E+07
Am-241	2.11E-01	1.46E+06	5.72E-02	1.14E+05
Am-243	7.16E-01	4.30E+05	6.67E-02	9.78E+04
C-14	1.95E-06	1.58E+11	5.35E-17	1.22E+20
Cm-244	3.23E-03	9.55E+07	9.75E-04	6.68E+06
Co-60	1.63E-05	1.89E+10	1.20E-08	5.42E+11
Cs-135	1.71E-02	1.80E+07	7.73E-07	8.43E+09
Cs-137	1.93E-01	1.60E+06	1.52E-04	4.28E+07
Eu-152	1.48E-02	2.08E+07	1.22E-05	5.34E+08
Eu-154	1.53E-03	2.02E+08	1.25E-06	5.20E+09
H-3	6.34E-10	4.86E+14	2.81E-09	2.32E+12
I-129	3.39E-01	9.08E+05	1.09E-04	5.96E+07
K-40	8.84E-01	3.48E+05	4.13E-04	1.58E+07
Np-237	5.57E+00	5.52E+04	8.23E-02	7.85E+04
Pa-231	9.48E+00	3.24E+04	2.10E-01	3.11E+04
Pu-238	8.89E-02	3.46E+06	2.68E-02	2.43E+05
Pu-239	2.17E-01	1.42E+06	6.47E-02	1.01E+05
Pu-240	2.15E-01	1.43E+06	6.42E-02	1.02E+05
Pu-241	7.23E-03	4.26E+07	1.96E-03	3.32E+06
Pu-242	2.06E-01	1.49E+06	6.21E-02	1.05E+05
Ra-226	1.25E+01	2.46E+04	8.94E-03	7.29E+05
Sb-125	1.60E-11	1.92E+16	1.45E-14	4.50E+17
Se-79	5.48E-02	5.62E+06	1.54E-06	4.23E+09
Sm-151	2.71E-05	1.14E+10	2.10E-06	3.11E+09
Sr-90	2.37E-01	1.30E+06	2.03E-05	3.21E+08
Tc-99	4.06E-01	7.59E+05	1.44E-06	4.52E+09
Th-228	8.69E-16	3.54E+20	8.65E-18	7.54E+20
Th-230	4.62E+00	6.65E+04	5.21E-02	1.25E+05
Th-232	1.23E+01	2.50E+04	3.07E-01	2.12E+04
U-232	2.28E+00	1.35E+05	5.97E-02	1.09E+05
U-234	6.66E-02	4.62E+06	2.04E-02	3.20E+05
U-235	6.60E-01	4.65E+05	2.34E-02	2.78E+05
U-236	4.22E-02	7.30E+06	1.89E-02	3.45E+05
U-238	1.17E-01	2.63E+06	1.80E-02	3.62E+05
Zr-93	4.57E-04	6.72E+08	4.85E-05	1.34E+08

a. ACW = average concentration in waste that yields a dose of 100 mrem/yr and 500 mrem/yr for chronic and acute intruder scenarios.

8.2 Waste Acceptance Criteria Based on Groundwater Pathway

Based on the results of the PA simulations, WAC have been calculated for the PA contaminants of concern. The WAC are calculated based on the predicted maximum aquifer concentrations over the 1,000-year compliance period, the 25-mrem/yr all-pathways dose performance criteria (Table 8-2), and the MCLs (Table 8-3) for the ICDF PA contaminants of concern plus C-14. These ICDF PA groundwater pathway WAC are then compared to the intruder WAC calculated in Section 8.1 and the ICDF design WAC, which are presented in Section 8.3. The minimum of WAC from the analyses is the most restrictive and was chosen as the WAC for the ICDF. The ICDF PA groundwater pathway WAC, based on the 1,000-year compliance period, are highlighted in Tables 8-2 and 8-3.

Carbon-14 was added to the ICDF PA list of contaminants of concern because the LFRG review team questioned the C-14 ICDF landfill inventory. Therefore it was necessary to evaluate whether a WAC based on the ICDF PA groundwater pathway analysis would be smaller than the ICDF design WAC. As shown in Section 8.3, the ICDF design WAC are much smaller than the PA WAC and are protective.

As a sensitivity analysis, the ICDF PA WAC were calculated for peak predicted concentrations (past the 1,000-year compliance period) and predicted all-pathways doses. These results are also presented in Tables 8-2 and 8-3.

As shown in Table 8-2, the WAC inventory is significantly larger than the adjusted design inventory for all contaminants of concern and over all time when the WAC are based on the 25-mrem/yr performance objective. As shown in Table 8-3, the WAC inventory based on the MCLs is significantly larger than the adjusted design inventory for all contaminants of concern over the 1,000-year compliance period. The sensitivity of the I-129 WAC to the design life of the ICDF cover has been evaluated and the results are presented in Section 8.4.

8.3 Sensitivity of Groundwater I-129 WAC to Cover Life

Compliance with DOE performance objectives were evaluated using the conservative cover scenario (Scenario Number 4). The conservative cover scenario assumes that the cover remains intact for 500 years and then degrades to background infiltration (1 cm/yr) over the next 500 years. All-pathways performance criteria were met for all cover scenario cases for all times in the future. However the I-129 MCL was exceeded for some cover scenarios (Scenario 5, 6, and 7) during the 1,000-year time of compliance. For this reason, the I-129 WAC based on the I-129 MCL was computed for each of the cover scenarios where the I-129 MCL was exceeded, and the conservative cover scenario that the deterministic results are based on.

The three scenarios where the I-129 MCL was exceeded were the catastrophic failure scenario (Scenario 7), the extreme degradation scenario (Scenario 6), and the rapid degradation scenario (Scenario 5). Maximum I-129 concentrations in the aquifer for the 1,000-year compliance time period were 2.8 pCi/L for the rapid degradation scenario, 6.3 pCi/L for the extreme degradation scenario, and 6.9 pCi/L for the catastrophic degradation scenario. The WAC was calculated by

$$WAC = I_0 \frac{MCL}{C_{max}} \quad (8-1)$$

Table 8-2. Groundwater pathway WAC calculations for the PA contaminants of concern based on 25 mrem/yr performance objective.

Nuclide	Adjusted Design Inventory (Ci)	Predicted Peak Dose		ICDF Landfill WAC (0–1,000 yr)		ICDF Landfill WAC (0–infinity)	
		0–1,000 Years (mrem/yr)	>1,000 Years (mrem/yr)	Soil Concentration (pCi/g)	Inventory (Ci)	Soil Concentration (pCi/g)	Inventory (Ci)
C-14	3.5E-05	1.78E-08	1.52E-06	64,784	49,157	758.7	575.7
I-129	0.985	4.6E-02	4.45	698	530	7.3	5.5
Np-237	0.488	0	0.49	NA ^a	NA	33	25
Pu-239	5.06	0	2.6E-05	NA	NA	6.3E+06	4.8E+06
Pu-240	1.14	0	1.5E-05	NA	NA	2.5E+06	1.9E+06
Tc-99	4.37	2.0E-04	0.11	7.21E+05	5.5.E+05	1,353	1,027
U-234	4.57	0	0.53	NA	NA	283	215
U-238	1.48	0	0.13	NA	NA	377	286

a. NA = not applicable.

Table 8-3. Groundwater pathway WAC calculations for the PA contaminants of concern based on the groundwater MCLs.

Nuclide	Adjusted Design Inventory (Ci or g)	Predicted Peak Concentration		MCL (pCi/L or mg/L)	ICDF Landfill WAC (0–1,000 yr)		ICDF Landfill WAC (0–infinity)	
		0–1,000 Years (pCi/L or mg/L)	>1,000 Years (pCi/L or mg/L)		Soil Conc. (pCi/g)	Inventory (Ci)	Soil Conc. (pCi/g or g/g)	Inventory (Ci or g)
C-14	3.5E-05	3.21E-06	2.73E-04	2,000	28,739	21,807	338	256
I-129	0.985	0.1	9.8	1	13	9.9	0.13	0.10
Np-237	0.488	0	0.14	15	NL ^a	NL	69	52.3
Pu-239	5.06	0	4.9E-06	0.152	NL	NL	2.07E+05	1.6E+05
Pu-240	1.14	0	3.8E-11	0.152	NL	NL	6.01E+09	4.6E+09
Tc-99	4.37	0.059	31.6	900	8.79E+04	6.7E+04	164	124
U-234	4.57	0	1.5	NA ^b	NL	NL	115	87
U-238	1.48	0	0.53	NA	NL	NL	37	28
U-234 (mass)	732	0	2.4E-07	NA	NA	NA	NA	NA
U-238 (mass)	4.4E+06	0	1.6E-03	NA	NA	NA	NA	NA
Total U (mass)	4.4E+06	0	1.6E-03	3E-02	NA	NL	1.1E+08	8.4E+07

a. NL = no limit.
b. NA = not applicable.

where

- I_o = the I-129 inventory used in the conservative cover scenario simulation (0.985 Ci)
- C_{max} = the maximum I-129 concentration for a given cover scenario (pCi/L)
- MCL = the I-129 maximum contaminant level (1 pCi/L).

The calculated I-129 WAC based on meeting the groundwater MCL for I-129 for each of the cover scenarios are presented in Table 8-4. Note that the WAC calculated in Table 8-4 will differ from the WAC that are based on the 25-mrem/yr all-pathways dose. For I-129, the WAC based on meeting the MCL will be lower than the WAC based on the 25-mrem/yr all-pathways dose. The I-129 WAC based on the conservative scenario was 9.85 Ci and was an order of magnitude greater than the adjusted design inventory of 0.985 Ci. Therefore, the adjusted design inventory is protective in terms of meeting the performance criteria during the compliance time. The I-129 WAC calculated for the other scenarios all resulted in inventories less than the design inventory for I-129. Therefore, the poor performance of the cover as described by these scenarios will result in excursions above the I-129 MCL during the 1,000-year compliance time window assuming the actual I-129 inventory in the ICDF is equivalent to the adjusted design inventory. The worst-case cover scenario (catastrophic scenario) results in an I-129 WAC of 0.14 Ci.

Table 8-4. Peak I-129 concentration and WAC values based on meeting the I-129 MCL of 1 pCi/L for the different cover integrity scenarios.

Scenario	Cover Life (yr)	Time of Complete Failure (yr)	Predicted Maximum Groundwater Concentration Over 1,000 yr (pCi/L)	WAC Based on Predicted Maximum Over 1,000 yr (Ci)
Conservative Scenario (4)	500	500	0.1	9.85
Rapid Degradation Scenario (5)	250	250	2.8	0.35
Extreme Degradation Scenario (6)	100	100	6.3	0.16
Catastrophic Scenario (7)	100	20	6.9	0.14

8.4 WAC Modifications Based on ICDF PA

Table 8-5 compares the original ICDF design WAC to the WAC based on the PA results for the acute and chronic intruder drilling scenarios and the groundwater pathway. The results from the acute and chronic drilling scenarios indicate that the original ICDF design WAC need to be adjusted lower for Cs-137 and Sr-90 from 1.7E+09 Ci to 1.2E+06 Ci and from 2.7E+09 Ci to 9.9E+05 Ci, respectively.

The groundwater pathway results based on meeting the 25-mrem/yr performance objective and/or MCL indicate that the original ICDF design WAC are protective of the groundwater.

Table 8-5. Development of ICDF radionuclide WAC based on the minimum WAC from the chronic and acute intruder drilling scenarios and groundwater pathway PA results and the ICDF design WAC.

Nuclide	Waste Acceptance Criteria					
	PA Design Inventory (Ci)	PA Chronic (Ci)	PA Acute (Ci)	PA Groundwater (Ci)	ICDF Design (Ci)	Minimum (Ci)
Ag-108m	2.809E-09	7.7E+04	5.2E+07	ND ^a	6.1E+02	6.1E+02
Am-241	1.81E+01	1.1E+06	8.7E+04	ND	7.6E+03	7.6E+03
Am-243	2.53E-04	3.3E+05	7.4E+04	ND	2.5E-01	2.5E-01
C-14	3.50E-05	1.2E+11	9.3E+19	2.18E+04	2.3E+00	2.3E+00
Cm-244	1.37E-03	7.2E+07	5.1E+06	ND	1.4E+00	1.4E+00
Co-60	1.47E+02	1.4E+10	4.1E+11	ND	1.4E+05	1.4E+05
Cs-135	2.72E-02	1.4E+07	6.4E+09	ND	2.7E+01	2.7E+01
Cs-137	1.85E+04	1.2E+06	3.2E+07	ND	1.7E+09	1.2E+06
Eu-152	7.34E+02	1.6E+07	4.1E+08	ND	7.4E+05	7.4E+05
Eu-154	6.23E+02	1.5E+08	3.9E+09	ND	6.2E+05	6.2E+05
H-3	3.76E+01	3.7E+14	1.8E+12	ND	3.8E+04	3.8E+04
I-129	9.85E-01	6.9E+05	4.5E+07	9.9E+00	2.4E+00	2.4E+00
K-40	1.45E+00	2.6E+05	1.2E+07	ND	1.8E+02	1.8E+02
Np-237	4.88E-01	4.2E+04	6.0E+04	NL ^b	4.9E+02	4.9E+02
Pa-231	5.30E-05	2.5E+04	2.4E+04	ND	5.2E-02	5.2E-02
Pu-238	1.77E+02	2.6E+06	1.8E+05	ND	7.6E+03	7.6E+03
Pu-239	5.06E+00	1.1E+06	7.7E+04	NL	5.1E+03	5.1E+03
Pu-240	1.14E+00	1.1E+06	7.7E+04	NL	1.1E+03	1.1E+03
Pu-241	4.85E+01	3.2E+07	2.5E+06	ND	4.9E+04	4.9E+04
Pu-242	1.83E-04	1.1E+06	8.0E+04	ND	1.8E-01	1.8E-01
Ra-226	3.60E-01	1.9E+04	5.5E+05	ND	3.6E+02	3.6E+02
Sb-125	7.04E+00	1.5E+16	3.4E+17	ND	7.1E+03	7.1E+03
Se-79	1.26E-01	4.3E+06	3.2E+09	ND	1.2E+02	1.2E+02
Sm-151	2.56E+02	8.7E+09	2.4E+09	ND	2.6E+05	2.6E+05
Sr-90	1.74E+04	9.9E+05	2.4E+08	ND	2.7E+09	9.9E+05
Tc-99	4.37E+00	5.8E+05	3.4E+09	6.7E+04	4.4E+03	4.4E+03
Th-228	2.50E-02	2.7E+20	5.7E+20	ND	1.2E+01	1.2E+01
Th-230	1.32E-01	5.0E+04	9.5E+04	ND	1.1E+01	1.1E+01
Th-232	1.18E-01	1.9E+04	1.6E+04	ND	1.3E+01	1.3E+01
U-232	4.06E-04	1.0E+05	8.3E+04	ND	4.0E-01	4.0E-01
U-234	4.57E+00	3.5E+06	2.4E+05	NL	4.6E+03	4.6E+03
U-235	8.37E-02	3.5E+05	2.1E+05	ND	8.3E+01	8.3E+01
U-236	1.53E-01	5.5E+06	2.6E+05	ND	1.5E+02	1.5E+02
U-238	1.48E+00	2.0E+06	2.7E+05	NL	1.5E+03	1.5E+03
Zr-93	6.50E-01	5.1E+08	1.0E+08	ND	6.4E+02	6.4E+02

a. ND = no data.

b. NL = no limit.

9. ALARA ANALYSIS

DOE's approach to radiation protection for LLW disposal is based on two key components. One component is the performance objectives described in Section 1.5.1, which specify maximum doses for various pathways. The other component requires doses to be maintained "as low as reasonably achievable" (ALARA).

The goal of the ALARA process is attainment of the lowest practical dose level after taking into account social, technical, economic, and public policy considerations. Therefore, in addition to providing a reasonable expectation that the performance objectives described in Section 1.5.1 will not be exceeded, the performance assessment also needs to show that LLW disposal is being conducted in a manner that maintains releases of radionuclides to the environment ALARA. This ALARA analysis presents the doses estimated in the ICDF landfill performance assessment and evaluates options that could reduce these doses.

The all-pathways dose was estimated to be 0.05 mrem/yr, well below the DOE O 435.1 standard of 25 mrem/yr. The estimated dose of 0.05 mrem/yr through the groundwater all-pathways was for a member of the public located 100 m downgradient from the ICDF landfill during the postinstitutional control period, in the year 2118. The majority of the dose is due to I-129. The dose is based on a single family farm/home garden scenario, so the affected population would also be small, probably involving no more than 10 people based on an average family size that ranges from 2.78 to 4.28 in the counties that surround the INEEL. Based on an affected population of 10 people, the annual collective dose is estimated to be 0.0005 person-rem. For this same population, the annual collective dose from background radiation on the ESRP is 3.6 person-rem (DOE-ID 2000c). The estimated ICDF collective dose represents 0.01% of background levels.

Several options are evaluated for reducing these doses. In the first option, removal, treatment, and off-Site disposal are examined as an alternative to disposal at the ICDF landfill. Soils will be selectively excavated to reduce the soil volume, packaged, and transported by truck or rail to a permitted engineered disposal facility located off-Site. Waste will be treated off-Site at the receiving facility, if necessary, to satisfy land disposal restrictions. The net present value cost of this alternative is \$208.4M (DOE-ID 1999). Based on a monetary equivalence of \$1000 to \$10,000 per person-rem per DOE guidance, off-Site disposal would not be cost-effective from an ALARA standpoint given the low doses already estimated in this ALARA analysis.

In the second option, the use of high-integrity containers was evaluated. Cost estimates for high-integrity containers are about \$20,000 per container (Maheras et al. 1997). Based on a monetary equivalence of \$1,000 to \$10,000 per person-rem, a single high-integrity container would be cost-effective from an ALARA standpoint if it resulted in a dose reduction of 2 to 20 person-rem. Given the small collective doses already estimated in this ALARA analysis, it is unlikely that the widespread use of high-integrity containers would be cost-effective from an ALARA standpoint.

In the third option, the use of an engineered landfill liner and leachate collection system are evaluated. The ICDF landfill was designed and built with a double composite liner system and leachate collection system and leachate detection recovery system. None of which were factored into the conservative modeling efforts in the performance assessment. Design and construction of the ICDF landfill was based on state-of-the-art engineering for LLW landfills. If all the cover and bottom liners and leachate collection components were factored into the performance assessment, modeling doses would be substantially less.

Other options that could be considered include extending the period of institutional control and expanding the areal extent of institutional control. However, both of these options are written into the ROD (DOE-ID 1999) and will be implemented should the ICDF pose a threat to human health and the environment.

In summary, the proposed waste disposal practices at the ICDF landfill will be protective of human health and environment with very small estimates of dose to members of the public relative to background levels. Several options were evaluated for reducing these doses but, based on a monetary equivalence of \$1,000 to \$10,000 per person-rem, most options will probably not be cost-effective from an ALARA standpoint.

10. PREPARERS

James M. McCarthy, Ph.D.

Ph.D., Civil Engineering, University of California, Los Angeles, 1988

M.S., Water Resource Systems, University of California, Los Angeles, 1984

B.S., Environmental Resources Engineering, California State University, Humboldt, 1981

Dr. McCarthy has 14 years of experience related to groundwater hydrology, surface water hydrology, and water resource systems. During the last 11 years he has focused his efforts on performance assessment and risk assessment related projects. He has been the principal investigator on a number of environmental restoration and waste management related subsurface flow and transport studies including most recently, the composite analysis evaluation for a low-level radioactive waste disposal facility at the Radioactive Waste Management Complex, at the Idaho National Engineering and Environmental Laboratory.

For this PA report, Dr. McCarthy has been one of the principal investigators contributing to the project coordination, technical aspects, as well as document preparation.

Marilyn J. Case

M.S., Environmental Engineering/Health Physics, University of Florida, Gainesville, Florida, 1981

M.S., Botany/Systems Ecology, University of Florida, Gainesville, Florida, 1976

B.A., Biology, Susquehanna University, Selinsgrove, Pennsylvania, 1973

Marilyn Case is an environmental engineer and health physicist with over 20 years of experience in the assessment of pollutants in the environment and in environmental modeling. She has designed and conducted monitoring programs for environmental radioactivity. She has developed models for and applied a variety of computer codes in the calculation of radionuclide movement in air, surface and groundwater, and food chains, and the subsequent radiation dose to individuals and populations. She has conducted assessments of health impacts from nuclear waste disposal facilities, nuclear reactors, and non-reactor facilities.

Currently, Ms. Case is an advisory engineer/scientist for Bechtel BWXT Idaho. Her achievements over the past two years have included conducting radiological and nonradiological risk assessments of thermal oxidation units, contaminated pond sediments, in situ vitrification, wild fires at the INEEL, and air emissions from various INEEL facilities. Highly visible projects include a performance assessment of the Radioactive Waste Management Complex and development of waste acceptance criteria, required by DOE Order 435.1.

For this PA, Ms. Case has been one of the principal investigators, focusing on surface pathways and intruder analyses, as well as document preparation.

Karen N. Keck

M.S. Hazardous Waste Management, University of Idaho, Moscow, 1991

B.S. Watershed Science, Colorado State University, Fort Collins, 1981

Ms. Keck is an advisory scientist for Bechtel BWXT Idaho with 20 years of experience in the field of surface water and groundwater hydrology and hazardous waste management. She prepares surface-water storm evaluation studies for RCRA Part B permitting of hazardous waste storage facilities. She has performed hydrologic modeling of landfill cover designs for a mixed-waste landfill using EPA code HELP. She has prepared several human health risk assessments in support of CERCLA/RCRA investigations. More recently she was involved in the technical aspects and overall document preparation of the INEEL Radioactive Waste Management Complex Composite Analysis and subsequent development of performance assessment and composite analysis action levels, required by DOE Order 435.1.

For this performance assessment, Ms. Keck has been one of the principal investigators providing technical assistance and document preparation.

Arthur S. Rood

M.S., Health Physics/Radioecology, Colorado State University, Fort Collins, 1987

B.S., Geology, Mesa State College, Grand Junction Colorado, 1982

Arthur Rood is an environmental engineer and health physicist with over 18 years of experience in developing and applying models of contaminant fate and transport in the environment. He developed the groundwater model used in this performance assessment and also co-authored the food chain model for the MACCS reactor consequence code. Mr. Rood has also been involved in numerous environmental assessments at the INEEL including other performance assessments. Additionally, he performed much of the environmental transport modeling for the Rocky Flats Historical Public Exposures Studies.

Currently, Mr. Rood is an advisory engineer/scientist for Bechtel BWXT Idaho. His achievements over the past two years have included a detailed analysis of subsurface tritium migration at the Radioactive Waste Management Complex. Highly visible projects include a performance assessment of the Radioactive Waste Management Complex and development of waste acceptance criteria, required by DOE Order 435.1.

For this PA, Mr. Rood has been one of the principal investigators, focusing on groundwater fate and transport pathways and Monte Carlo uncertainty analysis, as well as document preparation.

11. REFERENCES

- 10 CFR 61, 2002, "Licensing Requirements for Land Disposal of Radioactive Waste," *Code of Federal Regulations*, Office of the Federal Register, February 2002.
- 10 CFR 830.120, 1999, "Quality Assurance Requirements," *Code of Federal Regulations*, Office of the Federal Register, January 2000.
- 40 CFR 61, 2002, "National Emission Standards for Hazards Air Pollutants," *Code of Federal Regulations*, Office of the Federal Register, February 2002.
- 40 CFR 61, Subpart H, 2002, "National Emission Standards for Emissions of Radionuclides Other than Radon from Department of Energy Facilities," *Code of Federal Regulations*, Office of the Federal Register, February 2002.
- 40 CFR 61, Subpart Q, 2002, "National Emission Standards for Radon Emissions from Department of Energy Facilities," *Code of Federal Regulations*, Office of the Federal Register, February 2002.
- 40 CFR 141, 2002, "National Primary Drinking Water Regulations," *Code of Federal Regulations*, Office of the Federal Register, March 2002.
- 40 CFR 264, Subpart F, 1999, "Releases From Solid Waste Management Units," *Code of Federal Regulations*, Office of the Federal Register, July 1999.
- 40 CFR 264, Subpart G, 1999, "Closure and Post-Closure," *Code of Federal Regulations*, Office of the Federal Register, July 1999.
- 40 CFR 264, 2002, Subpart N, "Landfills," *Code of Federal Regulations*, Office of the Federal Register, April 2002.
- 40 CFR 264.301, 2002, "Design and Operating Requirements," *Code of Federal Regulations*, Office of the Federal Register, February 2002.
- 40 CFR 264.302, 2002, "Action Leakage Rate," *Code of Federal Regulations*, Office of the Federal Register, February 2002.
- 40 CFR 264.310, 2002, "Closure and Post-Closure Care," *Code of Federal Regulations*, Office of the Federal Register, February 2002.
- 40 CFR 268.49, 2002, "Alternative LDR Treatment Standards for Contaminated Soil," *Code of Federal Regulations*, Office of the Federal Register, February 2002.
- 40 CFR 761.75, 2002, "Chemical Waste Landfills," *Code of Federal Regulations*, Office of the Federal Register, February 2002.
- 54 FR 19820, 1989, "National Priorities List for Uncontrolled Hazardous Waste Sites: Update #9— Federal Facility Sites," *Federal Register*, U.S. Environmental Protection Agency, July 14, 1989.
- 54 FR 48184, 1989, "National Priorities List of Uncontrolled Hazardous Waste Sites," Final Rule, *Federal Register*, U.S. Environmental Protection Agency, November 21, 1989.

- 65 FR 78, 2000, "National Primary Drinking Water Regulations; Radionuclides; Notice of Data Availability," Proposed Rule, *Federal Register*, U.S. Environmental Protection Agency, pp. 21576-21628, April 21, 2000.
- Abbott, M.A., 1998, *INEEL Air Modeling Protocol*, INEEL/INT-98-00236, Idaho National Engineering and Environmental Laboratory, 1998.
- Ackerman, D. J., 1991, *Transmissivity of the SRPA at the Idaho National Engineering Laboratory Site, Idaho*, U.S. Geological Survey Water-Resources Investigations Report 91-4058, DOE/ID-22097, 1991.
- Anderson, S. R., 1991, *Stratigraphy of the Unsaturated Zone and Uppermost Part of the SRPA at the Idaho Chemical Processing Plant and Test Reactor Area, Idaho National Engineering Laboratory, Idaho*, U.S. Geological Survey Water-Resources Investigations Report 91-4010, DOE/ID-22095, 1991.
- Anderson, S. R., and R. C. Bartholomay, 1995, "Use of Natural Gamma Logs and Cores for Determining the Stratigraphic Relationship at the Radioactive Waste Management Complex, Idaho National Engineering Laboratory, Idaho," *Journal of the Idaho Academy of Science*, Vol. 31, No. 1, 1995, pp.1-10.
- Anderson, J. E., K. T. Ruppel, J. M. Glennon, K. E. Holte, and R. C. Rope. 1996a, *Plant communities, ethnoecology, and flora of the Idaho National Engineering Laboratory*. Environmental Science and Research Foundation Report No. 005. Environmental Science and Research Foundation, Idaho Falls, ID, 1996, 111pp.
- Anderson, S. R., D. J. Ackerman, and M. J. Liszewski, 1996b, *Stratigraphic Data for Wells at and near the Idaho National Engineering Laboratory, Idaho*, U.S. Geological Survey Open-File Report 96-248, DOE/ID-22127, 1996.
- Anderson, S. R., M. J. Liszewski, and L. D. Cecil, 1997, "Geologic Ages and Accumulation Rates of Basalt- Flow Groups and Sedimentary Interbeds in Selected Wells at the Idaho National Engineering Laboratory, Idaho," U.S. Geological Survey Water-Resources Investigations Report 97-4010, 1997.
- Arthur, W. J., 1982, "Radionuclide Concentrations in Vegetation at a Solid Radioactive Waste Disposal Area in Southeastern Idaho," *Journal of Environmental Quality*, Vol. 11, No. 3, 1982, pp. 394-399.
- Arthur, W. J., J. C. Grant, and O. D. Markham, 1983, *Importance of Biota in Radionuclide Transport at the SL-1 Radioactive Waste Disposal Area*, Idaho National Engineering Laboratory Radioecology and Ecology Programs, 1983 Progress Report, DOE/ID-12098, 1983.
- Baes, C. F. III, and T. H. Orton, 1979. "Production of Agriculture Crops and Forage, Y_v ," *A Statistical Analysis of Selected Parameters for Predicting Food Chain Transport and Internal Dose of Radionuclides*, NUREG/CR-1004, U.S. Nuclear Regulatory Commission, Washington, DC, November 1979.
- Baes, C. F. III, and R. D. Sharp, 1983, "A Proposal for Estimation of Soil Leaching and Leaching Constants for Use in Assessment Models," *Journal of Environmental Quality*, 12(1): pp. 17-28, 1983.

- Baes, C. F. III, R. D. Sharp, A. L. Sjoreen, and R. W. Shore, 1984, *A Review and Analysis of Parameters for Assessing Transport of Environmentally Released Radionuclides through Agriculture*, ORNL 5786, Oak Ridge National Laboratory, Oak Ridge, TN, 1984.
- Barraclough, J.T., W.E. Teasdale, J.B. Robertson, and R. G. Jensen, 1967, "Hydrology of the National Reactor Testing Station," Idaho, 1966, U.S. Geological Survey Water-Resources Open File Report, IDO-22049, 1967.
- Barraclough, J. T., and R. G. Jensen, 1976, *Hydrologic Data for the Idaho National Engineering Laboratory Site, Idaho 1971 to 1973*, IDO-22055, U.S. Geological Survey Water Resources Division, Idaho Falls, Idaho, Open-File Report 75-318, 1976.
- Barraclough, J. T., B. D. Lewis, and R. G. Jensen, 1981, "Hydrologic Conditions at the Idaho National Engineering Laboratory, Idaho Emphasis: 1974–1978," U.S. Geological Survey, Water Resource Investigation Open File Report 81-526, IDO-22060, April 1981.
- Bartholomay, R. C., and B. J. Tucker, 2000, *Distribution of Selected Radiochemical and Chemical Constituents in Perched Ground Water, Idaho National Engineering and Environmental Laboratory, Idaho, 1996-98*, DOE/ID-22168, U.S. Geological Survey Water Resources Investigations Report 00-4222, October 2000.
- Bates, R. L., and J. A. Jackson, 1980, *Glossary of Geology*, 2nd Ed., American Geological Institute, Falls Church, VA.
- BEA (Bureau of Economic Analysis), 1997, "REIS - Regional Economic Information System 1969-95" (CD-ROM), U.S. Department of Commerce, Economics and Statistics Administration, Bureau of Economic Analysis, Washington, DC, 1997.
- Bennett, C. M., 1986, "Capacity of the Diversion Channel Below the Flood-Control Dam on the Big Lost River at the Idaho National Engineering Laboratory," U.S. Geological Survey, Water-Resources Investigations Report 86-4204, 1986.
- Bennett, C. M., 1990, *Streamflow Losses and Groundwater Level Changes along the Big Lost River at the INEL, Idaho*, USGS Water-Resources Investigation Report 86-4204, DOE/ID-22091, 1990.
- Benson, C. H., and M. A. Othman, 1993, "Hydraulic Conductivity of Compacted Clay Frozen and Thawed In Situ," *Journal of Geotechnical Engineering*, Vol. 119, No. 2, p. 276.
- Berenbrock, C., and L. C. Kjelstrom, 1998, *Preliminary Water-Surface Elevations and Boundary of the 100-Year Peak Flow in the Big Lost River at the Idaho National Engineering and Environmental Laboratory, Idaho*, U.S. Geological Survey Water Resources Investigations Report 98-4065, DOE/ID-22148, 1998.
- Blackwell, D. D., 1989, "Regional implications of heat flow of the Snake River Plain, Northwestern United States;" *Tectonophysics*, v.164, p.323-343.
- Blackwell, D. D., and Steele, J. L., 1992, "Geothermal map of North America," DNAG Continent-Scale Map-006, Geological Society of America, Decade of North American Geology series.
- Blom, P. E., W. H. Clark, and J. B. Johnson, 1991. "Colony Densities of the Seed Harvesting Ant *Pogonomyrmex salinus* in Seven Plant Communities on the Idaho National Engineering Laboratory." *Journal of the Idaho Academy of Sciences*, 27, 1 pp. 28–36, 1991.

- Burgess, J. D., to Chris Kent, 1991, "ICPP 25-Year/24-Hour Flood Characterization," EG&G Idaho, Inc. Idaho Falls, Idaho, Interoffice Correspondence JDB-05-91.
- Case, M. J., A. S. Rood, J. M. McCarthy, S. O. Magnuson, B. H. Becker, and T. K. Honeycutt, 2000, Technical Revision of the Radioactive Waste Management Complex Low-Level Waste Radiological Performance Assessment for Calendar Year 2000, INEEL/EXT-2000-01089, Idaho National Engineering and Environmental Laboratory, September 2000.
- CDC, 1994, *Rare, Threatened, and Endangered Plants and Animals of Idaho*, 3rd ed., Conservation Data Center, Idaho Department of Fish and Game, Boise, Idaho, 1994, 39 pp.
- Cecil, L. D., B. R. Orr, T. Norton, and S. R. Anderson, 1991, *Formation of Perched Ground-water Zones and Concentrations of Selected Chemical Constituents in Water, Idaho National Engineering Laboratory, Idaho 1986-1988*, U.S. Geological Survey Water-Resources Investigations Report 91-4166, DOE/ID-22100, 1991.
- Cecil, L. D., J. R. Pittman, T. M. Beasley, R. L. Michel, P. W. Kubik, P. Sharma, U. Fehn, and H. Gove, 1992, "Water Infiltration Rates in the Unsaturated Zone at the Idaho National Engineering Laboratory Estimated by Chlorine-36 and Tritium Profiles, and Neutron Logging," in *Proceedings of the 7th International Symposium on Water-Rock Interactions*, WRI-7, Y. K. Kharaka and A. S. Meest (eds.), Park City, Utah, July 13-18, 1992.
- Cecil, L. D., and J. R. Green, 1999, "Chlorine-36 in water, snow, and mid-latitude glacial ice of North America: Meteoric and weapons-tests production in the vicinity of the INEEL, Idaho," WRIR 99-4037, 1999.
- Clawson, K. L., G. E. Start, and N. R. Ricks, 1989, *Climatology of the Idaho National Engineering Laboratory*, DOE/ID-12118, 2nd ed., U.S. Department of Commerce, National Oceanic and Atmospheric Administration, Environmental Research Laboratories, Air Resources Laboratory, Field Research Division, Idaho Falls, Idaho, December 1989.
- Codell, R. B., K. T. Key, and G. Whelan, 1982, "A Collection of Mathematical Models for Dispersion in Surface Water and Groundwater," NUREG-0868, U.S. Nuclear Regulatory Commission, 1982.
- Decisioneering Inc., 1993, *Crystal Ball Version 3.0: Forecasting and Risk Analysis for Spreadsheet Users*, Decisioneering Inc., Denver, Colorado, 1993.
- DOC, 1963, *Maximum Permissible Body Burdens and Maximum Permissible Concentrations of Radionuclides in Air or Water for Occupational Exposure*, National Bureau of Standards Handbook 69, U.S. Department of Commerce, Amended August 1963.
- DOC, 1990, "Census of Population: General Population Characteristics, Idaho, 1990," Economics and Statistics Administration, Bureau of the Census, Washington, DC, CP-1-14, 1990.
- DOC, 1997a, "Estimates of the Population of Counties and Demographic Components of Population Change: Annual Time Series, July 1, 1990, to July 1, 1996," Economics and Statistics Administration, Bureau of the Census, Washington, DC, CO-96-8, 1997.
- DOC, 1997b, "Estimates of the Population of Places: Annual Time Series, July 1, 1991, to July 1, 1996," Economics and Statistics Administration, Bureau of the Census, Washington, DC, SU-96-7, 1997.

- DOC, 2001, "Census of Population and Housing—Idaho," Profiles of General Demographic Characteristics, Economics and Statistics Administration, U.S. Census Bureau, May 2001.
- DOE, 1995, *Department of Energy Programmatic Spent Nuclear Fuel Management and Idaho National Engineering Laboratory Environmental Restoration and Waste Management Programs Final Environmental Impact Statement*, DOE/EIS-0203-F, U.S. Department of Energy, April 1995.
- DOE, 1999, "Remarks by Secretary of Energy Bill Richardson, Land Transfer Event, Idaho National Engineering and Environmental Laboratory, July 17, 1999," U.S. DOE Secretarial Notices, available at: <http://www.energy.gov/HQDocs/speeches/1999/julss/landtrans.htm>, Web page updated July 27, 1999, Web page visited December 4, 2001.
- DOE, 2002, *Idaho High-Level Waste & Facilities Disposition Draft Environmental Impact Statement*, DOE/EIS-0287, U.S. Department of Energy, September 2002.
- DOE O 231.1, Change 2, 1996, "Environment, Safety, and Health Reporting," U.S. Department of Energy, November 7, 1996.
- DOE O 414.1A, Change 1, 2001, "Quality Assurance," U.S. Department of Energy, July 12, 2001.
- DOE M 435.1-1, Change 1, 2001, "Radioactive Waste Management Manual," U.S. Department of Energy, June 19, 2001.
- DOE O 435.1, Change 1, 2001, "Radioactive Waste Management Manual," U.S. Department of Energy, August 18, 2001.
- DOE O 5400.1, 1988, "General Environmental Protection Program," U.S. Department of Energy, November 9, 1988. (canceled by DOE O 231.1)
- DOE O 5400.5, Change 2, 1993, "Radiation Protection of the Public and the Environment," U.S. Department of Energy, January 7, 1993.
- DOE O 5820.2A, 1998, "Radioactive Waste Management," U.S. Department of Energy, September 26, 1998 (superceded by DOE O 435.1).
- DOE-ID, 1987, *Environmental Assessment: Fuel Processing and Restoration at the Idaho National Engineering Laboratory*, DOE/EA-0306, U.S. Department of Energy Idaho Operations Office, 1987.
- DOE-ID, 1989, *Guidelines for Revegetation of Disturbed Sites at the INEL*, DOE/ID-12114, U.S. Department of Energy Idaho Operations Office, 1989.
- DOE-ID, 1991, *Federal Facility Agreement and Consent Order for the Idaho National Engineering Laboratory*, U.S. Department of Energy, State of Idaho Department of Health & Welfare, U.S. Environmental Protection Agency, Region 10, December 1991.
- DOE-ID, 1993a, *Groundwater Protection Management Program*, DOE/ID-10274, U.S. Department of Energy Idaho Operations Office, March 1993.
- DOE-ID, 1993b, *Idaho National Engineering Laboratory Groundwater Monitoring Plan*, DOE/ID-10441, U.S. Department of Energy Idaho Operations Office, June 1993.

DOE-ID, 1993c, *Idaho National Engineering Laboratory Storm Water Pollution Prevention Plan for Construction Activities*, DOE/ID-10425, U.S. Department of Energy Idaho Operations Office, September 1993.

DOE-ID, 1994, *Track 2 Sites: Guidance for Assessing Low Probability Hazard Sites at the INEL*, DOE/ID-10389, U.S. Department of Energy Idaho Operations Office, January 1994.

DOE-ID, 1995, *Long-Term Land-Use Future Scenarios for the Idaho National Engineering Laboratory*, DOE/ID-10440, Rev. 0, U.S. Department of Energy Idaho Operations Office, August 1995.

DOE-ID, 1996a, *Idaho National Engineering and Environmental Laboratory Comprehensive Facility and Land Use Plan*, DOE/ID-10514, U.S. Department of Energy Idaho Operations Office, March 1996.

DOE-ID, 1996b, *1995 INEL National Emissions Standards for Hazardous Air Pollutants- Radionuclides*, DOE/ID-10342(95), U.S. Department of Energy Idaho Operations Office, June 1996.

DOE-ID, 1997a, *Comprehensive RI/FS for the Idaho Chemical Processing Plant OU 3-13 at the INEL - Part A, RI/BRA Report*, DOE/ID-10534, Rev. 0, U.S. Department of Energy Idaho Operations Office, November 1997.

DOE-ID, 1997b, *Idaho National Engineering and Environmental Laboratory Site Environmental Report for Calendar Year 1996*, DOE-ID-12082(96), U.S. Department of Energy Idaho Operations Office, August 1997.

DOE-ID, 1997c, *1996 INEEL National Emissions Standard for Hazardous Air Pollutants - Radionuclides*, DOE/ID-10342(96), U.S. Department of Energy Idaho Operations Office, June 1997.

DOE-ID, 1997d, *Comprehensive Remedial Investigation/Feasibility Study for the Test Area North Operable Unit 1-10*, DOE/ID-10557, Rev. 0, U.S. Department of Energy Idaho Operations Office, November 1997.

DOE-ID, 1998, *Idaho National Engineering and Environmental Laboratory Storm Water Pollution Prevention Plan for Industrial Activities*, DOE/ID-10431, Rev. 30, U.S. Department of Energy Idaho Operations Office, October 1998.

DOE-ID, 1999, *Final Record of Decision, Idaho Nuclear Technology and Engineering Center, Operable Unit 3-13*, DOE/ID-10660, Rev. 0, U.S. Department of Energy Idaho Operations Office; U.S. Environmental Protection Agency, Region 10; and State of Idaho Department of Health and Welfare, October 1999.

DOE-ID, 2000a, *Geotechnical Report for the Conceptual Design of the INEEL CERCLA Disposal Facility at Waste Area Group 3, Operable Unit 3-13*, DOE/ID-10812, Rev. 0, U.S. Department of Energy Idaho Office Operations, December 2000.

DOE-ID, 2000b, *CERCLA Waste Inventory Database Report for the Operable Unit 3-13 Waste Disposal Complex*, DOE/ID-10803, Rev. 0, U.S. Department of Energy Idaho Operations Office, December 2000.

DOE-ID, 2000c, *Idaho National Engineering and Environmental Laboratory Site Environmental Report for Calendar Year 1998*, DOE-ID-12082(98), U.S. Department of Energy Idaho Operations Office, July 2000.

DOE-ID, 2001a, *Performance Assessment for the Tank Farm Facility at the Idaho National Engineering and Environmental Laboratory*, DOE/ID-10966, Rev. 0, U.S. Department of Energy Idaho Operations Office, December 2001.

DOE-ID, 2001b, *National Emissions Standards for Hazardous Air Pollutants – Year 2000 INEEL Report for Radionuclides*, DOE/ID-10890, U.S. Department of Energy Idaho Operations Office, 2001.

DOE-ID, 2002a, *Composite Analysis for Tank Farm Closure*, DOE/ID-10974, U.S. Department of Energy Idaho Operations Office, March 2002.

DOE-ID, 2002b, *INEEL CERCLA Disposal Facility Remedial Design/Construction Work Plan*, DOE/ID-10848, Rev. 1, U.S. Department of Energy Idaho Operations Office, May 2002.

DOE-ID, 2002c, *Waste Acceptance Criteria for ICDF Landfill*, DOE/ID-10865, Rev 2, U.S. Department of Energy Idaho Operations Office, May 2002.

DOE-ID, 2002d, *Idaho National Engineering and Environmental Laboratory Groundwater Monitoring Plan Update*, DOE/ID-11034, Rev. 0, U.S. Department of Energy Idaho Operations Office, September 2002.

DOE-ID, 2002e, *Quality Assurance Project Plan for Waste Area Groups 1, 2, 3, 4, 5, 6, 7, 10, and Inactive Sites*, DOE/ID-10587, Rev. 7, U.S. Department of Energy Idaho Operations Office, September 2002.

DOE-ID, 2003a, *Composite Analysis for the INEEL CERCLA Disposal Facility Landfill*, DOE/ID-10979, Rev. 0, U.S. Department of Energy Idaho Operations Office, August 2003.

DOE-ID, 2003b, *ICDF Complex Operations and Maintenance Plan*, DOE/ID-11000, Rev. 0, U.S. Department of Energy Idaho Operations Office, February 2003.

DOE-ID, 2003c, *ICDF Complex Waste Verification Sampling and Analysis Plan*, DOE/ID-10985, Rev. 0, U.S. Department of Energy Idaho Operations Office, February 2003.

DOE-ID, 2003d, *INEEL CERCLA Disposal Facility Complex Remedial Action Work Plan*, DOE/ID-10984, Rev. 0, U.S. Department of Energy Idaho Operations Office, February 2003.

DOE-ID, 2003e, *Phase I Monitoring Well and Tracer Study Report for Operable Unit 3-13, Group 4, Perched Water*, DOE/ID-10967, Rev. 1, U.S. Department of Energy Idaho Operations Office, June 2003.

EDF-ER-264, 2002, “INEEL CERCLA Disposal Facility Design Inventory,” Rev. 1, Idaho National Engineering and Environmental Laboratory, December 2002.

EDF-ER-266, 2002, “Subsurface Consolidation,” Rev. 1, Idaho National Engineering and Environmental Laboratory, May 2002.

- EDF-ER-267, 2002, "Landfill Compaction Subsidence Study," Rev. 1, Idaho National Engineering and Environmental Laboratory, May 2002.
- EDF-ER-268, 2002, "Slope Stability Assessments," Rev. 1, Idaho National Engineering and Environmental Laboratory, May 2002.
- EDF-ER-269, 2002, "Leachate Generation Study," Rev. 1, Idaho National Engineering and Environmental Laboratory, May 2002.
- EDF-ER-270, 2001, "Storm Water Drainage Calculations," Rev. 0, Idaho National Engineering and Environmental Laboratory, July 2001.
- EDF-ER-272, 2001, "Soil Amendment Study," Rev. 0, Idaho National Engineering and Environmental Laboratory, July 2001.
- EDF-ER-274, 2002, "Leachate/Contamination Reduction Time," Rev. 1, Idaho National Engineering and Environmental Laboratory, May 2002.
- EDF-ER-275, 2002, "Fate and Transport Modeling Results and Summary Report," Rev. 2, Idaho National Engineering and Environmental Laboratory, May 2002.
- EDF-ER-278, 2002, "Liner/Leachate Compatibility Study," Rev. 1, Idaho National Engineering and Environmental Laboratory, May 2002.
- EDF-ER-279, 2002, "Hydrologic Modeling of Final Cover," Rev. 2, Idaho National Engineering and Environmental Laboratory, May 2002.
- EDF-ER-280, 2002, "Landfill Leachate Collection System Design Analysis," Rev. 1, Idaho National Engineering and Environmental Laboratory, May 2002.
- EDF-ER-281, 2002, "Liner and Final Cover Long Term Performance Evaluation and Final Cover Life Cycle Expectation," Rev. 1, Idaho National Engineering and Environmental Laboratory, May 2002.
- EDF-ER-286, 2002, "Waste Placement Plan," Rev. 1, Idaho National Engineering and Environmental Laboratory, May 2002.
- EDF-ER-296, 2002, "Process and Treatment Overview for the Minimum Treatment Process," Rev. 0, Idaho National Engineering and Environmental Laboratory, March 2002.
- EPA, 1983, "Interim Guidelines and Specifications for Preparing Quality Assurance Project Plans," QAMS-005/80, U.S. Environmental Protection Agency, Office of Environmental Information, 1983.
- EPA, 1988, "Limiting Values of Radionuclide Intake and Air Concentration and Dose Conversion Factors for Inhalation, Submersion, and Ingestion; Federal Guidance Report 11," EPA-520/1-88-020, U.S. Environmental Protection Agency, Office of Radiation Programs, 1988.
- EPA, 1989a, "Requirements for Hazardous Waste Landfill Design, Construction, and Closure," EPA/624/4-89/022, Seminar Publication, U.S. Environmental Protection Agency, Center for

- Environmental Research Information, Office of Research and Development, Cincinnati, Ohio, 1989.
- EPA, 1989b, "Technical Guidance Document: Final Covers on Hazardous Waste Landfills and Surface Impoundments," U.S. Environmental Protection Agency, Office of Solid Waste Management, Washington, DC, 1989.
- EPA, 1989c, "Risk Assessment Guidance for Superfund," Volume I: Human Health Evaluation Manual, Interim Final, EPA/540/1-89/001, Office of Solid Waste and Emergency Response, Washington, DC, 1989.
- EPA, 1989d, "Risk Assessment Methodology, Environmental Impact Statement, NESHAP for Radionuclides," Background Information Document - Volume 1. EPA/520/1-89-005. Office of Solid Waste and Emergency Response, Washington, DC, 1989.
- EPA, 1990, "EPA Support Document for the EPA Designation of the Eastern SRPA as a Sole Source Aquifer," EPA 910/9-0-020, August 1990.
- EPA, 1994, "EPA Requirements for Quality Assurance Project Plans for Environmental Data Operations, QA/R-5, U.S. Environmental Protection Agency, Office of Environmental Information, 1994.
- Farnsworth, R.K., and C.R. Hymas, 1989, "The Compatibility of Various Polymeric Liner and Pipe Materials with Simulated Double-Shell Slurry Feed at 90°C," Hanford Grout Technology Program, Pacific Northwest Laboratory, Richland, Washington, 1989.
- Gorman, V. W., and R. C. Guenzler, 1983, "The 1983 Borah Peak Earthquake and INEL Structural Performance," EG&G Informal Report, EGG-EA-6501, 76 p, 1983.
- Groves, C. R., and B. L. Keller, 1983, "Ecological Characteristics of Small Mammals on a Radioactive Waste Disposal Area in Southeastern Idaho," *The American Midland Naturalist*, 109, 2, pp 253-265, 1983.
- Hackett, W. R., and R. P. Smith, 1992, "Quaternary Volcanism, Tectonics, and Sedimentation in the Idaho National Engineering Laboratory Area," *Field Guide to Geologic Excursions in Utah and Adjacent Areas of Nevada, Idaho, and Wyoming*, J.K. Wilson ed., Utah Geological Survey, Miscellaneous Publication 92-3, 1992, pp. 1-17.
- Hackett, W. R., J. Pelton, and C. Brockway, 1986, *Geohydrologic Story of the Eastern Snake River Plain and the INEL*, Idaho National Engineering Laboratory, 1986.
- Hahn, G. J., and W. Q. Meeker, 1991, *Statistical Intervals A Guide for Practitioners*. New York: John Wiley & Sons Incorporated, 1991.
- Harniss, R. O., and N. E. West, 1973, "Vegetation Patterns of the National Reactor Testing Station, Southeastern Idaho," *Northwest Science*, Vol. 47, pp. 30-43.
- Holtz, R. D., and W. D. Kovacs, 1981, *An Introduction to Geotechnical Engineering*, Prentice-Hall, New York, N.Y.

- Hsuan Y.G., and Guan Z., 1998, "Antioxidant Depletion During Thermal Oxidation of High Density Polyethylene Geomembranes," *Proceedings from the Sixth International Conference on Geosynthetics*, pp. 375-380, Industrial Fabrics Association International, Roseville, MN, 1998.
- Hull, L. C., 1989, *Conceptual Model and Description of the Affected Environment for the TRA Warm Waste Pond (Waste Management Unit TRA-03)*, EGG-ER-8644, 1989.
- ICRP, 1960, *Recommendations of the International Commission on Radiological Protection. Report of Committee II on Permissible Dose for Internal Radiation*, ICRP Publication 2, Oxford: Pergamon Press; 1960.
- IDAPA 58.01.05.008, 2003, "Standards for Owners and Operators of Hazardous Waste Treatment, Storage and Disposal Facilities," Idaho Administrative Procedures Act, Idaho Department of Environmental Quality, May 2003. (as promulgated as of December 1999)
- IDAPA 58.01.11, 1997, "Ground Water Quality Rules," Idaho Administrative Procedures Act, Idaho Department of Environmental Quality, March 1997.
- IDFG, Idaho Department of Fish and Game web site '<http://www2.state.id.us/fishgame.html>'.
- INEEL, 1998, *Idaho Chemical Processing Plant Safety Document, PSD-4.2, Aqueous Liquid Waste Management*," Rev. 10, Idaho National Engineering and Environmental Laboratory, 1998.
- Irving, J. S., 1993, *Environmental Resource Document for the Idaho National Engineering Laboratory*, EGG-WMO-10279, July 1993.
- Jackson, S. M., 1985, "Acceleration Data from the 1983 Borah Peak, Idaho, Earthquake Recorded at the Idaho National Engineering Laboratory," in Workshop XXVIII on the Borah Peak, Idaho, Earthquake, U.S. Geological Survey Open-File Report, 85-290, 1985, pp. 385-400.
- Jackson, S. M., I. G. Wong, G. S. Carpenter, D. M. Anderson, and S. M. Martin, 1993, "Contemporary Seismicity in the Eastern Snake River Plain, Idaho, Based on Microearthquake Monitoring," *Bulletin of the Seismological Society of America*, Vol. 83, pp. 680-695.
- Jeppson, R. J., and K. E. Holte, 1978, "Flora of the Idaho National Engineering Laboratory Site," Ecological Studies on the Idaho National Engineering Laboratory Site, 1978 Progress Report, IDO-12087, 1987.
- Jenkins, T., DOE-ID, to Marty Doornbos, INEEL, July 3, 2001, "Kd Values for INTEC Groundwater Modeling."
- Johnson, T. M., R. C. Roback, T. L. McLing, T. D. Bullen, D. J. DePaolo, C. Doughty, R. J. Hunt, M. T. Murrell, and R. W. Smith, 2000, "Groundwater Fast Paths in the SRPA: Radiogenic Isotope Ratios as Natural Groundwater Tracers," *Geology*, 28, 871-874.
- Kennedy, W. E., Jr., and R. A. Peloquin, 1988, "Intruder Scenarios for Site-Specific Low-Level Radioactive Waste Classification," DOE/LLW-71T, 1988.
- Kennedy, W. E., and D. L. Strenge, 1992, "Residual Radioactive Contamination from Decommissioning," NUREG/CR-5512, U.S. Nuclear Regulatory Commission, Washington, DC, 1992.

- Killough, G. G., R. E. Moore, and J. E. Till, 1991, "DECHEM Version 3.02: An All Pathway Assessment Procedure for Determining Acceptable Concentrations of Chemicals in Soil of Waste Sites," Radiological Assessment Corporation, Rt 2 Box 122, Neeses, SC 29107, 1991.
- Kjelstrom, L. C., and C. Berenbrock, 1996, "Estimated 100-Year Peak Flows and Flow Volumes in the Big Lost River and Birch Creek at the Idaho National Engineering Laboratory, Idaho," U.S. Geological Survey, Water-Resources Investigations Report 96-4163, 1996.
- Kozak, M. W., M. S. Y. Chu, and C. P. Harlan, 1990, "Performance Assessment Methodology for Low-Level Waste Facilities," NUREG/CR-5532. U.S. Nuclear Regulatory Commission, Washington, DC, 1990.
- Kuntz, M. A., H. R. Covington, and L. J. Schorr, 1992, "An Overview of Basaltic Volcanism of the Eastern Snake River Plain, Idaho," in P. K. Link, M. A. Kuntz, L. B. Platt (editors), *Regional Geology of Eastern Idaho and Western Wyoming*, Memoir 179, Geological Society of America, Denver, CO, pp. 227-267.
- Lamke, R. D., 1969, "Stage Discharge Relations on Big Lost River Within National Reactor Testing Station, Idaho," U.S. Geological Survey Open File Report, ID0-22050, 1969.
- Ligotke, M. W., 1993, "Soil Erosion Rates Caused By Wind and Saltating Sand Stresses In a Wind Tunnel," Pacific Northwest Laboratory, Richland, Washington, 1993.
- Maheras, S. J., A. S. Rood, S. O. Magnuson, M. E. Sussman, and R. N. Bhatt, 1994, *Radioactive Waste Management Complex Low-Level Waste Radiological Performance Assessment*, EGG-WM-8773, Idaho National Engineering Laboratory, 1994.
- Maheras, S. J., A. S. Rood, S. O. Magnuson, M. E. Sussman, and R. N. Bhatt, 1997, *Addendum to Radioactive Waste Management Complex Low-Level Waste Radiological Performance Assessment (EGG-WM-8773)*, INEL/EXT-97-00462, Idaho National Engineering Laboratory, 1997.
- Malde, H. E., 1991, "Quaternary geology and structural history of the Snake River Plain, Idaho and Oregon;" in R.B. Morrison, ed., *Quaternary Non-Glacial Geology, Coterminous United States*; Boulder Colorado, Geological Society of America, The Geology of North America, Vol. K-2, pp. 251-281.
- Markham, O. D., 1987, *Summaries of the Idaho National Engineering Laboratory Radioecology and Ecology Programs Research Projects*, DOE/ID-12111, Department of Energy Idaho Field Office, 1987.
- McBride, R. N. R. French, A. H. Dahl, and J. E. Detmer, 1978, *Vegetation Types and Surface Soils of the Idaho National Engineering Laboratory Site*, IDO-12084, 1978.
- McKinney, J.D., 1985, "Big Lost River 1983-1984 Flood Threat," PPD-FPB-002, EG&G Idaho, Inc., Idaho National Engineering Laboratory, 1985.
- McLing, T. L., 1994, *The Pre-Anthropogenic Groundwater Evolution at the Idaho National Engineering Laboratory*, Master of Science Thesis: Idaho State University, Pocatello, Idaho.

- Mitchell, J. C., L. L. Johnson, and J. E. Anderson, 1980, "Geothermal Investigations in Idaho, Part 9: Potential for Direct Heat Application of Geothermal Resources," Water Information Bulletin No. 30, Plate 1, Idaho Department of Water Resources, Boise.
- Morris, R. C., and R. D. Bleu, 1997, "Annual Technical Report Calendar 1996," Environmental Science and Research Foundation Report Series, Number 17, Idaho National Engineering Laboratory.
- Morris, R. C., 1999, "Potential Use of Habitats Within and Surrounding Facilities at the Idaho National Engineering and Environmental Laboratory by Sensitive Species: A Biological Assessment," Draft ESRF-026, Environmental Science and Research Foundation, Idaho Falls, Idaho.
- Mundorff, M. J., E. G. Crosthwaite, and C. Kilburn, 1964, "Groundwater for Irrigation in the Snake River Basin in Idaho," U.S. Geological Survey Water Supply Paper 1654, 1964.
- NCRP, 1984, "Radiological Assessment: Predicting the Transport, Bioaccumulation, and Uptake by Man of Radionuclide Released to the Environment," NCRP Report 76, National Council on Radiation Protection and Measurements, March 1984.
- NCRP, 1996, "Screening Models for Release of Radionuclides to Atmosphere, Surface Water, and Ground," NCRP Report No. 123 I & II, National Council on Radiation Protection and Measurements, January 1996.
- Noss, R. F., E. T. LaRoe III, and J. M. Scott, 1995, "Endangered Ecosystems of the United States: A Preliminary Assessment of Loss and Degradation," Biological Report 28, National Biological Service, U.S. Department of the Interior, 1995.
- Ng, Y. C., et al., 1978, "Methodology for Assessing Dose Commitment to Individuals and to the Population from Ingestion of Terrestrial Foods Contaminated by Emissions from a Nuclear Fuel Reprocessing Plant at the Savannah River Plant," UCID-17743, Lawrence Livermore Laboratory, March 1978.
- NOAA, 2001, *Air Resources Library Field Research Division Web Site*, www.NOAA.INEL.gov/frd/weather, National Oceanic and Atmospheric Administration, Washington, DC, 2001.
- Noss, R. F., E. T. LaRoe III, and J. M. Scott, 1995, "Endangered Ecosystems of the United States: A Preliminary Assessment of Loss and Degradation," Biological Report 28, National Biological Service, U.S. Department of the Interior, 1995.
- NRC, 1977, "Calculation of Annual Doses to Man from Routine Releases of Reactor Effluents for the Purpose of Evaluating Compliance With 10 CFR Part 50 Appendix I," Regulatory Guide 1.109, Revision 1, U.S. Nuclear Regulatory Commission, Washington, DC, 1997.
- NRC, 1982, *Final Environmental Impact Statement on 10 CFR Part 61 "Licensing Requirements for Land Disposal of Radioactive Waste*, NUREG-0945, Volumes 1-3, U.S. Nuclear Regulatory Commission, Washington, DC, 1982.
- NRC, 1986, "Methodologies For Evaluating Long-Term Stabilization Designs of Uranium Mill Tailings Impoundments," NUREG/CR-4620, U.S. Nuclear Regulatory Commission, Washington, DC, 1986.

- Olmsted, F. H., 1962, *Chemical and Physical Character of Groundwater in the National Reactor Testing Station*, Idaho, IDO-22043, 1962.
- Ostenaar, D. A., D. R. Levish, R. E. Klinger, and D. R. H. O'Connell, 1999, "Phase 2 Paleohydrologic and Geomorphic Studies for the Assessment of Flood Risk for the Idaho National Engineering and Environmental Laboratory, Idaho," Report 99-7, Geophysics, Paleohydrology, and Seismotechnics Group, Technical Service Center, U.S. Bureau of Reclamation, Denver, Colorado, July 1999.
- Overton, C. K., et al., 1976, "Big Lost River Fisheries," Summaries of the Idaho National Engineering Laboratory Site Ecological Information Meeting, July 10–11, 1975, U.S. Energy Research and Development Administration, Idaho Operations Office, 1976, pp. 42–43.
- Oztunali, O. I., and G. W. Roles, 1986, *Update of Part 61 Impacts Analysis Methodology*, NUREG/CR-4370, Vol. 1, U.S. Nuclear Regulatory Commission, Washington, DC, 1982.
- Parkhurst, D.L. and C.A.J. Appelo, 1999, "User's Guide to PHREEQC (Version 2)-A Computer Program for Speciation, Batch-Reaction, One-Dimensional Transport, and Inverse Geochemical Calculations," *U.S. Geological Survey Water-Resources Investigations Report 99-4259*, 312 p. Compiled program (Version 2.3) available at <http://water.usgs.gov/software/phreeqc.html>.
- Parks, B., *CAP88-PC Version 2.0 User's Guide*, U.S. Department of Energy, June 1997.
- Payne, S. J., V. W. Gorman, S. A. Jensen, M. E. Nitzel, M. J. Russell, and R. P. Smith, 2000, *Development of Probabilistic Design Basis Earthquake (DBE) Parameters for Moderate and High Hazard Facilities at INEEL*, INEEL/EXT-99-00775, Idaho National Engineering and Environmental Laboratory, 2000.
- Pelton, J. R., R. J. Vincent, and N. J. Anderson, 1990. "Microearthquakes in the Middle Butte/East Butte area, Eastern Snake River Plain, Idaho," *Bulletin of the Seismological Society of American*, Vol. 80, No. 1, pp. 209–212.
- Peterson, H. T. Jr., 1983, "Terrestrial and Aquatic Food Chain Pathways," *Radiological Assessment - A Textbook on Environmental Dose Analysis*, J.E. Till and H.R. Meyer (eds.), NUREG/CR-3332, U.S. Nuclear Regulatory Commission, Washington, DC, 1983.
- Peyton, R. L., and P. R. Schroeder, 1990, "Evaluation of Landfill-Liner Designs," *Journal of Environmental Engineering*, American Society of Civil Engineers, Vol. 116, No. 3.
- PLN-694, 2000, "Project Management Plan - Environmental Restoration Program Management," Rev. 0, Idaho National Engineering and Environmental Laboratory, November 2000.
- PNNL, 1996, *Subsurface Transport Over Multiple Phases Description "STOMP," Theory Guide*, PNNL-11217, Pacific Northwest National Laboratory, Richland, Washington, 1996.
- PNNL, 2000, *Subsurface Transport Over Multiple Phases Description "STOMP," Users Guide*, PNNL-12034, Pacific Northwest National Laboratory, Richland, Washington, 2000.
- Poeter, E. P., and M. C. Hill, 1998, "Documentation of UCODE, A Computer Code for Universal Inverse Modeling," WRIR 98-4080, U.S. Geological Survey, 1998.

- Press, W. H., B. P. Flannery, S. A. Teukolsky, and W. T. Vetterling, 1992, *Numerical Recipes: The Art of Scientific Computing*, Cambridge: Cambridge University Press, 1992.
- Rathburn, S. L., 1991, *Quaternary Channel Changes and Paleoflooding Along the Big Lost River, Idaho National Engineering Laboratory*, EGG-WM-9909, January 1991.
- Reynolds, T. D., 1994, "Idaho National Environmental Research Park. p. 19–22," DOE/ER-065 IP, In: Department of Energy National Environmental Research Parks, Washington, DC: U.S. Department of Energy, Office of Energy Research, 1994.
- Reynolds, T. D., J. W. Connelly, D. K. Halford, and W. J. Arthur, 1986, "Vertebrate Fauna of the Idaho National Environmental Research Park," *Great-Basin Naturalist*, Vol. 46, pp. 513–527.
- Reynolds, T. D., and L. Fraley, Jr., 1989, "Root Profiles of Some Native and Exotic Plant Species in Southeastern Idaho," *Environmental and Experimental Botany*, Vol. 29, pp. 241–248.
- Reynolds, T. D., and J. W. Laundre, 1988, "Vertical Distribution of Soil Removed by Four Species of Burrowing Rodents in Disturbed and Undisturbed Soils," *Health Physics*, Vol. 54, No. 4.
- Reynolds, T. M., and W. L. Wakkinen 1987, "Characteristics of the Burrows of Four Species of Rodents in Undisturbed Soils in Southeastern Idaho," *The American Midland Naturalist*, 118, 2, pp. 245-250, 1987.
- Roback R. C., T. M. Johnson, T. L. McLing, M. T. Murrell, S. Luo, and T. L. Ku, 2001, "Uranium Isotopic Evidence for Groundwater Chemical Evolution and Flow Patterns in the Eastern SRPA, Idaho," *Geological Society of America Bulletin*, 113, pp. 1133–1141.
- Robertson, J. B., R. Schoen, and J. T. Barraclough, 1974, "The Influence of Liquid Waste Disposal on the Geochemistry of Water at the National Reactor Testing Station, 1952-1970," U.S. Geological Survey Open-File Report, IDP-22053, TID-4500, February 1974.
- Rood, A. S., R. C. Arnett, and J. T. Barraclough, 1989, *Contaminant Transport in the SRPA: Phase I, Part 1: Simple Analytical Models of Individual Plumes*, EGG-ER-8623, Idaho National Engineering Laboratory, May 1989.
- Rood, S. M., G. A. Harris, and G. J. White, 1996, *Background Dose Equivalent Rates and Surficial Soil Metal and Radionuclide Concentrations for the Idaho National Engineering Laboratory*, INEL-94/0250, Rev. 1, Idaho National Engineering Laboratory, 1996.
- Rood, A. S., 1999, "GWSCREEN: A Semi-Analytical Model for Assessment of the Groundwater Pathway from Surface or Buried Contamination, Theory and User's Manual," Version 2.5, INEEL/EXT-98-00750, Idaho National Engineering and Environmental Laboratory, 1999.
- Rupp, E. M., 1980, "Age-Dependent Value of Dietary Intake for Assessing Human Exposures to Environmental Pollutants," *Health Physics*, 39, pp. 151–163, 1980.
- Saab, V., and T. D. Rich, 1997, "Large-scale conservation assessment of neotropical migratory landbirds in the Interior Columbia River Basin," USDA Forest Service, Pacific Northwest Research Station, General Technical Report. PNW-GTR-389. Portland, Oregon, 1997.

- Sagendorf, J., 1996, "Precipitation Frequency and Intensity at the Idaho National Engineering Laboratory," ARLFRD 94-100, U.S. Department of Commerce, National Oceanic Atmospheric Administration, Environmental Research Laboratories, Air Resources Laboratory Field Research Division, Idaho Falls, ID, 1996.
- SAR-II-8.4, 2003, "TMI-2 Safety Analysis Report," Rev. 3, March 2003. (Available only in the INEEL Document Control Web Site (EDMS): <http://zeus.inel.gov:8080/index.htm>.)
- Scrabble, K. W., C. S. French, G. Chabot, and A. Major, 1974, "A General Equation for the Kinetics of Linear First Order Phenomena and Suggested Applications," *Health Physics*, 27: pp. 155–157, 1974.
- Seitz, R. R., A. S. Rood, G. A. Harris, and M. Kotecki, 1991, "Sample Application of Sensitivity/Uncertainty Analysis Techniques to a Groundwater Transport Problem," DOE/LLW-108, U.S. Department of Energy, 1991.
- Sheppard, M. J., and D. H. Thibault, 1990, "Default Soil Solid/Liquid Partition Coefficients Kds for Four Major Soil Types: A Compendium," *Health Physics* 59(4)471-482, 1990.
- Smith, C. S., and C. A. Whitaker, 1993, *Independent Verification and Limited Benchmark Testing of the GWSCREEN Computer Code, Version 2.0*, EGG-GEO-10799, Idaho National Engineering Laboratory, 1993.
- Smith, R. W., and T. L. McLing, 2001, "Relationship between Physical and Chemical Heterogeneity in Geologic Media: the Role of Surface Area," *American Geophysical Union Annual Meeting 2001*.
- Till, J. E., and H. R. Meyer (eds), 1983, *Radiological Assessment: A Textbook on Environmental Dose Analysis*, NUREG/CR-3332, U.S. Nuclear Regulatory Commission, Washington, DC, 1983.
- Tucker, B. J., and B. R. Orr, 1998, *Distribution of Selected Radiochemical and Chemical Constituents in Perched Ground Water, Idaho National Engineering Laboratory, Idaho, 1989-91*, DOE/ID-22144, U.S. Geological Survey Water Resources Investigations Report 98-4028, 1998.
- USFWS, 1996, Letter from the U.S. Fish and Wildlife Service to T. Reynolds, Environmental Science and Research Foundation, SP# 1-4-96-SP-185 update to SP# 1-4-95-SP-255, File #506.0000, April 30, 1996.
- USFWS, 1997, Letter from the U.S. Fish and Wildlife Service to T. Reynolds, Environmental Science and Research Foundation, SP# 1-4-97-SP-242, update to 1-4-96-SP-185 File #506.0000, July 16, 1997.
- USFWS, 2001, Letter from the U.S. Fish and Wildlife Service to Roger Blew, Stoller Corporation, "90-day Confirmation of Species List – Department of Energy, Idaho National Engineering and Environmental Laboratory", File # 506.0000 1-4-02-SP-179, December 2001.
- VWG (Volcanism Working Group), 1990, *Assessment of Potential Volcanic Hazards for the New Production Reactor Site at the Idaho National Engineering Laboratory*, EGG-NPR 10624, EG&G Idaho, Idaho Falls, Idaho, October 1990.

- WCFS (Woodward-Clyde Federal Services), 1996, *Site-Specific Probabilistic Seismic Hazard Analyses for the Idaho National Engineering Laboratory*, Volume 1, Final Report, and Volume 2, Appendix, INEL-95/0536, Lockheed Idaho Technologies Company, Idaho Falls, Idaho, May 1996.
- Whelan, G., J.P. McDonald, and C. Sato, 1996, *Multimedia Environmental Pollutant Assessment System (MEPAS) Groundwater Pathway Formulations*, PNNL-10907, Pacific Northwest National Laboratory, Richland, Washington, 1996.
- Whelan, G., J.P. McDonald, E.K. Gnanapragasam, G.F. Leniak, C.S. Lew, W.B. Mills, and C. Yu, 1999. "Benchmarking of the Vadose-Zone Module Associated with Three Risk Assessment Models: RESRAD, MMSOILS, and MEPAS." *Environmental Engineering Science*, 16(1), January/February 1999.
- Whitehead, R. L., 1992, "Geohydrologic Framework of the Snake River Plain Regional Aquifer System, Idaho and Eastern Oregon," U.S. Geological Survey Paper 1408-B, 32 pp., 6 pls. in pocket.
- Wing, N. R., 1993, "Permanent Isolation Surface Barrier: Functional Performance," Westinghouse Hanford Company, Richland, WA.
- Wood, W. W., and W. H. Low, 1988, "Aqueous Geochemistry and Digenesis in the Eastern SRPA System, Idaho," *Geological Society of America Bulletin*, v. 97, p. 1456–1466
- Yu, C. A. J. Zielen, J.J. Cheng, Y. C. Yuan, L. G. Jones, D. J. Lepoire, Y. Y. Wang, C. O. Loureiro, E. Gnanapragasam, E. Faillace, A. Wallo III, W.A. Williams, and H. Peterson, 1993, *Manual for Implementing Residual Radioactive Material Guidelines Using RESRAD*, Version 5.0, ANL/EAD/LD-2 Argonne National Laboratory, Argonne, IL, 1993.

Appendix A
Cover Design Life

Appendix A

Cover Design Life

Several engineering analyzes were completed along with commitments made by the Department of Energy (DOE) to achieve approval of the INEEL CERCLA Disposal Facility (ICDF) Remedial Design/Construction Work Plan (DOE-ID 2002) by U.S. Environmental Protection Agency (EPA), Region X; Idaho Department of Environmental Quality (IDEQ); and DOE-ID. The first subsection will address potential postclosure impacts to cover systems. The next subsection will summarize the engineering analyses and DOE commitments. This section will be concluded with a discussion of long-term ICDF cover performance expectation.

A-1. POTENTIAL POSTCLOSURE IMPACTS TO COVER SYSTEMS

Water and wind erosion, lack of vegetation, excessive sunlight, disturbance by soil-dwelling animals (or by people), and freeze-thaw of compacted clay layers all are potential problems for landfill cover systems (EPA 1989). Each of these will be discussed separately as follows.

A-1.1 Water and Wind Erosion

Heavy water and wind erosion of the top cover layer can lead to exposure of the waste itself. The potential for erosion depends on local weather patterns, soil type in the cover, and length and slope of the surface. Overbuilding the cover thickness where additional depth of cover material is provided to account for erosion estimated over the cover service life will compensate for erosion (EPA 1989).

A-1.2 Lack of Vegetation

The top layer of the landfill cover is the vegetative layer. This layer prevents wind and water erosion, minimizes the percolation of surface water into the waste layer and maximizes evapotranspiration, the loss of water from the soil by evaporation and transpiration (EPA 1989). Long-term considerations in vegetation selection include periods of drought or fire and local plant species based upon vegetation studies for disturbed areas. Selecting appropriate vegetation for the landfill cover will provide sufficient transpiration and erosion control.

A-1.3 Excessive Sunlight

Excessive sunlight (ultraviolet light and ozone) degrades flexible membrane liners. This degradation can be minimized by adequately burying the flexible membrane liners used in the cover system. Typical soil depths of liners range from 3 to 6 ft in thickness (EPA 1989).

A-1.4 Disturbance by Soil-Dwelling Animals

The effects of animals can be minimized by adequately burying the cover system. Typical soil depths of liners range from 3 to 6 ft in thickness are adequate. Large rocks can also thwart the intrusion of animals into the cover system. Biotic barriers can be used to prevent intrusion of burying animals into the cover system. Posting signs and/or erecting fences can usually prevent human intrusion, either accidental or intentional (EPA 1989).

A-1.5 Freeze-Thaw of Compacted Clay Layers

The impact of freeze-thaw cycles on clay is still not known. Because of this lack of knowledge, clay liners should be placed below the frost penetration layer (EPA 1989).

A-2. COVER ENGINEERING DESIGN AND ANALYSIS ADDRESSING IMPACTS

The following information summarizes the engineering analyses for designing the ICDF landfill cover system. The complete design analysis is presented in Engineering Design File (EDF), “Liner and Final Cover Long-Term Performance Evaluation and Final Cover Life Cycle Expectation” (EDF-ER-281).

A-2.1 Record of Decision Design and Operating Objectives

The ICDF Complex must also comply with the design and operating objectives identified in the Record of Decision (ROD) (DOE-ID 1999). These objectives are listed below:

- Maintain the cover placed over the closed ICDF landfill to prevent the release of leachate to underlying groundwater, which would result in exceeding a cumulative carcinogenic risk of 1×10^{-4} , a total hazard index (HI) of 1, or applicable State of Idaho groundwater quality standards (i.e., maximum contaminant levels [MCLs]) in the Snake River Plain Aquifer (SRPA).
- In 2095, and beyond, ensure that SRPA groundwater does not exceed a cumulative carcinogenic risk of 1×10^{-4} , a total HI of 1, or applicable State of Idaho groundwater quality standards (i.e., MCLs).
- Minimize precipitation run-on and maximize precipitation run-off to effectively reduce infiltration through the contaminated soils and debris.
- Minimize subsidence of the waste and landfill cap.
- Ensure that the design is protective of human and ecological receptors.
- Ensure that the final cover is designed to serve as an intrusion barrier for a period of at least 1,000 years.

The performance specifications for the ICDF landfill and evaporation pond (SPC-332) describe the performance and other requirements for the liner and cover system. Specifically, for the ICDF landfill design must meet all applicable or relevant and appropriate requirements (ARARs), which include the substantive requirements listed below:

- Comply with the substantive requirements of the Resource Conservation and Recovery Act (RCRA) Subtitle C design standards specified in Idaho Administrative Procedures Act (IDAPA) 58.01.05.008 (40 CFR 264.301 and 40 CFR 264.302) and the polychlorinated biphenyls (PCBs) chemical waste landfill design requirements (40 CFR 761.75).
- Comply with the substantive requirements of RCRA Subtitle C closure requirements specified in IDAPA 58.01.05.008 (40 CFR 264.310), which include the following:
 - Provide long-term minimization of migration of liquids through the closed landfill.
 - Function with minimum maintenance.
 - Promote drainage and minimize erosion or abrasion of the cover.

- Accommodate settling and subsidence so that integrity of the cover is maintained.
- Have permeability less than or equal to the permeability of any bottom liner system or natural subsoils present.
- Maintain the integrity and effectiveness of the final cover, including making repairs to the cover as necessary to correct the effects of settling, subsidence, erosion, or other events.
- Maintain and monitor the groundwater monitoring system.
- Prevent run-on and run-off from eroding or otherwise damaging the final cover.
- Protect and maintain surveyed benchmarks used in complying with 40 CFR 264.309.

A-2.2 Description of Cover System

The ICDF landfill will be capped with a robust state-of-the-practice cover barrier to minimize long-term infiltration. The cover system will vary from approximately 28 to 54 ft above ground surface. The sides of the cover system will be sloped 2.5 to 1 and will be covered with approximately 2 ft of basalt riprap (5- to 12-in. diameter). The height and covering the sides slopes with riprap will make the cover a very predominate feature in a flat sagebrush plain. The ICDF Complex is sited in a sagebrush plain southwest of the INTEC Facility and it is not near any other facilities. So the final state of ICDF will be a 54-ft-high mound with steep side slopes with a width and length of approximately 1,000 ft. The cover system will meet the remedial action objectives to minimize infiltration and maximize run-off and protect against inadvertent intrusion for minimum of a 1,000 years and meet ARARs under the IDAPA and RCRA Subtitle C requirements for closure of a hazardous waste landfill.

The cover system will minimize infiltration and maximize run-off by maintaining a sloped surface, storing water for later release to the atmosphere, lateral drainage, and providing a low-permeability composite liner barrier system. The cover can be divided by function into three main sections. Each section and its function are listed below:

- Upper section: The upper water storage component (top 9 ft of the cover) provides water storage during wet periods for later release into the atmosphere during dry periods.
- Middle section: The biointrusion component provides protection from burrowing animals and a capillary break. This layer is immediately below the upper section and is approximately 4.5 ft thick where the top of the section is at least 9 ft below the surface of the cover.
- Lower section: The lower section includes a composite liner system that has a permeability less than or equal to the permeability of the landfill bottom liner system that complies with IDAPA 58.01.05.008 [40 CFR 264.310]. Lateral drainage can occur above the composite liner system through a high-permeability drainage material in the middle section. This layer is immediately below the middle section and is a minimum of 4 ft thick and 13 ft below the surface of the cover.

Each component in the cover profile is shown in Figures A-1 and A-2.

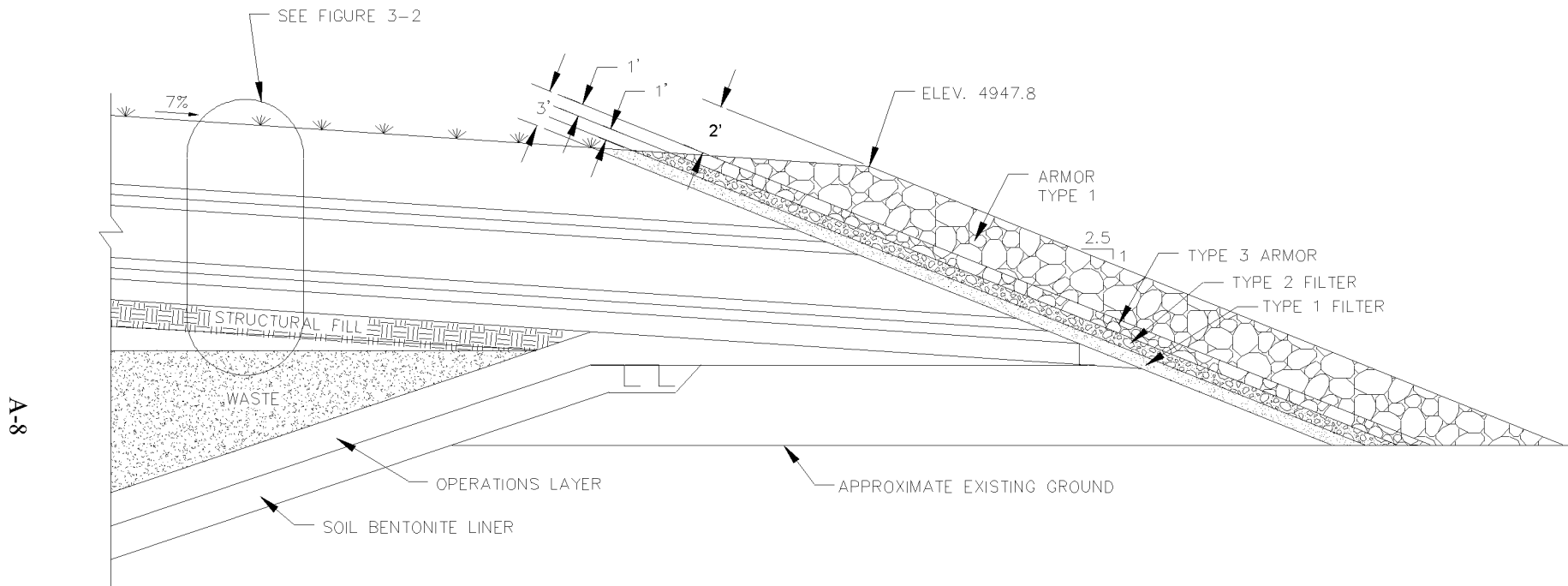


Figure A-1. Landfill cover section.

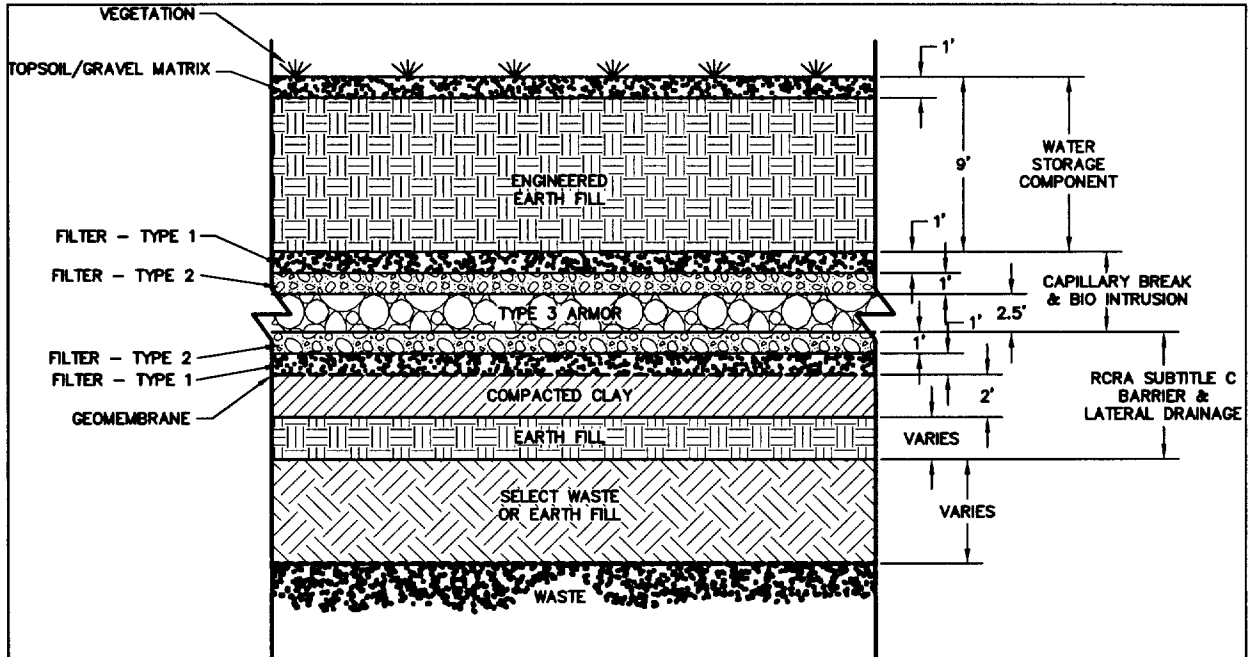


Figure A-2. Landfill cover profile.

A-2.3 Cover Surface Grade and Erosion Protection

The ICDF landfill cover surface grade and erosion protection meets or exceeds the requirements of RCRA Subtitle C design standards specified in IDAPA 58.01.05.008 (40 CFR 264.301 and 40 CFR 264.302). It is designed to provide long-term minimization of migration of liquids through the closed landfill, function with minimum maintenance, and minimize erosion.

The function of the surface of the cover is to promote surface water drainage away from the waste, minimize erosion, and provide a medium for vegetation. The surface will be sloped so that surface water run-off is directed to the side slopes of the landfill lined with basalt riprap armoring. The riprap armor will dissipate eroding forces from stormwater until the stormwater reaches the existing ground surface at a distance of over 100 ft from the edge of the waste mass.

The cover settlement has been evaluated in the “Landfill Compaction Subsidence Study” (EDF-ER-267). Based on the settlement determined in this study and the other design considerations (subsidence, erosion, and abrasion) provided herein, a final grade of 7% was determined for the cover. This will ensure that a minimum slope of 3% is maintained after consolidation to promote surface water drainage off the cover system through its life cycle.

Surface water and wind erosion analyses were performed to determine the amount of soil loss from the cover due to sheet flow. Erosion due to surface water was completed using the Modified Universal Soil Loss Equation (MUSLE) as recommended by the Nuclear Regulatory Commission (NRC) for long-term (i.e., 1,000-year) soil loss (NRC 1986). The surface of the cover was assumed to be fine-grained soils such as those found at the Rye Grass Flats area at the Idaho National Engineering and Environmental Laboratory (INEEL) without accounting for the protection of the soil/gravel matrix. The analysis consisted of determining the probable maximum precipitation (PMP) event and calculating soil loss per year using the MUSLE equation. Approximately 2 ft of soil could erode from the surface of the cover over a 1,000-year time period. The minimum water storage layer thickness needed to maximize

water storage is 6.5 ft based on the “Hydrologic Modeling of the Final Cover” (EDF-ER-279). The water storage layer will be constructed with an additional 2.5 ft of material to provide a sacrificial layer in the event that the surface would erode due to water erosion.

Extensive wind tunnel studies performed at the Hanford facility show that a mixture of fine-grained soil and pea gravel significantly reduced erosion due to wind forces. Soil/pea gravel armoring can reduce erosion rates from 96.5 to more than 99% at wind speeds of 45, 56, and 67 mph (Ligotke 1993). The average wind speed at the INEEL based on the period of record is 9 mph with peak gusts up to 82 mph (NOAA 2001). Based on these studies, a soil/pea gravel matrix will provide sufficient protection against wind and aeolian forces for the ICDF cover through its life cycle, and conceivably beyond.

The top surface of the cover will consist of a vegetated soil/gravel matrix system sloped to minimize infiltration and maximize run-off. Vegetation will enhance the evapotranspiration properties of the upper cover portion and provide erosion control. The soil/gravel matrix will prevent excessive soil loss due to wind and surface water run-off. The design of the cover surface and erosion protection is a combination of ICDF site-specific studies and off-site studies performed at the Hanford facility to support the development of long-term protective covers.

A-2.3.1 DOE Commitments

Long-term performance of the cover is based upon the vegetation that will be well established. The cover will be periodically monitored as part of the INEEL’s long term stewardship program and maintained as necessary.

Institutional controls anticipated to be implemented as part of long-term stewardship include the following:

- Access restrictions to prevent intrusions into the closed area, including the creation of a buffer zone surrounding the capped ICDF and supporting structures
- Access controls, monitoring, and maintenance will remain in place for as long as the contents of the landfill remain a threat to human health or the environment if uncontrolled.

The ICDF landfill closure requirements will include access restrictions with a buffer zone that will be maintained around the landfill for as long as the landfill contents remain a threat to human health and the environment. The institutional controls are designed to prevent disturbance of closed areas and to maintain a cumulative carcinogenic risk of less than 1×10^{-4} and a total HI of 1. The access restrictions are designed to prevent intrusion into a closed area and establish a buffer zone of protection. Access controls, monitoring, and maintenance will remain in place as long as the contents of landfill remain a threat to human health and environment (cumulative carcinogenic risk of greater than 1×10^{-4} and a total HI greater than 1).

The DOE-ID is required to monitor the ICDF Complex after its operational life is completed. The institutional controls for this facility will include proper signage, security, and monitoring. The long-term management of the ICDF Complex and associated monitoring, maintenance, etc., will be transferred to the INEEL Long-Term Stewardship Program. The DOE-ID will place easily visible permanent markers at all the corner boundaries for each cell of the landfill and identify the potential hazards. In addition, the DOE-ID will maintain all institutional controls until that responsibility is passed, along with management of the property, to another federal agency such as the Bureau of Land Management (BLM).

In the ROD, Table 11-1, the Agencies agreed to rely upon institutional controls as part of the selected remedy (DOE-ID 1999). In general, institutional controls will be designed to limit site access after closure of the ICDF. The institutional controls address two time frames—current DOE operations and DOE control postoperations. The controls under current DOE operations include operating ICDF as an industrial Radiologically Controlled Area with visible access restrictions (warning signs, copies of surveyed maps, etc.). Activities such as drilling or excavating will be controlled. In addition, surveillance to ensure controls are in-place includes periodic inspections by DOE and IDEQ/EPA reviews. The frequency of the surveillance is determined in the ICDF Remedial Action Work Plan and includes a combination of daily and weekly inspections.

The institutional controls for postoperations include restricting access to the landfill such that there will be no unauthorized intrusion into the capped area, drilling and excavating will be controlled. Only Federal Facility Agreement and Consent Order (FFA/CO) -approved operations and maintenance (O&M) activities will be authorized. Controls under the postoperations time frame include visible access restrictions (warning signs), notice to affected stakeholders, and property lease requirements. Notice to affected stakeholders (e.g., BLM, Fish and Wildlife Service, Sho Ban Tribal Council, local county governments, State, and EPA) will be made regarding notice of any change in land use designation, restriction, land users or activities. Warning signs will be installed and maintained to warn intruders of the risks of remaining in the area. These warnings would be to unauthorized trespassers if current DOE radiological site controls were no longer used. DOE will control postoperations of the ICDF site such that the landfill will have no unauthorized intrusion into the capped area. Also, DOE will maintain the integrity of the cap. The effectiveness of the institutional controls will be periodically evaluated during 5-year reviews. The 5-year reviews will continue until these reviews are no longer needed by the Agencies. Specifically, the 5-year reviews will continue as long as contaminants exist at levels that result in restricted access or limited site usage at ICDF. The remedy will be evaluated no less than every 5 years to ensure it is functioning as intended and remains effective in reducing risks and complying with applicable or relevant and appropriate requirements. These long-term requirements minimize the potential for cap degradation and inadvertent intrusion because DOE institutional controls will be maintained for a sufficiently adequate time period until restricted access is no longer necessary due to unacceptable levels of contamination.

A-2.4 Side Slope Erosion and Stability

The landfill cover side slopes will be sloped at 2.5H:1V (2.5 horizontal to 1 vertical) from the edge of the cover to the existing ground surface as shown in Figure A-1. The side slopes will be armored with durable basalt rock native to the INEEL area. The rock armor was designed to dissipate erosional forces from surface water run-off and protect the underlying cover layer and waste. The side slope erosion protection and stability analysis will ensure that the cover maintains its integrity over the long term.

The primary function of the side slope armor is to maintain the integrity of the cover system and waste mass. It will dissipate the energy from water run-off from the cover and protect the cover from an unlikely event of a flood. Its secondary function is to provide a biobarrier for the landfill. The side slope armor will be comprised of earthen materials sized to maintain the cover's integrity through the 1,000-year design life cycle. The rock armor size varies from 5 to 12 in. in diameter depending on the weight of the individual rock piece.

A-2.5 Evapotranspiration Component

The evapotranspiration component consists of silty loam-type soils that provide water storage during wet periods for later release into the atmosphere during dry periods. Coupled with a capillary break provided by the underlying sand and gravel layers, it will store moisture from long-term, low-probability precipitation events for later release to the atmosphere by evapotranspiration. The evapotranspiration layer in the cover is an integral component that provides long-term minimization of migration of liquids through the closed landfill while functioning for the long term with minimal maintenance.

The primary function of the evapotranspiration component is to store and release moisture and provide a medium for plant growth. It also provides a buffer zone between the waste and ecological receptors. Hydrologic modeling has shown that the evapotranspiration component can recover after cycles of extreme precipitation events and will continue to function through its 1,000-year design life and conceivably years beyond.

The thickness of the evapotranspiration layer was determined based on hydrologic modeling provided in the “Hydrologic Modeling of Final Cover” (EDF-ER-279). Sensitivity analysis was performed that determined an optimal layer thickness between 5 and 6.5 ft. The sensitivity analysis shows clearly that increasing the water storage thickness beyond the optimal thickness increases water storage capacity, but does not reduce the percolation rate. Insignificant changes in percolation occur for the water storage layer thickness beyond 6.5 ft. Additional material was added to the water storage layer to address erosion protection described in Section A-2.3.

A-2.6 Biointrusion/Drainage

Small animals and insects such as badgers and ants have been known to burrow into landfills, bringing waste materials to the surface and leaving defects in the cover system. Past barrier studies at INEEL, Hanford, and other facilities have shown that a thin layer of gravel is effective in preventing animals and ants from penetrating underlying waste materials (Morris and Bleu 1997; Wing 1993). The ICDF landfill cover will include a 2.5-ft-thick, Type 3 armor layer comprised of 2- to 5-in.-diameter gravel. This biointrusion layer is shown on Figure A-2. The Type 3 armor will also provide lateral drainage in the event breakthrough occurs through the upper cover layers. The primary function of the biointrusion layer is to prevent burrowing animals indigenous to the INEEL area from penetrating the underlying cover components and the waste material. It also provides a high-permeable drainage media if water were to percolate from the upper portions of the cover system.

The biointrusion design was primarily based on review of past studies performed at INEEL. The increase in infiltration due to holes left in the evapotranspiration component were evaluated in the “Hydrologic Modeling of Final Cover” (EDF-ER-279). The biointrusion design evaluated both plant and animal intrusion. Based on the total cover thickness varies from 17.5 to 21.5 ft below the cover surface, biointrusion will not be a concern because this depth is greater than known burrowing depths at the INEEL. The biointrusion material will consist of gravel screened from the local available alluvium at INEEL. The alluvium gravels at INEEL are composed of granite, quartz, and other durable minerals that make it ideally suited for long-term applications.

A-2.7 Barrier Layers

The primary mechanism for minimizing infiltration through the cover is the upper evapotranspiration cover layer. Barrier layers are included in the lower portions of the cover for redundancy and regulatory compliance. The barrier consists of a single high-density polyethylene (HDPE) geomembrane/soil-bentonite liner (SBL) composite system. Similar to the landfill liner system beneath the waste, the composite system will intercept water in the event breakthrough occurred from upper cover sections and divert it laterally through the overlying sand and gravel layers. The cover barrier layer complies with the substantive requirements of Subtitle C hazardous waste closure specified in IDAPA 58.01.05.008 (40 CFR 264.310) and will have a permeability less than or equal to the permeability of the ICDF bottom liner system. The function of the barrier layer is to provide a redundancy in the cover system and divert water away from the waste if it were to break through the upper cover sections. The earthen SBL is expected to perform through the 1,000-year design life of the cover.

Stresses will be induced in the cover SBL and geomembrane barrier components due to settlement in the foundation soils waste, and the cover itself. When the cover settles, the geomembranes will compress, resulting in a reduction in stress. However, the SBL could crack due to excessive settlement. The proposed cover surface will have a slope of 7%. The cover could accommodate an additional settlement (after surface consolidation, cover settlement, and the maximum strains are accounted for) of 13 ft. Approximately 54% (i.e., 6 ft) of the allowable settlement are predicted over the long term. Consequently, the strain in the SBL will not cause cracking and increased permeability.

Landfill covers must maintain a positive slope to promote surface water runoff (40 CFR 264.310). The EPA recommends a final top slope between 3 and 5%, after settlement has occurred. The proposed cover surface will have a slope of 7% (EDF-ER-281) and a length of 387 ft measured on its shortest side. The final top slope after settlement will be approximately 3%.

SBL can sustain irreversible damage caused by freeze-thaw cycles. Water added during construction for compaction can freeze, increasing the hydraulic permeability through formation of cracks, microcracks, and interconnected macro pores (Benson and Othman 1993). Extreme frost penetration at INEEL is estimated to be 3.75 ft. The ICDF landfill SBL will be protected from frost by 15.5 ft of overlying soil layers in the cover.

A-2.8 Filter Layers

The cover will be comprised of two filter-type materials to prevent fine-grained material from migrating to other components of the cover system. The filter layers provide a smooth transition from one material to another while maintaining the capillary break and lateral drain between the sections. Filter layers also provide capillary breaks due to the contrast in unsaturated permeabilities. Filters are included between the upper soil storage layer and biointrusion, between the biointrusion and SBL, and beneath the side slope armor.

Filters allow water to pass while keeping soil particles in place. They are typically comprised of sand and gravel or manufactured from synthetic materials. The filter layers in the landfill cover system will be composed of graded sands and gravels screened from the alluvium material that exists at the INEEL. The gradation of each filter is designed to prevent fine materials from the overlying layer from migrating downward. The filter layers will perform their function through the 1,000-year design life cycle. A summary of rock armor and filter sizes is provided in Tables A-1 and A-2, respectively.

Table A-1. Summary of rock armor sizes.

Armor/Filter	D ₅₀ ^a (in.)	Percent Finer Than						
		12 in.	8 in.	6 in.	4 in.	3 in.	2 in.	1.5 in.
Type 1—Side slope armor	10–12	100	35–60	15–35	0–5			
Type 3—Armor biointrusion barrier	2.5–4			100	100–40	100–25	30–0	0–1

a. D₅₀ is the medium diameter of the material.

Table A-2. Summary of filter sizes.

Armor/ Filter	D ₅₀ ^a (in.)	Percent Finer Than											
		3 in.	2 in.	1.5 in.	3/4 in.	3/8 in.	#4	#10	#20	#40	#60	#100	#200
Type 2— Coarse filter material	0.15– 0.5	100	100– 85	100– 77	86–57	68–42	55– 30	40–15	23–0	10–0	3.0		
Type 1— Fine filter material							100	100– 80	90– 58	75– 43	65– 33	55– 25	40– 12

a. D₅₀ is the medium diameter of the material.

A-2.9 Vegetation

The landfill cover surface will be seeded and fertilized to promote plant growth. Vegetation will minimize erosion and accelerate removal of water from the water storage layer. Long-term considerations include periods of drought or fire so erosion and hydrologic modeling studies have assumed a poor stand of vegetation. The vegetation will consist of local plant species based on vegetation studies performed for disturbed areas at INEEL (DOE-ID 1989). This should produce a healthier stand of vegetation than natural conditions, providing more transpiration and better erosion control.

Vegetation is expected to be present through the 1,000-year design life. Vegetation is expected to continue with periods of drought or fire. Vegetation based on native plant species will include the following:

- Secar bluebunch wheatgrass
- Bottlebrush squirreltail
- Sandberry bluegrass
- Sodar streambank wheatgrass
- Green rabbit brush.

The maximum allowable noxious weed percentage (by dry weight) will be 0.5%. The maximum allowable wet and other crop percentage will be 1.5%. The engineered seed mix will provide superior vegetation providing more transpiration and erosion control than the surrounding natural vegetation.

A-3. LONG-TERM COVER PERFORMANCE EXPECTATION

The only long-term performance consideration for the ICDF landfill is potential of cover system degradation over the long-term service life. Material degradation could potentially change the physical properties that would impact the performance of the cover. The soil and rock materials used will not be problematic with respect to degradation if the current materials specified are used during cover construction. These materials have a long track record with respect to degradation based on extensive studies associated with geology. The physical characteristics of geologic materials, such as soil and rock, do change with time, but these changes take a very long time, usually on the order of millions of years.

The ICDF cover system will consist of natural and synthetic materials. A description of each material and its long-term performance characteristics is presented below to determine the viability of the performance requirements being met.

A-3.1 Natural Materials

The majority of the cover system will consist of the natural materials. These materials will include the following: soil, rock, and vegetation.

The engineering properties of these materials are well understood and have obvious longevity. They will be engineered to perform a specific function in the ICDF such as hydraulic barriers, water storage, transpiration, erosion control, filtration, and drainage. Descriptions of the materials' natural properties (e.g., low permeability, capillary potential, energy dissipation) that make them well suited for their function are provided in the subsections below. Long-term degradation issues are described such as desiccation and freeze-thaw issues in clay soil or erosion potential in rock.

SBLs have a natural low saturated permeability due to the clay mineral crystalline structure. Clay is found in abundance in nature as a result of the chemical and physical erosion of rock. Geologically (millions of years), clay will continue to change chemically and physically if exposed to the environment. The clay mineral used in the SBL (e.g., bentonite, montmorillonite) is electrically unbalanced and has an affinity for water. This results in a swelling effect when water is available. Conversely, moisture loss will cause drying and shrinking, which results in cracking. Cracks or desiccation will increase permeability in SBLs. Clays are also subject to freeze-thaw cycles that can increase permeability.

The SBL used for the landfill cover will be protected by the overlying cover materials 15.5 ft thick. The frost depth at INEEL is approximately 3.75 ft below the ground surface. The SBL in the landfill bottom cover will be below the frost depths. Additionally, at this depth, the SBL will retain its moisture and maintain its low permeability characteristic.

Sands and gravel will be used in the cover system for filtration and drainage. There is an abundance of alluvial soils at INEEL that can be engineered to provide the required gradation and drainage properties for each layer in the landfill cover. The alluvium gravels at INEEL are comprised of granite, quartz, and other durable minerals that make it ideally suited for long-term applications.

The upper portion of the cover will be comprised of fine-grained soils that provide good water storage capabilities. These soils are also available at INEEL and have been shown to provide good water storage and release characteristics in engineered barrier studies performed at INEEL. Soil is a product of the decomposition of rock and will retain its properties for the long-term life of the cover. However, its fine-grained composition makes it vulnerable to erosional forces such as wind and water.

A soil/pea gravel mulch and vegetation providing an armor against erosion will protect the upper portion of the cover. The cover will also be overbuilt as a contingency in the unlikely event that the soil/pea gravel is eroded, exposing the upper fine-grained water storage material to long-term erosional forces.

Rock armor will line the side slopes of the ICDF landfill. Shallow formations of basalt underlie INEEL and can be easily mined for erosion protection. Basalt is a durable volcanic rock that provides excellent erosion protection, however, it may vary in its density and competency. Los Angeles Abrasion Tests (ASTM C535) will be performed on the rock armor selected for the ICDF cover prior to construction to determine its long-term durability. Based on the results of these tests, rock armor will be oversized if necessary to ensure that it performs its function for the life of the cover system.

A-3.2 Human Intrusion

To deter the inadvertent intrusion of humans into the waste, a marker system will be used to warn future generations of the dangers of the buried waste. DOE intends to maintain active control of INEEL (using fences, patrols, alarms, and monitoring instruments) for the foreseeable future (next 100 years). If these measures should cease, other passive-type measures will warn the inadvertent intruder from waste buried beneath the permanent cover barrier. The measures may include recognizable warning markers and other physical features. Site information will be provided on an Internet website, U.S. Geological Survey maps, libraries, and other information repositories that would be readily available to the public.

The ICDF landfill will have a steep rocky side slope of basalt riprap. This feature clearly delineates the boundaries of the surface barrier by providing a distinct contrast with the surrounding flat terrain. These side slopes are engineered structures that will be obvious that humans had built the structure. These distinct riprap side slopes in combination with warning signs will minimize the risk of human intrusion.

If ownership of any portion of the land is ever proposed for transfer outside the federal government, the DOE-ID will fulfill the requirements of 42 USC 9620 (Comprehensive Environmental Response, Compensation and Liability Act [CERCLA] §120[h]) to provide the transferee with complete notification and warranty of completed RA. At such time, the federal government will establish, in cooperation with local governments, appropriate land use restrictions, zoning restrictions, and deed restrictions on the ICDF landfill and its adjacent buffer zone, which will preclude industrial, institutional, or residential development until unacceptable risk no longer exists. These documents will include disposal records and the marker locations. These conditions will be verified as part of the EPA, IDEQ, and DOE 5-year review.

A-3.3 Potentially Disruptive Natural Events

Potential disruptive events would include a high wind condition, earthquake, or massive flood event. The likelihood and magnitude of these events at the INEEL are discussed in the following paragraphs. How the cover would be affected by these catastrophic events is discussed below.

Tornado-type winds are expected to be extremely rare at the ICDF Complex. The side slope armor will consist of large heavy basalt riprap that will resist tornado-type winds. The surface of the permanent cover will consist of vegetation and soil/pea gravel matrix. The soil/pea gravel matrix has shown to be resistant to high wind forces generated in wind tunnel tests performed at the Hanford facility.

The ICDF Complex is situated outside the 100-year and 500-year Big Lost River floodplains predicted by the United States Geological Survey (Berenbrock and Kjelstrom 1998) and United States Bureau of Reclamation (BOR 1999), respectively. As a conservative check, the ICDF landfill was

analyzed for the effect of the 500-year flood event flowing past the side slopes. Floodwaters at the base of the cover were assumed to rise to an elevation of 4,925 or 4 ft below the crest of the landfill berm. At this level, the estimated flow velocity is approximately 2.5 ft per second. Even during active landfill operations, this flow velocity and potential erosion can be resisted using native vegetation on the slopes.

Although the permanent ICDF cover barrier has a design life of 1,000 years, it could conceivably perform beyond this time. Its earthen material composition allows the permanent cover to perform like a geological structure requiring many years to break down its outer shell of rock armor. Forces of a catastrophic nature would be required to compromise the 17.5-ft cover comprised of soil, gravels, rock, and clay. Consequently, there is a likely probability that the cover will continue to perform after its 1,000-year design life.

In summary the ICDF cover system addresses all potential postclosure impacts as follows:

- An additional 2.5 ft of soil and pea gravel are added to the water storage layer to address water and wind erosion for 1,000-year design life.
- A vegetative cover including native plant species is expected to continue during its 1,000-year design life with periods of drought and fire.
- All flexible membrane liners are adequately buried to avoid degradation and are expected to continue during its 1,000-year design life.
- Biointrusion layer is placed at a depth greater known burrowing depths and is expected to continue during its 1,000-year design life.
- The sloped sides of the cover will have rock armor to minimize intrusion and is expected to continue during its 1,000-year design life.
- The soil bentonite liner is protected from frost and is expected to continue during its 1,000-year design life.

A-4. INFILTRATION RATE THROUGH THE COVER

Several engineering analyses were completed to achieve approval of the *ICDF Remedial Design/Construction Work Plan* (DOE-ID 2002) by EPA, Region X; IDEQ; and DOE-ID. One of these engineering analyses focused upon hydrologic modeling of cover to determine the design infiltration rate. The first subsection will address proposed cover design and conceptual model used to determine the design infiltration rate through the ICDF landfill cover. The next subsection will summarize the engineering design and modeling analyzes to achieve approval of the cover infiltration rate. The third subsection will summarize the results of the sensitivity analyses. This section will be concluded with a discussion regarding the design infiltration rate through the ICDF cover. The complete modeling for the cover is presented in "Hydrologic Modeling of Final Cover," EDF-ER-279.

A-4.1 Cover Design

The ICDF landfill will be capped with a robust, state-of-the practice cover to minimize long-term infiltration. The cover system must meet the remedial action objectives (RAOs) to minimize infiltration and maximize run-off and protect against inadvertent intrusion for greater than 1,000 years (DOE-ID 1999). The cover system must also meet applicable or relevant and appropriate requirements under the IDAPA and RCRA Subtitle C requirements for closure of a hazardous waste landfill.

The cover system will minimize infiltration and maximize run-off by maintaining a sloped surface, storing water for latter release to the atmosphere, lateral drainage, and providing a low-permeability composite liner barrier system. Each component in the cover profile is shown in Figure A-3.

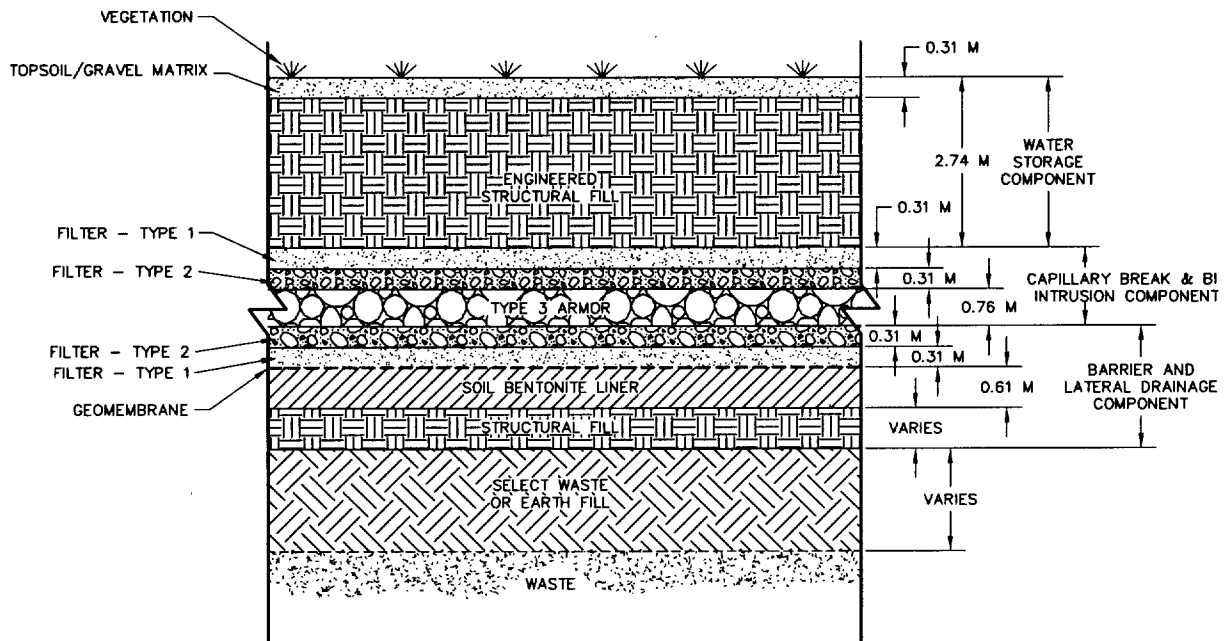


Figure A-3. Schematic of modeled cover section.

The cover can be divided by function into three main sections. Each section and its function are listed below:

- Upper section: The upper water storage component provides water storage during wet periods for latter release into the atmosphere during dry periods.

- Middle section: The biointrusion provides protection from burrowing animals and a capillary break to reduce infiltration.
- Lower section: The lower section includes a composite liner system that has a permeability less than or equal to the permeability of the landfill bottom liner system that complies with IDAPA 58.01.05.008 (40 CFR 264.310). Lateral drainage can occur above the lower section of the liner system through a high-permeability drainage material.

A-4.2 Conceptual Model

Figure A-4 shows the overall cover system model configuration. The arrows in Figure A-4 represent the layers that were evaluated to determine the ultimate percolation from the base of the SBL, Point F. The layers are represented by observation points and are referenced throughout this section to provide a point of reference for the analyses. Each point is described below:

- Point A: Precipitation on the cover surface
- Point B: Evapotranspiration from the cover surface
- Point C: Surface water run-off from the cover surface
- Point D: Breakthrough from the base of the water storage layer
- Point E: Lateral drainage
- Point F: Percolation from the base of the SBL.

NOTE: *Percolation was determined at the base of Layers D and F across the cover, not at a specific point.*

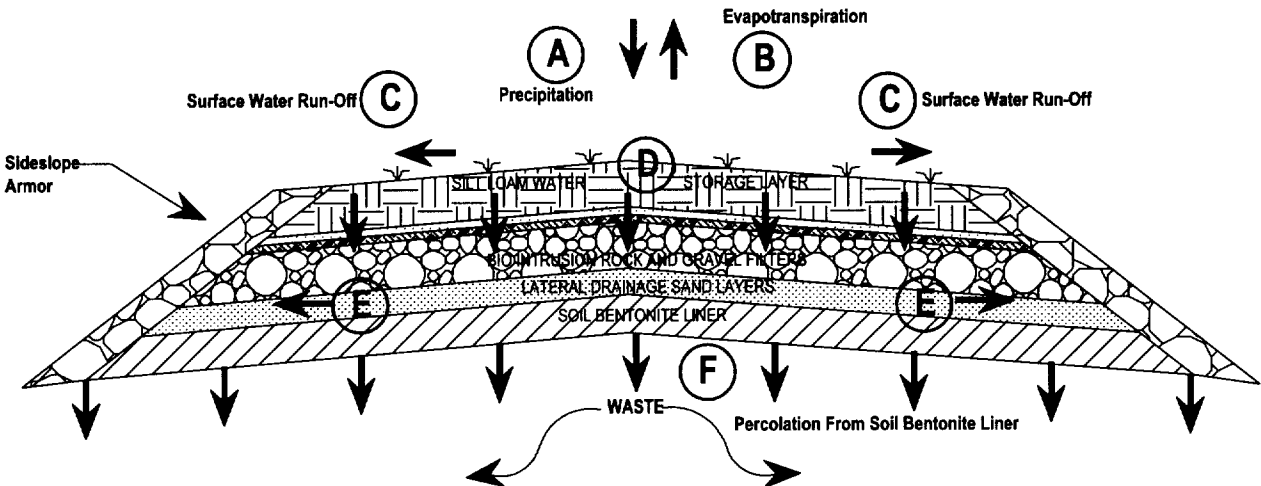


Figure A-4. Hydrologic model geometry and location of layers.

A-4.3 Design and Modeling Analyses

Climatological data, surface run-off, evapotranspiration, infiltration, biological intrusion, lateral drainage, and the modeled infiltration rate analyses and information from “Hydrologic Modeling of Final Cover” (EDF-ER-279) will be summarized in the following subsections.

A-4.3.1 Climatological Data

The hydrologic modeling of the final cover studies evaluated two climate scenarios that included a 10-year period having the conditions that most likely would break through the upper section at Point D shown in Figure A-4 and an extreme condition to address potential long-term climate changes. The extreme condition included back-to-back years that had precipitation amounts greater than the 90th percentile. Figure A-5 shows the period of climate data and the selected 10-year base case period. The 10-year period selected was from October 1, 1967, through September 30, 1976, with an average annual precipitation of 237 mm. This period provides the most likely chance of cover breakthrough from the upper section since the 10-year average annual precipitation (237 mm) is greater than the average annual precipitation (218 mm) for the period of record. Moreover, the selected 10-year period includes higher-than-normal precipitation events during the initial years that “load” the water storage cover layer with moisture, allowing the model to simulate the cover’s recovery capability after large precipitation events.

Figure A-6 shows the years selected for the extreme scenario. The 90th percentile for the period of record was 306 mm/yr. As shown, the years with precipitation greater than the 90th percentile were 1957, 1963, 1964, 1968, and 1995. These years, back-to-back (with the exception of 1968, which was included in the average climatic scenario), were used to determine break through from the upper section for long-term, worst-case climate conditions.

Maximum and minimum daily temperatures for the simulated years were included in the input data sets for the unsaturated flow model, Soil Cover 2000. Daily precipitation, maximum and minimum relative humidity, and wind speed data from these years were also input to the model. As a result of the lack of relative humidity data for the years simulated (only 2 years of data were available), monthly averages for minimum and maximum relative humidity were used in the model.

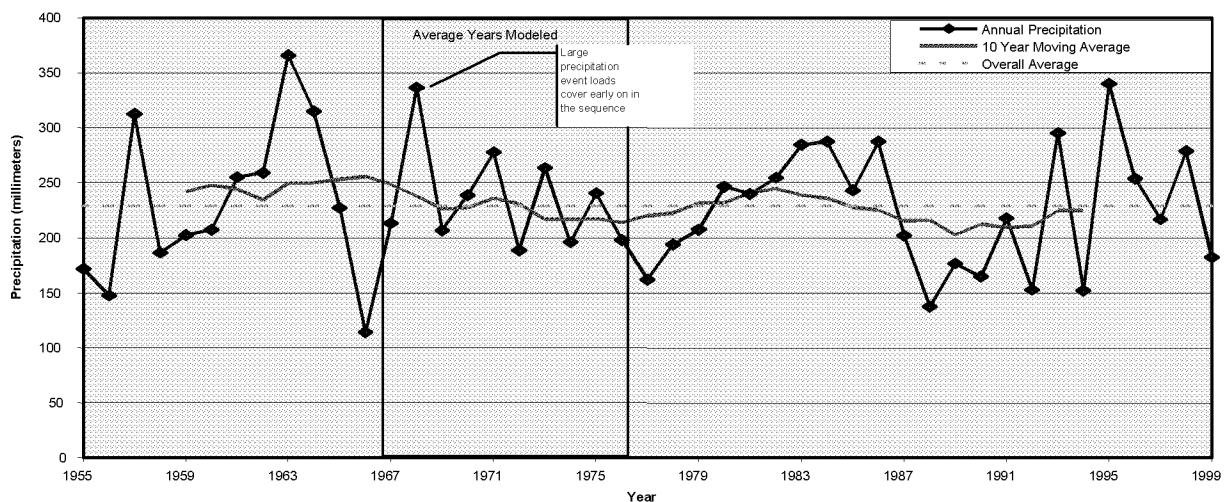


Figure A-5. INEEL annual precipitation.

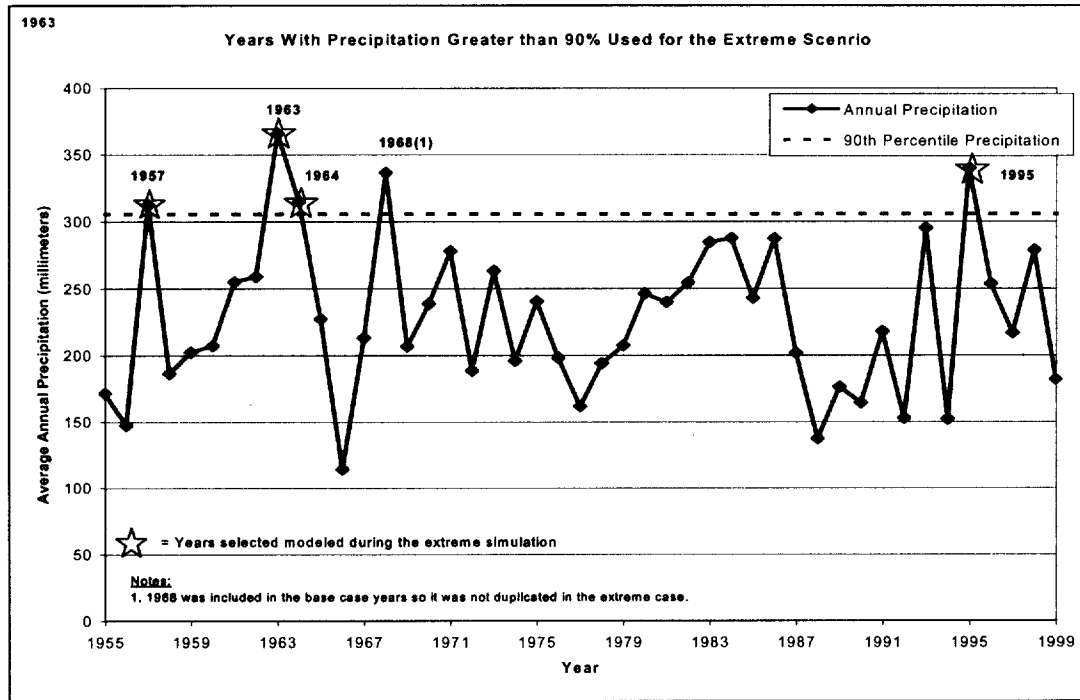


Figure A-6. Extreme precipitation events.

Global solar radiation data were synthetically generated using the Weather Generating Program (WGEN) computer code, which takes into account observed precipitation and temperature data (Martian 1995). These data were converted to net radiation using the method provided in the Handbook of Hydrology (Maidment 1993).

The climatological data for the extreme case were used in this study to determine the worst-case percolation through the base of the cover. Additionally, typical storms for Idaho Falls are of short duration (i.e., less than 6 hours) with high intensity resulting in run-off with little time for infiltration. Storm events for the hydrologic cover model were distributed over 12 hours, maximizing infiltration.

A-4.3.2 Surface Run-off

The surface water run-off component of the model is shown as Point C in Figure A-4. Surface water run-off was calculated using the curve number method developed by the Soil Conservation Service (SCS). Total run-off during the base case simulation period was calculated using the SCS method as 1.3 mm/yr, which represents approximately 0.6% of the total annual precipitation. The run-off for the extreme case simulation was 3.33 mm/yr, which is approximately 1% of the total annual precipitation. To account for the run-off in the hydrologic model, the daily precipitation values were adjusted by subtracting the run-off from the recorded precipitation. The observation point location in the model for run-off is shown at Point C in Figure A-4.

A-4.3.3 Biological Intrusion

Studies performed at INEEL and the Hanford facility have shown that small mammals can burrow into the cover and in some cases potentially deep enough to reach waste materials. Waste can be transported upward and holes left behind can increase infiltration into the cover. Observed burrow depths based on biointrusion studies were 1.47 m for pocket gophers, 1.40 m for pocket mice, and 1.14 m for the

Townsend ground squirrel. A report cited in the Hanford study indicates that the great basin pocket mouse can burrow as deep as 1.93 m (CH2M HILL 2002). Biobarrier demonstration plots at INEEL showed that 1- to 2-in.-size cobbles were effective in preventing animals from burrowing to underlying soil layers (Laundre 1996).

Of the animals that may introduce penetrating burrows to engineered soil structures such as the ICDF final cover, mammals such as badgers (*Taxidea taxus*) and coyotes (*Canis latrans*) may produce the largest-diameter burrows. These animals, however, are not likely to present dense populations on a structure such as the ICDF cover. Badgers tend to be solitary and excavated coyote dens tend to not be closely spaced. Both badgers and coyotes may create substantial excavations when hunting for smaller mammalian prey (Audubon Society 1992).

Small mammals such as the Great Basin pocket mouse (*Perognathus parvus*) and the northern pocket gopher (*Thomomys talpoides*) are expected to be common residents of the INEEL and may be expected, over time, to establish residence within disturbed areas of the ICDF Complex (Audubon Society 1992). Studies conducted at the INEEL and at DOE's Hanford Site in Washington State confirmed the presence of both species on, and near, retired waste sites. One study reported a pocket mouse burrow frequency of 2.9 burrows per 100 meters (m) along study transects. Pocket gopher burrows were observed at a frequency of 1.9 borrows per 100 m along the same transects (Smallwood 1996). The same study also reported observation of harvester ant colonies at a frequency of 1.2 colonies per 100 m. Another study of a pocket gopher population on a retired waste site at Hanford reported an average gopher density of 25.3 gophers per hectare over a two-year study (Hedlund and Rogers 1976).

The characteristics and habits of common burrowing animals indicate that the potential exists for such animals to populate an unmaintained engineered soil structure. In addition, the nature of the burrows produced by these populations could possibly increase water infiltration through the ICDF final cover to an unacceptable rate. The increase in infiltration through the upper section water storage layer from a burrow was determined assuming a mammal left a hole that could be flooded during precipitation events. It was assumed that the animal created one hole in the cover with a diameter of 20 cm that went through the upper section of the cover to the bio-intrusion layer. This hole drained an area 10 times the diameter of the hole, 200 cm. All precipitation contacting this area was added to the infiltration at Point D of Figure A-4.

The infiltration through the water storage layer resulting from one hole through the upper portion of the cover was computed as 0.01 mm/yr for the base case and 0.02 mm/yr for the extreme case. The infiltration through the water storage layer due to a hole that partially penetrates the upper portion of the cover was computed as 0.005 mm/yr for the base case and 0.01 mm/yr for the extreme case. The infiltration at Point D shown in Figure A-4 through the water storage layer due to animal burrows was 0.015 mm/yr and 0.03 mm/yr for the base and extreme cases, respectively.

Considering the burrow density of the pocket mouse, the additional infiltration through the water storage layer would only be 0.16 mm/yr. The pocket mouse density of 2.9 burrows per 100 m would produce a total number of burrow holes on the landfill of approximately 16. Based on an infiltration through each burrow hole of 0.01 mm/yr, the total additional infiltration through the water storage layer would be 0.16 mm/yr, which would provide a total infiltration rate of 0.62 mm/yr through the water storage layer. This infiltration rate is less than the infiltration rate required to produce total breakthrough at the bottom of the clay barrier of 0.1 mm/yr.

A-4.4 Lateral Drainage

Hydraulic head in the drainage layer was determined using the vertical downward infiltration at Point D shown in Figure A-4 determined by the SoilCover program plus the infiltration due to bio-intrusion. The volume of water that can be removed by the drainage layer is a function of its slope, length, and permeability. For the base and extreme climate scenarios, the drainage layer can remove approximately 112 and 136 m³/yr of water given the amount of hydraulic head on the SBL. The water removal capacity of the drainage layer was compared to the infiltration rate from the upper cover section to determine potential infiltration into the compacted SBL and build-up of hydraulic head in the drainage layer. Spreading the volume of water that can be removed from the drainage layer over the area of the cover results in 894 and 1,094 mm/yr water removal rate for the base and extreme climate scenarios, respectively. Comparing these values to the predicted infiltration from the upper cover section of 0.41 and 0.48 mm/yr (including 0.01 mm/yr due to defects caused by biointrusion) for the base and extreme climate scenarios, respectively, indicates that drainage will exceed infiltration, minimizing percolation from the base of the SBL.

A-4.5 Modeled Infiltration Rate

The percolation at the base of the cover in the lower cover section of the model is shown as Point F in Figure A-4. Infiltration at this point can enter the waste mass, potentially generating leachate and migration of contaminants in the waste. Hydrologic simulations of landfill bottom liner systems using EPA's HELP model have been performed to determine the effectiveness of bottom liner systems. Correlations between infiltration and percolation through landfill liner systems were developed to determine the minimum saturated permeability requirement of 1×10^{-7} cm/sec. an average annual percolation rate of 0.1 mm/yr is estimated to drain from the base of the ICDF landfill cover and contact the underlying waste mass. Although a small value, the average annual percolation rate of 0.1 mm/yr is conservative since it would require a near steady source of infiltrating water through the landfill cover system.

Two-dimensional finite element modeling was completed using SEEP/W to determine the percolation at the base of the lower cover section shown as Point F in Figure A-4. Steady-state simulations were performed using three inflow rates into the drainage layer in the range of the vertical downward infiltration at Point D shown in Figure A-4 determined by the SoilCover program plus the infiltration due to bio-intrusion. The volume of water exiting the based of the compacted SBL is a function of its slope, length, and permeability. The amount of water exiting the base of the compacted SBL was compared to the infiltration rate from the upper cover section to determine the percentage of the infiltration traveling vertically through the SBL base. Comparing these values to the predicted infiltration from the upper cover section of 0.40 and 0.46 mm/yr, the percolation from the SBL is provided in Table A-3.

Based on the SEEP/W modeling, the SBL can reduce the unsaturated inflow by 99.9%. The in-percolation estimated using the HELP studies is approximately an order of magnitude higher, thereby simulating a conservatively larger volume of water to percolate through the SBL.

Table A-3. Lower cover section vertical drainage.

Input Weather	3% Slope		7% Slope	
	SBL Percolation (mm/yr)	Percent Reduction	SBL Percolation (mm/yr)	Percent Reduction
Base case weather	0.0002	99.9%	0.0003	99.9%
Extreme case weather	0.0003	99.9%	0.0003	99.9%

A-5. SENSITIVITY ANALYSIS

Sensitivity analyses were conducted to determine effects of changes in thickness of the silt loam layer, increased precipitation, and changing climatic conditions on the cover's performance. This subsection specifically addresses sensitivity of the cover to the variations mentioned above. Observation Point D was used as the point of interest for evaluating infiltration. A summary of the sensitivity analyses is provided below.

A-5.1 Water Storage Layer

Changes in thickness of the silt loam layer of the water storage section were evaluated using the base and extreme climate scenarios. The modeling methodology was the same as was used to determine the infiltration at Point D in previous models. The silt loam water storage layer thickness was varied from 0.25 to 3.5 m.

At a thickness of 0.25 m, average annual infiltration was reduced to approximately 18 mm/yr. Increasing the cover thickness to 0.5 m reduced the average annual infiltration to approximately 10 mm/yr. A cover thickness of 1.5 m reduced infiltration to less than 2 mm/yr. Average annual infiltration was less than 1 mm/yr for cover thickness of 2 m and greater.

The sensitivity analysis shows clearly that increasing the water storage thickness beyond the optimal thickness does not provide added water storage. Based on the analysis, the optimal water storage layer thickness is between 1.5 and 2 m. Insignificant changes in infiltration occur for the water storage layer thickness beyond 2 m. A minimum water storage layer thickness of 2 m is recommended for the ICDF landfill cover. Additional material may be required to address erosion control and aeolian effects. A thicker water storage layer may be needed so that the minimum thickness is maintained after long-term erosion. This information was summarized in Section A-2.2 above.

A-5.2 Increased Precipitation

The effect of increased precipitation on infiltration through the water storage layer of the cover was analyzed using an average year of weather and multiples of the average year's precipitation. The weather data for the year were repeated until the soil profile reached a quasi-steady state. The year with total precipitation closest to average was 1975, which had 269 mm of precipitation including 51 mm of water-equivalent snowfall. The average precipitation for the period of record is 218 mm/yr including 37 mm of water-equivalent snowfall.

The one-dimensional computer was run using one, two, three, and four times the 1975 precipitation. Twenty years were modeled for each precipitation interval using two 10-year simulations. Based on the analysis, the upper cover may become ineffective when exposed to an average annual precipitation of greater than 810 mm/yr. This also assumes all other climate parameters remain constant. The resulting infiltration at the Point D layer is 0.17 mm/yr at three times the average annual precipitation, which is less than the 0.46 mm/yr infiltration based on the extreme climatological scenario. The four times precipitation resulted in significant breakthrough from the water storage cover.

A-5.3 Climate Change

The effect of decreased evaporation on infiltration through the water storage layer of the cover was analyzed using the Penman equation. The Penman equation determines potential evaporation from the soil surface based on temperature, net radiant energy, wind speed, and relative humidity. Changes in these

climate conditions at the ICDF in the long term could potentially reduce evaporation from the surface of the cover increasing infiltration.

Based on the analysis, long-term climate changes could reduce evaporation from the cover between 14 to 28% of the potential evaporation determined from the hydrologic model. The resulting infiltration at the Point D layer would then increase between 14 and 28% from what was predicted by the hydrological model, conservatively assuming that a change in potential evaporation is directly proportional to the change in infiltration. For the base case climate scenario used in the hydrologic model, the infiltration could increase between 0.45 to 0.51 mm/yr. For the extreme case climate scenario, the infiltration could increase between 0.52 to 0.60 mm/yr.

A-6. DESIGN INFILTRATION RATE

Eight different steady-state models were run for this exercise using the SEEP/W. Four models were run with a cover slope of 3%, which is a worst-case cover slope scenario and 7%, which is the design cover slope. All the models utilized the same geometry and materials types with a range of inflow fluxes in the lateral drainage layer. The 3% cover (worst-case) model output indicates that a steady influx into the lateral drainage layer of approximately 0.85 mm/yr or greater is required to obtain a percolation rate of more than 0.1 mm/yr from the bottom of the SBL. The value of 0.1 mm/yr is used as input into the fate and transport model.

Based on the results from the simulations for the ICDF landfill cover, results from experimental studies at the INEEL, and experimental and modeling results from other sites in the western U.S., it is believed that the cover design proposed for the ICDF landfill represents a state-of-the-practice design for a landfill cover that minimizes infiltration into the waste. Any leakage that occurs through the cover due to defects or extreme changes in climate is likely to be intercepted by the lateral drainage layers at the base of the cover. A conservative estimate of 0.1 mm/yr of percolation from the base of the cover was determined based on the estimated break through from the upper section of the cover. Based on the results reported in this EDF, it is believed that the cover design, which incorporates a store and release soil cover underlain by a capillary break and composite liner system, represents the best technology for minimizing infiltration into the landfill given site-specific climatic conditions.

A-7. REASONABLY CONSERVATIVE ESTIMATE OF INFILTRATION

The above results indicate 0.1 mm/yr of infiltration through the lower section of the soil cover into the waste. This is considered reasonably conservative for the reasons listed below:

- All snow was assumed to melt in a 22-day period each year, stressing the cover's water storage capacity.
- A poor stand of grass was assumed to simulate drought or post-fire conditions.
- The daily precipitation was distributed over 12 hours increasing infiltration into the cover.
- The years selected for the weather data included large precipitation events early on in the simulation to stress the recovery capacity of the cover.
- An extreme case was modeled that assumed four years of back-to-back precipitation events that were above the 90th percentile based on the period of record.
- Bio-intrusion does not account for increased evaporation from lower depths of the soil resulting from increased air circulation or for evaporation and dispersion resulting from precipitation moving through the soil.
- The 20% of the break through that percolates from the base of the SBL is an order of magnitude higher than two-dimensional modeling results using SEEP/W.
- The two-dimensional modeling was based on a steady-state inflow versus less conservative transient conditions.

The sensitivity results show that the cover will perform as modeled for precipitation up to three times the annual average. Increasing the water storage layer thickness greater than 2 m results in minimal improvement in hydraulic performance. Extreme changes in temperature, net solar radiation, wind speed, and humidity could increase influx into the lateral drainage layer, resulting in a percolation from the base of the SBL of less than 0.1 mm/yr.

Water movement was calculated from the cover layer represented by the observation points shown in Figure A-7. The average annual percolation from the base of the cover is provided in Table A-4.

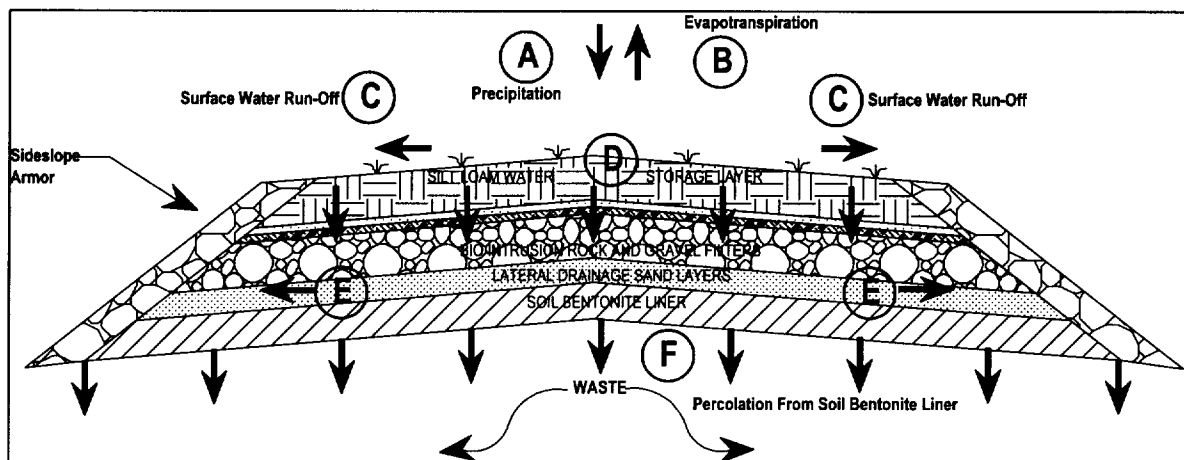


Figure A-7. Hydrologic model geometry and location of observation points.

The values listed in Table A-4 represent average annual flow from the main components of the cover system. The flux or break through from the water storage layer represented by Point D is assumed to be the same at the crest and downslope areas. The difference between the flux at the crest and downslope portion of the cover is expected to be small, since surface run-off is small and the lateral movement of water within the water storage layer will be minimal, due to its low saturated permeability and gradual slope. Using the conservative estimate of infiltration, the safety factors for the base and extreme cases are 3.0 and 2.6, respectively. With this infiltration due primarily from a depression in the SBL, these safety factors reflect a conservative viewpoint of cap degradation and performance.

Table A-4. Summary of water movement from base of cover.

Point	Description	Base Case		Extreme Case	
		Value	Direction	Value	Direction
D	Influx into lateral drainage layer (mm/yr)	0.42	Downward	0.49	Downward
E	Lateral drainage (mm/yr)	0.41	Lateral	0.40	Lateral
F	Percolation due to depression in SBL (mm/yr)	0.03	Downward	0.03	Downward
F	Percolation due to upper cover section influx (mm/yr)	0.003	Downward	0.009	Downward
Total Percolation from base of cover (mm/yr)		0.033	Downward	0.039	Downward

A-8. REFERENCES

- 40 CFR 264.301, 2002, "Design and operating requirements," *Code of Federal Regulations*, Office of the Federal Register, July 2002.
- 40 CFR 264.302, 2002, "Action leakage rate," *Code of Federal Regulations*, Office of the Federal Register, July 2002.
- 40 CFR 264.309, 2002, "Surveying and recordkeeping," *Code of Federal Regulations*, Office of the Federal Register, July 2002.
- 40 CFR 264.310, 2002, "Closure and post-closure care," *Code of Federal Regulations*, Office of the Federal Register, July 2002.
- 40 CFR 761.75, 2002, "Chemical waste landfills," *Code of Federal Regulations*, Office of the Federal Register, February 2002.
- 42 USC 9601, 1980, "Comprehensive Environmental Response, Compensation, and Liability Act of 1980," as amended. (Note: The 1986 amendment is cited as "Superfund Amendments and Reauthorization Act of 1986," [SARA].)
- 42 USC 9620, 1986, "Federal Facilities," as amended.
- ASTM C535, 2001, "Standard Test Method for Resistance to Degradation of Large-Size Coarse Aggregate by Abrasion and Impact in the Los Angeles Machine," American Society for Testing and Materials, June 10, 2001.
- Audubon Society, 1992, *The Audubon Society Field Guide to North American Mammals*, Alfred A. Knopf, New York, New York, 1992.
- Benson, C. H., and M. A. Othman, 1993, "Hydraulic Conductivity of Compacted Clay Frozen and Thawed In Situ," *Journal of Geotechnical Engineering*, Vol. 119, No. 2, p. 276.
- Berenbrock, C., and L. C. Kjelstrom, 1998, *Preliminary Water-Surface Elevations and Boundary of the 100-Year Peak Flow in the Big Lost River at the Idaho National Engineering and Environmental Laboratory, Idaho*, U.S. Geological Survey Water Resources Investigations Report 98-4065, DOE/ID-22148, 1998.
- BOR, 1999, *Phase 2 Paleohydrologic and Geomorphic Studies for the Assessment of Flood Risk for the Idaho National Engineering and Environmental Laboratory, Idaho*, US Department of the Interior, Bureau of Reclamation, Technical Service Center, Geophysics, Paleohydrology, and Seismotectonics Group, Denver, CO.
- CH2M HILL, 2002, *Hanford Biological Intrusion Questions for Cap/Barrier Alternative Formulation and Analysis*, Unpublished study provided by CH2M HILL, Hanford.
- DOE-ID, 1989, *Guidelines for Revegetation of Disturbed Sites at the INEL*, DOE/ID-12114, U.S. Department of Energy Idaho Operations Office, 1989.

- DOE-ID, 1999, *Final Record of Decision, Idaho Nuclear Technology and Engineering Center, Operable Unit 3-13*, DOE/ID-10660, Rev. 0, U.S. Department of Energy Idaho Operations Office, U.S. Environmental Protection Agency Region 10, and State of Idaho Department of Health and Welfare, October 1999.
- DOE-ID, 2002, *INEEL CERCLA Disposal Facility Remedial Design/Construction Work Plan*, DOE/ID-10848, Rev. 1, U.S. Department of Energy Idaho Operations Office, May 2002.
- EDF-ER-267, 2002, "Landfill Compaction Subsidence Study," Rev. 1, Environmental Restoration Program, Idaho National Engineering and Environmental Laboratory, May 2002.
- EDF-ER-279, 2002, "Hydrologic Modeling of Final Cover," Rev. 2, Environmental Restoration Program, Idaho National Engineering and Environmental Laboratory, May 2002.
- EDF-ER-281, 2002, "Liner and Final Cover Long-Term Performance Evaluation and Final Cover Life Cycle Expectation," Rev. 1, Environmental Restoration Program, Idaho National Engineering and Environmental Laboratory, May 2002.
- EPA, 1989, "Technical Guidance Document: Final Covers on Hazardous Waste Landfills and Surface Impoundments," U.S. Environmental Protection Agency, Office of Solid Waste Management, Washington, DC, 1989.
- Hedlund, J.D. and L.E. Rogers, 1976, *Characterization of Small Mammal Populations Inhabiting the B-C Cribs Environs*, Battelle Pacific Northwest Laboratory, Richland, Washington, BNWL-2181, December 1976.
- IDAPA 58.01.05.008, 2002, "Standards of Owners and Operators of Hazards Waste Treatment, Storage, and Disposal Facilities," Idaho Administrative Procedures Act, Idaho Department of Environmental Quality, March 2002.
- Laundre, J. W., 1996, *Mitigating Long Term Impacts of Small Mammal Burrowing on the Closure of Hazardous Waste Areas*, Idaho State University, Pocatello, Idaho.
- Ligotke, M. W., 1993, "Soil Erosion Rates Caused By Wind and Saltating Sand Stresses In a Wind Tunnel," Pacific Northwest Laboratory, Richland, Washington, 1993.
- Maidment, 1993, *Handbook of Hydrology*, McGraw-Hill, Inc., San Francisco, California.
- Martian, P., 1995, *UNSATH Infiltration Model Calibration at the Subsurface Disposal Area*, INEL-95/0596, Idaho National Engineering Laboratory, Idaho Falls, Idaho.
- Morris, R. C., and R. D. Bleu, 1997, "Annual Technical Report Calendar 1996", Environmental Science and Research Foundation Report Series, Number 17, Idaho National Engineering Laboratory.
- NOAA, 2001, *Air Resources Library Field Research Division Web Site*, www.noaa.inel.gov/frd/weather, National Oceanic and Atmospheric Administration, Washington, DC, 2001.
- NRC, 1986, "Methodologies For Evaluating Long-Term Stabilization Designs of Uranium Mill Tailings Impoundments," NUREG/CR-4620, U.S. Nuclear Regulatory Commission, Washington, DC, 1986.

- Smallwood, K.S., 1996, *Second Assessment of the BIOPORT Model's Parameter Values for Pocket Gopher Burrowing Characteristics and other Relevant Wildlife Observations*, Letter Report, Davis, California, August 1996.
- Wing, N. R., 1993, "Permanent Isolation Surface Barrier: Functional Performance", Westinghouse Hanford Company, Richland, WA, 1993.

Appendix B

Monte Carlo Simulation of the ICDF Cover System for Infiltration and Longevity

Appendix B

Monte Carlo Simulation of the ICDF Cover System for Infiltration and Longevity

B-1. INTRODUCTION

One of the issues that was identified during the review of the performance assessment (PA) and composite analysis (CA) reports for the Idaho National Engineering and Environmental Laboratory (INEEL) Comprehensive Environmental Restoration, Compensation and Liability Act (CERCLA) Disposal Facility (ICDF), was the lifetime that the cover system would last. The reviewers were concerned that the design life of the cover system (1,000 years) greatly exceeded the duration of the institutional controls. A second issue identified was the infiltration rate though the cover system apparently was not conservative in the value used.

During the development of the design for the ICDF landfill (DOE-ID 2002), both the U.S Environmental Protection Agency (EPA) and Idaho Department of Environment Quality (IDEQ) questioned the infiltration rate and project lifetime that the cover system would perform as designed. Two engineering design files (EDF-ER-279 and EDF-ER-281) prepared as part of the design deal specifically with the infiltration rate and lifetime of the cover system. In these two engineering design files (EDF-ER-279 and EDF-ER-281), the resulting infiltration rate was calculated, including the effects of climatological changes, along with the effects for degradation of cover system, including biointrusional and erosional effects.

As a result of the review of the ICDF PA and CA reports, it was recommended that a Monte Carlo analysis be conducted to assess the effects of the various parameters for the cover system. To conduct the Monte Carlo analysis it is necessary to establish factors that are changed as a result of the changes in the parameters. For the Monte Carlo analysis, it is important to understand the range of parameters to be considered. Also, it is necessary to understand how the distribution of the observed INEEL data (climatological and other data) vary by parameter.

For the design documentation, a sensitivity analysis was conducted on various parameters in the engineering design files. Most of these sensitivity analysis results used the data from 1975 as the base case and then varied the parameters around the 1975 data. To conduct the Monte Carlo analysis, it is necessary to establish relationships between the 1975 results and the range of the parameters being evaluated. Several sections below evaluate the 1975 data against the entire data set (1955 to 1999) and develop relationships (normalized equations). Other parameters that are being evaluated in this Monte Carlo analysis do not have relationships with the 1975 data, but there are equations that are used to determine the effect from these parameters.

No attempt has been made to deal with several potential impacts to the infiltration rate for the ICDF landfill cover system. These potential impacts include subsidence of the clay layer and erosion from the wind. However, the equations, relationships, and climatological data are presented below along with the results of the Monte Carlo analysis. The Monte Carlo analysis presented below deals with the major impacts on both the infiltration rate into the waste zone and the lifetime of the cover system.

B-2. INEEL CLIMATOLOGICAL INFORMATION

There are five climatological factors that need to be considered in the Monte Carlo analysis of the infiltration rate through the cover system. These factors directly influence the infiltration rate through the storage layer (upper part of the ICDF landfill cover system). Precipitation, temperature, net radiant energy, wind speed, and relative humidity are the climatological parameter being evaluated for the Monte Carlo analysis. Each of these climatological parameters is discussed below.

B-2.1 INEEL Precipitation

To determine that range of possible annual precipitation amounts it is necessary to start with the existing information and then extrapolate to the other values. The extrapolation can be accomplished using a number of different methods. At the INEEL, there is 45 years of climatological (precipitation) data available (1955 to 1999). These yearly precipitation values were presented in Figure 3-1 of EDF-ER-279. Using the EDF-ER-279 information, the distribution of the yearly precipitation can be evaluated. The precipitation data was split into a series of bins with a width of 10 mm/yr. A histogram for the annual INEEL precipitation data was developed by using the number of times that an annual precipitation amount occurred in the precipitation bins. Figure B-1 shows the frequency distribution (histogram) of the annual INEEL precipitation.

From the information used to develop Figure B-1, the statistics for the annual INEEL precipitation are as follows: minimum=116 mm/yr; maximum=366 mm/yr; average=230 mm/yr; and standard deviation=58 mm/yr. Also in looking at Figure B-1, the distribution of the annual precipitation has a nearly "normal" distribution. It is recognized that there are several bins that have a lower count that would be expected from a normal distribution. With additional years of annual precipitation data, it is expected that the distribution would assume a more complete "normal" distribution.

Prediction of the range of potential precipitation events likely to occur over time can be developed using the known precipitation data. There are a number of methods that can be used to develop these range estimates. As shown in Figure B-1, the distribution of precipitation amounts can be considered to be a normal distribution. The equation presented below is taken from a book on hydrology (Gupta 1989). While this equation is generally used to determine the volume of flood flow, the equation can also be used to estimate the range of precipitation events with respect to a particular return period. Using the average and standard deviation values presented above, the equation presented below, and the information presented in Table 8.6 from Gupta (1989), the range of potential annual precipitation can be calculated. Table B-1 presents the results of these calculations. While the equation does not directly calculate the dry side of the distribution, this is accomplished by subtracting the KS term from the average value instead of adding to the average value.

$$X = \bar{X} + K * S$$

X = annual precipitation for a given return period (mm/yr)

\bar{X} = average precipitation of the INEEL historical data (mm/yr)

K = frequency factor

S = standard deviation of the INEEL historical data (mm/yr).

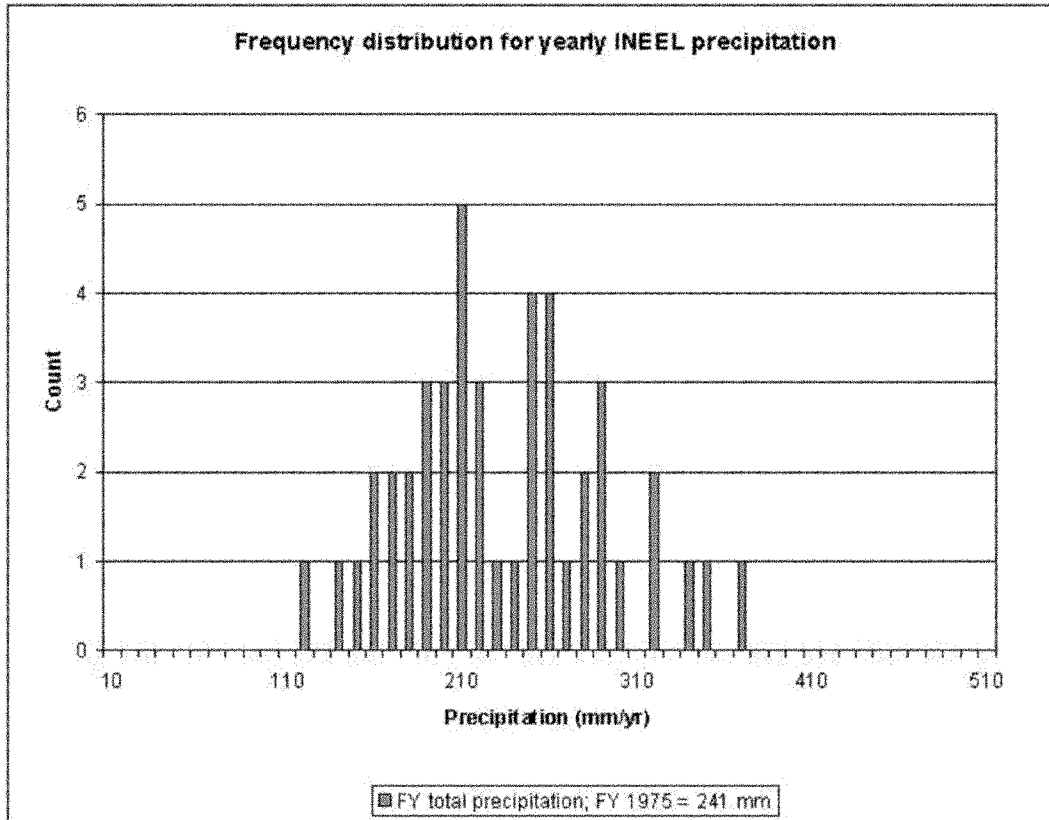


Figure B-1. Frequency distribution of the annual INEEL precipitation from the year 1955 through 1999 organized into frequency bins of 10 mm/yr.

Table B-1. Potential annual INEEL precipitation amounts calculated for different return periods with both the wet and dry sides of the distribution presented.

Exceedence Probability	Return Period	K	X (upper side) (mm/yr)	X (lower side) (mm/yr)
0.0001	10,000	3.719	445	14
0.0005	2,000	3.291	421	39
0.001	1,000	3.090	409	50
0.005	200	2.576	379	80
0.01	100	2.326	365	95
0.05	20	1.645	325	134
0.1	10	1.282	304	155
0.5	2	0.000	230	230

A range of precipitation events was hydrologically modeled in EDF-ER-279 for the ICDF cover system. This range included two, three, and four times the average precipitation amount. From Table B-1, it can be seen that two times the annual INEEL precipitation amount (460 mm/yr) exceeds the expected precipitation from a 10,000-year event.

In EDF-ER-279, the sensitivity of the storage layer to annual precipitation was evaluated. It is important to note that the 1975 precipitation amount was 241 mm/yr, which is greater than the average of 230 mm/yr. The sensitivity analysis was based on using the 1975 data and scaled up and down in relation to the base 1975 data. Using the information presented in EDF-ER-279, Table E-1, the resulting infiltration through the storage layer from increasing or decreasing the annual precipitation can be evaluated. The resulting equation for infiltration through the storage layer as a result of precipitation up to two times that average annual value is shown below. From this equation it can be seen that at precipitation of less than 78 mm/yr, the infiltration through the storage layer is zero.

$$y = 0.000965 * x - 0.0750$$

y = infiltration rate through storage layer (mm/yr)

x = annual precipitation rate (mm/yr).

B-2.2 INEEL Temperature

In EDF-ER-279, the sensitivity of the storage layer to temperature was evaluated. It is important to note that the 1975 average daily temperature was 6.5°C, which is greater than the average daily temperature of 5.2°C. The sensitivity analysis was based on using the 1975 data and scaled up and down in relation to the base 1975 data.

As the sensitivity analysis for temperature effects was based on 1975 data, it is important to determine how the 1975 daily temperature data compares to the rest of the daily temperature data. The daily temperatures for both the entire data set (1955 to 1999) and the 1975 data were plotted. Figure B-2 presents a graphic of the temperatures against the number of times that temperature occurred for both the entire data set and the 1975 data. From Figure B-2, the 1975 data are similar to the entire data set. There are temperatures in the 1975 data set that do not completely mimic the entire data set, but the 1975 data set is a reasonable approximation of the entire data set. This allows for predictions of predictions based on the 1975 data to be reasonable when applied to the entire data set and future projections.

Using the information presented in EDF-ER-279, Section E.3 and Figure E-3, the resulting infiltration through the storage layer from increasing or decreasing the average annual temperature can be evaluated. From the information in EDF-ER-279, Section E.3, the potential evaporation (PE) is about 3.95 times greater than the actual evaporation (AE) when all of the soil cover sensitivity analysis is considered. This value includes the consideration of both the changes in the thickness of the storage layer and changes in the annual precipitation. With Figure E-3, the potential evaporation versus temperature was plotted. As the information in Figure E-3 is potential evaporation, it is necessary to change this into a usable value and against a normalized temperature. By normalizing the temperatures in Figure E-3 to the 1975 data and dividing the PE by the ratio of PE to AE discussed above. With linear regression, the resulting equation for change in infiltration through the storage layer as a result of temperature changes can be developed. The resulting equation is shown below. From this equation it can be seen that large temperature changes are needed to significantly change the resulting infiltration.

$$y = 0.032 * x + 0.951$$

y = normalized change infiltration rate at normalized analysis temperature

$$x = \text{normalized temperature} \left(\frac{\text{analysis temperature}}{1975 \text{ average annual temperature}} \right)$$

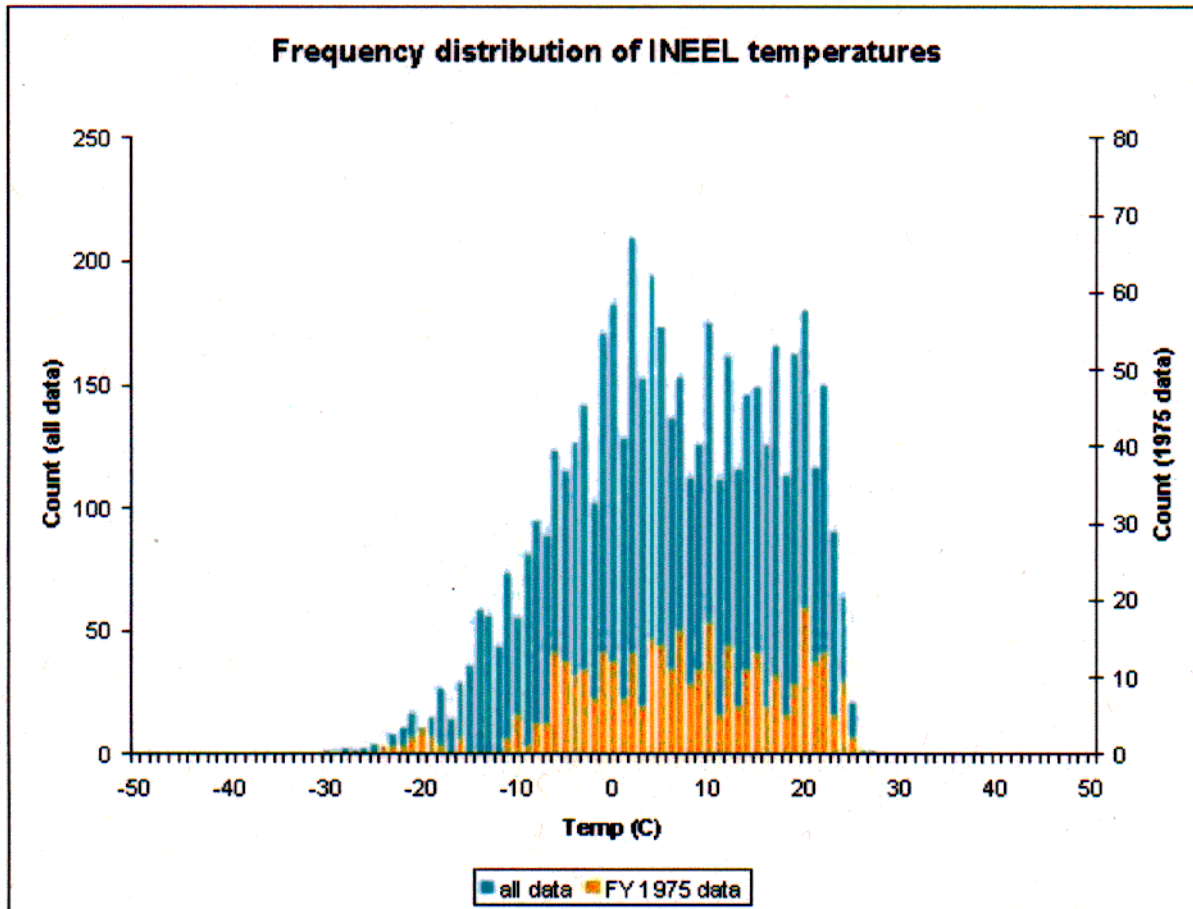


Figure B-2. Frequency distribution of the average daily temperatures at the INEEL for both the entire data set (1955 to 1999) and the 1975 data set.

B-2.3 INEEL Net Radiant Energy

In EDF-ER-279, the sensitivity of the storage layer to net radiant energy was evaluated. It is important to note that the 1975 average net radiant energy was 8.1 MJ/m²-day (3.26 mm/day), which is very similar to the average net radiant energy of 8.2 MJ/m²-day (3.30 mm/day). The sensitivity analysis was based on using the 1975 data and scaled up and down in relation to the base 1975 data.

As the sensitivity analysis for net radiant energy effects was based on 1975 data, it is important to determine how the 1975 net radiant energy data compares to the rest of the net radiant energy data. The net radiant energy for both the entire data set (1955 to 1999) and the 1975 data were plotted. Figure B-3 presents a graphic of the net radiant energy against the number of times that net radiant energy occurred for both the entire data set and the 1975 data. From Figure B-3, the 1975 data are similar to the entire data set. There are net radiant energies in the 1975 data set that do not completely mimic the entire data set, but the 1975 data set is a reasonable approximation of the entire data set. This allows for predictions of predictions based on the 1975 data to be reasonable when applied to the entire data set and future projections.

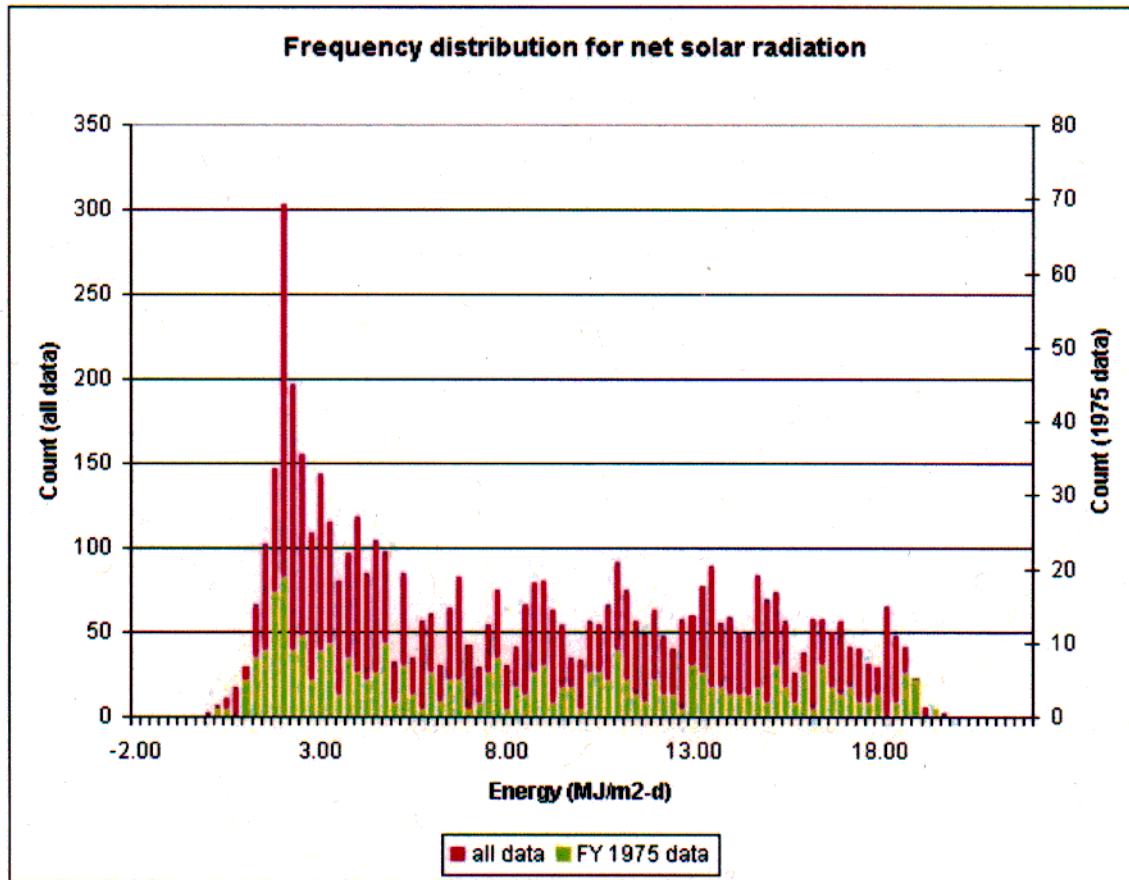


Figure B-3. Frequency distribution of the daily net radiant energy at the INEEL for both the entire data set (1955 to 1999) and the 1975 data set.

Using the information presented in EDF-ER-279, Section E.3 and Figure E-4, the resulting infiltration through the storage layer from increasing or decreasing the average net radiant energy can be evaluated. From the information in EDF-ER-279, Section E.3, the PE is about 3.95 times greater than the AE when all of the soil cover sensitivity analysis is considered. This value includes the consideration of both the changes in the thickness of the storage layer and changes in the annual precipitation. With Figure E-4, the potential evaporation versus net radiant energy was plotted. As the information in Figure E-4 is potential evaporation, it is necessary to change this into a usable value and against a normalized net radiant energy. By normalizing the net radiant energies in Figure E-4 to the 1975 data and dividing the PE by the ratio of PE to AE discussed above. With linear regression, the resulting equation for change in infiltration through the storage layer as a result of net radiant energy changes can be developed. The resulting equation is shown below. From this equation it can be seen that moderate net radiant energy changes are needed to significantly change the resulting infiltration.

$$y = 0.380 * x + 0.529$$

y = normalized change in infiltration at normalized net radiant energy

$$x = \text{normalized net radiant energy} \left(\frac{\text{analysis net radiant energy}}{\text{1975 average net radiant energy}} \right)$$

B-2.4 INEEL Wind Speed

In EDF-ER-279, the sensitivity of the storage layer to wind speed was evaluated. It is important to note that the 1975 average wind speed was 16.6 km/hr, which is similar (but higher) to the average wind speed of 13.7 km/hr. The sensitivity analysis was based on using the 1975 data and scaled up and down in relation to the base 1975 data.

As the sensitivity analysis for wind speed effects was based on 1975 data, it is important to determine how the 1975 wind speed data compares to the rest of the wind speed data. The wind speed for both the entire data set (1955 to 1999) and the 1975 data were plotted. Figure B-4 presents a graphic of the wind speed against the number of times that wind speed occurred for both the entire data set and the 1975 data. From Figure B-4, the 1975 data are similar to the entire data set. There are wind speeds in the 1975 data set that do not completely mimic the entire data set, but the 1975 data set is a reasonable approximation of the entire data set. This allows for predictions of predictions based on the 1975 data to be reasonable when applied to the entire data set and future projections.

Using the information presented in EDF-ER-279, Section E.3 and Figure E-5, the resulting infiltration through the storage layer from increasing or decreasing the average wind speed can be evaluated. From the information in EDF-ER-279, Section E.3, the PE is about 3.95 times greater than the AE when all of the soil cover sensitivity analyses are considered. This value includes the consideration of both the changes in the thickness of the storage layer and changes in the annual precipitation. With

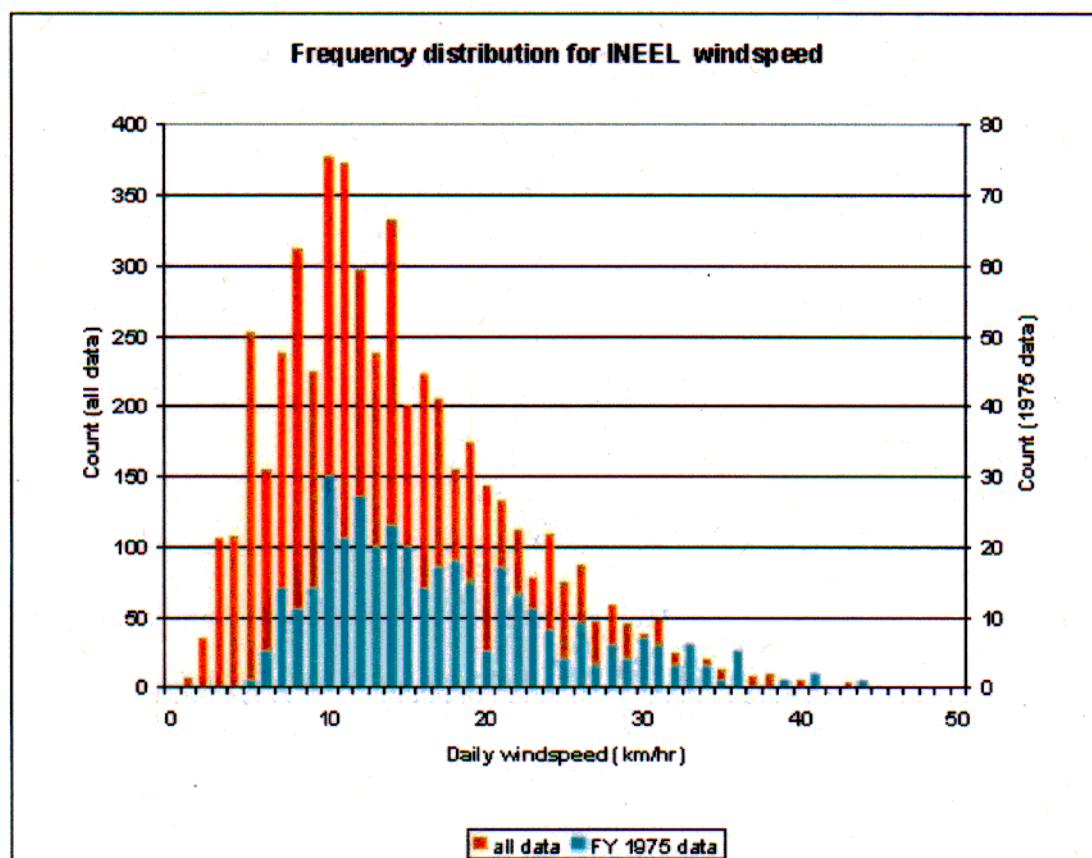


Figure B-4. Frequency distribution of the daily wind speeds at the INEEL for both the entire data set (1955 to 1999) and the 1975 data set.

Figure E-5, the potential evaporation versus wind speed was plotted. As the information in Figure E-5 is potential evaporation, it is necessary to change this into a usable value and against a normalized wind speed. By normalizing the wind speeds in Figure E-5 to the 1975 data and dividing the PE by the ratio of PE to AE discussed above. With linear regression, the resulting equation for change in infiltration through the storage layer as a result of wind speed changes can be developed. The resulting equation is shown below. From this equation it can be seen that moderate wind speed changes are needed to significantly change the resulting infiltration. Although the wind speed versus potential evaporation presented in Figure E-5 does not go up to the 1975 value of 16.6 km/hr, the effect of changing wind speed versus potential evaporation is a highly linear equation allowing for projections beyond the limits of the analysis.

$$y = 0.420 * x + 0.557$$

y = normalized change in infiltration rate at normalized wind speed

$$x = \text{normalized wind speed} \left(\frac{\text{wind speed at analysis}}{\text{1975 average wind speed}} \right).$$

B-2.5 INEEL Relative Humidity

In EDF-ER-279, the sensitivity of the storage layer to relative humidity was evaluated. It is important to note that the 1975 average relative humidity was 0.65, which is very similar to the average relative humidity of 0.59. The sensitivity analysis was based on using the 1975 data and scaled up and down in relation to the base 1975 data.

As the sensitivity analysis for relative humidity effects was based on 1975 data, it is important to determine how the 1975 relative humidity data compares to the rest of the relative humidity data. The relative humidity for both the entire data set (1955 to 1999) and the 1975 data were plotted. Figure B-5 presents a graphic of the relative humidity against the number of times that relative humidity occurred for both the entire data set and the 1975 data. From Figure B-5, the 1975 data are similar to the entire data set. There are relative humidity values in the 1975 data set that do not completely mimic the entire data set, but the 1975 data set is a reasonable approximation of the entire data set. Overall, the 1975 data have a higher relative humidity without the corresponding low humidity events in the entire data set. Also, it should be recognized that the data sets for relative humidity are actually the high and low values for the months within the data set with the other days within the month using the monthly values. This allows for predictions of predictions based on the 1975 data to be reasonable (within the range of values) when applied to the entire data set and future projections.

Using the information presented in EDF-ER-279, Section E.3 and Figure E-6, the resulting infiltration through the storage layer from increasing or decreasing the average net radiant energy can be evaluated. From the information in EDF-ER-279, Section E.3, the PE is about 3.95 times greater than the AE when all of the sensitivity analysis is considered. This value includes the consideration of both the changes in the thickness of the storage layer and changes in the annual precipitation. With Figure E-6, the potential evaporation versus relative humidity was plotted. As the information in Figure E-6 is potential evaporation, it is necessary to change this into a usable value and against a normalized relative humidity. By normalizing the relative humidity in Figure E-6 to the 1975 data and dividing the PE by the ratio of PE to AE discussed above, the change in the infiltration from relative humidity can be calculated. With linear regression, the resulting equation for change in infiltration through the storage layer as a result of relative humidity changes can be developed. The resulting equation is shown below. From this equation it can be seen that small relative humidity changes are needed to significantly change the resulting infiltration.

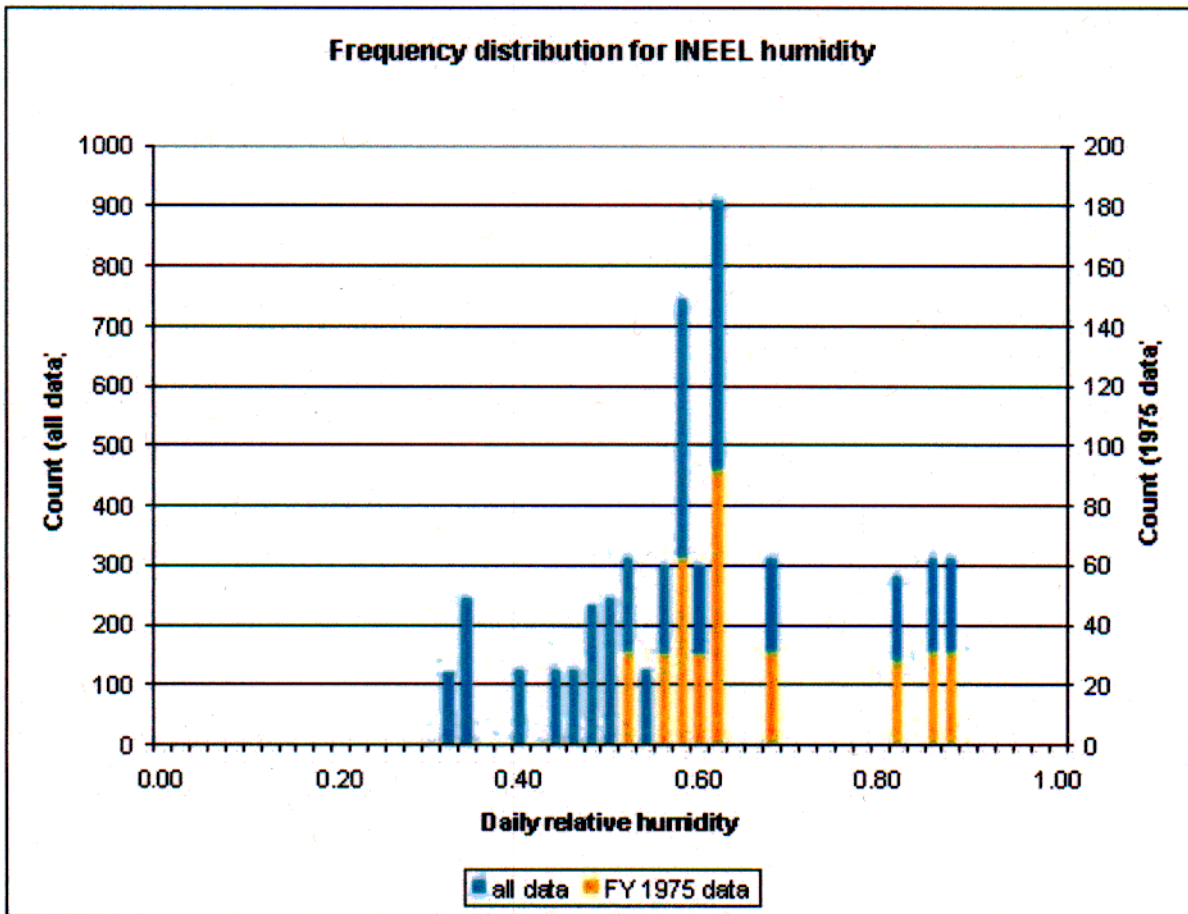


Figure B-5. Frequency distribution of the relative humidity at the INEEL for both the entire data set (1955 to 1999) and the 1975 data.

$$y = -4.77 * x + 1.61 * x^2 + 4.08$$

y = normalized changed in infiltration from relative humidity

$$x = \text{normalized relative humidity} \left(\frac{\text{relative humidity for analysis}}{\text{1975 average annual relative humidity}} \right)$$

x² = square of the normalized relative humidity.

B-3. SELECTION OF CLIMATOLOGICAL PARAMETER RANGES

To conduct the Monte Carlo analysis it is necessary to set range on the variable that will be used. With the existing INEEL information and the equations established presented above, the limits for the parameters can be set. To determine how the INEEL data are distributed in relation to linear equations, the cumulative count for the particular values was plotted against the parameter of concern. Each of the parameter ranges is discussed below.

B-3.1 Precipitation

To determine how the INEEL precipitation data relates to a linear curve, it is necessary to plot the precipitation against a cumulative count. Figure B-6 presents the precipitation versus the cumulative count. A linear curve is also presented in Figure B-6. This linear curve is a "best fit" to the existing data. From this figure it can be seen that there is a nearly linear area between precipitation values of 130 and 310 mm/yr. In Table B-1, the potential range of annual precipitation amounts was presented. While the 10,000-year return period values is outside of the linear range (should be based on the potential for occurrence), the Monte Carlo analysis will need to include this potential level of precipitation. For the range of annual precipitation to be considered, a range from approximately 50 mm/yr (1,000-year return period on the dry side) to 466 mm/yr (exceeding the 10,000-year return period on the wet side) will be used. To simplify the Monte Carlo analysis, uniformly distributed random numbers for precipitation will be used. The impact of this is that large precipitation events will have the same probability as the statistically average precipitation amount. This will bias the results to higher precipitation amounts than would normally be encountered over the lifetime of the cover system resulting in a conservative analysis for the precipitation amount considered.

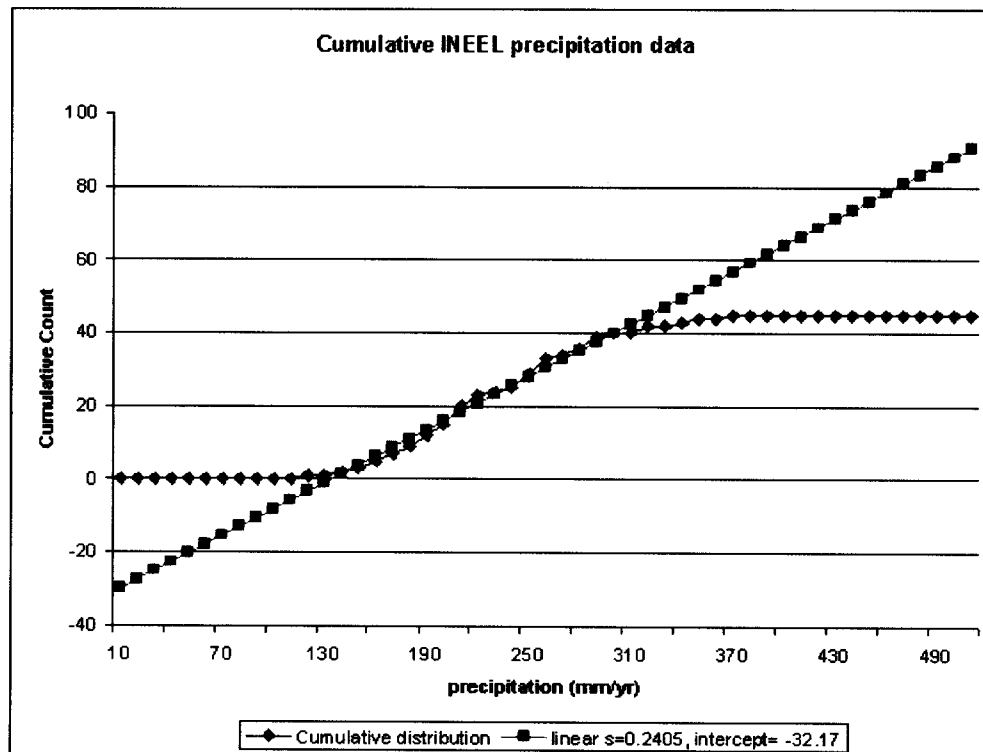


Figure B-6. INEEL precipitation range plotted against the cumulative count for the precipitation amounts.

B-3.2 Temperature

To determine how the INEEL temperature data relate to a linear curve, it is necessary to plot the temperature against a cumulative count. Figure B-7 presents the temperature versus the cumulative count. A linear curve is also presented in Figure B-7. This linear curve is a "best fit" to the existing data. From this figure it can be seen that there is a nearly linear area between temperature values of -6°C and 23°C. While the range of temperature values is linear over a wide range, the temperature include all of the temperature data. For the Monte Carlo analysis, a narrower range of temperature should be considered as the analysis is based on the average annual temperature. As stated above, the average annual INEEL temperature is 5.2°C. When EDF-ER-279 was developed, it was agreed to use a range of 1/3 the average annual temperature to determine the impact from reduced temperature. The Monte Carlo analysis will also need to evaluate a range of temperature, but needs to include also increased temperatures. Using the rational from EDF-ER-279, the range will be 1/3 to 1.5 times to the INEEL average temperature.

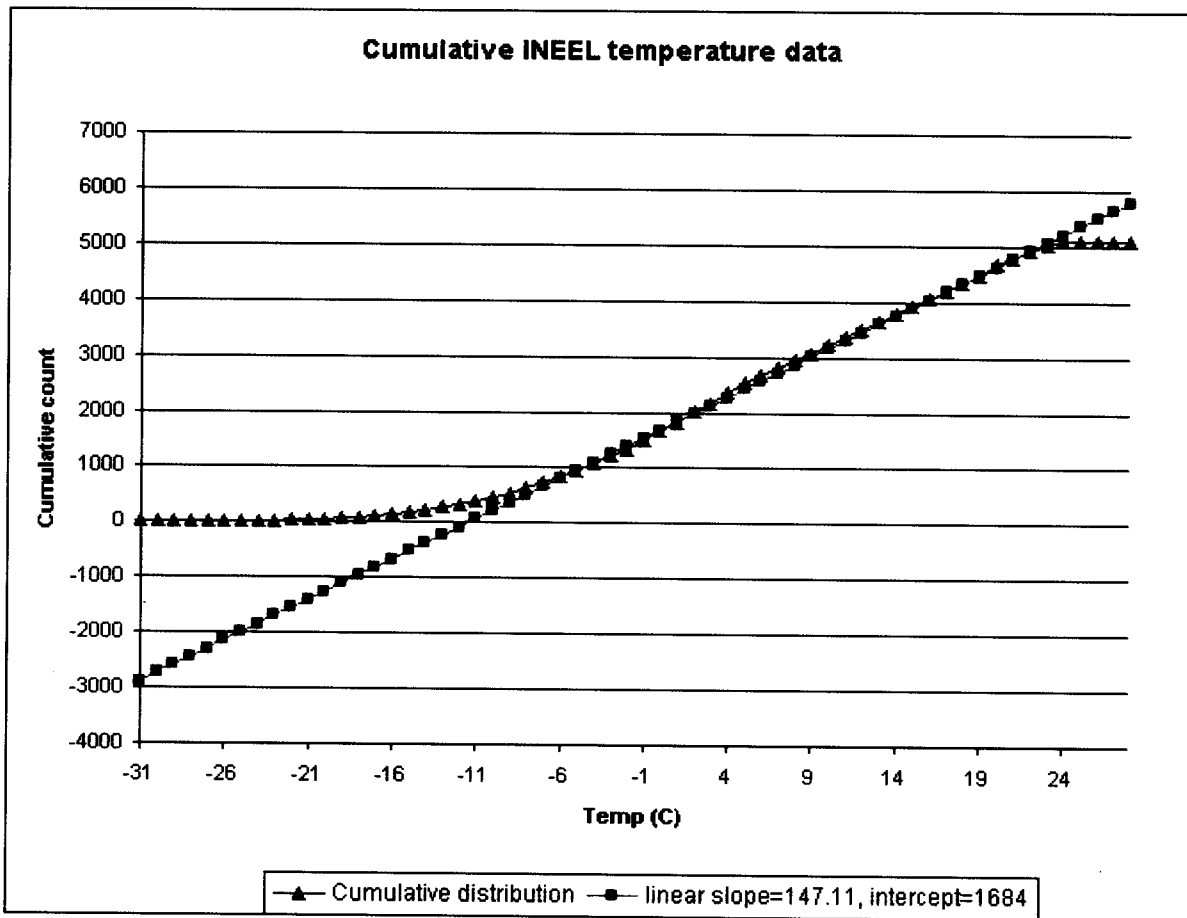


Figure B-7. INEEL temperature range plotted against the cumulative count for the temperature data.

Along with the linear curve presented in Figure B-6, an equation was developed and is presented below. While the equation of a line is generally developed in terms of solving for the “y value” based on a given “x value,” this is not an easy and simple solution. In this case, the desired value is the “x value” of precipitation with a given random number for the “y value.” As such the resulting linear curve equation was rearranged to present the equation in terms of a result based on the random number.

$$x = \left(\frac{y + 32.2}{0.241} \right)$$

x = resulting annual precipitation (mm/yr)

y = random number for precipitation with a range of -20 to +80.

For the range of annual temperature to be considered, a range from approximately 1.7°C (cold side) to 7.8°C (hot side) will be used. To simplify the Monte Carlo analysis, uniformly distributed random numbers for precipitation will be used. The impact of this is that low temperatures and high temperatures will have the same probability as the statistically average annual temperature.

Along with the linear curve presented in Figure B-7, an equation was developed and is presented below. While the equation of a line is generally developed in terms of solving for the “y value” based on a given “x value”, this is not an easy and simple solution. In this case, the desired value is the “x value” of temperature with a given random number for the “y value”. As such the resulting linear curve equation was rearranged to present the equation in terms of a result based on the random number.

$$x = \left(\frac{y - 1680}{147} \right)$$

x = resulting average annual temperature (C)

y = random number for the temperature with a range of 1,934 to 2,831.

B-3.3 Net Radiant Energy

To determine how the INEEL net radiant energy data relates to a linear curve, it is necessary to plot the net radiant energy against a cumulative count. Figure B-8 presents the net radiant energy versus the cumulative count. A linear curve is also presented in Figure B-8. This linear curve is a “best fit” to the existing data. From this figure it can be seen that there is a nearly linear area between net radiant energies of 19.0 MJ/m²-day (7.63 mm/day) and 3.50 MJ/m²-day (1.41 mm/day). While the range of net radiant energy values is linear over a wide range, the net radiant energies include all of the net radiant energy data. For the Monte Carlo analysis, a narrower range of net radiant energies should be considered as the analysis is based on the average annual net radiant energy. As stated above, the average annual INEEL net radiant energy is 8.19 MJ/m²-day (3.29 mm/day). When EDF-ER-279 was developed, it was agreed to use a range of 1/3 the average annual net radiant energy to determine the impact from reduced net radiant energy. The Monte Carlo analysis will also need to evaluate a range of net radiant energy, but needs to include also increased net radiant energies.

To simplify the Monte Carlo analysis, uniformly distributed random numbers for net radiant energy will be used. Using the rationale from EDF-ER-279, the bottom end range for the net radiant energy can be reduced to 1/3 (2.73 MJ/m²-day) of the INEEL average net radiant energy. However, it is not reasonable to consider the upper range to be 3 times (24.6 MJ/m²-day) the INEEL average net radiant energy. This value is outside of the net radiant energies measured at the INEEL and is likely outside of the potential

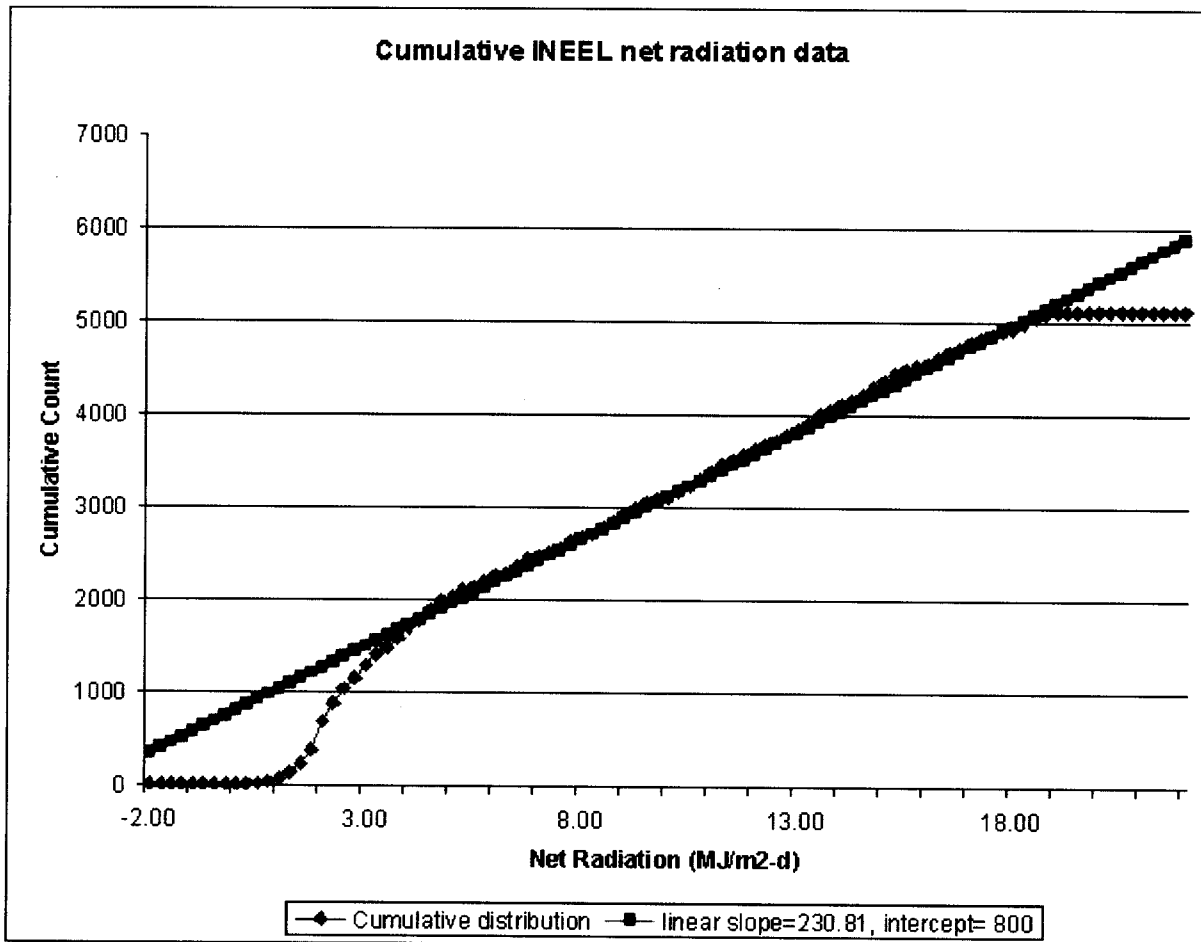


Figure B-8. INEEL net radiant energies range plotted against the cumulative count for the net radiant energies.

values for the INEEL based on location and other considerations for the ICDF landfill. One and one-half times the INEEL average net radiant energy ($12.3 \text{ MJ/m}^2\text{-day}$) is within the range of net radiant energies measured at the INEEL. Therefore, the range of average net radiant energies to be used for the Monte Carlo analysis will be from $2.73 \text{ MJ/m}^2\text{-day}$ (1.10 mm/day) to $12.3 \text{ MJ/m}^2\text{-day}$ (4.94 mm/day).

To simplify the Monte Carlo analysis, uniformly distributed random numbers for net radiant energy will be used. The impact of this is that small net radiant energy events will have the same probability as the statistically average net radiant energy amount. With the high side being a smaller change from the average than the low side, this will bias the results to lower net radiant energy amounts than would normally be encountered over the lifetime of the cover system resulting in a conservative analysis for the net radiant energy amount considered. Along with the linear curve presented in Figure B-8, an equation was developed and is presented below. While the equation of a line is generally developed in terms of solving for the “y value” based on a given “x value,” this is not an easy and simple solution. In this case, the desired value is the “x value” of temperature with a given random number for the “y value.” As such the resulting linear curve equation was rearranged to present the equation in terms of a result based on the random number.

$$x = \left(\frac{y - 800}{231} \right)$$

x = resulting average annual net radiant energy

y = random number for the net radiant energy with a range of 1,430 to 3,639.

B-3.4 Wind Speed

To determine how the INEEL wind speed data relate to a linear curve, it is necessary to plot the wind speed against a cumulative count. Figure B-9 presents the wind speed versus the cumulative count. A linear curve is also presented in Figure B-9. This linear curve is a "best fit" to the existing data. From this figure it can be seen that there is a nearly linear area between wind speeds of 3 km/hr and 20 km/hr. While the range of wind speeds is not completely linear over this range, the linear curve is a reasonable approximation of the wind speeds for all of the data set. For the Monte Carlo analysis, a range of wind speeds that represent the conditions that the ICDF landfill need to be considered. As stated above, the average annual INEEL wind speed is 13.7 km/hr. When EDF-ER-279 was developed, it was agreed to use a range of 1/3 the average annual wind speed to determine the impact from reduced wind speed. The Monte Carlo analysis will also need to evaluate a range of wind speeds, but needs to include also increased wind speeds.

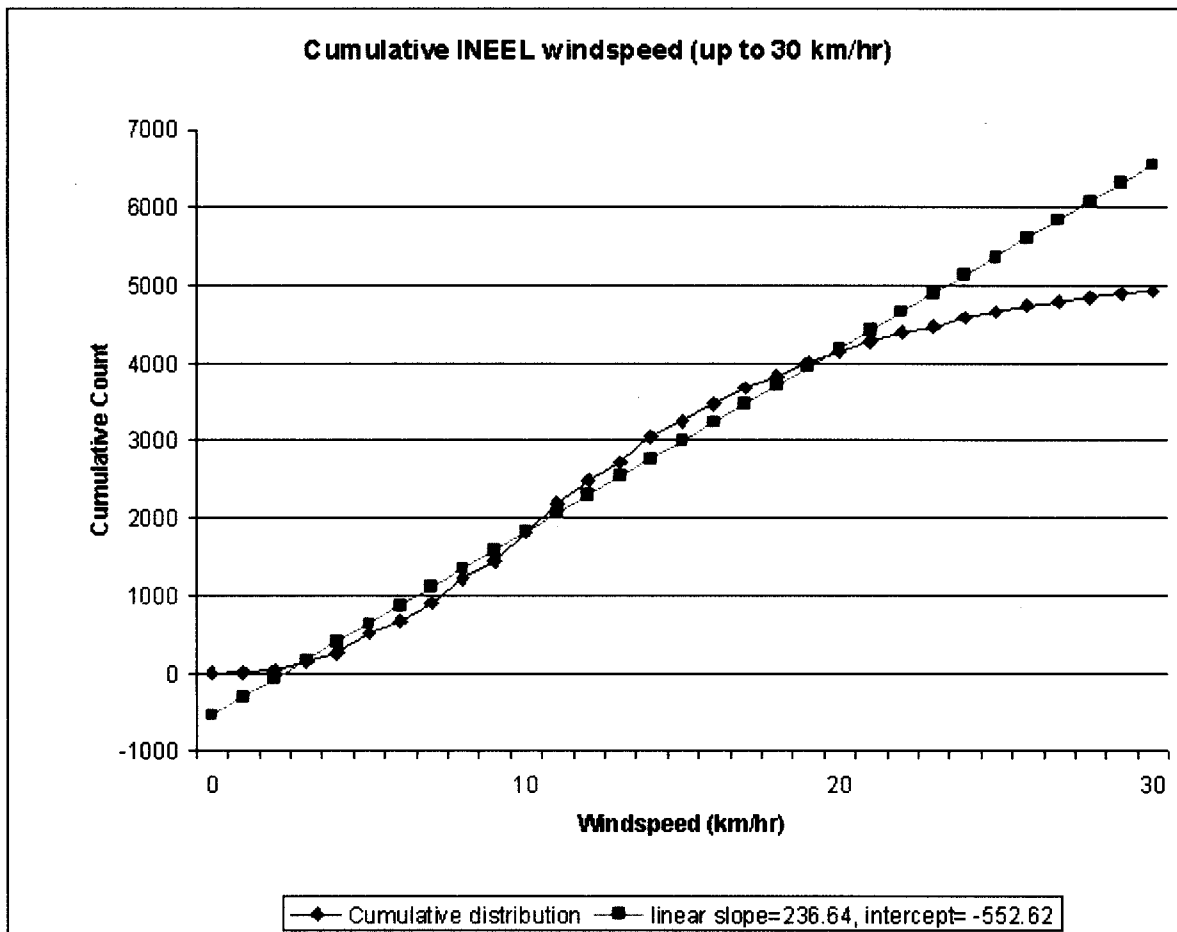


Figure B-9. INEEL wind speed range plotted against the cumulative count for daily wind speeds.

To simplify the Monte Carlo analysis, uniformly distributed random numbers for wind speed will be used. Using the rational from EDF-ER-279, the bottom end range for the wind speed can be reduced to 1/3 (4.57 km/hr) of the INEEL average wind speed. However, it is not reasonable to consider the upper range to be three times (41.1 km/hr) the INEEL average wind speed. These values are outside of most of the measured wind speeds at the INEEL and is likely outside of the potential values for the INEEL based on location and other considerations for the ICDF landfill. One point six times the INEEL average wind speed (21.9 km/hr) is within the range of wind speeds measured at the INEEL. Therefore, the range of average wind speeds to be used for the Monte Carlo analysis will be from 4.57 km/hr to 21.9 km/hr.

To simplify the Monte Carlo analysis, uniformly distributed random numbers for wind speed will be used. The impact of this is that low wind speeds will have the same probability as the statistically average INEEL wind speed. With the high side being a smaller change from the average than the low side, this will bias the results to lower net radiant energy amounts than would normally be encountered over the lifetime of the cover system resulting in a conservative analysis for the wind speeds considered.

Along with the linear curve presented in Figure B-9, an equation was developed and is presented below. While the equation of a line is generally developed in terms of solving for the “y value” based on a given “x value,” this is not an easy and simple solution. In this case, the desired value is the “x value” of temperature with a given random number for the “y value.” As such the resulting linear curve equation was rearranged to present the equation is terms of a result based on the random number.

$$x = \left(\frac{y + 553}{237} \right)$$

x = resulting average annual wind speed (km/hr)

y = random number for the wind speed with a range of 528 to 4,630.

B-3.5 Relative Humidity

To determine how the INEEL relative humidity data relate to a linear curve, it is necessary to plot the relative humidity against a cumulative count. Figure B-10 presents the relative humidity versus the cumulative count. A linear curve is also presented in Figure B-10. This linear curve is a “best fit” to the existing data. From this figure it can be seen that the relative humidity data do not fit a linear relationship against the cumulative count. However, the linear curve is the “bet fit” and more data points would likely make the distribution more linear. However, there is a somewhat linear area between relative humidity of 0.32 and 0.89. While the range of relative humidity is not completely linear over this range, the linear curve is a reasonable approximation of the relative humidity for all of the data set. For the Monte Carlo analysis, a range of relative humidity that represent the conditions that the ICDF landfill need to be considered. As stated above, the average annual INEEL relative humidity is 0.59. When EDF-ER-279 was developed, it was agreed to increase the relative humidity to determine the impact. It is physically not possible to increase the relative humidity to three times the INEEL values (1.77). Instead, the relative humidity was increased to 0.75 to simulate conditions similar to Seattle, WA. The Monte Carlo analysis will also need to evaluate a range of relative humidity, but needs to include also decreased relative humidity.

To simplify the Monte Carlo analysis, uniformly distributed random numbers for relative humidity will be used. Using the rational from EDF-ER-279, the upper end range for the relative humidity can be increased to 0.75. Also to evaluate the decreased relative humidity, the relative humidity cab be reduced

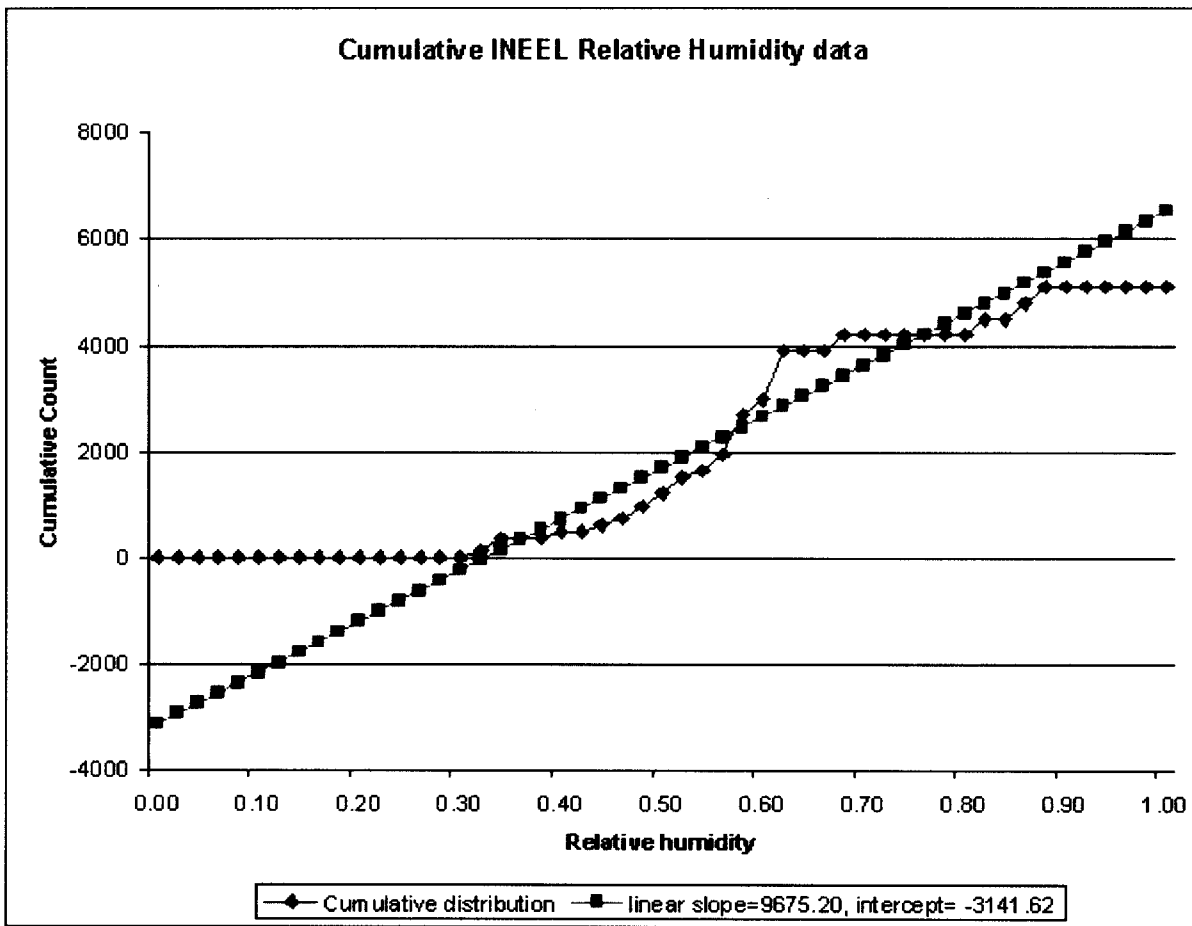


Figure B-10. INEEL relative humidity range plotted against the cumulative count for relative humidity.

to 0.43. Both of these values are with the measured values at the INEEL. Therefore, the range of average relative humidity to be used for the Monte Carlo analysis will be from 0.43 to 0.75.

To simplify the Monte Carlo analysis, uniformly distributed random numbers for relative humidity will be used. The impact of this is that high relative humidity will have the same probability as the statistically average INEEL relative humidity.

Along with the linear curve presented in Figure B-10, an equation was developed and is presented below. While the equation of a line is generally developed in terms of solving for the “y value” based on a given “x value,” this is not an easy and simple solution. In this case, the desired value is the “x value” of temperature with a given random number for the “y value.” As such the resulting linear curve equation was rearranged to present the equation in terms of a result based on the random number.

$$x = \left(\frac{y + 3140}{9680} \right)$$

x = resulting average relative humidity

y = random number for the relative humidity with a range of 1,018 to 4,115.

B-4. OTHER FACTORS INFLUENCING THE INFILTRATION RATES

There are four other factors that need to be considered in the Monte Carlo analysis of the infiltration rate through the cover system. These factors are not directly related to the climatological parameters, with the exception of the biointrusion. Of the four factors, three deal with changes to the affecting the infiltration through the storage layer. These three factors consist of the thickness of the storage layer, the erosion of the storage layer over time, and biointrusion from animals. The other factor is the amount of infiltration through the clay layer. Each of these factors is discussed below.

B-4.1 Thickness of the Storage Layer

To determine how the thickness of the storage layer controls the infiltration rate, a sensitivity analysis was conducted in EDF-ER-279. As can be seen from Figure E-1 in EDF-ER-279, there is a strong effect on the infiltration rate from the reduction in the thickness of the storage layer. The analysis of the other parameters used a thickness of 2 meters, which is one of the points shown on Figure E-1.

For the Monte Carlo analysis, the thickness of the storage layer will be varied to account for the erosional effects. Because the other sensitivity analysis for the other parameters used a thickness of 2 meters, it is necessary to normalize the thickness of the storage layer to a thickness of 2 meters. This will allow for the change in storage layer infiltration rate to be considered. Using Figure E-1, both the thickness and average annual infiltration rate were normalized against the 2-meter-thick results. Neither the points on Figure E-1 or the normalized values do not fit a linear relationship. To account for the normalized values, a 5th order polynomial was needed to accurately (within reason) fit the sensitivity analysis points. The equation for the normalized infiltration versus the normalized thickness is presented below:

$$y = -153.5 * x + 251.5 * x^2 - 208.8 * x^3 + 86.27 * x^4 - 14.09 * x^5 + 39.54$$

y = normalized change in the infiltration rate as a result of the storage layer thickness

x = normalized thickness of the storage layer

x² = square of the normalized thickness

x³ = cube of the normalized thickness

x⁴ = fourth power of the normalized thickness

x⁵ = fifth power of the normalized thickness.

B-4.2 Erosion of the Storage Layer

There are several parameters that affect how the cover system will be eroded during the lifetime of the cover system. These parameters include the soil properties (soil classification), location of the facility, and other factors. The U.S. Department of Agriculture (USDA) universal soil loss equation (EPA 1982) is used to calculate the rate of soil loss from an acre based on the parameters used.

Classification of the upper portion of the storage layer (protective layer) is designed to be comprised of a base soil (Rye Grass Flats) and some "pea gravel (1/4 in. to 3/8 in.)". The average soil properties for the Rye Grass Flats soil were presented on page E-3 of EDF-ER-281. The average silt and sand content were 88% and 12% respectively. As Rye Grass Flats soil is susceptible to erosion, the design calls for protecting the top surface of the storage layer by the addition of pea gravel into the protective

layer. It is desired for the protective layer to have 20% pea gravel. This results in the silt being 70% and the sand 10%. Based on this mixture, the soil is classified as “silt loam” in accordance with the USDA soil classification as presented in Figure 2-1 from EPA/625/4-89/022 (EPA 1989).

In the USDA universal soil loss equation, there are six parameters as shown in the Table B-2 and the following equation:

$$A = R * K * L * S * C * P$$

A = average annual soil loss (tons/acre)

R = rainfall and runoff erosivity index

K = soil – erodibility factor (tons/acre)

L = slope – length factor

S = slope – steepness factor

C = cover – management factor

P = practice factor.

Using the parameters above for the USDA universal soil loss equation, the calculated result is 2.208 tons/acre/yr. This value can be converted to a value of 4,416 lbs/acre or 0.1014 lb/ft². A soil density of 110 lbs/ft³ was presented in Appendix E of EDF-ER-281. With the density considered, the erosional rate is 0.000922 ft/yr (0.000281 m/yr).

B-4.3 Increased Storage Layer Infiltration from Biointrusion

To determine how the infiltration through the storage layer is impacted by animals (biointrusion), it is necessary to evaluate the potential biointruders. While plants present a biointrusion effect, the expected root depth is less than the depth of the cover system. Also, the roots of plants are going to seek out areas with sufficient water to maintain the plant life. The storage layer is design to hold water and then remove the water through a combination of two processes (evaporation and transpiration). This limits the depth and location that the roots of plants will be found in the landfill cover system.

Table B-2. Parameters selected for the conditions at the ICDF landfill for consideration in the erosion rate for the cover system.

Parameter	Value	Selection Criteria
R	20.0	Figure 20 in SW-867 (EPA 1982) for the location of the INEEL
K	0.48	Table 5 in SW-867 (EPA 1982) for “silt loam” based on the USDA soil classification presented above
L	1.15	Table 6 in SW-867 (EPA 1982) for 5% (mid point between 3% and 7%) slope and a slope length of 450 feet; note this is a combined parameter for L and S
S	-----	Combined with the L parameter into the LS parameter
C	0.20	Table 7 in SW-867 (EPA 1982) for grass in a meadow with poor to low productivity (extrapolated) for the ICDF expected vegetation
P	1.00	Table 8 in SW-867 (EPA 1982) for no support practice

Animal intrusion is not limited to where the water is expected to be stored or found in sufficient quantities to support life. The limiting factor on animal intrusion is the depth of the burrow for the particular biointruder. However, there are design features that can be included in a cover system to limit or prevent the biointrusion through the cover system. These design features have been included in the ICDF landfill cover system design.

Four biointruders (animals) have been identified that potentially could impact the ICDF landfill cover system. While there are other potential biointruders, the four selected are representative of the damage that can be expected and represent a variety of sizes and burrowing depths. Table B-3 presents the biointruders expected to be found at the ICDF landfill. In EDF-ER-279, the depths of the biointruder burrows and frequency of occurrence was presented. However, the frequency of occurrence was presented in terms of burrows per 100 m of transect distance. To use this information, it is necessary to convert the occurrence frequency into a count over the entire landfill storage layer surface area. As the measure of frequency was 100 m transects, this was assumed to represent a 70.7 m by 70.7 m area (diagonal of the stated area is 100 m). From Drawing C-304 (presented in EDF-ER-281, page E-23), the area of the ICDF landfill storage layer area was calculated to be 607,600 ft² (56,477 m² or 13.95 acres).

Using the area of the ICDF landfill cover system and burrow frequency, the number of burrow expected on the closed landfill was determined (rounded up to whole integer number, which is conservative). During the development of EDF-ER-279, it was agreed to by the EPA and IDEQ to use an area of 10 times the size of the burrow to assess the area drained from the burrow. The equation shown below is used to calculate the total area drained by the particular biointruder.

$$A_{\text{biointruder}} = \frac{N * \pi * (D_{\text{bio-hole}} * 10)^2}{4}$$

$A_{\text{biointruder}}$ = area drained by the particular biointruder

N = number of biointruder holes for the particular biointruder in the landfill cover system

$D_{\text{bio-hole}}$ = diameter of the burrow hole for the particular biointruder.

Table B-3. Biointruders identified for ICDF landfill cover system infiltration impact analysis including the size of the burrow, depth of burrowing, number of burrows, and total area drained by the biointruders.

Biointruder	Burrowing Depth (m)	Burrow Diameter (cm)	Burrow Frequency (per 100 m)	Burrows in Closed Landfill	Area Drained by Burrows in the Closed Landfill (cm ²)
Pocket gophers	1.47	7.6	1.9	22	99,802
Pocket mice	1.40	2.5	2.9	33	16,199
Harvester ants	1.83	0.5	1.2	14	275
Badger ^a	1.83	20	1	2	62,832

a. Two badgers considered for the entire area of the closed landfill due to their solitary nature.

With the areas drained by the biointruders, the impacts on the infiltration can be evaluated. Rather than try to simulate the development of the burrows in the ICDF cover system storage layer, the approach is to assume that all of the burrows exist following closure and remain intact for the duration of the Monte Carlo analysis. For the Monte Carlo analysis, there are two parameters in addition to the area drained by the biointruders that change the infiltration rate.

$$I_{\text{biointruder}} = \left(\frac{P * A_{\text{biointruder}} * \frac{D}{T}}{A_{\text{landfill}}} \right)$$

$I_{\text{biointruder}}$ = average annual infiltration from biointruder

P = annual precipitation (mm/yr)

$A_{\text{biointruder}}$ = total area of the biointruders burrow holes

D = burrow depth for the biointruder

T = thickness of the storage layer

A_{landfill} = surface area of the storage layer for the landfill.

The first additional parameter is the annual precipitation for the Monte Carlo analysis calculations. This parameter is varied for every iteration of the Monte Carlo analysis. Storage layer thickness is the second parameter that changes over the lifetime of the cover system due to erosion. This parameter is varied only at the end of every time interval iteration to account for the erosion for that year. The equation to calculate the infiltration due to biointrusion is presented below.

B-4.4 Infiltration Through the Clay Layer

To determine how much water infiltrates into the waste zone, there is an additional barrier that the infiltrating water must pass through. In the ICDF landfill cover system design, there is a 2-ft-thick layer of compacted clay with a hydraulic conductivity of no greater than 10^{-7} cm/sec. The clay layer at the bottom of the landfill that was actually constructed had a hydraulic conductivity lower than 10^{-7} cm/sec. According to the applicable regulations, the hydraulic conductivity of the clay layer in the cover system must be “no greater than” the hydraulic conductivity of the bottom layer of the landfill cell. The analysis conducted in EDF-ER-279 used a value of 7×10^{-7} cm/sec, but the bottom layer of the landfill cell had a hydraulic conductivity of approximately 5×10^{-7} cm/sec. This means that the hydraulic conductivity of the clay layer for the cover system must be reduced, which will result in even less water infiltrating into the waste zone.

For the Monte Carlo analysis, the properties will not change over time. However, the infiltration into the waste zone is highly dependent on the water infiltrating through the storage layer, including the contribution for biointrusion. Figure F-6 in EDF-ER-279 presented the relationship between infiltration through the storage layer and resulting infiltration through the clay layer. The points on Figure F-6 from EDF-ER-279 do not fit a linear relationship, but involve a much more complicated relationship. A complicated curve was fit to the points on Figure F-6 for the 3% slope curve. As the cover system is designed to be constructed on a 7% slope and with some settlement, the slope will be reduced. The slope of 3% is a conservative analysis of the magnitude of settlement that could occur during the ICDF landfill

lifetime. Use of the 3% slope is a conservative approach for the infiltration through the clay layer. The equation for the infiltration through the clay layer from infiltrating water through the storage layer is presented below. From the fitted curve, no water infiltrates through the clay layer with an infiltration rate for the storage layer of 0.38 mm/yr. In addition, the fitted curve allows for projections of the resulting infiltration up to a storage layer infiltration rate of 1.30 mm/yr normalized infiltration versus the normalized thickness is presented below:

$$y = \frac{-5.52}{1 - 23300 * \exp^{-6.97*x}}$$

y = infiltration through the clay layer (mm/yr)

x = infiltration through the storage layer (mm/yr).

B-5. MONTE CARLO ANALYSIS

To conduct the Monte Carlo analysis, it is necessary to define the problem, set up the problem into a mathematical model, and generate the results.

B-5.1 Problem Definition

In the case of defining the problem, there was a question raised concerning the infiltration rate through the cover system that will be used to close the ICDF landfill. Also, associated with the infiltration rate was how long will the cover system function. The cover system for the ICDF landfill was designed to remain functional for a period of “at least 1,000 years”. Along with the performance period, the ICDF landfill cover system was designed to function with minimal maintenance. With the requirement for minimal maintenance, it is necessary to evaluate the infiltration rate and cover system longevity without taking credit for maintenance and allowing for biointrusion into the storage layer of the cover system. Therefore, the defined problem is how long will the ICDF landfill cover system perform as designed and what is the infiltration rate over time without maintaining the cover system.

B-5.2 Development of Mathematical Model

To set up the problem into a mathematical model, it is necessary to know what variables will be considered in the analysis and the range limits for each variable. In the two engineering design files (EDF-ER-279 and EDF-ER-281) that were developed as part of the design for the ICDF landfill cover system, a number of variables were considered. This Monte Carlo analysis considers the same variables, but uses the deterministic results from the previous engineering design files results as the starting points. For the mathematical model, the effects from the precipitation, temperature, net radiant energy, wind speed, relative humidity, thickness of the storage layer, erosion of the storage layer, effect on biointrusion through the storage layer, and the resulting infiltration rate through the clay layer are considered. There are several other effects that could be considered in the analysis, such as wind erosion, that were not considered. In the case of wind erosion, the upper foot of the storage layer has been designed to minimize the effects on wind erosion by the addition of pea gravel.

The first part of mathematical development was to evaluate the impact and effect from the deterministic analysis that was conducted in the previous engineering design files. Discussed above were the evaluation of the deterministic results. For the climatological variables (precipitation, temperature, net radiant energy, wind speed, and relative humidity), the distribution of the climatological data was considered. This analysis resulted in equations to represent the effects of the changes in climatological variables as a function against the 1975 data. These “normalized” effects are then considered as factors affecting the results in the Monte Carlo analysis. Also, as part of the evaluation of the climatological data, the range for these parameters were developed.

In addition to the climatological parameters, four other factors were considered that effect the resulting infiltration rate. These other factors were the thickness of the storage layer, which as time progresses following the installation of the ICDF landfill cover system is reduced. This reduction is a result of another factor considered (erosion). The erosion rate is fixed rate over time. Biointrusion through the storage layer is another factor effecting the infiltration rate. This factor is a combination of fixed (amount of area drained) and variable (burrow depth changing in relation to the thickness of the storage layer and average annual precipitation). The final factor was the infiltration through the clay layer, which is dependent upon the total infiltration though the storage layer (precipitation and biointrusion).

With the effect equations and ranges determined, the computer code to generate the results was developed. The computer code (Appendix B-A) was developed in Microsoft Visual Basic

(Microsoft 1998). The flow and general logic of the computer code is presented in Figure B-11. Generally the computer code follows the following logic and sequence:

- Figure B-11 begins with initialization of the computer program.
- Next, the parameters used in the computer model that do not change as a result of climatological variables are then calculated.
- The thickness of the storage layer is initialized.
- The outer loop (lifetime) is initialized along with the variables used in this loop. This loop controls the number of year of Monte Carlo analysis evaluates. As the result for infiltration were expected to change over time (lifetime loop), the changes can then be used to determine when the cover system no longer functions as expected.
- The inner loop (effect) is initialized along with the variable used in this loop. This loop controls the number of evaluations within a given year (lifetime) of the Monte Carlo analysis. As the effects are dependent upon the climatological values, this loops allows for the range of climatological values to be simulated.
- The climatological values within the inner loop are then calculated. These climatological values are derived using the equations discussed above and a random number (uniform distribution).
- The normalized effects related to the climatological and thickness values are then calculated.
- With the normalized effects calculated, the average annual infiltration through the storage layer is then calculated by using the infiltration through the storage layer as a result of the precipitation rate.
- The infiltration rate is then adjusted with the normalized effects by multiplying the infiltration rate by the various normalized effects.
- The infiltration from biointrusion is then calculated considering both the precipitation and depth of the burrows (burrow depth remains constant even as the thickness of the storage layer is eroded).
- The total resulting infiltration through the storage layer is calculated by adding the precipitation and biointrusion infiltrations together.
- The average annual infiltration through the clay layer is then calculated.
- The calculated climatological average annual values are written to an output text (raw.txt) file. This output file also includes the counters for the two control loops.
- The calculated climatological average annual values and the infiltration rate through the clay layer are loaded into the arrays that will be used to determine the average values for the year (lifetime loop result).
- A determination is made concerning whether the number of iterations within the inner loop have been completed. If the number of iteration is completed, the program continues onto the other parts of the program outside of the inner loop. Otherwise, the program continues for another iteration through resulting calculations and determinations.

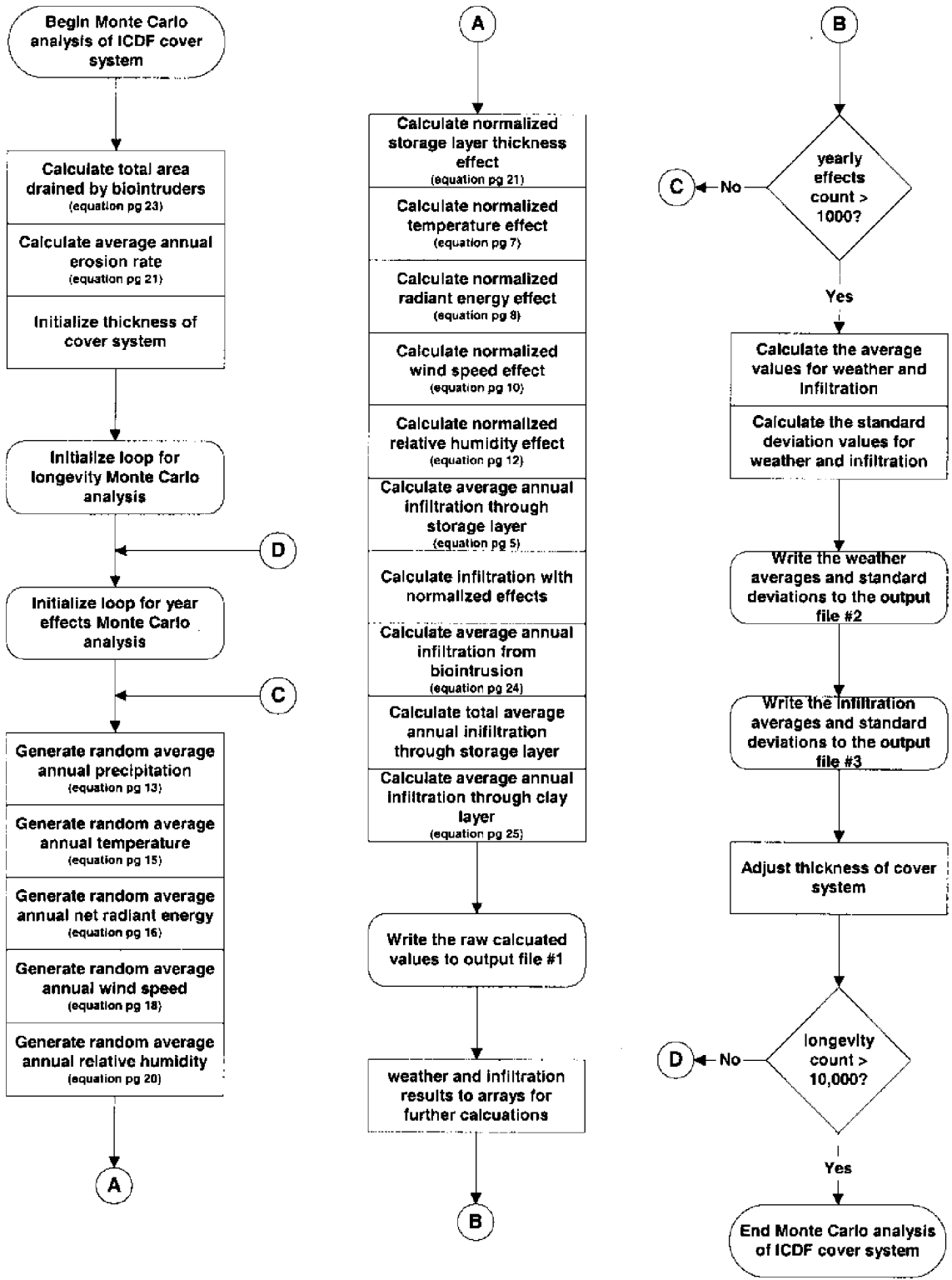


Figure B-11. Flow chart showing the various steps included in the computer model for the Monte Carlo analysis of the ICDF landfill cover system.

- Using the information in the arrays, both the average annual and standard deviation for the climatological and infiltration rate through the clay layer are then calculated.
- The calculated average annual and standard deviation for the climatological values are written to an output text file (weather.txt). This output file also includes the counters for the two control loops.
- The calculated average annual and standard deviation for the resulting average annual infiltration through the clay layer values are written to an output text file (results.txt). This output file also includes the counters for the two control loops.
- The thickness of the storage layer is adjusted (made thinner) by accounting for the annual erosion of the storage layer.
- A determination is made concerning whether the number of iterations within the outer loop have been completed. If the number of iteration is completed, the program ends. Otherwise, the program continues for another iteration through resulting calculations and determinations.

B-5.3 Results from the Computer Model

Although the computer program generates three output files, only two are used in the subsequent Monte Carlo analysis of the ICDF landfill cover system performance. The first file considered for the Monte Carlo analysis is the file containing the average and standard deviation results for the climatological parameters (weather.txt). The second file (results.txt) contains average and standard deviation results for infiltration through the clay layer. Both of these text files were imported into a Microsoft Excel (Microsoft 1999) spreadsheet for subsequent analysis and results presentation.

Using the results from the output files, a calculation of two times the standard deviation above and below the average values was conducted. These boundaries along with the average values were then presented in graphical form. Each of the climatological parameters along with the infiltration through the clay layer is presented this way as shown below. Although the computer program was designed to generate an analysis for 10,000 years, the computer program only generated the results for 9,765 years. In addition, the presentation of results was stopped at 6,000 years.

- Figure B-12 presents the Monte Carlo results for the average annual precipitation.
- Figure B-13 presents the Monte Carlo results for the average annual temperature.
- Figure B-14 presents the Monte Carlo results for the average annual net radiant energy.
- Figure B-15 presents the Monte Carlo results for the average annual wind speed.
- Figure B-16 presents the Monte Carlo results for the average annual relative humidity.
- In the case of the resulting infiltration through the clay layer, Figure B-17 presents the results. Only the average and two times the standard deviation above the average are presented in Figure B-17 for the infiltration rate. Also, the thickness of the storage layer as a function of time is presented on Figure B-17.

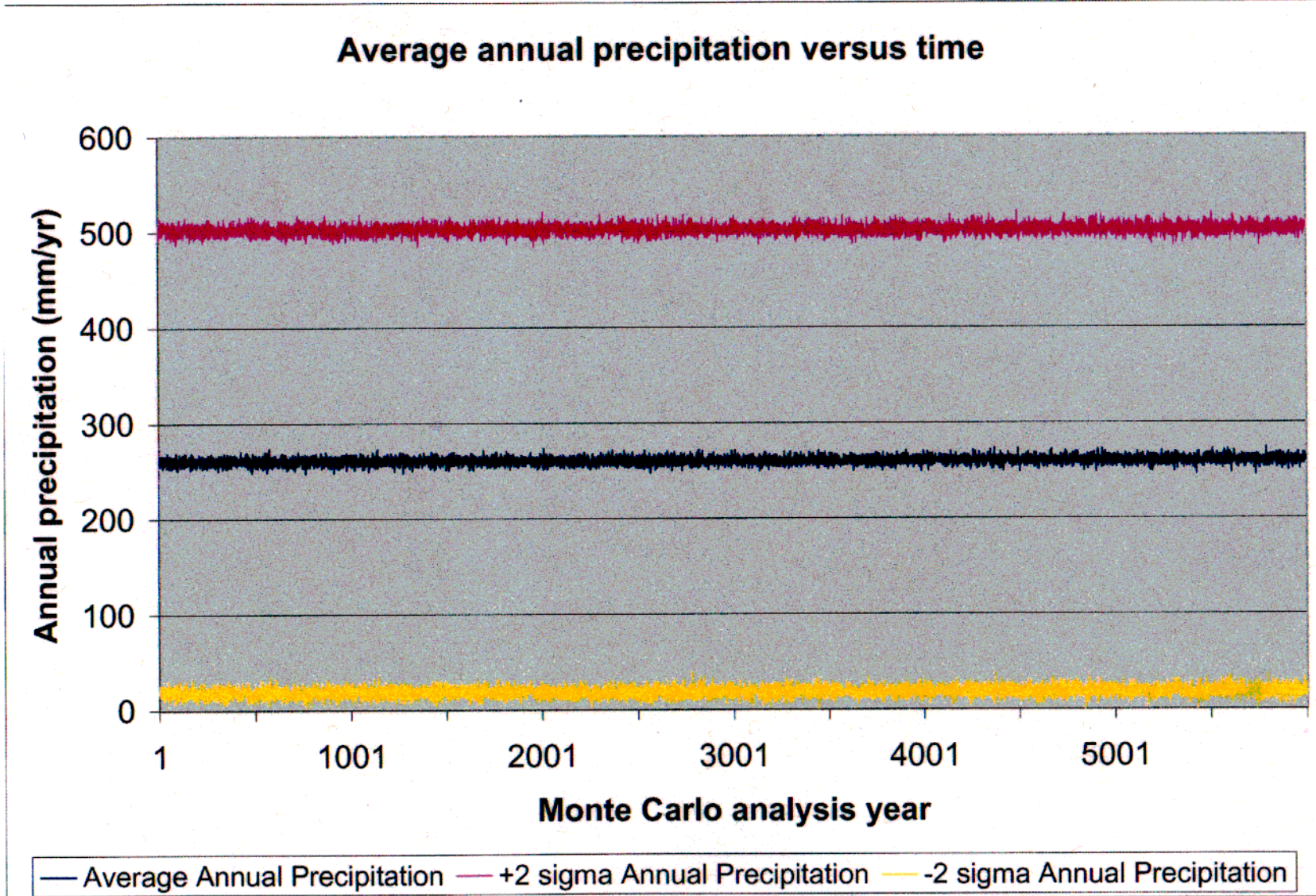


Figure B-12. Average annual precipitation results over the 6,000 years of the Monte Carlo analysis showing the average precipitation along with both two standard deviations above and below the average value for the duration of the analysis.

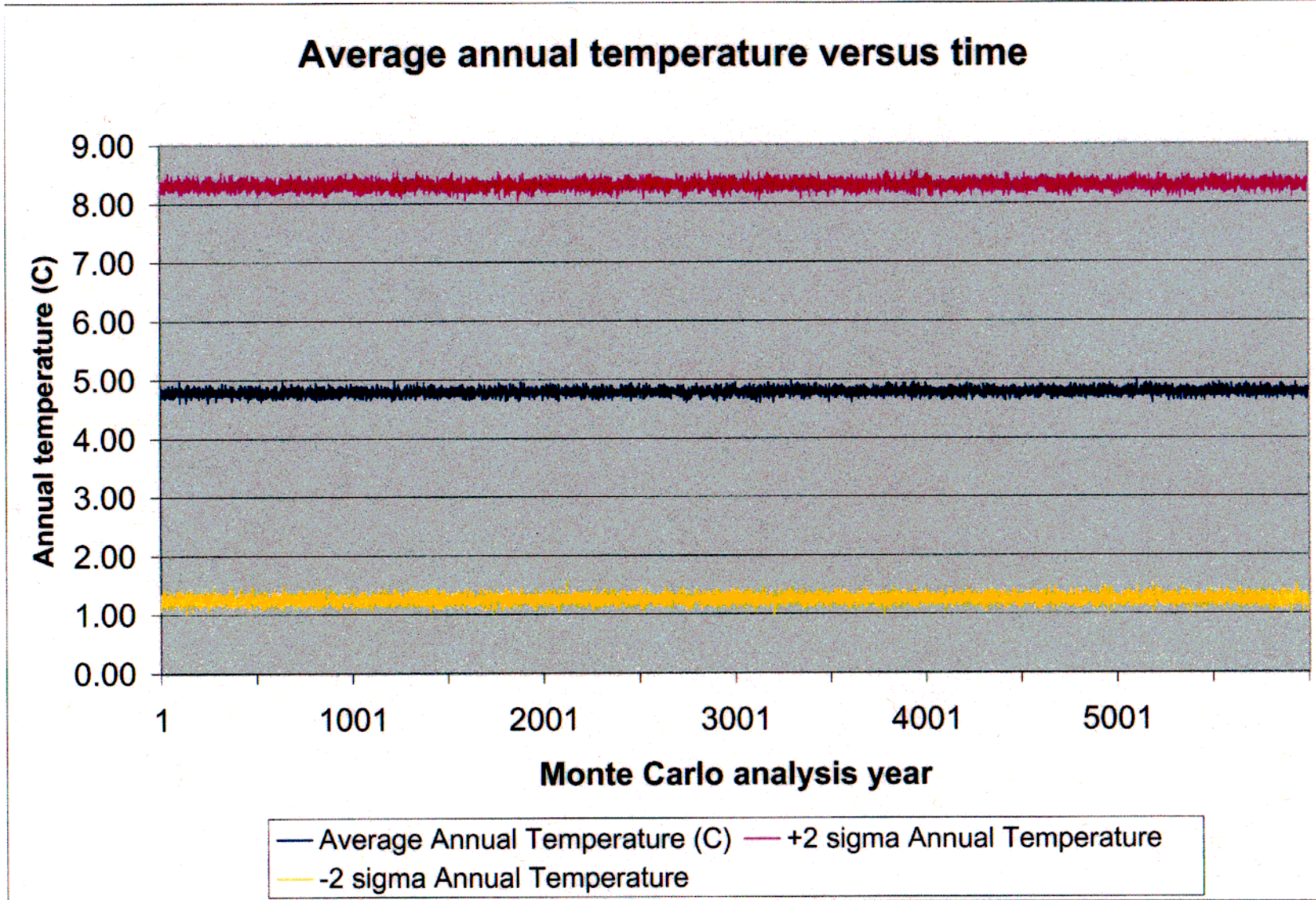


Figure B-13. Average annual temperature results over the 6,000 years of the Monte Carlo analysis showing the average temperature along with both two standard deviations above and below the average value for the duration of the analysis.

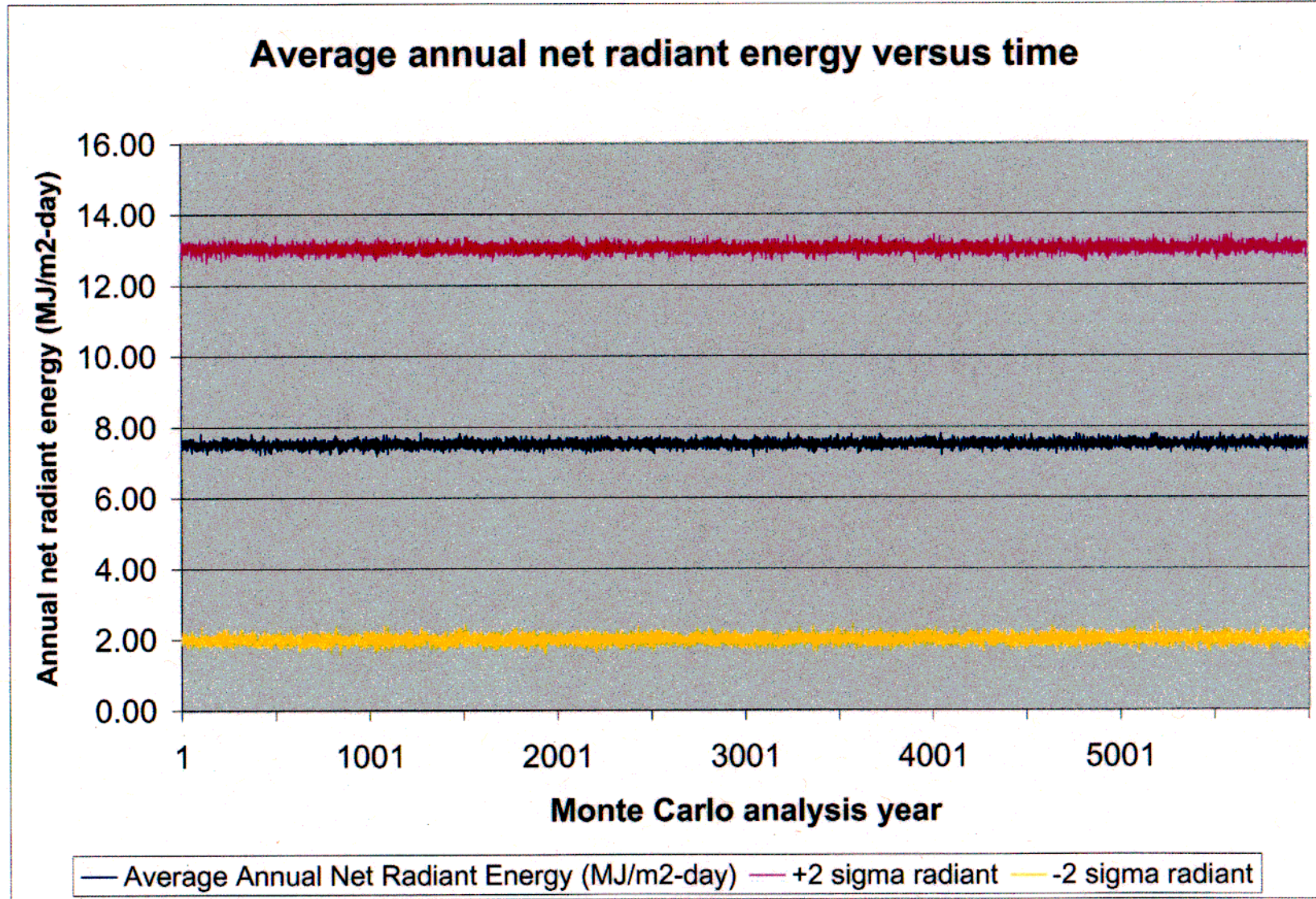


Figure B-14. Average annual net radiant energy over the 6,000 years of the Monte Carlo analysis showing the average net radiant energy along with both two standard deviation above and below the average value for the duration of the analysis.

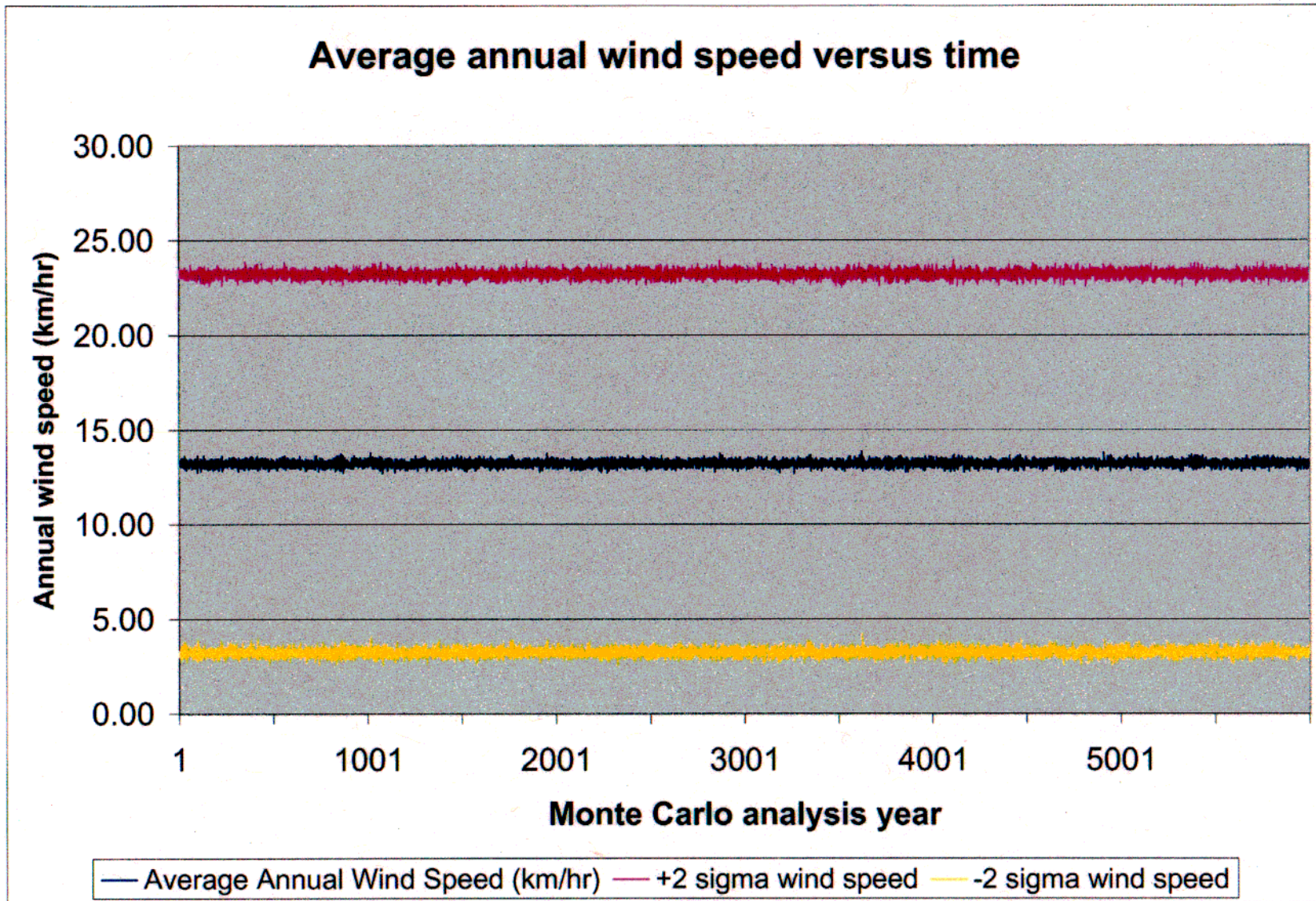


Figure B-15. Average annual wind speed results over the 6,000 years of the Monte Carlo analysis showing the average wind speed along with both two standard deviations above and below the average value for the duration of the analysis.

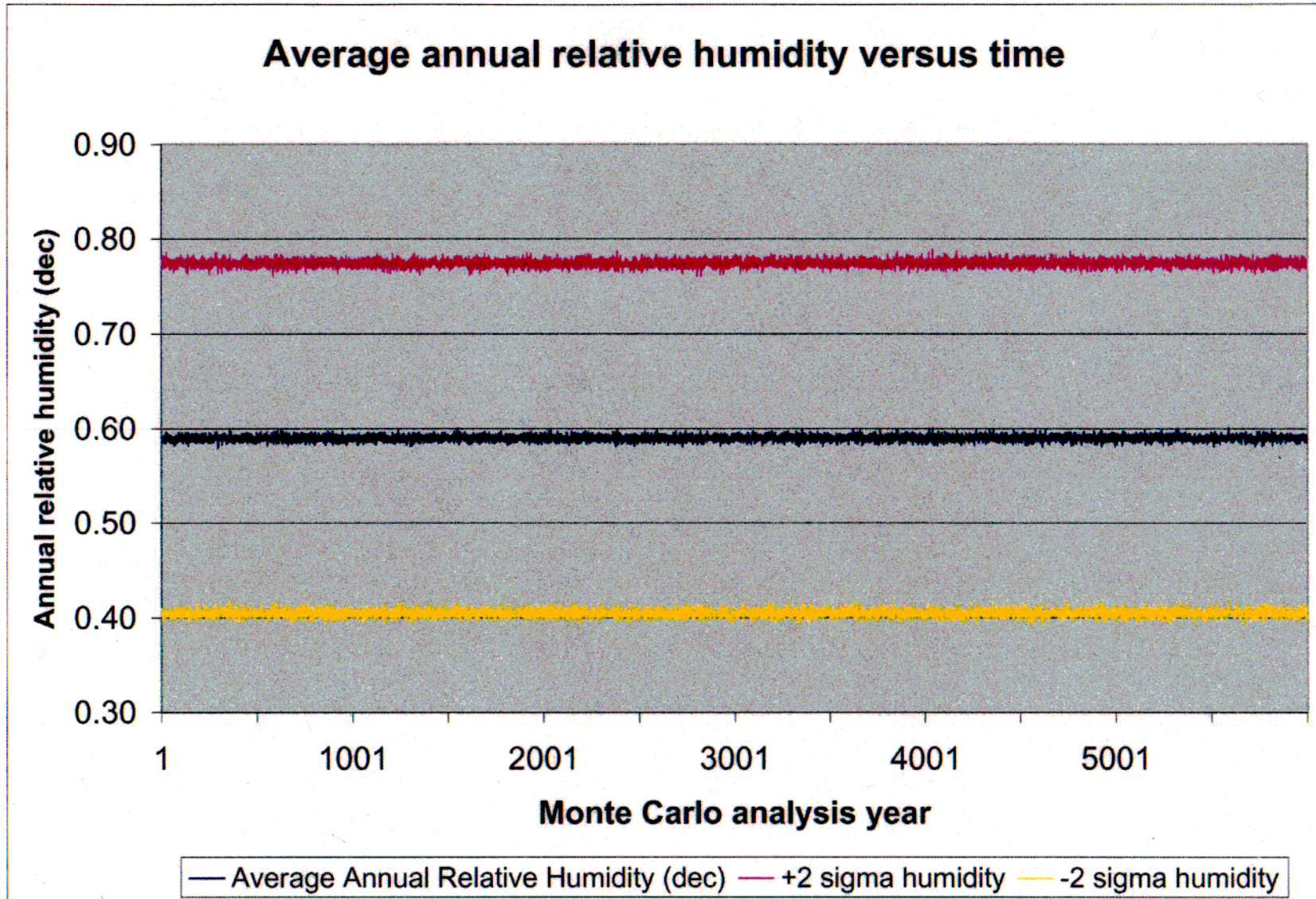


Figure B-16. Average annual relative humidity results over the 6,000 years of the Monte Carlo analysis showing the average relative humidity along with both two standard deviations above and below the average value for the duration of the analysis.

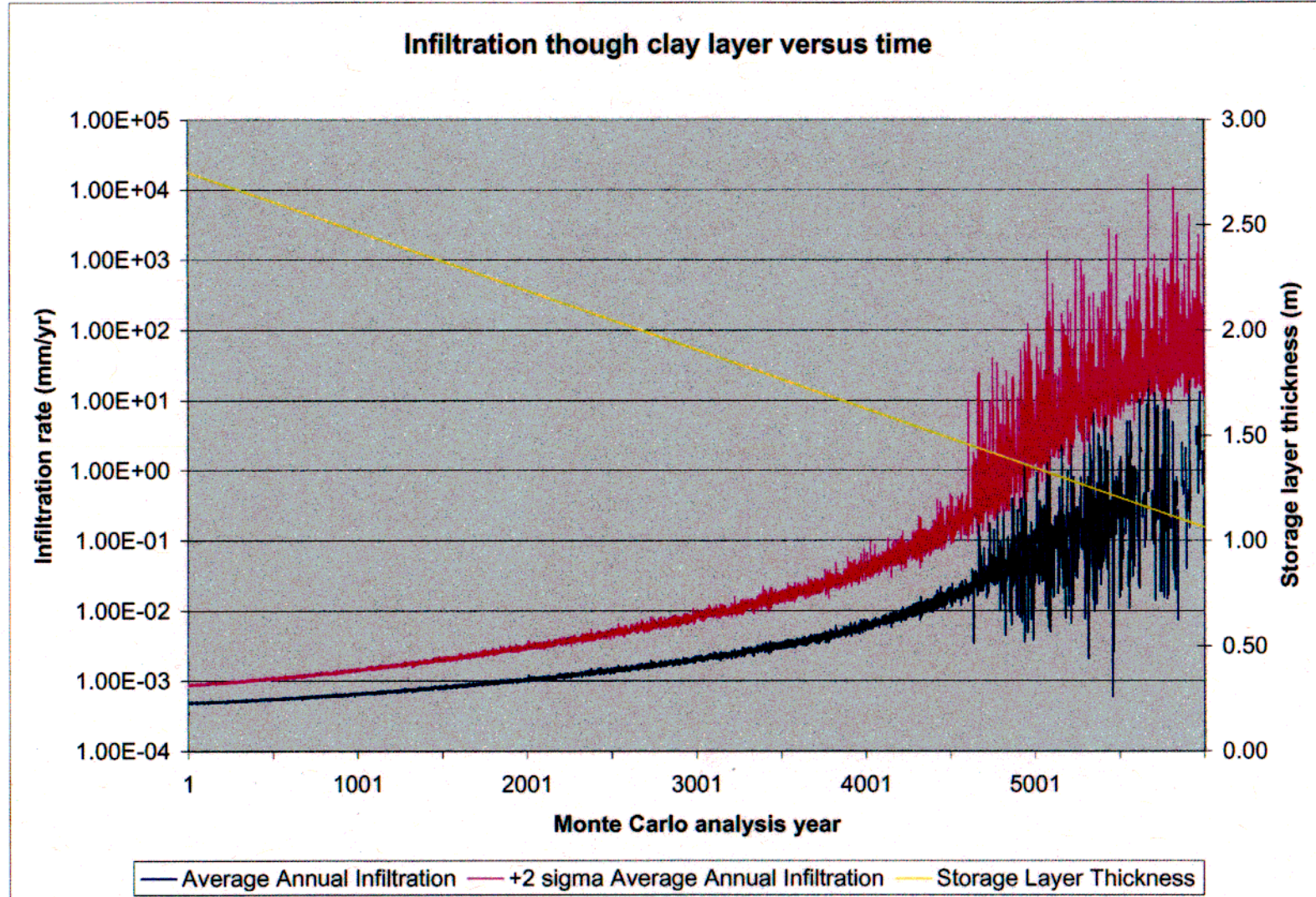


Figure B-17. Average annual infiltration through the clay layer in the ICDF landfill cover system results from the 6,000 years of Monte Carlo analysis along with two standard deviations above the average that is available for the leaching and transport of contaminants to the SRPA and the thickness of the storage layer in the ICDF landfill cover system.

B-6. CONCLUSIONS

Presented in Table B-4 is a summary of the Monte Carlo climatological results for Figures B-12 through B-16. In Table B-4, it is clear that the average Monte Carlo analytical results are conservative in relation to the analytical results for the previous engineering design files (EDF-ER-279 and EDF-ER-281) developed to support the ICDF landfill design. Also, the Monte Carlo results at the 2 sigma limit exceed the limits that were set for the computer model. Each of the climatological results is further discussed below.

Table B-4. Comparison table showing the climatological results of the Monte Carlo analysis including the degree of confidence that the +/- 2 sigma results correspond to along with the ranges for the climatological parameters and the actual climatological data from all years (1955 to 1999) and 1975 data.

	Average	High ^a	Low ^a	Confidence Level
Precipitation (mm/yr)				
Monte Carlo results	260	521	-2	>99%
Monte Carlo range	258	466	50.6	
All climatological data	230			
1975 climatological data	241			
Temperature (C)				
Monte Carlo results	4.78	8.57	0.98	>99%
Monte Carlo range	4.78	7.83	1.73	
All climatological data	5.2			
1975 climatological data	6.5			
Net radiant energy (MJ/m²-day)				
Monte Carlo results	7.51	13.4	1.56	>99%
Monte Carlo range	7.51	12.3	2.73	
All climatological data	8.2			
1975 climatological data	8.1			
Wind speed (km/hr)				
Monte Carlo results	13.2	24.0	2.51	>99%
Monte Carlo range	13.2	21.9	4.56	
All climatological data	13.7			
1975 climatological data	16.6			
Relative humidity (dec.)				
Monte Carlo results	0.59	0.79	0.39	>99%
Monte Carlo range	0.59	0.75	0.43	
All climatological data	0.59			
1975 climatological data	0.65			

a. The high and low values correspond to +/- 2 sigma for the results or range limits for the range.

For the precipitation, the average from the actual climatological data is considerably less than the Monte Carlo results (230 versus 260 or 88% of the Monte Carlo result). The Monte Carlo average precipitation also exceeded the 1975 data (260 versus 241) that was used as the basis for the previous sensitivity analysis. At the 2 sigma limits, the precipitation values exceed the range that was specified in the computer model (521 versus 466 and -2 versus 50.6). In fact, the 2 sigma levels for the Monte Carlo analysis result in a very high degree of confidence (>99%). Based on this, the Monte Carlo analysis portion for precipitation results in a very conservative analysis of the precipitation climatological factor.

For the temperature, the average from the actual climatological data is greater than the Monte Carlo results (5.20 versus 4.78 or 109% of the Monte Carlo result). The Monte Carlo average temperature was also significantly less than the 1975 data (4.78 versus 6.50) that was used as the basis for the previous sensitivity analysis. At the 2 sigma limits, the temperature values exceed the range that was specified in the computer model (8.57 versus 7.83 and 0.98 versus 1.73). In fact, the 2 sigma levels for the Monte Carlo analysis result in a very high degree of confidence (>99%). Based on this, the Monte Carlo analysis portion for temperature results in a very conservative analysis of the temperature climatological factor.

For the net radiant energy, the average from the actual climatological data is greater than Monte Carlo results (8.20 versus 7.51 or 109% of the Monte Carlo result). The Monte Carlo average net radiant energy was also less than the 1975 data (7.51 versus 8.10) that was used as the basis for the previous sensitivity analysis. At the 2 sigma limits, the net radiant energy values exceed the range that was specified in the computer model (13.4 versus 12.3 and 1.56 versus 4.56). In fact, the 2 sigma levels for the Monte Carlo analysis result in a very high degree of confidence (>99%). Based on this, the Monte Carlo analysis portion for net radiant energy results in a very conservative analysis of the precipitation climatological factor.

For the wind speed, the average from the actual climatological data is greater than the Monte Carlo results (13.7 versus 13.2 or 104% of the Monte Carlo result). The Monte Carlo average wind speed was also less than the 1975 data (13.2 versus 16.6) that was used as the basis for the previous sensitivity analysis. At the 2 sigma limits, the precipitation values exceed the range that was specified in the computer model (24.0 versus 21.9 and 2.51 versus 4.56). In fact, the 2 sigma levels for the Monte Carlo analysis result in a very high degree of confidence (>99%).

Based on this, the Monte Carlo analysis portion for wind speed results in a very conservative analysis of the precipitation climatological factor.

For the relative humidity, the average from the actual climatological data is the same as the Monte Carlo results (0.59 or 100% of the Monte Carlo result). The Monte Carlo relative humidity was less than the 1975 data (0.59 versus 0.65) that was used as the basis for the previous sensitivity analysis. At the 2 sigma limits, the precipitation values exceed the range that was specified in the computer model (0.79 versus 0.75 and 0.39 versus 0.43). In fact, the 2 sigma levels for the Monte Carlo analysis result in a very high degree of confidence (>99%). Based on this, the Monte Carlo analysis portion for relative humidity results in a very conservative analysis of the precipitation climatological factor.

From Figure B-17, it is clear that the cover system designed for the ICDF landfill will perform to the required infiltration rate of 0.1 mm/yr for a period of no less than 1,000 years even at the +2 sigma level. Presented in Table B-5 is a summary of the Monte Carlo infiltration rate through the clay layer results over time for Figure B-17. Table B-5 also presents the thickness over time of the storage layer component of the ICDF landfill cover system. In Table B-5, it is clear that the use of 0.1 mm/yr for the infiltration through the clay over the 1,000-year period is conservative and supports the analysis presented in the previous engineering design files (EDF-ER-279 and EDF-ER-281) developed to support the ICDF landfill design. Also, the Monte Carlo results at the +2 sigma limit is also significantly less than the required 0.1 mm/yr performance requirement over the 1,000-year period.

Table B-5. Monte Carlo analysis results of the infiltration through clay layer including the degree of confidence that the +2 sigma results correspond.

Monte Carlo analysis year	Average (mm/yr)	Avg +2 sigma (mm/yr)	Storage layer thickness (m)	confidence level
1	4.81E-04	8.56E-04	2.750	>99%
500	5.40E-04	1.07E-03	2.610	>99%
1000	6.39E-04	1.44E-03	2.469	>99%
1500	7.86E-04	1.89E-03	2.329	>99%
2000	1.06E-03	3.23E-03	2.188	>99%
2500	1.33E-03	4.76E-03	2.048	>99%
3000	2.03E-03	9.23E-03	1.907	>99%
3500	3.34E-03	1.81E-02	1.767	>99%
4000	7.04E-03	4.80E-02	1.626	>99%
4500	1.45E-02	1.17E-01	1.486	>99%
5000	8.61E-02	5.08E+00	1.345	>99%
5500	1.57E-02	6.60E+00	1.205	>99%
6000	-1.29E-01	1.11E+01	1.064	>99%

From Figure B-17 and Table B-5, it is clear that the cover system as designed for the ICDF landfill will meet the performance requirements of 0.1 mm/yr for the period of 1,000 years. In fact, based on the Monte Carlo analysis at the +2 sigma level (>99% confidence level), the cover system will meet a performance level of 0.1 mm/yr for a period of greater than 4,000 years.

From Figure B-17, there appears to be something occurring in the system after 4,500 years. At this point the storage layer has eroded to a depth of less than the biointruder burrows. At this point, the program continues to evaluate the biointruder burrow depth against the thickness of the storage layer. As a result, the volume of infiltrating water is greater than the volume drained by the biointruder drainage areas. This is an artifact of the simplistic modeling approach, but the results are still valid before this point in the analysis.

Another parameter that was not considered was the increased erosion from the wind. However, with the addition of the pea gravel to the upper part of the storage layer, the wind erosion is minimized and would not greatly increase the rate of erosion. Also, the issue of subsidence was not considered in the Monte Carlo analysis. The requirements for placement and compaction of waste in the ICDF landfill is designed to minimize the degree of settlement. In addition, there are limits for the void space for nonbulk waste and when dealing with other bulk nonsoil wastes there are additional constraints that will minimize the settlement issue long term.

Therefore, the cover system for the ICDF landfill is designed to perform to a level of 0.1 mm/yr infiltration rate through the clay layer for a period exceeding 1,000 years.

B-7. REFERENCES

- DOE-ID, 2002, *INEEL CERCLA Disposal Facility Remedial Design/Construction Work Plan*, DOE/ID-10848, Revision 1, U.S. Department of Energy Idaho Operations Office, May 2002.
- EPA, 1982, *Evaluating Cover Systems for Solid and Hazardous Waste*, SW-867, U.S. Environmental Protection Agency, Office of Solid Waste and Emergency Response, Washington D.C., September 1982.
- EPA, 1989, *Seminar Publication - Requirements for Hazardous Waste Landfill Design, Construction, and Closure*, EPA/625/4-89/022, U.S. Environmental Protection Agency, Office of Research and Development, Washington D.C., August 1989.
- Gupta, R. S., 1989, *Hydrology and Hydraulic System*, Prentice Hall, Englewood Cliffs, New Jersey.
- EDF-ER-279, "Hydrological Modeling of Final Cover," Rev. 2, Idaho National Engineering and Environmental Laboratory, May 2002.
- EDF-ER-281, "Liner and Final Cover System Long Term Performance Evaluation and Final Cover Life Cycle Expectation," Rev. 1, Idaho National Engineering and Environmental Laboratory, May 2002.
- Microsoft, 1998, "Microsoft Visual Basic - computer programming environment and application development", Microsoft Corporation, Redmond, WA.
- Microsoft, 1999, "Microsoft Excel - computer spreadsheet application", Microsoft Corporation, Redmond, WA.

Appendix B-A

Microsoft Visual Basic Computer Code Used To Generate the Monte Carlo Analysis Results

(Only the subroutine dealing with the results generation and resulting output)

Private Sub cmdCalculate_Click()

' This program performs a Monte Carlo analysis on the cover system
' for the ICDF landfill. The Monte Carlo analysis considers the
' impacts or effects from biointrusion (burrowing animals), erosion
' of the storage layer of the cover system, average annual precipitation,
' average annual temperature, average annual net radiant energy, average
' annual wind speed, and average annual relative humidity. These effects
' are simulated by generating a random number for each run within the
' Monte Carlo analysis. The resulting impacts are based on the sensitivity
' analysis performed in EDF-ER-279 and EWDF-ER-281. This allows for the
' effects of temperature, net radiant energy, wind speed, and relative humidity
' to be normalized to the base case (1975) from the previous sensitivity
' analysis.

' This program will use two loops to control the Monte Carlo analysis. The
' outer loop (cover system longevity - lifetime) determines the number of
' years of Monte Carlo analysis that are evaluated. The inner loop (average
' annual results - effects) simulates the range of conditions for the cover
' system for each year of analysis.

' For this Monte Carlo analysis, the biointruders are assumed to be present
' from the beginning of the analysis with fully developed burrows. The size
' and number of burrows does not change over the duration of the Monte Carlo
' analysis. However, as the cover system is eroded away, the depth of the
' biointruder burrows continues to remain constant (bottom of burrow moves

' downward through the cover system) over the lifetime of the Monte Carlo
' analysis.

' This program will generate an output file containing the results of the
' Monte Carlo analysis. The output file will contain three sets of data.
' The first column of data will be the year within the Monte Carlo analysis
' followed by the average of the average annual infiltration through the clay
' layer. The final column will be the standard deviation of the average
' annual infiltration rate though the clay layer.

Dim intRawFile As Integer ' File number for raw calculated results

Dim intWeatherFile As Integer ' File number for average and standard deviation
 ' weather results

Dim intResultsFile As Integer ' File number for average and standard deviation
 ' infiltration results

intRawFile = FreeFile ' Get first file #

Open "C:\temporary\Raw.txt" For Output As intRawFile

intWeatherFile = FreeFile ' Get second file #

Open "C:\temporary\Weather.txt" For Output As intWeatherFile

intResultsFile = FreeFile ' Get third file #

Open "C:\temporary\Results.txt" For Output As intResultsFile

' Calculate the total area drained by biointruders from Table B-3 of report

Const Gopher1 = 9980200 ' area drained by pocket gophers (99,802 cm²)

Const Mice1 = 1619900 ' area drained by pocket mice (16,199 cm²)

```

Const Ants1 = 27500    ' area drained by harvester ants (275 cm2)
Const Badger1 = 6283200 ' area drained by badgers (62,832 cm2)
Const Gopher2 = 1.47  ' depth of pocket gopher burrows (1.47 m)
Const Mice2 = 1.4     ' depth of pocket mice burrows (1.40 m)
Const Ants2 = 1.83    ' depth of harvester ant burrows (1.83 m)
Const Badger2 = 1.83  ' depth of badger burrows (1.83 m)
Const dblLandfill = 56477000000# ' total area of the cover system storage layer
Const dblErosion = 0.000281 ' erosional rate for the storage layer in the cover
                               ' system (mm/yr)
Dim dblThick As Double
dblThick = 2.75              ' initial thickness of the cover system storage
                               ' layer (mm)
Dim intLifetime As Integer ' counter for number of years (10,000) of analysis

For intLifetime = 1 To 10000
    Dim dblYearPrecip As Double
    Dim dblRanPrecip As Double
    Dim dblYearTemp As Double
    Dim dblRanTemp As Double
    Dim dblYearRad As Double
    Dim dblRanRad As Double
    Dim dblYearWind As Double
    Dim dblRanWind As Double
    Dim dblYearHumidity As Double
    Dim dblRanHumidity As Double
    Dim dblThickNorm As Double

```



```

        ' annual wind speed results
Dim dblHumidity(1 To 1000) As Double ' array to hold the within year average
        ' annual humidity results
Dim dblInfiltration(1 To 1000) As Double ' array to hold the within year
        ' average annual infiltration
        ' through clay layer results

Randomize

Dim intEffect As Integer ' counter for number (1,000) of analysis within
        ' a yearly time period

For intEffect = 1 To 1000
    dblRanPrecip = ((80 - -20 + 1) * Rnd + -20) ' generate a random number
        ' with a range from -20
        ' to +80
    dblYearPrecip = (dblRanPrecip + 32.2) / 0.241
    dblRanTemp = ((2831 - 1934 + 1) * Rnd + 1934) ' generate a random number
        ' with a range from 1934
        ' to 2831
    dblYearTemp = (dblRanTemp - 1680) / 147
    dblRanRad = ((3639 - 1430 + 1) * Rnd + 1430) ' generate a random number
        ' with a range from 1430
        ' to 3639
    dblYearRad = (dblRanRad - 800) / 231
    dblRanWind = ((4630 - 528 + 1) * Rnd + 528) ' generate a random number

```

```

        ' with a range from 528
        ' to 4630
dblYearWind = (dblRanWind + 553) / 237
dblRanHumidity = ((4115 - 1018 + 1) * Rnd + 1018) ' generate a random
        ' number with a range
        ' from 1018 to 4115
dblYearHumidity = (dblRanHumidity + 3140) / 9680
dblThickNorm = dblThick / 2# ' Normalize thickness against the
        ' 2.0 meter thick analysis
dblThickChange = -153.5 * dblThickNorm + 251.5 * dblThickNorm ^ 2 - 208.8 * dblThickNorm ^ 3
+ 86.27 * dblThickNorm ^ 4 - 14.09 * dblThickNorm ^ 5 + 39.54
dblTempNorm = dblYearTemp / 6.5 ' Normalize temperature against the
        ' 1975 data (6.5 C)
dblTempChange = 0.0322 * dblTempNorm + 0.951
dblRadNorm = dblYearRad / 8.1 ' Normalize Net Radiant Energy against
        ' the 1975 data (8.1 MJ/m2-day)
dblRadChange = 0.38 * dblRadNorm + 0.529
dblWindNorm = dblYearWind / 16.6 ' Normalize Wind Speed against the
        ' 1975 data (16.6 km/hr)
dblWindChange = 0.42 * dblWindNorm + 0.557
dblHumidityNorm = dblYearHumidity / 0.65 ' Normalize Relative Humidity
        ' against the 1975 data (0.65)
dblHumidityChange = -4.77 * dblHumidityNorm + 1.61 * dblHumidityNorm ^ 2 + 4.08
dblInfilPrecip = 0.000965 * dblYearPrecip - 0.075 ' calculate gross
        ' precipitation
        ' through storage layer

```

$\text{dblStorageInfil} = \text{dblInfilPrecip} * \text{dblThickChange} * \text{dblTempChange} * \text{dblRadChange} * \text{dblWindChange} * \text{dblHumidityChange}$

$\text{dblGopherInfil} = (\text{dblYearPrecip} * \text{Gopher1} * (\text{Gopher2} / \text{dblThick})) / \text{dblLandfill}$

$\text{dblMiceInfil} = (\text{dblYearPrecip} * \text{Mice1} * (\text{Mice2} / \text{dblThick})) / \text{dblLandfill}$

$\text{dblAntsInfil} = (\text{dblYearPrecip} * \text{Ants1} * (\text{Ants2} / \text{dblThick})) / \text{dblLandfill}$

$\text{dblBadgerInfil} = (\text{dblYearPrecip} * \text{Badger1} * (\text{Badger2} / \text{dblThick})) / \text{dblLandfill}$

$\text{dblBioInfil} = \text{dblGopherInfil} + \text{dblMiceInfil} + \text{dblAntsInfil} + \text{dblBadgerInfil}$

$\text{dblTotalInfil} = \text{dblStorageInfil} + \text{dblBioInfil}$

Dim dblTemp0 As Double

Dim dblTemp1 As Double

Dim dblTemp2 As Double

Dim dblTemp3 As Double

Dim dblTemp4 As Double

Dim dblTemp5 As Double

$\text{dblTemp0} = -6.9690711 * \text{dblTotalInfil}$

$\text{dblTemp1} = \text{Exp}(\text{dblTemp0})$

$\text{dblTemp2} = -23306.8 * \text{dblTemp1}$

$\text{dblTemp3} = 1 + \text{dblTemp2}$

$\text{dblAnnualInfil} = -5.52 / \text{dblTemp3}$

Print #intRawFile, intLifetime, intEffect, dblThick, dblYearPrecip, dblYearTemp, dblYearRad, dblYearWind, dblYearHumidity

' writes the raw data to the raw data output file

$\text{dblPrecip}(\text{intEffect}) = \text{dblYearPrecip}$

```
dblTemp(intEffect) = dblYearTemp
dblRadiant(intEffect) = dblYearRad
dblWind(intEffect) = dblYearWind
dblHumidity(intEffect) = dblYearHumidity
dblInfiltration(intEffect) = dblAnnualInfil
```

Next intEffect

```
Dim dblPreX2 As Double
Dim dblTempX2 As Double
Dim dblRadX2 As Double
Dim dblWindX2 As Double
Dim dblHumX2 As Double
Dim dblInfilX2 As Double
Dim dblPreSum As Double
Dim dblTempSum As Double
Dim dblRadSum As Double
Dim dblWindSum As Double
Dim dblHumSum As Double
Dim dblInfilSum As Double
Dim intCount As Integer
```

```
dblPreX2 = 0#
dblTempX2 = 0#
dblRadX2 = 0#
dblWindX2 = 0#
```

dblHumX2 = 0#

dblInfilX2 = 0#

dblPreSum = 0#

dblTempSum = 0#

dblRadSum = 0#

dblWindSum = 0#

dblHumSum = 0#

dblInfilSum = 0#

For intCount = 1 To 1000

dblPreX2 = dblPreX2 + dblPrecip(intCount) ^ 2

dblPreSum = dblPreSum + dblPrecip(intCount)

dblTempX2 = dblTempX2 + dblTemp(intCount) ^ 2

dblTempSum = dblTempSum + dblTemp(intCount)

dblRadX2 = dblRadX2 + dblRadiant(intCount) ^ 2

dblRadSum = dblRadSum + dblRadiant(intCount)

dblWindX2 = dblWindX2 + dblWind(intCount) ^ 2

dblWindSum = dblWindSum + dblWind(intCount)

dblHumX2 = dblHumX2 + dblHumidity(intCount) ^ 2

dblHumSum = dblHumSum + dblHumidity(intCount)

dblInfilX2 = dblInfilX2 + dblInfiltration(intCount) ^ 2

dblInfilSum = dblInfilSum + dblInfiltration(intCount)

Next intCount

Dim dblAvgPrecip As Double

Dim dblStdPrecip As Double

Dim dblAvgTemp As Double

Dim dblStdTemp As Double

Dim dblAvgRadiant As Double

Dim dblStdRadiant As Double

Dim dblAvgWind As Double

Dim dblStdWind As Double

Dim dblAvgHumidity As Double

Dim dblStdHumidity As Double

Dim dblAvgInfiltration As Double

Dim dblStdInfiltration As Double

dblAvgPrecip = dblPreSum / 1000

dblAvgTemp = dblTempSum / 1000

dblAvgRadiant = dblRadSum / 1000

dblAvgWind = dblWindSum / 1000

dblAvgHumidity = dblHumSum / 1000

dblAvgInfiltration = dblInfilSum / 1000

dblTemp1 = 0#

dblTemp1 = 1000# * (1000# - 1#)

dblTemp2 = 0#

dblTemp3 = 0#

dblTemp4 = 0#

dblTemp2 = dblPreSum ^ 2

```
dblTemp3 = 1000 * dblPreX2
dblTemp4 = (dblTemp3 - dblTemp2) / dblTemp1
dblStdPrecip = Sqr(dblTemp4)
```

```
dblTemp2 = 0#
dblTemp3 = 0#
dblTemp4 = 0#
dblTemp2 = dblTempSum ^ 2
dblTemp3 = 1000 * dblTempX2
dblTemp4 = (dblTemp3 - dblTemp2) / dblTemp1
dblStdTemp = Sqr(dblTemp4)
```

```
dblTemp2 = 0#
dblTemp3 = 0#
dblTemp4 = 0#
dblTemp2 = dblRadSum ^ 2
dblTemp3 = 1000 * dblRadX2
dblTemp4 = (dblTemp3 - dblTemp2) / dblTemp1
dblStdRadiant = Sqr(dblTemp4)
```

```
dblTemp2 = 0#
dblTemp3 = 0#
dblTemp4 = 0#
dblTemp2 = dblWindSum ^ 2
dblTemp3 = 1000 * dblWindX2
dblTemp4 = (dblTemp3 - dblTemp2) / dblTemp1
```

$\text{dblStdWind} = \text{Sqr}(\text{dblTemp4})$

$\text{dblTemp2} = 0\#$

$\text{dblTemp3} = 0\#$

$\text{dblTemp4} = 0\#$

$\text{dblTemp2} = \text{dblHumSum} \wedge 2$

$\text{dblTemp3} = 1000 * \text{dblHumX2}$

$\text{dblTemp4} = (\text{dblTemp3} - \text{dblTemp2}) / \text{dblTemp1}$

$\text{dblStdHumidity} = \text{Sqr}(\text{dblTemp4})$

$\text{dblTemp2} = 0\#$

$\text{dblTemp3} = 0\#$

$\text{dblTemp4} = 0\#$

$\text{dblTemp2} = \text{dblInfilSum} \wedge 2$

$\text{dblTemp3} = 1000 * \text{dblInfilX2}$

$\text{dblTemp4} = (\text{dblTemp3} - \text{dblTemp2}) / \text{dblTemp1}$

$\text{dblStdInfiltration} = \text{Sqr}(\text{dblTemp4})$

Print #intWeatherFile, intLifetime, dblAvgPrecip, dblStdPrecip, dblAvgTemp, dblStdTemp, dblAvgRadiant, dblStdRadiant, dblAvgWind, dblStdWind, dblAvgHumidity, dblStdHumidity

' writes the weather data to the weather output file

Print #intResultsFile, intLifetime, dblThick, dblAvgInfiltration, dblStdInfiltration

' writes the storage layer thickness and infiltration data to the infiltration output file

$\text{dblThick} = \text{dblThick} - \text{dblErosion}$

Next intLifetime

Close intRawFile

Close intWeatherFile

Close intResultsFile

End Sub

Appendix C
K_d Values for INTEC Groundwater Modeling



Department of Energy

Idaho Operations Office
850 Energy Drive
Idaho Falls, Idaho 83401-1563

July 3, 2001

Mr. Martin Doornbos
BBWI
2525 North Fremont Ave., MS 3930
Idaho Falls, ID 83415

SUBJECT: Kd values for INTEC groundwater modeling (EM-ER-01-115)

Dear Mr. Doornbos:

Attached is the Selection of Kd values for INTEC Groundwater Modeling. In the attachment, Kd values from six references are presented and the selection of the Kds to be used for groundwater modeling in the INTEC area discussed. The report documents the approach, assumptions, and results for the elements on the periodic table from hydrogen (H) through californium (Cf). The attached report presents Kd values for different media types (waste soils, alluvium soils, clay materials, barrier soils, sedimentary interbed materials, vadose zone basalt, and Snake River Plain Aquifer basalt). Several of the contaminants of concern for the groundwater modeling are presented as follows. The complete list is presented in Table 1 of the attached report with the specifics from each reference presented in the Appendix A to the attached report.

Element	Symbol	waste soils (ml/g)	clean alluvium (ml/g)	clay materials (GCL) (ml/g)	barrier soils (CCL) (ml/g)	interbeds materials (ml/g)	vadose zone basalt (ml/g)	SRPA basalt (ml/g)
Strontium	Sr	12	24	200	200	12	0	0.48
Technetium	Tc	0.2	0.2	1	1	0.2	0	0.008
Iodine	I	0	0	1	1	0	0	0
Cesium	Cs	500	500	1500	1500	500	0	20
Uranium	U	6	6	63	63	6	0	0.24
Neptunium	Np	8	8	55	55	8	0	0.32
Plutonium	Pu	140	140	1700	1700	22	0	0.88

Changes from the values presented above and in the attached report should be explained and the rationale for selection of alternative Kd values presented in the modeling documents. If you have any questions, please me at (208) 526-4978.

Sincerely,

Talley Jenkins, DOE-ID WAG 3 Manager
Environmental Restoration Program

Attachment

EXTERNAL bcc DISTRIBUTION:

D. Kuhns, BBWI, MS 3930
D. Vernon, BBWI, MS 3930
ARDC, BBWI, MS 3922

ID DISTRIBUTION:

K. Hain (EM/ER), MS 1117
T. Jenkins (EM/ER), MS 1117
R. Kimmel (EM/INTEC), MS 1154

CONCURRENCE:

(y) EM _____
(w)
(w)

RECORD NOTES:

1. This letter was prepared to transmit the Kd values to be used for INTEC groundwater modeling to BBWI.
2. This letter and the attachment were prepared by T. ^{TWJ 7/3/01}Jenkins (EM/ER).
3. This letter/memo closes OATS number N/A.
4. The attached correspondence has no relation to the Naval Nuclear Propulsion Program. Naval Reactors concurrence is not required.

TWJenkins (EM/ER): File: Kd values for INTEC groundwater modeling.wpd

Selection of Kd values for INTEC Groundwater Modeling

1 INTRODUCTION

In groundwater modeling, many parameters are used to predict subsurface contaminant movement. One of the more important major parameters is the retardation coefficient. This parameter is calculated based on several other parameters, including the distribution coefficient. For groundwater modeling, the linear distribution coefficient, referred to as the Kd value, is generally utilized. The different types of media (i.e., soils, basalt, clay, etc.) have corresponding Kd values that are not necessarily the same. This report evaluates several sources of information concerning Kd values. In addition, this report recommends Kd values for groundwater modeling at the Idaho Nuclear Technology and Engineering Center (INTEC) area for each of the different media evaluated.

2 METHODOLOGY

In considering the design of the Idaho National Engineering and Environmental Laboratory (INEEL) Comprehensive Environmental Response, Compensation, and Liability Act (CERCLA) Disposal Facility (ICDF) landfill, there were seven media types identified. Each of these media types have different physical and chemical properties, along with modeling assumptions. For this report, the seven media types are 1) waste soils, 2) alluvium soils, 3) clay materials, 4) barrier soils, 5) interbed materials, 6) vadose zone basalt, and 7) Snake River Plain Aquifer (SRPA) basalt. The specifics of each of these media types is discussed in the subsequent sections.

In reviewing the available literature, it was determined that not all references had the same Kd values for the various elements on the periodic table. As such, it was necessary to develop a selection preference for the Kd values to be utilized for the INTEC groundwater modeling. Generally, the preference was to select the values used in the preliminary groundwater modeling for the ICDF landfill conceptual design (INEEL 2000). The second choice was generally the Kd value used in the Operable Unit (OU) 3-13 Remedial Investigation/Baseline Risk Assessment (RI/BRA) (DOE-ID 1997). Finally, the Kd values from the Track 1 Guidance document (DOE-ID 1992) were used for the groundwater modeling. Deviations and the selection preferences for each of the media types are discussed in the subsequent sections.

In reviewing the sources of information on Kd values, several of the elements were missing. To fill in these missing elements, chemical analogs were considered and used. The missing elements and associated chemical analog rationale are discussed below. As the chemical elements react the same regardless of the media type, there was only one set of chemical analogs developed.

The elements of helium (He), oxygen (O), neon (Ne), and argon (Ar) are all gaseous elements and therefore are expected to move through the subsurface environment as gases.

The element lithium (Li) is an alkali metal like sodium (Na) potassium (K) (CRC 1980) and therefore is expected to move through the subsurface as other alkali metals. Potassium was used as the analog for lithium in selecting the Kd values for subsurface movement of lithium.

The element boron (B) is chemically similar to carbon (C) (CRC 1980) and therefore is expected to move through the subsurface as carbon. Non-gaseous carbon was used as the analog in selecting the Kd values for subsurface movement of boron.

The element nitrogen (N) is a component of nitrate and therefore has the same Kd that is used for nitrate

The element magnesium (Mg) has a valence state of +2 and is in the same group (2A) on the periodic table as calcium (Ca) with calcium being directly beneath magnesium on the periodic table of elements (CRC 1980). In addition, magnesium is found in nature in deposits along with calcium. Therefore, magnesium is expected to move through the subsurface similar to calcium and calcium was used for the analog in selecting Kd values for magnesium.

The element titanium (Ti) has valence states of +2, +3, and +4 (most common) and is in the same group (4B) on the periodic table as zirconium (Zr) with zirconium being directly beneath titanium on the periodic table of elements (CRC 1980). Therefore, titanium is expected to move through the subsurface similar to zirconium and zirconium was used for the analog in selecting Kd values for titanium.

The element gallium (Ga) has a valence state +3 and is in the same group (3A) on the periodic table as aluminum (Al) with aluminum being directly above gallium on the periodic table of elements (CRC 1980). Therefore, gallium is expected to move through the subsurface similar to aluminum and aluminum was used for the analog in selecting Kd values for gallium.

The element germanium (Ge) has valence states of +2 and +4 and is in the same group (4A) on the periodic table as silicon (Si) with silicon being directly above germanium on the periodic table of elements (CRC 1980). Therefore, germanium is expected to move through the subsurface similar to silicon and silicon was used for the analog in selecting Kd values for germanium.

The rare earth elements of dysprosium (Dy), erbium (Er), thulium (Tm), ytterbium (Yb) and lutetium (Lu) are similar to the other rare earth elements of praseodymium (Pr), neodymium (Nd), promethium (Pm), and samarium (Sm). The rare earth elements tend to occur in the same minerals in nature (CRC 1980). Therefore, these rare earth elements are expected to move through the subsurface similar to neodymium and neodymium was used for the analog in selecting Kd values for these rare earth elements.

The element platinum (Pt) has valence states of +2 and +4 and is in the same group (8) on the periodic table as palladium (Pd) with palladium being directly above platinum on the periodic table of elements. Therefore, platinum is expected to move through the subsurface similar to palladium and palladium was used for the analog in selecting Kd values for platinum.

The element astatine (At) is a halogen with chemical properties similar to iodine (I) (CRC 1980). Therefore, astatine is expected to move through the subsurface similar to iodine and iodine was used for the analog in selecting Kd values for astatine.

The element francium (Fr) is an alkali metal like cesium (Cs) (CRC 1980) and therefore is expected to move through the subsurface as other alkali metals. Cesium was used as the analog for francium in selecting the Kd values for subsurface movement of francium.

The element berkelium (Bk) is an actinide with valence states of +3 and +4 and occur next on the periodic table of element following curium (Cm). Therefore, berkelium is expected to move through the subsurface similar to curium and curium was used for the analog in selecting Kd values for berkelium.

In addition, the element carbon is assume to not migrate as a gas, but as a solid material. Also, chromium (Cr) is not assumed to exist in the hexavalent state, but as the elemental, bivalent or trivalent states.

2.1 Waste Soils

Most of the contaminated soils being considered for disposal in the ICDF landfill are from releases at INTEC. The soil type at INTEC is generally described as sands and gravels. One of the sources of Kd values (Sheppard and Thibault 1990) distinguished between these different soil types and for waste soils at INTEC the sand values were used from that reference. For the groundwater modeling at INTEC of contaminated soils, sand is the generic description used for waste soils being considered for the ICDF landfill.

Six references were used in the selection of Kd values for the waste soils media type. The references and preference for selection are as follows. As the releases at INTEC were modeled and assessed in the OU 3-13 RI/BRA (DOE-ID 1997), the first preference was the OU 3-13 RI/BRA Kd values presented in Table 5-1 and 5-2 for the waste soils. The second preference was the Kd values utilized for the ICDF conceptual design groundwater modeling as presented in EDF-ER-170 (INEEL 2000) on Table 3-2). For the third preference, the Track 1 Guidance Document (DOE-ID 1992) Table G-1 was used. Sheppard and Thibault (1990) Table 1 sand values were used as the fourth preference and Table 4.1 from NCRP 123 (1996) was used as the fifth preference. The sixth preference was and EPA document (EPA 1999) containing information on Kds.

When using the EPA document, it is necessary to know the expected environmental conditions that the contaminants will be subjected in order to select appropriate Kd values. Table 1

presents the environmental conditions that were used for selection of the Kd values from the EPA document.

The Kd values from the references and selected Kds for waste soils are presented in Appendix A, Table A-1.

2.2 Alluvium soils

The ICDF Complex will be constructed next to INTEC on soils that are generally described as sands and gravels. One of the sources of Kd values (Sheppard and Thibault 1990) distinguished between these different soil types and for the alluvium soils at INTEC the sand values are utilized from that reference. For the groundwater modeling at INTEC of alluvium soils, this is the generic description used for alluvium soils being considered for the ICDF landfill.

Six references were used in the selection of Kd values for the alluvium soils media type. The references and preference for selection are as follows. The first preference was the Kd values utilized for the ICDF conceptual design groundwater modeling as presented in EDF-ER-170 (INEEL 2000) on Table 3-2). The second preference was OU 3-13 RI/BRA (DOE-ID 1997) Kd values presented in Table 5-1 and 5-2 for the waste soils. For the third preference, the Track 1 Guidance Document (DOE-ID 1992) Table G-1 was used. Sheppard and Thibault (1990) Table 1 sand values were used as the fourth preference and Table 4.1 from NCRP 123 (1996) was used as the fifth preference. The sixth preference was an EPA document (EPA 1999) containing information on Kds.

When using the EPA document, it is necessary to know the expected environmental conditions that the contaminants will be subjected in order to select appropriate Kd values. Table 1 presents the environmental conditions that were used for selection of the Kd values from the EPA document.

The Kd values from the references and selected Kds for waste soils are presented in Appendix A, Table A-2.

2.3 Clay Materials

Clay materials have much different properties than soils (alluvium or waste). The Kd values selected for the clay materials in this report are to represent materials such as bentonite clays that can be contained in a geosynthetic clay liner (GCL) or as a stand alone layer. For the groundwater modeling at INTEC of clay materials, this is the generic description used for clay materials being considered for the ICDF landfill.

Six references were used in the selection of Kd values for the clay materials media type. The references and preference for selection are as follows. The first preference was the Kd values utilized for the ICDF conceptual design groundwater modeling as presented in EDF-ER-170 (INEEL 2000) on Table 3-2). The second preference was Sheppard and Thibault (1990) Table 1 clay values. For the third preference, the OU 3-13 RI/BRA (DOE-ID 1997), Kd values

presented in Table 5-1 and 5-2 were utilized. Track 1 Guidance Document (DOE-ID 1992) Table G-1 was used as the fourth preference and Table 4.1 from NCRP 123 (1996) was used as the fifth preference. The sixth preference was an EPA document (EPA 1999) containing information on Kds.

When using the EPA document, it is necessary to know the expected environmental conditions that the contaminants will be subjected to in order to select appropriate Kd values. Table 1 presents the environmental conditions that were used for selection of Kd values from the EPA document.

The Kd values from the references and selected Kds for waste soils are presented in Appendix A, Table A-3.

2.4 Barrier Soils

Barrier soils have much different properties than soils (alluvium or waste). The Kd selected for barrier soils in this report are to represent materials such as loam soils from areas like the Rye Grass Flats (RGF), which are being considered for the compacted clay liner (CCL) admixture soils in the INTEC landfill. One of the sources of Kd values (Sheppard and Thibault 1990) distinguished between the different soil types and for barrier soils the loam values are utilized from that reference. For the groundwater modeling at INTEC of barrier soils, this is the generic description used for barrier soils being considered for the ICDF landfill.

Six references were used in the selection of Kd values for the barrier soils media type. The references and preference for selection are as follows. The first preference was the Kd values utilized for the ICDF conceptual design groundwater modeling as presented in EDF-ER-170 (INEEL 2000) on Table 3-2). The second preference was Sheppard and Thibault (1990) Table 1 clay values. For the third preference, the OU 3-13 RI/BRA (DOE-ID 1997), Kd values presented in Table 5-1 and 5-2 were utilized. Track 1 Guidance Document (DOE-ID 1992) Table G-1 was used as the fourth preference and Table 4.1 from NCRP 123 (1996) was used as the fifth preference. The sixth preference was an EPA document (EPA 1999) containing information on Kds.

When using the EPA document, it is necessary to know the expected environmental conditions that the contaminants will be subjected to in order to select appropriate Kd values. Table 1 presents the environmental conditions that were used for selection of Kd values from the EPA document.

The Kd values from the references and selected Kds for waste soils are presented in Appendix A, Table A-4. An additional reference (Dicke 1997) was evaluated and is presented for comparison purposes.

2.5 Sedimentary Interbed Materials

Sedimentary interbed materials, in the INTEC area, generally have similar properties to that of alluvium soils. The sedimentary interbed materials at INTEC are generally sands and fine

gravels, which is the generic class of soils for the INTEC interbeds, between the basalt flows in the INTEC area. One of the sources of Kd values (Sheppard and Thibault 1990) distinguished between the difference soils type and for waste soils the sand values are utilized from that reference. For the groundwater modeling at INTEC of sedimentary interbed materials, this is the generic description used for sedimentary interbed materials being considered for the ICDF landfill.

Six references were used in the selection of Kd values for the waste soils media type. The references and preference for selection are as follows. The first preference was the Kd values utilized for the ICDF conceptual design groundwater modeling as presented in EDF-ER-170 (INEEL 2000) on Table 3-2). The second preference was OU 3-13 RI/BRA (DOE-ID 1997) Kd values presented in Table 5-1 and 5-2 for the waste soils. For the third preference, the Track 1 Guidance Document (DOE-ID 1992) Table G-1 was used. Sheppard and Thibault (1990) Table 1 sand values were used as the forth preference and Table 4.1 from NCRP 123 (1996) was used as the fifth preference. The sixth preference was and EPA document (EPA 1999) containing information on Kds.

When using the EPA document, it is necessary to know the expected environmental conditions that the contaminants will be subjected in order to select appropriate Kd values. Table 1 presents the environmental conditions that were used for selection of Kd values from the EPA document.

The Kd values from the references and selected Kds for waste soils are presented in Appendix A, Table A-5.

Table 1. Environmental conditions used for selection of Kd values (minimum values) from the EPA document for waste soils, alluvium soils, clay materials, barrier soils, and interbed materials.

contaminant	waste soils	alluvium soils	clay materials	barrier soils	interbed materials
chromium (Cr) Table 5.7	DCB extractable Fe 0.26 to 0.29 mmol/g soluble sulfate 0 to 1.9 mg/l pH 6.1 to 7.0	DCB extractable Fe 0.26 to 0.29 mmol/g soluble sulfate 0 to 1.9 mg/l pH 6.1 to 7.0	DCB extractable Fe 0.26 to 0.29 mmol/g soluble sulfate 0 to 1.9 mg/l pH 6.1 to 7.0	DCB extractable Fe 0.26 to 0.29 mmol/g soluble sulfate 0 to 1.9 mg/l pH 6.1 to 7.0	DCB extractable Fe 0.26 to 0.29 mmol/g soluble sulfate 0 to 1.9 mg/l pH 6.1 to 7.0
strontium (Sr) Table 5.13	cation exchange capacity 3 to 10 meq/100 g clay content 4% to 20% pH 5 to 8	cation exchange capacity 3 to 10 meq/100 g clay content 4% to 20% pH 5 to 8	cation exchange 10 to 50 meq/100 g clay content 20% to 60% pH 5 to 8	cation exchange capacity 10 to 50 meq/100 g clay content 20% to 60% pH 5 to 8	cation exchange capacity 3 to 10 meq/100 g clay content 4% to 20% pH 5 to 8
cadmium (Cd) Table 5.4	pH 5 to 8	pH 5 to 8	pH 5 to 8	pH 5 to 8	pH 5 to 8
cesium (Cs) Table 5.5	cation exchange capacity 3 to 10 meq/100 g clay content 4% to 20% pH 5 to 8	cation exchange capacity 3 to 10 meq/100 g clay content 4% to 20% pH 5 to 8	cation exchange capacity 10 to 50 meq/100 g clay content to 20% to 60% pH between 5 to 8	cation exchange capacity 10 to 50 meq/100 g clay content 20% to 60% pH 5 to 8	cation exchange capacity 3 to 10 meq/100 g clay content 4% to 20% pH 5 to 8
lead (Pb) Table 5.9	equilibrium lead concentration 100 to 200 ug/l pH 6.4 to 8.7	equilibrium lead concentration 100 to 200 ug/l pH 6.4 to 8.7	equilibrium lead concentration 100 to 200 ug/l pH 6.4 to 8.7	equilibrium lead concentration 100 to 200 ug/l pH 6.4 to 8.7	equilibrium lead concentration 100 to 200 ug/l pH 6.4 to 8.7
Radon (Rn)	Kd value of 0	Kd value of 0	Kd value of 0	Kd value of 0	Kd value of 0
thorium (Th) Table 5.15	pH 5 to 8 dissolved thorium $<10^{-9}$ moles/l	pH 5 to 8 dissolved thorium $<10^{-9}$ moles/l	pH 5 to 8 dissolved thorium $<10^{-9}$ moles/l	pH 5 to 8 dissolved thorium $<10^{-9}$ moles/l	pH 5 to 8 dissolved thorium $<10^{-9}$ moles/l
uranium (U) Table 5.17	pH 7	pH 7	pH 7	pH 7	pH 7
plutonium (Pu) Table 5.11	clay content 0% to 30% soluble carbonate 3 to 4 meq/l	clay content 0% to 30% soluble carbonate 3 to 4 meq/l	clay content 51% to 70% soluble carbonate 5 to 6 meq/l	clay content 51% to 70% soluble carbonate 5 to 6 meq/l	clay content 0% to 30% soluble carbonate 3 to 4 meq/l

2.6 Vadose Zone Basalt

For vadose zone basalt, Kd values of 0 ml/g have been historically used for groundwater modeling at INTEC. The nature of the basalt flows at INTEC (e.g., varying thickness and fractured) results in the assumption that transport through the basalt flows is dominated by the transport of water without significant interaction between the dissolved contaminants and the vadose zone basalt flows. As a result, the use of a Kd of 0 ml/g for the contaminants through the vadose zone basalts will continue to be utilized.

2.7 Snake River Plain Aquifer Basalts

For SRPA basalt, Kds of 1/25 of the Kd for the sedimentary interbed have been historically used for groundwater modeling at INTEC (DOE-ID 1997). The nature of the basalt flows at INTEC (e.g., varying thickness and fractured) results in the assumption that transport through the basalt flows is dominated by the transport of water without significant interaction between the dissolved contaminants and the vadose zone basalt flows. However, there are some in filling of the fractures in the SRPA basalts which do retard the movement of contaminants to some extent. As a result, the use of a Kds of 1/25 of values for the sedimentary interbed materials will continue to be utilized

3 RESULTS

Using the selection approach discussed above, Kd values were selected for all seven geological media types. The selected Kd values are presented in Table 1. As can be seen in Table 1, the Kd values vary greatly depending on the geologic media type. In addition, the specific element (contaminant) have varying Kd values. The Kd values presented in Table 1 should be utilized for groundwater modeling in the INTEC area. Changes from these values are acceptable, however, there changes should be explained and the rationale for selection of alternative Kd values presented in the modeling documents.

Table 2. Selected Kd values for the various media type for groundwater modeling within the INTEC area.

Element	Symbol	waste soils (ml/g)	clean alluvium (ml/g)	clay materials (GCL) (ml/g)	barrier soils (CCL) (ml/g)	interbeds materials (ml/g)	vadose zone basalt (ml/g)	SRPA basalt (ml/g)
Hydrogen	H	0	0	0	0	0	0	0
Helium	He	0	0	0	0	0	0	0
Lithium	Li	15	15	75	55	15	0	0.6
Beryllium	Be	250	250	1300	800	250	0	10
Boron	B	5	5	1	20	5	0	0.2
Carbon	C	5	5	1	20	5	0	0.2
Nitrogen	N	0	0	0	0	0	0	0
Oxygen	O	0	0	0	0	0	0	0
Fluorine	F	0	0	0	0	0	0	0
Neon	Ne	0	0	0	0	0	0	0
Sodium	Na	76	76	76	76	76	0	3.0
Magnesium	Mg	5	5	50	30	5	0	0.2
Aluminum	Al	250	250	250	250	250	0	10
Silicon	Si	35	35	180	110	35	0	1.4
Phosphorous	P	5	5	35	25	5	0	0.2
Sulfur	S	14	14	14	14	14	0	0.56
Chlorine	Cl	0	0	0	0	0	0	0
Argon	Ar	0	0	0	0	0	0	0
Potassium	K	15	15	75	55	15	0	0.6
Calcium	Ca	5	5	50	30	5	0	0.2
Scandium	Sc	310	310	310	310	310	0	12
Titanium	Ti	600	600	3300	2200	600	0	24
Vanadium	V	6	6	6	6	6	0	0.24
Chromium	Cr	30	30	1500	30	30	0	1.2
Manganese	Mn	50	50	180	750	50	0	2
Iron	Fe	220	220	165	800	220	0	8.8
Cobalt	Co	10	10	550	1300	10	0	0.4
Nickel	Ni	100	100	650	300	100	0	4
Copper	Cu	20	20	20	20	20	0	0.8
Zinc	Zn	16	16	2400	1300	16	0	0.64
Gallium	Ga	250	250	250	250	250	0	10
Germanium	Ge	35	35	180	110	35	0	1.4
Arsenic	As	3	3	7	7	3	0	0.12
Selenium	Se	4	4	740	500	4	0	0.16
Bromine	Br	15	15	75	50	15	0	0.6
Krypton	Kr	0	0	0	0	0	0	0
Rubidium	Rb	55	55	270	180	55	0	2.2
Strontium	Sr	12	24	200	200	12	0	0.48
Yttrium	Y	170	170	1000	720	170	0	6.8
Zirconium	Zr	600	600	3300	2200	600	0	24
Niobium	Nb	100	100	900	550	100	0	4
Molybdenum	Mo	10	10	90	125	10	0	0.4
Technetium	Tc	0.2	0.2	1	1	0.2	0	0.008
Ruthenium	Ru	55	55	800	1000	55	0	2.2

Element	Symbol	waste soils (ml/g)	clean alluvium (ml/g)	clay materials (GCL) (ml/g)	barrier soils (CCL) (ml/g)	interbeds materials (ml/g)	vadose zone basalt (ml/g)	SRPA basalt (ml/g)
Rhodium	Rh	52	52	52	52	52	0	2.1
Palladium	Pd	55	55	270	180	55	0	2.2
Silver	Ag	90	90	180	120	90	0	3.6
Cadmium	Cd	6	6	560	40	6	0	0.24
Indium	In	390	390	390	390	390	0	516
Tin	Sn	130	130	670	450	130	0	5.2
Antimony	Sb	50	50	250	150	50	0	2
Tellurium	Te	125	125	720	500	125	0	5
Iodine	I	0	0	1	1	0	0	0
Xenon	Xe	0	0	0	0	0	0	0
Cesium	Cs	500	500	1500	1500	500	0	20
Barium	Ba	50	50	50	50	50	0	2
Lanthanum	La	1200	1200	1200	1200	1200	0	48
Cerium	Ce	500	500	20000	8100	500	0	20
Praseodymium	Pr	240	240	240	240	240	0	9.6
Neodymium	Nd	240	240	240	240	240	0	9.6
Promethium	Pm	240	240	240	240	240	0	9.6
Samarium	Sm	240	240	1300	800	240	0	9.6
Europium	Eu	340	340	340	340	340	0	314
Gadolinium	Gd	240	240	240	240	240	0	9.6
Terbium	Tb	240	240	240	240	240	0	9.6
Dysprosium	Dy	240	240	240	240	240	0	9.6
Holmium	Ho	250	250	1300	800	250	0	10
Erbium	Er	240	240	240	240	240	0	9.6
Thulium	Tm	240	240	240	240	240	0	9.6
Ytterbium	Yb	240	240	240	240	240	0	9.6
Lutetium	Lu	240	240	240	240	240	0	9.6
Hafnium	Hf	450	450	2400	1500	450	0	18
Tantalum	Ta	220	220	1200	900	220	0	8.8
Tungsten	W	100	100	100	100	100	0	4
Rhenium	Re	10	10	60	40	10	0	0.4
Osmium	Os	190	190	190	190	190	0	7.6
Iridium	Ir	91	91	91	91	91	0	.4
Platinum	Pt	55	55	270	180	55	0	2.2
Gold	Au	30	30	30	30	30	0	1.2
Mercury	Hg	100	100	710	710	100	0	4
Thallium	Tl	100	100	100	100	100	0	4
Lead	Pb	100	100	710	710	100	0	4
Bismuth	Bi	100	100	600	450	100	0	4
Polonium	Po	150	150	3000	400	150	0	6
Astatine	At	0	0	1	1	0	0	0
Radon	Rn	0	0	0	0	0	0	0
Francium	Fr	500	500	1500	1500	500	0	20
Radium	Ra	100	100	9100	36000	100	0	4
Actinium	Ac	450	450	2400	1500	450	0	18
Thorium	Th	100	100	1700	1700	100	0	4

Element	Symbol	waste soils (ml/g)	clean alluvium (ml/g)	clay materials (GCL) (ml/g)	barrier soils (CCL) (ml/g)	interbeds materials (ml/g)	vadose zone basalt (ml/g)	SRPA basalt (ml/g)
Protactinium	Pa	550	550	2700	1800	550	0	22
Uranium	U	6	6	63	63	6	0	0.24
Neptunium	Np	8	8	55	55	8	0	0.32
Plutonium	Pu	140	140	1700	1700	22	0	0.88
Americium	Am	340	340	340	340	340	0	314
Curium	Cm	4000	4000	6000	4000	4000	0	160
Berkelium	Bk	4000	4000	6000	4000	4000	0	160
Californium	Cf	510	510	510	510	510	0	20

4 REFERENCES

CRC, 1980, *CRC Handbook of Chemistry and Physics*, CRC Press Inc., 61st Edition, 1980-1981.

DOE-ID, 1992, *Track 1 Sites: Guidance for Assessing Low Probability Hazard Sites at the INEL*, U.S. Department of Energy, Idaho Operations Office, DOE/ID-10340(92), Revision 1, July.

DOE-ID, 1997, *Comprehensive RI/FS for the Idaho Chemical Processing Plant OU 3-13 at the INEL - Part A, RI/BRA Report*, U.S. Department of Energy, Idaho Operations Office, DOE/ID-10534, Revision 0, November.

EPA, 1999, *Understanding Variation in Partition Coefficients K_d Values, Volume II: Review of Geochemistry and Available K_d Values for Cadmium, Cesium, Chromium, Lead, Plutonium, Radon, Strontium, Thorium, Tritium (³H) and Uranium*, U.S. Environmental Protection Agency, EPA 402-R-99-004A, August.

INEEL, 2000, *Engineering Design File - Screening Model Results of a Mixed Low-Level Waste Disposal Facility Proposed for the Idaho National Engineering and Environmental Laboratory*, Idaho National Engineering and Environmental Laboratory, EDF-ER-170, Revision 0, November.

NCRP, 1996, *Screening Models for Release of Radionuclides to Atmosphere, Surface Water, and Ground*, National Council on Radiation Protection and Measurements, NCRP Report No. 123 I, January.

Sheppard and Thibault, 1990, *Default Soil Solid/Liquid Partition Coefficients, K_ds, for Four Major Soil Types: A Compendium*, Health Physics, Vol 59, No. 4, October.

APPENDIX A

Table A-1. Kd values for waste soils from various references along with the preference for selection and resulting selected Kds.

Element	Symbol	Track 1 (Table G- 1, default values)	NCRP 123 (Table 4.1)	Sheppard and Thibault (Table 1, Sand)	EPA 402- R-99- 004A, Volume II	OU 3-13 RI/BRA (Appendix F, Tables 5-1 & 5-2)	EDF-ER- 170 (Table 3-2)	Selected Kd Value (ml/g)
preference for selection		#3	#5	#4	#6	#1	#2	
Hydrogen	H	0	0			0		0
Helium	He							0
Lithium	Li							15
Beryllium	Be	250	240	250		250		250
Boron	B							5
Carbon	C	0	6.7	5				5
Nitrogen	N					0		0
Oxygen	O							0
Fluorine	F	0	87			0		0
Neon	Ne							0
Sodium	Na		76					76
Magnesium	Mg							5
Aluminum	Al					250		250
Silicon	Si			35				35
Phosphorous	P		8.9	5				5
Sulfur	S		14					14
Chlorine	Cl		1.7			0		0
Argon	Ar							0
Potassium	K	15	18	15		15		15
Calcium	Ca	5	8.9	5				5
Scandium	Sc		310					310
Titanium	Ti							600
Vanadium	V	1000				6		6
Chromium	Cr	1.2	30	70	70	1.2		30
Manganese	Mn	50	50	50		50		50
Iron	Fe	220	160	220				220
Cobalt	Co	10	60	60		10		10
Nickel	Ni	100	400	400		100		100
Copper	Cu	20	30			20		20
Zinc	Zn	16	200	200				16
Gallium	Ga							250
Germanium	Ge							35
Arsenic	As	3	110			3	3	3
Selenium	Se	4	140	150		4		4
Bromine	Br	15	14	15				15
Krypton	Kr		0					0
Rubidium	Rb		52	55				55
Strontium	Sr	24	15	15	15	12	12	12
Yttrium	Y		190	170				170
Zirconium	Zr	600	580	600				600
Niobium	Nb		160	160		100		100
Molybdenum	Mo		10	10				10

A-1

Element	Symbol	Track 1 (Table G- 1, default values)	NCRP 123 (Table 4.1)	Sheppard and Thibault (Table 1, Sand)	EPA 402- R-99- 004A, Volume II	OU 3-13 RI/BRA (Appendix F, Tables 5-1 & 5-2)	EDF-ER- 170 (Table 3-2)	Selected Kd Value (ml/g)
preference for selection		#3	#5	#4	#6	#1	#2	
Technetium	Tc		0.1	0.1		0.2	0.2	0.2
Ruthenium	Ru		55	55		0		55
Rhodium	Rh		52					52
Palladium	Pd		52	55				55
Silver	Ag	90	90	90		90		90
Cadmium	Cd	6	40	80	8	6		6
Indium	In		390					390
Tin	Sn		130	130				130
Antimony	Sb	50	45	45		50		50
Tellurium	Te		140	125				125
Iodine	I	0	1	1		0	0	0
Xenon	Xe		0					0
Cesium	Cs	500	270	280	30	500	500	500
Barium	Ba	50	52			50		50
Lanthanum	La		1200					1200
Cerium	Ce	500	500	500				500
Praseodymium	Pr		240					240
Neodymium	Nd		240					240
Promethium	Pm		240					240
Samarium	Sm		240	245				240
Europium	Eu		240			340		340
Gadolinium	Gd		240					240
Terbium	Tb		240					240
Dysprosium	Dy							240
Holmium	Ho		240	250				250
Erbium	Er							240
Thulium	Tm							240
Ytterbium	Yb							240
Lutetium	Lu							240
Hafnium	Hf			450				450
Tantalum	Ta			220				220
Tungsten	W		100					100
Rhenium	Re		14	10				10
Osmium	Os		190					190
Iridium	Ir		91					91
Platinum	Pt							55
Gold	Au		30					30
Mercury	Hg	100	19			100	100	100
Thallium	Tl		390			100		100
Lead	Pb	100	270	270	710		100	100
Bismuth	Bi	100	120	100				100
Polonium	Po		150	150				150
Astatine	At							0
Radon	Rn		0		0			0

Element	Symbol	Track 1 (Table G-1, default values)	NCRP 123 (Table 4.1)	Sheppard and Thibault (Table 1, Sand)	EPA 402-R-99-004A, Volume II	OU 3-13 RI/BRA (Appendix F, Tables 5-1 & 5-2)	EDF-ER-170 (Table 3-2)	Selected Kd Value
preference for selection		#3	#5	#4	#6	#1	#2	(ml/g)
Francium	Fr							500
Radium	Ra	100	500	500				100
Actinium	Ac		420	450				450
Thorium	Th	100	3200	3200	1700		100	100
Protactinium	Pa		510	550				550
Uranium	U	6	15	35	63	6	6	6
Neptunium	Np		5	5		8	8	8
Plutonium	Pu	22	550	550	80	22	140	140
Americium	Am	340	1900	1900		340	340	340
Curium	Cm		4000	4000				4000
Berkelium	Bk							4000
Californium	Cf		510					510

Table A-2. Kd values for alluvium soils from various references along with the preference for selection and resulting selected Kds.

Element	Symbol	Track 1 (Table G- 1, default values)	NCRP 123 (Table 4.1)	Sheppard and Thibault (Table 1, Sand)	EPA 402- R-99- 004A, Volume II	OU 3-13 RI/BRA (Appendix F, Tables 5-1 & 5-2)	EDF-ER- 170 (Table 3-2)	Selected Kd Value (ml/g)
preference for selection		#3	#5	#4	#6	#2	#1	
Hydrogen	H	0	0			0		0
Helium	He							0
Lithium	Li							15
Beryllium	Be	250	240	250		250		250
Boron	B							5
Carbon	C	0	6.7	5				5
Nitrogen	N					0		0
Oxygen	O							0
Fluorine	F	0	87			0		0
Neon	Ne							0
Sodium	Na		76					76
Magnesium	Mg							5
Aluminium	Al					250		250
Silicon	Si			35				35
Phosphorous	P		8.9	5				5
Sulfur	S		14					14
Chlorine	Cl		1.7			0		0
Argon	Ar							0
Potassium	K	15	18	15		15		15
Calcium	Ca	5	8.9	5				5
Scandium	Sc		310					310
Titanium	Ti							600
Vanadium	V	1000				6		6
Chromium	Cr	1.2	30	70	70	1.2		30
Manganese	Mn	50	50	50		50		50
Iron	Fe	220	160	220				220
Cobalt	Co	10	60	60		10		10
Nickel	Ni	100	400	400		100		100
Copper	Cu	20	30			20		20
Zinc	Zn	16	200	200				16
Gallium	Ga							250
Germanium	Ge							35
Arsenic	As	3	110			3	3	3
Selenium	Se	4	140	150		4		4
Bromine	Br	15	14	15				15
Krypton	Kr		0					0
Rubidium	Rb		52	55				55
Strontium	Sr	24	15	15	15	12	24	24
Yttrium	Y		190	170				170
Zirconium	Zr	600	580	600				600
Niobium	Nb		160	160		100		100
Molybdenum	Mo		10	10				10

Element	Symbol	Track 1 (Table G-1, default values)	NCRP 123 (Table 4.1)	Sheppard and Thibault (Table 1, Sand)	EPA 402-R-99-004A, Volume II	OU 3-13 RI/BRA (Appendix F, Tables 5-1 & 5-2)	EDF-ER-170 (Table 3-2)	Selected Kd Value (ml/g)
		#3	#5	#4	#6	#2	#1	
preference for selection								
Technetium	Tc		0.1	0.1		0.2	0.2	0.2
Ruthenium	Ru		55	55		0		55
Rhodium	Rh		52					52
Palladium	Pd		52	55				55
Silver	Ag	90	90	90		90		90
Cadmium	Cd	6	40	80	8	6		6
Indium	In		390					390
Tin	Sn		130	130				130
Antimony	Sb	50	45	45		50		50
Tellurium	Te		140	125				125
Iodine	I	0	1	1		0	0	0
Xenon	Xe		0					0
Cesium	Cs	500	270	280	30	500	500	500
Barium	Ba	50	52			50		50
Lanthanum	La		1200					1200
Cerium	Ce	500	500	500				500
Praseodymium	Pr		240					240
Neodymium	Nd		240					240
Promethium	Pm		240					240
Samarium	Sm		240	245				240
Europium	Eu		240			340		340
Gadolinium	Gd		240					240
Terbium	Tb		240					240
Dysprosium	Dy							240
Holmium	Ho		240	250				250
Erbium	Er							240
Thulium	Tm							240
Ytterbium	Yb							240
Lutetium	Lu							240
Hafnium	Hf			450				450
Tantalum	Ta			220				220
Tungsten	W		100					100
Rhenium	Re		14	10				10
Osmium	Os		190					190
Iridium	Ir		91					91
Platinum	Pt							55
Gold	Au		30					30
Mercury	Hg	100	19			100	100	100
Thallium	Tl		390			100		100
Lead	Pb	100	270	270	710		100	100
Bismuth	Bi	100	120	100				100
Polonium	Po		150	150				150
Astatine	At							0
Radon	Rn		0		0			0

Element	Symbol	Track 1 (Table G-1, default values)	NCRP 123 (Table 4.1)	Sheppard and Thibault (Table 1, Sand)	EPA 402-R-99-004A, Volume II	OU 3-13 RI/BRA (Appendix F, Tables 5-1 & 5-2)	EDF-ER-170 (Table 3-2)	Selected Kd Value
preference for selection		#3	#5	#4	#6	#2	#1	(ml/g)
Francium	Fr							500
Radium	Ra	100	500	500				100
Actinium	Ac		420	450				450
Thorium	Th	100	3200	3200	1700		100	100
Protactinium	Pa		510	550				550
Uranium	U	6	15	35	63	6	6	6
Neptunium	Np		5	5		8	8	8
Plutonium	Pu	22	550	550	80	22	140	140
Americium	Am	340	1900	1900		340	340	340
Curium	Cm		4000	4000				4000
Berkelium	Bk							4000
Californium	Cf		510					510

Table A-3. Kd values for clay materials from various references along with the preference for selection and resulting selected Kds.

Element	Symbol	Track 1 (Table G- 1, default values)	NCRP 123 (Table 4.1)	Sheppard and Thibault (Table 1, Clay)	EPA 402- R-99- 004A, Volume II	OU 3-13 RI/BRA (Appendix F, Tables 5-1 & 5-2)	EDF-ER- 170 (Table 3-2)	Selected Kd Value 9m(g)
preference for selection		#4	#5	#2	#6	#3	#1	
Hydrogen	H	0	0			0		0
Helium	He							0
Lithium	Li							75
Beryllium	Be	250	240	1300		250		1300
Boron	B							1
Carbon	C	0	6.7	1				1
Nitrogen	N					0		0
Oxygen	O							0
Fluorine	F	0	87			0		0
Neon	Ne							0
Sodium	Na		76					76
Magnesium	Mg							50
Aluminum	Al					250		250
Silicon	Si			180				180
Phosphorous	P		8.9	35				35
Sulfur	S		14					14
Chlorine	Cl		1.7			0		0
Argon	Ar							0
Potassium	K	15	18	75		15		75
Calcium	Ca	5	8.9	50				50
Scandium	Sc		310					310
Titanium	Ti							3300
Vanadium	V	1000				6		6
Chromium	Cr	1.2	30	1500	70	1.2		1500
Manganese	Mn	50	50	180		50		180
Iron	Fe	220	160	165				165
Cobalt	Co	10	60	550		10		550
Nickel	Ni	100	400	650		100		650
Copper	Cu	20	30			20		20
Zinc	Zn	16	200	2400				2400
Gallium	Ga							250
Germanium	Ge							180
Arsenic	As	3	110			3	7	7
Selenium	Se	4	140	740		4		740
Bromine	Br	15	14	75				75
Krypton	Kr		0					0
Rubidium	Rb		52	270				270
Strontium	Sr	24	15	110	200	12	200	200
Yttrium	Y		190	1000				1000
Zirconium	Zr	600	580	3300				3300
Niobium	Nb		160	900		100		900
Molybdenum	Mo		10	90				90

Element	Symbol	Track 1 (Table G-1, default values)	NCRP 123 (Table 4.1)	Sheppard and Thibault (Table 1, Clay)	EPA 402- R-99- 004A, Volume II	OU 3-13 RI/BRA (Appendix F, Tables 5-1 & 5-2)	EDF-ER- 170 (Table 3-2)	Selected Kd Value
		#4	#5	#2	#6	#3	#1	9ml/g)
preference for selection								
Technetium	Tc		0.1	1		0.2	1	1
Ruthenium	Ru		55	800		0		800
Rhodium	Rh		52					52
Palladium	Pd		52	270				270
Silver	Ag	90	90	180		90		180
Cadmium	Cd	6	40	560	8	6		560
Indium	In		390					390
Tin	Sn		130	670				670
Antimony	Sb	50	45	250		50		250
Tellurium	Te		140	720				720
Iodine	I	0	1	1		0	1	1
Xenon	Xe		0					0
Cesium	Cs	500	270	1900	210	500	1500	1500
Barium	Ba	50	52			50		50
Lanthanum	La		1200					1200
Cerium	Ce	500	500	20000				20000
Praseodymium	Pr		240					240
Neodymium	Nd		240					240
Promethium	Pm		240					240
Samarium	Sm		240	1300				1300
Europium	Eu		240			340		340
Gadolinium	Gd		240					240
Terbium	Tb		240					240
Dysprosium	Dy							240
Holmium	Ho		240	1300				1300
Erbium	Er							240
Thulium	Tm							240
Ytterbium	Yb							240
Lutetium	Lu							240
Hafnium	Hf			2400				2400
Tantalum	Ta			1200				1200
Tungsten	W		100					100
Rhenium	Re		14	60				60
Osmium	Os		190					190
Iridium	Ir		91					91
Platinum	Pt							270
Gold	Au		30					30
Mercury	Hg	100	19			100	710	710
Thallium	Tl		390			100		100
Lead	Pb	100	270	550	710		710	710
Bismuth	Bi	100	120	600				600
Polonium	Po		150	3000				3000
Astatine	At							1
Radon	Rn		0		0			0

Element	Symbol	Track 1 (Table G- 1, default values)	NCRP 123 (Table 4.1)	Sheppard and Thibault (Table 1, Clay)	EPA 402- R-99- 004A, Volume II	OU 3-13 RI/BRA (Appendix F, Tables 5-1 & 5-2)	EDF-ER- 170 (Table 3-2)	Selected Kd Value
preference for selection		#4	#5	#2	#6	#3	#1	9ml/g)
Francium	Fr							1500
Radium	Ra	100	500	9100				9100
Actinium	Ac		420	2400				2400
Thorium	Th	100	3200	5800	1700		1700	1700
Protactinium	Pa		510	2700				2700
Uranium	U	6	15	1600	63	6	63	63
Neptunium	Np		5	55		8	55	55
Plutonium	Pu	22	550	5100	2440	22	1700	1700
Americium	Am	340	1900	8400		340	340	340
Curium	Cm		4000	6000				6000
Berkelium	Bk							6000
Californium	Cf		510					510

Table A-4. Kd values for barrier soils from various references along with the preference for selection and resulting selected Kds.

Element	Symbol	Track 1 (Table G-1, default values)	NCRP 123 (Table 4.1)	Sheppard and Thibault (Table 1, Loam)	EPA 402-R-99-004A, Volume II	OU 3-13 RI/BRA (Appendix F, Tables 5-1 & 5-2)	EDF-ER-170 (Table 3-2)	Dicke 1997 (Table 4, RWMC sediments)	Selected Kd Value (ml/g)
		#4	#5	#2	#6	#3	#1		
preference for selection									
Hydrogen	H	0	0			0		0	0
Helium	He								0
Lithium	Li								55
Beryllium	Be	250	240	800		250		250	800
Boron	B								20
Carbon	C	0	6.7	20				5	20
Nitrogen	N					0		0	0
Oxygen	O								0
Fluorine	F	0	87			0			0
Neon	Ne								0
Sodium	Na		76					0	76
Magnesium	Mg								30
Aluminum	Al					250			250
Silicon	Si			110					110
Phosphorous	P		8.9	25					25
Sulfur	S		14						14
Chlorine	Cl		1.7			0		0	0
Argon	Ar								0
Potassium	K	15	18	55		15			55
Calcium	Ca	5	8.9	30					30
Scandium	Sc		310						310
Titanium	Ti								2200
Vanadium	V	1000				6			6
Chromium	Cr	1.2	30	30	70	1.2		30	30
Manganese	Mn	50	50	750		50			750
Iron	Fe	220	160	800					800
Cobalt	Co	10	60	1300		10		1000	1300
Nickel	Ni	100	400	300		100		300	300
Copper	Cu	20	30			20			20
Zinc	Zn	16	200	1300					1300
Gallium	Ga								250
Germanium	Ge								110
Arsenic	As	3	110			3	7		7
Selenium	Se	4	140	500		4			500
Bromine	Br	15	14	50					50
Krypton	Kr		0						0
Rubidium	Rb		52	180					180
Strontium	Sr	24	15	20	15	12	200	60	200
Yttrium	Y		190	720					720
Zirconium	Zr	600	580	2200					2200
Niobium	Nb		160	550		100		500	550
Molybdenum	Mo		10	125					125

Element	Symbol	Track 1 (Table G-1, default values)	NCRP 123 (Table 4.1)	Sheppard and Thibault (Table 1, Loam)	EPA 402-R-99-004A, Volume II	OU 3-13 RI/BRA (Appendix F, Tables 5-1 & 5-2)	EDF-ER-170 (Table 3-2)	Dicke 1997 (Table 4, RWMC sediments)	Selected Kd Value (ml/g)
preference for selection		#4	#5	#2	#6	#3	#1		
Technetium	Tc		0.1	0.1		0.2	1	0	1
Ruthenium	Ru		55	1000		0			1000
Rhodium	Rh		52						52
Palladium	Pd		52	180					180
Silver	Ag	90	90	120		90			120
Cadmium	Cd	6	40	40	8	6		40	40
Indium	In		390						390
Tin	Sn		130	450					450
Antimony	Sb	50	45	150		50		7	150
Tellurium	Te		140	500					500
Iodine	I	0	1	5		0	1	0.1	1
Xenon	Xe		0						0
Cesium	Cs	500	270	4600	30	500	1500	1000	1500
Barium	Ba	50	52			50			50
Lanthanum	La		1200						1200
Cerium	Ce	500	500	8100					8100
Praseodymium	Pr		240						240
Neodymium	Nd		240						240
Promethium	Pm		240						240
Samarium	Sm		240	800					800
Europium	Eu		240			340		400	340
Gadolinium	Gd		240					400	240
Terbium	Tb		240						240
Dysprosium	Dy								240
Holmium	Ho		240	800					800
Erbium	Er								240
Thulium	Tm								240
Ytterbium	Yb								240
Lutetium	Lu								240
Hafnium	Hf			1500					1500
Tantalum	Ta			900					900
Tungsten	W		100						100
Rhenium	Re		14	40					40
Osmium	Os		190						190
Iridium	Ir		91						91
Platinum	Pt								180
Gold	Au		30						30
Mercury	Hg	100	19			100	710	176	710
Thallium	Tl		390			100			100
Lead	Pb	100	270	16000	710		710	270	710
Bismuth	Bi	100	120	450					450
Polonium	Po		150	400					400
Astatine	At								1
Radon	Rn		0		0				0

Element	Symbol	Track 1 (Table G- 1, default values)	NCRP 123 (Table 4.1)	Sheppard and Thibault (Table 1, Loam)	EPA 402- R-99- 004A, Volume II	OU 3-13 RI/BRA (Appendix F, Tables 5-1 & 5-2)	EDF-ER- 170 (Table 3-2)	Dicke 1997 (Table 4, RWMC sediments)	Selected Kd Value (ml/g)
		#4	#5	#2	#6	#3	#1		
Francium	Fr								1500
Radium	Ra	100	500	36000				575	36000
Actinium	Ac		420	1500				400	1500
Thorium	Th	100	3200	3300	1700		1700	500	1700
Protactinium	Pa		510	1800				8	1800
Uranium	U	6	15	15	63	6	63	6	63
Neptunium	Np		5	25		8	55	8	55
Plutonium	Pu	22	550	1200	2010	22	1700	5100	1700
Americium	Am	340	1900	9600		340	340	450	340
Curium	Cm		4000	18000				400	4000
Berkelium	Bk								4000
Californium	Cf		510						510

Table A-5. Kd values for sedimentary interbed materials from various references along with the preference for selection and resulting selected Kds.

Element	Symbol	Track 1 (Table G- 1, default values)	NCRP 123 (Table 4.1)	Sheppard and Thibault (Table 1, Sand)	EPA 402- R-99- 004A, Volume II	OU 3-13 RI/BRA (Appendix F, Tables 5-1 & 5-2)	EDF-ER- 170 (Table 3-2)	Selected Kd Value (ml/g)
preference for selection		#3	#5	#4	#6	#2	#1	
Hydrogen	H	0	0			0		0
Helium	He							0
Lithium	Li							15
Beryllium	Be	250	240	250		250		250
Boron	B							5
Carbon	C	0	6.7	5				5
Nitrogen	N					0		0
Oxygen	O							0
Fluorine	F	0	87			0		0
Neon	Ne							0
Sodium	Na		76					76
Magnesium	Mg							5
Aluminum	Al					250		250
Silicon	Si			35				35
Phosphorous	P		8.9	5				5
Sulfur	S		14					14
Chlorine	Cl		1.7			0		0
Argon	Ar							0
Potassium	K	15	18	15		15		15
Calcium	Ca	5	8.9	5				5
Scandium	Sc		310					310
Titanium	Ti							600
Vanadium	V	1000				6		6
Chromium	Cr	1.2	30	70	70	1.2		30
Manganese	Mn	50	50	50		50		50
Iron	Fe	220	160	220				220
Cobalt	Co	10	60	60		10		10
Nickel	Ni	100	400	400		100		100
Copper	Cu	20	30			20		20
Zinc	Zn	16	200	200				16
Gallium	Ga							250
Germanium	Ge							35
Arsenic	As	3	110			3	3	3
Selenium	Se	4	140	150		4		4
Bromine	Br	15	14	15				15
Krypton	Kr		0					0
Rubidium	Rb		52	55				55
Strontium	Sr	24	15	15	15	12	12	12
Yttrium	Y		190	170				170
Zirconium	Zr	600	580	600				600
Niobium	Nb		160	160		100		100
Molybdenum	Mo		10	10				10

Element	Symbol	Track 1 (Table G- 1, default values)	NCRP 123 (Table 4.1)	Sheppard and Thibault (Table 1, Sand)	EPA 402- R-99- 004A, Volume II	OU 3-13 RI/BRA (Appendix F, Tables 5-1 & 5-2)	EDF-ER- 170 (Table 3-2)	Selected Kd Value (ml/g)
		#3	#5	#4	#6	#2	#1	
Technetium	Tc		0.1	0.1		0.2	0.2	0.2
Ruthenium	Ru		55	55		0		55
Rhodium	Rh		52					52
Palladium	Pd		52	55				55
Silver	Ag	90	90	90		90		90
Cadmium	Cd	6	40	80	8	6		6
Indium	In		390					390
Tin	Sn		130	130				130
Antimony	Sb	50	45	45		50		50
Tellurium	Te		140	125				125
Iodine	I	0	1	1		0	0	0
Xenon	Xe		0					0
Cesium	Cs	500	270	280	30	500	500	500
Barium	Ba	50	52			50		50
Lanthanum	La		1200					1200
Cerium	Ce	500	500	500				500
Praseodymium	Pr		240					240
Neodymium	Nd		240					240
Promethium	Pm		240					240
Samarium	Sm		240	245				240
Europium	Eu		240			340		340
Gadolinium	Gd		240					240
Terbium	Tb		240					240
Dysprosium	Dy							240
Holmium	Ho		240	250				250
Erbium	Er							240
Thulium	Tm							240
Ytterbium	Yb							240
Lutetium	Lu							240
Hafnium	Hf			450				450
Tantalum	Ta			220				220
Tungsten	W		100					100
Rhenium	Re		14	10				10
Osmium	Os		190					190
Iridium	Ir		91					91
Platinum	Pt							55
Gold	Au		30					30
Mercury	Hg	100	19			100	100	100
Thallium	Tl		390			100		100
Lead	Pb	100	270	270	710		100	100
Bismuth	Bi	100	120	100				100
Polonium	Po		150	150				150
Astatine	At							0
Radon	Rn		0		0			0

Element	Symbol	Track 1 (Table G-1, default values)	NCRP 123 (Table 4.1)	Sheppard and Thibault (Table 1, Sand)	EPA 402-R-99-004A, Volume II	OU 3-13 RI/BRA (Appendix F, Tables 5-1 & 5-2)	EDF-ER-170 (Table 3-2)	Selected Kd Value
preference for selection		#3	#5	#4	#6	#2	#1	(ml/g)
Francium	Fr							500
Radium	Ra	100	500	500				100
Actinium	Ac		420	450				450
Thorium	Th	100	3200	3200	1700		100	100
Protactinium	Pa		510	550				550
Uranium	U	6	15	35	63	6	6	6
Neptunium	Np		5	5		8	8	8
Plutonium	Pu	22	550	550	80	22	22	22
Americium	Am	340	1900	1900		340	340	340
Curium	Cm		4000	4000				4000
Berkelium	Bk							4000
Californium	Cf		510					510

